Contrast-Enhanced Ultrasound in Pediatric Imaging

Paul S. Sidhu
Maria E. Sellars
Annamaria Deganello
Editors

Springer

Contrast-Enhanced Ultrasound in Pediatric Imaging

Paul S. Sidhu • Maria E. Sellars
Annamaria Deganello
Editors

Contrast-Enhanced Ultrasound in Pediatric Imaging

Springer

Editors
Paul S. Sidhu
Department of Radiology
King's College Hospital
London
UK

Maria E. Sellars
Department of Radiology
King's College Hospital
London
UK

Annamaria Deganello
Department of Radiology
King's College Hospital
London
UK

ISBN 978-3-030-49690-6 ISBN 978-3-030-49691-3 (eBook)
https://doi.org/10.1007/978-3-030-49691-3

This Springer imprint is published by the registered company Springer Nature Switzerland AG
The registered company address is: Gewerbestrasse 11, 6330 Cham, Switzerland

This book is dedicated to two pioneers of contrast-enhanced ultrasound and our colleagues who contributed immensely to the development of the technique, who both are sadly no longer with us.

***Professor David O. Cosgrove** (1938–2017) was the "father figure" of ultrasound in the United Kingdom, using ultrasound clinically in the 1970s and embracing the development of contrast-enhanced ultrasound from the very beginning. An internationally recognized and respected figure in ultrasound, mentor, and colleague to all of us.*

***Professor Martin J.K. Blomley** (1959–2006) a respected colleague, a pioneer in the early days of contrast-enhanced ultrasound, destined for great things, but a life cruelly cut short.*

A large number of people have helped over the years to develop the pediatric contrast-enhanced ultrasound service both in clinical terms and with research, too many to mention, but contributing to this new area of ultrasound imaging. In addition, I am grateful for the patience of my family—Monica, Francesca, and Gianluca who, I believe, continue to support me.

Paul S. Sidhu

To my clinical pediatric colleagues at Kings College Hospital who have supported us and continue to trust us with their patients. Also, to my father, Professor Sean Sellars who sadly passed away last summer, my husband Steve, four children, Anna, Matthew, Rebecca, and Emily and Emma, all of whose love and support has been invaluable to me.

Maria E. Sellars

To my husband Tommaso, who is always supportive of my academic work and keeps me on my toes, and to my children Marino and Maddalena, my daily reminder of what unconditional love means. Also, to my parents, Paola and Vittorio, who are always there for me and have shaped who I am today.

Annamaria Deganello

Foreword

In the past two decades, the acoustic microbubble has graduated from a scientific curiosity to a clinical contrast agent that has become an indispensable part of the ultrasound armamentarium. Injectable microbubbles have been approved for diagnostic indications in the heart, vascular system, and abdomen in dozens of jurisdictions. Over an estimated 10 million patient studies, they have proven to be safe and exceptionally well tolerated by patients. Several generations of guidelines for their clinical use have been published by both European and World ultrasound federations. Yet none of these guidelines, and until recently none of these approvals, have been for their use in children. In spite of this, a burgeoning number of pediatric radiologists and other specialists have been investigating their off-label use for many applications in children, assiduously recording and pooling data on safety and effectiveness. Principal among them have been the authors of this book, who have both led and brought together many of their international colleagues, all committed to bringing the evident advantages of contrast-enhanced ultrasound to pediatric diagnosis. The shear breadth of the titles of the contributions here both testifies to their commitment and confirms this book as the most up-to-date and comprehensive guide to the use of this new imaging modality in children.

The book is particularly timely in view of another, uniquely North American, story. Microbubble agents were first approved for abdominal diagnosis in European Union countries in 2002, which were soon joined by China, Canada, Australasia, and many Asian and south American jurisdictions. But in spite of continuous efforts by both manufacturers and medical organizations, the United States FDA allowed no approvals outside the heart until finally, in 2016, they announced acceptance of the same agent and the same indications that were approved in Europe nearly 15 years previously. However, when they did so, they extended the approved indications to children. This was something of a surprise, as it was known that the dossier presented to them contained no pivotal safety or efficacy studies in this population. It subsequently became clear that they had consulted the data that had been gathered by the authors of this book and their colleagues. While it is notoriously hazardous to divine the thinking of the FDA, it seems most likely that they were considering the well-documented overuse of body CT in children in the United States and the significant risk of needless radiation exposure to this radiogenically vulnerable population. That contrast-enhanced ultrasound has been shown to achieve diagnostic equivalence to CT in detection of liver

metastases or in the characterization of focal liver lesions in adults suggests that these might be important applications in children, where there is the additional hazard of sedation associated with CT and MR examinations, as well as the nephrotoxic risk of their contrast agents. For those interested in pursuing contrast-enhanced ultrasound as a means to reduce reliance on contrast CT and MR in children, there is no better starting point than this book.

But microbubbles offer some truly unique properties that allow them to go further than simple equivalence. They are relatively large, as nearly as big as red blood cells, so cannot diffuse through vessel walls, as do molecular iodine and gadolinium compounds. Thus, they have no interstitial phase, and in particular do not leak through hyperpermeable tumor vascular endothelium. In practice, this means that liver tumor "washout" in the portal phase is a more reliable sign of malignancy on CT or MR. As a pure blood pool agent, they provide a direct image of the intravascular volume of an organ or of a tumor, useful for gauging response to targeted therapies. And uniquely among contrast agents in medical imaging, they can be manipulated by the imaging process itself. Thus by the press of a key, the bubbles can instantly be eliminated from the imaging plane and their replenishment monitored in real time, showing vascular morphology and providing a new method to quantitate flow. The use of such techniques is well documented in the adult radiology literature and the authors demonstrate in practical detail that almost all are translatable to the pediatric patient.

The book begins with a description of the principles of contrast imaging: by now, the techniques employed by the scanners have matured, settling on one or two contrast-specific modes that are easy to understand. But as with all ultrasound imaging, understanding is important because the images are produced and interpreted in real time by the operator, and it is essential to understand the effect of the many parameters under his or her control. It is extraordinary to contemplate that the basis of these methods—that ultrasound stimulates the bubbles into resonant oscillation so that they ring like microscopic bells—is no more than a serendipity of physics that the size of a bubble determines that their resonance lies in the diagnostic frequency range. Current machines are so sensitive to this resonance that they can resolve in real time an individual bubble in a microvessel deep in an adult abdomen, a feat unmatched by any other clinical modality. A discussion of the excellent safety profile of ultrasound contrast agents includes summaries of the significant safety studies published to date in children, whose enrolment will hopefully increase now that post-marketing surveillance of the approved agent is underway. A chapter on artifacts peculiar to the contrast study follows, written by the principal and most senior author. Novices to the field may well be puzzled by the openly competitive enthusiasm shown by experienced sonographers for imaging artifacts; their appreciation is one of the hallmark pleasures of ultrasound imaging. A detailed, step-by-step guide to the performance of a contrast examination is then provided, from initial planning to final reporting.

Subsequent chapters are devoted to a comprehensive description of a series of key clinical applications of contrast in pediatric diagnosis, including focal liver lesions, organ transplantation, abdominal trauma, the kidneys,

spleen, and scrotum; in pneumonia, inflammatory bowel, oncology, and specialist applications in interventional radiology, intraoperative neuroimaging, and in the neonatal nursery. Each chapter is written by experts in the field, in many cases those with the most experience worldwide, beginning with practical basics and progressing to the limit of current knowledge. Additional chapters give the clinician's perspective, in the liver and from the trauma room. An important chapter is included on the principal extravascular indication for ultrasound contrast (also approved by the FDA), of vesicoureteral reflux. It is written by one of the originators of the method and presents convincing arguments for its use over X-ray and radionuclide alternatives. Finally, an analysis of cost-effectiveness of contrast-enhanced ultrasound in children comes from the academic medical center of the main authors, and though inevitably linked to the particulars of their own healthcare system, nonetheless provides a prima facie case for any healthcare administrator to support its use.

As these applications continue to find their place, research propels the acoustic bubble in new directions. Those currently approved are designed to circulate passively within the vascular system; new ones have surface ligands that attach to endothelial cells expressing VEGF, indicative of vascular proliferation, or VCAMs, associated with inflammation. Disrupting them in situ allows measure of expression of these molecules. As alluded to in Chap. 2, bubbles in oscillation near cell membranes can permeabilize them, allowing the selective enhancement of drug delivery under ultrasound guidance. Bubbles can even open the blood–brain barrier in regions selected by an ultrasound beam through the skull or into the spinal cord. And liquid nanodroplets can act as precursors of bubbles, diffusing into tissue and transforming into bubbles under the ultrasound beam, releasing drugs or providing a diagnostic beacon. Exciting and original though the benefits derived by pediatric patients from the applications described in this book may be, they surely are just the beginning.

Peter N. Burns
University of Toronto
Toronto, ON, Canada

Sunnybrook Research Institute
Toronto, ON, Canada

Preface

There has been a wealth of experience accumulated over the last 25 years with regard to the application of contrast-enhanced ultrasound in adult practice. From the initial stages of the application of early ultrasound contrast agents for "Doppler rescue" to the science of gene and drug delivery therapy, the field has been constantly changing, improving, and most importantly remaining innovative. Initially, this was mostly driven by practitioners in Europe, exploring clinical applications outside the few licenced uses, constantly discovering new areas, and extending the usefulness of this novel extension of the ultrasound examination.

The ultrasound physicists made enormous advances in the understanding of the interaction of the microbubble in an acoustic field, opening up tremendous opportunity to image right down to the capillary level, reflecting the unique intravascular nature of the microbbuble contrast agent. Multiple advances in numerous areas made the development of the technique a fascinating journey for those involved in the evolutionary process.

We as a team here at King's College Hospital evolved with this unfolding scenario, "tagging" along with the many greats of the field, experimenting and innovating as much as we could, dragged along by the momentum generated by enthusiastic and skilled practitioners. The developments, particularly on the technical aspects, rapidly advanced with usefulness of the technique so blatantly obvious to the enthusiast.

Around the early part of this century, we were approached by our pediatric clinical colleagues to help with reducing the amount of imaging they were obliged to request when incidental abnormalities in the liver were picked up on our ultrasound imaging. The hospital serves as a large tertiary referral for chronic pediatric liver disease, with children on surveillance ultrasound at regular intervals, with new focal liver lesions needing workup with computed tomography and magnetic resonance imaging, often nearly always benign. This additional "imaging" demands all those aspects that you should avoid in children; sedation, general anesthesia, radiation, potentially harmful contrast agents, which ultrasound avoids.

We had already an established adult liver contrast-enhanced ultrasound service, and without hesitation we embarked on expanding pediatric applications into our contrast-enhanced ultrasound practice. We targeted the focal liver lesions in these children, but we had previously been using contrast-enhanced ultrasound following liver transplantation in both adults and children, in pursuit of the elusive hepatic artery. This initiative proved to be

successful; the parents readily agreed to the procedure as carefully explained by the referring clinical team, the children had no fear of the "test" in the friendly supported examination room and furthermore the accuracy of the test matched that being seen in adults. The issue of "off-licence" was elegantly detailed to the parent by the referring clinical team; most drug intervention is "off-licence" in children but we do it for the betterment of healthcare for our children.

We published our results, as did other groups across Europe, many using this technique on an "ad hoc" basis, with an international questionnaire indicating this was not an uncommon occurrence. The application of intravesical contrast ultrasound (licenced application) was relatively common practice, with intravenous applications in many organs documented by this survey.

Subsequently, the application of contrast ultrasound in the assessment and follow-up of blunt abdominal trauma began to emerge in the adult population, with almost immediate transfer to the management of trauma in children. This seems to be an obvious option to apply contrast-enhanced ultrasound to the follow-up of a resolving focal solid single organ injury, avoiding the need to do repeated computed tomography examinations in the child. This has now also become accepted practice in many trauma centers in Europe.

Many other groups have developed the applications of contrast-enhanced ultrasound in children, and this book summarizes this experience. We are at the beginning, and as we look back over the last 20 years of our own practice and see how far we come, we are sure the transformation over the next 20 years will be unrecognizable today. We owe it to the children to image gently and ultrasound is ideal for this. Adding a contrast agent to an ultrasound examination avoids all the aspects of computed tomography and magnetic resonance imaging procedures that may not always be needed or even be detrimental to the child.

London, UK Paul S. Sidhu
London, UK Maria E. Sellars
London, UK Annamaria Deganello

Contents

About the Editors

Paul S. Sidhu, BSc, MBBS, MRCP, FRCR, DTM&H is Professor of Imaging Sciences at King's College London and a Consultant Radiologist in the Department of Radiology at King's College Hospital. He qualified from St. Mary's Hospital Medical School (now part of Imperial College London) in 1982, with Honors. He completed his internship at St. Mary's Hospital in Paddington on the Professorial Medical Unit, before completing Senior House Officer Positions at the Brompton Hospital, Hammersmith Hospital, Hospital for Tropical Diseases and Guy's Hospital. He did his radiology training at the Hammersmith Hospital and King's College Hospital. He was appointed a Consultant Radiologist at King's College Hospital in 1996, with a role in Ultrasound and Interventional Radiology. He was made Professor of Imaging Sciences in 2012. He is Clinical Director of Radiology at King's College Hospital, London. He has published extensively on many aspects of ultrasound particularly in relation to male health and liver transplantation and has pioneered the introduction of contrast-enhanced ultrasound in the United Kingdom. He is recognized as an authority in the application of contrast-enhanced ultrasound in clinical practice. He is the Editor of 6 books and has published over 600 scientific articles, book chapters, and conference abstracts. He lectures widely with over 500 presentations at national and international meetings. He is currently the Editor of the *European Journal of Ultrasound* and previously the Deputy Editor of the *British Journal of Radiology*. He is an Associate Editor of Radiology. He is Past-President of the British Medical Ultrasound Society and the Past-

President of the Section of Radiology of the Royal Society of Medicine. He is recent Past-President of the European Federation of Societies in Ultrasound in Medicine and Biology. His current research interests include the application of contrast-enhanced ultrasound to the testis, radiation dose reduction in children, and non-invasive ultrasound in the assessment of liver disease.

Maria E. Sellars, MBChB, FRCR is a consultant pediatric radiologist at King's College Hospital London since 2002. After completing her medical training and Internship in 1991 at the University of Cape Town, she spent five years working in Emergency Medicine while lecturing in Anatomy at the University of Cape Town. She began specialist training in Radiology at Groote Schuur Hospital in Cape Town, joining the training program in the Department of Radiology at King's College in London, where she was awarded the FRCR in 2000. She has a special interest in the imaging of pediatric hepatobiliary disease in particular complex hepatobiliary, pancreatic/pediatric surgical disorders and pediatric liver transplantation and pediatric trauma. She is the author and co-author of a number of peer-reviewed publications and has lectured at national and international meetings.

Annamaria Deganello, MD is a Consultant Pediatric Radiologist in the Department of Radiology at King's College Hospital, London, and an Honorary Senior Lecturer at King's College London. She qualified in 2004 from the Faculty of Medicine and Surgery of the University of Padova (Italy), having also trained for a year at the Faculty of Medicine of the University of Granada (Spain). She trained in Clinical Radiology at the Policlinico Universitario Hospital of Padova and at King's College Hospital, and she was awarded the Specialization Diploma in Clinical Radiology in Italy in 2009. She subspecialized in Pediatric Radiology at King's College Hospital and worked at the Evelina Children's Hospital in London. She was appointed Consultant Radiologist at King's College Hospital in 2013, with a role in pediatric radiology and hepatobiliary pediatric imaging.

Dr. Deganello has a special interest in the imaging of pediatric hepatobiliary diseases and liver transplantation and pediatric trauma. She is the author and co-author of over 40 peer-reviewed publications and book chapters; she has been a Visiting Professor at the Children's Hospital of Philadelphia and an invited lecturer for her expertise at over 30 national and international congresses. She is a member of the Editorial Board of the *Journal of Ultrasound* and a co-opted member of Council of the British Medical Ultrasound Society.

1 Physics of Microbubble Contrast Agents

Kirsten Christensen-Jeffries
and Robert J. Eckersley

1.1 Introduction

Ultrasound (US) has become a routine clinical imaging modality due to its ability to provide safe, non-invasive, real-time images of soft tissue structures, with costs far below that of other common clinical imaging techniques. Furthermore, detecting blood flow in patients has been facilitated through the use of Doppler US. Nevertheless, flow within small vessels or vessels at depth has been limited due to the poor reflectivity of blood and the strong echoes from the tissue. Visualization of the vasculature in clinical US has since been greatly enhanced with the development of microbubbles as ultrasound contrast agents (UCAs) [1–3].

Both the advancement in microbubble engineering [4] and the improved understanding of microbubble behavior [5] has facilitated the progress of contrast-enhanced ultrasound (CEUS) imaging into a routine diagnostic procedure [6]. Comprehensive reviews of the mechanical properties, acoustic response, application, challenges and future directions of microbubbles have been published, which demonstrates the wide recognition of these UCAs as a valuable diagnostic tool [5–7]. In this chapter, a summary of the physics of microbubbles for CEUS is provided.

1.2 Microbubble Contrast Agents

Microbubble UCAs are injected into the bloodstream to enhance the backscatter signal from the blood. Microbubble UCAs have gained increasing interest since their introduction, and CEUS has become a rapidly evolving field with extensive clinical applications, including the assessment of the macro- and micro-vasculature, the quantification of organ perfusion, and the identification and characterization of abdominal lesions. This has been achieved due to the safe profile and the increased stability of microbubbles, which are able to persist in the bloodstream for several minutes. Furthermore, the availability of specialized contrast-specific US imaging techniques has allowed considerable improvement in the contrast resolution and signal suppression from stationary tissues.

1.2.1 Efficacy of Microbubbles as Contrast Agents

The blood itself is a weak scatterer of US. In 1968, before the introduction of commercial agents, the

K. Christensen-Jeffries (✉) · R. J. Eckersley
Department of Biomedical Engineering, School of Biomedical Engineering and Imaging Sciences, King's College London, St Thomas' Hospital, London, UK
e-mail: kirsten.christensen-jeffries@kcl.ac.uk; robert.eckersley@kcl.ac.uk

P. S. Sidhu et al. (eds.), *Contrast-Enhanced Ultrasound in Pediatric Imaging*,
https://doi.org/10.1007/978-3-030-49691-3_1

increased backscattering effect caused by gas bubbles was observed during cardiac catheterization, where gas bubbles were formed during the injection of saline solution [8]. Ultrasound insonation of gas bubbles not only creates increased backscattering due to the presence of gas within the surrounding media, but its compressibility allows bubbles to undergo compression and expansion in response to the peaks and troughs of the acoustic wave. This produces a strong backscattered signal, which can provide a bright contrast within the blood pool. Nevertheless, gas cavities such as these are unstable and unlikely to survive the pulmonary circulation. Nowadays, bubbles are engineered using different shell and core compositions to improve both their persistence in the bloodstream and their effectiveness as contrast agents.

1.2.2 Composition of Microbubble Contrast Agents

Microbubble UCAs are typically 1–7 μm in size, and are composed of a gas core encapsulated by a shell. Currently, many engineered commercial microbubbles are available worldwide, with varying compositions and attributes depending on their desired application (Table 1.1).

1.2.2.1 Core

Air bubbles of this size are inherently unstable because of the surface tension between the gas core and surrounding liquid; the gas tries to diffuse into the liquid. By using a core gas with a lower solubility and lower diffusivity than air (e.g., perfluorocarbon or sulfur hexafluoride), the microbubble stability is increased. Commercial agents are typically created with a low-density gas core. This choice of gas has another benefit that it creates a large impedance mismatch between the bubble and its surrounding media, and thus increases the resulting backscatter when it is hit with an ultrasound wave. At the end of the bubble's lifetime, this gas from the core dissolves in the blood and is exhaled via the lungs (around 10–15 min after injection).

1.2.2.2 Shell Types

The microbubble shell also helps to stabilize the bubble. These usually have a thickness of around 10–200 nm and are usually composed of biocompatible materials, including proteins, lipids, or biopolymers [9]. These can make the shell stiff (e.g., polymers, denaturated albumin) or flexible (e.g., phospholipids). Therefore, the properties of the shell (as well as the gas core) affect the microbubble response to acoustic radiation. For example, stiff polymer-coated microbubbles do not expand and contract at low acoustic pressures, and buckle when acoustic pressure is high, while a flexible phospholipid shell will allow the microbubble to strongly oscillate in response to low pressure acoustics without rupturing [10]. The returning echo is thus much stronger than that from similar-sized incompressible objects, such as red blood cells.

Table 1.1 The core gas and shell material of commercial microbubble contrast agents

Company name	Agent	Gas	Shell
Mallinckrodt	Albunex	Air (Nitrogen)	Albumin
Schering	Echovist	Air (Nitrogen)	Galactose
	Levovist	Air (Nitrogen)	Galactose
	Sonavist	Air (Nitrogen)	Cyanoacrylate
Quadrant	Myomap	Air (Nitrogen)	Albumin
	Quantison	Air (Nitrogen)	Albumin
Bracco	SonoVue	Sulfur hexafluoride	Phospholipid
	BR14	Perfluorobutane	Phospholipid
Bristol–Myers Squibb Medical Imaging	Definity	Octafluoropropane	Phospholipid
Alliance	Imagent–Imavist	Perfluorohexane	Phospholipid
GE Healthcare	Optison	Perfluorobutane	Albumin
	Sonazoid	Perfluorobutane	Phospholipid

Information acquired from [8]

1.2.2.3 Size

Microbubbles have a similar size to red blood cells, which is advantageous for two reasons. Firstly, this means the microbubbles remain within the vascular space: acting as a microvascular marker and allowing multiple passages through the lungs [1]. Secondly, their size means they have a resonance frequency that falls within the medical US frequency range [11], resulting in a dramatic increase in the amplitude of their response. This will be described further in the following section.

1.2.3 Microbubble Behavior in Acoustic Fields

The high compressibility typical of microbubbles means that they are capable of large volumetric oscillations in response to an acoustic pulse [2]. When a wave hits the microbubble, the bubble alternately compresses and expands due to the positive and negative sections of the wave respectively, as shown for SonoVue™ (*Bracco* SpA, Milan) microbubbles (Fig. 1.1). This volume pulsation causes the surrounding medium to oscillate. The returning echo is much stronger than that from similar-sized incompressible objects, such as red blood cells.

1.2.3.1 Linear Response

At low acoustic pressures, the expansion and compression phases of the microbubble are equal in response to the incident wave. This is known as linear oscillation and results in symmetrical scattered signals with the same frequency as the transmitted pulse. This volume pulsation is frequency-dependent. Volumetric oscillations are at a maximum at a specific frequency, which is referred to as the natural resonant frequency of the microbubble, and this is inversely related to its size. At the resonant frequency, the microbubble absorbs and scatters sound very efficiently. This is illustrated further within models described in Sect. 1.2.4.

1.2.3.2 Nonlinear Response

If the insonation pressure is sufficiently high, the microbubble can vibrate with asymmetrical oscillations, where the expansion and compression amplitudes become unequal [5, 12]. This "nonlinear" response to the acoustic pressure wave generates a broad spectrum of radiated energy at multiples and integer sub-multiples of the insonating frequency, termed harmonics and subharmonics [11]. The nonlinear response of microbubbles is not typically shown by tissue, and thus this offers the possibility of separating the response of bubbles from that of surrounding tissue. There have been many signal processing

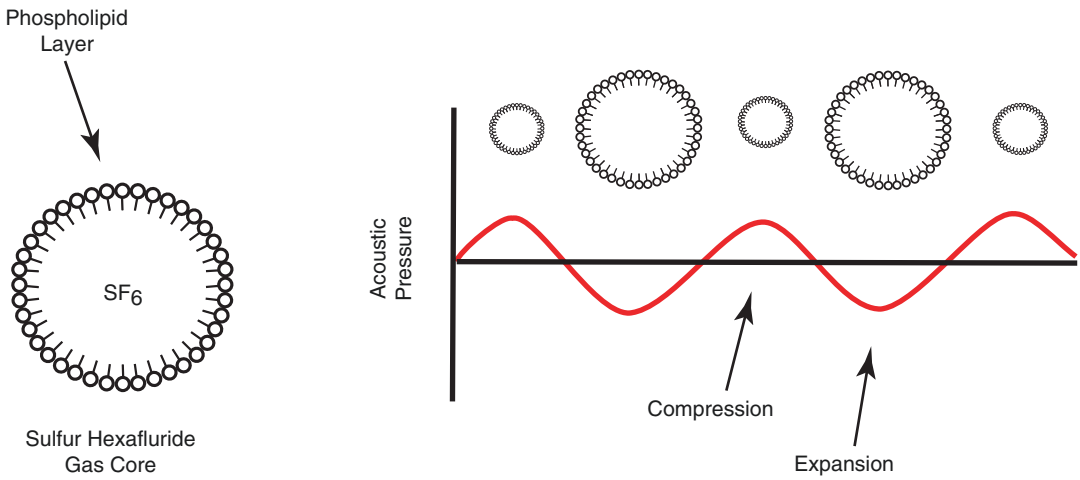

Fig. 1.1 SonoVue™ microbubble and its response to a sound wave. Microbubbles are comprised of a phospholipid monolayer and a sulfur hexafluoride (SF6) gas core. When insonated with an acoustic wave, the bubble undergoes compression and expansion phases, resulting in the creation of a backscatter echo. https://kclpure.kcl.ac.uk/portal/files/83192542/2017_Christensen_Jeffries_Kirsten_Mia_1254928_ethesis.pdf

techniques developed to detect these echoes, which will be discussed in Sect. 1.3.3.

1.2.3.3 Microbubble Destruction

At even higher acoustic pressures, the microbubble shell is compromised at a threshold negative pressure and the microbubbles are destroyed. Disruption of the microbubble shell allows the contained gas to be released and dissolution occurs. This phenomenon, though unfavorable in many imaging strategies, can be advantageous in certain situations. The destruction of the microbubble causes the scattering level to increase for a short period of time, as well as being highly nonlinear, which can allow its detection [13]. Furthermore, techniques such as destruction–replenishment, where, following disruption, the replenishment of microbubble flow into a region of interest is monitored in real time, allow the estimation of dynamic blood flow and volume information in a tissue region [14].

1.2.4 Models of Microbubble Dynamics

Since 1917, a variety of theoretical models have been developed to study gas bubble dynamics in liquids. A fundamental equation of bubble dynamics was developed by Rayleigh and Plesset [15–18], which models the simplest case of a free microbubble driven by a low amplitude sound field in an infinite fluid. Rayleigh-Plessetbased equations have been used extensively in the field to model the behavior of contrast agents. By neglecting liquid compressibility effects for an unshelled bubble, and assuming that the gas pressure in the bubble is uniform and obeys the polytropic law, this can be given by:

$$\rho\left(\ddot{R}R+\frac{3}{2}\dot{R}^2\right)=p_g(t)-p_0-p_i(t)-\frac{4\eta\dot{R}}{R}-\frac{2\sigma}{R}, \tag{1.1}$$

where $\dot{R}$ and $\ddot{R}$ represent respectively the first- and second-order time derivatives of the bubble radius $\dot{R}$, p_0 is the hydrostatic pressure, $p_i(t)$ is the incident ultrasound pressure in the liquid at an infinite distance, $p_g(t)$ is the uniform gas pressure within the bubble and ρ, σ, and η are the density, surface tension, and viscosity of the bulk fluid, respectively.

Using a small-amplitude oscillation assumption, the Rayleigh–Plesset equation has been widely applied to study many aspects of bubble dynamics such as acoustic scattering characteristics and thermal damping effects. Furthermore, at these small amplitudes of displacement where the bubble radius is approximated by simple harmonic oscillation, the bubble will have its own resonance frequency. When the US driving frequency is at this resonance frequency, the bubble will oscillate vigorously. The acoustic resonance frequency, f_0, of a single bubble can be given by [19, 20]:

$$f_0=\frac{1}{2\pi R}\sqrt{\frac{3\gamma}{\rho}\left[P_0\left(1-\frac{1}{3\gamma}\right)\frac{2\sigma}{R}\right]-\left(\frac{2\eta}{\rho R}\right)^2}, \tag{1.2}$$

where γ is the adiabatic ideal gas constant and P_0 is the ambient fluid pressure. Neglecting the effects of surface tension and viscosity, the expression simplifies to

$$f_0\approx\frac{1}{2\pi R}\sqrt{\frac{3\gamma P_0}{\rho}}. \tag{1.3}$$

This shows that the resonance frequency is inversely proportional to the bubble radius. Indeed, such models contain many assumptions, while real-life situations often involve more complex situations, such as those involving encapsulated bubbles traveling within small blood vessels often containing high concentrations of red blood cells and driven by high amplitude sound fields. In order to accurately model the behavior of microbubbles in vivo, and improve agreement between theory and measurements, a series of increasingly complex models have been developed which are not included here. These still include a number of assumptions and simplifications in each case, but may be more complete models for specific scenarios. A Rayleigh–Plesset-based model describing the dynamics of encapsulated microbubbles has been developed by Church, which relates backscatter and attenuation coefficients to shell parameters such as its thickness and rigidity [21]. Hoff et al. [22] developed a model using viscous and elastic properties

of the shell to describe polymeric microbubble behavior. Modified Rayleigh–Plesset equations have also been developed for thin and thick viscoelastic-shelled agents, examining shell viscosity and elasticity effects [23]. Other work has also modeled the behavior of unshelled bubbles within a bubble cloud [24] and the behavior of a single microbubble non-spherically oscillating within a small vessel [25].

An important effect arising from the resonance of a gas bubble is the significant increase in scattering that results. The simplest mathematical description of the scattering of sound waves from a particle whose diameter is much smaller than the incident wavelength, $d \ll \lambda$ or $ka \ll 1$, is Rayleigh scattering [26], proposed in 1871 by Lord Rayleigh where d is the particle diameter, λ is the wavelength of the incident acoustic wave, $k = 2\pi/\lambda$ is the acoustic wavenumber and $R = \frac{1}{2}d$ is the particle radius. For a microbubble, the scattering cross section, σ_s, is the quotient of the acoustic power scattered in all directions per unit incident and is given by [27]

$$\sigma_s = 4\pi R^2 (kR)^4 \left[\left(\frac{K - K_0}{3K} \right)^2 + \frac{1}{3} \left(\frac{\rho - \rho_0}{2\rho + \rho_0} \right)^2 \right], \tag{1.4}$$

or

$$\sigma_s = \frac{\pi^5 d^6 f^4}{v^4} \left[\left(\frac{K - K_0}{3K} \right)^2 + \frac{1}{3} \left(\frac{\rho - \rho_0}{2\rho + \rho_0} \right)^2 \right], \tag{1.5}$$

where v is the speed of sound in the medium. Rayleigh scattering, therefore, depends on the fourth power of the frequency and sixth power of particle diameter. The bracketed term describes the dependence of scattering on the particle material parameters, given by the density,

$$\rho = \frac{m}{V}, \tag{1.6}$$

where m is the mass and V is the volume of the scatterer, The bulk modulus, K, is defined by

$$K = -V \frac{\Delta p}{\Delta V}, \tag{1.7}$$

where Δp is the change in pressure and ΔV is the change in volume, and thus is a measure of the compressional stiffness. As can be seen from Eq (1.5), the scattering cross section varies dramatically with frequency. At resonance, the scattering cross section reaches its maximum, which is orders of magnitude larger than the bubble geometric cross section. Knowledge of the resonant frequency of a bubble can drastically improve the backscatter signals achievable from microbubble contrast agents.

1.3 Ultrasound Imaging with Contrast

1.3.1 Ultrasound Imaging

Ultrasound is a wide-ranging and continually advancing field, where innovations through the application of physics and engineering are paving the way for new and improved imaging technologies for diagnosis, treatment assessment, and therapy guidance [1, 28, 29]. Some excellent reviews provide an insight into developments in the extensive field of US imaging [11, 28, 30]. The following review focuses on the general characteristics and physics of US imaging, and more specifically, CEUS.

Ultrasound waves are defined as longitudinal waves which have a frequency above 20 kHz, higher than the range humans are capable of hearing. Clinical US imaging generally involves the use of frequencies in the range of 1–10 MHz. Transducers are used to transmit and receive sound signals. Modern transducers have an array of several elements and can operate over a range of frequencies defined by their bandwidth. Sound waves propagating into the body are partly absorbed by tissue but are also reflected, or scattered, back to the transducer where they are detected [31]. Given an estimate for the average speed of sound in the medium, and the time taken for the pulse to be reflected, the distance to a particular boundary can be very simply calculated. The processing capabilities of US scanners allow for the creation of real-time images for diagnostic use. Standard Brightness mode (B-mode) grayscale images are constructed using the amplitude of the received echo [32].

1.3.2 Mechanical Index (MI)

An important system parameter is the user-defined mechanical index (MI), which is directly related to the peak negative pressure of the transmitted acoustic wave, p_N in kPa, and the frequency, f, in MHz, of the transducer, and is defined by

$$\mathrm{MI} = \frac{p_N}{\sqrt{f}}. \tag{1.8}$$

The MI is an indication of the potential for mechanical bio-effects created by the US insonation. In the United States, the Food and Drug Administration (FDA) specifies a maximum MI of 1.9 MPa $\mathrm{MHz}^{-1/2}$ for clinical investigations [33]. However, it must be noted that the value of MI given by Eq. (1.1) is only an approximation. The real MI value is spatially variant since the acoustic wave will be subject to attenuation and diffraction during propagation.

In the case of CEUS, at high acoustic pressures, the microbubble shell is compromised at a threshold negative pressure, and microbubbles are disrupted. This releases the contained gas, and dissolution occurs. Therefore, CEUS commonly uses a considerably lower MI than the FDA approved level stated above of between 0.05–0.4 MPa $\mathrm{MHz}^{-1/2}$ to minimize bubble disruption [33]. However, it should be noted that the system-displayed MI in itself has not been shown to directly predict the amount of microbubble destruction, with other factors related to scanner and transducer settings also contributing to the outcome [34].

1.3.3 Contrast-Enhanced Ultrasound Imaging (CEUS)

Through the development of microbubbles as UCAs and the advent of advanced techniques to exploit the unique nonlinear response of microbubbles, US imaging specificity and sensitivity have improved. This section gives an overview of the contrast imaging methods that are currently available or under investigation. Excluding fundamental B-Mode imaging, these all exploit the unique signature of microbubbles that distinguish them from tissue, as discussed previously. A key term used to describe the performance of imaging techniques is the ratio of the scattered power from the contrast agent to the scattered power from the tissue and is termed "contrast-to-tissue ratio" (CTR).

1.3.3.1 Fundamental B-Mode Imaging

In this mode, a microbubble enhances the backscatter signal and therefore the intensity level in the image. However, since fundamental B-Mode imaging has been designed for tissue imaging, this technique can result in a poor CTR [13].

1.3.3.2 Harmonic B-Mode Imaging

Harmonic imaging was the first technique to exploit the nonlinear behavior of microbubbles to enhance imaging CTR. Since echoes from microbubbles typically contain considerably more harmonic energy than tissue, most notably at twice the insonating frequency, in this mode the system transmits US at a particular frequency, and receives signals preferentially at twice this frequency [13]. As a result, this selective imaging enhances the bubble signals and suppresses signals from tissue. Nevertheless, to perform harmonic imaging with a single transducer, the frequency bandwidths of both the transmit and receive must fit within the bandwidth of the transducer to ensure the system sensitivity is high enough. To do this, narrowband signals are needed, which in turn reduces the spatial resolution of the imaging system. Therefore, harmonic imaging generally involves optimizing the trade-off between imaging resolution and contrast detectability [13].

1.3.3.3 Harmonic Power Doppler

Conventional Doppler US estimates the velocity of blood flow by estimating the motion of scattering objects in the blood in an area of interest. Power Doppler US provides information about the strength, or power, of the returned signal, but does not provide information about the direction of the flow. Harmonic Doppler US performs the same as conventional Doppler US technique, but receives signals at twice the frequency of the transmitted signals. The addition of contrast agents for harmonic power Doppler US makes the

technique particularly sensitive to flow from small vessels with a typically higher signal-to-noise ratio (SNR) than the conventional technique.

1.3.3.4 Multi-Pulse Contrast-Enhanced Imaging

Multi-pulse imaging procedures such as pulse inversion (PI) and amplitude modulation (AM) [8] have provided improved resolution and SNR, and have been shown to provide enhanced lesion visibility and diagnostic confidence [35]. These techniques exploit the nonlinear signature of microbubble scattering in order to detect the contrast agent in the blood while suppressing linear signals. This can provide enhanced visualization of perfusion, an example abdominal contrast-enhanced image is shown alongside a simultaneously acquired B-mode scan of the same region (Fig. 1.2). Here, visualization of a liver lesion is greatly enhanced with the use of multi-pulse CEUS.

Pulse Inversion (PI)

Unlike harmonic imaging, pulse inversion (PI), also known as pulse subtraction or phase inversion mode, is able to use broader transmit and receive bandwidths, and therefore overcomes the contrast detectability and imaging resolution trade-off characteristic of other techniques. PI involves the transmission of two successive pulses along each scan line, 180° phase shifted with respect to one another, the echoes of which are then summed on return [36, 37]. When these pulses are reflected by a linear scatterer, the two received echoes will cancel each other out when summed since they are out of phase. In the case of a nonlinear scatterer, however, the sum of the two echoes is non-zero as the initial phase difference of 180° is not conserved (Fig. 1.3) [38]. As a result, the fundamental component of the echo cancels, but the harmonic component adds, doubling the magnitude of the harmonic level of a single echo [39]. This technique has the advantage over harmonic imaging and harmonic power Doppler US that it avoids bandwidth limitations associated with separating harmonic signals from the transmitted fundamental signal, and therefore provides better imaging resolution. Furthermore, since PI imaging has been shown to work well at low MI, the lifetime of the contrast agent is prolonged. Nevertheless, the nature of this as a multi-pulse scheme means that any tissue motion between frames can result in incomplete removal of tissue and artifact.

Amplitude Modulation (AM)

In AM [8], also known as power modulation, instead of inverting the polarity between the two pulses, as in PI, the pulses are modified in amplitude. For example, two consecutive pulses can be sent with amplitudes (½, 1), and the scattered response from the half amplitude pulse is scaled by a factor of two and subtracted from the full amplitude response [40]. This approach works in a similar manner to PI, in which an appropriate combination of the returned echoes will result in

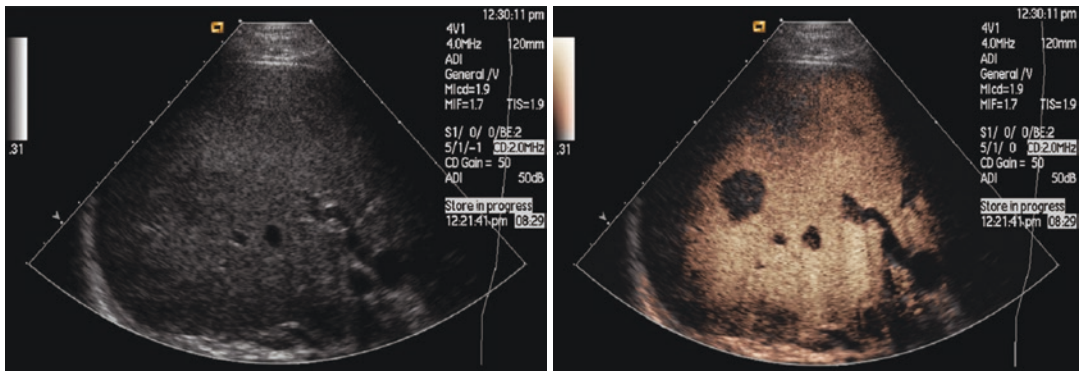

Fig. 1.2 Abdominal US B-mode scan alongside sequentially acquired CEUS imaging, where a weakly perfused region corresponding to a liver lesion can be clearly visualized with the introduction of microbubble contrast agents. (Figure acquired from Hammersmith Hospital courtesy of Prof. David Cosgrove)

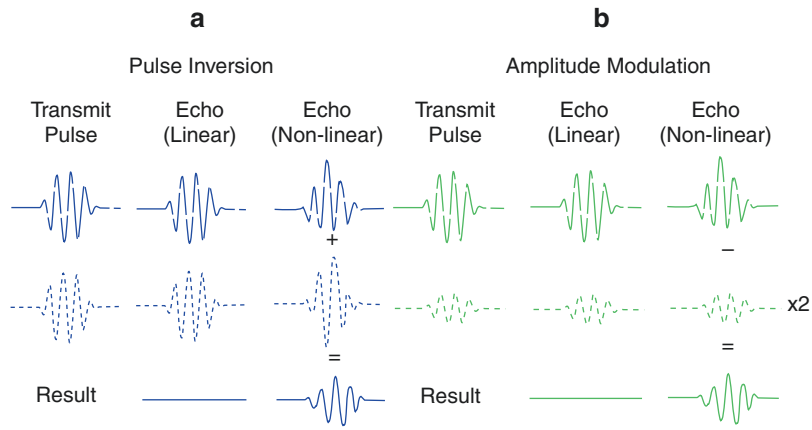

Fig. 1.3 Principles of pulse inversion (PI) and amplitude modulation (AM). (**a**) PI: A positive (dashed line) and inverted (dotted line) pulses are transmitted sequentially along one scan line. Linear targets produce symmetric scattered echoes, while non-linear targets produce asymmetric echoes to those transmitted. Linear targets thus cancel upon summation, whereas residual signal remains for non-linear echoes. (**b**) AM: A full amplitude (dashed line) and scaled-down version of the same pulse (dotted line) are transmitted as successive pulses, here shown for a scaling factor of 2. The amplitude difference will be compensated using a scaling factor before subtracting the signals, to remove the linear scattering. Alternatively, three consecutive pulses can be sent with amplitudes (½, 1, ½), and the scattered response from the half amplitude pulses is subtracted from the full amplitude response

complete signal cancellation for stationary linear scatterers, while echoes from non-linear microbubbles will produce residual signals. These residual signals occur because the microbubbles respond nonlinearly to the different amplitude pulses, e.g., a pulse with double the amplitude will not produce an echo with twice the amplitude, whereas for tissue this would be the case.

Importantly, an advantage of AM over PI is that it can detect nonlinear signals both at the fundamental frequency and at harmonic frequencies, nevertheless, the second harmonic part is lower than in PI [32]. This conservation of the odd harmonic components holds some advantages over PI such as the ability to detect pressure dependent nonlinear effects and increased sensitivity. This is because the fundamental component contains more energy than in any other harmonic component and the echo suffers less attenuation due to its lower frequency than higher harmonic components [41]. Furthermore, the transducer efficiency is greater since its center frequency can match that of the fundamental, whereas for second harmonic detection both the transmitted (fundamental) frequency and the second harmonic generally lie in the less efficient parts of the transducer's frequency response.

Alternative Multi-Pulse Sequences

Multi-pulse sequences where the amplitude of the pulses is modified, as well as inverting the phase, such as pulse inversion amplitude modulation (PIAM), have the advantage of both gaining a stronger second harmonic component than AM and a fundamental component which is not present in PI, while also maintaining the suppression of the linear signals [41]. Contrast pulse sequencing (CPS) refers to a more general strategy involving the transmission of a number of amplitude and phase modified pulses along each scan line, with corresponding weighting factors. By summing echoes from a suitable choice of transmission pulses and with appropriate weighting factors, detection or suppression of specific harmonics is possible [39, 42]. Typically, only two pulse amplitudes are used, one being half that of the other, and phase shifts of either 0° or 180°, although variations of these do exist. Manufacturers of clinical imaging systems often have their own version of multi-pulse contrast sequences, which use variations of these principles to enhance contrast signals. A mode known as Cadence™ CPS used in Siemen's systems involves the transmission of three pulses with amplitudes (½, −1, ½) and weightings (1, 1, 1). Methods such as these

have been shown to have high microbubble sensitivity since the echoes generated have a large second harmonic component [14].

1.3.3.5 Super- and Sub-Harmonic Imaging

Despite the benefits of second harmonic imaging, nonlinear propagation (see Sect. 1.3.3.6) through tissue can still degrade the image by limiting contrast and tissue discrimination. It has been shown that discrimination between the perfused tissue and contrast agents can be improved as a function of the order of the harmonic frequency [43]. Therefore, to further increase the CTR, the detection of higher harmonics, for example, the third to fifth, referred to as super-harmonics, or super-harmonic imaging (SHI) can be used [44]. However, the use of SHI implies a large dynamic range and requires a sufficiently sensitive array over a frequency range from the transmission frequency up to the chosen higher harmonic (often bandwidth >130%). In current systems, the transducer bandwidth is often limited to 70–80%, which makes it hard or impossible to perform SHI imaging. Therefore, interleaved dual-frequency arrays have been designed primarily for SHI.

It is also known that bubbles are not only able to generate harmonics, and super-harmonics, but also ultra-harmonics at 3/2f, 5/2f, etc., and sub-harmonics at 1/2f, 1/3f etc. Unlike harmonic imaging, the contribution to these from tissue is negligible at typical diagnostic frequencies, and sub-harmonics have the advantage of being less affected by frequency dependent attenuation effects. However, the generation of sub-harmonics depends on both the frequency and pressure of the transmitted wave, where transmission at twice the resonant frequency of the bubble, and pressure above a certain pressure leads to generation of sub-harmonics [45–47].

1.3.3.6 Potential Harmonic Imaging Artifacts

Imaging techniques that rely upon the nonlinearity of bubble echoes for detection require a high enough acoustic pressure to induce non-linear bubble behavior. At these US pressures, slight nonlinearities in sound propagation can occur through tissue, which gradually deform the wave as it travels, introducing harmonic frequencies into the wave. This is known as "nonlinear propagation," and is known to limit the maximal CTR achievable for harmonic filtering methods. Additionally, the second harmonic signal undergoes greater attenuation than the fundamental, which can further reduce the CTR. This is due to the frequency-dependent attenuation effects.

1.4 Summary

The availability of new generations of engineered UCAs has stimulated extensive research and development of US technology to image these contrast agents. Selective detection strategies that exploit the unique responses of these bubbles have led to many effective contrast specific imaging methods, many of which are available on clinical imaging systems. Techniques that can effectively distinguish bubble echoes from those of the surrounding tissue have considerably improved image quality and sensitivity. A comprehensive understanding of the physics of microbubbles and their interaction with US will continue to improve current imaging techniques and the development of new ones.

References

1. Becher H, Burns PN. Handbook of contrast echocardiography: left ventricular function and myocardial perfusion. New York: Springer; 2000. 184 p. Available from: http://books.google.co.uk/books/about/Handbook_of_contrast_echocardiography.html?id=9QRsAAAAMAAJ&pgis=1.
2. Cosgrove D, Lassau N. Imaging of perfusion using ultrasound. Eur J Nucl Med Mol Imaging. 2010;37(Suppl 1):S65–85. Available from: http://www.ncbi.nlm.nih.gov/pubmed/20640418.
3. Pysz MA, Foygel K, Panje CM, Needles A, Tian L, Willmann JK. Assessment and monitoring tumor vascularity with contrast-enhanced ultrasound maximum intensity persistence imaging. Invest Radiol. 2011;46(3):187–95. Available from: http://www.pubmedcentral.nih.gov/articlerender.

fcgi?artid=4457398&tool=pmcentrez&rendertype=abstract.
4. Stride E, Edirisinghe M. Novel microbubble preparation technologies. Soft Matter. 2008;4(12):2350. Available from: http://pubs.rsc.org/en/content/articlehtml/2008/sm/b809517p.
5. Stride E, Saffari N. Microbubble ultrasound contrast agents: a review. Proc Inst Mech Eng Part H. 2003;217(6):429–47. Available from: http://pih.sagepub.com/content/217/6/429.short.
6. Lindner JR. Microbubbles in medical imaging: current applications and future directions. Nat Rev Drug Discov. 2004;3(6):527–32. Available from:. https://doi.org/10.1038/nrd1417.
7. Goldberg BB, Liu J-B, Forsberg F. Ultrasound contrast agents: a review. Ultrasound Med Biol. 1994;20(4):319–33. Available from: http://www.sciencedirect.com/science/article/pii/0301562994900019.
8. Gramiak R, Shah PM. Echocardiography of the aortic root. Investig Radiol. 1968;3(5):356–66. Available from: https://insights.ovid.com/crossref?an=00004424-196809000-00011.
9. Quaia E. Classification and safety of microbubble-based contrast agents. In: Contrast media in ultrasonography. Berlin: Springer-Verlag; 2005. p. 3–14. Available from: http://link.springer.com/10.1007/3-540-27214-3_1.
10. Faez T, Emmer M, Kooiman K, Versluis M, van der Steen AFW, de Jong N. 20 Years of ultrasound contrast agent modeling. IEEE Trans Ultrason Ferroelectr Freq Control. 2013;60(1):7–20. Available from: http://www.ncbi.nlm.nih.gov/pubmed/23287909.
11. Cosgrove D. Ultrasound contrast agents: an overview. Eur J Radiol. 2006;60(3):324–30. Available from: http://www.sciencedirect.com/science/article/pii/S0720048X06003007.
12. de Jong N, Bouakaz A, Frinking P. Basic acoustic properties of microbubbles. Echocardiography. 2002;19(3):229–40. Available from: http://doi.wiley.com/10.1046/j.1540-8175.2002.00229.x.
13. Goldberg BB, Raichlen JS, Forsberg F. Ultrasound contrast agents: basic principles and clinical applications. 2nd ed. London: Martin Dunitz; 2001.
14. Wei K, Jayaweera AR, Firoozan S, Linka A, Skyba DM, Kaul S. Quantification of myocardial blood flow with ultrasound-induced destruction of microbubbles administered as a constant venous infusion. Circulation. 1998;97(5):473–83. Available from: http://circ.ahajournals.org/content/97/5/473.full.
15. Plesset MS. The dynamics of cavitation bubbles. J Appl Mech. 1949;16:277–82. Available from: https://authors.library.caltech.edu/48246/1/TheDynamicsofCavitationBubbles.pdf.
16. Vokurka K. On Rayleigh's model of a freely oscillating bubble. I. Basic relations. Czechoslov J Phys. 1985;35(1):28–40. Available from: http://link.springer.com/10.1007/BF01590273.
17. Plesset MS, Prosperetti A. Bubble dynamics and cavitation. Annu Rev Fluid Mech. 1977;9(1):145–85. Available from: http://www.annualreviews.org/doi/10.1146/annurev.fl.09.010177.001045.
18. Rayleigh L. On the pressure developed in a liquid during the collapse of a spherical cavity. London Edinburgh Dublin Philos Mag J Sci. 1917;34(200):94–8. Available from: https://www.tandfonline.com/doi/full/10.1080/14786440808635681.
19. Miller DL. Ultrasonic detection of resonant cavitation bubbles in a flow tube by their second-harmonic emissions. Ultrasonics. 1981;19(5):217–24. Available from: https://www.sciencedirect.com/science/article/abs/pii/0041624X81900068.
20. Minnaert M. On musical air-bubbles and the sounds of running water. London Edinburgh Dublin Philos Mag J Sci. 1933;16(104):235–48. Available from: http://www.tandfonline.com/doi/abs/10.1080/14786443309462277.
21. Church CC. The effects of an elastic solid surface layer on the radial pulsations of gas bubbles. J Acoust Soc Am. 1995;97(3):1510–21. Available from: http://asa.scitation.org/doi/10.1121/1.412091.
22. Hoff L, Sontum PC, Hovem JM. Oscillations of polymeric microbubbles: effect of the encapsulating shell. J Acoust Soc Am. 2000;107(4):2272–80. Available from: http://www.ncbi.nlm.nih.gov/pubmed/10790053.
23. Morgan KE, Allen JS, Dayton PA, Chomas JE, Klibaov AL, Ferrara KW. Experimental and theoretical evaluation of microbubble behavior: effect of transmitted phase and bubble size. IEEE Trans Ultrason Ferroelectr Freq Control. 2000;47(6):1494–509. Available from: http://www.ncbi.nlm.nih.gov/pubmed/18238696.
24. Hamilton MF, Ilinskii YA, Meegan GD, Zabolotskaya EA. Interaction of bubbles in a cluster near a rigid surface. Acoust Res Lett Online. 2005;6(3):207–13. Available from: http://asa.scitation.org/doi/10.1121/1.1930967.
25. Qin S, Ferrara KW. Acoustic response of compliable microvessels containing ultrasound contrast agents. Phys Med Biol. 2006;51(20):5065–88. Available from: http://www.ncbi.nlm.nih.gov/pubmed/17019026.
26. Rayleigh JWSB, Lindsay RB. The theory of sound, vol. 1. New York: Courier Corporation; 1945. 520 p. Available from: https://books.google.com/books?id=v4NSAlsTwnQC&pgis=1.
27. Hoff L. Acoustic characterization of contrast agents for medical ultrasound imaging. Dordrecht: Springer Netherlands; 2001. Available from: http://link.springer.com/10.1007/978-94-017-0613-1.
28. Wells PNT. Ultrasound imaging. Phys Med Biol. 2006;51(13):R83–98. Available from: http://iopscience.iop.org/0031-9155/51/13/R06/pdf/pmb6_13_r06.pdf.
29. Foster FS, Burns PN, Simpson DH, Wilson SR, Christopher DA, Goertz DE. Ultrasound for the visualization and quantification of tumor microcirculation. Cancer Metastasis Rev. 2000;19(1–2):131–8. Available from: http://www.ncbi.nlm.nih.gov/pubmed/11191052.

30. Fenster A, Downey DB. 3-D ultrasound imaging: a review. IEEE Eng Med Biol Mag. 1996;15(6):41–51. Available from: http://ieeexplore.ieee.org/articleDetails.jsp?arnumber=544511.
31. Ng A, Swanevelder J. Resolution in ultrasound imaging. Cont Educ Anaesth Crit Care Pain. 2011;11(5):186–92. Available from: http://ceaccp.oxfordjournals.org/content/11/5/186.full.
32. Szabó TL. Diagnostic ultrasound imaging: inside out. Amsterdam: Academic Press; 2004. 549 p. Available from: http://books.google.com/books?id=-Fd1Pkeh2T0C&pgis=1.
33. Tang M-X, Mulvana H, Gauthier T, Lim AKP, Cosgrove DO, Eckersley RJ, et al. Quantitative contrast-enhanced ultrasound imaging: a review of sources of variability. Interface Focus. 2011;1(4):520–39. Available from: http://rsfs.royalsocietypublishing.org/content/1/4/520.
34. Forsberg F, Shi WT, Merritt CRB, Dai Q, Solcova M, Goldberg BB. On the usefulness of the mechanical index displayed on clinical ultrasound scanners for predicting contrast microbubble destruction. J Ultrasound Med. 2005;24(4):443–50. Available from: http://www.ncbi.nlm.nih.gov/pubmed/15784762.
35. Desser TS, Jeffrey RB. Tissue harmonic imaging techniques: physical principles and clinical applications. Semin Ultrasound CT MR. 2001;22(1):1–10. Available from: http://www.ncbi.nlm.nih.gov/pubmed/11300583.
36. Burns PN, Hope Simpson D, Averkiou MA. Nonlinear imaging. Ultrasound Med Biol. 2000;26(Suppl 1):S19–22. Available from: http://www.ncbi.nlm.nih.gov/pubmed/10794866.
37. Burns PN, Wilson SR, Simpson DH. Pulse inversion imaging of liver blood flow: improved method for characterizing focal masses with microbubble contrast. Invest Radiol. 2000;35(1):58–71. Available from: http://www.ncbi.nlm.nih.gov/pubmed/10639037.
38. Ultrasound imaging system employing phase inversion subtraction to enhance the image. 1997 [cited 2015 Sept 7]. Available from: http://www.google.com/patents/US5632277.
39. Quaia E. Contrast media in ultrasonography: basic principles and clinical applications. New York: Springer Science & Business Media; 2006. 414 p. Available from: https://books.google.com/books?id=givPAvaL2-kC&pgis=1.
40. Hoskins PR, Martin K, Thrush A. Diagnostic ultrasound: physics and equipment. Cambridge: Cambridge University Press; 2010. Available from: https://books.google.com/books?id=W8LB26lsHjMC&pgis=1.
41. Eckersley RJ, Chin CT, Burns PN. Optimising phase and amplitude modulation schemes for imaging microbubble contrast agents at low acoustic power. Ultrasound Med Biol. 2005;31(2):213–9. Available from: http://www.umbjournal.org/article/S030156290400300X/fulltext
42. Phillips PJ. Contrast pulse sequences (CPS): imaging nonlinear microbubbles. In: 2001 IEEE ultrasonics symposium proceedings an international symposium (Cat No. 01CH37263). IEEE; 2001 [cited 2015 Aug 26]. p. 1739–45. Available from: http://ieeexplore.ieee.org/articleDetails.jsp?arnumber=992057.
43. Bouakaz A, Frigstad S, Ten Cate FJ, de Jong N. Super harmonic imaging: a new imaging technique for improved contrast detection. Ultrasound Med Biol. 2002;28(1):59–68. Available from: http://www.ncbi.nlm.nih.gov/pubmed/11879953.
44. Van Neer PLMJ, Matte G, Danilouchkine MG, Prins C, Van Den Adel F, De Jong N. Super-harmonic imaging: development of an interleaved phased-array transducer. IEEE Trans Ultrason Ferroelectr Freq Control. 2010;57(2):455–68. Available from: http://www.ncbi.nlm.nih.gov/pubmed/20178912.
45. Sijl J, Dollet B, Overvelde M, Garbin V, Rozendal T, de Jong N, et al. Subharmonic behavior of phospholipid-coated ultrasound contrast agent microbubbles. J Acoust Soc Am. 2010;128(5):3239–52. Available from: http://www.ncbi.nlm.nih.gov/pubmed/21110619.
46. Eller A, Flynn HG. Generation of subharmonics of order one-half by bubbles in a sound field. J Acoust Soc Am. 1969;46(3B):722–7. Available from: http://asa.scitation.org/doi/10.1121/1.1911753.
47. Lotsberg O, Hovem JM, Aksum B. Experimental observation of subharmonic oscillations in Infoson bubbles. J Acoust Soc Am. 1996;99(3):1366–9. Available from: http://asa.scitation.org/doi/10.1121/1.414715.

Safety of Contrast-Enhanced Ultrasound

2

Gail ter Haar

2.1 Introduction

Contrast-enhanced ultrasound (CEUS) is often chosen instead of other imaging modalities because of the perception that it is a "safe" technique that does not involve the use of ionizing radiation. In this chapter, the evidence for this stance for non-cardiac applications is examined. In a recent survey of members of the U.S. Society for Pediatric Radiology, the main reasons given for the use of CEUS were as a replacement for fluoroscopy, computed tomography (CT), or magnetic resonance (MR) imaging, with other reasons given including lack of nephrotoxicity (since the microbubbles do not have to clear through the kidneys), the availability of ultrasound (US), low cost, and point of care availability [1].

There is little doubt from pre-clinical in vitro and in vivo experiments involving studies of the US exposure of microbubble ultrasound contrast agents (UCAs) that they present a potential hazard since biological effects have been seen, but the question to be answered is whether such exposures are safe in clinical use, that is, do they present an unacceptable risk? Here, risk is defined as the probability of occurrence of harm, and its severity. For imaging, and especially in pediatrics, the risk to benefit ratio should remain very low.

Ultrasound contrast agents take the form of stabilized microbubbles encapsulated in a lipid, albumin, or other shell. This stabilization is necessary as "unshelled" air bubbles will dissolve in minutes in the blood. The microbubble core is an inert gas such as perfluorocarbon or sulfur hexafluoride. The microbubble diameter (1–5 μm) is designed to be about the same size as that of red blood cells, allowing them to transit the lungs intact and to remain in the blood pool. Once the microbubble is dissolved, the shell can be metabolized by the liver, and the gas is exhaled. These microbubbles are designed to be strong scatterers of US. They enhance the echogenicity of well-vascularized regions, revealing parenchymal vessels and blood pools, and allowing functional imaging using wash in/wash out techniques [2–4]. The number of clinically approved UCA is limited, with different countries taking different stances on approval of their use. Assessment is not made easier by the change in the name of agents as they cross continental borders. Contrast agents currently approved for clinical use are SonoVue™ (Lumason™ in the United States, Bracco Diagnostics), Optison™ (GE Healthcare), Luminity™ [3] (Definity™ outside Europe; Lantheus Medical Imaging), and Sonazoid™ (GE Healthcare) [4]. Although non-cardiac appli-

G. ter Haar (✉)
The Institute of Cancer Research, Sutton, UK
e-mail: gail.terhaar@icr.ac.uk

P. S. Sidhu et al. (eds.), *Contrast-Enhanced Ultrasound in Pediatric Imaging*,
https://doi.org/10.1007/978-3-030-49691-3_2

cations were approved outside the United States in the early 2000s, the use of Lumason™ was approved by the Food and Drug Administration (FDA) for adult and pediatric liver examinations only in 2016. It was approved by the FDA for intravesical use in children in the same year [5].

Three different ways of delivering UCA to children have been described—oral, intravenous (IV), and intracavitary (IC), although the oral route has only been reported once, for the diagnosis of gastro-oesophageal reflux [6]. Intravenous administration follows the same procedure as used in adults, and is increasingly accepted as, in contrast to CT examinations, it avoids ionizing radiation, and does not require the sedation needed for peditric MR imaging. These considerations are in addition to the well-documented advantages of portability and low cost of US devices. Intra-cavitary UCAs are used for the diagnosis of vesico-ureteric reflux in children. Here, the CEUS images that are acquired during voiding are a more acceptable technique in children than the other available options, which involve radionuclide imaging.

As with contrast agents for other imaging modalities, it is important to know whether UCAs can give rise to anaphylactoid reactions. The incidence of these is lower than that for X-ray contrast agents, but comparable with that for MR imaging. In one study, a rate of 0.01% has been reported [7].

2.2 Biophysics and Bio-effects

The design of microbubbles is such that they not only scatter sound more effectively than the red blood cells around them in the vasculature due to their reflective cores, but also have a non-linear response to the incident US wave that results in scattered frequencies that are different from those by which the microbubbles are driven [3, 8]. Ultrasound contrast agents oscillate in response to the incident sound field. In contrast to the behavior of free gas bubbles, the response of the encapsulated microbubbles used for biomedical applications is determined by a number of factors, including the interfacial tension between the microbubble and its surroundings, and the viscosity of its shell [8].

At very low incident pressures, UCAs undergo approximately linear oscillations—growing and shrinking by the same amount each pressure cycle. As the US pressure increases, the motion becomes non-linear, with the microbubble expanding more than it contracts in each cycle, and the periodicity of this motion becomes less uniform. This process is known as stable, or non-inertial, cavitation. If the acoustic pressure is increased still further, the oscillations become increasingly chaotic and the microbubble may undergo violent collapse, creating a shock wave and fragmenting into smaller microbubbles. This behavior is known as collapse, or inertial, cavitation and is locally extremely destructive to the surrounding medium. A stably oscillating microbubble produces echoes containing not only the fundamental imaging frequency but integer multiples of it (harmonics). These higher frequencies allow differentiation of microbubble echoes from those echoes coming from tissues, and are used by sophisticated signal processing techniques to produce high contrast images [2, 3, 8].

Acoustic streaming patterns are created around an oscillating microbubble [8–12]. The nature of these patterns varies, depending on the proximity of surfaces and of other microbubbles. These circulating flows create shear stresses that can result in biological effects at nearby cell membranes. It is thought that this is the mechanism by which intracellular uptake of therapeutic drugs is enhanced, but at high microbubble oscillation amplitudes this streaming can lead to membrane disruption.

The most common damage seen following US exposure of UCAs in pre-clinical models is to the microvasculature. This is most likely to arise from the destruction of the microbubbles. This microvessel disruption has been shown in the heart, muscle, kidney, liver, and intestine following clinical diagnostic US exposure levels [13–22]. A study of flash replenishment contrast imaging in rodent kidneys was unable to show any hemorrhage either 4 h or 6 weeks after exposure [23].

In an attempt to provide the user with information about the safety of an US examination,

two indices, MI (mechanical index) and TI (thermal index) have been introduced [24–26]. One or both of these are displayed on the screen during the US examination. The MI is designed to address safety related to mechanical effects, predominantly due to cavitation. The TI addresses the potential for thermal effects arising from an US exposure. In the absence of microbubbles, thermal effects are more likely than non-thermal effects. MI is the more relevant index when considering the safety of CEUS. It is defined by the equation $MI = p^{-}/\sqrt{f}$ where p^{-} is the peak negative pressure and f is the fundamental frequency of the US beam. An MI of 0.7 is taken as the threshold for cavitation in tissues in which there are existing nuclei from which microbubbles can grow [27] and MI = 0.3 is taken as the threshold at which capillary bleeding can occur in gas-containing organs such as the lungs or intestine. In general, it is sensible to conduct CEUS examinations for conditions under which MI remains ≤ 0.4 [2]. At this level, UCAs are likely to remain intact, but it should be remembered that the formulation of MI was undertaken to address the behavior of free (unshelled) microbubbles. While it serves as a useful indicator of the potential for non-thermal effects during CEUS, it is likely to give only a rough estimate.

2.3 Safety of CEUS in Pediatrics: Clinical Evidence

The safety of UCAs when used clinically in children has been the subject of a number of studies. In 2013 the Society for Pediatric Radiology and the International Contrast Ultrasound Society reviewed papers describing this off-label practice for non-cardiac applications [6]. Both IV and IC delivery of UCAs were analyzed. Only minor adverse events were reported, with an incidence of 0.1–0.5% in patients receiving IV UCAs ($n = 1071$), and 0.8% for those in whom they were administered intra-vesically ($n = 2951$). The adverse events were transient, and the higher incidence in the latter group was attributed to problems of bladder catheterization. More recent reports have borne out these findings. Piskunowicz et al. (2015) again reviewed the literature and found that of 502 children, there was one incidence of anaphylactic shock and nine mild, transitory adverse effects [28]. These included altered taste, lightheadedness, headaches, and transient nausea. Similar results are reported by Rosado and Riccabona (2016) who found literature relating to the use of SonoVue™, Optison™, and Definity™ [29]. A single center, prospective study from China involved 312 children [30], found three incidents of hypotension, and three of the development of a rash, all of which resolved readily. Yusuf et al. (2017) reviewed the records of 305 pediatric patients who had had CEUS investigations [31]. They saw no immediate adverse reactions, but in two patients (0.7%) they saw delayed, transient, hypertension in one, and tachycardia in another. The authors point out that these delayed effects occurred after the UCA components would have been expected to have cleared and so may not have been a direct result of the CEUS procedure. An EFSUMB position statement points out that although many CEUS examinations involve the "off-label" use of UCA, this is not a barrier, as this is fairly common for any pharmaceutical agents prescribed in children [5]. The conclusion from all these reports indicates that adverse events are similar in children to those found in adults, and so the use of CEUS in pediatrics is acceptable from a safety standpoint.

2.4 Recommendations for Ensuring Safe Use of UCAs in Pediatric Patients

There are some basic precautions that should be taken in order to ensure the continuing safety of CEUS in pediatrics [32]:

- Examine at low MI. Where possible, choose an MI with 0.4 as the default output setting. Increase this level only where there is a clinical need for a better image. Keep a record of the highest MI encountered during each examination.
- Keep the exposure time as short as possible, providing the required clinical information is acquired.

- Use the lowest dose of UCA that gives the required information.
- Always have resuscitation facilities available, in case of anaphylaxis.
- Ensure that anyone conducting the CEUS examination has had proper training.

References

1. Back SJ, Maya C, Darge K, Acharya PT, Barnewolt CE, Coleman JL, Dillman JR, Fordham LA, Hwang M, Lim A, McCarville MB. Pediatric contrast-enhanced ultrasound in the United States: a survey by the contrast-enhanced ultrasound task force of the society for pediatric radiology. Pediatr Radiol. 2018;48(6):852–7.
2. Chong WK, Papadopoulou V, Dayton PA. Imaging with ultrasound contrast agents: current status and future. Abdom Radiol. 2018;43(4):762–72.
3. Frinking P, Segers T, Luan Y, Tranquart F. Three decades of ultrasound contrast agents: a review of the past, present and future improvements. Ultrasound Med Biol. 2020;46:892–908.
4. Rafailidis V, Huang DY, Yusuf GT, Sidhu PS. General principles and overview of vascular contrast-enhanced ultrasonography. Ultrasonography. 2020;39(1):22–42.
5. Sidhu PS, Cantisani V, Deganello A, Dietrich CF, Duran C, Franke D, Harkanyi Z, Kosiak W, Miele V, Ntoulia A, Piskunowicz M. Role of contrast-enhanced ultrasound (CEUS) in paediatric practice: an EFSUMB position statement. Ultraschall Med—Eur J Ultrasound. 2017;38(1):33–43.
6. Darge K, Papadopoulou F, Ntoulia A, Bulas DI, Coley BD, Fordham LA, Paltiel HJ, McCarville B, Volberg FM, Cosgrove DO, Goldberg BB. Safety of contrast-enhanced ultrasound in children for non-cardiac applications: a review by the Society for Pediatric Radiology (SPR) and the International Contrast Ultrasound Society (ICUS). Pediatr Radiol. 2013;43(9):1063–73.
7. Piscaglia F, Bolondi L. The safety of SonoVue® in abdominal applications: retrospective analysis of 23188 investigations. Ultrasound Med Biol. 2006;32(9):1369–75.
8. Azmin M, Harfield C, Ahmad Z, Edirisinghe M, Stride E. How do microbubbles and ultrasound interact? Basic physical, dynamic and engineering principles. Curr Pharm Des. 2012;18(15):2118–34.
9. Gormley G, Wu J. Observation of acoustic streaming near Albunex® spheres. J Acoust Soc Am. 1998;104(5):3115–8.
10. Liu X, Wu J. Acoustic microstreaming around an isolated encapsulated microbubble. J Acoust Soc Am. 2009;125(3):1319–30.
11. Collis J, Manasseh R, Liovic P, Tho P, Ooi A, Petkovic-Duran K, Zhu Y. Cavitation microstreaming and stress fields created by microbubbles. Ultrasonics. 2010;50(2):273–9.
12. Boluriaan S, Morris PJ. Acoustic streaming: from Rayleigh to today. Int J Aeroacoust. 2003;2(3):255–92.
13. Miller DL, Quddus J. Diagnostic ultrasound activation of contrast agent gas bodies induces capillary rupture in mice. Proc Natl Acad Sci. 2000;97(18):10179–84.
14. Miller DL, Averkiou MA, Brayman AA, Everbach EC, Holland CK, Wible JH Jr, Wu J. Bioeffects considerations for diagnostic ultrasound contrast agents. J Ultrasound Med. 2008;27(4):611–32.
15. Wu J, Nyborg WL. Ultrasound, cavitation bubbles and their interaction with cells. Adv Drug Deliv Rev. 2008;60(10):1103–16.
16. Miller DL, Gies RA. The influence of ultrasound frequency and gas-body composition on the contrast agent-mediated enhancement of vascular bioeffects in mouse intestine. Ultrasound Med Biol. 2000;26(2):307–13.
17. Miller DL, Dou C, Wiggins RC. Frequency dependence of kidney injury induced by contrast-aided diagnostic ultrasound in rats. Ultrasound Med Biol. 2008;34(10):1678–87.
18. Miller DL, Dou C, Wiggins RC. Contrast-enhanced diagnostic ultrasound causes renal tissue damage in a porcine model. J Ultrasound Med. 2010;29(10):1391–401.
19. Miller DL, Lu X, Dou C, Fabiilli ML, Church CC. The dependence of glomerular capillary hemorrhage induced by contrast enhanced diagnostic ultrasound on microbubble diameter. Ultrasound Med Biol. 2018;44(3):613–21.
20. Lu X, Dou C, Fabiilli ML, Miller DL. Capillary hemorrhage induced by contrast-enhanced diagnostic ultrasound in rat intestine. Ultrasound Med Biol. 2019;45(8):2133–9.
21. Miller DL, Lu X, Fabiilli M, Dou C. Hepatocyte injury induced by contrast-enhanced diagnostic ultrasound. J Ultrasound Med. 2019;38(7):1855–64.
22. Skyba DM, Price RJ, Linka AZ, Skalak TC, Kaul S. Direct in vivo visualization of intravascular destruction of microbubbles by ultrasound and its local effects on tissue. Circulation. 1998;98(4):290–3.
23. Nyankima AG, Kasoji S, Cianciolo R, Dayton PA, Chang EH. Histological and blood chemistry examination of the rodent kidney after exposure to flash-replenishment ultrasound contrast imaging. Ultrasonics. 2019;98:1–6.
24. Meltzer RS. Food and Drug Administration ultrasound device regulation: the output display standard, the "mechanical index," and ultrasound safety. J Am Soc Echocardiogr. 1996;9(2):216.
25. Forsberg F, Shi WT, Merritt CR, Dai Q, Solcova M, Goldberg BB. On the usefulness of the mechanical index displayed on clinical ultrasound scanners for predicting contrast microbubble destruction. J Ultrasound Med. 2005;24(4):443–50.
26. ter Haar G. Safety and bio-effects of ultrasound contrast agents. Med Biol Eng Comput. 2009;47(8):893–900.

27. Apfel RE, Holland CK. Gauging the likelihood of cavitation from short-pulse, low-duty cycle diagnostic ultrasound. Ultrasound Med Biol. 1991;17(2):179–85.
28. Piskunowicz M, Kosiak W, Batko T, Piankowski A, Połczyńska K, Adamkiewicz-Drożyńska E. Safety of intravenous application of second-generation ultrasound contrast agent in children: prospective analysis. Ultrasound Med Biol. 2015;41(4):1095–9.
29. Rosado E, Riccabona M. Off-label use of ultrasound contrast agents for intravenous applications in children: analysis of the existing literature. J Ultrasound Med. 2016;35(3):487–96.
30. Muyi M, Bei X, Weiling C, Xiaojie G, Jun Y, Shoulin L, Bin W, Huirong M, Sixi L, Feiqiu W, Yungen G. The safety and effectiveness of intravenous contrast-enhanced sonography in Chinese children—a single center and prospective study in China. Front Pharmacol. 2019;10:1447.
31. Yusuf GT, Sellars ME, Deganello A, Cosgrove DO, Sidhu PS. Retrospective analysis of the safety and cost implications of pediatric contrast-enhanced ultrasound at a single center. Am J Roentgenol. 2017;208(2):446–52.
32. Barnett SB, Duck F, Ziskin M. Recommendations on the safe use of ultrasound contrast agents. Ultrasound Med Biol. 2007;33(2):173–4.

3 Quantitative Contrast-Enhanced Ultrasound

Martin Krix

3.1 Introduction

Quantitative approaches beyond basic measurements of size are not yet common in imaging-based diagnosis. The diagnostic assessment often relies on a subjective, descriptive image interpretation by the diagnostic physician. This implies that this may also be the method of the evaluation for contrast enhancement and related information about tissue characterization, perfusion, or function. Traditionally, nuclear medicine has been different since quantification of radiotracer uptake is routinely integrated into the diagnostic algorithm. However, quantification of imaging-based information is rarely performed in magnetic resonance (MR) imaging, computed tomography (CT) imaging, or other X-ray-based methods. Or, if quantification is existence, such as Hounsfield units in CT, related data are not reported or not implemented in routine diagnostic approaches. In this respect, contrast-enhanced ultrasound (CEUS) has also followed a similar path, with limited use of quantification methods. However, a few relevant applications for quantitative perfusion already exist, particularly using CT methods in stroke imaging, highlighting the usefulness of quantification assessment. Furthermore, there is also an increasing medical need for diagnostic procedures that provide quantitative parameters, e.g., for follow-up evaluation of modern treatment in oncology [1, 2]. In pediatric indications, its use may even be more limited [3]. Future trends in medicine such as large data analysis or artificial intelligence may require or result in more quantitative approaches. Thus, for ultrasound (US) and CEUS quantitative methods may become crucial, particularly considering when over time these imaging modalities will thrive, eventually routinely providing objective and standardized data.

In the following chapter, it is described how to perform quantitative CEUS, which technical aspects should be kept in mind and which examination methods exist to quantitatively analyze CEUS [4]. Applications of quantitative CEUS in pediatrics are briefly reviewed.

3.2 Requirements for Quantification of CEUS Data

To quantitatively assess CEUS, the whole contrast dynamics over time is usually evaluated. As 3D transducers with CEUS capabilities are not yet routinely available, this implies that an US section (e.g., of the liver) needs to be identified and chosen as representing the clinical question,

M. Krix (✉)
Global Medical and Regulatory Affairs, Bracco Imaging Germany, Konstanz, Germany
e-mail: Martin.Krix@bracco.com

P. S. Sidhu et al. (eds.), *Contrast-Enhanced Ultrasound in Pediatric Imaging*,
https://doi.org/10.1007/978-3-030-49691-3_3

and then the position of the US transducer needs to be kept constant during the examination. Any patient-related movement should be minimized. For in-plane motion, correction algorithms have been developed and automatic quantification software tools exist which implement any motion correction options [5].

Ultrasound contrast agents (UCAs) consist of microbubbles which interact with the insonating US wave (see Chap. 1—Physics of Microbubble Contrast Agents). In a perfect CEUS technique, solely the UCA causes signals, with no signal from the native tissue. Furthermore, for a perfect quantification, these signals need to be linear to the amount of microbubbles present. Quantification would cause misleading results if insufficient background suppression would be interpreted incorrectly as UCA signals. Linearity, or in general a clearly defined proportionality between the amount of UCA detected and its signal is a fundamental requirement for the quantification of enhancement. Put simply, a body area in which is present twice (or trice) as much UCA as compared to another area of the same size should also have exactly twice (or trice) as much CEUS signals as compared to the other area. Finally, these results need to be reproducible, i.e., the same amount of UCA in the same body structure should always provide the same signal enhancement as long as the patho-physiology does not change, independent of the examiner, the surrounding acoustic conditions, or the US device used [4, 5].

The first issue requires the use of modern CEUS-specific techniques which strongly reduce the background signal from non-enhancing structures. Currently, these are all low mechanical index (MI) techniques. Ideally, the US images before contrast should be completely black, if necessary, the US gain as well as the MI should be reduced. However, any change in the US settings later on during the examination, needs to be avoided to maintain reproducibility. Body structures or surfaces with strong backscattering (e.g., calcification) are sometimes difficult to suppress completely. In such occurrences, these structures should be excluded from the quantification analysis (e.g., do not include them in the to be placed region of interest, ROI), or as a secondary choice, subtract the baseline signal from the contrast-enhanced signals.

Non-linearity of contrast enhancement is not just an issue in CEUS, it is also well described in MR imaging. Saturation effects in MR imaging can occur when body areas with high contrast uptake do not show a corresponding high contrast signal, but non-linearly increasing with the contrast dose. For a qualitative assessment usually this is not problematic, however, for quantification, the CEUS signals need to be linearized. This can be achieved with self-developed tools, or more conveniently, by using commercially available options. These tools are sometimes already integrated onto dedicated US platforms, and external quantification software exists which operates as device and vendor-independent techniques (e.g., VueBox™, Bracco) [5].

3.3 Options for Quantification of CEUS Exams

"Quantification" of CEUS in its broadest sense starts with the use of scores that assess the degree of CEUS signals. Such scores are typically used to assess if the lesion is, for example, hyper-, iso- or hypo-enhancing compared to the surrounding tissue or to describe the degree of enhancement or its pattern of enhancement (homogeneous, inhomogeneous, rim etc.) [6]. This information can be applied in conjunction with other "quantitative" assessment systems such as CEUS LI-RADS [7]. Quantitation with CEUS examinations is to primarily develop approaches for categorization or to generate quantitative parameters of data that were originally just qualitative findings. It does not equate to a real quantification of CEUS signals.

The following focuses only on these actual quantitative methods.

3.3.1 Time Intensity Curves

The typical quantitative approach in CEUS is to inject a UCA bolus and to observe and record the whole UCA dynamics over time in a chosen US

plane. The contrast dose given generally is the same as a standard non-quantitative CEUS examination. Then, regions of interest (ROI) can be placed inside relevant or representative body areas. The linearized US signal in these ROIs is then measured over time, which results in time–intensity curves (TIC). The typical shape of such TIC (Fig. 3.1) is often characterized by a relatively short and sharp bolus according to the distribution of the microbubbles, which remain strictly intravascular in the human body (fast arterial inflow followed by the venous outflow). Its shape may vary depending on the examined organ or pathology, e.g., the bolus can be prolonged in liver tissue due to the additional portal venous blood supply, or rarely can also show a plateau-like enhancement when blood flow/microbubbles are trapped, e.g., in certain liver hemangiomas.

Various quantitative parameters may be derived from a TIC, such as the peak intensity, the time to peak, the slope to maximum intensity, or the area under the curve (AUC) (Fig. 3.1). Quantification is complicated by the fact that the method to derive a single parameter may not be precisely standardized. Parameters calculated from original CEUS data may be different compared to parameters derived from any "smoothed" fitting curves based on this original data. Actually, a smoothing of the "raw" data should always be performed first, prior to quantification, since original data often may be influenced by noise or motion artifacts, and outliers can cause non-representative values. Existent quantitative software tools automatically provide such fittings. However, the fitting algorithm is based on perfusion model assumptions which then can result in different but more or less optimum fitting curves. A widely used perfusion model is the lognormal perfusion model [8]. In addition, on occasion, the definition of a certain parameter may not be standardized. For instance, the parameter "slope" of the TIC can represent the maximum slope of the wash-in phase (the extreme of the derivative of the curve) or the mean slope during a certain time period of the TIC (e.g., between 10% and 90% of maximum).

Of note, these parameters are primarily mathematical variables which describe the shape of the TIC, and the interpretation may be variable.

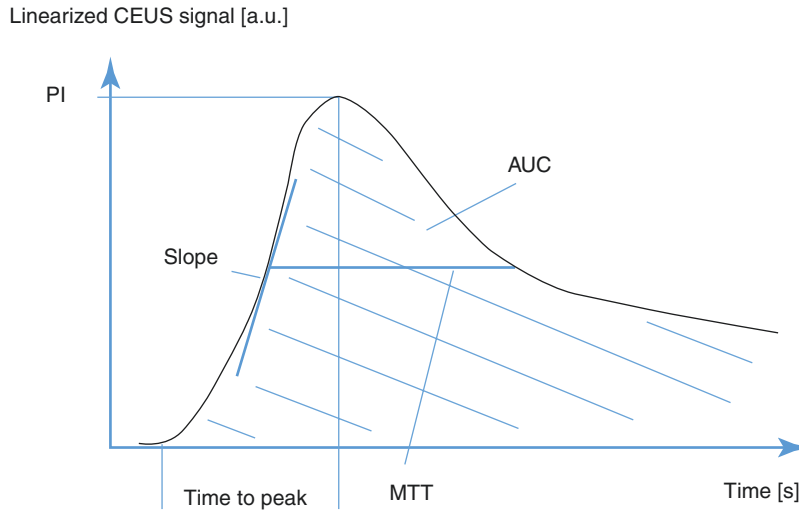

Fig. 3.1 Time–intensity curve (TIC) after bolus injection of ultrasound contrast agent and its parameters. (PI, peak intensity at time to peak [= time at peak intensity − arrival time]; slope, slope to maximum, also the slope of the wash out after the maximum can be calculated; AUC, area under the whole TIC curve, also the wash in AUC [area up to maximum peak] and wash out AUC [area from maximum peak on] can be calculated; a.u., arbitrary units, FWHM is the full width of the TIC curve at half maximum; when adding perfusion models also parameters such as the mean transit time (MTT) can be derived)

By adding mathematical models' other parameters (such as the mean transit time, MTT) can be calculated which may be a closer association to certain vascularization parameters such as the local blood flow.

The approach for quantification of CEUS is generally similar to perfusion examinations with other imaging modalities, e.g., CT or MR imaging. A general limitation is that the underlying models are valid only under certain conditions, which may not be applicable generally. Quantification may also depend on the clinical indication. Specific perfusion models may be beneficial in dedicated situations, e.g., in highly spatially organized perfusion such as in the kidneys, or when certain "sub"-aspects of perfusion are of interest, e.g., to characterize the degree of vascular dis-organization in tumors. It should be emphasized that due to its high spatial and temporal resolution, CEUS is particularly useful for such dedicated assessments. On the other hand, other modalities like MR or CT imaging can obtain input functions (blood flow in afferent vessels), a consequence of the three-dimensional nature of the modality. This is not usually feasible in CEUS, and the typical parameters derived from CEUS TIC curves are relative values (given by arbitrary units) and not absolute values of blood flow (mL/min), blood volume (mL), or perfusion (mL/min/mg). Furthermore, several of the pure "TIC describing" parameters are not related to a single vascularization quantity, but are affected by more than one. For example, the peak of a TIC curve may increase if the local blood volume of the body area is higher than in a different ROI ("more blood—more CEUS signal"), but at the same time, this value is also affected by a change of the local blood flow ("higher flow—sharper bolus CEUS signal").

The acoustic conditions and the examination conditions in such quantitative CEUS exams need to be standardized as much as possible. Experience indicates that the signal enhancement in a certain CEUS examination may be considerably different compared to a previous examination of the same body area, even in the same patient, not because of different pathophysiological findings, but solely a consequence of different imaging conditions. It is obvious that such variations can dramatically influence quantification and may even negate any meaningful assessment of quantification. Parameters that are more prone to such bias are parameters related to the CEUS signal such as the peak intensity or the AUC. Single measurements (peak enhancement) may also be more affected than integrals such as AUCs. In addition to standardization, parameter normalization can improve the reliability of such measurements. Normalization is the process where values obtained in a certain ROI (e.g., a tumor or an affected organ) are set and measured in relation to a "normal" ROI, e.g., to normal liver parenchyma.

Time-dependent parameters such as arrival times or the time to maximum intensity are less influenced by individual variations of the acoustic conditions, but they are influenced by the individual circulatory circumstances of a patient. With issues of inconsistent circulatory time, any parameters that are mainly based on the time of injection should be avoided. Any variation in the general body circulation can affect these parameters, not any potential local, relevant changes being investigated. Instead, time parameters that are based on the arrival time in the local ROI are less prone to circulatory variations if the contrast bolus injection protocol is standardized.

A key question is which of the various quantitative CEUS parameters should be used to assess a certain clinical disease or condition; currently, there is no definitive answer. A preselection of the parameters may be projected, depending on the main clinical problem, as certain parameters may be more suited to the general "vascularity" or blood volume of a body region (e.g., AUC), while others may be better suited to the dynamics of blood supply (the perfusion) such as the slope or the time to peak. However, as mentioned above, a strict assignment of CEUS parameters to a certain vascularization parameter is often not feasible. The robustness of the method is crucial, which would allow a preference to choose parameters such as the AUC to provide usable quantification [9].

Finally, it often may not be clear which parameter may really be best suited for the evaluation of

a certain clinical aspect. For instance, monitoring of anti-angiogenic treatment in oncology may at first glance suggest using a parameter that monitors the general "perfusion" of a tumor. However, it has been discussed that certain anti-angiogenic therapies do not really reduce perfusion in general but rather may normalize or just change certain aspects of the blood supply. Then, more sophisticated vascularization parameters may be needed which currently are not routinely used.

3.3.2 Replenishment Kinetics

An alternative approach for quantification with CEUS is to destroy the UCA within the region of interest with a "flash-pulse," with a number of high-energy US pulses (high MI) and then observe the refilling (the replenishment) of UCA in the area under observation; UCA entering from outside the field of view while reverting to a contrast-specific low MI US technique to image the UCA. This method requires a steady-state situation of the UCA signal within the body circulation, and therefore, a continuous infusion of UCA is required instead of a single bolus injection. In adults often larger contrast doses are given (e.g., the maximum dose of 4.8 mL for SonoVue over a few minutes), with little experience of this technique existing in children.

The transducer again strictly needs to be held at the same position throughout the procedure. The signal intensity over time is recorded, again as a TIC, although the term TIC is not usually used for replenishment curves. The shape of these curves is different from TIC after standard bolus injection (Fig. 3.2). As a special feature, a parameter β can be calculated which provides an absolute quantification of the local blood flow velocity (in m/s). This quantitative CEUS technique is able to provide more than relative quantitative values. The plateau of the refilling curve is considered to be proportional to the local volume, and blood flow is then related to the product of blood flow velocity × blood volume. Due to the less often used continuous infusion of microbubbles, this technique is generally less prevalent than the TIC analysis, although it is an established approach in echocardiography for analysis of myocardial perfusion, typically in a semi-quantitative approach, and after a bolus injection of UCA [8].

A simplified quantitative CEUS method is to measure arrival times of a contrast bolus, e.g., to assess peripheral arterial occlusive disease, or in liver CEUS for diagnosis of occult liver lesions. Here, it is not the aim to directly measure perfusion, but rather to indirectly detect alternations of the blood supply. CEUS and its data analysis is an ongoing field of research and in the future,

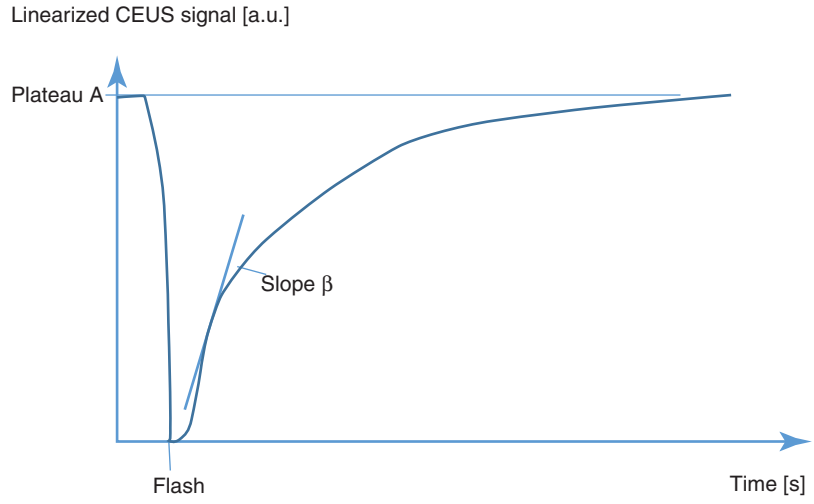

Fig. 3.2 Flash replenishment kinetics, a flash (high MI pulses) destroys CEUS signal (steady state) due to the destruction of microbubbles. (Slope β describes the refilling kinetics and is proportional to the blood flow velocity [m/s]; Plateau A, maximum signal obtained after complete refilling, is related to the local blood volume; a.u., arbitrary units)

additional options for quantification of CEUS may occur, e.g., using developments that aim at the tracking of the microbubbles signal.

3.3.3 Quantitative CEUS in Children

In general, the indications for quantification in CEUS do not differ between children and adults. However, as for other topics in medicine in general, reports of this technique in pediatrics are considerably lower than in adults. In addition, off-label use of a drug in children is a common issue, as is so for CEUS where limited licensing for pediatrics is encountered (see Chap. 4—Artifacts in Contrast-Enhanced Ultrasound Examinations) [10]. There is no difference between quantitative CEUS and "standard" CEUS except maximum dose considerations in cases where quantification would require an additional injection of UCA [11].

A current major application of quantitative CEUS is for monitoring of novel oncological treatments like with antiangiogenic drugs where simple size measurement on CT imaging (RECIST) is not sufficient. This has been reported in children, where peak enhancement and wash-in AUC were predictors of early progression in various tumors entities and body locations [3].

Quantitative CEUS is also used in diseases that are typical in younger patients. The use of quantitative CEUS has been investigated in the evaluation of Crohn's disease activity [12]. Perfusion of vascular malformations was quantified by CEUS in patients including children before and after percutaneous interventional treatment [13]. Of particular interest for pediatrics are US applications, including quantitative CEUS exams, in those indications where its use is particularly beneficial in children (and less in adults), e.g., in neuro-sonography. CEUS has been studied in the quantification of brain perfusion in children, e.g., to assess neonatal hypoxic injury [14, 15].

3.4 Summary

Quantification of CEUS provides objective data about organ or lesion vascularity and perfusion. Standardization and normalization of the data are required in order to compare between patients or for longitudinal data collection. Commercially available software tools have facilitated its use, but currently is still not common practice, in particular, in pediatric CEUS. However, future developments such as artificial intelligence and large data analysis may result in more quantitative examinations. In pediatrics US and CEUS should be preferred as an alternative to using other imaging modalities. Considering this, quantitative CEUS seems to be underutilized.

References

1. Lassau N, Chebil M, Chami L, Bidault S, Girard E, Roche A. Dynamic contrast-enhanced ultrasonography (DCE-US): a new tool for the early evaluation of antiangiogenic treatment. Target Oncol. 2010;5:53–8.
2. Lassau N, Chapotot L, Benatsou B, Vilgrain V, Kind M, Lacroix J, et al. Standardization of dynamic contrast-enhanced ultrasound for the evaluation of antiangiogenic therapies: the French multicenter support for innovative and expensive techniques study. Investig Radiol. 2012;47(12):711–6.
3. McCarville MB, Coleman JL, Guo J, Li Y, Li X, Honnoll PJ, et al. Use of quantitative dynamic contrast-enhanced ultrasound to assess response to antiangiogenic therapy in children and adolescents with solid malignancies: a pilot study. Am J Roentgenol. 2016;206:933–9.
4. Dietrich CF, Averkiou MA, Correas JM, Lassau N, Leen E, Piscaglia F. An introduction into dynamic contrast-enhanced ultrasound (DCE-US) for quantification of tissue perfusion. Ultraschall Med. 2012;33:344–51.
5. Tranquart F, Mercier L, Frinking P, Gaud E, Arditi M. Perfusion quantification in contrast-enhanced ultrasound (CEUS) ready for research projects and routine clinical use. Ultraschall Med. 2012;33:S31–8.
6. Bakas S, Chatzmichail K, Hunter G, Labbe B, Sidhu PS, Makris D. Fast semi-automatic segmentation of focal liver lesions in contrast-enhanced ultrasound, based on a probabilistic model. Comput Methods Biomech Biomed Eng. 2017;5:329–38.

7. Kono Y, Lyshchik A, Cosgrove D, Dietrich CF, Jang HJ, Kim TK, et al. Contrast enhanced ultrasound (CEUS) liver imaging reporting and data system (LI-RADS): the official version by the American College of Radiology (ACR). Ultraschall Med. 2017;38(1):85–6.
8. Hudson JM, Karshafian R, Burns PN. Quantification of flow using ultrasound and microbubbles: a disruption replenishment model based on physical principles. Ultrasound Med Biol. 2009;35(12):2007–20.
9. Lassau N, Bonastre J, Kind M, Vilgrain V, Lacroix J, Cuinet M, et al. Validation of dynamic contrast-enhanced ultrasound in predicting outcomes of antiangiogenic therapy for solid tumors: the French multicenter support for innovative and expensive techniques study. Investig Radiol. 2014;49(6296):794–800.
10. Seitz K, Strobel D. A milestone: approval of CEUS for diagnostic liver imaging in adults and children in the USA. Ultraschall Med. 2016;37:229–32.
11. Sidhu PS, Cantisani V, Deganello A, Dietrich CF, Duran C, Franke D, et al. Role of contrast-enhanced ultrasound (CEUS) in paediatric practice: an EFSUMB position statement. Ultraschall Med. 2017;38:33–43.
12. Kljucevsek D, Vidmar D, Urlep D, Dezman R. Dynamic contrast-enhanced ultrasound of the bowel wall with quantitative assessment of Crohn's disease activity in childhood. Radiol Oncol. 2016;50(4):347–54.
13. Wiesinger I, Schreml S, Wohlgemuth WA, Stoszczynski C, Jung EM. Perfusion quantification of vascular malformations using contrast enhanced ultrasound (CEUS) with time intensity curve analysis before and after treatment: first results. Clin Hemorheol Microcirc. 2016;62:283–90.
14. Hwang M, Sridharan A, Darge K, Riggs B, Sehgal C, Flibotte J, et al. Novel quantitative contrast-enhanced ultrasound detection of hypoxic ischemic injury in neonates and infants: pilot study 1. J Ultrasound Med. 2019;38(8):2025–38.
15. Hwang M, De Jong Jr RM, Herman S, Boss R, Riggs B, Tekes-Brady A, et al. Novel contrast-enhanced ultrasound evaluation in neonatal hypoxic ischemic injury: clinical application and future directions. J Ultrasound Med. 2017;36(11):2379–86.

4 Artifacts in Contrast-Enhanced Ultrasound Examinations

Paul S. Sidhu, Gibran T. Yusuf, Cheng Fang, and Vasileios Rafailidis

4.1 Introduction

The clinical application of contrast-enhanced ultrasound (CEUS) has been widespread in Europe and Asia for some time, with the United States recently permitting the application of ultrasound contrast agents (UCAs) in the investigation of focal liver lesions in both adults and children [1]. In the early period, when the UCAs were employed as "Doppler" rescue agents, artifacts associated with imaging the vascular system were those related to issues surrounding color Doppler ultrasound (US) sensitivity, and largely expected, with similar issues surrounding the spectral Doppler US spectral tracings [2–4]. With the advent of low mechanical imaging (MI) techniques, combined with phase inversion, CEUS imaging artifacts were largely unknown, but a better understanding has developed, allowing for a full appreciation of these artifacts and importantly, the ability to overcome or suppress these artifacts [5, 6]. The inadvertent destruction of microbubbles can lead to significant misdiagnosis as a hallmark of the malignant liver lesion is the "wash-out," and this inadvertent destruction unless identified as an artifact of CEUS, causes misinterpretation.

There are a number of artifacts detailed in this chapter, some are common on the B-mode US and accentuated with the use of UCAs, others are unique to a CEUS examination [7]. The description and explanation of each artifact are embellished by appropriate images to reinforce the visual aspect of the artifact, with an explanation on recognizing, minimizing, and appreciating the limitation of a CEUS examination when not under the control of the operator.

4.2 Ultrasound Contrast Agents

There are a number of UCAs available, with the main experience outside cardiology with the agents Definity™ (Lantheus Medical Imaging), Sonazoid™ (GE Healthcare), and SonoVue™ (Bracco SpA) using low MI contrast specific imaging. The early experience with the now obsolete agent Levovist™ (Schering), predominantly as a "Doppler-rescue" agent, using conventional color, spectral Doppler US and high MI techniques, had specific artifacts. The current experience is predominantly with low MI continuous and real-time techniques and the main agent predominantly used worldwide being SonoVue™ (Lumason™ in the United States). This agent is composed of a phospholipid shell, encapsulating a relatively insoluble perfluorocarbon gas, sulfur

P. S. Sidhu (✉) · G. T. Yusuf · C. Fang · V. Rafailidis
Department of Radiology, King's College Hospital, London, UK
e-mail: paulsidhu@nhs.net; Gibran.yusuf@nhs.net; chengfang@nhs.net; v.rafailidis@nhs.net

P. S. Sidhu et al. (eds.), *Contrast-Enhanced Ultrasound in Pediatric Imaging*,
https://doi.org/10.1007/978-3-030-49691-3_4

hexafluoride, with stability for several minutes after intravenous injection, eventually shrinking and becoming undetectable [8]. During the recirculation of the UCA, there is ample opportunity to optimize the imaging, identify and correct any artifacts and produce diagnostic imaging.

The UCA behaves differently with the degree of energy of the acoustic pulse and this leads to different groups of artifacts. Conventional US, using color Doppler US techniques, will expose the microbubble to prolonged diagnostic levels of MI, and shorten the duration of recirculation. With higher levels of MI, the phospholipid shell is destabilized and fractures, the gas is released and becomes too small to detect. This microbubble destruction can be induced by conventional Doppler US using a short burst of high MI, a phenomenon termed stimulated acoustic emission (SAE), where stationary Kupffer cell (or reticuloendothelial cell) uptake of the UCA allows for late-phase imaging (>5 min after injection) when the vascular component has ceased [9]. The US machine identifies this destruction as a Doppler shift, and the movement on conventional color Doppler imaging, recording a color signal. This phenomenon is transient, lasting less than 1 s. This is an artifact as there is not really any movement, but microbubble destruction is perceived as a movement.

Increasing the MI briefly, with the microbubbles still in the vascular compartment may also be used to interpret the image and record replenishment patterns. In this case, the microbubble in the field of view is destroyed, and replenishment occurs from vascular recirculation, a technique described as "flash" imaging with low MI techniques. With low MI, as used in contrast-specific modes, the UCA oscillates, producing harmonics, with a longer duration of recirculation as less microbubbles are destroyed. Prolonged imaging in one constant area will also accelerate microbubble destruction.

4.3 Artifacts Associated with High Mechanical Index Imaging

The early use of UCA agents aimed to improve the diagnostic capability of the color Doppler US examination, where the UCA enhanced the Doppler signal. This was of use in several areas including the carotid artery, peripheral arteries, portal vein, and in transcranial imaging [10–13]. With the increase in Doppler signal, artifacts were an issue which limited the window of opportunity to examine the vessel under consideration, without manipulation of the US machine settings. The artifacts of this type of high MI color and spectral Doppler US techniques included the following:

4.3.1 Blooming Artifact

With the presence of the UCA there is an increase in the backscatter signal intensity, with even the lowest velocities, previously undetected, being readily visualized. The overload of the Doppler signal registration, determined by these strong signals, results in the blooming of the color signal outside the vessel walls, with adjacent tissue signal increased. This artifact is easily recognized, and with manipulation of the color gain, persistence, wall filter, pulse repetition frequency, and MI, it can be controlled to produce diagnostic imaging. Furthermore, careful consideration of the optimal dose of the UCA will alleviate the tendency for any blooming, larger doses result in more pronounced blooming. The increased Doppler bandwidth may be interpreted as an area of turbulence, with underlying stenosis suspected. An infusion of the UCA will limit this artifact (Fig. 4.1).

4.3.2 Effects on the Spectral Doppler

There is an increase in both the color and spectral Doppler US signal intensity following administration of a UCA (Fig. 4.2), which, with the spectral Doppler signal, can result in a number of artifacts.

4.3.2.1 Pseudo-Increase in Systolic Peak Velocity

There may be an increase in the systolic peak velocity, by as much as 45% following the

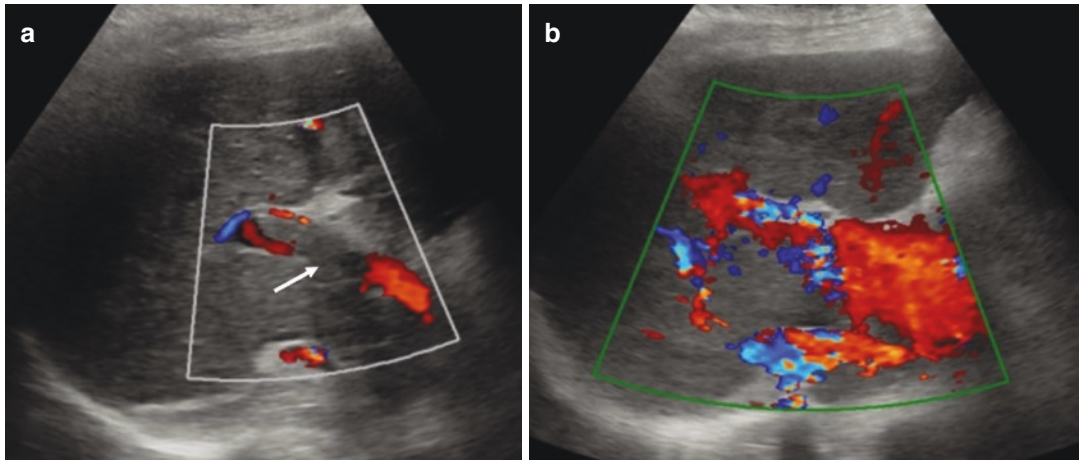

Fig. 4.1 Blooming contrast-enhanced ultrasound artifact on a conventional color Doppler examination of the portal vein. (**a**) Color Doppler image of the portal vein before the administration of the UCA, with minimal signal within the porta 1 vein (arrow). (**b**) During the CEUS examination, the color Doppler image shows an overwriting-blooming artifact caused by the increase of color Doppler signal induced by the UCA. This will obscure the interpretation of any thrombus within the vessel under investigation and requires manipulation of the Doppler settings

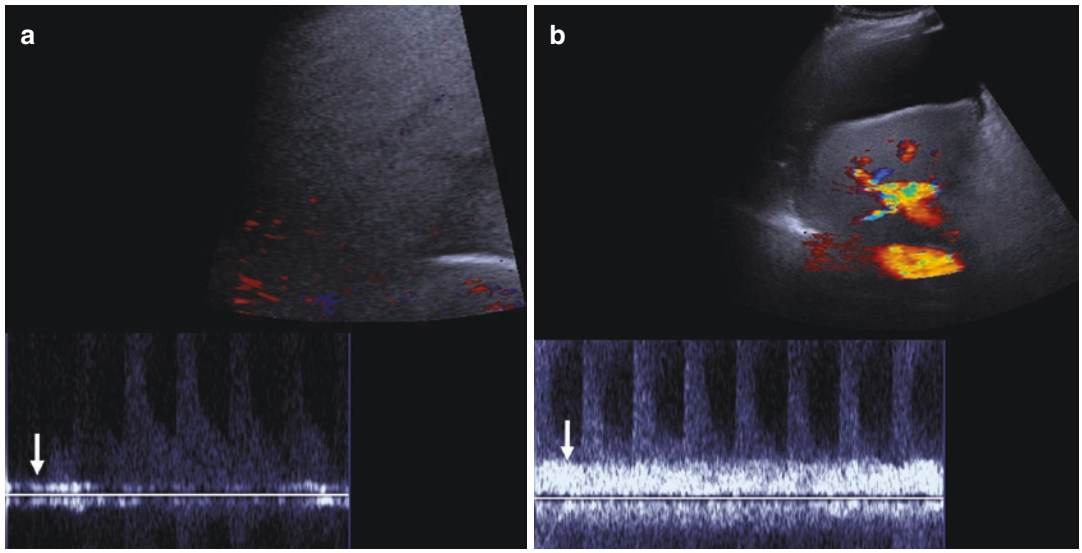

Fig. 4.2 There is an enhancement of both the color and spectral Doppler signals following the administration of a UCA. (**a**) Although there is limited color Doppler signal at the porta hepatis, a Doppler spectral waveform is obtained demonstrating a hyperdynamic hepatic artery, and a minimal signal from the portal vein (arrow). (**b**) Following the administration of a UCA, the portal vein spectral Doppler trace is enhanced (arrow), with the improvement of the color Doppler image

administration of UCA, attributed to the limited system dynamic range, non-linear conversion of backscattered signal and improved signal at very high velocities previously too weak to detect [2, 14, 15].

4.3.2.2 High-Intensity Transient Signals: "Spikes"

When the microbubbles collapse or cavitate along the sample line of the Doppler gate, sharp spikes are produced on the spectral Doppler

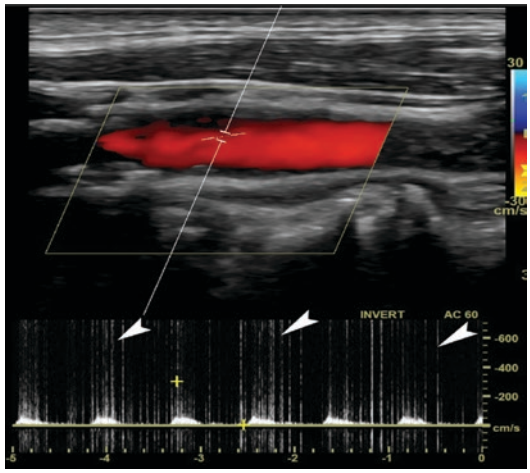

Fig. 4.3 Spectral wave Doppler technique in a patient imaged for the carotid arteries, acquired after the end of a CEUS examination. The image shows the appearance of bright linear signals (arrowheads) superimposed on a normal arterial waveform, representing "spikes" generated by the burst of microbubbles induced by the US beam

trace, and there is also an audible "crackling" sound (Fig. 4.3). This is readily recognized and may also appear as pixels of higher color on the color Doppler image.

4.3.2.3 Clutter

These are strong unwanted echoes from stationary or slow-moving tissue, produced by the movement between the US transducer and the unwanted tissue targets, primarily from operator movement, cardiac pulsation, and patient breathing [16].

4.3.2.4 Simulated Acoustic Emission

This artifact is produced when the microbubble is taken up and is stationary within a Kupffer cell in the liver or within the reticuloendothelial system within the spleen. At the late parenchymal stage, a high MI pulse destroys the microbubble, perceived as movement and color coded on the color Doppler analysis [9]. This technique was suitable for the UCA Sonazoid™, Levovist™, both with this late phase in the liver and spleen, and SonoVue™ which has only spleen uptake (Fig. 4.4). This artifact is very transient and was used to identify abnormal liver tissue, which failed to allow uptake of the UCA [17]. This technique has developed further using specific con-

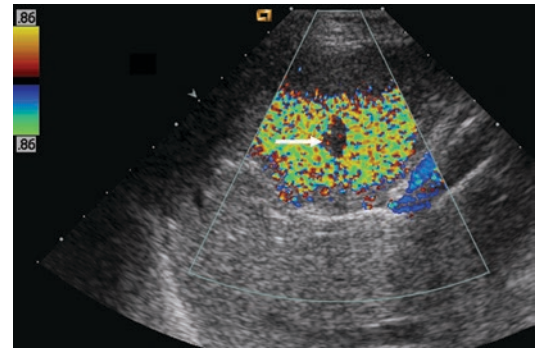

Fig. 4.4 A single image from the late phase of a Levovist™ liver study, using the Stimulated Acoustic Emission (SAE) technique. This is a very transient phenomenon, lasting <1 s, and only demonstrated in normal liver tissue. The focal nodular hyperplasia lesion shows SAE in all but the central scar (arrow) where there are no normal Kupffer cells

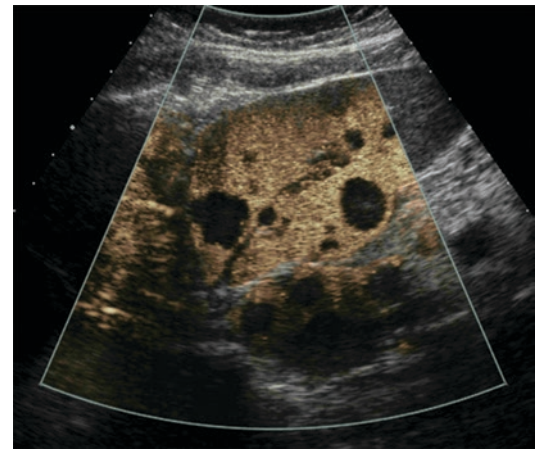

Fig. 4.5 Agent detection imaging demonstrating "black holes" where there is no UCA uptake (Levovist™) is seen in malignant areas. This is a transient phenomenon and is an artifact of the Doppler signal generated from cavitation of microbubbles

trast techniques (Agent Detection Imaging, ADI™, Siemens, Fig. 4.5) but was reliant on the UCA being taken up by Kupffer cells, which is not a property of the most commonly used UCA, SonoVue™ [18]. The ADI technique worked both with Levovist™ and Sonazoid™, but the more robust agent Sonazoid™ caused another artifact termed "veiling" with layers of microbubble collapse causing shadowing followed by more distal microbubble destruction (Fig. 4.6) [19].

4.4 Artifacts Associated with Low Mechanical Index Imaging

With the introduction of contrast-specific imaging techniques, and the use of low MI techniques, artifacts seen with a B-mode US examination may be exaggerated, and artifacts associated with UCA destruction may be identified.

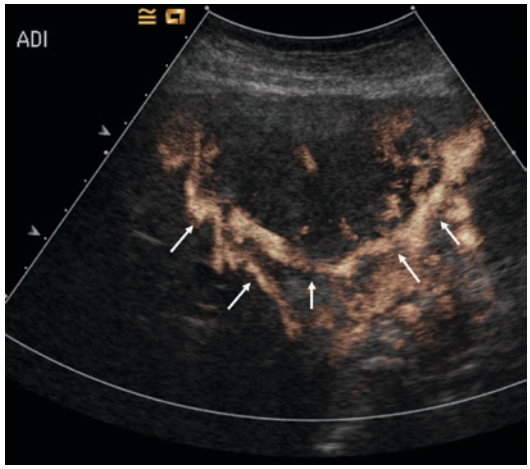

Fig. 4.6 Agent detection imaging with a more robust contrast agent Sonazoid™, with a line of microbubble cavitation (arrows) passing down through the liver as a "veil." This is best appreciated in real time

4.4.1 B-Mode Ultrasound Artifacts on CEUS

4.4.1.1 Posterior Acoustic Enhancement

This commonly encountered artifact on a B-mode examination is also present on the CEUS examination (Fig. 4.7), with a prominent depiction of the visualized microbubbles, and confirms a cystic structure. This exaggerated appearance allows smaller and more subtle cystic structures to be identified. The through transmission is more sharply demarcated, as spatial compounding and frame averaging are non-functioning in the contrast specific mode.

4.4.1.2 Acoustic Shadowing

The same principle applies to acoustic shadowing, with more sharply demarcated borders of the shadowing artifact, and possibly useful to identify smaller areas of calcification (Fig. 4.8).

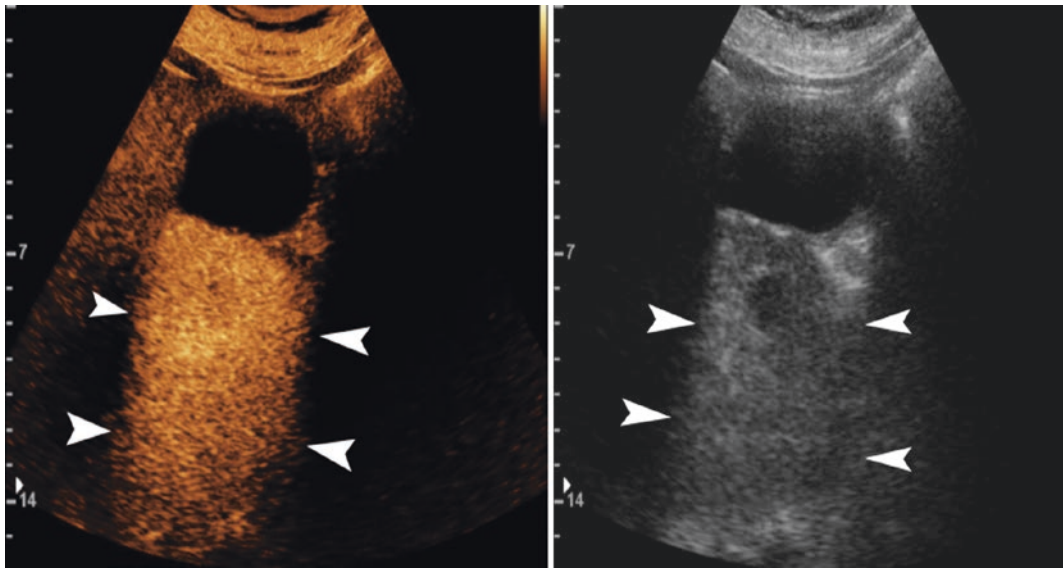

Fig. 4.7 Posterior acoustic enhancement caused by the gallbladder. Note the increased signal intensity (arrowheads) of the structures located deep to the gallbladder. This applies both in the contrast-specific image (left) and low-MI B-mode image (right)

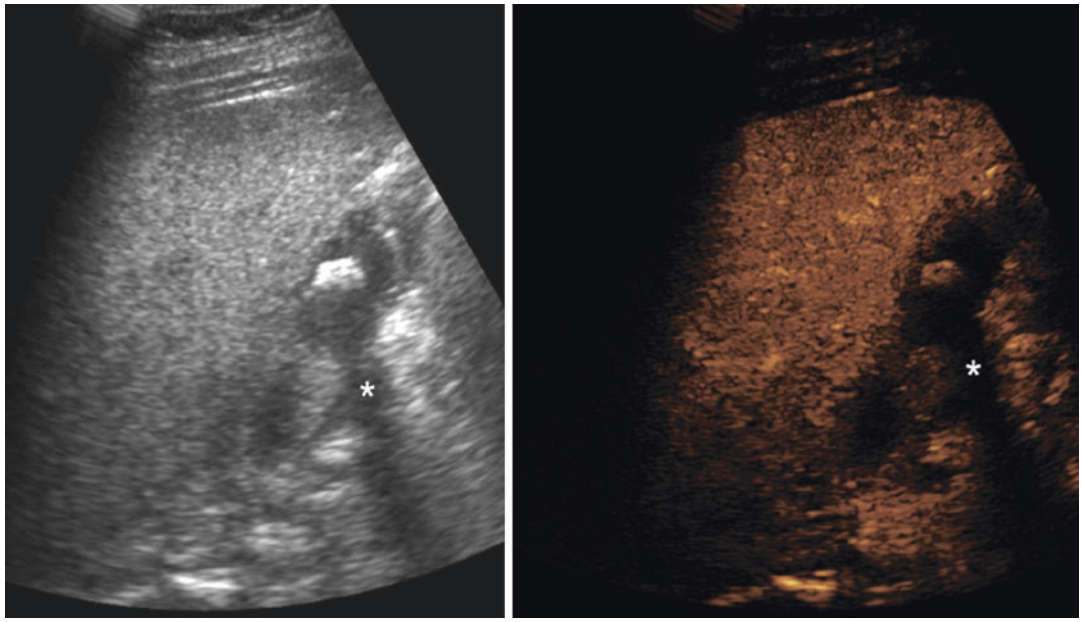

Fig. 4.8 Acoustic shadowing in a CEUS examination of the liver. Dual screen image showing a gallstone with acoustic shadowing (asterisk) in both low MI B-mode image (left) and contrast-specific image (right)

4.4.1.3 Mirror Image

A misregistration artifact, a consequence of highly reflective surfaces such as the diaphragm, causes the mirror image artifact, which will also demonstrate the CEUS lesion (Fig. 4.9). Similar CEUS artifacts found on B-mode imaging include side lobe artifacts, beam width and volume averaging can be seen.

4.4.2 Artifacts Associated Solely with CEUS

4.4.2.1 Non-linear Artifacts

Highly echogenic interfaces will result in signals that are not fully suppressed on the contrast-specific mode and will be inseparable from signals from microbubbles. Normally the simultaneous B-mode US image on the dual-screen format will make the artifact obvious, as this will be seen on the B-mode image, and will persist after UCA injection (Fig. 4.10). This artifact will be reduced by lowering the contrast image gain or decreasing output power (MI), this will also decreases the microbubble signal. A clue on the contrast image is the static nature of the high signal, with no movement of microbubbles observed.

4.4.2.2 Pseudo-Enhancement

Ineffective tissue subtraction is not a common phenomenon observed in the liver, as the liver normally presents a homogeneous reflective surface, but does occur with particularly echogenic lesions, for example, an area of focal fatty infiltration. An "enhancing" lesion may be visualized and misinterpreted. In addition, manipulation of gain, increasing this in order to better visualize the far-field or in the later phases of the study will unintentionally cause appearances of areas of enhancement (Fig. 4.11).

4.4.2.3 Signal Saturation

With higher UCA doses, particularly in the kidney, the signal received may exceed the display range of the contrast image, with the "glare" of uniform bright echoes. This will not adversely affect the angiographic or perfusion aspects of the examination, but may mask highly perfused lesions or blur the margin of well-defined lesions (Fig. 4.12). This artifact may be avoided with a decrease in UCA dose, contrast image gain, and decreasing pulse power.

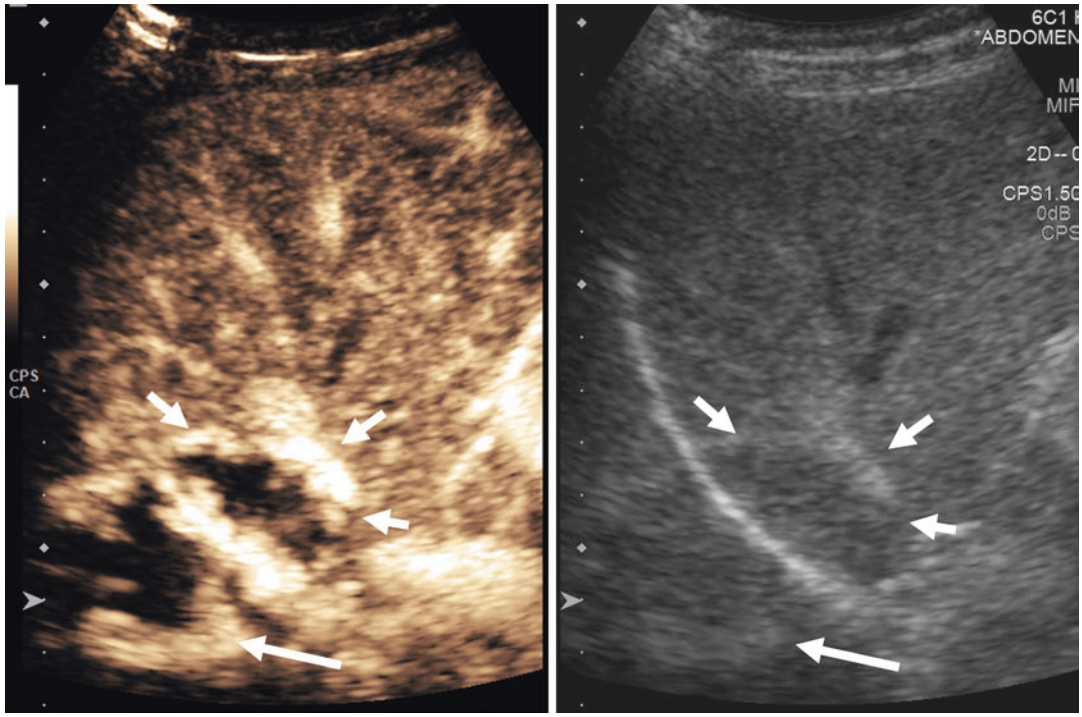

Fig. 4.9 Mirror artifact seen in a liver hemangioma. Note the presence of a lesion (short arrows) in a location near the hemidiaphragm. The mirror artifact seen with the conventional B-mode technique is also seen with CEUS, with the artifactual projection of the lesion over the diaphragm long (arrow)

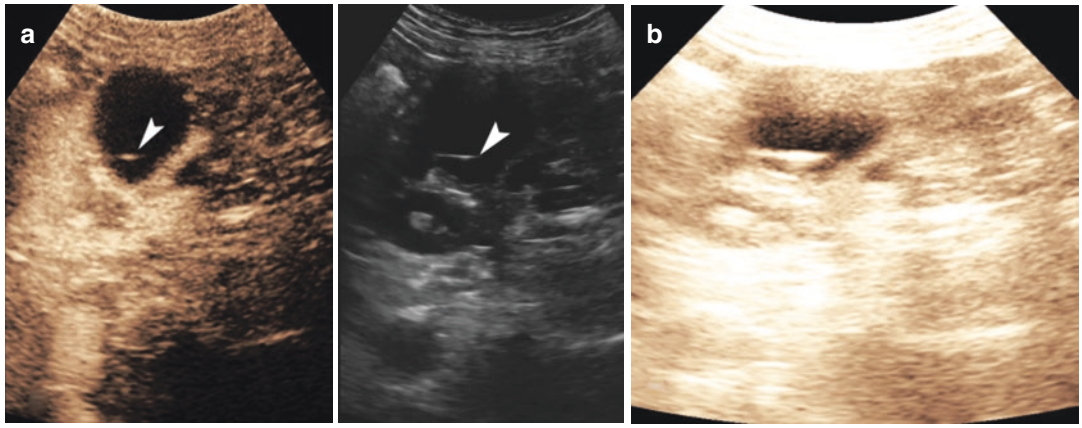

Fig. 4.10 Projection of echogenic structure on the contrast-specific image. (**a**) Dual screen image demonstrating a renal cyst with a septum (arrowheads that appear to be enhancing; an artifact produced by a poorly suppressed echogenic septum). This is readily appreciated by comparing the low-MI B-mode image, where the echogenic septum is seen (arrowhead). (**b**) By applying a high-MI pulse, a "flash" procedure, where all the microbubbles are destroyed, and observing the pattern of replenishment of the microbubbles, the nature of the echogenic area can be elucidated. (**c**) On observation of the arrival of microbubbles, the septum appears echogenic immediately after the pulse, indicating this is not truly enhancing but is caused by the projection of a poorly suppressed echogenic structure (arrowheads)

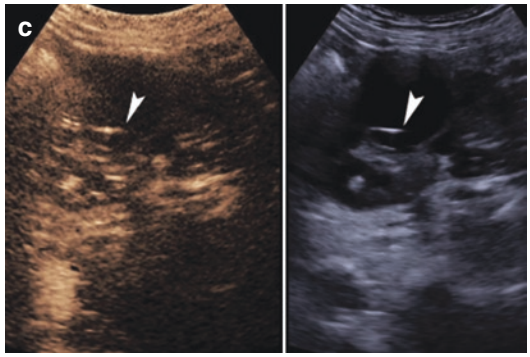

Fig. 4.10 (continued)

4.4.2.4 Shadowing

An area of concentrated microbubbles is highly attenuating, may cause shadowing in a similar fashion as that seen with a highly reflective surface, for example, bowel gas, and as such demonstrate far-field shadowing (Fig. 4.13). This artifact will alter over time as the concentration of microbubbles diminishes in the near field and is most often seen with the intra-cavitary use of UCA [20]. This artifact may be eliminated using a smaller dose of UCA or increasing the MI.

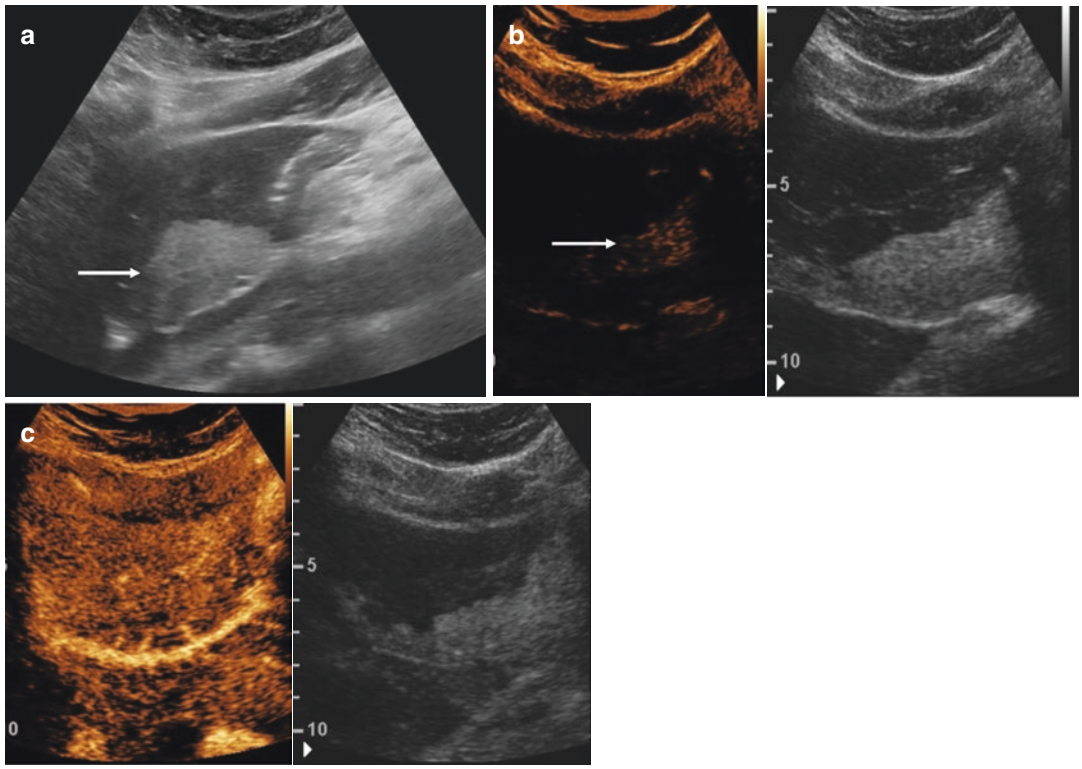

Fig. 4.11 Projection of echogenic structure on the contrast-specific image. (**a**) Conventional B-mode image showing an echogenic area in the liver parenchyma representing focal fatty infiltration. Dual screen CEUS image prior to the administration of microbubbles. (**b**) Shows echogenic signals in the contrast-specific image caused by the projection of the echogenic area due to incomplete suppression. This should not be misdiagnosed for enhancement. (**c**) Dual-screen CEUS image after the arrival of microbubbles shows the true and homogeneous enhancement of the lesion with the parenchyma

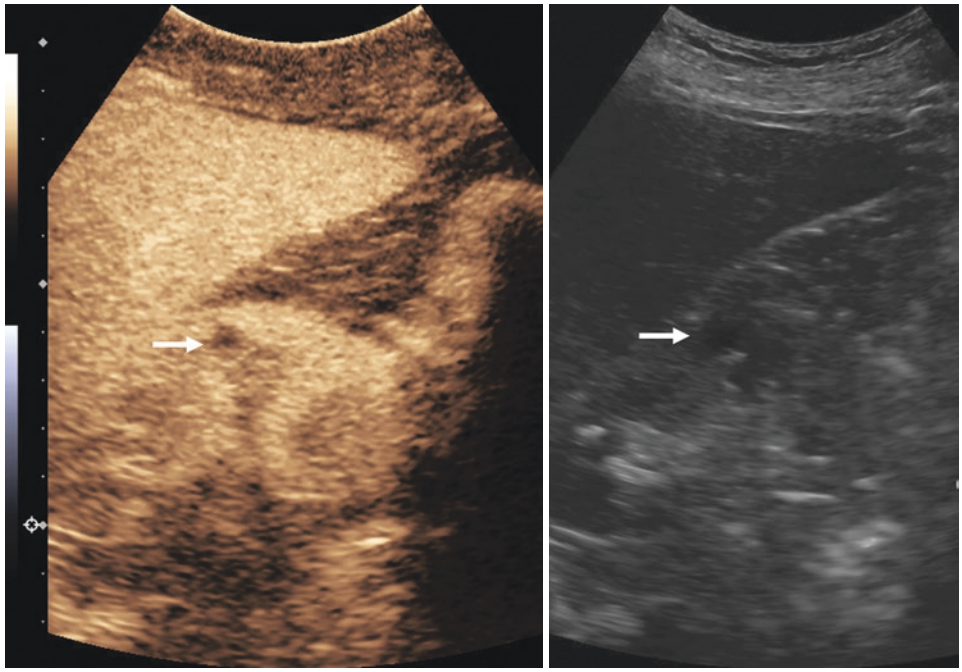

Fig. 4.12 Following the addition of a larger dose of UCA, the left kidney has become saturated with contrast, with the well-demarcated cyst on the B-mode ultrasound (arrow) becoming less obvious and smaller on the contrast image (arrow)

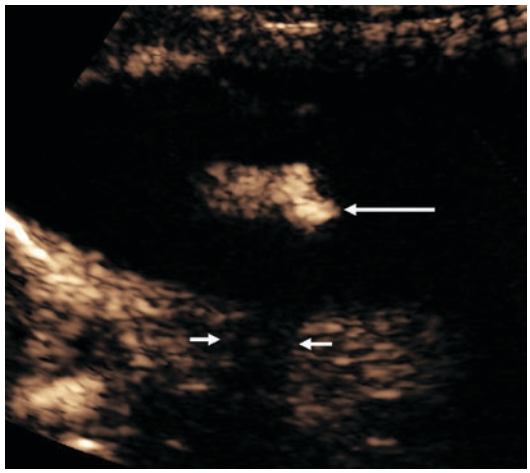

Fig. 4.13 An intra-cavitary application of a UCA, injected via an indwelling chest drainage catheter in a child with an empyema. A pocket of contrast (long arrow) lies within the anechoic pleural fluid causing distal shadowing (small arrows) of the lung parenchyma that is enhanced following a simultaneous intravenous UCA injection

4.4.2.5 Near-Field Signal Loss

There is a difference between the acoustic pressure in the near field and at the level of the focal zone, in comparison to the far-field during contrast-enhanced ultrasound. This will result in a progressive loss of signal in the near field with prolonged scanning even at low MI, with a band of "burn-off" close to the transducer (Fig. 4.14). This could be interpreted as an area of wash-out if the liver lesion being investigated is close to the surface of the liver. This artifact is much more prevalent at higher MI, higher transducer frequency, and higher frame rates. This may be avoided by not performing continuous scanning over the same area, but taking still images at fixed time periods during the examination, after the cessation of the initial phase exploring the arterial component of vascularization of a focal liver lesion [21].

4.4.2.6 Image Plane Signal Loss

An artifact that will occur after prolonged imaging at one site resulting in near field loss, or if an intermittent high MI "flash" procedure is used, is the phenomenon of image plane signal loss. This is encountered when a sweep is made through the liver, in an orthogonal plane, after a prolonged period of scanning in a single plane, where the artifact is visualized as a band of low signal (Fig. 4.15).

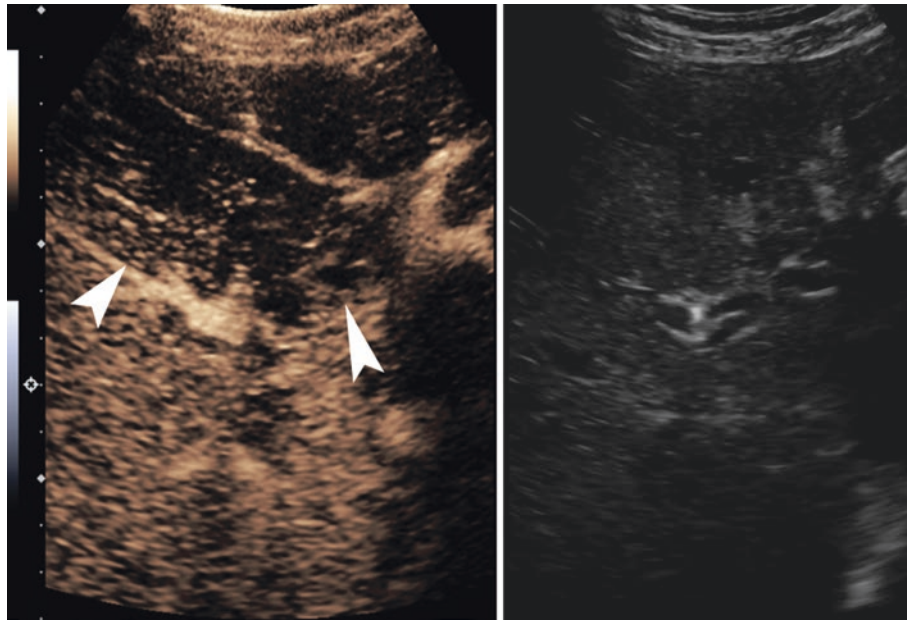

Fig. 4.14 A CEUS of the liver for characterization of a focal liver lesion. Note the near-field lower enhancement (arrowheads) after prolonged scanning at the same imaging plane. This is explained by the more intense disruption of microbubbles in this part of the image due to the disproportionate power deposition in the near field; "microbubble burn off"

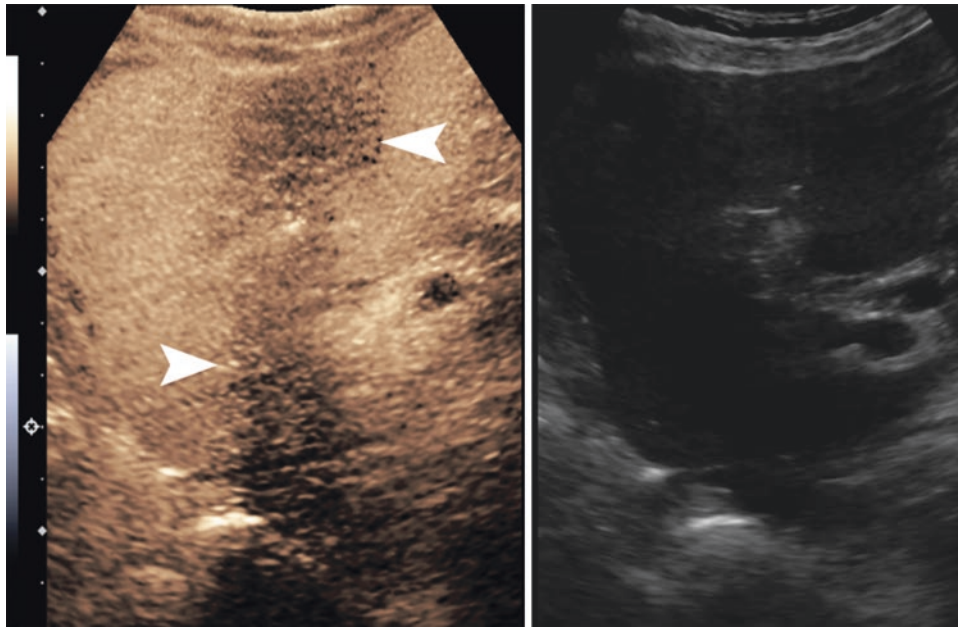

Fig. 4.15 A CEUS of the liver for focal liver lesion characterization. Note the vertically oriented linear zone of low enhancement (arrowheads). This is explained by the disproportionate disruption of microbubbles in this area, induced by the previous prolonged scanning on the same imaging plane (for the characterization of a focal lesion). The transducer was then turned 90° (in a different orthogonal plane) to visualize this artifact

This may be prevented by using low MI, decreasing the frame rate, and by using intermittent imaging. The "flash" image of a sudden burst of high MI is designed to destroy microbubbles and interpret the replenishment and is normally observer generated.

4.5 Conclusion

There are a number of artifacts associated with a CEUS examination, many are an exaggeration of well-known artifacts associated with a B-mode US or Doppler examination. Other artifacts are unique to the CEUS examination, very often obvious and recognizable with straightforward solutions to the avoidance of generating these artifacts. Once understood and recognized, this should not detract from a diagnostic CEUS examination.

References

1. Food & Drug Administration. Approved drug product list, Mar 2016. http://www.fda.gov/downloads/drugs/developmentapprovalprocess/ucm071120.pdf
2. Forsberg F, Liu JB, Burns PN, Merton DA, Goldberg BB. Artifact in ultrasonic contrast agents studies. J Ultrasound Med. 1994;13:357–65.
3. Schneider M. The past, present and future of ultrasound contrast agents. La Chimica e l'Industria. 2000;82:1–6.
4. Greis C. Technical aspects of contrast-enhanced ultrasound (CEUS) examinations: tips and tricks. Clin Hemorheol Microcirc. 2014;58:89–95.
5. Dietrich CF, Ignee A, Hocke M, Schreiber-Dietrich D, Greis C. Pitfalls and artefacts using contrast enhanced ultrasound. Z Gastroenterol. 2011;49:350–6.
6. Fetzer DT, Rafailidis V, Peterson C, Grant EG, Sidhu P, Barr RG. Artifacts in contrast-enhanced ultrasound: a pictorial essay. Abdom Radiol. 2018;43:977–97.
7. Hindi APC, Peterson C, Barr RG. Artifacts in diagnostic ultrasound. Rep Med Imag. 2013;6:29–48.
8. Schneider M. Characteristics of SonoVue. Echocardiography. 1999;16:743–6.
9. Blomley MJK, Albrecht T, Cosgrove DO, Eckersley RJ, Butler-Barnes J, Jayaram V, et al. Stimulated acoustic emission to image a late liver and spleen-specific phase of Levovist in normal volunteers and patients with and without liver disease. Ultrasound Med Biol. 1999;25:1341–52.
10. Kono Y, Pinnell SP, Sirlin CB, Sparks SR, Georgy B, Wong W, et al. Carotid arteries: contrast-enhanced US angiography—preliminary clinical experience. Radiology. 2004;230:561–8.
11. Sidhu PS, Allan PL, Cattin F, Cosgrove DO, Davies AH, Do DD, et al. Diagnostic efficacy of SonoVue(R), a second generation contrast agent, in the assessment of extracranial carotid or peripheral arteries using colour and spectral Doppler ultrasound: a multicentre study. Br J Radiol. 2006;79:44–51.
12. Marshall MM, Beese RC, Muiesan P, Sarma DI, O'Grady J, Sidhu PS. Assessment of portal venous patency in the liver transplant candidate: a prospective study comparing ultrasound, microbubble-enhanced colour Doppler ultrasound with arteriography and surgery. Clin Radiol. 2002;57:377–83.
13. Bartels E, Bittermann HJ. Transcranial contrast imaging of cerebral perfusion in patients with space-occupying intracranial lesions. J Ultrasound Med. 2006;25:499–507.
14. Gutberlet M, Venz S, Neuhaus R, Ehrenstein T, Lemke AJ, Vogl AJ, et al. Contrast agent enhanced duplex ultrasonography: visualization of the hepatic artery after orthotopic transplantation. Rofo Fortschr Geb Rontgenstr Neuen Bildgeb Verfahr. 1997;166:411–6.
15. Gutberlet M, Venz S, Zendel W, Hosten N, Felix R. Do ultrasonic contrast agents artificially increase maximum Doppler shift? In vivo study of human common carotid arteries. J Ultrasound Med. 1998;17(2):97–102.
16. Frinking P, Segers T, Luan Y, Tranquart F. Three decades of ultrasound contrast agents: a review of the past, present and future improvements. Ultrasound Med Biol. 2020;46(4):892–908.
17. Blomley MJK, Sidhu PS, Cosgrove DO, Albrecht T, Harvey CJ, Heckemann RA, et al. Do different types of liver lesions differ in their uptake of the microbubble contrast agent SH U 508A in the late liver phase? Early experience. Radiology. 2001;220:661–7.
18. Bryant TH, Blomley MJ, Albrecht T, Sidhu PS, Leen ELS, Basilico R, et al. Improved characterization of liver lesions with liver-phase uptake of liver-specific microbubbles: prospective multicenter study. Radiology. 2004;232:799–809.
19. Edey AJ, Ryan SM, Beese RC, Gordon P, Sidhu PS. Ultrasound imaging of liver metastases in the delayed parenchymal phase following administration of Sonazoid (TM) using a destructive mode technique (Agent Detection Imaging (TM)). Clin Radiol. 2008;63:1112–20.
20. Yusuf GT, Fang C, Huang DY, Sellars ME, Deganello A, Sidhu PS. Endocavitary contrast enhanced ultrasound (CEUS): a novel problem solving technique. Insights Imaging. 2018;9:303–11.
21. Deganello A, Sellars ME, Yusuf GT, Sidhu PS. How much should i record during a CEUS examination? Practical aspects of the real-time feature of a contrast ultrasound study. Ultraschall Med. 2018;39(5):484–6.

5 How to Perform an Intravenous Contrast-Enhanced Ultrasound (CEUS) Examination in a Child. Methodology and Technical Considerations

Benjamin Leenknegt, Zoltan Harkanyi, Annamaria Deganello, and Paul S. Sidhu

5.1 Introduction

The performance of a contrast-enhanced ultrasound (CEUS) examination, both the intravenous and the intracavitary route, requires an understanding not only of the technique of the procedure, but also the clinical question, and that of the patient's well-being during the course of the CEUS examination. Paramount to the CEUS examination is the skill of the operator, and a level of expertise is required to perform the CEUS examination adequately [1, 2]. The European Federation of Societies of Ultrasound and Medicine in Biology (EFSUMB) has detailed the requirements for competency in the performance of a CEUS examination [3]. The intravenous CEUS examination in the adult is now well established and the extension to use in the child is relatively simple, but the child does present some unique issues that need to be managed appropriately for a successful procedure. This chapter deals with the practicalities of an intravenous CEUS examination in a child, with the intracavitary application technique described elsewhere. A summary is detailed in Table 5.1.

5.2 Study Planning

The child is normally referred for a specific clinical or imaging indication for a CEUS examination, to establish the diagnosis, exclude a particular diagnosis or often as a "problem-solving" investigation. According to FDA the only registered CEUS indication in the child is for a focal liver lesion [4], and only in the United States using Lumason™ (Bracco Inc., NJ). Nevertheless, there is widespread use of SonoVue™ (Bracco Spa, Milan) for intravenous CEUS in Europe, for many pediatric applications [5].

Prior to the examination, the clinical history and previous imaging studies should be thoroughly reviewed in conjunction with the clinical referrer. This will determine whether a CEUS examination is appropriate and indicated to assess the diagnostic question. Potential contra-indications are identified. Manufacturers provide a standard list of possible contra-indications,

B. Leenknegt
Department of Radiology, Ghent University Hospital, Ghent, Belgium
e-mail: benjamin.leenknegt@ugent.be

Z. Harkanyi
Department of Radiology, Heim Pal National Pediatric Institute, Budapest, Hungary

A. Deganello · P. S. Sidhu (✉)
Department of Radiology, King's College Hospital, London, UK
e-mail: adeganello@nhs.net; paulsidhu@nhs.net

P. S. Sidhu et al. (eds.), *Contrast-Enhanced Ultrasound in Pediatric Imaging*,
https://doi.org/10.1007/978-3-030-49691-3_5

Table 5.1 Summary of five steps for a pediatric contrast-enhanced ultrasound (CEUS) examination

First step: Planning a CEUS study
- Review the relevant *clinical case history* of the patient. Determine whether a CEUS study is indicated for the diagnostic question.
- A detailed examination and documentation of the region of interest with *B-mode and color Doppler US.*
- Review of any *prior imaging studies* (US/CEUS/MR/CT: images and report.
- Assess patient for any *contraindication to CEUS*.
- Obtain *informed consent* from parents or the patient as appropriate.

Second step: Technical considerations
- Be certain that the *contrast-specific software* within the US scanner is functional. Be familiar with the factory CEUS protocol and use organ-based scanning protocol, if available.
- Select appropriate *US transducer and scanning parameters* for CEUS study.
- Ensure capability of US machine to record cine loops during the CEUS study.
- Ensure that treatment and life support are available for allergic reactions to UCA. Be sure that intensive care is available if needed.

Third step: Ultrasound contrast agent preparation
- Determine *dose of UCA* and saline flush (verify UCA expiration date).
- Prepare the UCA for injection based on company recommendations.
- *IV line*. Use a needle of 20–24 gauge for IV bolus injection. Three-way stop-cock.
- Central venous line can be used if the peripheral vein is not accessed.
- Have a *second person* present during the CEUS study to inject and monitor the patient.
- Be prepared for the treatment of potential UCA adverse reactions.

Fourth step: CEUS examination
- Practice respiratory movement with the patient before injection.
- Re-scan the region of interest after switching into contrast specific mode.
- Select optimal scanning parameters for the study (MI, depth, focus, gain, scan width).
- Go to split-screen, be sure the selected region of interest is displayed.
- Start timer at the moment of injection.
- Injection of UCA and saline flush.
- Start recording cine loop after the arrival of the first microbubbles for approximately 45–60 s and then record in the venous and late phase using short clips or static images (liver study).
- Decide if a repeated injection is needed.

Fifth step: Documentation and reporting
- Review the images (US system/PACS) and select still images with measurements.
- Report the CEUS examination.
- Record the UCA dose and consent in the report.
- Consider standard templates for the description of common focal liver lesions.

US ultrasound, *CT* computed tomography, *MR* magnetic resonance, *UCA* ultrasound contrast agent, *IV* intravenous, *MI* mechanical index, *PACS* picture archiving system

which include a history of known hypersensitivity to the active substance or excipients, children with right-to-left shunts, severe pulmonary hypertension, uncontrolled systemic hypertension, and uncertain pregnancy status where applicable [6]. Laboratory tests prior to the study are not required, as there are no hepato-, nephro-, or cardio-toxic effects.

If it is decided to perform a CEUS examination, the patient and the parents or guardians are informed of the diagnostic question and the details of a CEUS study, particularly the nature of the agent, the potential for adverse reactions, and the overall examination procedure from the patient's perspective. The issue of obtaining informed consent for the CEUS examination is complex and is dependent on the clinical indication ("on-label" vs. "off-label" use), the local hospital policy, and local jurisdiction, written consent may be mandatory in some healthcare systems. The key is to make available to the parents all the necessary information about the intravenous CEUS procedure, and a summary leaflet with this information may be useful.

5.3 Technical Considerations

The equipment required to perform a CEUS is an ultrasound machine with dedicated CEUS software, a catheter with a three-way stop-cock, an ultrasound contrast agent (UCA), a normal saline flush and two operators; the examiner and a person trained to administer the intravenous agents. A pediatric epinephrine-autoinjector should always be available in the event of a rare anaphylactoid reaction. The administration of any UCA must take place in an environment that supports the availability of a "team" that can lead to any resuscitation requirements in the event of a UCA reaction.

The technical considerations for ultrasound (US) imaging with a UCA are related to the unique properties of the UCA, and the interaction with the US beam. An understanding of these technical attributes is important to achieve a diagnostic study, and particular attention to artifacts as a consequence of the UCA/US interaction is essential [7]. The UCA can easily be destroyed by the energy of the US beam, and modern techniques using low mechanical index (MI) and non-linear imaging achieve good results [8]. If the shell of the UCA microbubble is disrupted and the gas diffuses from the microbubble, the microbubble loses its contrast capacity [9].

All modern high specification US machines will have the capability to perform a detailed and adequate CEUS examination, with software programs unique to each individual manufacturer. It is important to have the relevant software program enabled on the US machine and to be familiar with the process of obtaining a diagnostic study. For example, the location of the switches and buttons to start the program, the timer, cine loop recording, and still images are all used during the examination and the operator must familiarize themselves with these buttons in order to perform the dynamic examination smoothly and with a diagnostic outcome. Not ensuring that this set-up is exact, being hesitant with the buttons, may result in a repeat examination and further doses of the UCA.

The program should have the capacity to record cine loops, have an organ-based scanning protocol that can be selected for each individual case. The appropriate transducer should be selected for the lesion and organ under investigation. Usually, for technical reasons, the UCA resonates best at 3–4 MHz, the frequency normally used in the abdominal US examination. There is often the opportunity to use higher frequency transducers in children, this should be tempered against the possible loss of UCA signal with the higher frequency transducers. The transducer can be selected based on the B-mode US examination prior to the UCA administration. Parenchymal abdominal organs are most often imaged with curvilinear array transducers, using linear transducers with higher transmitting frequencies only for superficial lesions or if a higher spatial resolution is required. When a higher frequency transducer is used, a higher UCA dose may be necessary as the UCAs are less efficient nonlinear scatterers at higher frequencies. The current doses of SonoVue™ (Bracco Spa, Milan) used both in adult and pediatric practice for intravenous examinations are considerably lower than the doses originally projected to be diagnostic and higher and repeat doses are well tolerated and safe [10].

5.4 Intravenous Cannulation

It is advisable that a cannula be placed by an experienced pediatric physician or nurse, away from the US examination venue. This allows for the child to be guaranteed an examination when they arrive in the US department and also the child does not associate the pain and stress of cannulation with the US examination, particularly if very young. In most circumstances, an intravenous cannula is inserted in the left antecubital vein for the UCA injection, to avoid interaction with the right-sided examiner, the possible exception when the spleen or left kidney is targeted, with a right-sided cannula inserted. The diameter of the venous line should be 20–24 gauge. In difficult cannulation, the needle can be placed under US guidance. If present, a central venous line or a port system can be used if the system does not contain a filter requiring

high-pressure injection. Permission to use the central catheter should be obtained from the clinical team.

5.5 Ultrasound Contrast Agents and Safety

In adults, UCAs are considered safe and life-threatening side effects are extremely rare. An analysis of 23,188 CEUS studies established an incidence rate of serious adverse events of 0.0086% [11]. In children, the safety profile of UCA is less well known, with two small series suggesting the rate of adverse reactions is similar to adults [12, 13]. A European-based survey reported six minor events in 948 studies of intravascular CEUS (0.56%) and no adverse events in 4131 intravesical studies [14]. The most common adverse effects were skin reaction, unusual taste, and hyperventilation. Nonetheless, physicians administering UCAs should be able to react appropriately to an anaphylactic reaction, with a pediatric epinephrine-autoinjector available for immediate administration. All personnel involved with UCA administration in children should have basic skills in identifying and treating a contrast reaction in a child. Preferably, CEUS studies in children are only performed in a center with pediatric intensive care facilities.

5.6 Ultrasound Contrast Agents and Dosage

Two of the commercially available UCAs have been used in children: SonoVue™ (Bracco SpA, Milan) containing sulfur hexafluoride gas microbubbles and Optison™ (GE Healthcare Inc., Princeton, NJ) containing perflutren gas microbubbles. Previously the UCA, Levovist™ (Schering, Berlin) was used for intracavitary CEUS examinations, but this UCA is no longer available. The Food and Drug Administration (FDA) has authorized the use of SonoVue™ (Bracco SpA, Milan) under the commercial name Lumason™ (Bracco, NJ) for liver applications in pediatric patients in the United States [4].

There are no standardized dosage schemes of the UCA for CEUS in children. The UCA dose can be extrapolated from the licensed adult dose for hepatic applications, adjusted to the child's age, body surface or body weight, and the US equipment characteristics. For SonoVue™/Lumason™, FDA recommends a dosage for intravenous injection based on body weight: 0.03 mL/kg with a maximum of 2.4 mL per injection. Other groups advocate a dosage scheme based on the age of the patient; 0–6 years ¼ adult dose, 6–12 years ½ adult dose, and >12 years adult dose [12]. The dosage also varies for the different organs under consideration and may vary with the type of US machine used. In general, the adult doses for SonoVue™ (Bracco SpA, Milan), the most commonly used UCA, are as follows; 2.4 mL for the liver, 1.2 mL for the spleen and the kidney, and a dose of 4.8 mL for the testis and thyroid, with appropriate adjustment for children [15].

Before injection, the contrast agent expiration date and the company recommendations for injection of the UCA are verified. The UCA must be reconstituted strictly according to the manufacturer's guidelines; with SonoVue™ (Bracco SpA, Milan), the progression through the steps for reconstitution allows for the microbubbles to form correctly and assures the efficacy of the UCA. The UCA is suitable for use for a maximum of 6 h following reconstitution when it should be again shaken vigorously to obtain a "milky" appearance prior to injection. Besides the physician performing the ultrasound, a second person—preferably also a physician, is present to inject the UCA and monitor the patient after injection.

5.7 B-Mode Examination

Before starting the CEUS study, a B-mode US study is performed. This allows optimal positioning of the patient, which should be comfortable for the child and examiner, allowing for optimal identification of the region of interest and the imaging plane. The image plane is aligned along the axis of respiratory movement to minimize

respiratory out-of-plane displacement of the area of interest. A calm and continuous breathing cycle is practiced with the patient. A detailed examination and documentation of the region of interest is obtained, which should include color Doppler US observations. The region is rescanned after switching into the CEUS specific mode, to ensure that the region of interest remains visualized on the split-screen mode. It is important to appreciate that on this split-screen mode the MI is lower than in conventional B-mode imaging and the lesion under investigation may "disappear." Adjustments can be made at this stage to ensure that the lesion is visible on B-mode during the CEUS examination. Some manufactures supply a cursor that fixates on the lesion on the split-screen to allow for a maintained correct plane of imaging.

Before administering a UCA, the optimal scanning parameters for the study are selected. The MI, depth, focus, gain, and image width can be adjusted to the preferences of the physician. In general, a region of interest can be adequately assessed up to a depth of 12–15 cm, but this should not occur in most children. The mechanical index can be increased to improve penetration in this situation, but this increases microbubble destruction, especially in the nearfield [16]. The focus is positioned just deep to the target lesion to allow optimal visualization in most cases. A deeper focus position results in a more uniform acoustic field, improving UCA sensitivity and decreasing the risk of microbubble disruption [17]. Microbubble destruction by the US energy is time and depth-dependent, even at low acoustic power. This can reduce image quality or induce signal loss that can mimic washout [18]. Therefore, acoustic power is reduced when scanning more superficial target regions, and intermittent scanning also will reduce microbubble destruction.

5.8 CEUS Examination

A parent sits close to the child, and the child is fully versed in the expectations of the study procedure (if applicable for the patient age), and encouraged to watch the screen of the US machine, or else be entertained by any other suitable device. The child is reassured of the painless nature of the examination. The intravenous cannula is checked for patency by injecting a small volume of normal saline. A check is made that the examiner has achieved the ideal position for assessing the lesion, has activated the CEUS mode with dual-screen images and is poised to initiate examination timer and the cine-loop.

The UCA is injected, after the dose has been chosen to suit the patient age and site of the lesion, most commonly the liver. The UCA injection is followed by a normal saline flush, approximately 5–10 mL. The timer is started at the moment of UCA injection. After UCA injection, the target region is scanned continuously and a cine loop is recorded for approximately 45–60 s after the injection of the UCA [19]. A gentle movement of the transducer is preferred to a static transducer position to reduce microbubble destruction. In the late portal venous phase in the liver, scanning is intermittent at about 30–60 s interval, and this technique may also be deployed in assessing organs with a single blood supply. Single images or short clips can be stored to demonstrate the presence of washout, which can be for a further 5 min following UCA injection, sometimes longer with the assessment of a well-differentiated hepatocellular carcinoma in the adult patient. The UCA could last up to 7 min in the pediatric patient of normal body habitus. The UCA is rapidly removed from the blood pool, so the injection can be repeated if necessary, usually after a period of 10 min following the first injection of UCA.

The cannula may be removed in the US examination room following the CEUS examination period, or the patient may have the cannula removed on return to the ward or outpatient department. It is the manufacturer's recommendation that the patient is observed for 30 min following the administration of the UCA, and it is prudent that the cannula is removed at this point rather than immediately following completion of the US examination.

Depending on the organ under investigation, there are different phases of the examination; arte-

rial, early portal venous, and late portal venous in the liver with its unique dual blood supply. The two main diagnostic features of the examination are the vascular architecture of a lesion (in the arterial wash-in phase) and the enhancement of a lesion compared to the adjacent liver parenchyma (enhancement time course), identical in adults and children [20–22]. The wash-out of the UCA in the portal venous phase determines the benign versus malignant characteristic of a focal liver lesion. In the kidney, there is an intense enhancement of the renal cortex and delayed enhancement of the renal medulla, with abnormal vascularization of any lesion a hallmark of potential malignancy, or absence in a simple cyst. The pattern of splenic enhancement in the spleen is based on arterial enhancement and continuing enhancement in the venous phase, traumatic fractures showing no enhancement [1, 15].

5.9 Documentation and Reporting

Following the completion of the US examination, and with the departure of the patient, all images should be reviewed including the initial cine loop, particularly for the interpretation of the crucial arterial phase of any focal liver lesion. This could be from the US machine itself or a Picture Archiving Computer System (PACS). The observers may want to use a quantification program to further analyze the enhancement pattern of the UCA (e.g., in a focal liver lesion washout characteristic or with inflammatory bowel enhancement). Most machine manufacturers will have an in-built quantification software, but offline multi-machine commercial programs are available for analysis. The final interpretation should than be recorded in a formal report. The report should detail the method of obtaining consent for the CEUS examination, that is, verbal or written, and from the parents or guardian. The dose of the UCA agent should be recorded, and the number of injections used during the examination. Any adverse reactions should be recorded in the report, as well as reporting any adverse reaction to the manufacturers of the UCA and the relevant local health authority. The report should give the diagnosis achieved, or if no conclusion is reached then a recommendation for any further imaging techniques or management that would help. Finally, the report should be signed off by both the operators of the CEUS examination and any other physician involved in the interpretation of the findings.

5.10 Conclusion

The CEUS examination in the child follows the procedure of the CEUS examination in the adult, with reduced doses of the UCA needed in the smaller child. There is almost never the need for any sedation in the child as the presence of the parents is often sufficient to maintain compliance by the child for the procedure. A detailed explanation of the procedure to the parents and the older child ensures a successful examination. The placement of an intravenous cannula remote from the US examination room is desirable. The dose of UCA is based on body weight or an arbitrary fraction of the adult dose for the particular clinical scenario. The availability of resuscitation equipment and trained personal is mandatory. Monitoring of the patient following the UCA administration and recording of any adverse reactions should be undertaken. A clear, concise and informative report following the examination is key, as is the availability of images to encourage the use of this technique in the pediatric population.

References

1. Sidhu PS, Cantisani V, Deganello A, Dietrich CF, Duran C, Franke D, et al. Role of contrast-enhanced ultrasound (CEUS) in paediatric practice: an EFSUMB position statement. Ultraschall Med. 2017;38:33–43.
2. Dietrich CF, Averkiou M, Nielsen MB, Barr RG, Burns PN, Calliada F, et al. How to perform contrast-enhanced ultrasound (CEUS). Ultrasound Int Open. 2018;04:E2–E15.
3. Education and Practical Standards Committee, European Federation of Societies for Ultrasound in Medicine and Biology. Minimum training

requirements for the practice of medical ultrasound in Europe. Appendix 14: (CEUS) contrast enhanced ultrasound. Ultraschall Med. 2010;31:426–7.
4. Food & Drug Administration. Approved drug product list, Mar 2016. http://www.fda.gov/downloads/drugs/developmentapprovalprocess/ucm071120.pdf.
5. Rosado E, Riccabona M. Off-label use of ultrasound contrast agents for intravenous applications in children. Analysis of the existing literature. J Ultrasound Med. 2016;35:e21–30.
6. Sidhu PS, Huang DY, Fang C. Contrast enhanced ultrasound (CEUS) in pregnancy: is this the last frontier for microbubbles? Ultraschall Med. 2020;41(1):8–11.
7. Fetzer DT, Rafailidis V, Peterson C, Grant EG, Sidhu P, Barr RG. Artifacts in contrast-enhanced ultrasound: a pictorial essay. Abdom Radiol. 2018;43:977–97.
8. Wilson SR, Burns PN. Microbubble-enhanced US in body imaging: what role? Radiology. 2010;257:24–39.
9. Greis C. Technical aspects of contrast-enhanced ultrasound (CEUS) examinations: tips and tricks. Clin Hemorheol Microcirc. 2014;58:89–95.
10. Sidhu PS, Allan PL, Cattin F, Cosgrove DO, Davies AH, Do DD, et al. Diagnostic efficacy of SonoVue(R), a second generation contrast agent, in the assessment of extracranial carotid or peripheral arteries using colour and spectral Doppler ultrasound: a multicentre study. Br J Radiol. 2006;79:44–51.
11. Piscaglia F, Bolondi L. The safety of SonoVue in abdominal applications: retrospective analysis of 23188 investigations. Ultrasound Med Biol. 2006;32:1369–75.
12. Yusuf GT, Sellars ME, Deganello A, Cosgrove DO, Sidhu PS. Retrospective analysis of the safety and cost implications of pediatric contrast-enhanced ultrasound at a single center. AJR Am J Roentgenol. 2016;208:446–52.
13. Piskunowicz M, Kosiak W, Batko T, Piankowski A, Polczynska K, Adamkiewicz-Drozynska E. Safety of intravenous application of second generation ultrasound contrast agent in children: prospective analysis. Ultrasound Med Biol. 2015;41:1095–9.
14. Riccabona M. Application of a second-generation US contrast agent in infants and children—a European questionnaire-based survey. Pediatr Radiol. 2012;42:1471–80.
15. Sidhu PS, Cantisani V, Dietrich CF, Gilja OH, Saftoiu A, Bartels E, et al. The EFSUMB guidelines and recommendations for the clinical practice of contrast-enhanced ultrasound (CEUS) in non-hepatic applications: update 2017 (long version). Ultraschall Med. 2018;39:e2–e44.
16. Greis C. Technology overview: sonoVue. Euro Radiol Suppl. 2004;14:P11–5.
17. Averkiou MA, Bruce MF, Powers JE, Sheeran PS, Burns PN. Imaging methods for ultrasound contrast agents. Ultrasound Med Biol. 2019;46:498–517.
18. Dietrich CF, Ignee A, Hocke M, Schreiber-Dietrich D, Greis C. Pitfalls and artefacts using contrast enhanced ultrasound. Z Gastroenterol. 2011;49:350–6.
19. Deganello A, Sellars ME, Yusuf GT, Sidhu PS. How much should I record during a CEUS examination? Practical aspects of the real-time feature of a contrast ultrasound study. Ultraschall Med. 2018;39(5):484–6.
20. Claudon M, Dietrich CF, Choi BI, Kudo M, Nolsoe C, Piscaglia F, et al. Guidelines and good clinical practice recommendations for contrast enhanced ultrasound (CEUS) in the liver—update 2012. Ultraschall Med. 2013;34:11–29.
21. Jacob J, Deganello A, Sellars ME, Hadzic N, Sidhu PS. Contrast enhanced ultrasound (CEUS) characterization of grey-scale sonographic indeterminate focal liver lesions in paediatric practice. Ultraschall Med. 2013;34:529–40.
22. Fang C, Bernardo S, Sellars ME, Deganello A, Sidhu PS. Contrast-enhanced ultrasound in the diagnosis of pediatric focal nodular hyperplasia and hepatic adenoma: interobserver reliability. Pediatr Radiol. 2019;49(1):82–90.

6 How to Set Up a Contrast-Enhanced Ultrasound Service for Children

Paul D. Humphries

6.1 Introduction

Ultrasound (US) is one of the most widely used imaging modalities in pediatrics. The smaller size of children and reduced body fat compared to adults mean that exquisite imaging can be obtained. The dynamic and non-ionizing nature of US and the lack of a requirement for sedation or general anesthesia are further advantages over computerized tomography (CT) and magnetic resonance (MR) imaging.

Previously, a lack of physiological or biological functional imaging using US has been a relative disadvantage compared to CT or MR imaging. Modern US developments including elastography and contrast-enhanced ultrasound (CEUS) now allow operators to not only evaluate anatomy but also characterize and examine pathological tissues, further strengthening the role of US, particularly in children.

Compared to CT and MR imaging, US is more child friendly, has more rapid access, can be repeated more often and has health economic benefits for institutions. In this chapter, the challenges that may be encountered when attempting to set up a CEUS service in children and strategies for managing these are outlined.

P. D. Humphries (✉)
Great Ormond Street Hospital for Children and University College London Hospital, London, UK
e-mail: Paul.Humphries@gosh.nhs.uk

6.2 Local Approval Procedures

Each hospital will likely vary somewhat in the local process by which new services are introduced. There may be a central committee that considers service developments, evaluating each aspect of the new proposed service, including clinical indications, medicine administration, business costs, equipment procurement; usually a well-established process and well-known documentation. In other institutions, a number of different committees or managerial boards may need to be navigated for each part of the process. The first step is to identify to whom you need to apply for each of the considerations detailed below when setting up your CEUS service.

It is likely that introducing CEUS will require some form of medicines safety committee or prescribing board approval for the administration of an ultrasound contrast agent (UCA), normally SonoVue™/Lumason™ (Bracco SpA, Milan). The main points to consider when submitting your application to such a committee are:

6.2.1 Regulatory Considerations, Off-Label Use and Safety

The first step in the process is often to explain to the medicines/prescribing committee that CEUS is actually possible; a recognized and established procedure, explain the physiology of the UCA

P. S. Sidhu et al. (eds.), *Contrast-Enhanced Ultrasound in Pediatric Imaging*,
https://doi.org/10.1007/978-3-030-49691-3_6

and to detail the currently used agents. The remainder of this discussion will assume you will wish to use SonoVue™/Lumason™ (Bracco SpA, Milan), the only agent currently licensed for pediatric use and used widely. Other commercially available UCAs have not been or have rarely been used in children.

One of the first obstacles that may be encountered when setting up a pediatric CEUS service relates to the licensing of Sonovue™/Lumason™ in children. Lumason™ has been licensed by the US Food and Drug Administration for the characterization of liver lesions in both adults and children, as an intravenous injection [1], however, no such licensing exists elsewhere, and any use for unlicensed indications is therefore "off-label" [2]. This however should not be a hindrance to setting up a CEUS service in children, as there are no legal barriers to off-label use of medicines [3] and there are clearly defined guidelines for the use of off-label medicines [4].

In reality, if your practice is based at a children's hospital, it may be more straight forward to gain acceptance for off-label use of SonoVue™ in children compared to a facility where there is a limited pediatric practice, as many children are routinely administered off-label medicines, with surveys documenting more than 40% of children being in this situation [5–7], with the hospital administration more familiar to off-label use of medicines. Where the committee are less conversant with off-label use of medicines in children, the above arguments can be used to convince them [8].

The second barrier that may be encountered relates to the safety profile of SonoVue™, which any committee is unlikely to be acquainted. There is a growing body of evidence regarding the safety profile of UCA in both adults and, most importantly, children [9–11], which can be presented as an evidence base to persuade the committee of the safety of the agent. In addition, it is worth highlighting that UCAs have a lower reported rate of adverse events compared to iodinated contrast for CT, also used routinely off-label in pediatrics.

6.2.2 Pharmacy, Ordering and Stock

Once the medicines committee has granted approval for the use of the UCA, the process by which it is ordered and stored will need to be agreed with your pharmacy. The most practical way of facilitating a clinical service is to have a stock available in your US Department, with the departmental administration team notifying pharmacy when stock will need replenishing, such that you always have in-date UCA available. It is ideal to store the UCA as you would any medicinal product, within a locked cupboard in easy access to the procedure room. One potential hurdle that may be encountered is the pharmacy treating the UCA as a "drug" that requires a prescription for each administration. This should be argued against, as SonoVue™ is analogous to CT or MR contrast administration, which, in most countries, does not require prescribing on an individual basis. It should be noted that despite only a small volume injected in each case that it is highly likely that the medicines committee and pharmacy will insist that each vial is single use only and not split between several patients, notwithstanding the lower doses that are equally clinically effective [12].

6.3 Clinical Service Management and Business Case

The next group that you will need to convince when setting up your CEUS service is your clinical manager and the departmental service manager. It is likely that the immediate response to your proposal will be related to (a) longer scanning time per case and (b) new consumable previously not used, and ultimately the perceived increased cost. Your clinical manager will need convincing that CEUS has a role in the work up of pediatric patients for a wide variety of conditions, using both intravenous and intracavitary applications [13]. The best overview of these indications can be found in the EFSUMB position statement and correspondence and used as a basis for your discussion [14, 15].

While not able to replace all cross-sectional imaging or fluoroscopy, CEUS may be able to reduce the burden of these other investigations. For example, in cases where new or incidental liver lesions are found requiring prompt characterization, for the assessment of vesical–ureteric reflux and problem-solving in many other situations. Any child diverted away from other investigations that either requires sedation/general anesthesia and/or prolonged scanning times with CT or MR imaging, CT or MR contrast administration (and their attendant contraindications in the setting of renal dysfunction) provides a better patient experience and has significant cost reduction implications for the radiology service [16]. This is a powerful and persuasive argument for departmental managers to support the introduction of CEUS. In addition, the rapidity with which CEUS can be performed is a further advantage over waiting for over-subscribed cross-sectional imaging, in appropriate cases.

Any US equipment upgrades should be planned with CEUS in mind and the equipment specification should include the software package to enable CEUS to be performed. It may be necessary to secure funding to pay for installation on any pre-existing US systems within the department. All modern-day manufacturers include CEUS functionality on their high specification machines, and it is a personal choice as to the preferred manufacturer.

6.4 Clinical "Buy-In"

Ultimately, a nascent CEUS service will not grow and flourish without clinical "buy in" from your referring clinicians. This aspect can be one of the more challenging aspects of CEUS service development and requires enthusiasm and persuasion on the part of the US practitioner. Good relationships with clinical colleagues and being able to have open discussions about imaging options help in the development of a CEUS service. Multidisciplinary meetings are often a good way to introduce the idea of CEUS in cases, particularly, where there is good evidence that it will be beneficial. Be prepared to give an overview of the UCA physics, pharmacokinetic action, and practicality of performing a CEUS examination in children to your clinical colleagues to help them understand what is being proposed. Where there is uncertainty, one strategy is to initially offer CEUS in parallel with existing imaging techniques to allow both yourself and the clinical teams' time to become comfortable with the new service and see how and where it is effective for your patient population.

Another avenue that can help with the introduction of a CEUS service is to identify research that can be complemented by CEUS within the study protocol and collaborate with colleagues undertaking such studies. One example is using CEUS to assess the anti-angiogenic properties of new therapies in oncology trials [17]. Such collaborations may also assist with funding for new equipment or installation of CEUS software packages on existing equipment, including commercially available quantification software to assist with analysis.

6.5 Learning and Development

An important part of any new service is the training of other practitioners, audit, and feedback. Attendance at any formal CEUS educational or practical course is necessary and clinical attachments at a center already performing CEUS is a very sensible approach during your learning phase.

It is vital to consider how your CEUS service will be delivered throughout the working week and how many practitioners will be needed to deliver this service. As a minimum, it is useful to have two practitioners trained and able to collaborate for service delivery. There is an inevitable learning curve when starting to use a new technique, and double reporting with a colleague is useful to ensure accuracy and improve familiarity with the technique. If possible, it is also helpful to have a more senior mentor who has more experience of CEUS, to whom you can consult for advice and support, who may be from another facility, willing to review images.

As with any new service, it is important to set up tools to allow regular audit of your practice in terms of side effects, technical adequacy, and diagnostic performance compared to either defined reference standards, for example, histology or alternative imaging modality assessment. A suggested strategy is a prospectively populated database of any CEUS examinations performed, which can be interrogated for audit purposes and can also be used to collaborate with colleagues at other pediatric CEUS centers, increasing patient numbers in any future research studies performed.

6.6 Summary

CEUS in children has many potential benefits, but there are challenges to institute such a service as described above. Having a clear thought process regarding the issues that may be encountered should assist in a successful outcome.

References

1. Seitz K, Strobel D. A milestone: approval of CEUS for diagnostic liver imaging in adults and children in the USA. Ultraschall Med. 2016;37:229–32.
2. Sidhu PS. Contrast-enhanced ultrasound: extended role outside 'regulations'. Ultrasound. 2016;24:4–5.
3. Barr RG. Off-label use of ultrasound contrast agents for abdominal imaging in the United States. J Ultrasound Med. 2013;32:7–12.
4. General Medical Council of the United Kingdom. Good practice in prescribing and managing medicines and devices. 2016. http://www.gmc-uk.org/2016 [updated 25 Feb 13; cited 27 Sept 2016]. Available from: https://www.gmc-uk.org/ethical-guidance/ethical-guidance-for-doctors/prescribing-and-managing-medicines-and-devices.
5. Knopf H, Wolf IK, Sarganas G, Zhuang W, Rascher W, Neubert A. Off-label medicine use in children and adolescents: results of a population-based study in Germany. BMC Public Health. 2013;13:631.
6. Conroy S, Choonara I, Impiccaitore P, Mohn A, Arnell H, Rane A, et al. Survey of unlicensed and off label drug use in paediatric wards in European countries. BMJ. 2000;320:79–82.
7. Bazzano ATF, Mangione-Smith R, Schonlau M, Suttorp MJ, Brook RH. Off-label prescribing to children in the United States outpatient setting. Acad Pediatr. 2009;9:81–8.
8. Sidhu PS, Choi BI, Nielsen MB. The EFSUMB guidelines and recommendations on the clinical practice of contrast enhanced ultrasound (CEUS): a new dawn for the escalating use of this ubiquitous technique. Ultraschall Med. 2012;32:5–7.
9. Piscaglia F, Bolondi L. The safety of SonoVue in abdominal applications: retrospective analysis of 23188 investigations. Ultrasound Med Biol. 2006;32:1369–75.
10. Piskunowicz M, Kosiak W, Batko T, Piankowski A, Polczynska K, Adamkiewicz-Drozynska E. Safety of intravenous application of second generation ultrasound contrast agent in children: prospective analysis. Ultrasound Med Biol. 2015;41:1095–9.
11. Coleman JL, Navid F, Furman WL, McCarville MB. Safety of ultrasound contrast agents in the pediatric oncologic population: a single-institution experience. AJR Am J Roentgenol. 2014;202:966–70.
12. Sidhu PS, Cantisani V, Dietrich CF, Gilja OH, Saftoiu A, Bartels E, et al. The EFSUMB guidelines and recommendations for the clinical practice of contrast-enhanced ultrasound (CEUS) in non-hepatic applications: update 2017 (long version). Ultraschall Med. 2018;39:e2–e44.
13. Yusuf GT, Sellars ME, Deganello A, Cosgrove DO, Sidhu PS. Retrospective analysis of the safety and cost implications of pediatric contrast-enhanced ultrasound at a single center. AJR Am J Roentgenol. 2016;208:446–52.
14. Sidhu PS, Cantisani V, Deganello A, Dietrich CF, Duran C, Franke D, et al. Role of contrast-enhanced ultrasound (CEUS) in paediatric practice: an EFSUMB position statement. Ultraschall Med. 2017;38:33–43.
15. Sidhu PS, Cantisani V, Deganello A, Dietrich CF, Duran C, Franke D, et al. Authors reply to letter: role of contrast-enhanced ultrasound (CEUS) in paediatric practice: an EFSUMB position statement. Ultraschall Med. 2017;38:447–8.
16. Sellars ME, Deganello A, Sidhu PS. Paediatric contrast-enhanced ultrasound (CEUS); a technique that requires co-operation for rapid implementation into clinical practice. Ultraschall Med. 2014;35:203–6.
17. McCarville MB, Coleman JL, Guo J, Li Y, Li X, Honnoll PJ, et al. Use of quantitative dynamic contrast-enhanced ultrasound to assess response to antiangiogenic therapy in children and adolescents with solid malignancies: a pilot study. Am J Roentgenol. 2016;206:933–9.

Pediatric Focal Lesions in the Liver: A Clinical Perspective

7

Emer Fitzpatrick

7.1 Introduction

Pediatric liver tumors may be benign or malignant, and frequencies of the different types of tumor occur at different ages [1]. A mass in infancy most often prompts concern over hepatoblastoma, whereas a fibrolamellar tumor occurs almost exclusively in those in late adolescence and adulthood. The presence of an underlying liver or systematic condition is also of importance. There is an increased risk of liver malignancy with most chronic liver diseases. In particular conditions such as tyrosinemia, bile salt export pump deficiency (BSEP), and sclerosing cholangitis carry a significant malignancy predisposition [2]. Portosystemic shunts or other disturbance to the perfusion of the liver predispose to focal nodular hyperplasia (FNH) or nodular regenerative hyperplasia. Metabolic conditions such as glycogen storage disease and hormonal imbalance may predispose to adenomata [3, 4]. Focal liver lesions may be single or multiple, which may in itself be a clue to diagnosis, and each requires a different management approach (Table 7.1).

E. Fitzpatrick (✉)
Pediatric Liver Centre, King's College London
Faculty of Life Sciences and Medicine at King's College Hospital, London, UK
e-mail: emer.fitzpatrick@kcl.ac.uk

7.2 Benign Liver Lesions

7.2.1 Focal Nodular Hyperplasia

This benign tumor of the liver accounts for 4% of all hepatic tumors in the pediatric population (Fig. 7.1). FNH are well-circumscribed lesions of various echotexture on ultrasound (US) imaging, often with a characteristic central scar. FNH may be seen in the context of vascular disturbance to the liver, for example, in the presence of porto-systemic shunts [5] or following chemotherapy/bone marrow transplantation [6, 7]. FNH may also be associated with Alagille syndrome or other chronic liver diseases in which there is a disturbance to vascular flow. In addition, children and adults with cardiac-related liver disease, for example, those with a Fontan circulation, are more predisposed to developing FNH [8]. The circulatory disturbance is postulated to result in a hyperplastic response of the parenchyma though the mechanism of this is not fully elucidated. An FNH occurs more commonly in girls and can present at any age but probably most frequently between 2 and 10 years [9]. The oral contraceptive pill has not been associated [10].

The presentation of FNH may be incidental or with abdominal pain and FNH may be small or large at presentation and single or multiple. An FNH may be identified as a slightly hypodense discrete lesion on an unenhanced computed tomography (CT) which following contrast, enhances homogenously in the arterial phase becoming isodense in delayed scan. The central

P. S. Sidhu et al. (eds.), *Contrast-Enhanced Ultrasound in Pediatric Imaging*,
https://doi.org/10.1007/978-3-030-49691-3_7

Table 7.1 Range of focal liver lesions distributed by age with characteristic clinical features and clinical management

Age	Likely diagnosis	Characteristic features	Management
<1 year	Hepatic hemangiomas Hepatoblastoma Mesenchymal hamartoma	Hemangioma - abdominal mass, cardiac failure Hepatoblastoma - Mass, abdominal distension	Hemangioma—propranolol supportive, hepatic artery ligation or embolization, resection Hepatoblastoma chemotherapy and resection Mesenchymal hamartoma—resection
0–5 years	Hepatoblastoma FNH Mesenchymal hamartoma	Mass, abdominal distension	Hepatoblastoma - Chemotherapy, resection FNH - Observation, resection Mesenchymal hamartoma - Resection
5–12 years	Adenoma FNH HCC Rarely hepatoblastoma	Mass, abdominal distension	Adenoma - Observation, stop OCP, resection FNH - Resection Malignancy - Chemotherapy, resection
Teenagers	Fibrolamellar/HCC FNH	Mass, abdominal distension	Fibrolamellar - Resection FNH - Resection

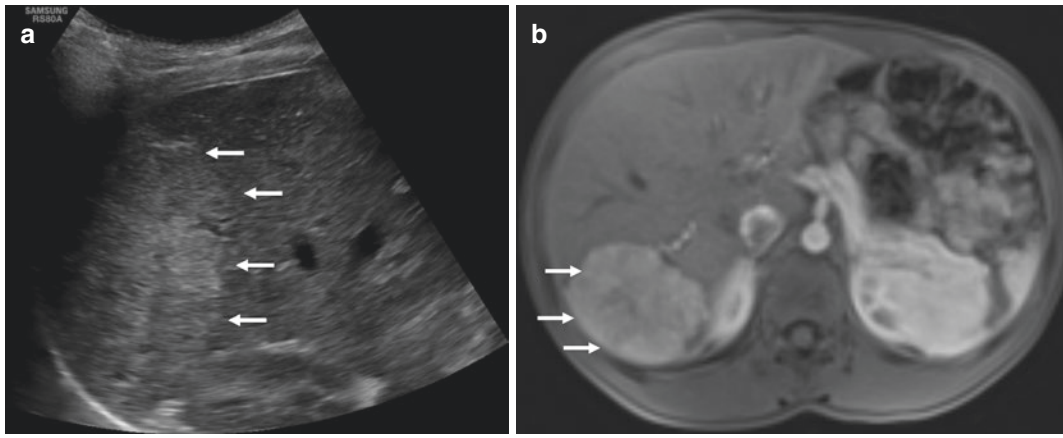

Fig. 7.1 Focal nodular hyperplasia in an 11-year-old girl. (**a**) B-mode ultrasound demonstrates a slightly hyperechoic abnormality in the posterior aspect of the right liver lobe (arrows), atypical for a focal nodular hyperplasia. (**b**) On T1 weighted Magnetic Resonance (MR) imaging, the lesion shows early homogeneous enhancement post administration of gadolinium, with evidence of a central, non-enhancing scar, confirming a focal nodular hyperplasia

scar is visible in 50% with delayed enhancement. The presence of a port-systemic shunt should be sought on imaging. In cases in which there is a doubt about the diagnosis, a biopsy is indicated. Microscopically FNH consist of hyperplastic hepatocytes supported by a well-developed reticulin framework. The septa are rich in vessels, and the immunohistochemical pattern differs from hepatocellular adenoma. The natural history of FNH is variable. Some 10% may undergo spontaneous regression, however, an FNH may also increase in size and there is the potential for malignant transformation [11].

Surgical resection is a possibility for FNH, which are increasing in size or are symptomatic or if there is concern regarding malignant transformation. If a portosystemic shunt is present, closure of the shunt whether radiologically or surgically, can result in regression of the FNH. If resection or shunt closure is not possible or desirable, close surveillance is advised with imaging on a 6–12 monthly basis.

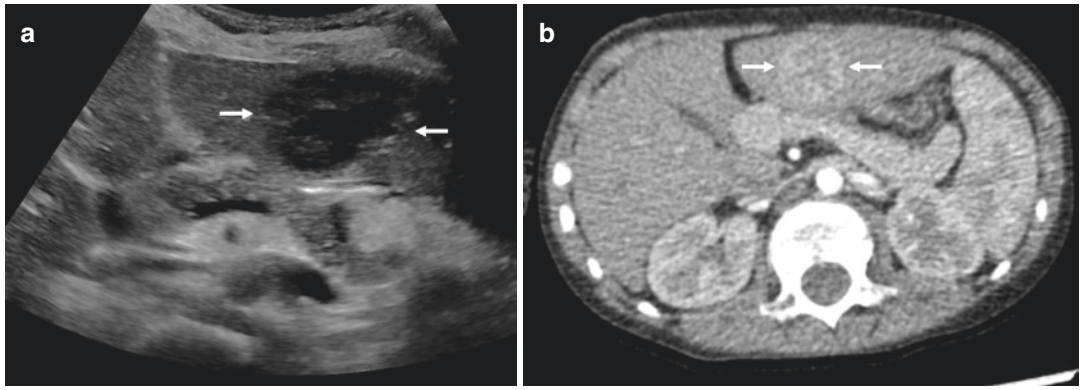

Fig. 7.2 Hepatocellular adenoma in a 6-year-old boy with underlying liver disease awaiting a transplant. (**a**) An atypical low reflective lesion in the left lobe of the liver (arrows). (**b**) On the contrast-enhanced CT, there is vascularization in the arterial phase (arrows)

7.2.2 Hepatocellular Adenoma

Hepatocellular adenoma (HCA) (Fig. 7.2) are benign liver tumors, less commonly found than FNH. Hepatocellular adenomas may be single or multiple and incidentally found on the background of a normal liver or in the context of underlying liver or metabolic disease. Hepatocellular adenoma are more common in females and associated with hormonal changes and particularly with the oral contraceptive pill [3]. Though benign, there is the potential for malignant transformation in certain situations, increasing size and bleeding into the tumor may also occur. Hepatocellular adenomas in adults have been associated with obesity with some case reports in children [12]. Glycogen storage diseases Type I, III, and IV, and McClune Albright Syndrome are also associated with the occurrence of HCAs [4].

Over the last 15 years, considerable advances have been made in the molecular understanding of this tumor. Genetic alterations of the HNF1 alpha transcription factor have been found in 50% of cases [13]. In addition, alterations in beta catenin exon 3 have been found in 10–15% of adenomas studied and beta catenin exon 7/8 in a further 5% [14, 15]. The HNF1 alpha inactivation results in altered expression of FAP (familial adenomatosis polypi) and is also linked to MODY 3 (maturity onset diabetes of the young) [16, 17].

Nault et al. [18] described the currently accepted classification of HCA as:

1. HNF1a inactivated HCA 40–50% overall. These HCAs may be associated with estrogen, and the presence of FAP and MODY3 should be sought.
2. Beta catenin exon 3 mutated HCA: 10–15%. This subtype is associated with an increased risk of malignant transformation. It may be associated with increased androgens and also with estrogen, alcohol consumption, also with vascular diseases of the liver in males.
3. Beta catenin mutated HCA exon 7/8: 5–10% not associated with malignant transformation.
4. Inflammatory HCA 35–45%. This subtype is associated with constitutive activation of the IL6/JAK/STAT pathway with over-expression of C-reactive protein (CRP) and serum amyloid A. Patients may present with an inflammatory syndrome/anemia and fever. Also associated with estrogen, obesity, and glycogen storage diseases.
5. Sonic hedgehog HCA associated with constitutive–activation of sonic hedgehog and occurring in 5% of all HCA. This subtype is associated with estrogen and obesity and a higher risk of bleeding.
6. Unclassified HCA accounts for 7% of HCA and is not otherwise defined by genetics or by signal pathway.

Hepatocellular adenomata are often difficult to distinguish from well-differentiated hepatocellular carcinoma (HCC) or FNH (particularly telangiectatic FNH) [19]. HCC may also carry a beta catenin mutation; this is obviously the most important differential diagnosis. European association for the Study of the Liver (EASL) has published a guideline for management of adenomas in adults, but similar guidance in pediatrics does not exist and must be extrapolated [20]. EASL guidelines suggest that resection is undertaken in all men and in the case of a proven beta catenin mutation because of the increased malignant potential. In women, the guideline recommends that resection is undertaken for lesions equal or greater than 5 cm and those which continue to increase in size. Lesions less than 5 cm in diameter should be reassessed at 1 year and annually thereafter. Lesions larger than this are at increased risk of bleeding. Actively bleeding lesions can be embolised and residual viable tumor then considered for resection [20].

Multiple hepatocellular adenomas may also occur. Underlying susceptibility should be investigated. The malignant risk and that of bleeding in patients with multiple HCAs are largely driven by the size of the largest tumor rather than the number of tumors. Options include resection of the largest HCA [21, 22]. Liver transplantation is recommended only in the case of underlying liver disease [23].

7.2.3 Hemangioma (Infantile and Congenital)

Hepatic hemangiomas (HH) are benign vascular tumors comprising 13% of all hepatic neoplasms [24].

Infantile hepatic hemangioma (HH) (Fig. 7.3) are the most common benign tumors of the liver in infancy [25]. Almost all infantile HH present before 6 months of age and mainly in the first 2 months of life. These tumors may be unifocal or multifocal and are Glut1 positive which differentiates them from congenital hemangiomas and other vascular tumors. Lymphatic markers are negative [26]. The tumors usually increase in size until 12 months of age followed by a gradual resolution more than 3–9 years [27]. These tumors may present with abdominal distension or a palpable mass and rarely with high output cardiac failure, anemia, failure to thrive and Kasabach–Merritt syndrome or liver failure, pulmonary hypertension, and respiratory distress. Infantile HH express 3-iodothyronine deiodinase that converts thyroid hormone to an inactive form thus hypothyroidism needs to be carefully and regularly screened for in these infants [28].

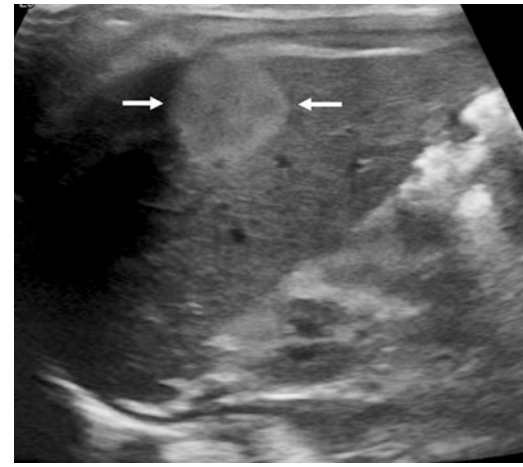

Fig. 7.3 Infantile hepatic hemangioma in a 6-month-old boy found incidentally on an ultrasound examination. There is a 15 × 14 mm echogenic well-circumscribed right liver lesion with characteristics of a hemangioma (arrows)

Congenital HH, in contrast, are fully formed at birth and either rapidly involuting by age 2, partially involuting, or non-involuting. These tumors are Glut1 and lymphatic markers negative [29]. They are predominantly unifocal and may have intra-tumoral calcification. Congenital HH may be diagnosed on antenatal scan or in the perinatal period when they may present with perinatal intra-tumoral bleeding (anemia, hypofibrinogenemia, thrombocytopenia).

On ultrasound, HH are well-circumscribed masses with large feeding and draining vessels.

Management of HH is observation only if asymptomatic and small/unifocal. It has been recommended to follow these lesions up to resolution [29]. For symptomatic or large/multifocal lesions, beta blockers are recommended as first line. In the event that additional management is required, steroids, alpha interferon, vincristine,

and cyclophosphamide have all been reported as treatments in case reports or series, but there is no consensus as to the efficacy [30].

Arterial embolization of a main feeding hepatic artery may decrease flow into the lesion. Likewise, surgical hepatic artery ligation or in some cases resection may be required. In the case of an unresectable lesion(s), liver transplant may occasionally be offered.

Hepatic hemangioendothelioma is best used as nomenclature for a separate entity, which occurs in older children and is intermediate between an HH and an angiosarcoma. Liver, lung, skin, and bone are the most commonly seen regions for these lesions [31].

7.2.4 Liver Cysts

As with any focal liver lesions, liver cysts may be single or multiple (Fig. 7.4). Solitary cysts may be congenital or acquired. The most common congenital cysts include simple cysts, mesenchymal hamartomata (which typically comprise both solid and cystic areas) (Fig. 7.5), intrahepatic choledochal cysts, ciliated hepatic foregut cysts, and biliary cysts [32]. Acquired may be infectious (pyogenic or amoebic abscess) parasitic (in particular hydatid), neoplastic (cystadenoma, sarcoma, teratoma), and biliary cysts (post-traumatic). Simple hepatic cysts may be antenatally detected and are often asymptomatic. Asymptomatic cysts do not require treatment and can be monitored using US. If they become symptomatic, for example with abdominal distension/pain, respiratory distress, and/or duodenal obstruction, if they enlarge significantly, or if imaging raises diagnostic uncertainty, they can be treated. Surgical excision is usually the best option but if this is not possible and there is no diagnostic concern about their nature then aspiration, sclerotherapy, or fenestration may also sometimes be considered.

7.2.5 Infective Cysts

Infective focal lesions in the liver include single or multiple pyogenic abscesses and parasitic cysts. Children may present with abdominal pain and fever. In the case of liver abscess, underlying pathology such as a ruptured appendix or immunodeficiency should be excluded. In particular, chronic granulomatous disease can present in this way [33]. Management of liver abscess is most commonly with prolonged intravenous antibiotics. Ideally, US-guided aspiration of pus will guide antimicrobial choice and confirm diagnosis.

Amoebiasis secondary to *Entamoeba histolytica* is most commonly found in the tropics and subtropics and can present with hepatic abscesses. Typically,

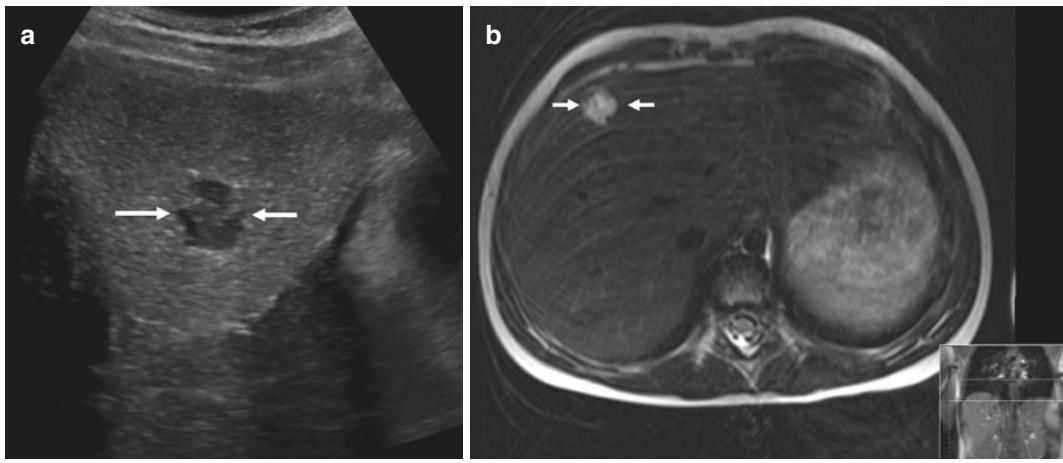

Fig. 7.4 Incidental finding in a 7-year-old girl on an ultrasound examination for abdominal pain, found to be a septated cystic structure. (**a**) Septate irregular hypoechoic lesion in the right lobe of the liver (arrows). (**b**) The MR imaging (T2 weighted sequence) confirms fluid content and the cystic nature of the lesion

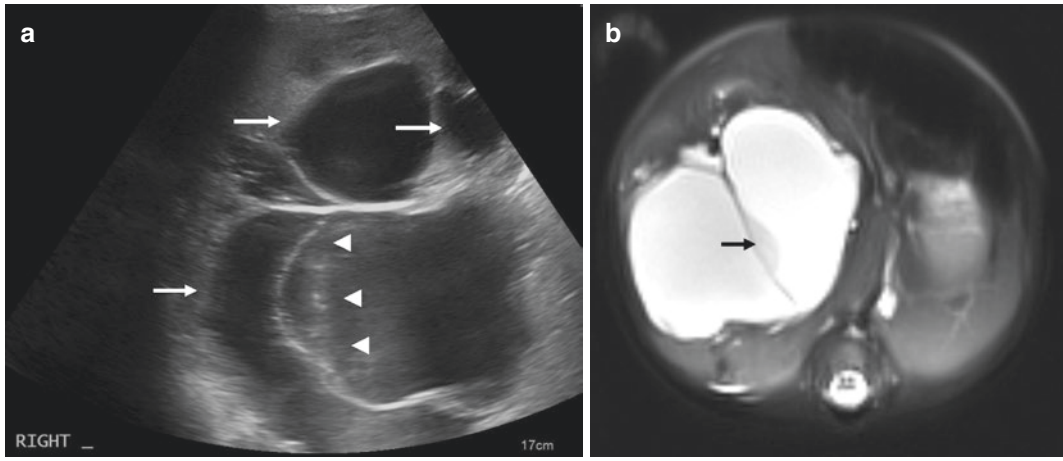

Fig. 7.5 A 7-month-old male infant with abdominal distension, found to have a mesenchymal hamartoma, which typically comprises both solid and cystic areas. (**a**) A lobulated cystic structure within the right liver lobe (arrows), with some more solid aspects (arrowheads). (**b**) A T2 weighted MR image showing the high signal cyst within the liver, and an intermediate signal of the solid component

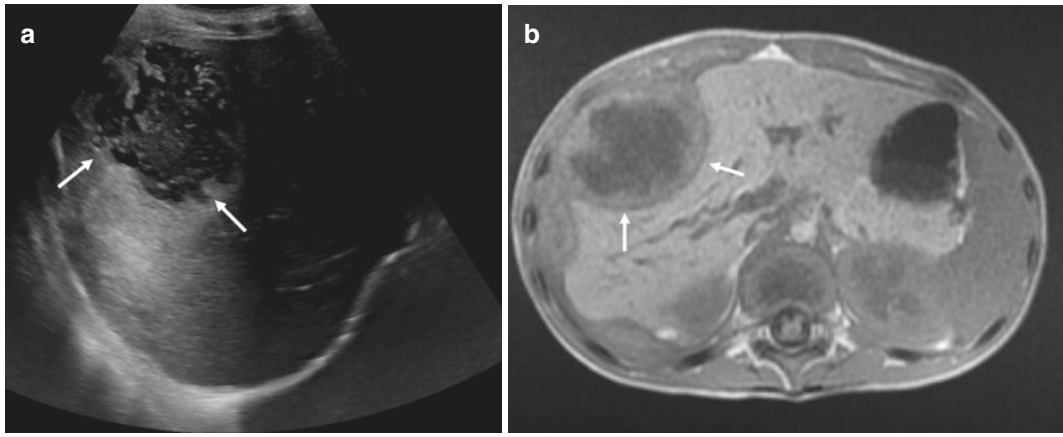

Fig. 7.6 A 11-year-old boy with a 4-month history of weight loss and fever, with an amoebic liver abscess. (**a**) A heterogeneous irregular lesion present in the right lobe of the liver (arrows), with posterior acoustic enhancement indicating a fluid collection with debris. (**b**) On the T1 weighted MR image, there is a well-demarcated mixed signal (arrows) lesion suggesting an abscess

a single abscess in the right lobe presenting with pyrexia, right upper quadrant pain. Less commonly nausea vomiting, diarrhea, and jaundice may be presenting features (Fig. 7.6). Aspiration may yield anchovy sauce-like pus. Treatment is usually with metronidazole with or without chloroquine for at least 2 weeks. A luminal amobicide, such as paromomycin, may also be given to eradicate gastrointestinal disease.

Hydatid disease is caused by the parasite *Echinococcus granulosus* (the dog tape worm) which can affect dogs who have been fed offal from infected live stock. The liver is the most frequent site for cyst formation. Children may present with liver enlargement, abdominal pain with nausea and vomiting, the development of portal hypertension, portal vein thrombosis, and biliary cirrhosis less common. Cysts may be single or multiple sometimes with internal daughter cysts and calcification present. Diagnosis can be made using serology and the detection of antibodies in blood. Definitive therapy is with complete cyst

removal though spillage of contents into the peritoneal cavity and anaphylaxis during surgery can occur. Small hydatid cysts may be treatment with mebendazlole and albendazole. Medical treatment pre-operatively may make extensive lesions cysts more amenable to surgery.

7.3 Biliary Cysts

Biliary cysts may be present in the context of cystic biliary atresia or in a post-Kasai operation patient who develops bile "pools or lakes" from ectatic bile ducts. Cholangitis is a particular concern in these patients. Biliary cysts may also be acquired from trauma. Rarely a cystoenterostomy may be required. In the case of cystic biliary atresia, a portoenterostomy is performed. Caroli disease is characterized by intrahepatic biliary cyst(s). Caroli syndrome manifests as multiple biliary cystic lesions in the presence of extrahepatic features, most commonly polycystic kidney disease and may be inherited in an autosomal dominant manner. In the case of diagnostic doubt between biliary and non-biliary cystic lesions, an HIDA nuclear medicine examination will distinguish whether or not the cyst contains bile.

7.4 Mesenchymal Hamartoma

Mesenchymal hamartoma is the second most common benign focal liver lesion. They usually present in infants and children less than 2 years with a large abdominal mass. Bleeding into the hamartoma or rupture may also be the presenting feature. The tumor is usually single, more often located in the right lobe and with both solid and cystic components. Management is generally full surgical resection, in part to confirm diagnosis as there is a possible malignant potential associated [34, 35].

7.4.1 Inflammatory Myofibroblastic Pseudotumor

This is a benign tumor which can arise anywhere in body. In the case of hepatobiliary involvement, fever, jaundice, and weight loss may be the presenting features [36]. There is a possibility of spontaneous regression, but recurrence has also been described. In the case that the lesion is symptomatic (the majority as the child will come to medical attention with symptoms as above), or if there is diagnostic uncertainty then surgical resection is considered. Local resection curative in most [37]. The histology is of spindle cell proliferation admixed with chronic inflammatory cell infiltrate or plasma cells, lymphocytes, and histiocytes. Anaplastic lymphoma kinase gene rearrangements noted in half; this is associated with localized disease at presentation and improve prognosis.

7.4.2 Calcified Lesions

Calcified lesions in the liver may be associated with antenatal infection or either antenatal or post-natal vascular accidents. Tumors such as teratomas or even hepatoblastomas may be partially calcified. Granulomatous disease such as sarcoid can rarely present with calcified lesions. The majority of calcified lesions in the liver do not need follow up.

7.5 Malignant Liver Lesions

7.5.1 Hepatoblastoma

Hepatocellular carcinoma (HCC) and hepatoblastoma (HB) account for 1% of all pediatric tumors. Incidence has been increasing possibly because of better survival of premature infants who have an increased risk of developing the tumor. The incidence of hepatoblastoma is between 0.5 and 1.5 per million population [38].

Hepatoblastoma occurs most commonly in the first 4 years of life with a median age at diagnosis of 18 months (Fig. 7.7). Hepatoblastoma can also present at birth or even rarely in utero. Characteristically the tumor is associated with an elevated α fetoprotein (AFP) in the blood. Unlike in HCC where there may be a modest rise in AFP, with hepatoblastoma the AFP is often >1,000,000 kIU/L. Risk factors include small birth weight

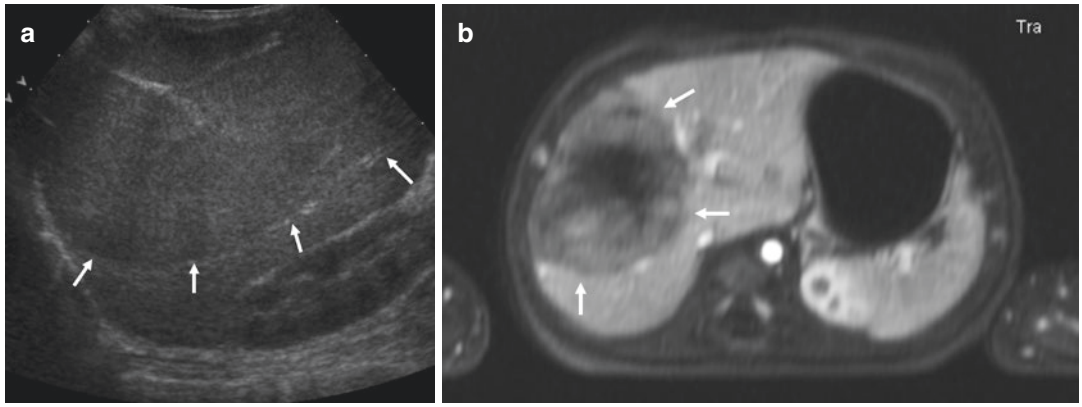

Fig. 7.7 A 1-year-old boy with an abdominal mass, presenting with a hepatoblastoma. (**a**) The ultrasound image demonstrates a focal large isoechoic liver mass (arrows), compressing surrounding liver parenchyma and displacing the right kidney. (**b**) The post-gadolinium T1-weighted MR image confirms a mixed signal large hepatoblastoma with patchy enhancement (arrows)

and prematurity in which case there the prognosis can be less favorable [39, 40]. Children with syndromes, such as Beckwith Wiedemann syndrome and Trisomy 18 [41], have an increased risk of developing HB, as well as those with a family history of FAP [42].

Children may present with abdominal pain and vomiting, failure to thrive, fever and more rarely jaundice, abdominal distention, or with an abdominal mass. Investigation will include some form of axial imaging following the initial US (CT or MR imaging) which delineates PRETEXT staging and on which a chemotherapy regime is based.

Regional international collaborations have different approaches to management with or without the use of neo-adjuvant chemotherapy prior to surgery (resection or transplant). The Pediatric Hepatic International Tumour Trial (PHITT) aims to resolve these differences and brings together the expertise of the European SIOPEL group, the Liver Tumour Committee of the Children's Oncology Group, USA (COG), and the Japanese Children's Cancer Group (JCCG).

Hepatoblastomas may be embryonal, mesenchymal, or mixed. Very well-differentiated fetal histology has the best prognosis with small cell undifferentiated the worst. Prognostic markers include age, AFP, and extrahepatic spread. For those children with low-risk disease, survival is 90% at 5 years though only 50% in those with high-risk disease [20].

7.5.2 Hepatocellular Carcinoma

Hepatocellular carcinoma is rarer than hepatoblastoma in children and tends to occur in an older age group (Fig. 7.8). An HCC may occur in the context of chronic liver disease such as Hepatitis B, metabolic disorders, intrahepatic cholestasis syndromes, or other cirrhosis [2]. Non-cirrhotic HCC can also occur and is less common than in adults. There has been some decrease in incidence of the tumor with the rise in Hepatitis B vaccination [43].

An HCC may present with abdominal pain and vomiting, jaundice, bleeding, or rupture of the tumor. An abdominal mass is often palpable at time of presentation with de novo tumors. AFP may be elevated but rarely to the extent of that in HB. It is important to screen for underlying liver disease. The optimal treatment is complete surgical resection if possible. Transplantation may be necessary but guidelines have been set (Milan criteria) as to when this is appropriate in adults. Often children may have mixed hepatocellular neoplasms and thus it is not clear to what extent

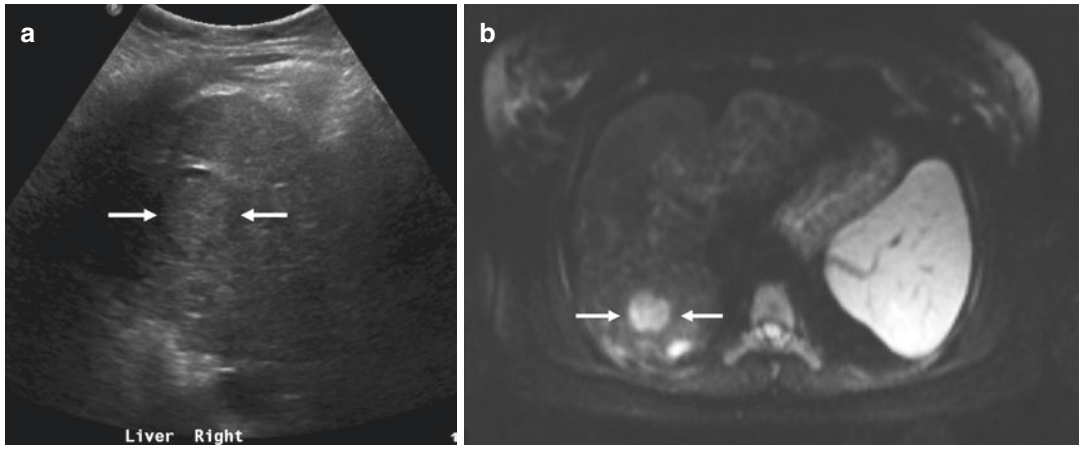

Fig. 7.8 A 12-year-old girl with chronic autoimmune liver disease presents with a "new" nodule on a routine ultrasound examination found to be a hepatocellular carcinoma, requiring a liver transplantation. (**a**) An isoechoic nodule in the mid aspect of the right liver lobe (arrows) with a halo, suggesting either a regenerative nodule of a hepatocellular carcinoma on the background of liver cirrhosis. (**b**) The MR image demonstrates the lesion (arrows) shows restricted diffusion on DWI, in keeping with a hepatocellular carcinoma

that these guidelines should extend to children. Some studies have looked at transplants in adults beyond the Milan criteria and reported good outcomes [44]. Thus, unless there is major vascular invasion or extrahepatic disease, children with HCC will more often be considered for liver transplantation, but transplantation usually has a very poor outcome in the presence of lung metastases [45].

Unfortunately, HCC is a relatively chemoresistant tumor though many new drugs are currently in clinical trials. The mainstay of management to date has been a combination of cisplatin and sorafenib. There is a 5-year survival reported of 70% with mortality largely due to recurrent disease.

7.5.3 Fibrolamellar Tumors

Fibrolamellar tumors are malignant neoplasms occurring mostly in adolescents and young adults and almost never under the age of 5 years. The median age at presentation is 21 years. Fibrolamellar tumors do not generally occur on the background of a cirrhotic liver. There may be an elevated AFP associated. By the time of presentation, these tumors are often large. In one series the average size at presentation was 12 cm [46]. Computed tomography imaging shows a large well-circumscribed lesion, which enhances strongly in both arterial and portal venous phases and isodense in delayed scans. A poorly enhancing central scar may sometimes be seen. Fibrolamellar tumors metastasize by lymphatic and blood. With full surgical resection, 5-year survival has been reported at 70%. Although liver transplant has been reported, outcomes have not been good for this tumor [47].

7.5.4 Transitional Tumors

Tumors in children may have mixed features of hepatoblastoma and hepatocellular carcinoma. This occurs more often in older children and AFP is usually elevated. Histologically these tumors are intermediate between a macro-trabecular variant HB and a trabecular HCC. Outcome is poorer for these transitional tumors than for HB. There is also a chemotherapy effect that may be seen so diagnostic biopsy taken before chemotherapy started is sometimes better able to distinguish tumor types than resection post chemotherapy.

7.5.5 Embryonal Sarcoma

Embryonal sarcomas comprise 5% of liver tumors in children. They most commonly occur between the ages of 6 and 10 years and in males, with a normal AFP. Several reports suggest that embryonal sarcomas may arise within mesenchymal hamartoma, an otherwise benign lesion. On US embryonal sarcomas are solid isoechoic demarcated tumors. On CT imaging, they are well-circumscribed hypoattenuating lesions with multiple enhancing septations. An enhancing pseudocapsule may be present. Metastases may be present at the time of presentation. Histologically these tumors have large areas of necrosis with areas of viable tumor. Characteristically stellate or spindle cells are loosely arranged in a myxoid matrix. Initial reports suggest that prognosis is poor [30]. Over the last two decades, a combination of chemotherapy, surgery, and transplantation has allowed a survival of 90% [36, 48].

7.5.6 Biliary Rhabdomyosarcoma

Biliary rhabdomyosarcoma is the most common cause of malignant biliary obstruction in children. Biliary rhabdomyosarcoma may affect any part of the extra or intrahepatic biliary tree including the gallbladder. The median age of presentation is 3 years and presenting features include jaundice and abdominal pain. Computed tomography imaging may show a dilated biliary tract with hypoattenuating tumor in the bile duct. Biopsy of the lesion may need to be via open surgery. Resection of the tumor may be possible using a hepatojejunostomy. Negative margins are very rarely achieved, however, and adjuvant chemotherapy/radiotherapy is required. The 5-year survival has been quantified as 66% (higher with metastases). Liver transplantation has been reported but radiotherapy may be an alternative [49].

7.5.7 Angiosarcoma

This is a highly malignant neoplasm occurring mostly in the older child with a poor prognosis. Resection may be an option, but metastases are frequently present at the time of diagnosis.

7.6 Conclusion

The approach to focal lesions in a child is first to determine benign versus malignancy. Benign lesions that are symptomatic or have malignant potential may also need an aggressive approach. The age of the child will suggest the differential diagnosis with hepatoblastoma and infantile hemangioma most common under the age of 5 years. Over 5 years, hepatocellular carcinoma, hepatic adenoma, focal nodular hyperplasia are more likely. The step-wise approach to diagnosis will include blood biomarkers such as AFP, imaging, and lesional histology.

References

1. Finegold MJ. Tumors of the liver. Semin Liver Dis. 1994;14(3):270–81.
2. Khanna R, Verma SK. Pediatric hepatocellular carcinoma. World J Gastroenterol. 2018;24(35):3980–99.
3. Edmondson HA, Henderson B, Benton B. Liver-cell adenomas associated with use of oral contraceptives. N Engl J Med. 1976;294(9):470–2.
4. Calderaro J, Labrune P, Morcrette G, Rebouissou S, Franco D, Prevot S, et al. Molecular characterization of hepatocellular adenomas developed in patients with glycogen storage disease type I. J Hepatol. 2013;58(2):350–7.
5. Witters P, Maleux G, George C, Delcroix M, Hoffman I, Gewillig M, et al. Congenital veno-venous malformations of the liver: widely variable clinical presentations. J Gastroenterol Hepatol. 2008;23(8 Pt 2):e390–4.
6. Towbin AJ, Luo GG, Yin H, Mo JQ. Focal nodular hyperplasia in children, adolescents, and young adults. Pediatr Radiol. 2011;41(3):341–9.
7. Valentino PL, Ling SC, Ng VL, John P, Bonasoni P, Castro DA, et al. The role of diagnostic imaging and liver biopsy in the diagnosis of focal nodular hyperplasia in children. Liver Int. 2014;34(2):227–34.
8. Engelhardt EM, Trout AT, Sheridan RM, Veldtman GR, Dillman JR. Focal liver lesions following Fontan palliation of single ventricle physiology: a radiology-pathology case series. Congenit Heart Dis. 2019;14:380–8.
9. Rela M, Reddy MS. Liver tumours in children. In: Guandalini S, Dhawan A, Branski D, editors. Textbook of pediatric gastroenterology, hepatology and nutrition. Cham: Springer; 2016.

10. Mathieu D, Kobeiter H, Maison P, Rahmouni A, Cherqui D, Zafrani ES, et al. Oral contraceptive use and focal nodular hyperplasia of the liver. Gastroenterology. 2000;118(3):560–4.
11. Dokmak S, Paradis V, Vilgrain V, Sauvanet A, Farges O, Valla D, et al. A single-center surgical experience of 122 patients with single and multiple hepatocellular adenomas. Gastroenterology. 2009;137(5):1698–705.
12. Oliveira S, Samba AK, Towbin AJ, Gupta A, Geller JI, Nathan JD, et al. Incidental inflammatory adenoma with beta-catenin activation in the setting of paediatric NASH. Pediatr Obes. 2018;13(1):70–3.
13. Bluteau O, Jeannot E, Bioulac-Sage P, Marques JM, Blanc JF, Bui H, et al. Bi-allelic inactivation of TCF1 in hepatic adenomas. Nat Genet. 2002;32(2):312–5.
14. Monga SP. Hepatic adenomas: presumed innocent until proven to be beta-catenin mutated. Hepatology. 2006;43(3):401–4.
15. Pilati C, Letouze E, Nault JC, Imbeaud S, Boulai A, Calderaro J, et al. Genomic profiling of hepatocellular adenomas reveals recurrent FRK-activating mutations and the mechanisms of malignant transformation. Cancer Cell. 2014;25(4):428–41.
16. Bacq Y, Jacquemin E, Balabaud C, Jeannot E, Scotto B, Branchereau S, et al. Familial liver adenomatosis associated with hepatocyte nuclear factor 1alpha inactivation. Gastroenterology. 2003;125(5):1470–5.
17. Reznik Y, Dao T, Coutant R, Chiche L, Jeannot E, Clauin S, et al. Hepatocyte nuclear factor-1 alpha gene inactivation: cosegregation between liver adenomatosis and diabetes phenotypes in two maturity-onset diabetes of the young (MODY)3 families. J Clin Endocrinol Metab. 2004;89(3):1476–80.
18. Nault JC, Paradis V, Cherqui D, Vilgrain V, Zucman-Rossi J. Molecular classification of hepatocellular adenoma in clinical practice. J Hepatol. 2017;67(5):1074–83.
19. Bioulac-Sage P, Rebouissou S, Sa Cunha A, Jeannot E, Lepreux S, Blanc JF, et al. Clinical, morphologic, and molecular features defining so-called telangiectatic focal nodular hyperplasias of the liver. Gastroenterology. 2005;128(5):1211–8.
20. European Association for the Study of the Liver. EASL clinical practice guidelines on the management of benign liver tumours. J Hepatol. 2016;65(2):386–98.
21. Bioulac-Sage P, Laumonier H, Couchy G, Le Bail B, Sa Cunha A, Rullier A, et al. Hepatocellular adenoma management and phenotypic classification: the Bordeaux experience. Hepatology. 2009;50(2):481–9.
22. Vetelainen R, Erdogan D, de Graaf W, ten Kate F, Jansen PL, Gouma DJ, et al. Liver adenomatosis: reevaluation of aetiology and management. Liver Int. 2008;28(4):499–508.
23. Wellen JR, Anderson CD, Doyle M, Shenoy S, Nadler M, Turmelle Y, et al. The role of liver transplantation for hepatic adenomatosis in the pediatric population: case report and review of the literature. Pediatr Transplant. 2010;14(3):E16–9.
24. Weinberg AG, Finegold MJ. Primary hepatic tumors of childhood. Hum Pathol. 1983;14(6):512–37.
25. Meyers RL. Tumors of the liver in children. Surg Oncol. 2007;16(3):195–203.
26. Burrows PE, Dubois J, Kassarjian A. Pediatric hepatic vascular anomalies. Pediatr Radiol. 2001;31(8):533–45.
27. Kulungowski AM, Alomari AI, Chawla A, Christison-Lagay ER, Fishman SJ. Lessons from a liver hemangioma registry: subtype classification. J Pediatr Surg. 2012;47(1):165–70.
28. Huang SA, Tu HM, Harney JW, Venihaki M, Butte AJ, Kozakewich HP, et al. Severe hypothyroidism caused by type 3 iodothyronine deiodinase in infantile hemangiomas. N Engl J Med. 2000;343(3):185–9.
29. Iacobas I, Phung TL, Adams DM, Trenor CC 3rd, Blei F, Fishman DS, et al. Guidance document for hepatic hemangioma (infantile and congenital) evaluation and monitoring. J Pediatr. 2018;203:294–300.e2.
30. Leaute-Labreze C, Hoeger P, Mazereeuw-Hautier J, Guibaud L, Baselga E, Posiunas G, et al. A randomized, controlled trial of oral propranolol in infantile hemangioma. N Engl J Med. 2015;372(8):735–46.
31. Lau K, Massad M, Pollak C, Rubin C, Yeh J, Wang J, et al. Clinical patterns and outcome in epithelioid hemangioendothelioma with or without pulmonary involvement: insights from an internet registry in the study of a rare cancer. Chest. 2011;140(5):1312–8.
32. Rogers TN, Woodley H, Ramsden W, Wyatt JI, Stringer MD. Solitary liver cysts in children: not always so simple. J Pediatr Surg. 2007;42(2):333–9.
33. Marciano BE, Spalding C, Fitzgerald A, Mann D, Brown T, Osgood S, et al. Common severe infections in chronic granulomatous disease. Clin Infect Dis. 2015;60(8):1176–83.
34. Ramanujam TM, Ramesh JC, Goh DW, Wong KT, Ariffin WA, Kumar G, et al. Malignant transformation of mesenchymal hamartoma of the liver: case report and review of the literature. J Pediatr Surg. 1999;34(11):1684–6.
35. Koganti SB, Thumma VM, Nagari B. Mesenchymal hamartoma of the liver: complete excision always necessary. Case Rep Surg. 2017;2017:8314102.
36. Walther A, Geller J, Coots A, Towbin A, Nathan J, Alonso M, et al. Multimodal therapy including liver transplantation for hepatic undifferentiated embryonal sarcoma. Liver Transpl. 2014;20(2):191–9.
37. Nagarajan S, Jayabose S, McBride W, Prasadh I, Tanjavur V, Marvin MR, et al. Inflammatory myofibroblastic tumor of the liver in children. J Pediatr Gastroenterol Nutr. 2013;57(3):277–80.
38. Spector LG, Birch J. The epidemiology of hepatoblastoma. Pediatr Blood Cancer. 2012;59(5):776–9.
39. Paquette K, Coltin H, Boivin A, Amre D, Nuyt AM, Luu TM. Cancer risk in children and young adults born preterm: A systematic review and meta-analysis. PLoS One. 2019;14(1):e0210366.

40. Ikeda K, Terashima M, Kawamura H, Takiyama I, Koeda K, Takagane A, et al. Pharmacokinetics of cisplatin in combined cisplatin and 5-fluorouracil therapy: a comparative study of three different schedules of cisplatin administration. Jpn J Clin Oncol. 1998;28(3):168–75.
41. Farmakis SG, Barnes AM, Carey JC, Braddock SR. Solid tumor screening recommendations in trisomy 18. Am J Med Genet A. 2019;179(3):455–66.
42. Zhang L, Jin Y, Zheng K, Wang H, Yang S, Lv C, et al. Whole-genome sequencing identifies a novel variation of WAS gene coordinating with heterozygous germline mutation of APC to enhance hepatoblastoma oncogenesis. Front Genet. 2018;9:668.
43. Lin CL, Kao JH. Review article: the prevention of hepatitis B-related hepatocellular carcinoma. Aliment Pharmacol Ther. 2018;48(1):5–14.
44. Xu X, Lu D, Ling Q, Wei X, Wu J, Zhou L, et al. Liver transplantation for hepatocellular carcinoma beyond the Milan criteria. Gut. 2016;65(6):1035–41.
45. Ikeda M, Ueda T, Shiba T. Reconstruction after total gastrectomy by the interposition of a double jejunal pouch using a double stapling technique. Br J Surg. 1998;85(3):398–402.
46. Schmid I, Haberle B, Albert MH, Corbacioglu S, Frohlich B, Graf N, et al. Sorafenib and cisplatin/doxorubicin (PLADO) in pediatric hepatocellular carcinoma. Pediatr Blood Cancer. 2012;58(4):539–44.
47. Kassahun WT. Contemporary management of fibrolamellar hepatocellular carcinoma: diagnosis, treatment, outcome, prognostic factors, and recent developments. World J Surg Oncol. 2016;14(1):151.
48. Ismail H, Dembowska-Baginska B, Broniszczak D, Kalicinski P, Maruszewski P, Kluge P, et al. Treatment of undifferentiated embryonal sarcoma of the liver in children—single center experience. J Pediatr Surg. 2013;48(11):2202–6.
49. Perruccio K, Cecinati V, Scagnellato A, Provenzi M, Milano GM, Basso E, et al. Biliary tract rhabdomyosarcoma: a report from the Soft Tissue Sarcoma Committee of the Associazione Italiana Ematologia Oncologia Pediatrica. Tumori. 2018;104(3):232–7.

8 Contrast-Enhanced Ultrasound of Pediatric Focal Liver Lesions

Maciej Piskunowicz, Cheng Fang, Annamaria Deganello, Maria E. Sellars, and Paul S. Sidhu

8.1 Introduction

Ultrasound (US) is usually the first-line investigation for abdominal symptoms, with any focal liver lesion (FLL) likely to be initially encountered with this US investigation, both in adults and children. Ultrasound is particularly well suited for the pediatric population, with less difficult abdominal habitus than an adult and is often used in many clinical settings in the child. Furthermore, US has many other advantages over other imaging methods in the child; there is no ionizing radiation, no need for any sedation or iodinated/gadolinium-based contrast agents, all potentially detrimental to the health of the child [1–4].

Traditionally, an US examination has been limited by the lack of any suitable contrast agents, but with the advent of microbubble ultrasound contrast agents (UCA), this has changed. Ultrasound contrast agents are gas-filled microbubbles with a stable shell, the most commonly used is SonoVue™ (Bracco SpA, Milan), which consists of a phospholipid shell filled with an inert gas, sulfur hexafluoride. Microbubble UCAs have an excellent safety profile with reported incidence of severe adverse reactions around 0.0086% in adults, with reports now indicating a similar reaction rate in children [5, 6]. These UCAs have been extensively used in the evaluation of focal liver lesions (FLLs) in adults for a number of years in European and Asian countries, with success, proving to be accurate and cost-effective [7–9]. The more recent approval by the Food and Drug Administration (FDA) in the United States for both adult and pediatric FLL assessment is the first time there has been a license for the intravenous use of UCA in children [10]. Despite this approval, there are few reports in the literature of the use of UCA in the assessment of FLL in children, but this may reflect the recent endorsement, and the cautious nature of the examining physician, relying on more established imaging methods for the assessment of an FLL in the child. The small number of reports originate from Europe, where the UCAs have been used off-label, but established their usefulness, safety, and accuracy in children [6, 11]. The registry of CEUS use in pediatric practice initiated by the European Federation and Society of Ultrasound in Medicine and Biology (EFSUMB) provides a platform for data collection of pediatric CEUS examinations performed for any indication in institutions across Europe and in time to develop a body of evidence for future evidence-based recommendations [12].

M. Piskunowicz (✉)
Department of Radiology, Medical University of Gdańsk, Gdańsk, Poland

C. Fang · A. Deganello · M. E. Sellars · P. S. Sidhu
Department of Radiology, King's College Hospital, London, UK
e-mail: chengfang@nhs.net; adeganello@nhs.net; maria.sellars@nhs.net

P. S. Sidhu et al. (eds.), *Contrast-Enhanced Ultrasound in Pediatric Imaging*,
https://doi.org/10.1007/978-3-030-49691-3_8

The aim of this chapter is to describe the use of CEUS in characterizing benign and malignant liver tumors in children.

8.2 Technical Aspects for Liver CEUS Imaging

Contrast-enhanced ultrasound (CEUS) can be used as an alternative imaging modality to magnetic resonance (MR) or computed tomography (CT) imaging for children with an FLL. The individual vascularization pattern of FLL makes CEUS a very specific and sensitive tool for detection and accurate characterization of any FLL. A CEUS examination may be performed in the clinic as well at the patient's bedside as an extension of the regular US examination. It can shorten the time for the patient and the family to obtain the final diagnosis and reduces the overall costs of diagnostic imaging [6]. In the pediatric population, the biggest benefits of using CEUS are in children with a single FLL and with a previous cancer history or comorbidity of another systemic disease, particularly with underlying chronic liver disease; confirmation of a benign lesion can be immediate.

The procedure for a CEUS examination in the child is no different from that in an adult, with the younger child usually having had placement of the intravenous cannula remote from the US examination room, placed by a pediatric nurse or physician.

With the US examination, the operator must optimize the grayscale US images to allow ideal viewing of the lesion, preferably in the center of the screen, moving along the plane of the transducer (usually longitudinal) in order to maintain lesion visualization throughout the examination. The intravenous dose of SonoVue™ (Bracco SpA, Milan) for liver imaging, the most commonly used UCA, as recommended by the manufacturer is 0.03 mL/kg. In practice, dosage of 0.1 mL/year of age has also been used [13]. It is practicable and safe to administer more than one dose during any CEUS examination, with attention given to the dissipation of the UCA before a second examination is performed, usually a minimum of 10 min [14]. In addition, the dose must be adjusted to the type of US scanner and transducer used. The arrival time of the UCA is dependent on the venous site of administration (central vs. peripheral vein), heart rate, and the volume of the circulating blood. In the youngest children, the arrival time is usually less than 10 s. The examination must be performed using contrast specific low mechanical index (MI) imaging, normally defined as an MI < 0.1. For investigating sub-capsular lesions, a linear higher frequency transducer may be used to obtain better spatial resolution; the MI can be increased to 0.12–0.16 in these cases, with a higher dose of the UCA, often needed. The US beam focus should be positioned below the examined lesion. Localizing deep lesions in the cirrhotic liver or liver overloaded with iron can be challenging due to reduced beam penetration through the liver parenchyma. Prolonged recording of the late portal venous phase up to 5 min with intermittent imaging of the lesion is recommended to elicit washout while not causing excessive microbubble disruption [15]. This is particularly important in case of suspicion of hepatocellular carcinoma (HCC), which often shows mild and late wash out.

8.3 Focal Liver Lesions

A focal liver lesion is often encountered in the adult population, often benign in the context of a patient referred from the community physician, where the majority are benign hemangioma, focal fatty sparing or infiltration, or the rarer benign hepatic adenoma or focal nodular hyperplasia. Rarely a newly encountered FLL on an initial US examination is malignant. Referral form any other source, for example, hospital-based oncology or hepatitis clinics will yield a greater number of FLL that are malignant [16, 17]. The same principles are likely to apply to the pediatric population, with any underlying chronic liver disease predisposing to the development of FLL, both benign and malignant [18].

Furthermore, the increasing prevalence of hepatic steatosis, both in the adult and child, renders the occurrence of areas of focal fatty sparing and infiltration increasingly endemic,

posing difficulty with a clear US diagnosis, causing both parental and clinical anxiety. Often further imaging with computed tomography (CT) or magnetic resonance (MR) imaging is needed to establish the diagnosis; the use of CEUS has the potential to resolve this dilemma and reduce the costs associated with this additional imaging.

The characteristics of the numerous FLL encountered in pediatric practice are discussed later, and Table 8.1 details the spectrum of FLL seen in the child with underlying chronic liver disease. Where the normal practice is the undergo US surveillance for the development of any new FLL in the child with chronic liver disease, using CEUS is particularly cost-effective [6], and this has also been demonstrated in adult patients [19].

Table 8.1 Spectrum of focal liver lesions in the pediatric patient with a normal underlying liver and a cirrhotic underlying liver

Age	Benign	Malignant
Normal liver		
<5 years	Hemangioendothelioma	Hepatoblastoma
	Mesenchymal hamartoma	Metastasis
>5 years	Hepatic adenoma	Hepatocellular carcinoma
	Focal nodular hyperplasia	Undifferentiated embryonal sarcoma
	Hemangioma	Metastasis/ lymphoma
Chronic disease	**Benign**	**Malignant**
Underlying cirrhotic liver		
Glycogen storage disease	Adenoma	
Tyrosinemia	Regenerative nodules	Hepatocellular carcinoma
Wilson's disease	Regenerative nodules	
Alpha 1 antitrypsin deficiency	Regenerative nodules	
Progressive familiar intrahepatic cholestasis	Regenerative nodules	Hepatocellular carcinoma
Biliary atresia	Regenerative nodules	Hepatocellular carcinoma

The practice of assessing FLL in the child is based on the principles well established in adult clinical practice and detailed in guidelines issued by EFSUMB, following the different enhancement patterns during the arterial and portal venous phase, paying particular attention to the pattern of arterial enhancement and the delayed washout of the FLL. It is good practice to base the interpretation of the findings on the late portal venous enhancement pattern; washout is likely malignant and retention of the UCA indicates a benign entity, with a pattern of arterial enhancement diagnostic (Fig. 8.1) [20].

8.4 Benign Focal Liver Lesions

Grayscale US with color Doppler imaging is the method of choice for the examination of children suspected of having a benign FLL. Most benign FLL can be detected on the grayscale US. The application of color Doppler US has benefits, but is limited by the sensitivity of the technique, being operator dependent and is not reproducible to give any particular diagnostic pattern of vessels depicted. However, the use of CEUS significantly increases sensitivity and specificity in benign lesions, particularly if the underlying grayscale US appearances are atypical, for example, a low reflective FLL in a fatty liver that is a hemangioma. It allows establishing the diagnosis and completing the diagnostic pathway, avoiding additional MR or CT imaging.

8.4.1 Focal Fatty Infiltration and Focal Fatty Sparing

A growing number of obese older children are found to have non-alcoholic fatty liver disease (NAFLD). This NAFLD is linked to the most common liver parenchyma changes seen in both adults and children, such as focal fatty infiltration (FFI) and focal fatty sparing (FFS) which are often detected during a routine grayscale US liver examination (Figs. 8.2 and 8.3). The majority of these fatty change lesions occur at typical locations (adjacent to the gallbladder fossa, around the porta

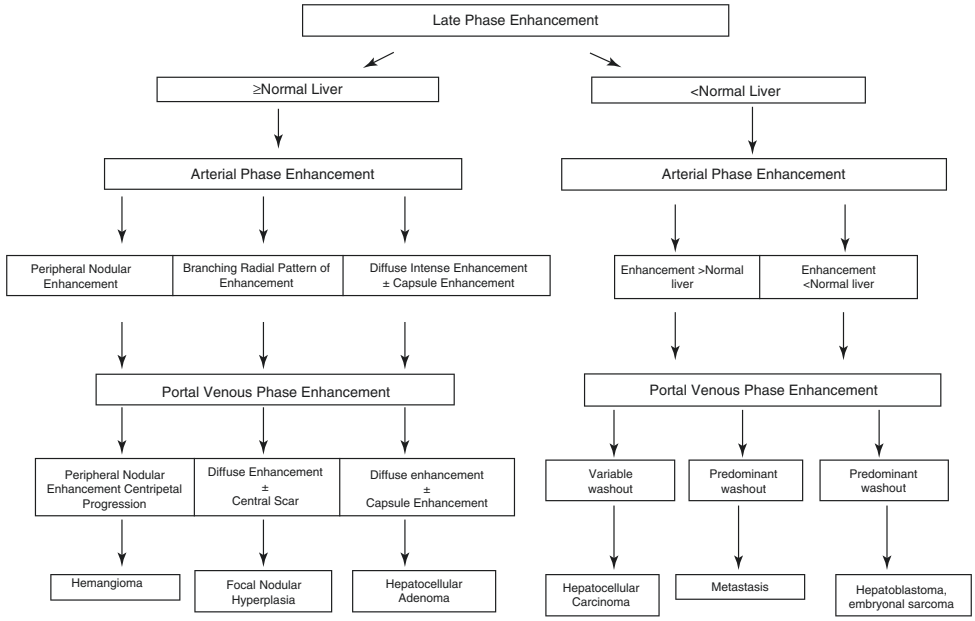

Fig. 8.1 A flow chart of the diagnostic interpretation of the vascular patterns of enhancement of focal liver lesions in a contrast-enhanced ultrasound examination, with interpretation working backward from the washout characteristics in the late portal venous phase

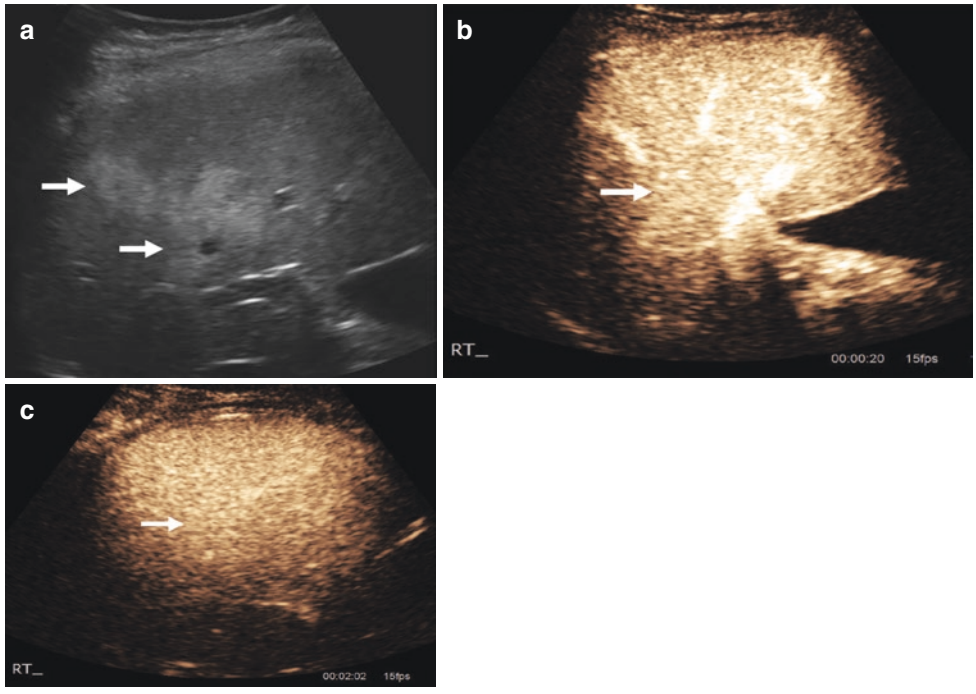

Fig. 8.2 Incidental finding of focal fat infiltration in an 11-year-old male, confirmed on magnetic resonance and computed tomography imaging. (**a**) Grayscale ultrasound shows a geographical pattern of hyperechoic abnormality (arrows) within the right liver. (**b**) On the arterial at 20 s, there is no hyper-or hypo-enhancement (arrow). (**c**) On the late portal venous phases at 122 s on the contrast-enhanced ultrasound images, focal fat infiltration shows iso-enhancement to the background liver (arrow)

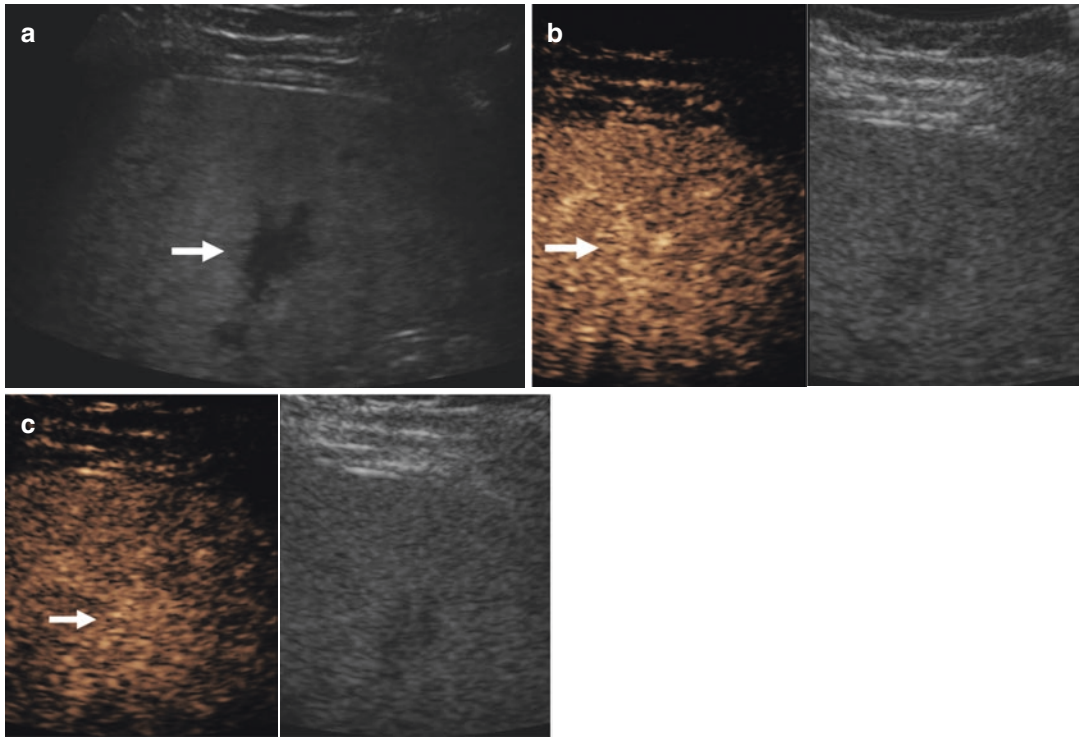

Fig. 8.3 Area of focal fat sparing in a 17-year-old obese male. This area "disappeared" on a 2-year follow up ultrasound examination. (**a**) Grayscale ultrasound shows a geographical area of hypoechoic abnormality (arrow) within the right liver. (**b**) On the arterial at 30 s there is no hyper-or hypo-enhancement (arrow). (**c**) On the portal venous phases at 75 s on the contrast-enhanced ultrasound images, focal fat sparing shows iso-enhancement to the background liver (arrow)

hepatis or falciform ligament) [21]. On grayscale US, the areas affected by FFS and FFI have geographical borders without the mass effect and distortion of the vessels. The echogenicity is increased in FFI and decreased in FFS. However, these FLL can mimic other benign or malignant lesions, with a resulting diagnostic dilemma on grayscale US, needing to proceed to further imaging with CT or MR imaging, but this is often not helpful. With a CEUS examination, an area of FFI and FFS cannot be distinguished from normal liver parenchyma, and on all vascular phases, have the same pattern of enhancement as the normal liver parenchyma, establishing the diagnosis. In particular, there is no washout of the UCA from the lesion [22].

8.4.2 Hemangioma

A hemangioma is a vascular malformation and the commonest incidentally discovered FLL in children [23]. The three subtypes of infantile hepatic hemangioma (IHH)—focal, multifocal, and diffuse can be seen during the first months of life. On grayscale US, an IHH presents as a well-defined, rounded, usually hypoechoic lesion. The smaller IHH is more homogeneous, whereas a large focal IHH can be inhomogeneous due to the presence of calcifications, necrosis, hemorrhage, and prominent intralesional arteries and veins. On a CEUS examination, the IHH demonstrates peripheral nodular arterial phase enhancement with centripetal progression during the portal phase and complete or near-complete fill-in in the late portal venous phase [13, 24, 25]. The nodules are hyper-enhancing comparing to the liver parenchyma during all phases. In older children, an incidentally discovered hemangioma is likely hyperechoic on grayscale US with the same enhancement pattern on CEUS as with adults. The CEUS assessment of small hyper vascularized hemangiomas can be challenging, as they

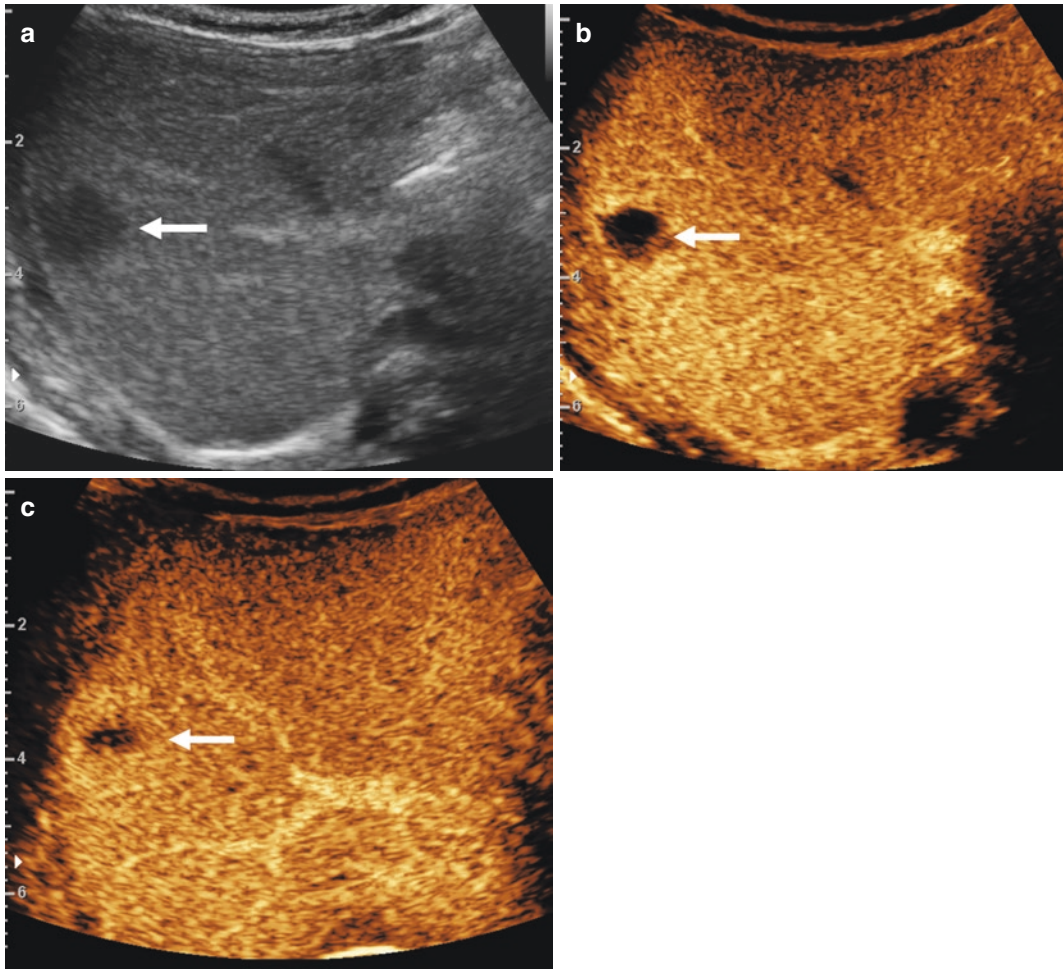

Fig. 8.4 Focal infantile hepatic hemangioma (IHH) in a 4-month-old child, which resolved on follow up ultrasound over 2 years. (**a**) Grayscale ultrasound shows focal hypoechoic subcapsular lesion (arrow) within the right liver. (**b**) The IHH shows peripheral nodular enhancement on the arterial phase at 19 s (arrow). (**c**) There is centripetal near complete filling in of contrast during delayed venous phase at 147 s (arrow)

can demonstrate rapid enhancement with a centripetal pattern of filling, which can be often only observed retrospectively when reviewing the cine loops frame by frame (Fig. 8.4).

8.4.3 Focal Nodular Hyperplasia

Focal nodular hyperplasia (FNH) is a form of a regenerative lesion composed of hyperplastic hepatocytes, malformed biliary drainage channels, which are not connected to the bile ducts and sinusoidal capillaries supplied by the hepatic artery with drainage to the hepatic veins without a portal venous supply [26]. An FNH has increased prevalence in long-term survivors after childhood cancers such as Wilms' tumor, neuroblastoma, germ cell tumor, and sarcomas due to the use of chemotherapy drugs, which induce hepatic vascular endothelial injury [27]. In these children, with a previous cancer history, the appearance of a new lesion in the liver is particularly concerning, as the FLL could represent disease recurrence or metastatic disease. On grayscale US, the detection of a smaller FNH (<2 cm) can be difficult because the FNH is usu-

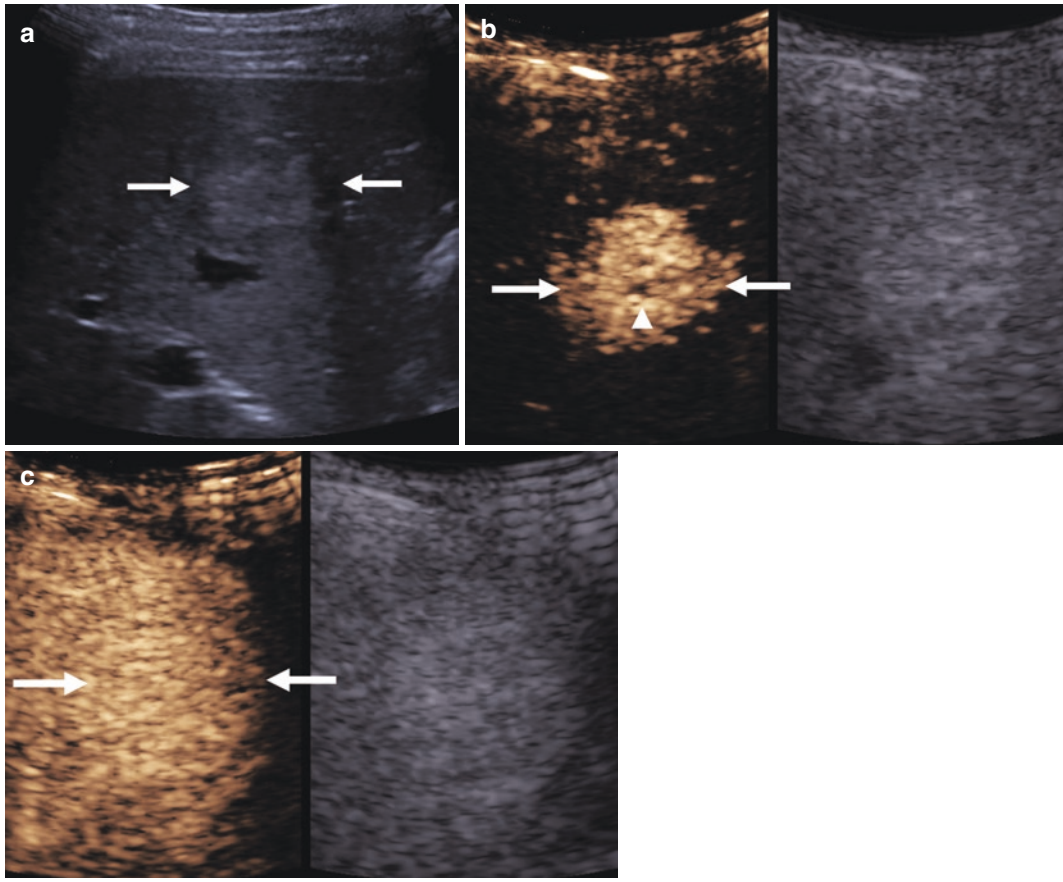

Fig. 8.5 Focal nodular hyperplasia (FHN) in a 7-year-old female. (**a**) Grayscale ultrasound shows a focal hyperechoic lesion (arrow) within the right liver. (**b**) On contrast enhancement ultrasound, arterial phase, the FNH demonstrates a spoke wheel enhancement pattern (arrows) with a small focal central "scar" (arrowhead). (**c**) The FNH remains isoenhancing (arrows) compared to the background liver parenchyma on the late portal venous phase at 180 s

ally isoechoic to the surrounding liver parenchyma. A larger lesion has a rounded contour and can be slightly hyperechoic or hypoechoic to the background liver, with areas of heterogeneous echotexture. Color Doppler US can demonstrate a central feeding artery with markedly increased blood flow [28]. Additional newer options for vessel detection (B-flow, superb microvascular imaging) as well as power Doppler US demonstrate a spoke-wheel pattern of vascularization in most of the larger lesions. This can be crucial for establishing the final diagnosis without the need for any further imaging examinations. On CEUS, an FNH shows early centrifugal filling and rapidly becomes homogeneously hyperenhancing (the spoke-wheel pattern usually can be seen on the cine loop frame by frame) on the late arterial phase [29]. During the early portal phase, an FNH is hyperenhancing compared to the liver parenchyma (Fig. 8.5). During the late portal venous phase, an FNH will sustain enhancement for a long time, therefore appearing slightly hyperenhancing or isoenhancing to the liver parenchyma. The central vascular scar can be visible in the portal and late portal venous phases as a linear/stellate filling defect in the middle of the lesion [29].

8.4.4 Hepatic Adenoma

A hepatic adenoma (HA) in a child is associated with underlying disorders such as glycogen storage disease, obesity, diabetes mellitus, in teenage

girls on the oral contraceptive pill, and young boys is associated with anabolic steroid ingestion [28]. On grayscale US, an HA is a round-shaped lesion with a well-demarcated edge, separated from the adjacent liver parenchyma. An HA can be hyperechoic due to lipid content or hemorrhage (can occur with larger lesions) or hypoechoic if the background liver parenchyma is fatty. On color Doppler US, an HA shows tortuous vessels with increased vascularity. On CEUS, an HA has a rapid, intense enhancement with centripetal or mixed centripetal/centrifugal pattern on the arterial phase imaging [29]. During the early portal venous phase, an HA can remain hyperenhancing or slowly becoming isoenhancing to liver parenchyma. During the late portal venous phase, the HA is isoenhancing (Fig. 8.6). The hemorrhagic regions within the lesion do not enhance in any phase. Hypoenhancement during the portal venous and late portal venous phase is rare and dependent on the type of HA classification [30], and this may then be misinterpreted as a malignant FLL [31]. In these cases, a short interval follow-up or tissue diagnosis is required

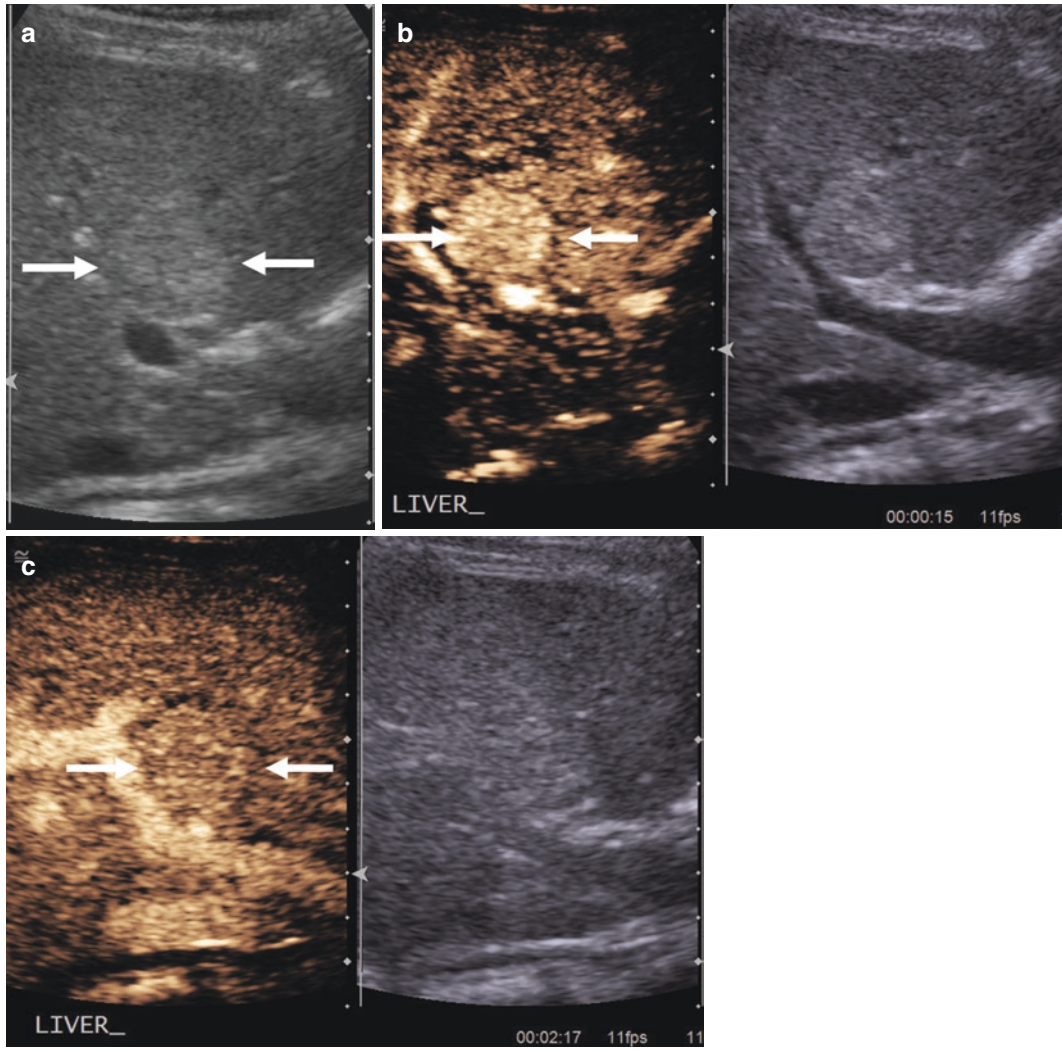

Fig. 8.6 Hepatic adenoma (HA) in a 16-year-old female. (**a**) Grayscale ultrasound image shows a focal hyperechoic lesion (arrows) within the right liver. (**b**) On contrast enhancement ultrasound, the lesion shows a mixed pattern of arterial hyperenhancement at 15 s (arrows), in a centrifugal direction. (**c**) The lesion appears iso-enhancing (arrows) compared to the background liver parenchyma on the late portal venous phase at 137 s

depending on the level of clinical suspicion. The HA does not show a central scar which can be seen in an FNH.

8.4.5 Cystic Lesions

Simple hepatic cysts on the grayscale US are well-circumscribed, round or ovoid lesions. The walls do not show thickening, and when larger demonstrate posterior acoustic enhancement, a classical sign of a cystic lesion. Cysts may contain intra-cystic debris; septations can pose a diagnostic dilemma by mimicking a solid component of an intramural solid nodule. On CEUS, benign cystic lesions do not show any internal enhancement, with very thin enhancing septations noted, and with no wall enhancement (Fig. 8.7). If on the CEUS examination, thickened septal, intramural, or mural enhancement is visible (Fig. 8.8), then a malignant cystic lesion is possible [32].

8.4.6 Hepatic Abscess

In developed countries, the most common hepatic abscess is bacterial in origin, whereas in developing countries, parasites are the most common pathogen, usually *Entamoeba histolytica* or *Echinococcus* spp. On grayscale US, bacterial abscesses have irregular edges, most are hypoechoic

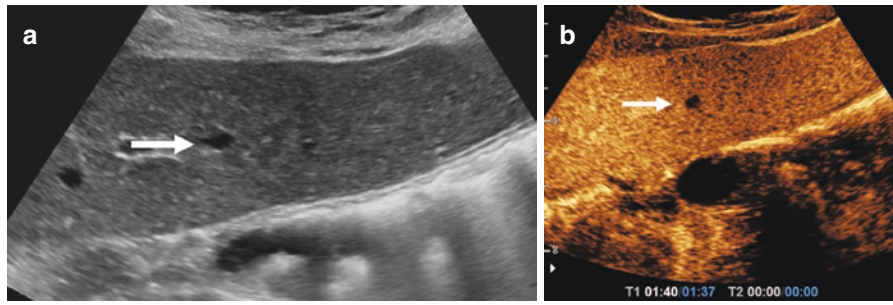

Fig. 8.7 Hepatic cyst in a 12-year-old male with liver transplantation due to biliary atresia. (**a**) Grayscale ultrasound shows a focal anechoic lesion within the left lobe of the liver, with some posterior acoustic enhancement. (**b**) On contrast enhancement ultrasound, the lesion is non-enhancing (arrow) in the late portal venous phase at 97 s

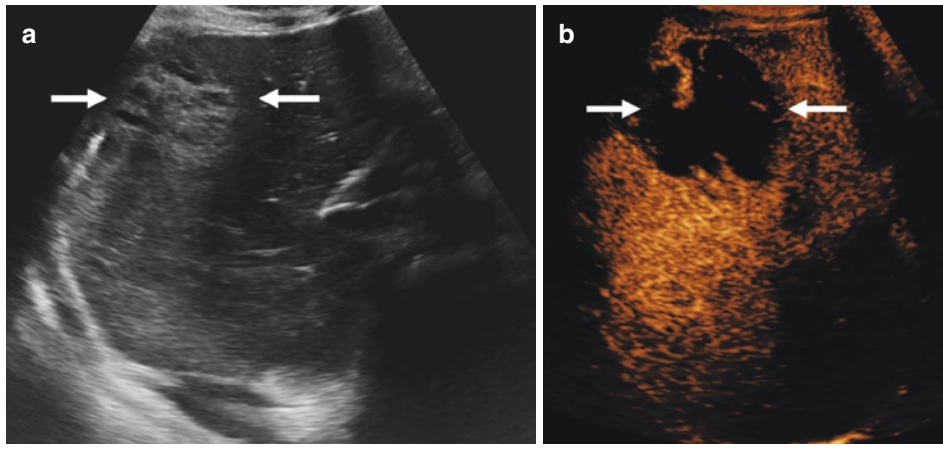

Fig. 8.8 Amoebic abscess in a 9-year-old-boy presenting with 3-month history of weight loss, lethargy, and fever. (**a**) Grayscale ultrasound shows a hyperechoic heterogeneous subcapsular mass (arrows) within the right lobe of the liver. (**b**) On contrast enhancement ultrasound there is peripheral rim enhancement, but the central fluid collection is non-enhancing with septations noted (arrows)

due to areas of the dense fluid collection with some internal hyperechogenic regions often from purulent inflammatory tissue, septations and on occasion, with gas-forming organisms, air may be seen. On arterial phase images, there is enhancement from the abscess wall (rim enhancement), septations or purulent inflammatory tissue within the abscess when present. Areas of fluid collection localized within the abscess, between septations will not enhance. On grayscale US, an *Echinococcus* abscess can appear as a simple cyst, cysts with internal membranes or internal daughter cysts with debris, cysts with intramural nodules or calcified areas. There is a paucity of data on the CEUS appearance of parasitic abscesses in children. However, in adults, with hepatic alveolar echinococcosis (HAE), the periphery of the HAE shows rapid rim-like strip of enhancement during the early arterial phase, with slow washout during the late portal venous phase (Fig. 8.9). No contrast enhancement was observed within the HAE lesions in the arterial, portal, and delayed phases [33].

8.4.7 Regenerative Nodular Hyperplasia

Regenerative nodular hyperplasia (RNH) is rare in children. In RNH the regular hepatic parenchyma is replaced by multiple, regenerative nodules of hyperplastic hepatocytes. Regenerative nodular hyperplasia can be associated with myeloproliferative and lymphoproliferative syndromes, lupus erythematosus, steroids, cytotoxic and immunosuppressive drugs. On grayscale US, RNH can be seen as solitary or multiple solid nodules that are either hypo- or isoechoic. The larger nodules can distort background liver architecture and will have a heterogeneous echogenicity [25]. On CEUS they are isoenhancing to the liver parenchyma during all phases (Fig. 8.10).

8.4.8 Mesenchymal Hamartoma of the Liver

Mesenchymal hamartoma of the liver (MHL) is a mass composed of fluid-filled cystic spaces within areas of degenerated mesenchyme [34]. It usually appears within the first 2 years of life and it is very uncommon in older children and adults. On grayscale US, MHL appears as large mass with a solid component, septation, and numerous cysts of different sizes. Mesenchymal hamartoma of the liver may have predominant mixed cystic and solid structures. Calcifications and hemorrhage are uncommon features. On CEUS, the solid components of the MHL are isoenhancing

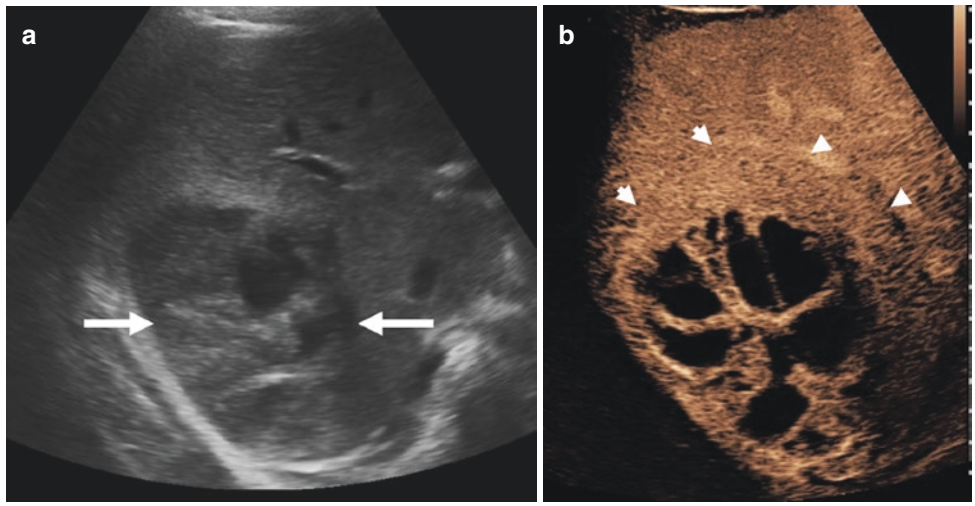

Fig. 8.9 Bacterial abscess in a 14-year-old female present with fever. (**a**) Grayscale ultrasound shows a subcapsular mass (arrows) with heterogeneous echogenicity within the right lobe of the liver. (**b**) On contrast enhancement ultrasound, there is thick peripheral rim enhancement (arrowheads). The central loculated fluid pockets are much better defined

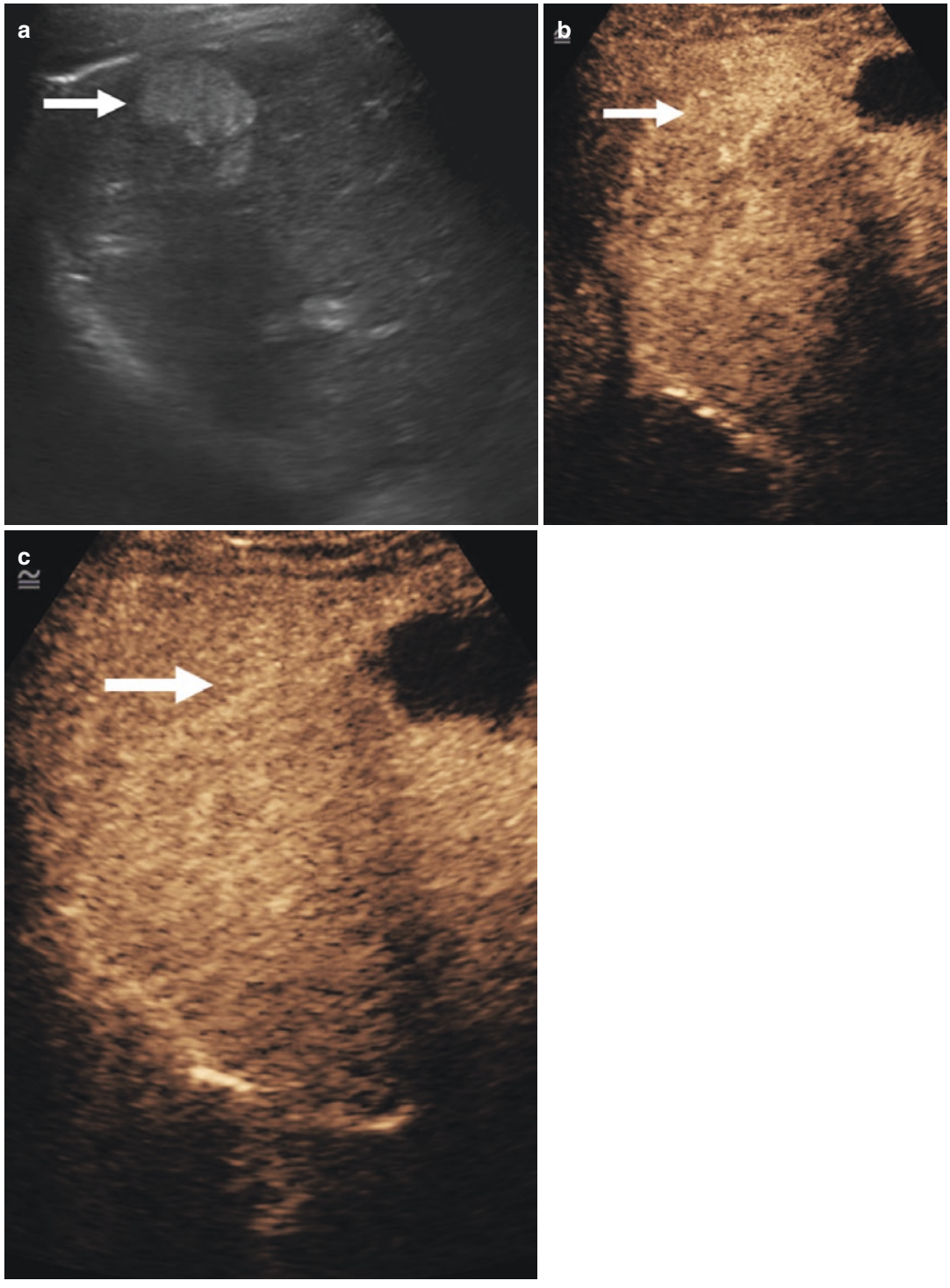

Fig. 8.10 Hepatic regenerative nodule in a 15-year-old female with cystic fibrosis-related liver disease and portal hypertension. (**a**) Grayscale ultrasound shows a hyperechoic nodule (arrow) in the right liver lobe, with underlying chronic liver parenchymal changes. (**b**) On contrast enhancement ultrasound, the regenerative nodule shows iso-enhancement compared to liver parenchyma during arterial at 15 s (arrow). (**c**) In the portal venous phase at 90 s, the lesion remains isoenhancing with the background liver (arrow)

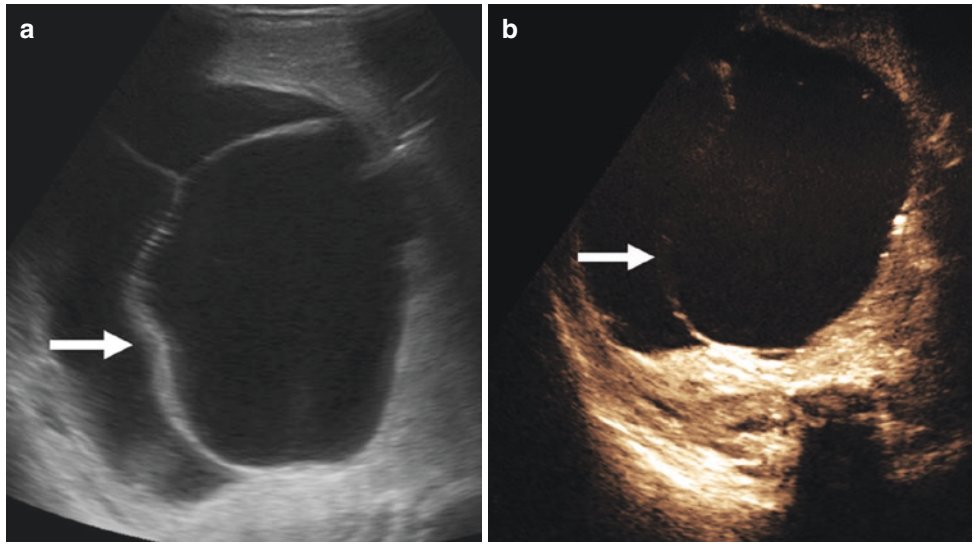

Fig. 8.11 Mesenchymal hamartoma in a 7-month-old male presenting with hepatomegaly. (**a**) Grayscale ultrasound shows a large cystic mass with internal septation (arrow). (**b**) On the contrast-enhanced ultrasound, the septation (arrow) enhances and remains isoenhancing to the liver on all phases, with the cystic component of the lesion well demarcated

to the liver in all phases, with no enhancement of the cystic parts (Fig. 8.11).

8.4.9 Bile Duct Hamartomas (von Meyenburg Complex) and Bile Duct Adenomas

Bile duct micro-hamartomas (BDMH), also known as von Meyenburg complex, have a cystic nature. They are composed of dilated intrahepatic bile ducts not communicating to the biliary tree, separated by fibrous septae and surrounded by fibrous, sometimes hyalinized stroma [35]. Bile duct micro-hamartomas can be associated with congenital hepatic fibrosis, Caroli disease, and autosomal dominant polycystic hepatorenal disease. Bile duct micro-hamartomas appear as innumerable, well-circumscribed hyperechoic or hypoechoic tiny nodules scattered in the liver parenchyma. Most BDMHs are <5 mm and do not tend to exceed 10 mm. A "comet tail" sign and posterior acoustic enhancement may be seen. Bile duct adenomas (BDAs) are composed of a proliferation of tightly packed small ductules with inapparent lumens lined by cuboidal epithelium. The ductules of BDA have small lumens and do not contain intraluminal secretions or bile-like dilatated channels of BDMH. On grayscale US, they are small (diameter <10 mm), solid well-circumscribed, usually hypoechoic lesions which predominantly present at the subscapular location. There is no data concerning pediatric CEUS appearance of BDMH or BDA. The reports about CEUS enhancement from adult populations are ambiguous, probably a consequence of mixing these two entities. Based on the histological appearances of the lesions, the authors suggest that BDMHs do not show enhancement in any phase whereas BDAs have a rapid wash-in with hyperenhancement during the arterial phase with wash-out during the portal venous phase and hypo-enhancement during late portal venous phase [36–38].

8.5 Malignant Focal Liver Lesions

Malignant FLL can be divided into primary and secondary. A primary hepatic malignancy in a child is rare and occurs more commonly in children predisposed by the presence of underlying medical conditions. Benign liver lesions, such as hepatic adenoma and dysplastic nodules, may also undergo malignant transformation. Malignant FLL can

have variable appearances on grayscale US, overlapping with benign lesions. The hallmark of a malignant hepatic lesion on CEUS is UCA washout during the portal venous and late portal venous phase [20]. The dynamic enhancement patterns together with the clinical information will help to narrow down the differential diagnosis.

8.5.1 Hepatoblastoma

Hepatoblastoma is the most common primary malignant tumor in children accounting for 60% of all cases, and more than 90% of malignant hepatic tumors occurring in children under the age of 5 years are hepatoblastoma [39], mostly occurring sporadically. The alpha-fetoprotein is markedly elevated in the majority of the cases. The presence of cystic areas, calcification, and necrosis in hepatoblastoma can differentiate these tumors from hepatocellular carcinoma. On grayscale US, a hepatoblastoma is a solid mass with heterogeneous echogenicity. On CEUS, hepatoblastoma shows arterial phase hyperenhancement and rapid early contrast washout (Fig. 8.12) [40].

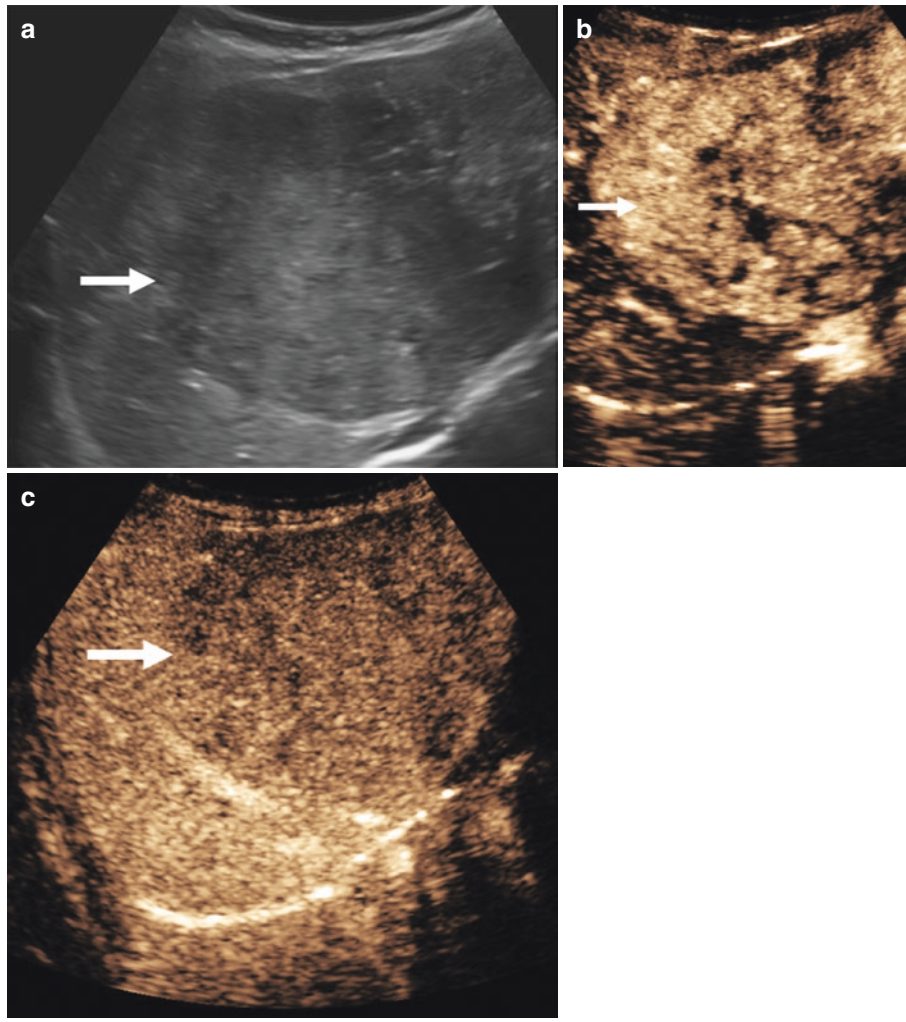

Fig. 8.12 Hepatoblastoma in a 2-year-old girl. (**a**) Grayscale ultrasound shows a large solid slightly hypoechoic mass in the right lobe of the liver (arrow), with no evidence of underlying parenchymal liver abnormality. (**b**) On contrast-enhanced ultrasound examination, the early arterial phase demonstrates avid patchy enhancement of the lesion (arrow). (**c**) In the portal venous phase, there is a washout, demarcating the lesion (arrow) against the normal contrast retention in the background liver

8.5.2 Hepatocellular Carcinoma

Pediatric hepatocellular carcinoma (HCC) often occurs in children with underlying liver disease including hepatitis B virus infection, metabolic disorders such as tyrosinemia, glycogen storage disease, congenital portosystemic shunts, long-standing hepatic venous tract outflow obstruction [41]. An HCC can also occur in children with no known underlying liver disease, either sporadically or in children with genetic cancer syndromes. An HCC is the second most common primary hepatic malignancy in children. On a CEUS examination, an HCC will demonstrate characteristic enhancement patterns, with ancillary features on the CEUS which have been described according to CEUS Liver Imaging Reporting and Data System (LI-RADS) in the adult population [42]. In children, although there are limited studies, similar enhancement patterns have been observed [18]. The HCC will show hyperenhancement without any rim-like enhancement, peripheral discontinuous nodular morphology on the arterial phase imaging between 10–20 and 30–45 s after the UCA injection. Washout in an HCC tends to be mild and late-onset compared to a hepatoblastoma (Fig. 8.13). Malignant transformation from dysplastic nodules should be suspected when these nodules show washout or display threshold growth in comparison to the previous examination.

8.5.3 Undifferentiated Embryonal Sarcoma

Undifferentiated embryonal sarcoma (UES) is a rare aggressive hepatic mesenchymal tumor that

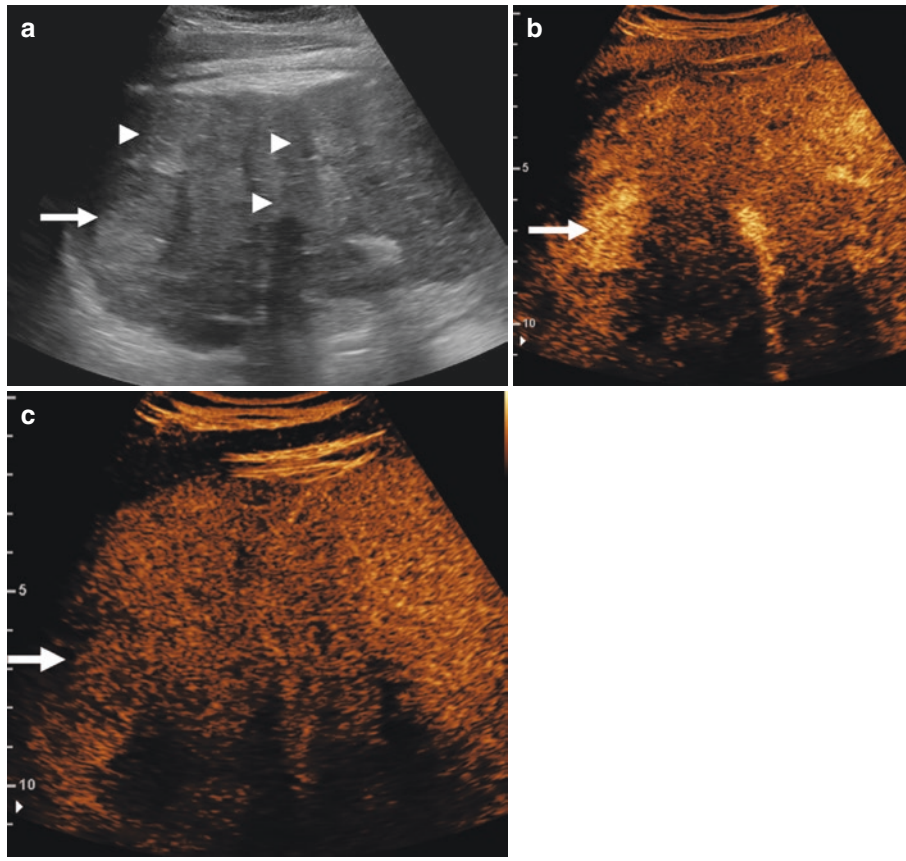

Fig. 8.13 Hepatocellular carcinoma in a 16-year-old female with a diagnosis of autoimmune hepatitis. (**a**) Grayscale ultrasound shows multiple hyperechoic nodules (arrows and arrowheads) within the right liver. (**b**) On contrast-enhanced ultrasound the large hyperechoic lesion (arrow) shows hyperenhancement on the early arterial phase, at 23 s. (**c**) On the late portal venous phase at 202 s the lesion demonstrates washout (arrow)

often has metastases to the lung, peritoneum, and pleura [43]. An UES exhibits no gender predilection and the majority occur in children aged 6–10 years [44]. They are typically large tumors (diameter >10 cm) and intralesional hemorrhage, necrosis, and cystic degeneration are often present. The pre-operative diagnosis of UES is challenging due to lack of specific imaging findings, serological markers, and the rarity of the disease. The appearances of misleading cystic appearances on CT and MR imaging can misdiagnose them as benign hydatid disease [45]. In distinction, grayscale US often shows more accurately the internal solid nature of the lesion with areas of small anechoic spaces. Discrepant finding between CT and US imaging is a recognized diagnostic feature [46–48] for UES. An UES is a hypo-vascular tumor on angiography [40, 49]. On CEUS, the UES demonstrates peripheral rim enhancement representing fibrous pseudo-capsule (Fig. 8.14).

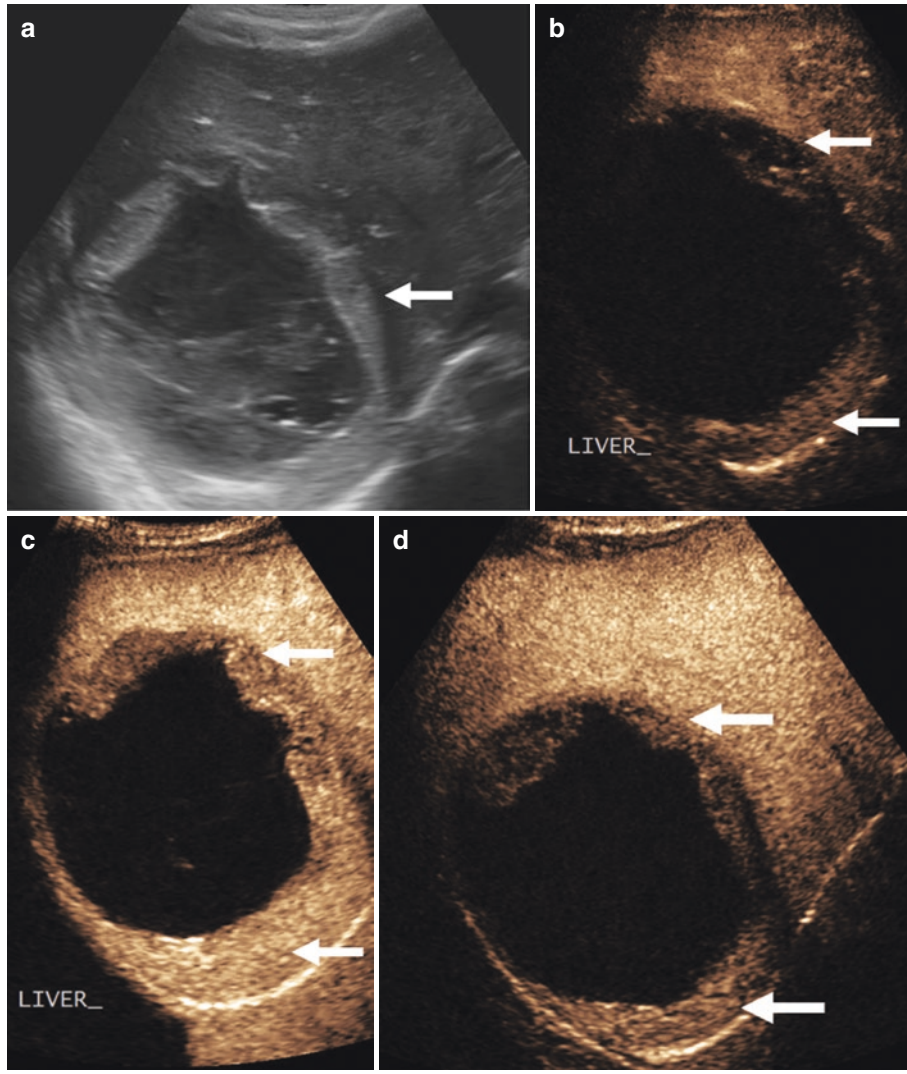

Fig. 8.14 Embryonal sarcoma in a 10-year-old female presenting with abdominal pain. (**a**) The grayscale ultrasound demonstrates a well-circumscribed, thick-walled partially cystic lesion within the right liver (arrow). (**b**) On the contrast-enhanced ultrasound, in the early arterial phase at 20 s, the solid component of the mass (arrows) shows lower enhancement compared to the background liver. (**c**) In the mid portal venous phase at 86 s, there is a differential enhancement of the lesion wall (arrows), with washout appearing on the anterior wall (arrows). (**d**) In the late portal venous phase at 201 s, this washout is more obvious (arrows) in comparison to the surrounding normal liver, particularly at the anterior surface

The internal architecture of the tumor shows little or no enhancement during the arterial phase, but heterogeneous internal nodular enhancement during the portal venous and late phase with the rim of the lesion showing faint washout [40].

8.5.4 Rhabdomyosarcoma

Rhabdomyosarcoma (RMS) is the most common childhood soft tissue sarcoma. The majority of RMS occurs in the head and neck (35–40%), genitourinary tract (25%), and limb extremities (20%) [50]. Although it only accounts for 1% of all RMS, an RMS is the most common pediatric tumor of the biliary tree. A hilar mass with associated biliary duct dilatation is a typical finding. RMS can also metastases to the liver surface [50]. Primary hepatic RMS is extremely rare with approximately 20 cases reported in the literature [51, 52] and they often appear as large cystic and solid masses, which may be associated with tumor rupture or hemorrhage. On grayscale US, the RMS is a well-defined solid irregular mass with heterogeneous echogenicity. The RMS shows non-specific imaging features on CEUS, with similar appearances to other hepatic malignancy demonstrating early portal venous phase washout, but with a variable arterial enhancement pattern on CEUS (Fig. 8.15) [40]. Another very

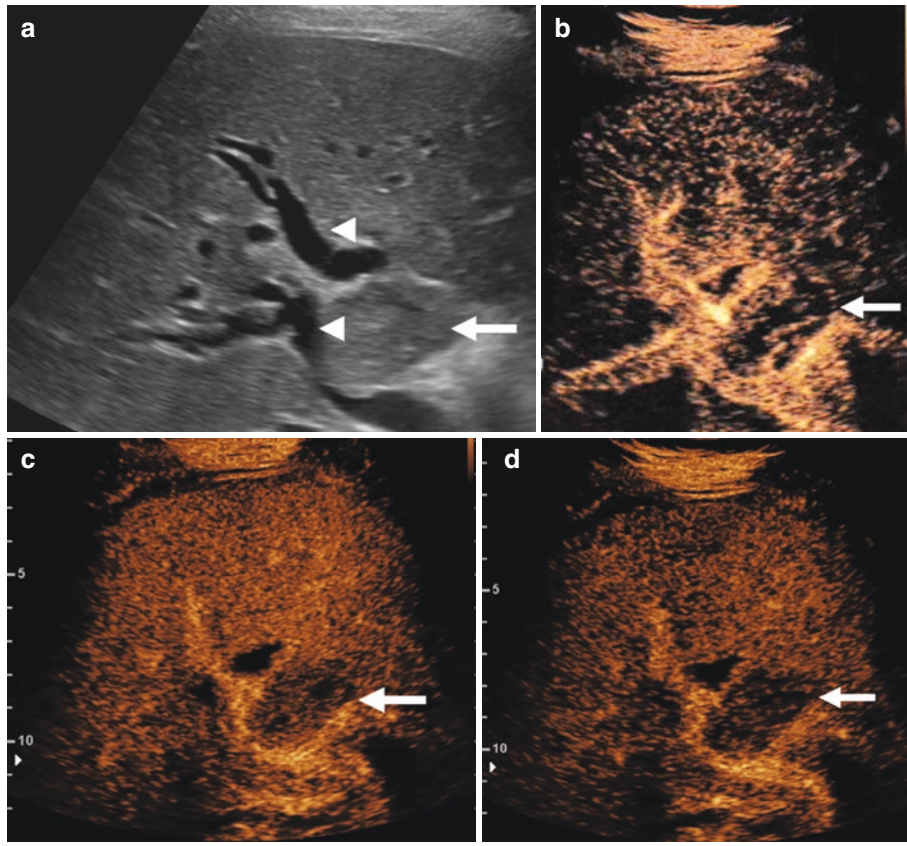

Fig. 8.15 Primitive germ cell tumor of the biliary tree in a 10-year-old female. (**a**) Grayscale ultrasound shows a well-circumscribed lesion (arrow) extending into the common hepatic duct with associated intrahepatic duct dilatation (arrowheads). (**b**) On the contrast-enhanced ultrasound, in the arterial phase at 17 s, the lesion shows patchy internal enhancement (arrow). (**c**) On the contrast-enhanced ultrasound, in the early portal venous phase, at 48 s, there is less enhancement in the lesion (arrow) in comparison to background normal liver. (**d**) On the contrast-enhanced ultrasound, in the late portal venous phase, at 90 s, there is washout appreciated in the lesion (arrow) in comparison to background normal liver

rare tumor of the biliary tree is a primitive germ cell tumor, which will cause biliary duct dilatation and demonstrates washout in the portal venous phase, indistinguishable from an RMS (Fig. 8.15).

8.5.5 Hepatic Lymphoma

Primary hepatic lymphoma (PHL) is rare and accounts for <1% of the presentation of non-Hodgkin lymphoma. Primary hepatic lymphoma most commonly appears as a discrete FLL but can also demonstrate a diffuse infiltrative pattern within the liver or as multiple ill-defined masses at porta hepatis [53]. Multiple hepatic masses or diffuse infiltrative pattern are more common in secondary hepatic lymphoma and is seen with post-transplant lymphoproliferative disease. In PHL, there tends to be a dominant lesion within the liver which is not evident in secondary hepatic lymphoma which presents with multiple focal lesions. A miliary pattern with numerous small nodules scattered throughout the liver is seen in 10% of Hodgkin lymphoma and secondary non-Hodgkin lymphoma of the liver [54]. On grayscale US, these focal hepatic lesions are hypoechoic without posterior acoustic enhancement. They may have a central hyperechoic area giving a "target" appearance. On CEUS, arterial hyper, iso, and hypo-enhancement has been demonstrated, but almost all of the lesions investigated were hypo-enhancing compared to the background liver during portal venous and late-phase imaging (Fig. 8.16) [55]. On CT imaging these lesions are typically hypo-attenuated on all phases [53].

8.5.6 Hepatic Metastasis

Hepatic metastases are usually from solid primary tumors in children, commonly from neuroblastoma (NB) or a Wilms' tumor. Other tumors that

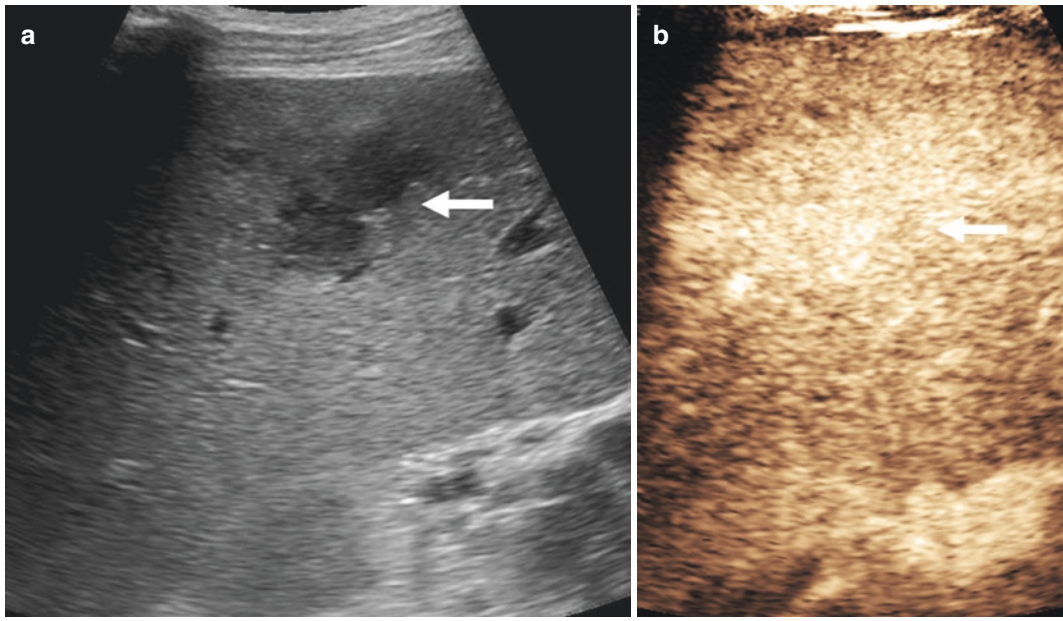

Fig. 8.16 Hepatic lymphoma in a 46-year-old female with HIV. (**a**) Grayscale ultrasound demonstrates an ill-defined irregular hypoechoic lesion (arrow) within the right liver. (**b**) On contrast-enhanced ultrasound, on the arterial phase at 15 s, the lesion (arrow) shows hyperenhancement. (**c**) On contrast-enhanced ultrasound, on the early portal venous phase at 60 s, there is rapid washout with a distinct "feathery" pattern of vascular change within the lesion

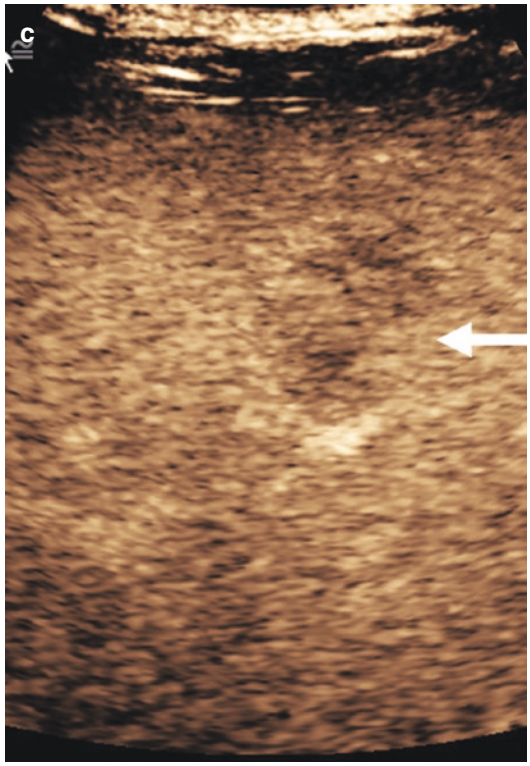

Fig. 8.16 (continued)

metastasize to the liver include germ cell tumors, osteosarcoma, and neuroendocrine tumors. Stage 4S NB can present with multiple ill-defined nodules or diffuse liver involvement, whereas stage 4 NB disease involving the liver usually presents with multiple discrete lesions. The appearances of hepatic metastasis are expected to mimic those in adulthood. On grayscale US, they are found to be predominantly hypoechoic (63.8%) and hyperechoic (28.3%); isoechoic (5.8%) and non-echoic metastasis (0.4%) and mixed echogenicity (1.7%) are rare [56]. On CEUS the majority of these metastases show diffuse homogenous hyperenhancement (55.4%) or rim-like hyperenhancement (33.3%) during the arterial phase. The vast majority, 99% of the lesions demonstrate washout occurring rapidly during the portal venous phase (97%) rather than with a delayed washout (2%). Hypervascular metastasis shows a significant longer washout time compared to hypo-vascular metastases (Fig. 8.17) [56].

A number of very rare malignant tumors are also found in children and include, cholangiocarcinoma (Fig. 8.18), combined HCC-

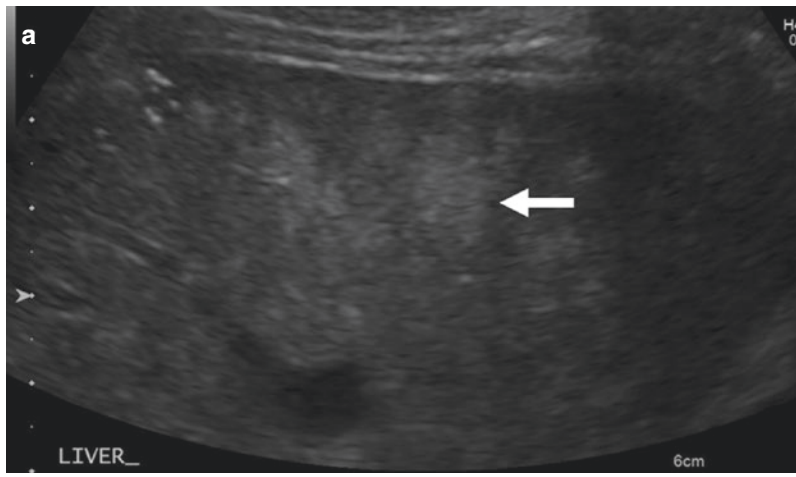

Fig. 8.17 Neuroendocrine metastasis in a 10-year-old male with an underlying pancreatic insulinoma. (**a**) Grayscale ultrasound shows a hyperechoic nodule (arrow) within a heterogeneous right liver lobe. (**b**) On the contrast-enhanced ultrasound, the arterial phase at 15 s demonstrates hyperenhancement (arrow). (**c**) On the contrast-enhanced ultrasound, washout out of the lesion (arrow) on the late portal venous phase at 120 s

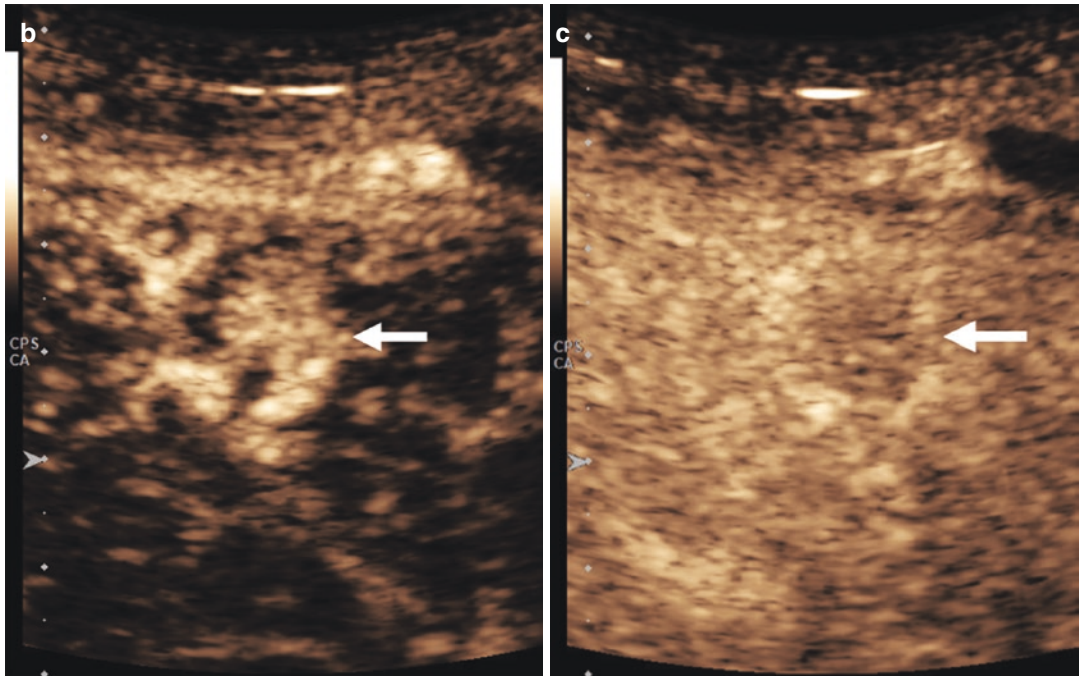

Fig. 8.17 (continued)

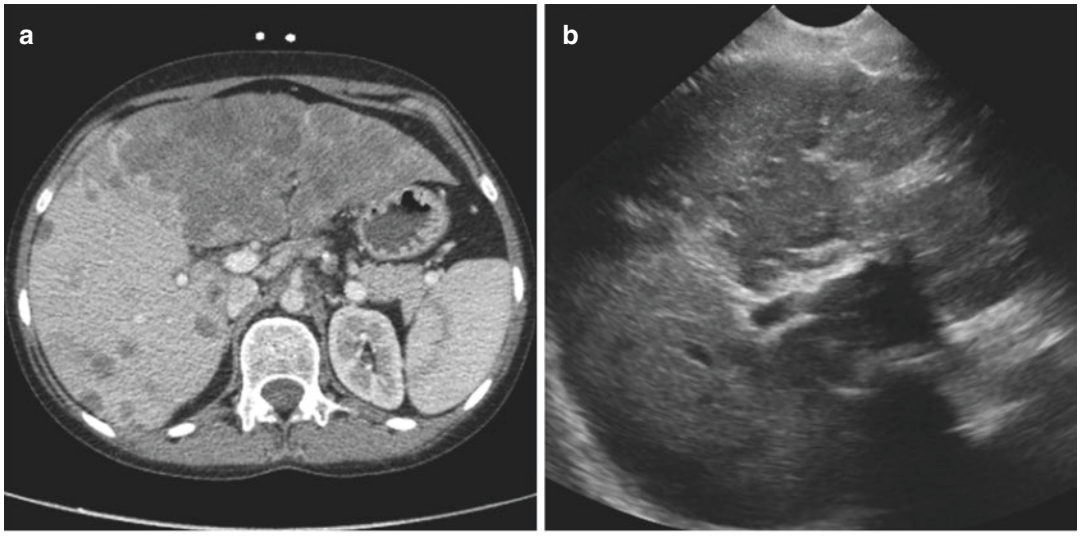

Fig. 8.18 Liver cholangiocarcinoma in a 16-year-old child. (**a**) Computed tomography in the venous phase shows multiple hypoechoic lesions in the liver. (**b**) Grayscale ultrasound demonstrates heterogeneous echogenicity within the liver. (**c**) The contrast-enhanced ultrasound examination demonstrates rapid peripheral and heterogeneous central hypoenhancement of the lesion on the arterial phase at 23 s. (**d**) The contrast-enhanced ultrasound examination demonstrates washout of during the late portal venous phase at 137 s

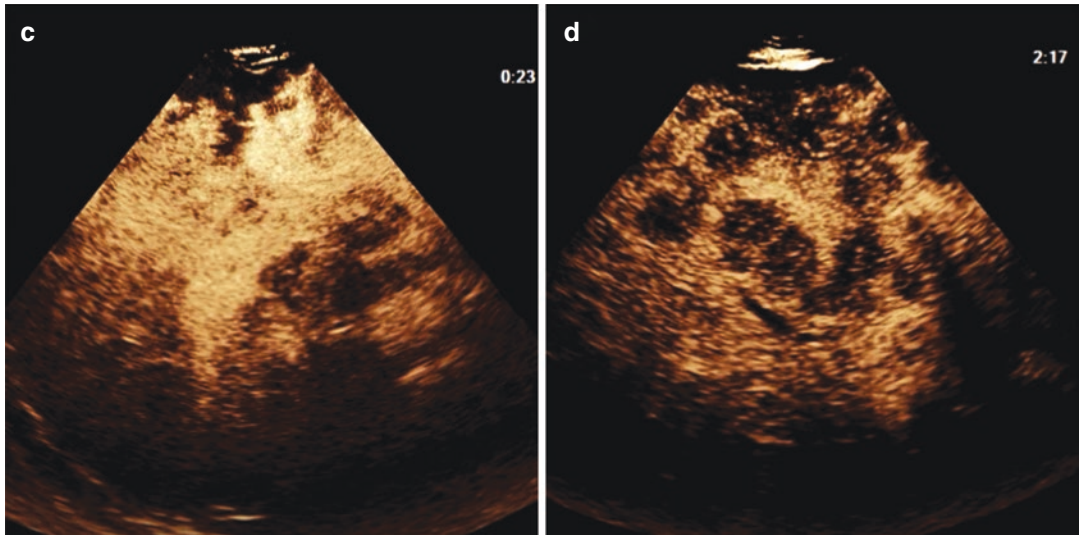

Fig. 8.18 (continued)

cholangiocarcinoma, fibrolamellar hepatocellular carcinoma, angiosarcoma, and epithelioid hemangioendothelioma [57].

8.6 Conclusion

The presence of an FLL found inadvertently in the child on an US examination can often be an anxious time for the parents, and presents a diagnostic dilemma for the referring clinical team. If there is underlying chronic liver disease, a known risk factor or an established primary tumor elsewhere, the clinical management and the imaging strategy are different from the finding of an FLL in an otherwise healthy child. The ability to undergo a CEUS examination, to safely and accurately characterize the FLL is immense to alleviate the anxiety of the parents and to allow subsequent appropriate clinical management. The introduction of CEUS in the assessment of an FLL in the child has implications for future imaging strategies and will be beneficial to the child reducing the need for MR and CT imaging.

References

1. Brenner DJ, Elliston C, Hall EJ, Berdon WE. Estimated risks of radiation-induced fatal cancer from pediatric CT. AJR Am J Roentgenol. 2001;176:289–96.
2. Pearce MS, Salotti JA, Little MP, McHugh K, Lee C, Kim KP, et al. Radiation exposure from CT scans in childhood and subsequent risk of leukaemia and brain tumours: a retrospective cohort study. Lancet. 2012;380:499–505.
3. Elbeshlawi I, AbdelBaki MS. Safety of gadolinium administration in children. Pediatr Neurol. 2018;86:27–32.
4. Andropoulos DB, Greene MF. Anesthesia and developing brains: implications of the FDA warning. N Engl J Med. 2017;376(10):905–7.
5. Piscaglia F, Bolondi L. The safety of SonoVue in abdominal applications: retrospective analysis of 23188 investigations. Ultrasound Med Biol. 2006;32:1369–75.
6. Yusuf GT, Sellars ME, Deganello A, Cosgrove DO, Sidhu PS. Retrospective analysis of the safety and cost implications of pediatric contrast-enhanced ultrasound at a single center. AJR Am J Roentgenol. 2016;208:446–52.
7. Seitz K, Strobel D, Bernatik T, Blank W, Friedrich-Rust M, von Herbay A, et al. Contrast-enhanced ultrasound (CEUS) for the characterization of focal liver lesions prospective comparison in clinical practice: CEUS vs. CT (DEGUM multicenter trial). Ultraschall Med. 2009;30:383–9.

8. Seitz K, Bernatik T, Strobel D, Friedrich-Rust M, Strunk H, Greis C, et al. Contrast-enhanced ultrasound (CEUS) for the characterization of focal liver lesions in clinical practice (DEGUM multicenter trial): CEUS vs. MRI—a prospective comparison in 269 patients. Ultraschall Med. 2010;31:492–9.
9. Strobel D, Seitz K, Blank A, Schuler A, Dietrich C, von Herbay A, et al. Contrast-enhanced ultrasound for the characterization of focal liver lesions—diagnostic accuracy in clinical practice (DEGUM multicenter trial). Ultraschall Med. 2008;225:499–505.
10. Seitz K, Strobel D. A milestone: approval of CEUS for diagnostic liver imaging in adults and children in the USA. Ultraschall Med. 2016;37:229–32.
11. Piskunowicz M, Kosiak W, Batko T, Piankowski A, Polczynska K, Adamkiewicz-Drozynska E. Safety of intravenous application of second generation ultrasound contrast agent in children: prospective analysis. Ultrasound Med Biol. 2015;41:1095–9.
12. Sidhu PS, Cantisani V, Deganello A, Dietrich CF, Duran C, Franke D, et al. Role of contrast-enhanced ultrasound (CEUS) in paediatric practice: an EFSUMB position statement. Ultraschall Med. 2017;38:33–43.
13. Stenzel M. Intravenous contrast-enhanced sonography in children and adolescents—a single center experience. J Ultrason. 2013;13:133–44.
14. Dietrich CF, Averkiou M, Nielsen MB, Barr RG, Burns PN, Calliada F, et al. How to perform contrast-enhanced ultrasound (CEUS). Ultrasound Int Open. 2018;04:E2–E15.
15. Deganello A, Sellars ME, Yusuf GT, Sidhu PS. How much should I record during a CEUS examination? Practical aspects of the real-time feature of a contrast ultrasound study. Ultraschall Med. 2018;39(5):484–6.
16. Bartolotta TV, Taibbi A, Midiri M, Matranga D, Solbiati L, Lagalla R. Indeterminate focal liver lesions incidentally discovered at gray-scale US role of contrast-enhanced sonography. Investig Radiol. 2011;46:106–15.
17. Beaton C, Cochlin DL, Kumar N. Contrast enhanced ultrasound should be the initial radiological investigation to characterise focal liver lesions. Eur J Surg Oncol. 2010;36:43–6.
18. Jacob J, Deganello A, Sellars ME, Hadzic N, Sidhu PS. Contrast enhanced ultrasound (CEUS) characterization of grey-scale sonographic indeterminate focal liver lesions in paediatric practice. Ultraschall Med. 2013;34:529–40.
19. Giesel FL, Delome S, Kayczor HU, Krix M. Contrast-enhanced ultrasound for the characterization of incidental liver lesions—an economical evaluation in comparison with multi-phase computed tomography. Ultraschall Med. 2009;30:259–68.
20. Claudon M, Dietrich CF, Choi BI, Kudo M, Nolsoe C, Piscaglia F, et al. Guidelines and good clinical practice recommendations for contrast enhanced ultrasound (CEUS) in the liver—update 2012. Ultraschall Med. 2013;34:11–29.
21. Piscaglia F, Lencioni R, Sagrini E, Pina CD, Cioni D, Vidili G, et al. Characterization of focal liver lesions with contrast-enhanced ultrasound. Ultrasound Med Biol. 2010;36(4):531–50.
22. D'Onofrio M, Crosara S, De Robertis R, Canestrini S, Mucelli RP. Contrast-enhanced ultrasound of focal liver lesions. AJR Am J Roentgenol. 2015;205:W56–66.
23. Gnarra M, Behr G, Kitajewski A, Wu JK, Anupindi SA, Shawber CJ, et al. History of the infantile hepatic hemangioma: from imaging to generating a differential diagnosis. World J Clin Pediatr. 2016;5(3):273–80.
24. Piorkowska MA, Dezman R, Sellars ME, Deganello A, Sidhu PS. Characterization of a hepatic haemangioma with contrast-enhanced ultrasound in an infant. Ultrasound. 2017;26(3):178–81.
25. Chiorean L, Cui XW, Tannapfel A, Franke D, Stenzel M, Kosiak W, et al. Benign liver tumors in pediatric patients—review with emphasis on imaging features. World J Gastroenterol. 2015;21(28):8541–61.
26. Franchi-Abella S, Branchereau S. Benign hepatocellular tumors in children: focal nodular hyperplasia and hepatocellular adenoma. Int J Hepatol. 2013;2013:215064.
27. Bouyn CI-D, Leclere J, Raimondo G, le Pointe HD, Couanet D, Valteau-Couanet D, et al. Hepatic focal nodular hyperplasia in children previously treated for a solid tumor. Cancer. 2003;97(12):3107–13.
28. Chung EM, Cube R, Lewis RB, Conran RM. Pediatric liver masses: radiologic-pathologic correlation part 1. Benign tumors. Radiographics. 2009;30(3):801–26.
29. Fang C, Bernardo S, Sellars ME, Deganello A, Sidhu PS. Contrast-enhanced ultrasound in the diagnosis of pediatric focal nodular hyperplasia and hepatic adenoma: interobserver reliability. Pediatr Radiol. 2019;49(1):82–90.
30. Katabathina VS, Menias CO, Shanbhogue AKP, Jagirdar J, Paspulati RM, Prasad SR. Genetics and imaging of hepatocellular adenomas: 2011 update. Radiographics. 2011;31(6):1529–43.
31. Dietrich CF, Schuessler G, Trojan J, Fellbaum C, Ignee A. Differentiation of focal nodular hyperplasia and hepatocellular adenoma by contrast-enhanced ultrasound. Br J Radiol. 2005;78:704–7.
32. Anupindi SA, Biko DM, Ntoulia A, Poznick L, Morgan TA, Darge K, et al. Contrast-enhanced US assessment of focal liver lesions in children. Radiographics. 2017;37:1632–47.
33. Tao S, Qin Z, Hao W, Yongquan L, Lanhui Y, Lei Y. Usefulness of gray-scale contrast-enhanced ultrasonography (SonoVue) in diagnosing hepatic alveolar echinococcosis. Ultrasound Med Biol. 2011;37(7):1024–8.
34. Makin E, Davenport M. Fetal and neonatal liver tumours. Early Hum Dev. 2010;86(10):637–42.
35. Chung EB. Multiple bile duct hamartomas. Cancer. 1970;26:287–96.
36. Berry JD, Boxer ME, Rashid HI, Sidhu PS. Microbubble contrast enhanced ultrasound

characteristics of multiple biliary hamartomas (von Meyenberg complexes). Ultrasound. 2004;12:95–7.
37. Ahn JM, Paik YH, Lee JH, Cho JY, Sohn W, Gwak GY, et al. Intrahepatic bile duct adenoma in a patient with chronic hepatitis B accompanied by elevation of alpha-fetoprotein. Clin Mol Hepatol. 2015;21(4):393–7.
38. Shi QS, Xing LX, Jin LF, Wang H, Lv XH, Du LF. Imaging findings of bile duct hamartomas: a case report and literature review. Int J Clin Exp Med. 2015;8(8):13145–53.
39. Darbari A, Sabin KM, Shapiro CN, Schwarz KB. Epidemiology of primary hepatic malignancies in U.S. children. Hepatology. 2003;38(3):560–6.
40. McCarville B, Deganello A, Harkanyi Z. Contrast enhanced ultrasound: the current state. In: Voss SD, McHugh K, editors. Imaging in pediatric oncology. 1st ed. Cham: Springer; 2019. p. 137–55.
41. Khanna R, Verma SK. Pediatric hepatocellular carcinoma. World J Gastroenterol. 2018;24(35):3980–99.
42. Lyshchik A, Kono Y, Dietrich CF, Jang HJ, Kim TK, Piscaglia F, et al. Contrast-enhanced ultrasound of the liver: technical and lexicon recommendations from the ACR CEUS LI-RADS working group. Abdom Radiol. 2018;43:861–79.
43. Stocker JT, Ishak KG. Undifferentiated (embryonal) sarcoma of the liver: report of 31 cases. Cancer. 1978;42(1):336–48.
44. Gao J, Fei L, Li S, Cui K, Zhang J, Yu F, et al. Undifferentiated embryonal sarcoma of the liver in a child: a case report and review of the literature. Oncol Lett. 2013;5(3):739–42.
45. Pachera S, Nishio H, Takahashi Y, Yokoyama Y, Oda K, Ebata T, et al. Undifferentiated embryonal sarcoma of the liver: case report and literature survey. J Hepatobiliary Pancreat Surg. 2008;15(5):536–44.
46. Faraj W, Mukherji D, El Majzoub N, Shamseddine A, Shamseddine A, Khalife M. Primary undifferentiated embryonal sarcoma of the liver mistaken for hydatid disease. World J Surg Oncol. 2010;8:58.
47. Moon WK, Kim WS, Kim IO, Yeon KM, Choi BI, Han MC. Undifferentiated embryonal sarcoma of the liver: US and CT findings. Pediatr Radiol. 1994;24(7):500–3.
48. Lashkari HP, Khan SU, Ali K, Sashikumar P, Mukherjee S. Diagnosis of undifferentiated embryonal sarcoma of the liver: importance of combined studies of ultrasound and CT scan. J Pediatr Hematol Oncol. 2009;31(10):797–8.
49. Ros PR, Olmsted WW, Dachman AH, Goodman ZD, Ishak KG, Hartman DS. Undifferentiated (embryonal) sarcoma of the liver: radiologic-pathologic correlation. Radiology. 1986;161(1):141–5.
50. Park K, van Rijn R, McHugh K. The role of radiology in paediatric soft tissue sarcomas. Cancer Imaging. 2008;8(1):102–15.
51. Yin J, Liu Z, Yang K. Pleomorphic rhabdomyosarcoma of the liver with a hepatic cyst in an adult: case report and literature review. Medicine (Baltimore). 2018;97(29):e11335.
52. Roebuck DJ, Yang WT, Lam WWM, Stanley P. Hepatobiliary rhabdomyosarcoma in children: diagnostic radiology. Pediatr Radiol. 1998;28(2):101–8.
53. Tomasian A, Sandrasegaran K, Elsayes KM, Shanbhogue A, Shaaban A, Menias CO. Hematologic malignancies of the liver: spectrum of disease. Radiographics. 2015;35(1):71–86.
54. Leite NP, Kased N, Hanna RF, Brown MA, Pereira JM, Cunha R, et al. Cross-sectional imaging of extranodal involvement in abdominopelvic lymphoproliferative malignancies. Radiographics. 2007;27(6):1613–34.
55. Trenker C, Kunsch S, Michl P, Wissniowski TT, Goerg K, Goerg C. Contrast-enhanced ultrasound (CEUS) in hepatic lymphoma: retrospective evaluation in 38 cases. Ultraschall Med. 2014;35:142–8.
56. Kong WT, Ji ZB, Wang WP, Cai H, Huang BJ, Ding H. Evaluation of liver metastases using contrast-enhanced ultrasound: enhancement patterns and influencing factors. Gut Liver. 2016;10(2):283–7.
57. Chavhan GB, Siddiqui I, Ingley KM, Gupta AA. Rare malignant liver tumors in children. Pediatr Radiol. 2019;49(11):1404–21.

9 Pediatric Contrast-Enhanced Ultrasonography (CEUS): Pediatric Transplantation

Doris Franke

Abbreviations

CEUS	Contrast-enhanced ultrasonography
EBV	Epstein–Barr virus
GvHD	Graft versus host disease
PTLD	Post-transplant lymphoproliferative disease
RI	Resistive indices
UCA	Ultrasound contrast-agent
US	Ultrasonography

9.1 Introduction

In the assessment before, during, and after solid organ and stem cell transplantation in children, ultrasonography (US) is the first-line imaging modality, especially in liver and kidney transplantation.

Doppler Sonography is used for confirmation of vessel patency and diagnosis of vessel pathologies like stenoses, arterio-venous-fistulas, or aneurysms. In some cases, however, it can be very troublesome even for an experienced investigator to find the hepatic artery in a complex liver transplantation or the artery after renal transplantation. The inability to identify the artery, a crucial finding, is one of the indications for contrast-enhanced ultrasonography (CEUS); Table 9.1. CEUS has the advantage of being available and applicable at any location, including the operating theater or the bedside in the bone marrow transplant patient, and pertinently in the intensive care unit with the very sick patient. CEUS is repeatable, cost-effective and, especially in children, safe. Most importantly, CEUS has the potential to reduce the overall radiation burden in children [1], which is of special impact in the field of pediatric transplantation as these children will already have an overall increased malignancy risk due to immunosuppression and underlying disease.

Furthermore, CEUS can be of help in pre-, peri-, and post-transplant complications including perfusion abnormalities, systemic infections, abscesses, or secondary malignancy, most commonly post-transplantation lymphoproliferative disorder (PTLD).

No imaging modality has the ability to diagnose *allograft rejection or calcineurin inhibitor toxicity*, but imaging can exclude or identify other complications in the differential diagnosis for rejection or transplant malfunction such as biliary or urinary obstruction, bilioma or impaired vessel patency. Ultrasound is routinely performed

D. Franke (✉)
Pediatric Ultrasonography, Department of Pediatric Kidney, Liver and Metabolic Diseases, Children's Hospital, Hannover Medical School, Hannover, Germany
e-mail: franke.doris@mh-hannover.de

P. S. Sidhu et al. (eds.), *Contrast-Enhanced Ultrasound in Pediatric Imaging*,
https://doi.org/10.1007/978-3-030-49691-3_9

Table 9.1 Indications for CEUS in pediatric transplantation

Vascular
Patency of vessels
Arterio venous-fistulas
Infarction
Pseudoaneurysm
Transplant renal artery stenosis
Non-vascular
Unclear masses
Unclear focal solid organ lesions
Complicated cysts
Abscess
Intra-cavitary CEUS (biliary system, vesicoureteral reflux, leakage, the position of drainage catheters)

as the initial screening imaging modality for the detection and follow-up of both early and delayed complications.

9.2 Liver Transplantation

Liver transplantation is performed for a variety of benign and malignant conditions of the liver and biliary system in children. The most common cause in infants is biliary atresia, followed by metabolic diseases and other conditions including hepatoblastoma. Depending on the donor-recipient graft size match, whole-organ grafts as well as right or left split liver grafts are transplanted from deceased donors. Living donated liver transplants in children are in the majority of cases left lateral segments (segments II and III) and only very exceptionally a right liver lobe. The early detection and treatment of postoperative complications have contributed significantly to improved graft and patient survival with reliable imaging playing a critical role [2–5].

Complications after liver transplantation may be distinguished in vascular and nonvascular. Early and correct diagnosis is of critical importance [4, 6–9]. Vascular complications include stenosis and thrombosis of the hepatic artery, portal vein, inferior vena cava or hepatic veins, hepatic artery pseudoaneurysm, and arteriovenous fistulae [5, 10].

Hepatic artery thrombosis is the most significant complication as it is usually associated with graft failure due to biliary complications and early development of secondary biliary cirrhosis as the bile ducts are solely supplied by the hepatic artery. Mostly, hepatic artery thrombosis occurs in the early postoperative phase. Due to the small vessel size in infants and possible anatomical variations, for example, in heterotaxy syndromes, the occurrence of hepatic artery thrombosis is high with an estimated incidence of 2–12% [9].

Post-operative Doppler US has high sensitivity and specificity for the detection of hepatic artery thrombosis, but the inability to depict very low flow in a patent hepatic artery due to either a post stenotic tardus parvus pattern, an overlaying turbulent portal vein or reduced cardiocirculatory perfusion remains a challenge [11–14]. CEUS can ensure the diagnosis of patency in the hepatic artery in questionable cases (Fig. 9.1a, b).

CEUS is a safe, non-invasive and rapid tool to detect potential complications and to enable early intervention following liver transplantation. When necessary CEUS has been used off-label for identifying circulatory complications after liver transplantation in children [2, 3].

Cho et al. investigated the influence of ultrasound contrast agents (UCA) on spectral Doppler analysis in liver transplantation recipients. The measured velocities of graft hepatic vessels tended to increase after administration of UCA, but without statistical significance. The comparison of serial Doppler parameters with or without injection of UCA is valid during Doppler surveillance in liver transplantation recipients [15].

Portal vein thrombosis occurs in about 3% and is characterizes by a filling defect on B-mode, Doppler, or CEUS in the case of a partial thrombosis or a complete lack of enhancement in occlusion of the portal vein stem or the intrahepatic branches.

Thrombosis of the inferior vena cava or the hepatic veins is rarer than stenosis of the anastomotic sites, in our experience.

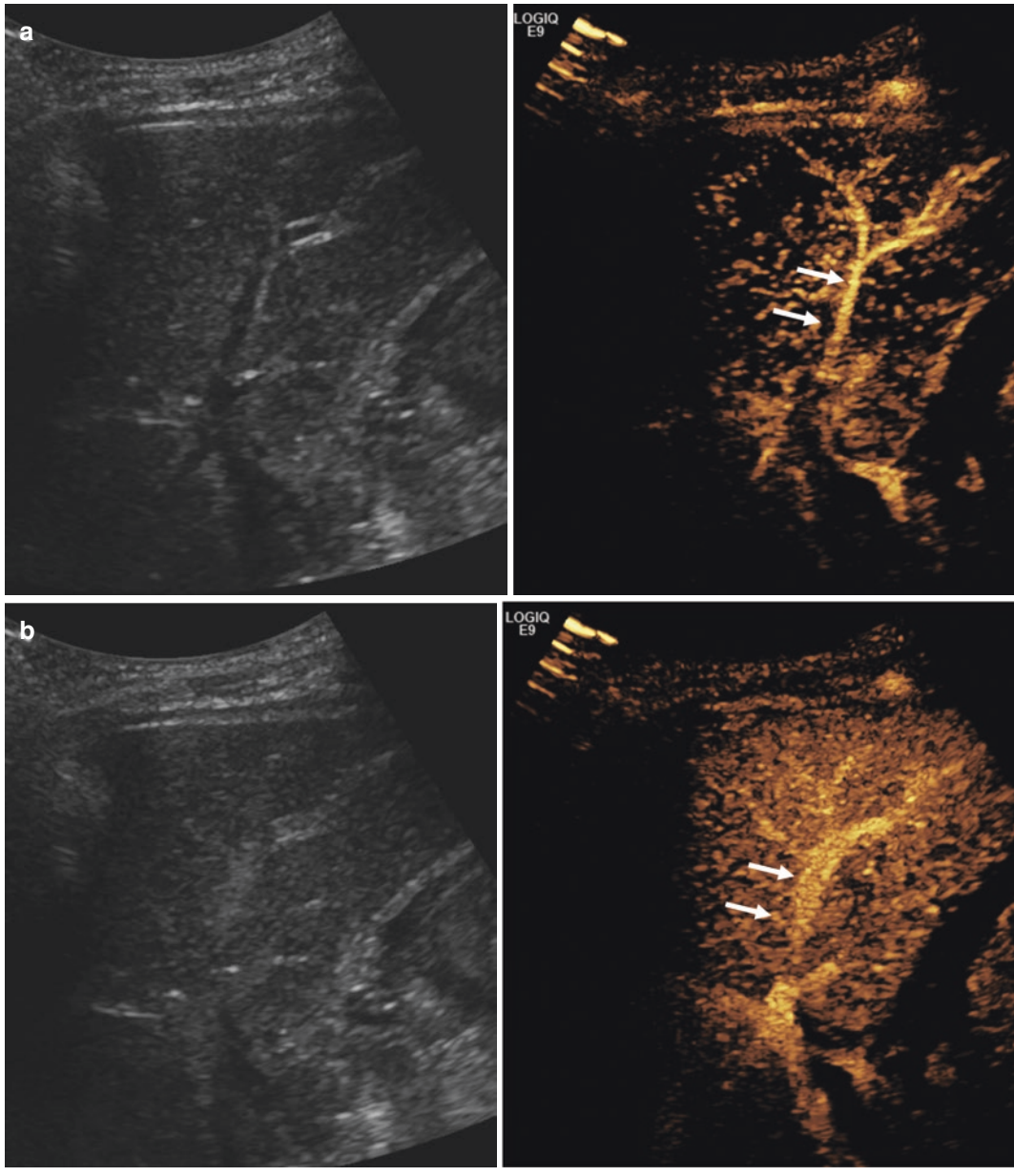

Fig. 9.1 (**a**) CEUS in a liver transplant patient (left lateral split liver) on the first day after the operation with questionable patency of the hepatic artery. Depiction of the hepatic artery 10 s post injection (arrows). The portal venous bed is still not enhancing. (**b**) Enhancement of the portal vein (arrows) and liver parenchyma 19 s post-injection

9.2.1 Biliary and other nonvascular complications

The biliary anastomoses are performed between the donor and recipient common bile duct in full-size liver transplantations and right lobe liver transplantations. In a left lateral split liver lobe transplantation, a Roux-Y hepatojejunostomy is performed. The gallbladder is always removed during transplantation. Biliary complications occur in about 10% and are usually seen in the early postoperative period (within in the first 3

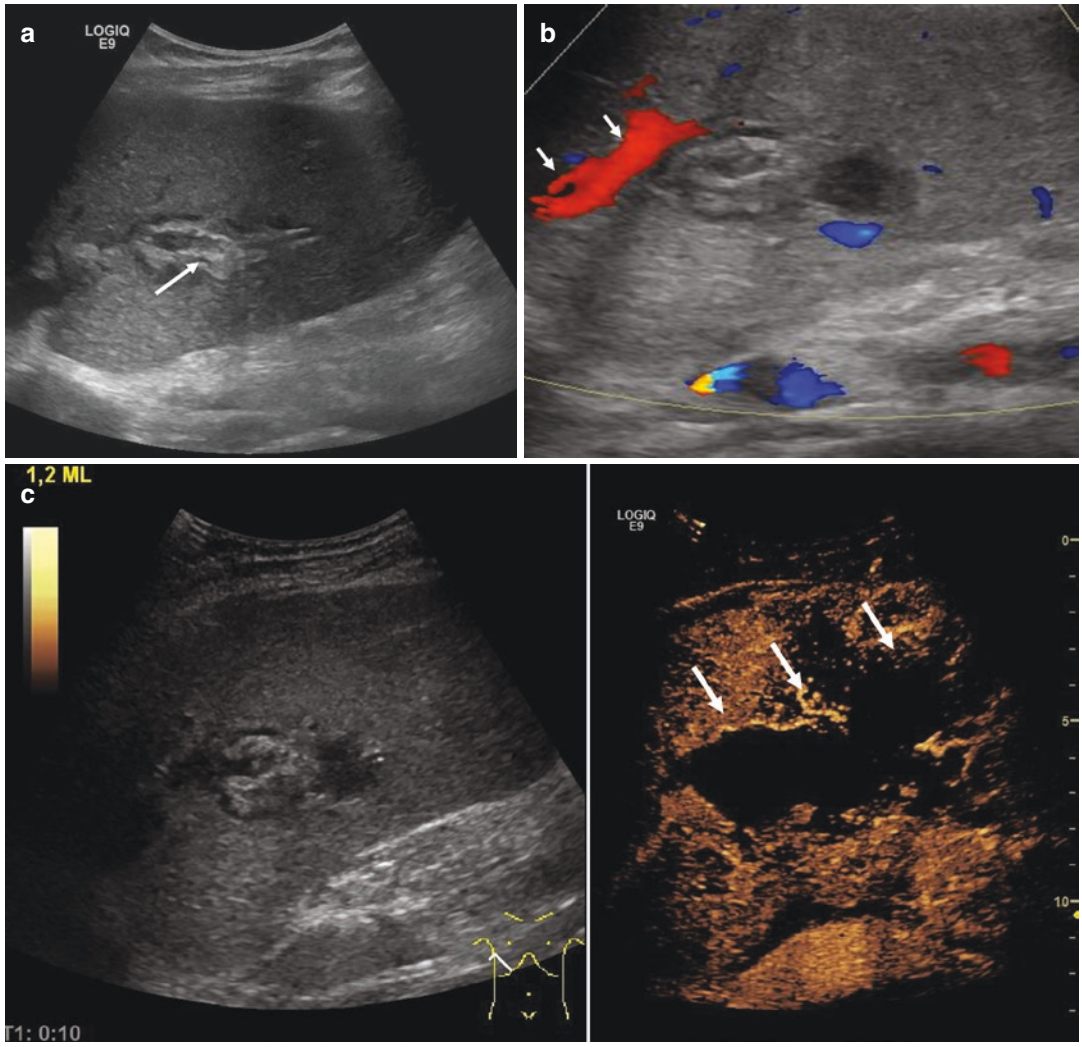

Fig. 9.2 Chologenic liver abscesses following an episode of severe cholangitis in a 14-year-old boy 7 years after left lateral split liver transplantation with Roux-Y-hepatojejunostomy. (**a**) B mode US imaging shows a broadened and inhomogeneous periportal area and dilated bile ducts (arrow). (**b**) Color Doppler US demonstrates that the portal vein and the hepatic artery are patent, with a focal area of altered reflectivity adjacent to the portal vein (arrows). (**c**) Contrast-enhanced ultrasonography (CEUS) demonstrates the real extent of the hepatic abscesses in association with the biliary tree, as intrahepatic areas of non-enhancement (arrows)

months), but may also present later due to recurrent cholangitis or inflammatory stenosis of the biliary system.

Biliary complications include obstruction due to anastomotic and non-anastomotic strictures, bile leak with biloma formation, recurrence of the primary disease (e.g., primary sclerosing cholangitis), infection, abscess formation, and development of intraductal stones (Fig. 9.2a–c). Peri-hepatic leaks (biloma) are often located along the resection site in split liver transplants. These bilomas may require an US-guided drainage or may resolve spontaneously.

Other complications are post-operative perihepatic *fluid collections*, which may be hematoma, seroma, or biloma.

More rare complications are abscesses due to cholangitis or systemic infections and post-transplant lymphoproliferative disease (PTLD).

Contrast-enhanced ultrasound may be useful in delineating non-vascularized areas, such as bile duct dilatation, biloma, or an abscess cavity considered for potential aspiration or catheter drainage.

9.3 Kidney transplanation

Similar to liver transplantation, early vascular complications in infants and young pediatric patients are more frequent than in adults because of the small vessel diameters [16]. Therefore, in small children, anastomosis of the donor renal artery and vein is usually performed with the recipient's aorta and inferior vena cava or common iliac vein. CEUS has a promising role in early and late imaging of vascular complications after renal transplantations such as thrombosis of renal vessels, patency of polar arteries, arteriovenous fistulas, pseudoaneurysm, renal artery stenosis, as well as in the characterization of indeterminate renal masses.

The lack of nephrotoxicity is a particular advantage in CEUS, particularly relevant in renal transplant patients.

After injection of UCA, three phases of enhancement are distinguished:

1. The cortical phase starts 8–14 s after UCA injection with initial intense enhancement in the renal cortex.
2. The medullary phase follows the cortical phase UCA enhancement, progressing from the outer to the inner aspects of the renal medullae.
3. In the late phase, UCA will disappear first from the medullae, later from the cortex. Due to the high renal perfusion, the transit time between renal artery enhancement and UCA arrival in the renal vein is very short, often in 2–3 s [17].

CEUS has been shown to be superior to Doppler US in the detection of renal artery stenosis, which is not unusual following renal transplantation, with an incidence of 5–10% [18]. With Doppler US, a high resistive index (RI) is associated with vascular complications. CEUS however reveals information about kidney allograft microvascular perfusion independent of the recipient's vascular compliance and may predict long-term allograft function [19, 20].

In children with delayed allograft function, vascular causes can be ruled out by Doppler US or if remaining uncertain, the addition of CEUS may help.

A frequent nonvascular complication after renal transplantation is pyelonephritis often associated with a clinical course of urosepsis, which max results in renal abscess formation (Fig. 9.3a–c). Contrast-enhanced ultrasound may help to delineate the abscess borders, and allow for percutaneous drainage.

9.4 Special indications and so on

9.4.1 Intra-Cavity CEUS

Intra-cavity CEUS can be performed in the same way as cholangiography via T-tube or nasobiliary line following liver transplantation [21]. Other indications for intra-cavitary CEUS include investigations for vesicoureteral reflux or urinary leakage after renal transplantation via a suprapubic or transurethral catheter. Furthermore, it is easy to control the position of drainage catheters using intra-cavitary CEUS. For all intra-cavitary investigations, only a very tiny amount of UCA diluted in sterile saline solution is necessary. It is important to use sterile solutions contained in plastic and not glass bottles, as glass can cause deactivation of the microbubbles.

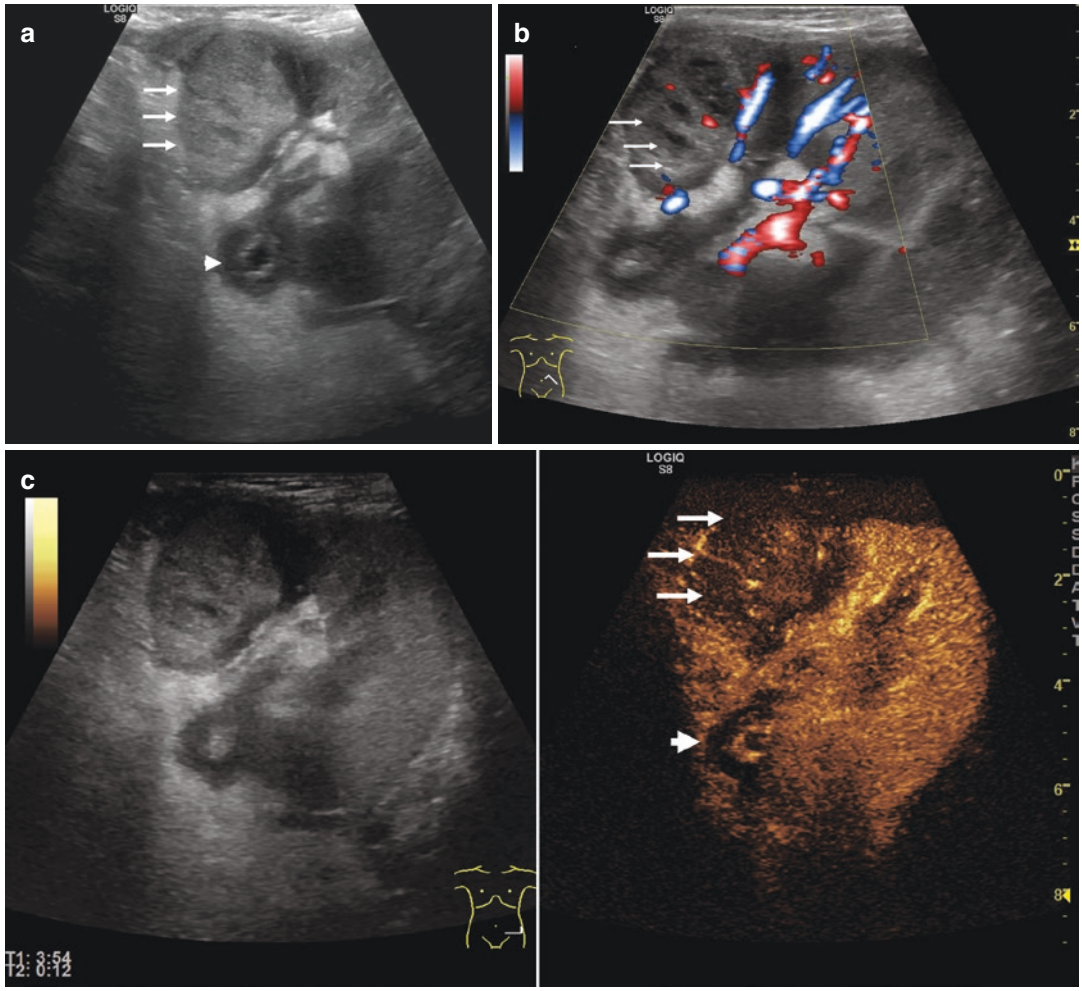

Fig. 9.3 (**a**) B-mode US image of a second renal transplant in the left fossa iliaca in a 12-year old boy with previous obstructive uropathy secondary to posterior urethral valves. On the first day of acute hospital admission with high fever, low blood pressure, and an overall poor clinical state. The US shows a massively increased total renal volume, swollen ureteral wall (arrowhead), and a hyperechoic ill-defined mass on the medial part of the kidney (arrows). (**b**) A color Doppler ultrasound image demonstrates an area of suspected decreased vascularization in the medial area (arrows) of an assumed renal transplant abscess. (**c**) Contrast-enhanced ultrasound (CEUS) reveals a roundish hypo-enhanced area of an early transplant abscess (arrows) and a markedly thickened hypoenhancing ureter (arrowhead) in the boy with transplant urosepsis

9.5 Gastrointestinal Graft Versus Host Disease (GvHD) After Stem Cell Transplantation

Acute gastrointestinal graft-versus-host disease (GvHD) is a life-threatening complication in patients after allogeneic stem cell transplantation. Weber et al. [22] suggested a score that comprised morphological and vascular changes using B-mode and Doppler sonography, changes of mural stiffness using compound elastography and dynamic microvascularization using CEUS. Contrast-enhanced ultrasound was found to be a promising, non-invasive tool for the diagnosis of acute gastrointestinal GvHD, Fig. 9.4a–c.

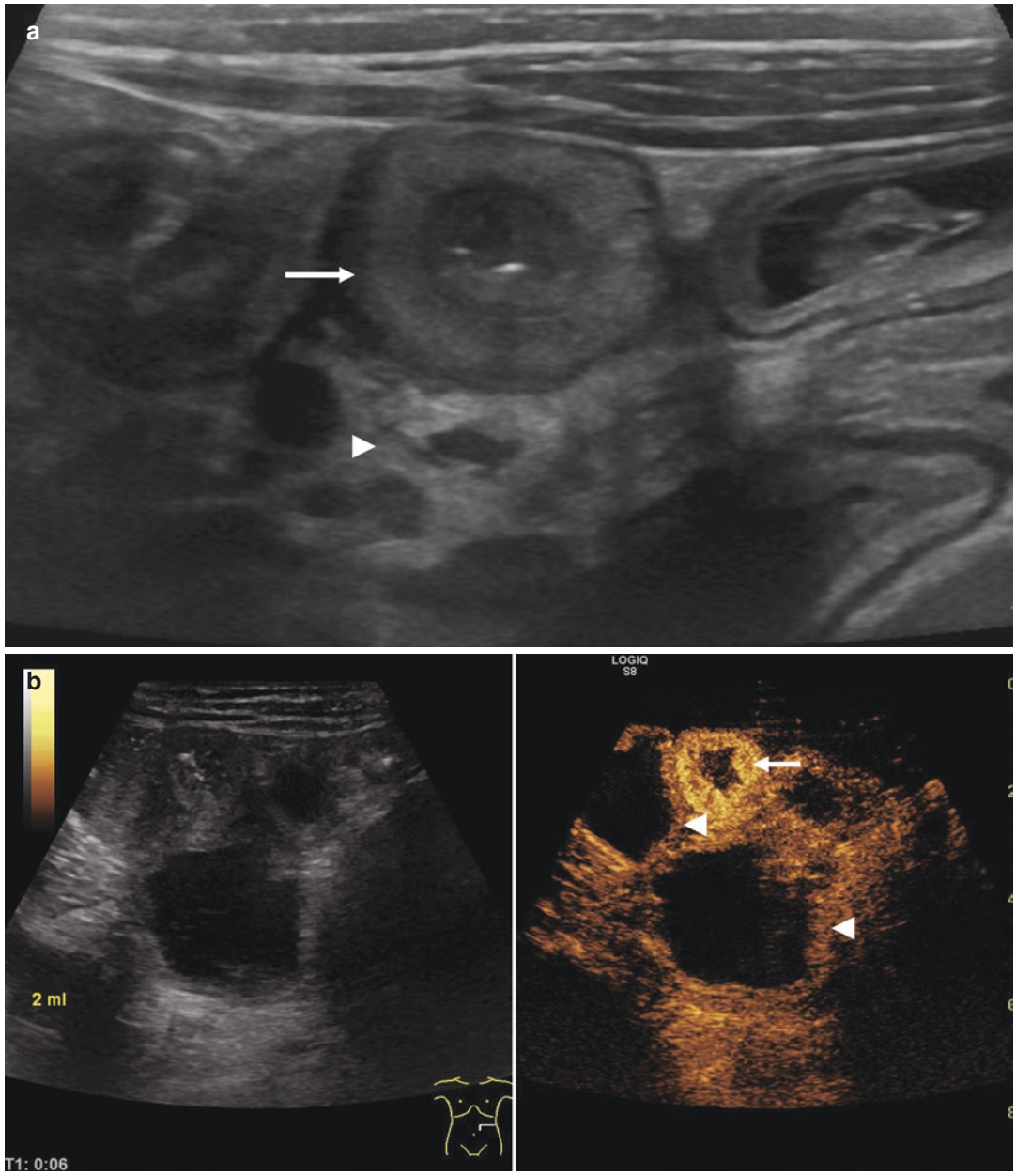

Fig. 9.4 Graft versus host disease (GVHD) of the small bowel. (**a**) Three-year-old boy with sickle-cell disease, 4 weeks following stem cell transplantation, presenting with profuse bloody diarrhea, inability to eat or drink, vomiting, and recurrent colicky abdominal pain. B mode US imaging demonstrates segmental small bowel wall thickening (arrow), increased echogenic reactivity of the fat surrounding the small bowel ("creeping fat," arrowhead), and bowel dilatation secondary to an increase in watery contents. (**b**) Contrast-enhanced ultrasound of the same segment of small bowel demonstrates patchy hyper-enhancement in the thickened segments, with wall thickening (arrow). The neighboring small bowel segments without wall thickening or hyperenhancement, but marked dilatation is also delineated (arrowheads). (**c**) Diagnosis of segmental inflammatory stenosis with marked dilatation of the proximal small bowel segment is much easier using CEUS compared to B-Mode US imaging (arrow). Inflammatory bowel stenosis can be distinguished from fibrotic stenosis by the presence of hyperenhancement of the stenotic bowel segment. Therefore, immunosuppressive and photopheresis treatment was continued

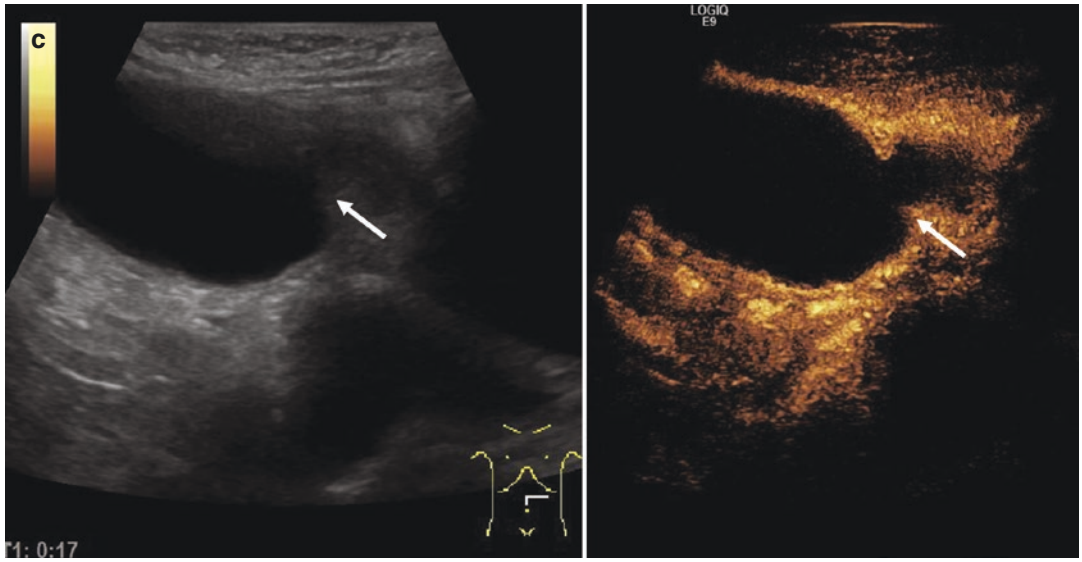

Fig. 9.4 (continued)

9.6 Post-Transplant Lymphoproliferative Disease (PTLD)

Post-transplant lymphoproliferative disease (PTLD) is a heterogeneous, potentially life-threatening condition, which shows a higher prevalence in children than in adults: the reported incidence after pediatric renal transplantation is 1–4% [16]. Early onset (<1 year post-transplantation) is common in young, Epstein–Barr virus (EBV), seronegative children during the high-dose immunosuppression phase of treatment and an EBV donor-recipient mismatch, resulting in an early high EBV viral load. PTLD treatment includes a reduction or even withdrawal of immunosuppressive therapy during chemotherapy and/or rituximab [23, 24]. PTLD location is frequently reported to be extranodal (81.3%) and mostly involved the gastrointestinal tract (68.8%) [25]. However, even a PTLD mass within a transplanted kidney has been described. After administration of UCA, the mass enhanced but with a persistent hypo enhancement throughout the examination [26]. PTLD may also be diagnosed in hyperplastic tonsils. During the therapy of PTLD, the possibility of acute or chronic rejection and even graft failure should have to be kept in mind [25].

References

1. Sidhu PS, Cantisani V, Deganello A, Dietrich CF, Duran C, Franke D, Harkanyi Z, Kosiak W, Miele V, Ntoulia A, Piskunowicz M, Sellars ME, Gilja OH. Role of contrast-enhanced ultrasound (CEUS) in paediatric practice: an EFSUMB position statement. Ultraschall Med. 2017;38(1):33–43. https://doi.org/10.1055/s-0042-110394. Epub 2016 Jul 14.
2. Teegen EM, Denecke T, Eisele R, Lojewski C, Neuhaus P, Chopra SS. Clinical application of modern ultrasound techniques after liver transplantation. Acta Radiol. 2016;57(10):1161–70. https://doi.org/10.1177/0284185116633910. Epub 2016 Feb 27.
3. Torres A, Koskinen SK, Gjertsen H, Fischler B. Clinical application of modern ultrasound techniques after liver transplantation. Contrast-enhanced ultrasound for identifying circulatory complications after liver transplants in children. Pediatr Transplant. 2019;23(1):e13327. https://doi.org/10.1111/petr.13327. Epub 2018 Dec 7.
4. Bonini G, Pezzotta G, Morzenti C, Agazzi R, Nani R. Contrast-enhanced ultrasound with SonoVue in the evaluation of postoperative complications in pediatric liver transplant recipients. J Ultrasound. 2007;10(2):99–106. https://doi.org/10.1016/j.jus.2007.02.008. Epub 2007 Jun 13.

5. Itri JN, Heller MT, Tublin ME. Hepatic transplantation: postoperative complications. Abdom Imaging. 2013;38(6):1300–33. https://doi.org/10.1007/s00261-013-0002-z.
6. Camacho JC, Coursey-Moreno C, Telleria JC, Aguirre DA, Torres WE, Mittal PK. Nonvascular post-liver transplantation complications: from US screening to cross-sectional and interventional imaging. Radiographics. 2015;35(1):87–104. https://doi.org/10.1148/rg.351130023.
7. Ma L, Lu Q, Luo Y. Vascular complications after adult living donor liver transplantation: evaluation with ultrasonography. World J Gastroenterol. 2016;22(4):1617–26. https://doi.org/10.3748/wjg.v22.i4.1617.
8. Ren J, Wu T, Zheng BW, Tan YY, Zheng RQ, Chen GH. Application of contrast-enhanced ultrasound after liver transplantation: current status and perspectives. World J Gastroenterol. 2016;22(4):1607–16. https://doi.org/10.3748/wjg.v22.i4.1607.
9. Singh AK, Nachiappan AC, Verma HA, et al. Postoperative imaging in liver transplantation: what radiologists should know. Radiographics. 2010;30(2):339. https://doi.org/10.1148/rg.302095124.
10. Luo Y, Fan YT, Lu Q, Li B, Wen TF, Zhang ZW. CEUS: a new imaging approach for postoperative vascular complications after right-lobe LDLT. World J Gastroenterol. 2009;15(29):3670–5.
11. Abdelaziz O, Attia H. Doppler ultrasonography in living donor liver transplantation recipients: intra- and post-operative vascular complications. World J Gastroenterol. 2016;22(27):6145–72. https://doi.org/10.3748/wjg.v22.i27.6145.
12. Hom BK, Shrestha R, Palmer SL, et al. Prospective evaluation of vascular complications after liver transplantation: comparison of conventional and microbubble contrast-enhanced US. Radiology. 2006;241(1):267–74.
13. Lee SJ, Kim KW, Kim SY, et al. Contrast-enhanced sonography for screening of vascular complication in recipients following living donor liver transplantation. J Clin Ultrasound. 2013;41(5):305–12. https://doi.org/10.1002/jcu.22044.
14. Berry JD, Sidhu PS. Microbubble contrast-enhanced ultrasound in liver transplantation. Eur Radiol. 2004;14(Suppl 8):P96–103.
15. Cho YS, Kim KW, Jang HY, Kim BH, Lee J, Song GW, Lee SG, Munkhbaatar D. Influence of ultrasound contrast agents on spectral Doppler analysis in recipients of liver transplantation. Clin Mol Hepatol. 2017;23(3):224–9. https://doi.org/10.3350/cmh.2016.0064. Epub 2017 Jul 4.
16. Nixon JN, Biyyam DR, Stanescu L, Phillips GS, Finn LS, Parisi MT. Imaging of pediatric renal transplants and their complications: a pictorial review. Radiographics. 2013;33(5):1227–51. https://doi.org/10.1148/rg.335125150.
17. Weskott H-P. Kidney. In: Weskott H-P, editor. Contrast-enhanced ultrasound. 2nd ed. Bremen: UNIMED Science; 2013. p. 152–4.
18. Pan FS, Liu M, Luo J, Tian WS, Liang JY, Xu M, Zheng YL, Xie XY. Transplant renal artery stenosis: evaluation with contrast-enhanced ultrasound. Eur J Radiol. 2017;90:42–9. https://doi.org/10.1016/j.ejrad.2017.02.031. Epub 2017 Feb.
19. Schwenger V, Hankel V, Seckinger J, Macher-Göppinger S, Morath C, Zeisbrich M, Zeier M, Kihm LP. Contrast-enhanced ultrasonography in the early period after kidney transplantation predicts long-term allograft function. Transplant Proc. 2014;46(10):3352–7. https://doi.org/10.1016/j.transproceed.2014.04.013.
20. Zeisbrich M, Kihm LP, Drüschler F, Zeier M, Schwenger V. When is contrast-enhanced sonography preferable over conventional ultrasound combined with Doppler imaging in renal transplantation? Clin Kidney J. 2015;8(5):606–14. https://doi.org/10.1093/ckj/sfv070. Epub 2015 Aug 8.
21. Chopra SS, Eisele R, Stelter L, Seehofer D, Grieser C, Warnick P, Denecke T. Contrast enhanced ultrasound cholangiography via T-tube following liver transplantation. Ann Transplant. 2012;17(4):108–12.
22. Weber D, Weber M, Hippe K, Ghimire S, Wolff D, Hahn J, Evert M, Herr W, Holler E, Jung EM. Noninvasive diagnosis of acute intestinal graft-versus-host disease by a new scoring system using ultrasound morphology, compound elastography, and contrast-enhanced ultrasound. Bone Marrow Transplant. 2018;54:1038. https://doi.org/10.1038/s41409-018-0381-4 [Epub ahead of print].
23. Simakachorn L, Tanpowpong P, Lertudomphonwanit C, Anurathapan U, Pakakasama S, Hongeng S, Treepongkaruna S, Phuapradit P. Various initial presentations of Epstein-Barr virus infection-associated post-transplant lymphoproliferative disorder in pediatric liver transplantation recipients: case series and literature review. Pediatr Transplant. 2019;23(2):e13357. https://doi.org/10.1111/petr.13357. Epub 2019 Jan 20.
24. Mendogni P, Henchi S, Morlacchi LC, Tosi D, Nosotti M, Tarsia P, Gregorini AI, Rosso L. Epstein-Barr virus-related post-transplant lymphoproliferative disorders in cystic fibrosis lung transplant recipients: a case series. Transplant Proc. 2019;51(1):194–7. https://doi.org/10.1016/j.transproceed.2018.05.032. Epub 2018 Jun 30.
25. Hsu CT, Chang MH, Ho MC, Chang HH, Lu MY, Jou ST, Ni YH, Chen HL, Hsu HY, Wu JF. Post-transplantation lymphoproliferative disease in pediatric liver recipients in Taiwan. J Formos Med Assoc. 2019;118:1537–45. pii: S0929-6646(18)30009-3. https://doi.org/10.1016/j.jfma.2018.12.023 [Epub ahead of print].
26. Lampe A, Duddalwar VA, Djaladat H, Aron M, Gulati M. Contrast-enhanced ultrasound findings of post-transplant lymphoproliferative disorder in a transplanted kidney: a case report and literature review. J Radiol Case Rep. 2015;9(10):26–34. https://doi.org/10.3941/jrcr.v9i10.2602. eCollection 2015 Oct.

Blunt Abdominal Trauma in Children: Clinical Perspective

10

Erica Makin

10.1 Introduction

Trauma is the leading cause of death in children aged more than 1 year in the United Kingdom. The predominant cause of mortality is traumatic brain injury. The highest case fatality rates are seen in asphyxia (71%) followed closely by drowning (58%). Approximately half (2 million) of all pediatric attendances to the emergency department in a year are due to an injury. Major trauma in childhood is commonest within the first year of life, the first 3 months of life having the highest incidence of non-accidental injury (accounting for 10% of all major trauma in childhood). Mortality due to isolated abdominal trauma is <5%, but raises to 14% when seen in conjunction with chest injuries, and again rising to 20% when combined with head trauma (i.e., with polytrauma) [1].

10.2 Incidence

Significant intra-abdominal injury occurs in approximately 12% of children admitted following trauma. Isolated abdominal injury is common in children (>60% cases) and has a low mortality at 2%, but when combined with head or thoracic injury, the mortality rises steeply to 20% [1].

10.3 Etiology and Patterns of Injury

Blunt force trauma is by far the commonest modality of injury in children (90%). However, this is skewed in areas of high interpersonal violence where penetrating trauma in children/adolescents is rising and accounts for up to 27% of all pediatric trauma victims. A detailed history of the mechanism of injury is essential, including accurate timelines. The commonest mechanism of injury is road traffic collisions (RTC), at 40% [1]. Table 10.1 highlights the distribution of the mechanism of trauma in children. The highest casualty rates in RTC are seen in pedestrians/cyclists rather than children correctly restrained within the vehicle. The possibility of non-accidental injury should always be considered if there is any inconsistency between the history and the nature of the injuries sustained.

The anatomy of the child, including a large head and pliable skeleton means that even relatively minor degrees of force can result in significant internal injury. Solid organs are more vulnerable to the effects of blunt trauma in children than in adults. Intra-abdominal organs are more exposed due to a wider more rotund abdominal cavity. The liver, spleen, and bladder

E. Makin (✉)
Department Pediatric Surgery, King's College Hospital, London, UK
e-mail: Erica.makin@nhs.net

P. S. Sidhu et al. (eds.), *Contrast-Enhanced Ultrasound in Pediatric Imaging*,
https://doi.org/10.1007/978-3-030-49691-3_10

Table 10.1 Mechanism of injury

	Mechanism	Incidence
Blunt trauma	Road traffic collisions	40%
	Falls height <2 m	20%
	Falls height >2 m	10%
	Blunt assault	10%
	Burns/scalds	<5%
	Asphyxia/drowning	<5%
Penetrating trauma	Geographical variation, London highest	<5–27%

are proportionally less protected by the incompletely ossified rib cage and lower pelvis than in adults and therefore more at risk to injury. Compression injuries (e.g., handlebar or seatbelt injuries) can also result in intestinal perforation and pancreatic injury. Deceleration forces from falls or RTC may cause mesenteric or great vessel tears. Bladder and urethral injuries are rare but may occur with pelvic trauma, even in the absence of obvious fractures. Abdominal injury in children <18 months of age should raise suspicion of non-accidental injury, particularly with latent pancreatic injury presentations.

10.4 Staging and Grading of Traumatic Injuries

Individual injuries are classified according to the Abbreviated Injury Scale (AIS), which in turn translates into an overall Injury Severity Score (ISS), calculated as a value between 0 and 75. In children, major trauma is classified as an ISS >15 and the most severely injured children will have an ISS >25 [2]. A more detailed staging of injury severity and prediction of outcome is the probability of survival (PS). The first version was described in 1984 in the United States using a Trauma Injury Severity Score (TRISS), calculated from the Revised Trauma Score, ISS, age, and method of injury (blunt/penetrating). The European model generated by the Trauma Audit Research Network (TARN) in 2004 included parameters of age, gender, ISS, and Glasgow Coma Scale (GCS). This model has now been recalibrated in 2019 (Ps19) to include comorbidities and true 30 day outcomes [3].

Solid organ injuries are classified according to their grade based on radiological findings on initial computed tomography (CT) imaging. This was developed by the American Association of the Surgery of Trauma (AAST) in 1987. This grading system has been used to guide non-operative management (NOM) of blunt abdominal trauma for 20 years [4]. However, this approach has not been adopted worldwide due to concerns regarding the scarcity of post-injury follow-up imaging.

10.5 Assessment and Damage Control Resuscitation

10.5.1 Immediate Clinical

Physiological changes start to happen at the point of trauma, resuscitation and management need to be directed by this. The deadly triad of acidosis, hypothermia, and coagulopathy begin immediately and the resulting acute traumatic coagulopathy can be fatal. Adult data demonstrate that if a patient arrives in the emergency department already coagulopathic, mortality is 40% within the first 24 h. In trauma, hypovolemia secondary to blood loss is the likely cause and so the principle that the "first clot is the best clot" is paramount. The estimated circulating blood volume of a child is 80 mL/kg. Recommendations are to commence with 5 mL/kg fluid resuscitation, if the child is obviously bleeding this should be packed cells, if not then crystalloid can be used. Any further fluid resuscitation should be in alignment with your hospital's Major Hemorrhage Protocol—i.e., packed cells, fresh frozen plasma (FFP)/Octaplas in people under 18 years, which is irradiated FFP and platelets in as close to a 1:1:1 ratio as possible. Tranexamic acid 15 mg/kg within the first 3 h. Second dose tranexamic acid considered after 8 h [5]. Once stabilized, maintenance fluids should be given separately and should include 5% dextrose (especially important in infants).

10.5.2 Investigations

An accurate history is essential as this may dictate investigations, imaging, and treatment pathways as well as being crucial for safeguarding the child. Careful examination (observation and re-examination) is vital in assessing the possibility of injury. Abnormal physiological parameters, tenderness, bruising, or distension should be considered evidence of injury until proven otherwise. Hematuria (microscopic or macroscopic) should lead to further investigation of the urinary tract. Pancreatic injuries may present late so an initial amylase and lipase at time of presentation should be requested although normal levels do not exclude pancreatic injuries, it can however be helpful as a serial marker for injury progression.

10.5.3 Radiological Imaging

The gold standard imaging for abdominal trauma remains the contrast-enhanced CT (CECT) when clinically indicated. However, due to increasing concern regarding irradiation in children, guidelines from the Royal College Radiologists have been drawn up to help minimize the use of CECT in pediatric trauma [6]. Recent publications from the Pediatric Emergency Care Applied Research Network (PECARN) propose a predictive rule to identify children with blunt abdominal trauma who are at low risk for clinically important intra-abdominal injury in whom CECT may be avoided [7, 8].

10.5.4 FAST Scan

Focused abdominal sonography for trauma (FAST) was first described in adults in the early 1970s. Initially it was used to assess free fluid within the abdomen (Morrison's and splenorenal pouch, pelvis) and, latterly extended to looking for fluid in the pericardium and pleural cavity. The primary goal of a FAST scan is to identify free intra-peritoneal fluid, which is inferred as a hemo-peritoneum and thus associated with an intra-abdominal injury. The volume of free fluid within the abdomen required for a positive FAST is in the region of 400 mL [9].

It is recognized that the sensitivity of FAST in detecting recognized that the sensitivity of FAST in detecting intra-abdominal injury (IAI) is low, ranging from 23% to 75% [10–13]. The specificity is higher at 80–98% [12, 13], with marginal negative predictive values (0.50), which have lead the majority to interpret a negative FAST scan as adding little to the decision-making process for detecting an intra-abdominal injury. The more worrying consequence of this is that "missed" injuries on a FAST scan may not be detected if not also subsequently screened for by conventional CECT. Taylor and Sivit found that 37% of intra-abdominal injuries were missed on FAST scan [14]. A negative FAST scan may provide false reassurance and should be viewed with caution. FAST scans are currently seen as a "rule in" diagnostic tool. A positive FAST scan is likely to infer significant intra-abdominal injury IAI. Conversely, a positive FAST scan may not always be indicative of bleeding. Perhaps when faced with a hemodynamically unstable child with a positive FAST scan, the presumption would be that there is ongoing active bleeding requiring urgent intervention either with interventional radiology or trauma laparotomy. However, it must not be forgotten that hollow viscus injuries can also occur and free fluid may be the result of intestinal/biliary fluid within the abdominal cavity. A recent randomized controlled trial looking at the effectiveness of FAST scanning on clinical care and outcomes did not support the routine use of FAST scanning in the pediatric population in detecting an intra-abdominal injury [15]. However, the extended FAST scan (eFAST) also looks at the pericardium and pleural cavity for pericardial tamponade/assessment of cardiac contractility. Ultrasound is useful in detecting and acts as a guide to percutaneous chest drain insertion for the treatment of hemo/pneumothoraces, and therefore should not be abandoned completely.

10.5.5 Clinical Management

Non-operative management can be achieved in more than 90% of blunt abdominal trauma in

children [16]. Since the publication of the ATOMAC guidelines, most centers are moving away from using the CECT grade of the injury alone to dictate non-operative management protocols. A more physiological assessment to guide length of stay, intensive care admission, and periods of bed rest is now recommended [17, 18].

10.6 Splenic Trauma

The mainstay for splenic trauma is non-operative management [19, 20]. Traditionally a splenectomy would have been more common place in managing high-grade splenic injuries in an unstable patient. Upadhyaya and Simpson [21] first reported their successful non-operative management of pediatric splenic trauma in 1968. Pediatric practice has led the way in conservative management resulting in many more children retaining splenic immunological function and therefore reducing the morbidity associated with asplenism (Figs. 10.1 and 10.2). An alternate approach to bleeding in the unstable patient is splenic artery embolization (Fig. 10.3). This has been shown to be safe and has increased the success rate of non-operative management of splenic trauma to 98% [22–24]. Recent guidelines from the UK TARN office require the Major Trauma Centers to be able to provide interventional radiology services for pediatric trauma. Complications associated with embolization include unwanted ischemia resulting in functional asplenism, which can be further complicated by abscess formation. Other rare complications include post embolization syndrome, which comprises abdominal pain, nausea, ileus, and fever. This is usually self-limiting. Less frequent complications include reactive pleural effusions, pneumonia, and embolization coil migration [22, 24, 25]. If embolization is unsuccessful and the patient remains unstable then trauma laparotomy is required. A total splenectomy may be required, but if some splenic tissue can be preserved then this is optimal.

Delayed complications that can occur include pseudocyst formation, pseudoaneurysms, abscesses, and delayed splenic rupture. Delayed splenic rupture although rare is perhaps the most severe with an incidence of up to 0.33%. This tends to occur from 4 to 28 days post injury [19, 26] and is felt to be due to rupture of capsular hematomas or pseudoaneurysms.

Pseudoaneurysms form following injury to an arterial wall resulting in leakage of blood, usually into a contained cavity (Figs. 10.1, 10.2, and 10.3). Communication with the arterial lumen is maintained, but this produces a pressure cavity with risk of life-threatening rupture. Studies using Doppler ultrasound as screening for a pseudoaneurysm post trauma show a splenic PA incidence of 5.4% [27]. Our institution routinely screens for a pseudoaneury sms using contrast-enhanced ultrasound at 5–7 days post injury. In the splenic cohort, the incidence of a pseudoaneurysm is 9% [28]. It would appear from our experience that a splenic pseudoaneurysm perhaps does have a more indolent course, with only one splenic pseudoaneurysm becoming symptomatic and requiring embolization over a 10-year study period. In addition, asymptomatic pseudoaneurysms (splenic and liver) appear to thrombose/resolve at a median of 1.7 (0.7–4.9) weeks post injury.

Fig. 10.1 Post-contrast CT examination performed during the arterial phase on a 17-year-old boy following a sports injury, shows a grade IV splenic traumatic lesion with two pseudoaneurysms (arrows) at day 5 post injury

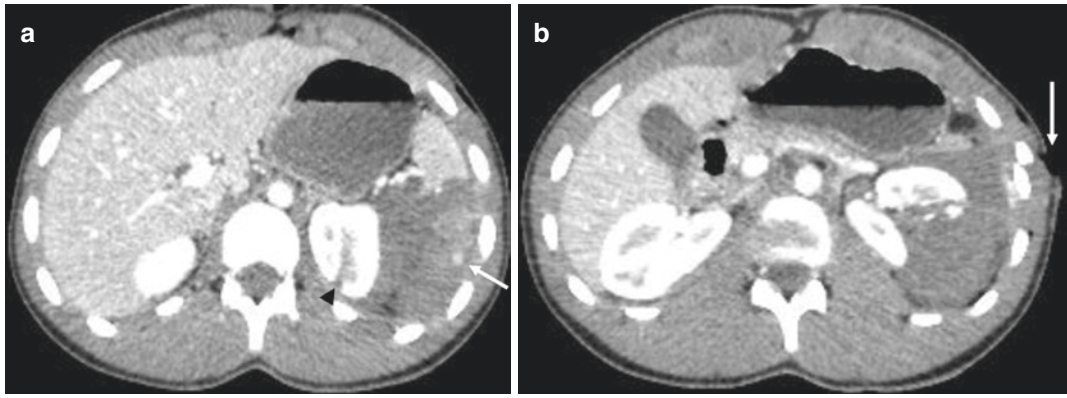

Fig. 10.2 A CT examination performed during the arterial phase on a 16-year-old boy with stabbing injuries. (**a**) The CT demonstrates a grade IV splenic and renal (arrowhead) lacerations with surrounding hematoma. There is active hemorrhage from the splenic artery (arrow). (**b**) The CT examination also indicates the stabbing entry wound on the skin (arrow)

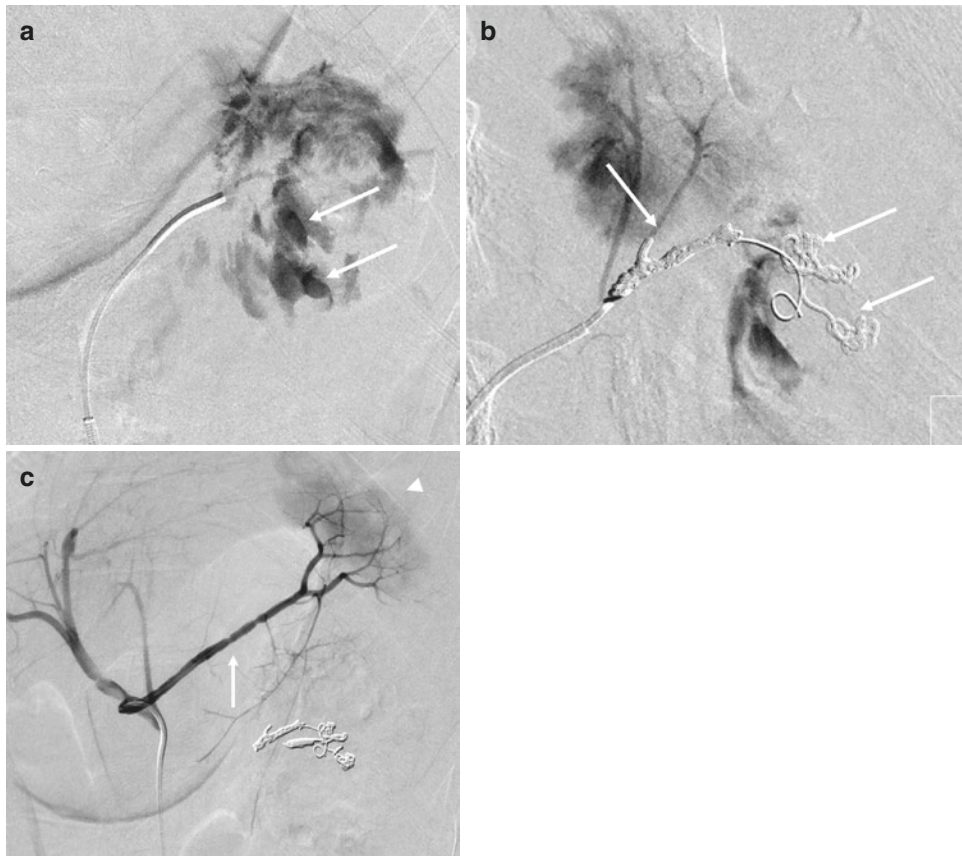

Fig. 10.3 The patient as in Fig. 10.2, is managed by interventional radiology with digital subtraction angiography and coil embolization. (**a**) Selective catherization of the splenic artery, with angiography images confirming active extravasation of contrast (arrows). (**b**) Selective coil embolization of a lower pole branch of the splenic artery, at multiple sites, was performed (arrows). (**c**) Post-procedural angiography of the coeliac axis confirms satisfactory embolization with cessation of hemorrhage, but with preservation of the upper pole branch of the splenic artery (arrow) with contrast blush of splenic preservation (arrowhead)

10.7 Liver Trauma

Injury to the liver occurs in up to 30% of blunt abdominal trauma and in the most part can be managed conservatively. The majority of cases will have raised transaminases aspartate aminotransferase (AST) and alanine aminotransferase (ALT) on admission which are released from damaged hepatocytes. There appears to be direct correlation with grade of injury and level of raised transaminases [29]. The gold standard imaging for hepatic trauma at initial presentation remains the CECT (Fig. 10.4). However, in certain cases of isolated abdominal trauma even if the patient is hemo-dynamically unstable, CEUS may be adequate. Similarly, as with splenic trauma, if there is active bleeding at presentation associated with physiological instability, then embolization should be considered prior to trauma laparotomy to reduce morbidity and mortality.

It is important to be aware of the complications of liver trauma and to actively look for them. With respect to a pseudoaneurysm, historically the incidence of hepatic PA was felt to be low, at 1.7% when assessed using Doppler ultrasound techniques [27]. With the use of CEUS, this incidence dramatically increases to 25% in liver trauma. In distinction to the splenic pseudoaneurysm, 40% of the liver pseudoaneurysms became symptomatic at a median of 7 (3–11) days post injury. These can be treated successfully with embolization with no deleterious effects [28]. It is felt that liver pseudoaneurysms are more volatile due to their occurrence deep within the parenchyma, particularly when the hepatic injury is related to the porta hepatis in conjunction with a bile leak (Fig. 10.5).

Fig. 10.4 A CT examination performed during the arterial phase in a 16-year-old boy with multiple stabbing injuries. The CT demonstrates a grade V liver laceration with intrahepatic (short arrows) and subcapsular (long arrows) hematomas. There is also a small pseudoaneurysm of the hepatic artery (arrowhead)

The second commonest complication following hepatic trauma is that of an intrahepatic biloma, peritoneal bile leak, and hemobilia. The mainstay of management of traumatic bile leaks is with endoscopic retrograde cholangiopancreatography (ERCP), transampullary biliary stenting with or without intraperitoneal drainage of any fluid collection to prevent infection. Complications of stent migration and biliary duct strictures can be managed successfully with repeated stenting, endoscopic dilatation, or open biliary reconstruction [30, 31].

10.8 Pancreatic Trauma

The incidence of pancreatic trauma is <2% and is most commonly seen when the body of the pancreas is compressed against the spinal column, most typically seen in handlebar injuries [32]. Diagnosis of pancreatic injuries can be challenging. Serum amylase/lipase is non-specific and may not always be raised even in the presence of ductal injury [33]. Due to the retroperitoneal position of the pancreas ultrasound imaging can difficult. A CEUS examination has been demonstrated to detect pancreatic injuries, including ductal injuries, but more detailed analysis is achieved by CECT or magnetic resonance cholangiopancreatography (MRCP) to delineate ductal anatomy [34]. Complications following pancreatic trauma are usually associated with ductal injury and include pseudocysts, fistula formation, intraperitoneal fluid collections/infections, strictures, and pleural effusions. If diagnosis and management are delayed, then the morbidity and mortality may increase to as high as 26% and 5%, respectively [35]. From personal

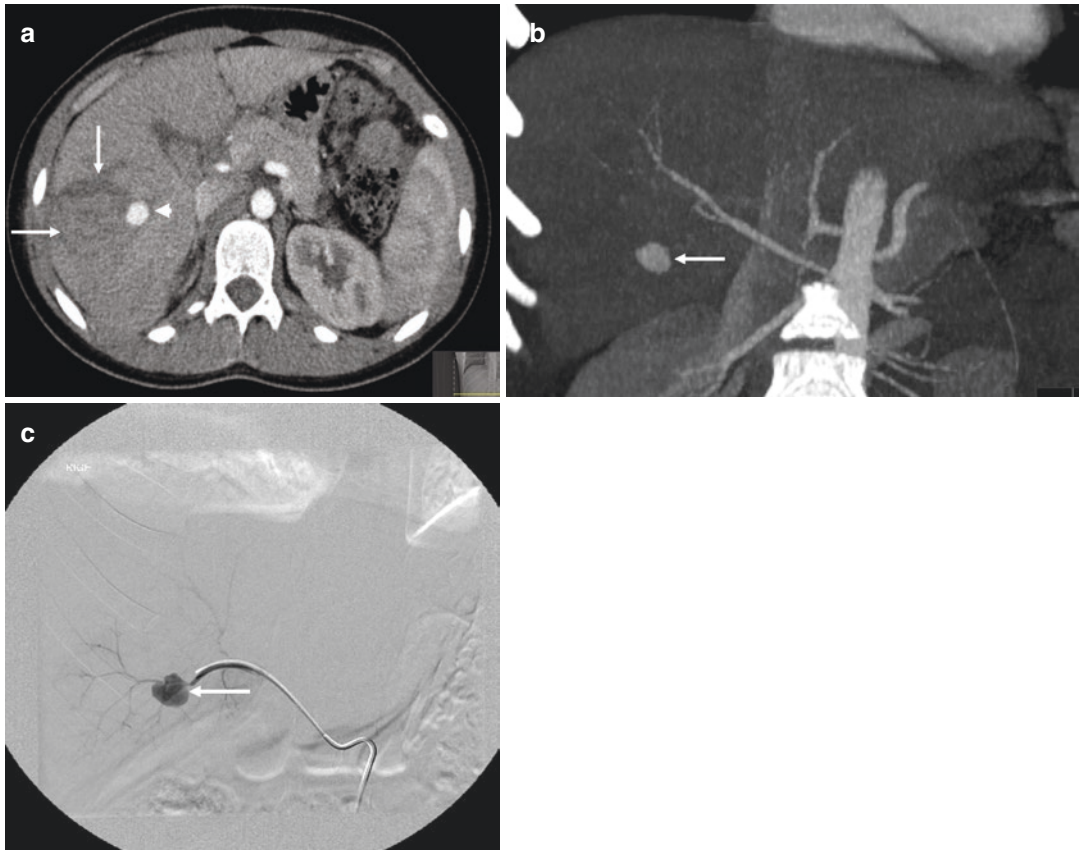

Fig. 10.5 A 14-year-old girl who was kicked by a horse. (**a**) An arterial phase CT examination reveals a grade 4 liver laceration (long arrows) with a large pseudoaneurysm of the hepatic artery (arrowhead). (**b**) A CT coronal maximum intensity projection (MIP) of the liver confirms the presence of a pseudoaneurysm in segment 6 (arrow). (**c**) The diagnostic arteriogram demonstrates that the traumatic pseudoaneurysm (arrow) is arising from the segment VI division of the hepatic artery, taking origin from the accessory right hepatic artery from the superior mesenteric artery

experience consideration of early (<48 h post injury) distal pancreatectomy with or without an early ERCP and transampullary stenting (within 7 days) appears to reduce the morbidity, increase time to enteral feeds, and reduce length of hospital stay (Fig. 10.6).

10.9 Renal Trauma

Kidneys are at an increased risk of trauma in children when compared to adults due to their lower position within the abdominal cavity and less protective perirenal fat. The majority will have hematuria (microscopic), however, Ishida et al. report a 17% normal urinalysis rate in renal trauma patients and therefore urinalysis cannot be exclusively relied upon as a screening mechanism [36]. Initial assessment is usually by CECT and non-operative management is achieved in 98% of cases [36]. In cases of hemo-dynamic instability and active bleeding, embolization can be considered. If surgery is required, renal parenchymal sparing surgery can be attempted. A CEUS examination has been shown to accurately diagnose renal pathology in the acute phase

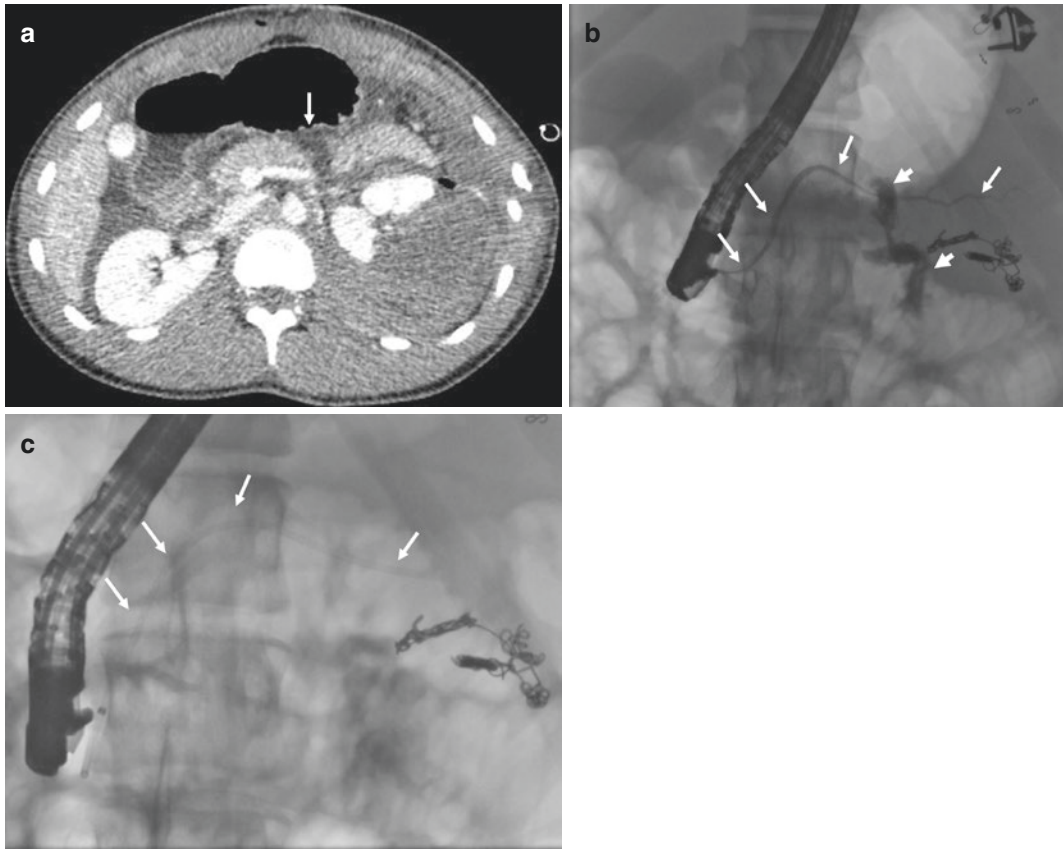

Fig. 10.6 The patient from Fig. 10.2, 16-year-old stabbing injury with a pancreatic transection. (**a**) The portal venous phase CT examination demonstrates a pancreatic transection (arrow). (**b**) The patient underwent an endoscopic retrograde cholangio pancreatography (ERCP) and cannulation of the pancreatic duct (arrows), with contrast injection demonstrating a pancreatic leak at the site of the transection (arrowheads). (**c**) A pancreatic stent (arrows) was placed in the pancreatic duct, across the transection plane, to control the continuing pancreatic duct leak

[37, 38]. In addition, CEUS is used as follow-up imaging to assess for pseudoaneurysms. The benefits of the agents used in a CEUS examination are that they are not nephrotoxic and therefore favored over CECT with the nephrotoxic iodinated agents used. The disadvantage of an ultrasound contrast agent is related to the mode of excretion, it is not renally excreted and therefore injury to the renal collecting system cannot be visualized [34]. Complications following renal trauma include pseudoaneurysm formation and urinoma, which can be managed by percutaneous drainage, with or without an endoscopic insertion of a double J stent.

10.10 Summary CEUS in Abdominal Trauma

CEUS has been shown to be superior to ultrasound for detecting solid organ injury with a sensitivity, specificity, positive predictive value, negative predictive value, and accuracy of 100%, 100%, 100%, 100%, and 100% for CEUS vs 38.8%, 100%, 100%, 12.8%, and 44% for ultrasound [39]. CEUS is reported to be almost as accurate at diagnosing solid organ injuries in the acute setting as CECT. It is essential for follow-up imaging to provide evidence of traumatic injury resolution and identification of complica-

tions such as PAs. This aids in streamlining the management plan for the children [34]. CEUS achieved high sensitivity (92.2%), specificity (100%), negative predictive value (100%), and positive predictive value (93.8%) in detecting solid organ injury at the initial presentation to the emergency department and may be able to replace CECT for intra-abdominal injury assessment in both the stable and unstable patient depending on user availability [40]. However, in cases of polytrauma, it remains prudent to obtain a CECT as first-line imaging.

References

1. Trauma Audit and Research Network (TARN). Severe injury in children 2015–16 report. https://www.tarn.ac.uk>content>downloads> Severe Injury in Children 15–16.
2. www.tarn.ac.uk>TheInjurySeverityScore–ISS.
3. www.tarn.ac.uk>TARN–PS.
4. Stylianos S, The APSA Committee. Evidence based guidelines for resource utilization in children with isolated spleen and liver injury. J Pediatr Surg. 2000;35:164–7.
5. Harris T, Davenport R, Mak M, Brohi K. The evolving science of trauma resuscitation. Emerg Med Clin North Am. 2018;36(1):85–106. Review. https://doi.org/10.1016/j.emc.2017.08.009.
6. Paediatric trauma imaging guidelines. www.rcr.ac.uk>field_publication_files>BFCR(14)8_paeds_trauma.
7. Holmes JF, Lillis K, Monroe D, et al. Identifying children at very low risk of clinically important blunt abdominal injuries. Ann Emerg Med. 2013;62:107–16.
8. Springer E, Barron Frazier S, Arnold DH, Vukovic AA. External validation of a clinical prediction rule for very low risk pediatric blunt abdominal trauma. Am J Emerg Med. 2019;37:1643–8.
9. Branney SW, Wolfe RE, Moore EE, et al. Quantitative sensitivity of ultrasound in detecting free intraperitoneal fluid. J Trauma. 1995;39:375–80.
10. Skerritt C, Haque S, Makin E. Focused assessment with sonography in trauma (FAST) scans are not sufficiently sensitive to rule out significant injury in pediatric trauma patients. Open J Pediatr. 2014;4:236–42.
11. Scaife ER, Rollins MD, Barnhart DC, et al. The role of focused abdominal sonography for trauma (FAST) in pediatric trauma evaluation. J Pediatr Surg. 2013;48:1377–83.
12. Fox JC, Boysen M, Gharahbaghian L, et al. Test characteristics of focused assessment of sonography for trauma for clinically significant abdominal free fluid in pediatric blunt abdominal trauma. Acad Emerg Med. 2011;18:477–82.
13. Holmes JF, Gladman A, Chang CH. Performance of abdominal ultrasonography in pediatric blunt trauma patients: a meta-analysis. J Pediatr Surg. 2007;42:1588–94. Review.
14. Taylor GA, Sivit CJ. Post traumatic fluid: is it a reliable indicator of intra-abdominal injury in children? J Pediatr Surg. 1995;30:1644–8.
15. Holmes JF, Kelley KM, Wooton-Gorges SL, et al. Effect of abdominal ultrasound on clinical care, outcomes, and resource use among children with blunt torso trauma. JAMA. 2017;317:2290–6.
16. Koyoma T, Skattum J, Engelsen P, Eken T, Gaardner C, Naess PA. Surgical intervention for paediatric liver injuries is almost history—a 12-year cohort from a major Scandanavian trauma centre. Scand J Trauma Resusc Emerg Med. 2016;29:139.
17. Notrica DM, Eubanks JW, Tuggle DW, et al. Nonoperative management of blunt liver and spleen injury in children: evaluation of the ATOMAC guidelines using GRADE. J Trauma Acute Care Surg. 2015;79:683–93.
18. Cunningham AJ, Lofberg KM, Krishnaswami S, et al. Minimizing variance in care of pediatric blunt solid organ injury through utilization of a hemodynamic-driven protocol: a multi-institution study. J Pediatr Surg. 2017;52:2026–30.
19. Jen HC, Tillou A, Cryer HG 3rd, Shew SB. Disparity in management and long-term outcome of pediatric splenic injury in California. Ann Surg. 2010;251(6):1162–6.
20. Martin K, VanHouwelingen L, Bütter A. The significance of pseudoaneurysms in the nonoperative management of pediatric blunt splenic trauma. J Pediatr Surg. 2011;46:933–7.
21. Upadhyaya P, Simpson JS. Splenic trauma in children. Surg Gynecol Obstet. 1968;126:781–90.
22. Skattum J, Gaarder C, Naess PA. Splenic artery embolization in children and adolescents—an 8 year experience. Injury. 2014;45:160–3.
23. Sweed Y, Singer-Jordan J, Papura S, Loberant N, Yulevich A. Angiographic embolization in pediatric trauma. IMAJ. 2016;18:665–8.
24. Kiankhooy A, Sartorelli KH, Vane DW, Bhave AD. Angiographic embolization is safe and effective therapy for blunt abdominal solid organ injury in children. J Trauma. 2010;68:526–31.
25. Coccolini F, Montori G, Catena F, et al. Splenic trauma: WSES classification and guidelines for adult and pediatric patients. World J Emerg Surg. 2017;12:40. https://doi.org/10.1186/s13017-017-0151-4.
26. Davis DA, Fecteau A, Himidan S, et al. What's the incidence of delayed splenic bleeding in children after blunt trauma? An institutional experience and review of the literature. J Trauma. 2009;67:573–7.
27. Safavi A, Beaudry P, Jamieson D, et al. Traumatic pseudoaneurysms of the liver and spleen in children: is routine screening warranted. J Pediatr Surg 2011;46:938–941.
28. Durkin N, Deganello A, Sellars ME, Sidhu PS, Davenport M, Makin E. Post traumatic liver and

splenic pseudoaneurysms in children: diagnosis, management and follow-up screening using contrast enhanced ultrasound (CEUS). J Pediatr Surg. 2016;51:289–92.
29. Bruhn PJ, Østerballe L, Hillingsø J, Svendsen LB, Helgstrand F. Posttraumatic levels of liver enzymes can reduce the need for CT in children: a retrospective cohort study. Scand J Trauma Resusc Emerg Med. 2016;24:104. https://doi.org/10.1186/s13049-016-0297-1.
30. Castagnetti M, Houben C, Patel S, et al. Minimally invasive management of bile leak leaks after blunt abdominal trauma in children. J Pediatr Surg. 2006;41:1539–44.
31. Bala M, Gazalla SA, Faroja M, et al. Complications of high grade liver injuries: management and outcome with focus on bile leaks. Scand J Trauma Resusc Emerg Med. 2012;20:20. https://doi.org/10.1186/1757-7241-20-20.
32. Miele V, Piccolo CL, Trinci M, Galluzzo M, Ianniello S, Brunese L. Diagnostic imaging of blunt abdominal trauma in pediatric patients. Radiol Med. 2016;121:409–30.
33. Matsuno WC, Huang CJ, Garcia NM, Roy LC, Davis J. Amylase and lipase measurements in paediatric patients with traumatic pancreatic injuries. Injury. 2009;40:66–71.
34. Trinci M, Piccolo CL, Ferrari R, et al. Contrast-enhanced ultrasound (CEUS) in pediatric blunt abdominal trauma. J Ultrasound. 2018;22:27–40.
35. Englum BR, Gulack BC, Rice HE, Scarborough JE, Adibe OO. Management of blunt pancreatic trauma in children: review of the national trauma data bank. J Pediatr Surg. 2016;51:1526–31.
36. Ishida Y, Tyroch AH, Emami N, McLean SF. Characteristics and management of blunt renal injury in children. J Emerg Trauma Shock. 2017;10:140–5.
37. Valentino M, Ansaloni L, Catena F, Pavlica P, Pinna AD, Barozzi L. Contrast-enhanced ultrasonography in blunt abdominal trauma: considerations after 5 years of experience. Radiol Med. 2009;114:1080–93.
38. Poletti PA, Platon A, Becker CD, et al. Blunt abdominal trauma: does the use of a second-generation sonographic contrast agent help to detect solid organ injuries? AJR. 2004;183:1293–301.
39. Menichini G, Sessa B, Trinci M, Galluzzo M, Miele V. Accuracy of contrast-enhanced ultrasound (CEUS) in the identification and characterization of traumatic solid organ lesions in children: a retrospective comparison with baseline US and CE-MDCT. Radiol Med. 2015;120:989–1001.
40. Valentino M, Serra C, Pavlica P, Labate AM, Lima M, Baroncini S, et al. Blunt abdominal trauma: diagnostic performance of contrast-enhanced US in children—initial experience. Radiology. 2008;246:903–9.

Contrast-Enhanced Ultrasound in Blunt Abdominal Trauma

11

Margherita Trinci, Annamaria Deganello, and Vittorio Miele

11.1 Introduction

In industrialized countries, blunt abdominal trauma is considered the leading cause of death in the age group of <40–50 years and the main cause of morbidity in pediatric patients [1, 2]. Depending on the mechanism, injuries are divided between high- and low-energy traumatic injuries. These two different types of trauma require different management, and this is valid both for adult and pediatric patients: in high-energy trauma management is well established, whereas for the low-energy trauma there is no common agreement. In hemodynamically stable patients who sustain high-energy trauma, contrast-enhanced computed tomography (CE-CT), is the reference standard diagnostic technique, as multiorgan involvement must be considered, and this technique allows to examine the patient from "head to toe" in a short time with high diagnostic accuracy [1, 3, 4].

In the setting of high-energy trauma with hemodynamically unstable patients, the diagnostic management of volemic shock is different and an abdominal-focused assessment with sonography for trauma (FAST) is performed, also extended to the thorax (E-FAST), which should identify causes for the volemic shock including hemoperitoneum, hemothorax, and pneumothorax. Once the patient has been treated and has become hemodynamically stable, a diagnostic CE-CT [5–12] should be carried out. In low-energy trauma, the situation is very different as the patient may only have superficial wounds without the involvement of internal organs, but equally they may have one or more internal organs injured; management is more controversial as it is likely to underestimate the severity of the injury. While road traffic accidents occur in all age groups, being the most frequent cause of high-energy trauma, in pediatric patients the causes of low energy trauma vary according to age. This follows the distinct phases of childhood development, as children practice different activities in different settings. Toddlers are often involved in domestic trauma, children in sports-related trauma and teenagers mainly sustain road traffic accidents and sports injuries [13]. In regard to non-accidental injury in the newborn and early childhood, different clinical and imaging evaluations are required, which will not be discussed further [1, 13].

M. Trinci
Department of Emergency Radiology, S. Camillo Hospital, Rome, Italy

A. Deganello
Department of Radiology, King's College Hospital, London, UK
e-mail: adeganello@nhs.net

V. Miele (✉)
Department of Radiology, Careggi University Hospital, Florence, Italy
e-mail: vmiele@sirm.org

P. S. Sidhu et al. (eds.), *Contrast-Enhanced Ultrasound in Pediatric Imaging*,
https://doi.org/10.1007/978-3-030-49691-3_11

Children have specific physical characteristics that differentiate them from adults and need a different clinical and imaging approach. These differences include a thinner abdominal wall, greater elasticity of the tissues, particularly the bone, closer proximity of internal organs to each other and the horizontal position of the diaphragm. All these factors are influential as even with low-energy trauma lesions of one or more internal organs can occur without any bone injury [4, 13]. In childhood, a head injury is most frequent, this is partly due to the disproportion between the skull and the rest of the body and also to the lower resistance of the cervical muscles; the abdomen is the second most common site of injury and blunt trauma accounts for 80–90% of abdominal injuries. In low-energy trauma, a single organ injury is most likely to occur, the spleen being the most frequently injured organ in the pediatric patient.

The clinical evaluation can be difficult, especially in the younger patient and/or in case of unconsciousness or lack of witnesses to the trauma episode. For these reasons, clinical history and examination alone are often unable to provide enough information about the presence and the extent of abdominal injury [14]. However, the presence of wounds or fractures on physical examination can orientate to the location and the severity of the trauma [1, 14–16]. In this scenario diagnostic imaging should play a key role in correctly and quickly differentiating between patients with or without organ injury, directing correct management and the possible need for further diagnostic tests [9, 17–20].

11.2 Guidelines and Recommendations

The European Federation of Societies for Ultrasound in Medicine and Biology (EFSUMB) first published guidelines and recommendations for the use of contrast-enhanced ultrasound (CEUS) in the context of trauma in 2008 [21]. Contrast-enhanced ultrasound was mentioned as potentially beneficial in those cases where computed tomography (CT) was of poor quality, to clarify equivocal CT results or as an addition to CT to facilitate follow-up and the main recommendation was to use CEUS in addition to ultrasound (US) and focused assessment with sonography for trauma (FAST) scanning in the evaluation of traumatic injuries to the liver, spleen, and kidneys. In the 2011 and 2017 updates with formal recommendations were produced with specific references to pediatric patients: the use of CEUS in trauma had been expanded to the evaluation of hemodynamically stable patients with isolated abdominal trauma as first-line investigation as an alternative to CT, both in adults and pediatric patients. In addition, CEUS is recommended as a supplementary investigation in cases of uncertain CT findings and the follow-up of patients managed conservatively, to reduce the number of repeated CT examinations, especially in children [22, 23].

11.3 Ultrasound Contrast Administration

Given the lengthy persistence of ultrasound contrast agent (UCA) microbubble enhancement in the solid organs, parenchymal lacerations and hematomas can be assessed easily and accurately with CEUS. However, considering the rapid cortical enhancement of the kidneys in the arterial phase, the examination should always start with the kidney on the affected side of injury, then proceed and examine the remaining solid upper abdominal viscera. Most commonly, the study should utilize two separate injections of UCA, allowing the examiner to evaluate initially the right kidney and adrenal, liver and pancreas and, following the second dose of contrast, the left kidney and adrenal and finally the spleen [22, 23]. In isolated, low-energy trauma, the examination may be focused on the suspected involved organ, allowing detailed examination in all phases of enhancement. This is particularly important with follow-up examinations, where there is a need to exclude the presence of arterial pseudoaneurysms within the injured organ [23].

11.4 Imaging Techniques: Indications and Limitations

11.4.1 Computed Tomography and Magnetic Resonance Imaging

Although CE-CT is considered the reference standard imaging method to highlight any type of traumatic lesion [24–26], it carries risks related to radiation exposure, and therefore should not be performed routinely. In addition, CE-CT is more expensive than CEUS and needs intravenous administration of iodinated contrast medium, exposing the patient to potential risks of an adverse reaction. For all these reasons, CE-CT should be used only in patients with a strong suspicion of an injury following low-energy blunt abdominal trauma. Despite the lack of radiation exposure, magnetic resonance (MR) imaging is not used routinely in emergency departments. MR examinations are more expensive, require a longer examination time, and depending on the patient's age, may require sedation. Furthermore, there is still a risk of adverse reaction to a gadolinium contrast medium, although this is considered lesser to iodinated contrast agents used in CE-CT, and the unknown long-term consequences of gadolinium deposition in the body [23].

11.4.2 Conventional Ultrasound Imaging

Baseline B-mode US is usually the first-line diagnostic imaging technique used for the assessment of patients with low-energy blunt abdominal trauma [27]. There are many reasons for this, largely due to the availability of US in emergency departments, bedside application, rapidity, and tolerability of the examination by the pediatric patient in the presence of the parents. The US examination can also be easily repeated and is relatively inexpensive for initial assessment and additionally for follow-up. The disadvantages include a dependency on the experience of the sonologist and the body habitus of the patient. Furthermore, US has poor sensitivity in detecting traumatic parenchymal lesions that often appear isoechoic to the underlying parenchyma [28–31].

When performing an US examination in trauma, the aim is not only to detect parenchymal lesions but to establish the relationship with the organ capsule and to assess the presence of free fluid, which can be an indirect sign of traumatic injury even in absence of a visible parenchymal injury. Ultrasound has a high sensitivity for the detection of free fluid, ranging from 63% to 99%, comparable with that of CE-CT [4–7, 28, 31, 32] and as such has, in an unstable patient, has replaced peritoneal lavage. Sensitivity in the detection of free fluid is however influenced both by the experience of the sonologist and the amount of free fluid present; sensitivity decreases with a small fluid volume [29, 30]. The accuracy of US in the detection of solid organ injury is low, reported at 45.7%, depending not only on the experience of the sonologist but also on the echogenicity of the fresh blood, which may be similar to that of the healthy organ parenchyma, especially surrounding the spleen [1, 3–5, 33, 34].

The anatomical position of the targeted organ influences the ability of US to detect a lesion; organs located below the diaphragmatic muscle or examined predominantly intercostally, like the spleen, are more difficult to evaluate. Similarly, retroperitoneal organs such as the kidneys and the pancreas may be difficult to examine, especially in a large patient but likely easier in the pediatric patient. Up to 29–34% of parenchymal traumatic lesions may be present and not seen on FAST in the absence of hemoperitoneum, [31, 35, 36] and as such the absence of free fluid should not be considered a reliable criterion to exclude the presence of a traumatic solid organ injury.

11.4.3 Contrast-Enhanced Ultrasound

When examining patients with abdominal trauma, negative prognostic factors that influence the patient's management must be considered besides the presence of free fluid, such as organ capsule and/or hilar region involvement, the pres-

ence of vascular lesions including post-traumatic pseudo-aneurysms and ongoing intralesional or extracapsular bleeding. B-mode US has limitations in the evaluation of these prognostic factors and in some cases, as in active bleeding, it has no role. To improve on the basic US examination, particularly with patients presenting with localized low-energy trauma, an often-non-conclusive baseline US is followed by a contrast-enhanced ultrasound (CEUS) examination. With the addition of a UCA, there is a significant improvement in detecting parenchymal solid organ injury, with the ability to observe all the vascular phases of the injured organ in real time, and repeatedly with safety. On a CEUS examination, healthy parenchyma shows uniform, avid enhancement in the venous and late phases, which allows better detection of parenchymal lesions, which are markedly hypoechoic with respect to healthy parenchyma as a consequence of the avascular nature of the lesion. This allows for an accurate and confident evaluation of the relationship between the lesion and the organ capsule. Furthermore, it is possible to highlight the presence of intralesional or extracapsular bleeding and detect vascular lesions such as pseudoaneurysm or artero-venous fistula [1, 13, 37, 38].

Contrast-enhanced ultrasound is established as more accurate than the B-mode US and almost as sensitive as CE-CT in the detection of traumatic injuries, with levels of sensitivity and specificity up to 95%. Using CEUS, it allows a safe discharge of a patient when no injuries are identified following low-energy blunt abdominal trauma, avoiding hospital stay and associated costs, as well as any further imaging examinations. By using CEUS, and avoiding a CE-CT, reduction in radiation exposure is achieved [1, 4, 19, 31, 33, 39–43].

Contrast-enhanced ultrasound carries the same limitations of conventional B-mode ultrasound; it is dependent on the experience of the sonologist, the patient's body habitus, it is not panoramic and it has difficulties in exploring deep regions, especially in patients unable to move or not collaborating. Specific CEUS limits are the additional cost of the UCA and potential allergic reactions, known to occur rarely. Lack of experience and awareness are likely to explain the low usage of this technique in trauma patients.

The UCA used in CEUS is purely intravascular, does not pass into the interstitial space, and is eliminated via the lungs and not via the kidneys, with a CEUS examination unable to evaluate abnormalities of the renal excretory system. However, the UCA can be safely used in patients with acute or chronic renal failure. If a traumatic lesion is depicted on CEUS, it is advisable to also perform a CE-CT examination, as CE-CT remains the reference standard, allowing for a global view of the abdomen. This panoramic view is warranted to exclude the presence of further injuries and other negative prognostic factors such as rupture of the urinary tract, active bleeding, or gastrointestinal injuries [39]. Another very important indication is the follow-up of trauma, even at the bed side, of known lesions both in high- and low-energy traumas, avoiding repeated radiation exposure.

11.5 Traumatic Solid Organ Injuries

On B-mode US, a recent traumatic lesion appears hyperechoic due to the presence of fresh blood. Any delay in presentation, the lesion will vary in echogenicity, from hyperechoic to isohypoechoic, but there may be only a subtle distortion of the normal echogenicity [40]. The lesions may be single or multiple, of various sizes, with an irregular shape and ill or well-defined border [1, 4, 33, 43]. After intravenous administration of the UCA, the parenchymal enhancement varies according to the differences in the vascularization of the organ under investigation.

11.5.1 Enhancement Patterns of Contrast-Enhanced Ultrasound

In relation to the intensity of the enhancement, the kidneys enhance avidly and more rapidly compared to the liver and spleen. In particular,

the renal cortex enhances very early while the medullary pyramids enhance approximately 30 s after the injection of the UCA, from the periphery to the center. The optimal time period for kidney assessment is up to 2.5 min. At CEUS, in comparison with the conventional US, it is easier to detect small amounts of retroperitoneal fluid in the perirenal space [1, 44]. The spleen has an inhomogeneous enhancement in the arterial phase, as in CE-CT, and therefore it is best evaluated in the venous phase when it shows avid and persistent enhancement (up to 6–8 min post-UCA administration). The liver and the pancreas show enhancement of intermediate intensity [1]. Contrast-enhanced ultrasound findings are related to the UCA distribution, which may be homogeneous in healthy parenchyma with vascular structures clearly recognizable (Fig. 11.1), heterogeneous, with areas of lack of perfusion, in case of injury, or absent in case of organ devascularization or hypovolemic shock. The venous phase is the best to appreciate the number, position, and extent of the traumatic lesions [31, 43].

11.5.1.1 Parenchymal Lesions: Lacerations, Hematoma, and Capsule Rupture

Traumatic lesions on a CEUS examination are visualized as hypoechoic or anechoic areas, due to the absence of UCA enhancement, clearly depicted within healthy, normally enhancing parenchyma. The margins of the lesion will readily demarcate, as will the integrity or the rupture of the organ capsule (Fig. 11.2). Similar to CE-CT, on a CEUS examination, the severity of a traumatic injury can be assessed based on the American Association for Trauma Surgery (AAST) classification [45, 46]. The type of parenchymal lesions that can be found following trauma is diverse depending on the degree of damage caused by the traumatic event. Contusions may result simply in an edematous or hypoechoic area, a manifestation of reduced perfusion. Lacerations can have different shapes and sizes: they may appear as small, anechoic, linear defects (Fig. 11.3) with branches or as larger, irregular or rounded areas in which there may be the presence of active bleeding foci. The laceration can reach the capsule at one or more points and possibly

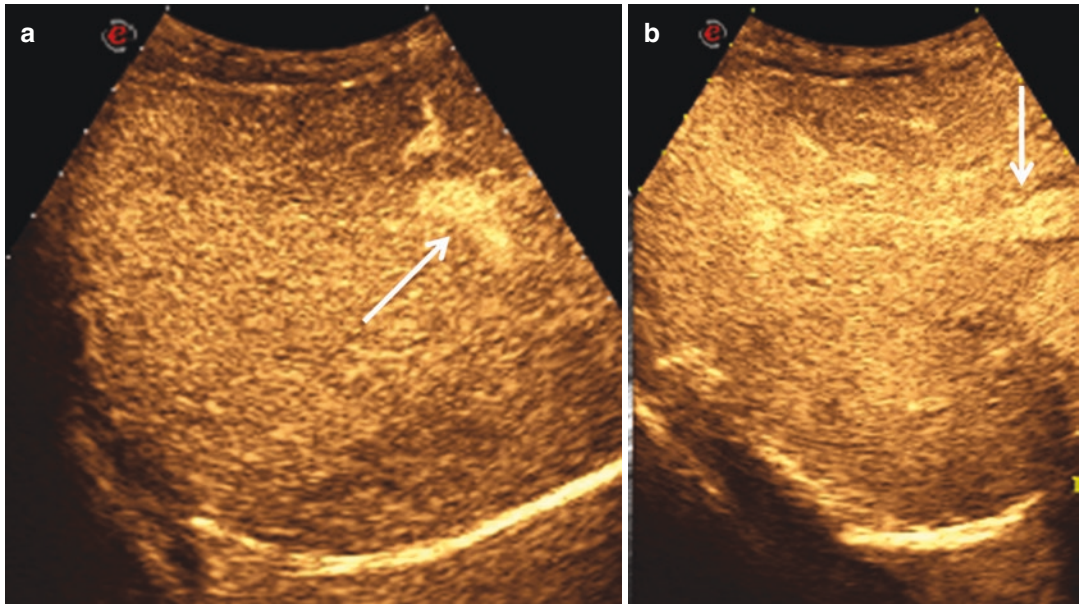

Fig. 11.1 Healthy hepatic parenchyma. (**a**, **b**) CEUS shows homogeneous enhancement of healthy hepatic parenchyma. Vascular structures are clearly depicted (arrows)

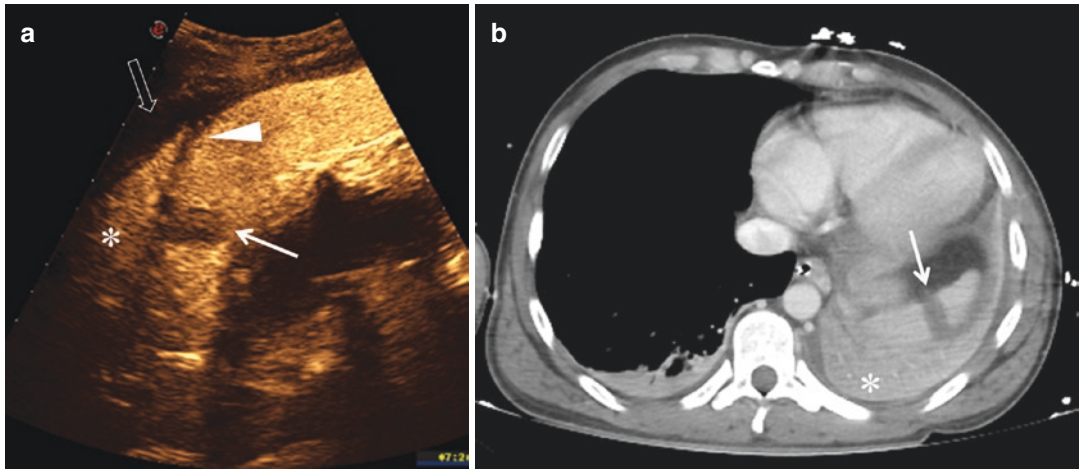

Fig. 11.2 Splenic trauma. (**a**) CEUS shows the laceration of the upper pole of the spleen, involving the splenic capsule (arrow); small amount of perisplenic hematoma (arrowhead). Collapsed parenchyma at the lung base is also shown (asterisk), with a small amount of pleural effusion (open arrow). (**b**) CT confirms the laceration of the spleen, involving the organ capsule (arrow) and the collapse of lung parenchyma (asterisk)

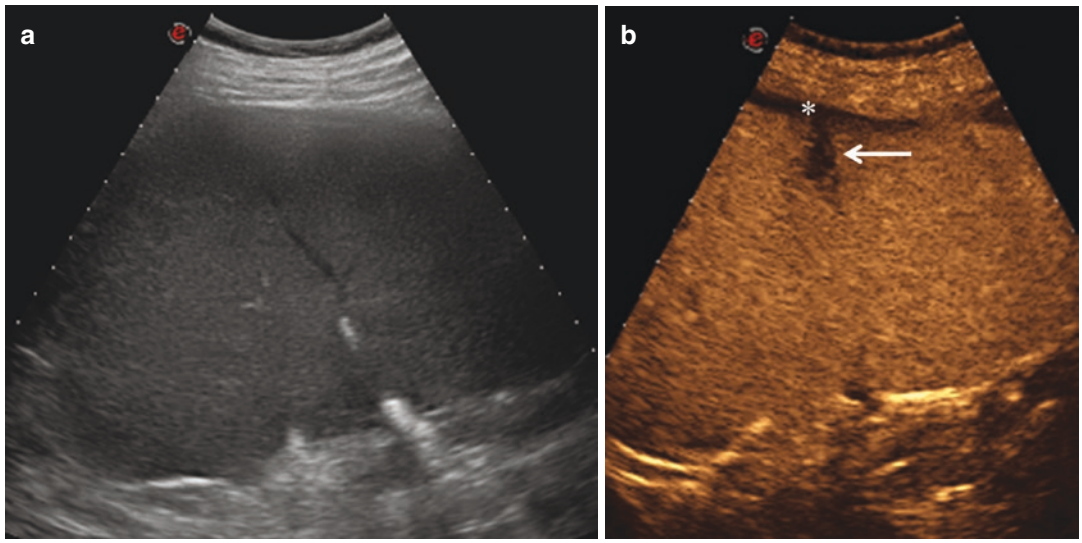

Fig. 11.3 Splenic trauma in patients with splenomegaly. (**a**) US shows homogeneous echostructure of splenic parenchyma; no injuries are appreciable. (**b**) CEUS shows a linear laceration of the spleen, involving the splenic capsule (arrow), with a thin subcapsular hematoma (asterisk)

breaching the capsule (Fig. 11.4), or may remain completely intraparenchymal (Fig. 11.5). The presence of subcapsular hematoma will appear as a lenticular hypoechoic or anechoic area (Fig. 11.6), surrounding the normal enhanced parenchyma, causing a mass effect (Fig. 11.7). Similarly, a parenchymal hematoma will be seen as a slightly hyperechoic area at B-mode US and as a non-enhancing area at CEUS.

11.5.1.2 Active Bleeding

Contrast-enhanced ultrasound can also detect the presence of intralesional or extracapsular active hemorrhage. The bleeding point will be

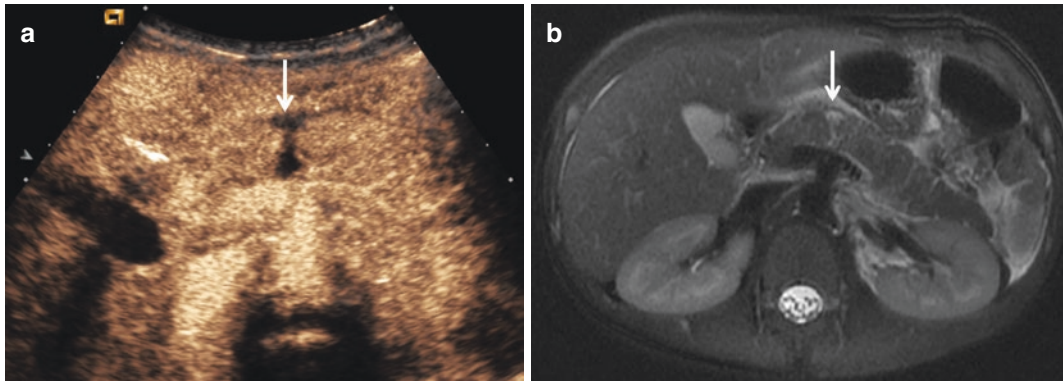

Fig. 11.4 Pancreatic injury. (**a**) CEUS shows a complete fracture of the pancreatic body, with subtle peripancreatic fluid collection (arrow). (**b**) MR imaging confirms the pancreatic lesion as a linear hyperintensity across the parenchyma and the peripancreatic small fluid collection (arrow)

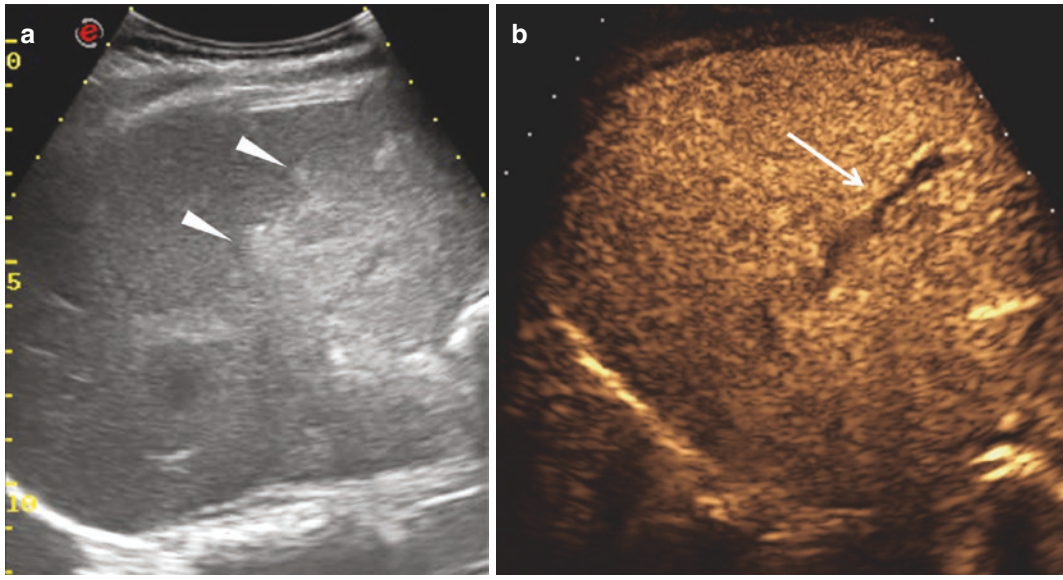

Fig. 11.5 Liver trauma. (**a**) US shows a large inhomogeneous hyperechoic area in the hepatic parenchyma (arrowheads). (**b**) CEUS clearly depicts a deep linear laceration of hepatic parenchyma (arrow), not involving the organ capsule

visualized as one or more round or oval hyperechoic focus of variable size, with alteration of the shape and echogenicity over a short time period, similar to that seen on a CE-CT (Fig. 11.8). Active hemorrhage is a very important prognostic marker, as the presence of hemorrhage alters the management of the patient from conservative to non-conservative, possibly requiring an embolization procedure [39]. Despite the ability of CEUS to demonstrate the ongoing extravasation of the UCA, the first-choice investigation for the visualization of both intralesional and extracapsular hemorrhage remains CE-CT, but often altered by a preceding CEUS examination. The literature reports variable sensitivities of CEUS in detecting contrast pooling [47–49]. A recent study [50] reported a sensitivity of 72.4% in the identification of sites of active hemorrhage on CEUS, compared to 81.2% on CE-CT [39]. Peritoneal or retroperito-

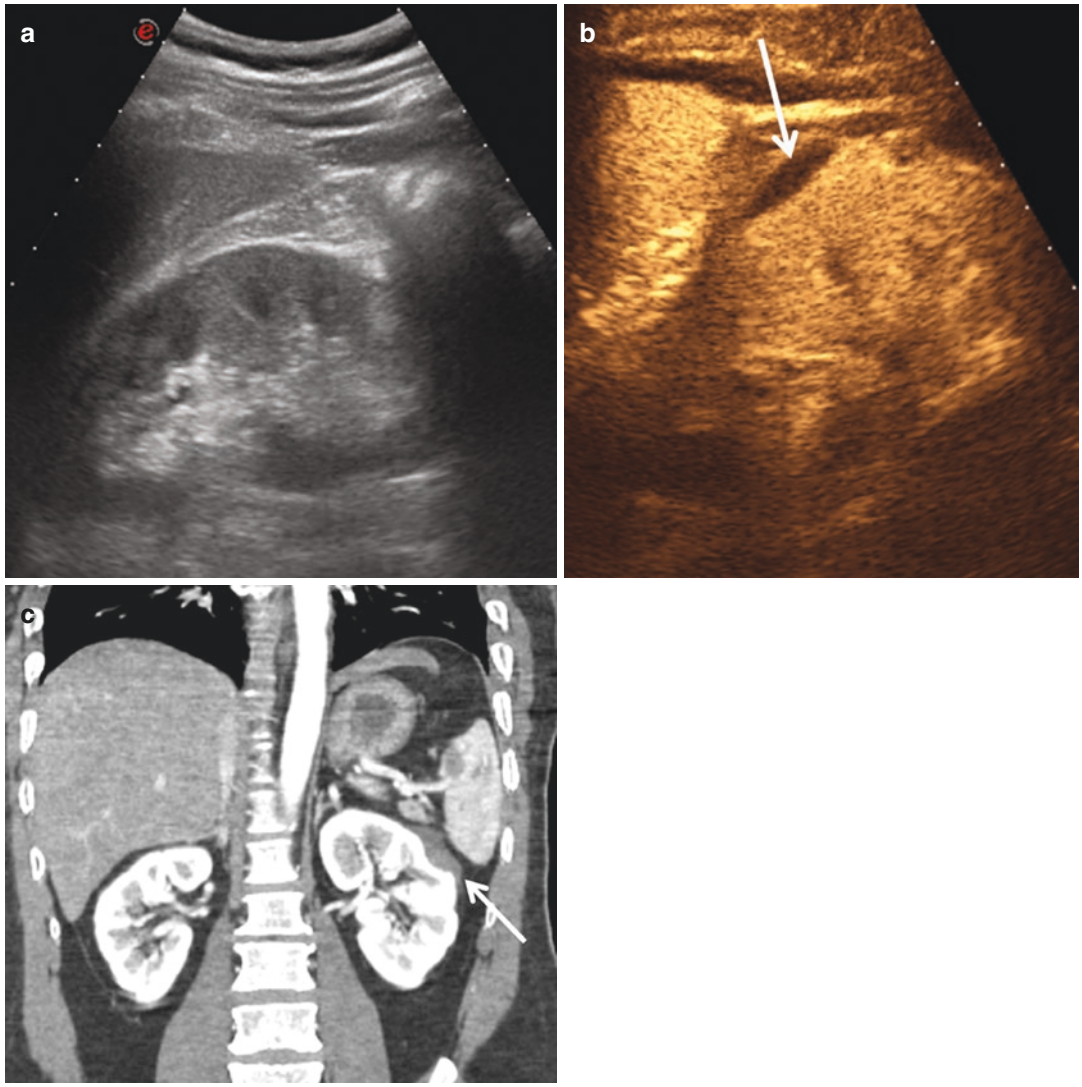

Fig. 11.6 Renal trauma. (**a**) B-mode US does not depict any renal injuries. (**b**) CEUS shows a lenticular subcapsular hematoma in the mid aspect of the left kidney (arrow). (**c**) CE-CT confirms the subcapsular hematoma (arrow)

neal active hemorrhage will be visualized in the early stage as extra parenchymal extravasation of hyperechoic UCA microbubbles [39].

The presence of a post-traumatic vascular lesion such as a pseudo-aneurysm, can be visualized on the B-mode US as anechoic areas located in the context of healthy parenchyma; color Doppler US evaluation shows the presence of blood flow inside the anechoic lesion. Contrast-enhanced ultrasound can confirm that the UCA is distributed within the lesion, with swirling under real-time observation. The complete lack of organ perfusion is indicative of major vascular injury and avulsion of the vascular pedicle. As the evaluation of the renal excretory system is not possible on CEUS, any visualization of parenchymal damage can be indicative of renal excretory impairment.

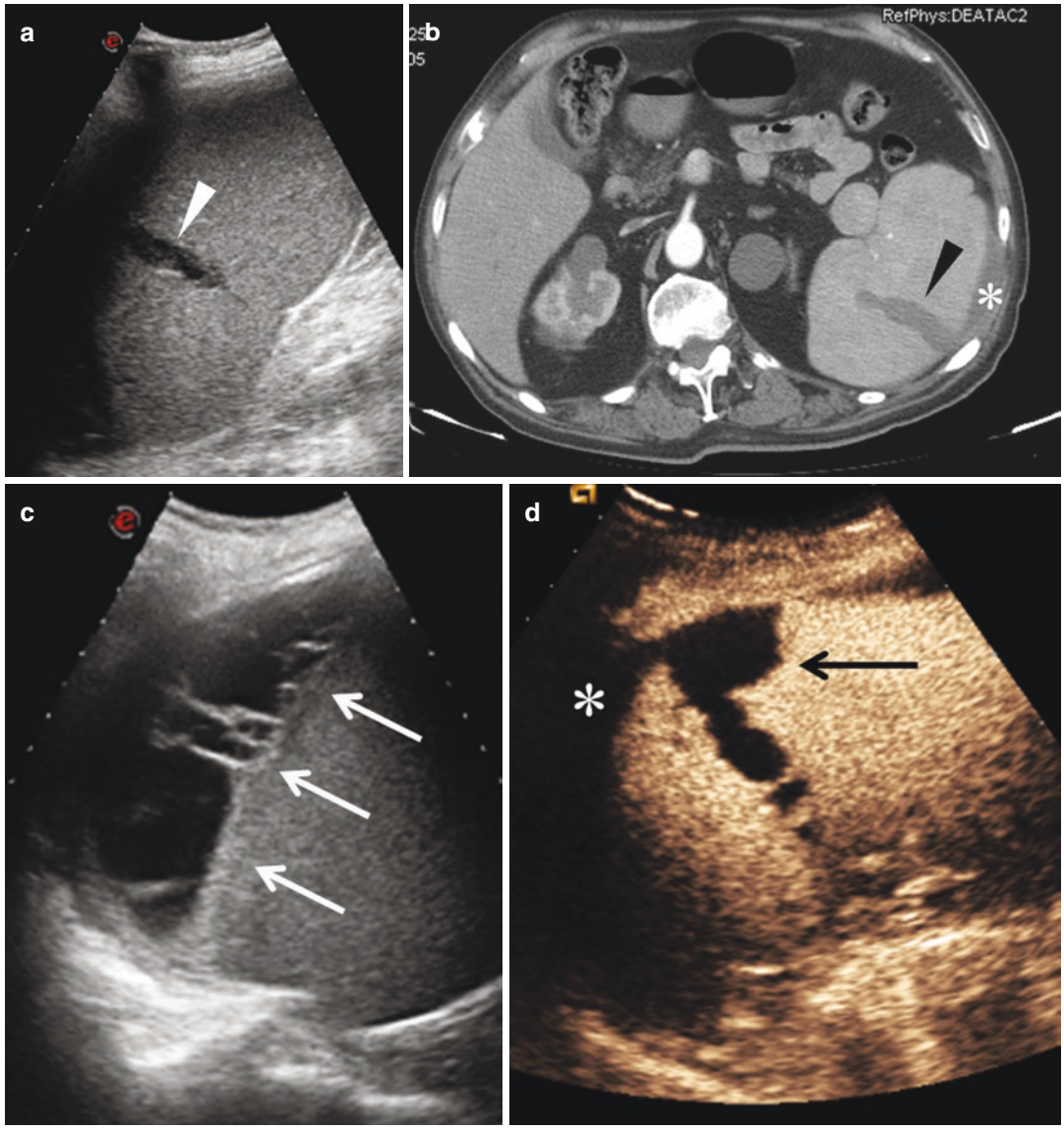

Fig. 11.7 Splenic trauma. (**a**) US shows a linear laceration of the spleen (white arrowhead), involving the capsule; (**b**) CE-CT confirms the lesion (black arrowhead). A perisplenic fluid collection is appreciable (asterisk). One month later, (**c**) follow-up US shows the organized subcapsular hematoma (white arrows) and (**d**) CEUS clearly depicts the large lacerations of the splenic parenchyma (black arrow) and the perisplenic fluid collection (asterisk)

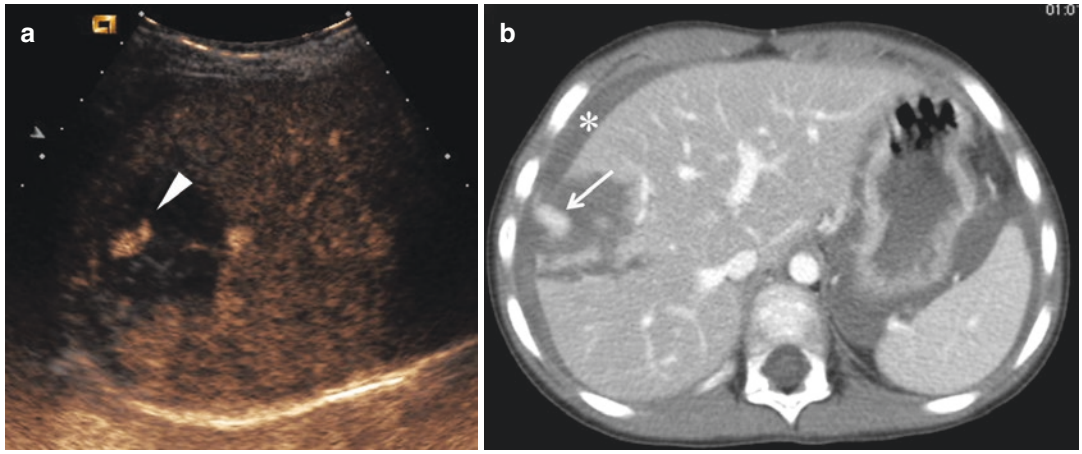

Fig. 11.8 Liver trauma. (**a**) CEUS demonstrates a large hematoma in the right lobe, with active bleeding (arrowhead). (**b**) CE-CT confirms the intraparenchymal and intraperitoneal active bleeding (arrow). A perihepatic fluid collection is also present (asterisk)

11.6 Conclusion

Contrast-enhanced ultrasound is a safe, reliable imaging modality to evaluate pediatric patients presenting to the emergency department with a history of low-energy trauma. It also plays an important role in triaging patients towards conservative management or intervention, especially when a CE-CT examination may not be indicated in the first instance. Moreover, its use in the follow-up of known solid organ injuries avoids unnecessary repeated radiation exposure and reduces costs.

References

1. Miele V, Piccolo CL, Galluzzo M, Ianniello S, Sessa B, Trinci M. Contrast-enhanced ultrasound (CEUS) in blunt abdominal trauma. Br J Radiol. 2016;89(1061):20150823.
2. Van Beeck EF, Van Roijen L, Mackenbach JP. Medical costs and economic production losses due to injuries in the Netherlands. J Trauma. 1997;42:1116–23. https://doi.org/10.1097/00005373-199706000-00023.
3. Poletti PA, Wintermark M, Schnyder P, Becker CD. Traumatic injuries: role of imaging in the management of the polytrauma victim (conservative expectation). Eur Radiol. 2002;12:969–78. https://doi.org/10.1007/s00330-002-1353-y.
4. Trinci M, Sessa B, Menichini G, Valentini V, Miele V. Abdominal trauma. In: Miele V, Trinci M, editors. Imaging trauma and polytrauma in pediatric patients. Cham: Springer International Publishing; 2015. p. 65–100. https://doi.org/10.1007/978-3-319-08524-1_4.
5. McKenney KL, Nuñez DB Jr, McKenney MG, Asher J, Zelnick K, Shipshak D. Sonography as primary screening technique for blunt abdominal trauma: experience with 899 patients. AJR Am J Roentgenol. 1998;170:979–85. https://doi.org/10.2214/ajr.170.4.9580140.
6. Brown MA, Sirlin CB, Hoyt DB, Casola G. Screening ultrasound in blunt abdominal trauma. J Intensive Care Med. 2006;18:253–60. https://doi.org/10.1177/0885066603256103.
7. Branney SW, Wolfe RE, Moore EE, Albert NP, Heinig M, Mestek M, et al. Quantitative sensitivity of ultrasound in detecting free intraperitoneal fluid. J Trauma. 1995;39:375–80. https://doi.org/10.1097/00005373-199508000-00032.
8. Paajnen H, Lahti P, Nordback I. Sensitivity of transabdominal ultrasonography in detection of intraperitoneal fluid in humans. Eur Radiol. 1999;9:1423–5.
9. Miele V, Andreoli C, Grassi R. The management of emergency radiology: key facts. Eur J Radiol. 2006;59:311–4. https://doi.org/10.1016/j.ejrad.2006.04.020.
10. Volpicelli G. Sonographic diagnosis of pneumothorax. Intensive Care Med. 2011;37:224–32.
11. Ianniello S, Di Giacomo V, Sessa B, Miele V. First-line sonographic diagnosis of pneumothorax in major trauma: accuracy of e-fast and comparison with multidetector computed tomography. Radiol Med. 2014;119:674–80.

12. Soldati G, Testa A, Sher S, Pignataro G, La Sala M, Gentiloni Silveri N. Occult traumatic pneumothorax: diagnostic accuracy of lung ultrasonography in the emergency department. Chest. 2008;133:204–11.
13. Miele V, Piccolo CL, Trinci M, Galluzzo M, Ianniello I, Brunese L. Diagnostic imaging of blunt abdominal trauma in pediatric patients. Radiol Med. 2016;121:409–30.
14. Schurink GW, Bode PJ, van Luijt PA, van Vugt AB. The value of physical examination in the diagnosis of patients with blunt abdominal trauma: a retrospective study. Injury. 1997;28:261–5.
15. Holmes JF, Sokolove PE, Brant WE, Palchak MJ, Vance CW, Owings JT, Kuppermann N. Identification of children with intra-abdominal injuries after blunt trauma. Ann Emerg Med. 2002;39:500–9.
16. Cotton BA, Beckert BW, Smith MK, Burd RS. The utility of clinical and laboratory data for predicting intraabdominal injury among children. J Trauma. 2004;56:1068–74.
17. Brown CK, Dunn KA, Wilson K. Diagnostic evaluation of patients with blunt abdominal trauma: a decision analysis. Acad Emerg Med. 2000;7:385–96.
18. Sivit C. Imaging children with abdominal trauma. AJR Am J Roentgenol. 2009;192:1179–89.
19. Sivit C. Contemporary imaging in abdominal emergencies. Pediatr Radiol. 2008;38(Suppl 4):S675–8.
20. Miele V, Di Giampietro I, Ianniello S, Pinto F, Trinci M. Diagnostic imaging in pediatric polytrauma management. Radiol Med. 2015;120:33–49.
21. Claudon M, et al. Guidelines and good practice recommendations for contrast enhanced ultrasound (CEUS)—update 2008. Ultraschall Med. 2008;29:28–44.
22. Piscaglia F, et al. The EFSUMB guidelines and recommendations on the clinical practice of contrast enhanced ultrasound (CEUS): update 2011 on non-hepatic applications. Ultraschall Med. 2012;33:33–59.
23. Sidhu PS, et al. The EFSUMB guidelines and reccomendations for the clinical practice of contrast enhanced ultrasound (CEUS) in non-hepatic applications: update 2017. Ultraschall Med. 2018;39:154–80.
24. Shuman WP. CT of blunt abdominal trauma in adults. Radiology. 1997;205:297–306.
25. Weishaupt D, Grozaj AM, Willmann JK, Roos JE, Hilfiker PR, Maricenk B. Traumatic injuries: imaging of abdominal and pelvic injuries. In: Baert AL, Gourtsoyannis N, editors. Categorical course ECR. Vienna: European Congress of Radiology; 2003. p. 123–39.
26. ACEP Clinical Policies Committee, Clinical Policies Subcommittee on Acute Blunt Abdominal Trauma. Clinical policy: critical issues in the evaluation of adult patients presenting to the emergency department with acute blunt abdominal trauma. Ann Emerg Med. 2004;43:278–90.
27. Kretschmer KH, Bohndorf K, Pohlenz O. The role of sonography in abdominal trauma: the European experience. Emerg Radiol. 1997;2:62–7.
28. Paajanen H, Lahti P, Nordback I. Sensitivity of transabdominal ultrasonography in detection of intraperitoneal fluid in humans. Eur Radiol. 1999;9:1423–5.
29. Poletti PA, Kinkel K, Vermeulen B, et al. Blunt abdominal trauma: should US be used to detect both free fluid and organ injuries? Radiology. 2003;227:95–103.
30. Rothlin MA, Naf R, Amgwerd M, et al. Ultrasound in blunt abdominal and thoracic trauma. J Trauma. 1993;34:488–95.
31. Valentino M, Serra C, Zironi G, De Luca C, Pavlica P, Barozzi L. Blunt abdominal trauma: emergency contrast-enhanced sonography for detection of solid organ injuries. AJR Am J Roentgenol. 2006;186:1361–7.
32. Rozycki GS, Ochsner MG, Jaffin JH. A prospective study of surgeon-performed ultrasound as the primary adjuvant modality for injured patient assessment. J Trauma. 1995;39:492–8.
33. Clevert DA, Weckbach S, Minaifar N, et al. Contrast enhanced ultrasound versus MS-CT in blunt abdominal trauma. Clin Hemorheol Microcirc. 2008;39:155–69.
34. Pearl WS, Todd KH. Ultrasonography for the initial evaluation of blunt abdominal trauma: a review of prospective trials. Ann Emerg Med. 1996;27:353–61.
35. Chiu WC, Cushing BM, Rodriguez A, et al. Abdominal injuries without hemoperitoneum: a potential limitation of focused abdominal sonography for trauma (FAST). J Trauma. 1997;42:617–25.
36. Shanmuganathan K, Mirvis SE, Sherbourne CD, Chiu WC, Rodriguez A. Hemoperitoneum as the sole indicator of abdominal visceral injuries: a potential limitation of screening abdominal US for trauma. Radiology. 1999;212:423–30.
37. Catalano O, Lobianco R, Sandomenico F, Siani A. Splenic trauma: evaluation with contrast-specific sonography and a second-generation contrast medium. J Ultrasound Med. 2003;22:467–77.
38. Miele V, Buffa V, Stasolla A, et al. Contrast enhanced ultrasound with second generation contrast agent in traumatic liver lesions. Radiol Med. 2004;107:82–91.
39. Sessa B, Trinci M, Ianniello S, Menichini G, Galluzzo M, Miele V. Blunt abdominal trauma: role of contrast-enhanced ultrasound (CEUS) in the detection and staging of abdominal traumatic lesions compared to US and CE-MDCT. Radiol Med. 2015;120:180–9.
40. Valentino M, De Luca C, Galloni SS, et al. Contrast enhanced US evaluation in patients with blunt abdominal trauma. J Ultrasound. 2010;13:22–7.
41. Tang J, Li W, Lv F, et al. Comparison of gray-scale contrast-enhanced ultrasonography with contrast-enhanced computed tomography in different grading of blunt hepatic and splenic trauma: an animal experiment. Ultrasound Med Biol. 2009;35:566–75.
42. Dietrich CF. Comments and illustrations regarding the guidelines and good clinical practice recommendations for contrast-enhanced ultrasound (CEUS)–update 2008. Ultraschall Med. 2008;29(Suppl 4):S188–202.

43. Pinto F, Miele V, Scaglione M, Pinto A. The use of contrast-enhanced ultrasound in blunt abdominal trauma: advantages and limitations. Acta Radiol. 2014;55:776–84. https://doi.org/10.1177/0284185113505517.
44. Cagini L, Gravante S, Malaspina CM, Cesarano E, Giganti M, Rebonato A, et al. Contrast enhanced ultrasound (CEUS) in blunt abdominal trauma. Crit Ultrasound J. 2013;5(Suppl. 1):S9. https://doi.org/10.1186/2036-7902-5-S1-S9.
45. Moore EE, Cogbill TH, Jurkovich GJ, et al. Organ injury scaling: spleen and liver (1994 revision). J Trauma. 1995;38:323–4.
46. Moore EE, Shackford SR, Pachter HL, et al. Organ injury scaling: spleen, liver and kidney. J Trauma. 1989;29:1664–6.
47. Catalano O, Cusati B, Nunziata A, Siani A. Active abdominal bleeding: contrast-enhanced sonography. Abdom Imaging. 2006;31:9–16.
48. Marmery H, Shanmuganatan K, Mirvis SE, et al. Correlation of multidetector CT findings with splenic arteriography and surgery: prospective study in 392 patients. J Am Coll Surg. 2008;206:685–93.
49. Hamilton JD, Kumaravel M, Censullo ML, et al. Multidetector CT evaluation of active extravasation in blunt abdominal and pelvic trauma patients. Radiographics. 2008;28:1603–16.
50. Lv F, Tang J, Luo Y, et al. Contrast-enhanced ultrasound imaging of active bleeding associated with hepatic and splenic trauma. Radiol Med. 2011;116:1076–82.

12 Contrast-Enhanced Ultrasound of the Pediatric Kidneys

Jeevesh Kapur and Zoltan Harkanyi

12.1 Introduction

Conventional ultrasound (US) has been the mainstay of imaging the renal system and abdominal organs in clinical practice, more so in the pediatric age group. With the advantages of being a non-irradiating modality and with real-time imaging, US has become absolutely essential in the radiological evaluation pathway in children. However, a conventional US of the kidneys may be suboptimal, particularly in the assessment of renal lesion characteristics. With the advent of contrast-enhanced ultrasound (CEUS), a new dimension has been added to this essential role, which has the potential of offering insights to enhancing patterns of abdominal organs and focal lesions similar to, if not better than, conventional computed tomography (CT) and magnetic resonance (MR) imaging [1–3]. In the last decade, CEUS has begun making headway, not subject to the same limitations of CT and MR imaging, and is particularly useful in patients with renal impairment. Following several consensus conferences since 2003, the European Federation of Societies for Ultrasound in Medicine and Biology (EFSUMB) study group has developed numerous guidelines and protocols for the use of CEUS, allowing a more standardized and reproducible practice of CEUS, culminating in a position paper on CEUS practice in pediatric patients [3].

12.2 Safety and Technical Considerations

As ultrasound contrast agents (UCA) consist of microbubbles and are true blood pool agents, they do not leave the blood vessels and are not subject to normal renal filtration or renal excretion, essentially behaving as "vascular tracers." The risk of iodinated CT contrast-induced nephrotoxicity and nephrogenic systemic fibrosis with gadolinium in patients with renal compromise has limited the role of contrast-enhanced CT and MR imaging in patients with renal impairment. Ultrasound contrast agents, with their established safety and low incidence of side effects, offer a unique perspective into renal imaging [4, 5]. These UCA are not nephrotoxic or cardiotoxic and components are excreted by the lungs or metabolized via the liver, their use does not require renal function biochemical tests prior to administration. Riccabona et al. have found UCA to be safe for use in children, and have incorporated it into guidelines of pediatric practice [6, 7]. In a large-scale retrospective analy-

J. Kapur (✉)
Department of Diagnostic Imaging, National University Hospital, Singapore, Singapore
e-mail: jeevesh@nus.edu.sg

Z. Harkanyi
Department of Radiology, Heim Pal National Pediatric Institute, Budapest, Hungary

P. S. Sidhu et al. (eds.), *Contrast-Enhanced Ultrasound in Pediatric Imaging*,
https://doi.org/10.1007/978-3-030-49691-3_12

sis, it was demonstrated that SonoVue™ (Bracco Spa, Milan) has a good safety profile in abdominal applications, with an adverse event reporting rate lower than or similar to that reported for radiologic and MR contrast agents [6–8]. Ultrasound contrast agents have a low serious adverse event rate of 0.006–0.009%, consisting primarily of anaphylactoid reactions that resolve and typically do not necessitate hospitalization; nevertheless, competent medical care for any reaction should be available. Less serious side effects that are also rare and typically transient include headache, dizziness, flushing, nausea, flank pain, and chest pain [4, 5].

SonoVue™ is the most commonly used UCA for intravascular renal assessment. This UCA is a phospholipid encapsulated sulfur hexafluoride microbubble with an average microbubble diameter of 2.5 μm. The adult dose is normally between 1.2 and 4.8 mL depending on the organ to be examined, and in the examination of the pediatric kidney, a dose of between 0.6 and 1.2 mL will suffice. The UCA is administered via a peripheral vein (in which a 20G intra-venous cannula has been inserted), followed by a rapid bolus injection of 5 mL of normal saline. We usually inject up to a maximum of two boluses of at an interval of 10–15 min when two kidneys are to be examined, but with a single lesion to be examined, rarely is more than one dose required.

When assessing a focal lesion, we select appropriate positions, depending on the different clinical requirements, to perform axial, coronal, sagittal examinations of the kidneys. Baseline grayscale US is conducted to observe lesion size, shape, echo intensity, and demarcation from adjacent tissues, while color Doppler US is used to examine the blood flow within and surrounding the lesion. Contrast-enhanced ultrasound is performed selecting the most appropriate transducer, remaining static over the most suitable view in order to obtain maximum information on the vascularity of the lesion.

With the role of CEUS being well established in the adult population, most of the modern high-end US machines are equipped with a contrast imaging mode. Vendor-specific workstations are able to process attributes such as areas under the curve and time to peak, which can be helpful for further insights and research into contrast-enhanced patterns in kidneys.

12.3 Imaging

After an intravenous injection of the UCA, renal lesions are compared with the corresponding normal renal cortex. Lesions with post-UCA administration enhancement higher than, lower than or equal to that of the cortical echogenicity are defined as hyperenhancing, hypoenhancing, and iso-enhancing respectively. In addition, the time in which the UCA washes-in and washes-out of the lesion is compared with that of the rest of the normal kidney. “Fast in” indicates that inflow into the lesion of the UCA precedes the enhancement of the renal cortex, whereas “fast out” indicates an outflow of the UCA from the lesion precedes that of the renal cortex. “Identical in” and “identical out” indicate that the UCA enters and exits the lesion in an identical manner when compared with the normal renal cortex. Furthermore, “slow in” and “slow out” indicate that inflow and outflow of the UCA are later in the lesion than in the normal renal cortex [9].

Renal lesions are often better assessed on CEUS due to its greater sensitivity in depicting intra-cystic septations and cystic contents such as hemorrhage [10]. Contrast-enhanced ultrasound has a higher temporal resolution, and that in combination with the lack of renal contrast excretion and background suppression of stationary tissue, is superior in the detection of microvascular flow within the septations or wall of any renal lesion [11–13]. Contrast-enhanced ultrasound also has a larger margin for error, allowing repeated scanning in a single session, although more often encountered in adults rather than pediatric patients.

12.4 Focal Renal Lesions

12.4.1 Bosniak Classification of Renal Cysts

Characterization of complex renal cyst remains a common and sometimes difficult diagnostic

dilemma for the referring urologist and the radiologist. These complex renal cysts are found incidentally on routine radiological investigations. Whether a cyst enhances or not, it is important in differentiating benign from malignant lesions as the chance of neoplasia increases to 40–80% when there is enhancement noted [12, 14]. Although contrast CT and MR imaging is considered the gold standard, CEUS has given the evaluation of complex renal cyst a new dimension. Contrast-enhanced ultrasound has the advantage of being able to visualize the thin fine septa better than CT or MR imaging due to the inherent resolution superiority of US [11, 15]. Contrast-enhanced ultrasound provides an accurate and reliable alternative to other cross-sectional imaging modalities, especially when evaluating solitary lesions and for their follow-up imaging (Figs. 12.1, 12.2, and 12.3).

As in all cross-sectional studies, contrast use is important in identifying solid enhancing components, and the Bosniak complex renal cyst classification is reproducible [16] with high accuracy in predicting malignancy as enhancing tissue [17, 18]. This classification system is suited to a CEUS examination [12, 19] with recent studies comparing CEUS and contrast-enhanced CT (CECT) showing no statistical difference between the two modalities in diagnosing renal malignancies [20]. Quaia et al. asserted superior CEUS characterization of complex renal cysts compared to CECT, with a sensitivity of 81–95% (vs. 86–95%), a specificity of 42–68% (vs. 63–79%), positive predictive value (PPV) of 61–74% (vs.74–82%), and negative predictive value (NPV) of 67–89% (vs. 83–92%) of CECT compared with CEUS across their three separate readers [11]. In another study comparing CEUS with MR imaging, Chen et al. concluded that CEUS had a higher diagnostic sensitivity and accuracy but lower specificity than MR imaging for classifying complex cystic renal masses (sensitivity 97.2% vs. 80.6%, specificity 71.4% vs. 77.1%, PPV 77.8% vs. 78.4%, and NPV 96.2%

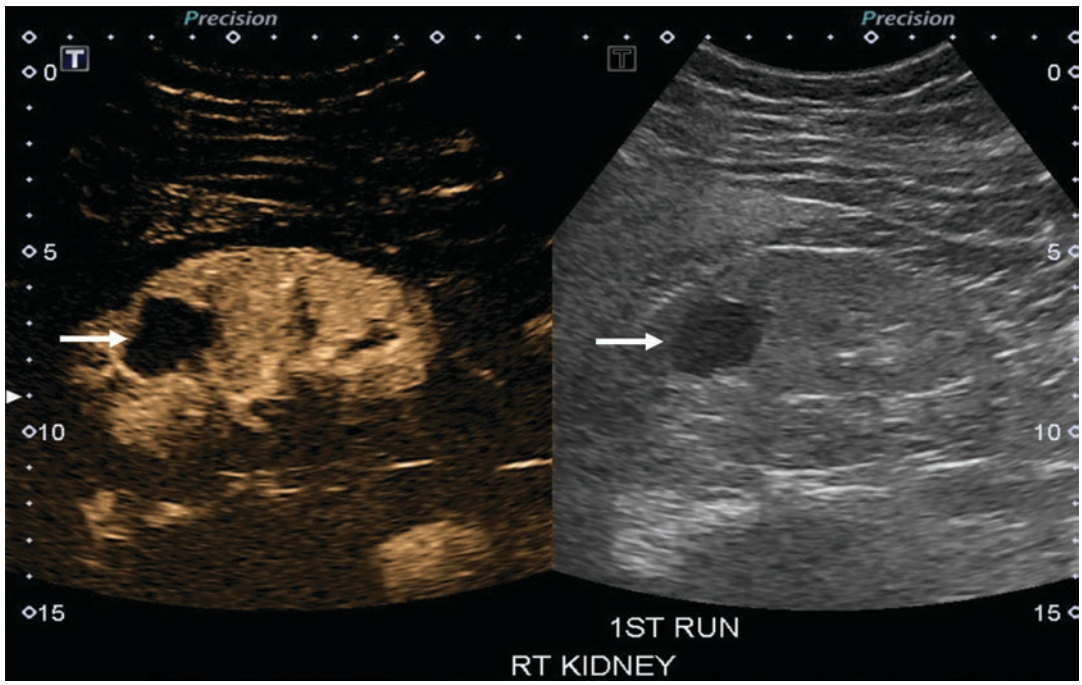

Fig. 12.1 Simple renal cyst shown on a split-screen view with the CEUS (left) and the baseline low mechanical index (MI) ultrasound image (right). CEUS shows the cyst with anechoic cyst without septa, calcification nor solid components (arrow). No enhancement after intravenous contrast agent injection. This is characteristic of a simple Bosniak Type I cyst and does not entail further investigation

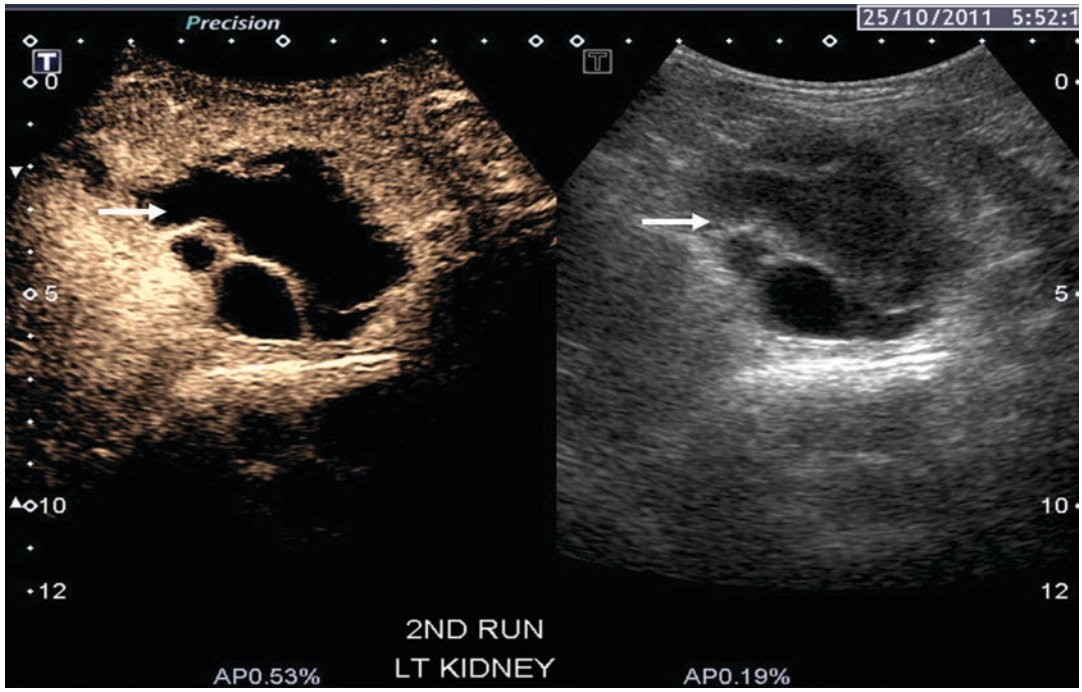

Fig. 12.2 Complex renal cyst, Bosniak IIF, shown on a split-screen view with the CEUS (left) and the baseline low mechanical index (MI) ultrasound image (right). Non-contrast US shows a large renal cyst with a solid echogenic component within the cyst (arrow). Post-contrast image shows no intra-cystic enhancement and the apparent echogenic solid lesion shows no arterial enhancement or washout. Minimal enhancement of the septa is noted, with no nodular enhancement or washout. It was proven on follow-up imaging to be a complicated cyst with some internal hemorrhage

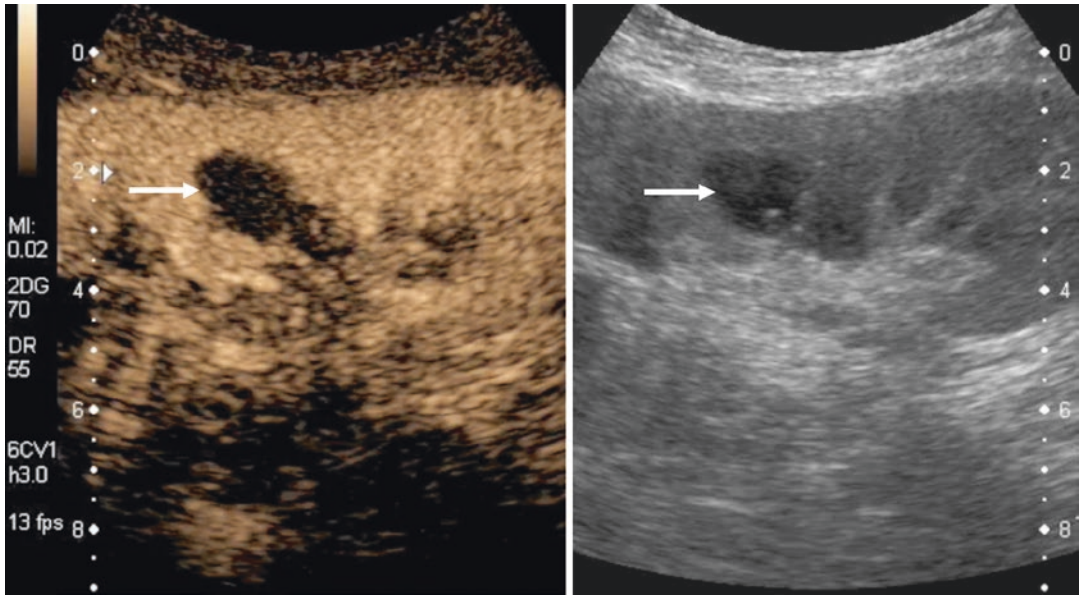

Fig. 12.3 Bosniak II cyst in a transplanted kidney shown on a split-screen view with the CEUS (left) and the baseline low mechanical index (MI) ultrasound image (right). Non-contrast image shows some thin septae within the cyst, whereas the post-contrast image shows no significant contrast enhancement within the septa, rendering the cyst to be Bosniak II

vs. 79.4%) [21]. Recently, a cohort of studies has published high sensitivity and NPV of CEUS. Barr et al. published sensitivity and NPV of 100% [22] while Li et al. reported a sensitivity of 93.3% and NPV of 99.2% respectively [23]. Our department study results support these assertions as applied to the pediatric patient, with a sensitivity of 95.5% and NPV of 98.0% [24].

A confounding factor in the interpretation of CEUS studies has been the differentiation of malignancy from benign tumors and in turn from an inflammatory lesion. This is due to the vascularity and enhancement of granulation tissue within these inflammatory lesions which can mimic tumors. Some studies have shown that approximately 30% of renal cell carcinoma (RCC) mimic angiomyolipoma (AML) on US and that half of the RCC can be hyperechoic [25] (Table 12.1).

Table 12.1 Summarizes the most frequent CEUS indications in pediatric patients with renal disorders

Indications of pediatric renal CEUS
• Renal focal solid lesions, assessment of vascularity
• Complex cystic renal lesions
• Complicated renal infection
• Renal transplant complication
• Renal trauma
• Renal artery stenosis[a]

[a]Renal artery stenosis: not commonly used but may have future indications

12.5 Renal Angiomyolipoma

Classically a renal AML shows in-filling of the UCA starting from the periphery of an echogenic lesion and slowly spreading to the center of the lesion with iso or hypoenhancement. This is most likely due to most of the blood vessels in AML being malformed with a tortuous course and disorganized blood vessels. These anatomical features associated with renal AML result in difficult inflow and slow outflow of the UCA: the start of the inflow and outflow of the UCA is later in the lesion than in the renal cortex. A typical renal AML is where the lesion is seen to be less enhancing than the adjacent normal renal parenchyma in all phases (i.e., arterial, early venous, and delayed phases (Fig. 12.4).

Fig. 12.4 Renal angiomyolipoma (AML) shown on a split-screen view with the CEUS (left) and the baseline low mechanical index (MI) ultrasound image (right). An 8-year-old boy, with an incidental note of a left kidney mass on bedside ultrasound. Non-contrast image shows a large echogenic exophytic mass (arrowheads), which shows post-contrast enhancement, which is less enhancing than the renal parenchyma (star) at all phases. No significant washout is seen within the lesion (arrows)

12.6 Renal Parenchyma Defects

Ultrasound contrast agents are truly intravascular and do not "leak" into the surrounding tissue (no "equilibrium" phase) and are not subjected to renal filtration; they behave like "vascular tracers." Using CEUS to identify the vessels, rather than color Doppler US, to track the course of the renal artery has been shown to be more accurate and shortens examination time, particularly with unfavorable body habitus, and can be used in patients with renal impairment [24, 26]. Contrast-enhanced ultrasound is an excellent modality to assess the perfusion pattern of a kidney, due to the unique ability to image microcirculation. After UCA injection, there is an immediate and prompt enhancement of the kidney, usually seen within 10 s. The main renal artery, its bifurcation, the arcuate and segmental arteries rapidly enhance with perfusion seen up to the periphery of the renal cortex (Fig. 12.5).

This ability to image the microcirculation to the peripheral renal cortex is useful in the assessment of any patient with a renal transplant. A cortical infarct often appears as a wedge-shaped defect in all phases of the contrast enhancement when compared to the rest of the renal cortex. Ischemia can be reliably differentiated from a true infarction, as in ischemia, some slow inflowing UCA will be visible [27]. Similarly, in trauma, lacerations and hematomas are seen as non-enhancing areas when compared to the surrounding enhancing renal parenchyma. Active bleeding and pseudoaneurysm formation are also easily identified. Renal transplant complications, including vascular compromise, vascular patency, cortical infarcts, and acute cortical necrosis (Fig. 12.6), can be investigated with a CEUS examination, with relative ease at the bedside, and with a confident interpretation.

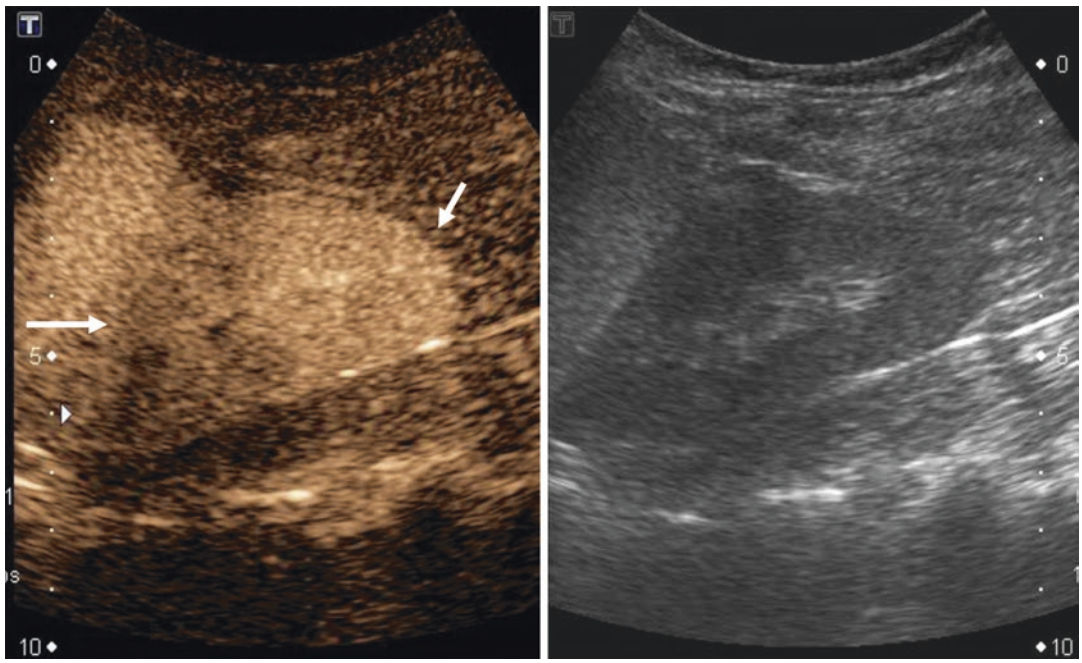

Fig. 12.5 Normal renal perfusion. Post-contrast US shows diffuse prompt homogenous uniform enhancement of the kidney (arrows), with no perfusion defects or areas of ischemia/necrosis. This appearance allows for the exclusion of the possibility of a renal thrombo-embolic episode

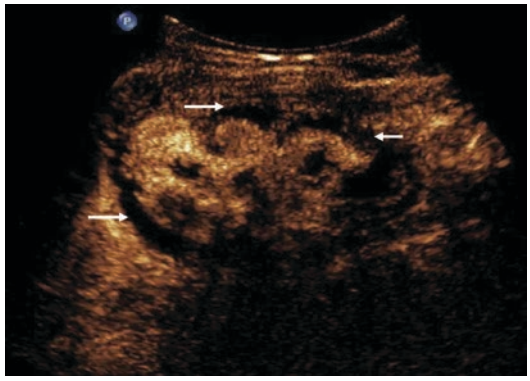

Fig. 12.6 Renal cortical necrosis. A patient with blunt abdominal trauma resulting in occlusion to the main left renal artery. Following the administration of an ultrasound contrast agent, there is an absence of enhancement to the renal cortex (arrows), consistent with subcapsular cortical necrosis

12.7 Focal Pyelonephritis and Abscess Formation

In the appropriate clinical context, CEUS can be used as an accurate tool in the assessment of renal infection and inflammatory renal masses. Focal nephronia can often present as a well-defined mass and presents a clinical conundrum for the referring pediatricians and concern for the parents; CEUS can improve the ability to differentiate a true renal malignancy from an area of benign change (Fig. 12.7). Often the characteristics on CT and MR imaging can be non-specific. Any regional difference in parenchymal enhancement is better detected than any global impairment to perfusion, as the adjacent normal parenchyma serves as an internal reference.

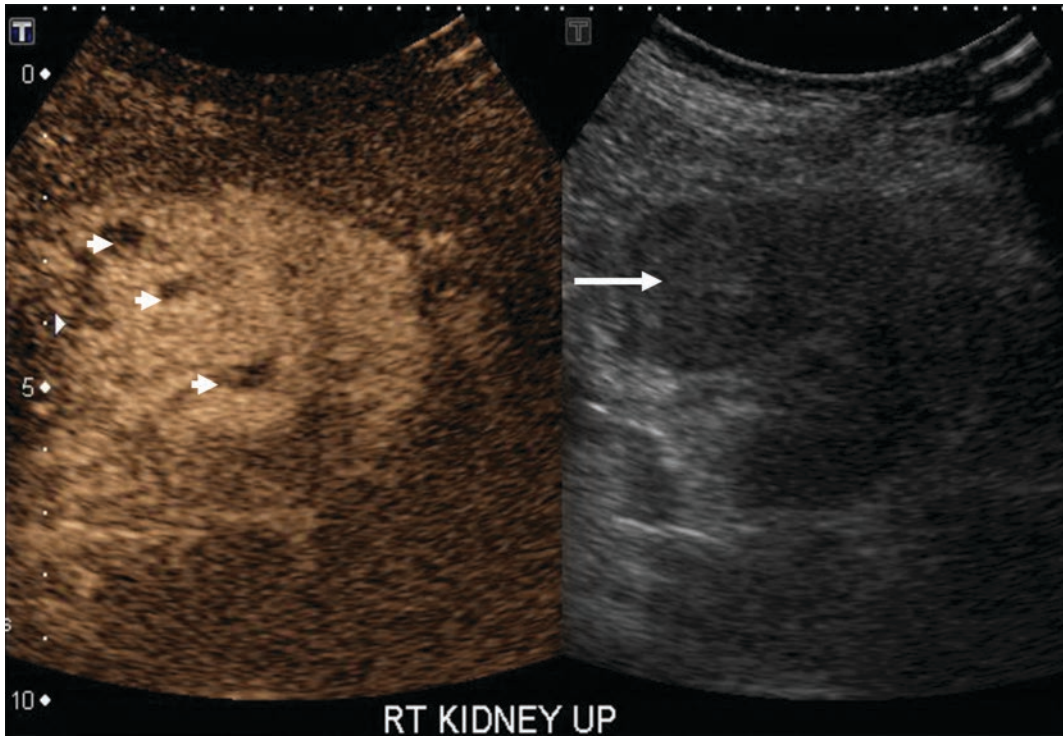

Fig. 12.7 Lobar nephronia shown on a split-screen view with the CEUS (left) and the baseline low mechanical index (MI) ultrasound image (right). This 16-year-old boy was being treated for urinary tract infection. A focal lesion is identified at the upper aspect of the right kidney arrow). Post-contrast US of the heterogeneous lesion demonstrates enhancement similar to the rest of the renal parenchyma, with areas of non-enhancement in the center of the lesion (arrowheads). No contrast washout was noted. These features are similar to CT imaging features of lobar nephronia

Children with pyelonephritis can develop renal abscesses as a complication. As conventional US is suboptimal at depicting, or confidently identifying an early renal abscess, especially when presenting on US as an indeterminate solid lesion. A CEUS examination is ideal to depict an abscess and will demonstrate a heterogeneous lesion with a central cavity, with a thick enhancing rim and often with a surrounding non-vascularized perinephric fluid collection. There is normally peripheral enhancement of the lesion on the CEUS examination, with the fluid central area of pus demonstrating no central enhancement. There is no washout on delayed images (Fig. 12.8).

12.8 Pseudotumors

A pseudotumor represents a number of normal renal anatomic variants that can be misinterpreted as a tumor on imaging. The most frequently encountered normal variants are: persistence of fetal lobulation, hypertrophied column of Bertin, and dromedary or splenic hump [28]. In conventional US and color Doppler US, pseudotumors have defined features. The addition of CEUS allows for the identification of a normal renal perfusion pattern, readily distinguished. This represents a major criterion for the diagnosis of a pseudotumor. There is limited evidence for this, but confident identification of a pseudotumor

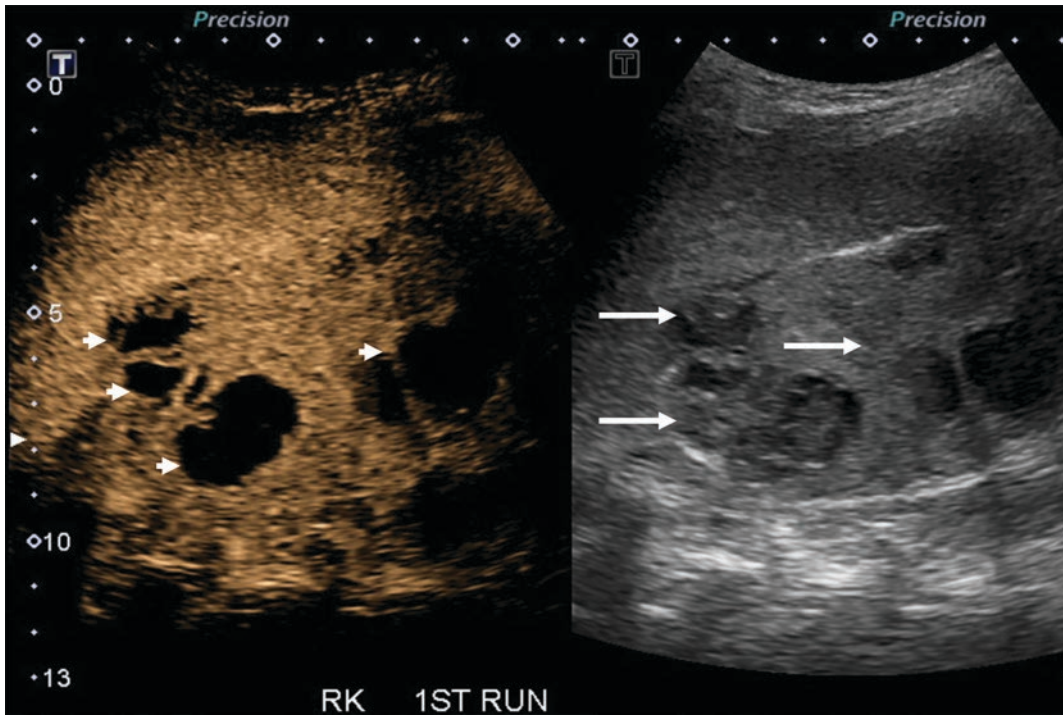

Fig. 12.8 Renal abscess shown on a split-screen view with the CEUS (left) and the baseline low mechanical index (MI) ultrasound image (right). A 10-year-old boy being treated for recurrent urinary tract infections. A bedside ultrasound was performed to look for secondary renal findings, due to persistent high fever, and elevated C-reactive protein markers. Non-contrast images show heterogeneous hypoechoic lesion (arrows). Post CEUS, there is a prompt enhancement of the periphery of the lesions, with no central enhancement (arrowheads) and no delayed washout. The enhancement timing is similar to the rest of the renal parenchyma

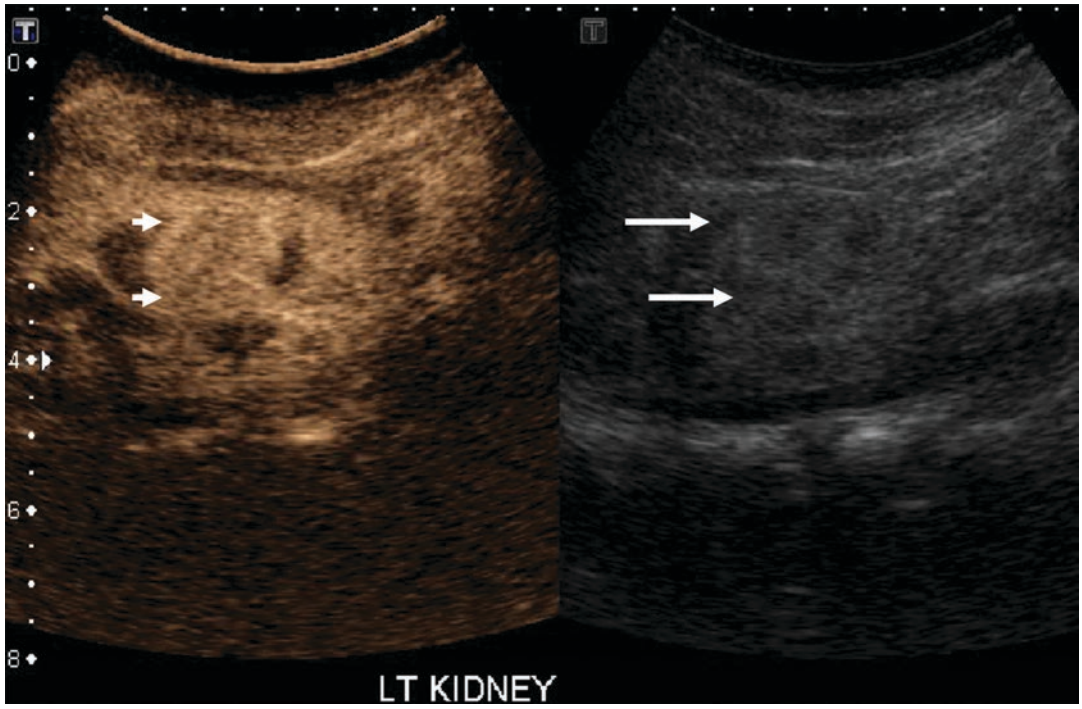

Fig. 12.9 Renal pseudotumor on a split-screen view with the CEUS (left) and the baseline low mechanical index (MI) ultrasound image (right). A 15-year-old girl, with incidental findings of a non-specific "mass" on her bedside ultrasound study. Non-contrast US shows an area of apparent altered echogenicity in the interpolar region of the kidney (arrows), which was suspicious for a possible renal tumor. Post-contrast US shows prompt and homogenous enhancement in this area (arrowheads), with similar enhancement to rest of the kidney, with no abnormal enhancement or washout, indicating the presence of normal renal tissue, likely a prominent column of Bertin

directly on US will avoid the need for further imaging with CT or MR (Fig. 12.9).

12.9 Malignant Renal Lesions

Renal lesions are common incidental findings in adult abdominal imaging, with cysts diagnosed in up to 35% of individuals after the seventh decade. In the pediatric population, a Wilms' tumor is the most prevalent renal malignancy. However, due to the usually large size of a Wilms' tumor at presentation, CT and MR imaging have normally been performed, with the usefulness of using CEUS not established. Although renal cell carcinoma (RCC) comprises only a small subset of renal lesions in the child [15], these tumors are often initially detected on imaging, preceding any clinical signs. Over 50% of RCC are initially diagnosed in this manner on imaging and with the insidious growth of an RCC, more than 60% of patients do not show any classic symptoms of hematuria, abdominal mass, or loin pain [29, 30]. Renal cell carcinomas are often identified by their increased vasculature, an important finding that is only seen with contrast-enhanced imaging [9, 11, 31, 32]. Although CT and MR imaging remains the modalities of choice, the limitations imposed by renal impairment, contrast allergies, radiation, and even technical and timing errors are disadvantageous.

An RCC is characterized by numerous thin-walled blood vessels with increased blood flow physiologically and intratumor necrosis with hemorrhage and calcification common [33]. The RCC enhances rapidly and intensely after UCA administration due to this increased blood flow (Figs. 12.10 and 12.11). The UCA than washes

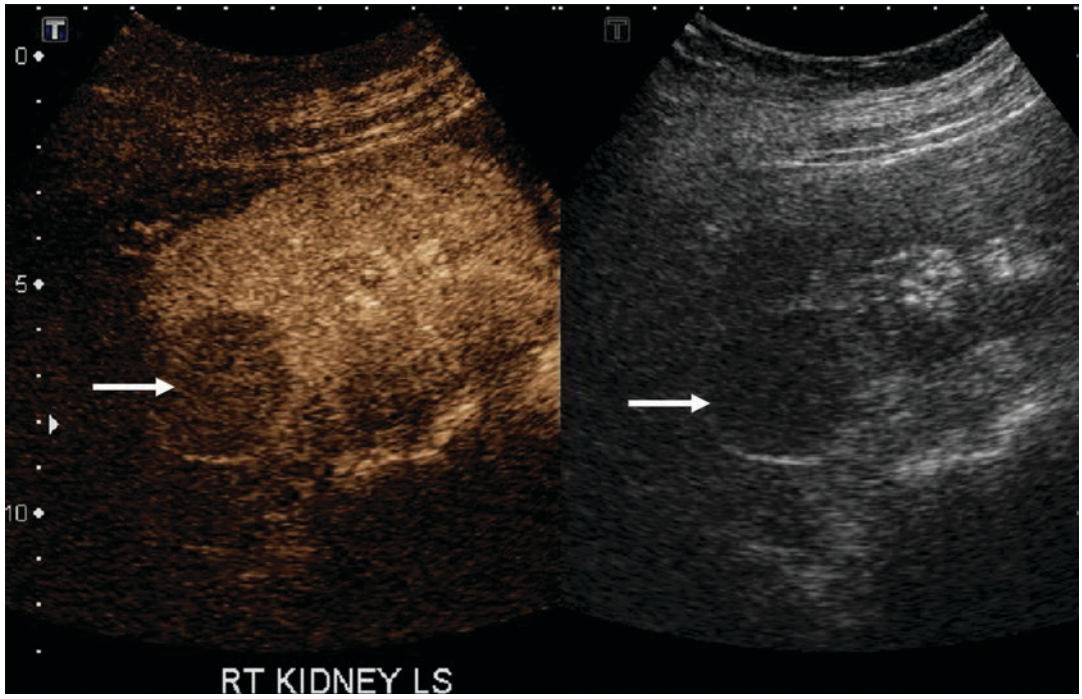

Fig. 12.10 Renal cell carcinoma shown on a split-screen view with the CEUS (left) and the baseline low mechanical index (MI) ultrasound image (right) in a 13-year-old boy presented with hematuria for investigation. Following UCA administration, the lesion showed homogenous central enhancement (arrow) within the lesion, which appeared less enhancing as compared to the rest of the renal parenchyma, and showed washout in the delayed images, suspicious for a malignant lesion

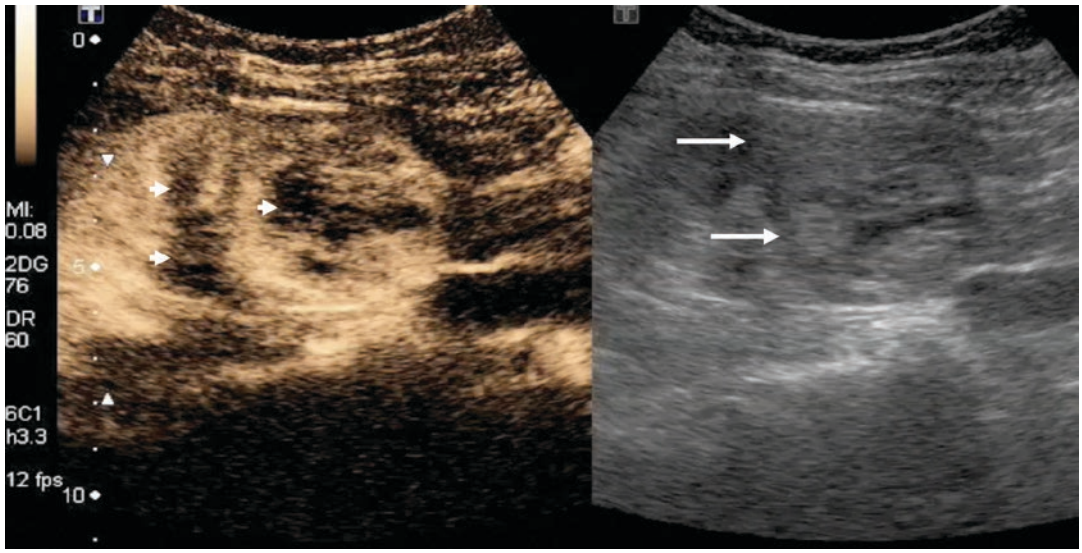

Fig. 12.11 Renal cell carcinoma shown on a split-screen view with the CEUS (left) and the baseline low mechanical index (MI) ultrasound image (right). A complex solid cystic encapsulated lesion at the lower pole of the left kidney (arrows) with immediate enhancement and areas of washout after intravenous contrast injection (arrowheads)

out rapidly in comparison to the adjacent liver/spleen [10]. Almost all malignant renal lesions show similar imaging characteristics on CEUS, with immediate contrast enhancement and rapid washout, appearing less enhancing than the adjacent renal parenchyma on delayed images [34]. Despite some conflicting data on RCC vascularization patterns, published studies have generally been positive [35]. Of note, Barr et al. evaluated the performance of CEUS in 1018 indeterminate renal lesions and showed high sensitivity 100%; specificity 95.0%; PPV 94.7%; and NPV of 100% [22]. The main advantage of CEUS is the avoidance of any renal damage and the issue with the increasing prevalence of acute kidney injury limiting the use of contrast-enhanced CT and MR [36]. Contrast-enhanced ultrasound will play a larger role in evaluating and differentiating benign from malignant renal lesions in the future.

12.10 Summary

Contrast-enhanced ultrasound is useful in children, as this reduces the radiation burden of CT, and this technique is likely to be beneficial in similar indications as in adults (such as differential of focal lesions in parenchymal organs, organ perfusion) [2, 5, 37, 38]. Contrast-enhanced ultrasound has proven to be an excellent tool in the assessment of renal perfusion, renal infection (abscess), solid and cystic renal masses (cysts, angiomyolipoma's, neoplastic lesions), and pseudo-tumors [27]. The main benefit of CEUS over other investigation modalities in assessing renal pathology in children is that UCAs are not nephrotoxic and can be employed safely in patients with impaired renal function. Such an advantage, coupled with a lack of ionizing radiation adds immense value in the assessment of renal diseases. Possible contraindication for the use of CEUS in the pediatric age group would be a history of the right to left shunts, severe cardiac rhythm disorders, and severe respiratory failure including respiratory distress syndrome, in keeping with the recommendations of the UCA manufacturer [39].

However, the use of CEUS as an imaging modality does have some limitations: a relatively short diagnostic window that might need two UCA injections for the same kidney or one injection for each kidney. Simultaneous assessment of more than one focal lesion may be difficult and may require multiple injections during the examination. In general, US is relatively harder to perform and interpret in the obese child and bowel gas can interfere with images. Patient compliance is required as the lesion may not be visible in one particular position or the patient may be required to hold his or her breath, which is not always possible with the child. As the UCA is not excreted by the kidney, it is not possible to assess the renal excretory function and detailed anatomy of the urinary collecting system. There is not universal approval for the use of UCA in children, and often these agents are used off-label, not an issue in medical practice [40]. With the approval of the use of an intravenous UCA in the United States, it is expected that the applications will increase.

In conclusion, CEUS is an accurate, inexpensive, non-radiation modality, with an accurate depiction of enhancement patterns of focal renal lesions. It is safe to be used in children with renal insufficiency and renal failure and appears to have minimal episodes of contrast allergy. Its accuracy is at least similar, if not better than CT or MR imaging in the assessment of focal renal lesions and can be used as a modality of choice for solitary focal renal lesions in presence of renal insufficiency. Its role in the pediatric age group has been less defined and further studies should be performed to validate its use as a safe and viable alternative to CT and MR imaging for renal diseases.

References

1. Claudon M, Dietrich CF, Choi BI, Kudo M, Nolsoe C, Piscaglia F, et al. Guidelines and good clinical practice recommendations for contrast enhanced ultrasound (CEUS) in the liver—update 2012. Ultraschall Med. 2013;34:11–29.

2. Sidhu PS, Cantisani V, Deganello A, Dietrich CF, Duran C, Franke D, et al. Role of contrast-enhanced ultrasound (CEUS) in paediatric practice: an EFSUMB position statement. Ultraschall Med. 2017;38:33–43.
3. Sidhu PS, Cantisani V, Dietrich CF, Gilja OH, Saftoiu A, Bartels E, et al. The EFSUMB guidelines and recommendations for the clinical practice of contrast-enhanced ultrasound (CEUS) in non-hepatic applications: update 2017 (short version). Ultraschall Med. 2018;39(2):154–80.
4. Piscaglia F, Bolondi L. The safety of SonoVue in abdominal applications: retrospective analysis of 23188 investigations. Ultrasound Med Biol. 2006;32:1369–75.
5. Yusuf GT, Sellars ME, Deganello A, Cosgrove DO, Sidhu PS. Retrospective analysis of the safety and cost implications of pediatric contrast-enhanced ultrasound at a single center. AJR Am J Roentgenol. 2016;208:446–52.
6. Riccabona M. Application of a second-generation US contrast agent in infants and children—a European questionnaire-based survey. Pediatr Radiol. 2012;42:1471–80.
7. Riccabona M, Avni FE, Damasio MB, Ording-Muller LS, Blickman JG, Darge K, et al. ESPR Uroradiology Task Force and ESUR Paediatric Working Group—Imaging recommendations in paediatric uroradiology, part V: childhood cystic kidney disease, childhood renal transplantation and contrast-enhanced ultrasonography in children. Pediatr Radiol. 2012;42:1275–83.
8. Darge K, Papadopoulu F, Ntoulia A, Bulas DI, Coley BD, Fordham LA, et al. Safety of contrast-enhanced ultrasound in children for non-cardiac applications: a review by the Society for Pediatric Radiology (SPR) and the International Contrast Ultrasound Society (ICUS). Pediatr Radiol. 2013;43:1063–73.
9. Wang XH, Wang YJ, Lei CG. Evaluating the perfusion of occupying lesions of kidney and bladder with contrast-enhanced ultrasound. Clin Imaging. 2011;35(6):447–51.
10. Setola SV, Catalano O, Sandomenico F, Siani A. Contrast-enhanced sonography of the kidney. Abdom Imaging. 2007;32(1):21–8.
11. Quaia E, Bertolotto M, Cioffi V, Rossi A, Baratella E, Pizzolato R, et al. Comparison of contrast-enhanced sonography with unenhanced sonography and contrast-enhanced CT in the diagnosis of malignancy in complex cystic renal masses. Am J Roentgenol. 2008;191:1239–49.
12. Ascenti G, Mazziotti S, Zimbaro G, Settineri N, Magno C, Melloni D, et al. Complex cystic renal masses: characterization with contrast-enhanced US. Radiology. 2007;243:158–65.
13. Clevert DA, Minaifar N, Weckbach S, Jung EM, Stock K, Reiser M, et al. Multislice computed tomography versus contrast-enhanced ultrasound in evaluation of complex cystic renal masses using the Bosniak classification system. Clin Hemorheol Microcirc. 2008;39:171–8.
14. Bertolotto M, Derchi LE, Cicero C, Iannelli M. Renal masses as characterized by ultrasound contrast. Ultrasound Clin N Am. 2013;8:581–92.
15. Park BK, Kim B, Kim SH, Ko K, Lee HM, Choi HY. Assessment of cystic renal masses based on Bosniak classification: comparison of CT and contrast-enhanced US. Eur J Radiol. 2007;61:310–4.
16. Graumann O, Osther SS, Karstoft J, Hørlyck A, Osther PJ. Bosniak classification system: inter-observer and intra-observer agreement among experienced uroradiologists. Acta Radiol. 2015;56(3):374–83.
17. Israel GM, Bosniak MA. An update of the Bosniak renal cyst classification system. Urology. 2005;66:484–8.
18. Bosniak MA. The current radiological approach to renal cysts. Radiology. 1986;158(1):1–10.
19. McArthur C, Baxter GM. Current and potential renal applications of contrast-enhanced ultrasound. Clin Radiol. 2012;67:909–22.
20. Xue LY, Lu Q, Huang BJ, Ma JJ, Yan LX, Wen JX, et al. Contrast-enhanced ultrasonography for evaluation of cystic renal mass: in comparison to contrast-enhanced CT and conventional ultrasound. Abdom Imaging. 2014;39(6):1274–83.
21. Chen Y, Wu N, Xue T, Hao Y, Dai J. Comparison of contrast-enhanced sonography with MRI in the diagnosis of complex cystic renal masses. J Clin Ultrasound. 2015;43(4):203–9.
22. Barr RG, Peterson C, Hindi A. Evaluation of indeterminate renal masses with contrast-enhanced US: a diagnostic performance study. Radiology. 2014;271:133–42.
23. Li X, Liang P, Yu X, Cheng Z, Han Z, Liu F, et al. Value of real-time contrast-enhanced ultrasound in diagnosis of renal solid renal lesions. Nan Fang Yi Ke Da Xue Xue Biao. 2014;34:890–5.
24. Yong C, Teo YM, Jeevesh K. Diagnostic performance of contrast-enhanced ultrasound in the evaluation of renal masses in patients with renal impairment. Med J Malaysia. 2016;71:193–8.
25. Forman HP, Middleton WD, Melson GL, McClennan BL. Hyperechoic renal cell carcinomas: increase in detection at US. Radiology. 1993;272:757–66.
26. Paspulati RM, Bhatt S. Sonography in benign and malignant renal masses. Radiol Clin N Am. 2006;44(6):787–803.
27. Harvey CJ, Alsafi A, Kuzmich S, Ngo A, Papadopoulou I, Lakhani A, et al. Role of US contrast agents in the assessment of indeterminate solid and cystic lesions in native and transplant kidneys. Radiographics. 2015;35(5):1419–30.
28. Marchal G, Verbeken E, Moerman F, Baert AL, Lauweryns J. Ultrasound of the normal kidney: a sonographic, anatomic and histologic correlation. Ultrasound Med Biol. 1986;12:999–1009.

29. Ozen H, Colowick A, Freiha FS. Incidentally discovered solid renal masses: what are they? Br J Urol. 1993;72:274–6.
30. Jayson M, Sanders H. Increased incidence of serendipitously discovered renal cell carcinoma. Urology. 1998;51(2):203–5.
31. Ignee A, Straub B, Brix D, Schuessler G, Ott M, Dietrich CF. The value of contrast enhanced ultrasound (CEUS) in the characterisation of patients with renal masses. Clin Hemorheol Microcirc. 2010;46:275–90.
32. Raj GV, Bach AM, Iasonos A, Korets R, Blitstein J, Hann L, et al. Predicting the histology of renal masses using preoperative Doppler ultrasonography. J Urol. 2007;177(1):53–8.
33. Reese JH. Renal cell carcinoma. Curr Opin Oncol. 1992;4:427–34.
34. Harvey CJ, Sidhu PS. Ultrasound contrast agents in genito-urinary imaging. Ultrasound Clin N Am. 2011;5:489–506.
35. Haendl T, Strobel D, Legal W, Frieser M, Hahn EG, Bernatik T. Renal cell cancer does not show a typical perfusion pattern in contrast-enhanced ultrasound. Ultraschall Med. 2009;30(01):58–63.
36. Jakobsen J, Oyen R, Thomsen HS, Morcos SK, Members of Contrast Media Safety Committee of European Society of Urogenital Radiology (ESUR). Safety of ultrasound contrast agents. Eur Radiol. 2005;15(5):941–5.
37. Fang C, Bernardo S, Sellars ME, Deganello A, Sidhu PS. Contrast-enhanced ultrasound in the diagnosis of pediatric focal nodular hyperplasia and hepatic adenoma: interobserver reliability. Pediatr Radiol. 2019;49(1):82–90.
38. Rafailidis V, Deganello A, Watson T, Sidhu PS, Sellars ME. Enhancing the role of paediatric ultrasound with microbubbles: a review of intravenous applications. Br J Radiol. 2016;90(1069):20160556.
39. Sellars ME, Deganello A, Sidhu PS. Paediatric contrast-enhanced ultrasound (CEUS); a technique that requires co-operation for rapid implementation into clinical practice. Ultraschall Med. 2014;35:203–6.
40. Sidhu PS, Choi BI, Bachmann NM. The EFSUMB guidelines and recommendations on the clinical practice of contrast enhanced ultrasound (CEUS): a new dawn for the escalating use of this ubiquitous technique. Ultraschall Med. 2012;32:5–7.

13 Pediatric Contrast-Enhanced Ultrasonography (CEUS) of the Spleen

Doris Franke and Zoltan Harkanyi

13.1 Introduction

The spleen is rarely affected by primary diseases, but secondary diffuse or focal alterations may be seen in a broad variety of causes. For all imaging modalities, including contrast-enhanced ultrasound (CEUS), characterization of focal or diffuse splenic lesions is more difficult than in the liver. Blood pool agents however allow a better description of the parenchymal perfusion and vascularization pattern. Contrast-enhanced ultrasound of the spleen increases the detection rate of splenic infarction, trauma, and splenuncula [1, 2] and is an ideal indication for CEUS in children in order to reduce the overall radiation burden [3].

13.2 Investigation Technique

The enhancement pattern of the ultrasound contrast agent (UCA) is described in the early arterial and later parenchymal phase as being hyper-, iso, or hypo-enhancing in comparison to the surrounding splenic tissue and the enhancement of the left kidney. The reasons for the comparably long duration and higher intensity of UCA enhancement of the spleen in relation to other organs are not fully understood. Pooling of the UCA in the sinusoids or splenic tropism [4, 5] is likely caused and under discussion.

The arterial phase in the spleen lasts for 5–60 s and the parenchymal phase up to 5 min (or even longer) after UCA injection [4]. Depending on the indication, the sonographic investigation should be performed in an intermittent manner in order to avoid bubble destruction. The dose depends on the age and weight of the child, the ultrasound device, the software and transducer used, the depth of the lesion, and lesion vascularity. The UCA dosage is usually less than the dosage for the liver or kidney due to the intense and long-lasting UCA enhancement in the spleen.

During scanning, UCA intensity, homogenicity, and focal lesions should be observed. Limitations for CEUS are the same as for B-mode US imaging: difficult viewing of the subdiaphragmatic and neighboring areas of the spleen due to lung or colon gas overlay, great depth, or small lesions (<1 cm).

In the arterial phase, a typically inhomogeneous pattern of UCA enhancement can be observed in many patients. This is termed the "tiger or zebra pattern" and thought to be caused by different UCA velocities in splenic capillaries,

D. Franke
Pediatric Ultrasonography, Department of Pediatric Kidney, Liver and Metabolic Diseases, Children's Hospital, Hannover Medical School, Hannover, Germany
e-mail: Franke.Doris@mh-hannover.de

Z. Harkanyi (✉)
Department of Radiology, Heim Pal National Pediatric Institute, Budapest, Hungary
e-mail: harkanyi@heimpalkorhaz.hu

P. S. Sidhu et al. (eds.), *Contrast-Enhanced Ultrasound in Pediatric Imaging*,
https://doi.org/10.1007/978-3-030-49691-3_13

pulpa, and sinusoids. Approximately 50 s post-injection, the UCA enhancement should be homogeneous throughout the spleen. General signs of benign lesions are persistent iso-enhancement or absent enhancement with avascularity of the lesion (e.g., a cyst). Signs of malignancy are a washout phenomenon or a hypo-enhancement in the late parenchymal phase.

13.3 Spenunculi or Accessory Spleens, Splenosis, and Polysplenia

Accessory spleens are very common and seen in an overall prevalence of 15% in a meta-analysis of 22,487 patients [2, 6]. Identification of splenunculi is particularly important in patients with immune thrombocytopenia requiring splenectomy as unrecognized accessory spleens may increase in size after splenectomy and responsible for refractory symptoms. The location of a spenculus is most often at the hilum or lower pole of the spleen, but may also be found within the pancreas or elsewhere in the abdomen. Splenunculi have the same B-mode ultrasonography (US) appearance and the same contrast enhancement characteristics of the normal spleen. This may be important in the diagnosis of ectopic splenic tissue in the pancreatic tail or elsewhere in the abdomen, particularly after traumatic splenic rupture, and in the differential diagnosis of lymph nodes at the splenic hilum. The post-traumatic splenic auto-transplantation of splenic tissue in the abdomen is called *splenosis*. Contrast-enhanced ultrasound can identify the characteristic persistent late-phase enhancement of splenic tissue and may be useful in splenosis [7]. *Polyspenia* is most commonly associated with syndromes such as heterotaxy and is usually diagnosed on the B-mode US.

13.4 Anomalies of Position: Wandering Spleen

A "wandering spleen" is a hyper-mobile, abnormally positioned ectopic spleen and may be an excellent indication for CEUS if painful torsion is suspected, congestion or infarction occurs due to the mobility [8, 9]. It is a rare and possibly congenital condition due to abnormally lax ligaments failing to keep the spleen in the anatomical position. The correct and early diagnosis is challenging, especially in children with symptoms ranging from none, recurrent abdominal pain to acute abdomen in case of torsion or infarction [9, 10]. The main CEUS finding is a non-enhancement in the infarcted areas (Fig. 13.1).

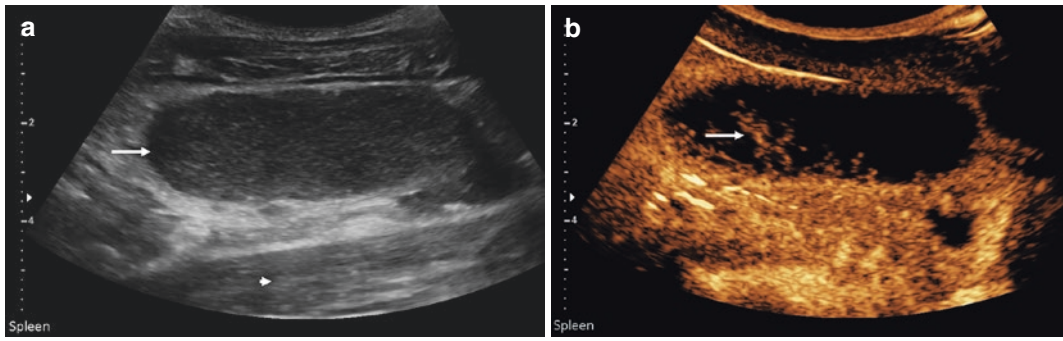

Fig. 13.1 Infarction of a wandering spleen. (**a**) The spleen (arrow) is present in the left iliac fossa, above the psoas muscle (arrowhead) in a 9-year old boy with 3 days of intractable abdominal pain, with identification of an abnormal position of the spleen. (**b**) Following the administration of an UCA, there is only hilar vessel enhancement (arrow) consistent with infarction in a "wandering spleen." (Courtesy of Annamaria Deganello and Maria Sellars)

13.5 Splenic Infarction

Splenic infarction is seen in children with sickle-cell disease, after septic embolism in bacterial endocarditis or myeloproliferative diseases. In the early phase, infarction of the spleen is often iso-echogenic (later hypo-echogenic), may be ill delineated on the B-mode US, and may, therefore, be overlooked. After administration of the UCA, non-enhancement is often triangular in the configuration in the spleen (wedge-shaped). Complications after splenic infarction are liquification of the affected parenchyma, hemorrhage, post-infarction splenic rupture, or splenic pseudoaneurysm, all of which may be diagnosed using CEUS [11, 12]. Splenic pseudoaneurysms are particularly clinically relevant for the child [13]. A study using CEUS in the assessment of upper left quadrant pain and splenic inhomogeneity on the B-mode US in adults with focal lesions found half of these lesions were splenic infarction [11]. Recurrent splenic infarction may lead to calcification, organ shrinkage, and eventually functional asplenia/hyposplenia. In functional asplenia, a reduced or even absent CEUS enhancement in the parenchymal phase can be suggestive [4].

13.6 Focal and Diffuse Lesions of the Spleen

13.6.1 Benign Focal Lesions of the Spleen

13.6.1.1 Cystic Lesions

Simple cysts have a characteristic B-mode US appearance; being round, anechoic with posterior enhancement, with no vascularization on color Doppler US and a thin smooth wall. Pseudo- or secondary cysts are thought to be of traumatic or inflammatory origin, containing blood or debris in the early stage and with a thickened or a calcified wall. In simple cysts, there is no indication for a CEUS examination, only if the cyst is thought complicated (Fig. 13.2). Hydatid cysts of the spleen are uncommon in comparison to the liver and seen in only 5% of patients with *Echinicoccal* disease. After administration of a UCA, there may be a hyper enhanced rim and no enhancement in the center of the cyst.

13.6.1.2 Hemangioma

Cavernous hemangiomas are the most common solid focal splenic lesion. Usually, hemangiomas appear well delineated, round, hyperechoic with sometimes with echo-poor regions

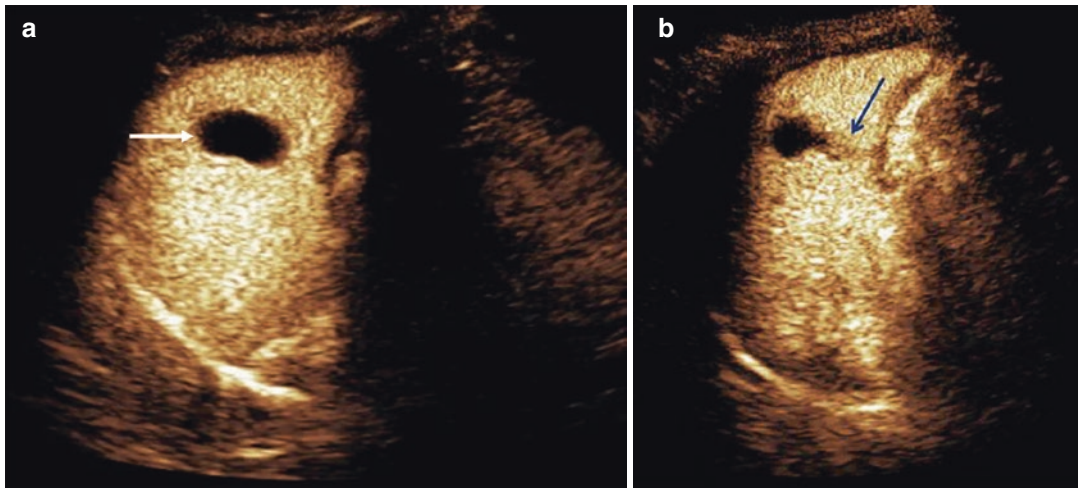

Fig. 13.2 Simple splenic cysts. (**a**) Contrast-enhanced ultrasound of a simple splenic cyst (arrow) sometimes following trauma to the left flank and an incidental finding on ultrasound. (**b**) A simple cyst (arrow) with a hypo-enhancing line (arrowheads) towards the capsule

and have no or few signals on color Doppler US due to the slow blood flow. Calcification may be present. On CEUS, a characteristic slow centripetal nodular rim enhancement can be detected similar to that in hepatic hemangiomas. Hemangiomas may present solitary or multiple (Fig. 13.3).

13.6.1.3 Lymphangioma

Lymphangiomas (lymphatic malformations) in children are benign and can be found anywhere in the body. Splenic manifestations are rare. Lymphangiomas present on the B-Mode US as an accumulation of well-delineated small or big cysts with septae, containing a lymph-like fluid and possibly debris. The cysts show no contrast enhancement, whereas the septae can enhance due to the presence of vessels (Fig. 13.4).

13.6.1.4 Hamartoma

Splenic hamartomas are also termed "splenoma," "nodular splenic hyperplasia" or "focal nodular hyperplasia of the spleen" are rare congenital benign vascular tumors, which are usually asymptomatic and diagnosed incidentally. Complications may be an increase in size and rupture. They are of variable B-mode US appearance: hypo-echoic and lobulated. The CEUS criteria are a persistent hyper-enhancement of the lesion and a spoke wheel pattern in the early phase (Fig. 13.5).

13.6.1.5 Malignant Solid Lesions

Metastasis

Primary malignancy of the spleen and splenic metastasis is rare in adults and children.

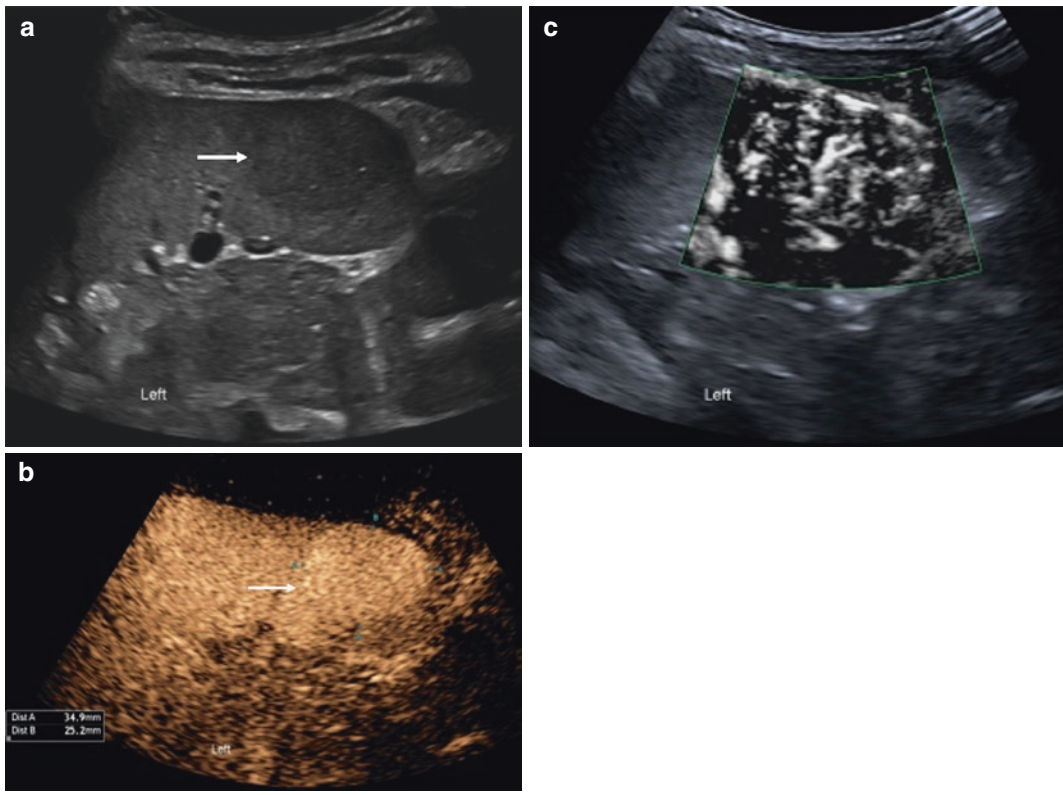

Fig. 13.3 Splenic hemangioma. (**a**) Hypoechoic solid mass (arrow) in the spleen in a 16-year-old boy with no prior clinical history. (**b**) On the CEUS image, the hypoechoic lesion is seen to enhance (arrow, between cursors) more than the surrounding spleen. (**c**) A microvascular CEUS mapping image of the mass

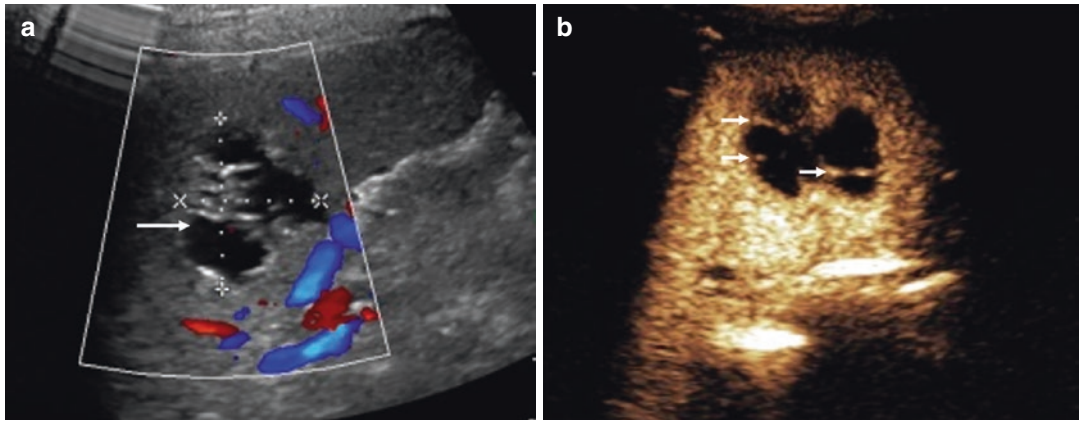

Fig. 13.4 Splenic lymphatic malformation. (**a**) Cystic mass (arrow, between cursors) with multiple septa with no vascularity on color Doppler US. (**b**) On the CEUS image of the mass, there is no enhancement of the cystic component but enhancement of the septations is present (arrows), typical of a rare isolated splenic lymphangioma

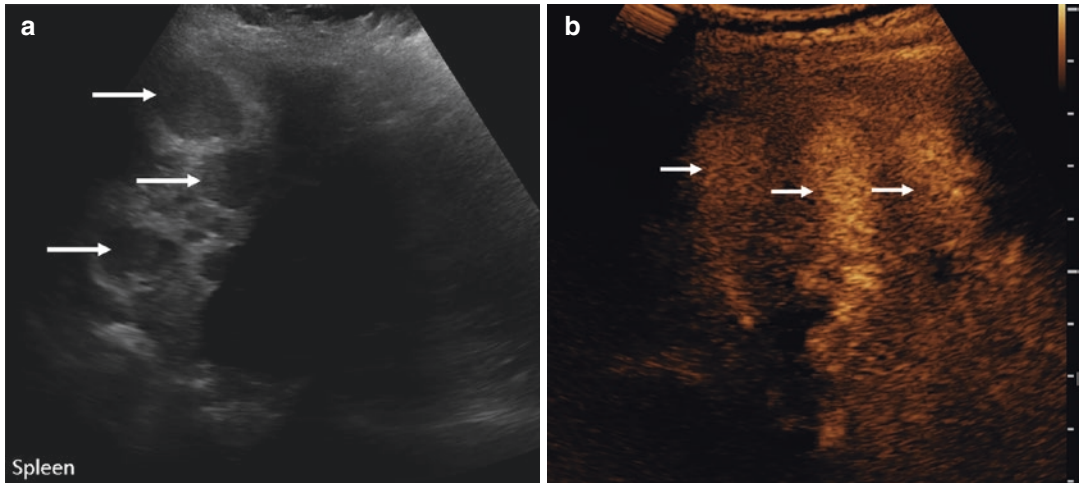

Fig. 13.5 Splenic hamartomas. (**a**) A 17-year-old patient with multiple hypoechoic rounded lesions (arrows) present in the spleen, with a history of sickle cell disease. (**b**) Following the CEUS examination, the lesions (arrows) are hyper-enhancing more than the adjacent spleen, and remain hyper-enhancing throughout the examination. (Courtesy of Maria Sellars)

Angiosarcoma and primary lymphoma are reported [14]. Lymphoma is the most common secondary lesion of the spleen in children and is described below. There is limited data for the role of CEUS in the detection and characterization of splenic metastasis in adults and none in children. Contrast-enhanced ultrasound was found to improve the imaging of metastasis with respect to sensitivity and specificity compared to B-Mode US by 40% [15]. Most of the metastasis was hypoenhancing (66%) or complex (25%) in the early arterial phase and 75% hypoenhancing in the later parenchymal phase using CEUS.

Lymphoma

Involvement of the spleen is seen in approximately 10–30% of patients in Hodgkin's lymphoma. The spleen may be enlarged and the lymphoma lesion in the spleen is usually hypo-echoic on B-Mode US, with no alteration of the splenic vessels on colour-

Doppler imaging. Following administration of the UCA, an often-progressive hypo-enhancement in the splenic lymphoma nodule is seen in the parenchymal phase (Fig. 13.6). However, splenic CEUS cannot detect diffuse or small-nodular lymphoma infiltration. Therefore, it is not a standard procedure in lymphoma staging and is reported to have no clear advantage in the diagnosis of lymphoma splenic involvement in adults [16]. However, it has been shown that CEUS provides higher sensitivity than computed tomography (CT) or positron emission tomography-CT (PET-CT) in the detection of splenic involvement in Hodgkin's lymphoma [17]. There are currently no studies in children.

13.6.1.6 Splenic Abscesses

Due to the immune competence of the spleen, the incidence of splenic abscesses is lower than for the liver. Hematological spread may occur in bacterial endocarditis or even be attributable to fungal infections in leukemia. The B-Mode US appearance may be variable: well-or ill-delineated, hypo-echoic or later hyper-echoic, micro- or macro-abscesses containing air, debris or liquid, with or without an abscess wall. A perilesional hyper-enhancement is highly suggestive of a splenic abscess during CEUS, with the center of the mass usually showing no enhancement (Fig. 13.7).

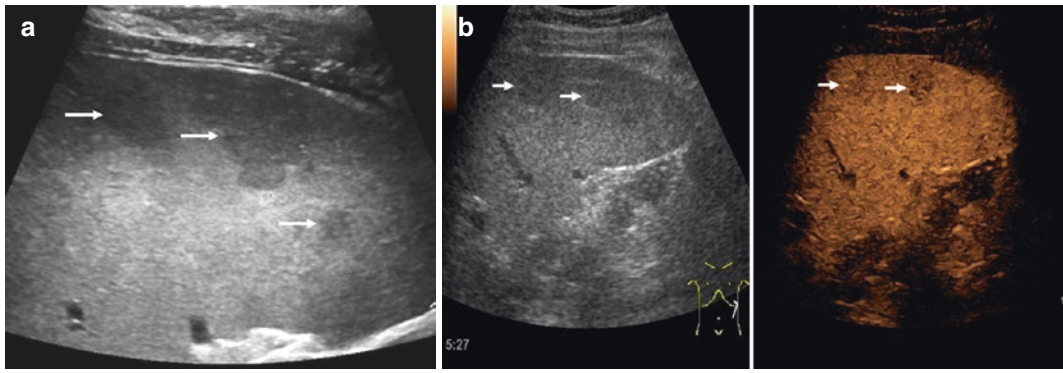

Fig. 13.6 Splenic lymphoma. (**a**) Hodgkin's lymphoma of the spleen in a 14-year-old boy, on B-mode with several hypoechoic focal lesions (arrows) in the spleen. (**b**) The CEUS examination depicts several lesions (arrows) with persistent hypo-enhancement. The continuity of the splenic vessels is respected

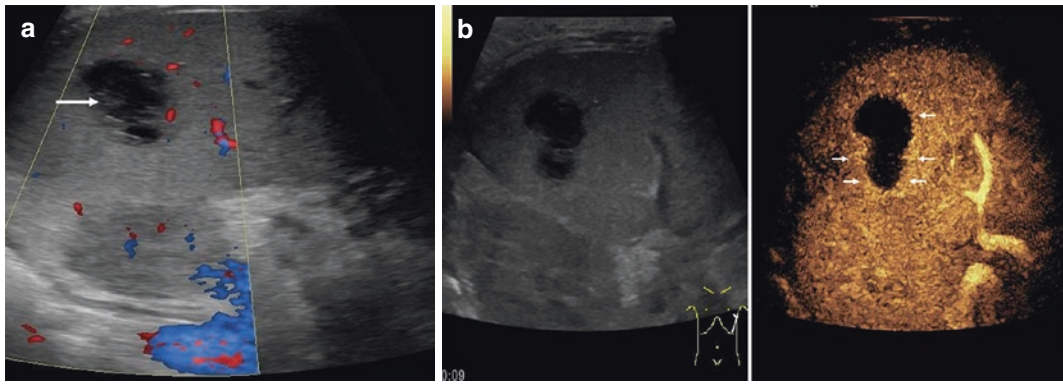

Fig. 13.7 Splenic abscess. (**a**) A 4-year-old child with pain and fever. Longitudinal section through the spleen with a hypoechoic round lesion and no vascularization on color Doppler study (arrow). (**b**) The CEUS shows non-enhancement within the lesion with a hyper-enhanced rim around the abscess (arrows)

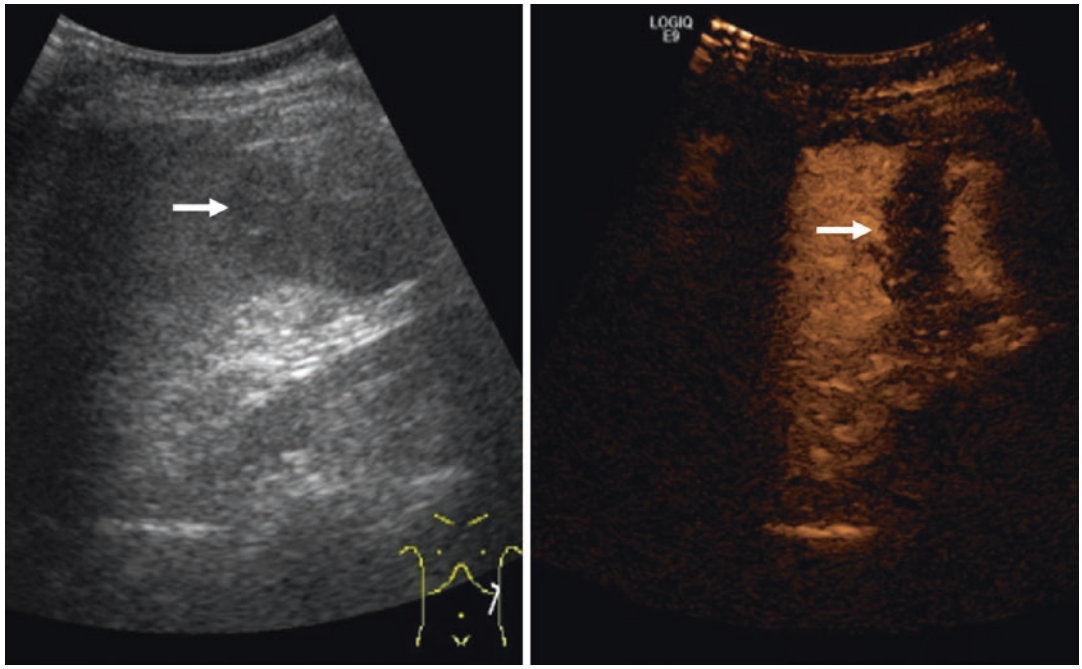

Fig. 13.8 Splenic trauma. Following a splenic biopsy, a splenic band-like hematoma (arrow) with clinical evidence of bleeding. The CEUS examination shows no enhancement over all phases at the hematoma site (arrow)

13.6.1.7 Splenic Trauma

In blunt or penetrating abdominal trauma, injury of the splenic is common, despite the intrathoracic position of the spleen. However, B-Mode US imaging is not sensitive in the detection of small lacerations, particularly in the first 2 days after the trauma. This is due to the initial isoechoic or hypo-echoic appearance of the laceration, and compression of the lesion a consequence of surrounding parenchymal edema (Fig. 13.8). Using UCA, the sensitivity of detection of a splenic laceration increases from 51% to 92% [18] as CEUS improves the visualization of any non-vascularized defect [19, 20]. For low-energy abdominal trauma, CEUS has been suggested as the first-line imaging modality, especially in children to minimize the radiation burden [21], and also for the detection and management of follow-up complications. In the detection of the splenic pseudoaneurysm, CEUS appears to be highly sensitive and specific for diagnosis and follow-up [13]. In a cohort of adult patients, Poletti et al. described a 75% sensitivity and 100% specificity of the CEUS examinations in abdominal trauma [22], concluding that CEUS may be useful for the screening of delayed traumatic splenic pseudoaneurysms. The incidence of post-traumatic splenic pseudoaneurysms may be higher than previously predicted with approximately 9% in a pediatric cohort [13]. A splenic of hepatic pseudoaneurysm has potentially life-threatening rupture often with a delayed presentation. The incidence of pseudoaneurysms in the liver seems to be higher than in the spleen. Monitoring after embolization or spontaneous thrombosis of the pseudoaneurysms can be performed using CEUS with possible detection of pseudoaneurysms smaller than 0.5 cm, where the detection frequency with CT would be lower. Using CEUS instead of contrast-enhanced CT, radiation exposure can be reduced, costs are lower, and bedside practice is possible. No association was found between the grade of trauma and the occurrence of pseudoaneurysms of the spleen or liver [13]. Follow-up CEUS after a splenic injury can be performed after major trauma, in suspected fractures or rupture of the spleen, delayed vascular injury, to rule out pseudoaneurysms, in hemodynamic unstable children, and in case of secondary active bleeding [23, 24] (Fig. 13.9).

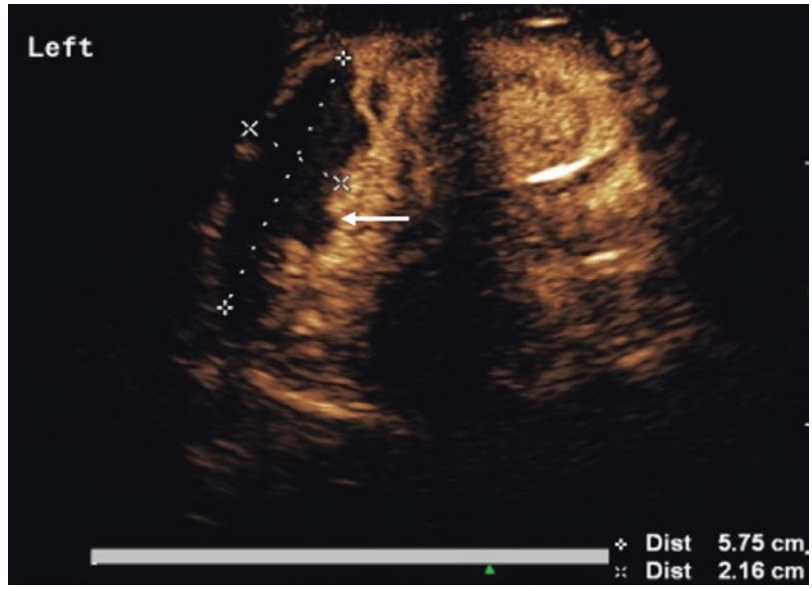

Fig. 13.9 Splenic contusion after blunt trauma. In a 10-year-old girl with blunt trauma to the spleen, the CEUS images demonstrate a large contusion (arrow, between cursors) of the spleen in the subdiaphragmatic region. The patient was treated conservatively

Table 13.1 Indications for pediatric CEUS of the spleen

Trauma
Unclear focal splenic lesions
Complicated cysts
Infarction
Functional asplenia/hyposplenia
Abscess

Table 13.2 Differential diagnosis of cystic and solid focal splenic lesions

Cystic focal lesions
• Congenital cyst
• Post-traumatic cyst
• Splenic abscess (cystic or mixed)
• Infectious cyst
• Splenic lymphangioma
• Hydatid disease
Solid focal lesions
• Hemangioma
• Lymphoma
• Hamartoma
• Granulomatosus disease (sarcoidosis, tuberculosis)
• Metastases

13.6.2 Diffuse Lesions of the Spleen

Diffuse splenic involvement may be caused by diffuse lymphoma infiltration, sarcoidosis with diffuse manifestation or small nodules, tuberculosis, fungal microabscesses from *Candida*, *Aspergillus* or *Cryptococcous*, and Niemann Pick disease. CEUS investigations may reveal a delayed global enhancement or a more prolonged early phase inhomogenicity. However, these changes are not constant or specific [25] (Tables 13.1 and 13.2).

13.7 Conclusion

Contrast-enhanced ultrasound has the potential to become a landmark in the diagnostic improvement of imaging of splenic lesions in children without the need for general anesthesia or radiation exposure.

References

1. Görg C, Bert T. Second-generation sonographic contrast agent for differential diagnosis of perisplenic lesions. AJR Am J Roentgenol. 2006;186(3):621–6.
2. Peddu P, Shah M, Sidhu PS. Splenic abnormalities: a comparative review of ultrasound, microbubble-enhanced ultrasound and computed tomography. Clin Radiol. 2004;59:777–92.
3. Sidhu PS, Cantisani V, Deganello A, Dietrich CF, Duran C, Franke D, Harkanyi Z, Kosiak W, Miele V, Ntoulia A, Piskunowicz M, Sellars ME, Gilja OH. Role of contrast-enhanced ultrasound (CEUS) in

paediatric practice: an EFSUMB position statement. Ultraschall Med. 2017;38(1):33–43.
4. Görg C. Spleen. In: Weskott H-P, editor. Contrast-enhanced ultrasound. 2nd ed. UNI-MED Science: Bremen; 2013. p. 140–51.
5. Lim AK, Patel N, Eckersley RJ, Taylor-Robinson SD, Cosgrove DO, Blomley MJ. Evidence for spleen-specific uptake of a microbubble contrast agent: a quantitative study in healthy volunteers. Radiology. 2004;231(3):785–8.
6. Vikse J, Sanna B, Henry BM, Taterra D, Sanna S, Pękala PA, Walocha JA, Tomaszewski KA. The prevalence and morphometry of an accessory spleen: a meta-analysis and systematic review of 22,487 patients. Int J Surg. 2017;45:18–28.
7. Kruger R, Freeman S. An unusual pelvic mass: contrast enhanced sonographic diagnosis of pelvic splenosis. J Clin Ultrasound. 2019;47(3):172–4.
8. Aguirre Pascual E, Fontanilla T, Pérez Í, Muñoz B, Carmona MS, Minaya J. Wandering spleen torsion-use of contrast-enhanced ultrasound. BJR Case Rep. 2016;3(1):20150342.
9. Franke D, Deeg KH. Doppler sonography of the spleen. CEUS of a wandering spleen. In: Deeg KH, Rupprecht T, Hofbeck M, editors. Doppler sonography in infancy and childhood. Cham: Springer; 2015. p. 410.
10. Di Crosta I, Inserra A, Gil CP, Pisani M. Ponticelli A abdominal pain and wandering spleen in young children: the importance of an early diagnosis. J Pediatr Surg. 2009;44(7):1446–9.
11. Görg C, Graef C, Bert T. Contrast-enhanced sonography for differential diagnosis of an inhomogeneous spleen of unknown cause in patients with pain in the left upper quadrant. J Ultrasound Med. 2006;25(6):729–34.
12. Catalano O, Lobianco R, Sandomenico F, D'Elia G, Siani A. Real-time contrast-enhanced ultrasound of the spleen: examination technique and preliminary clinical experience. Radiol Med. 2003;106(4):338–56.
13. Durkin N, Deganello A, Sellars ME, Sidhu PS, Davenport M, Makin E. Post-traumatic liver and splenic pseudoaneurysms in children: diagnosis, management, and follow-up screening using contrast enhanced ultrasound (CEUS). J Pediatr Surg. 2016;51(2):289–92.
14. Thompson WM, Levy AD, Aguilera NS, Gorospe L, Abbott RM. Angiosarcoma of the spleen: imaging characteristics in 12 patients. Radiology. 2005;235(1):106–15.
15. Neesse A, Huth J, Kunsch S, Michl P, Bert T, Tebbe JJ, Gress TM, Görg C. Contrast-enhanced ultrasound pattern of splenic metastases—a retrospective study in 32 patients. Ultraschall Med. 2010;31(3):264–9.
16. Görg C, Faoro C, Bert T, Tebbe J, Neesse A, Wilhelm C. Contrast enhanced ultrasound of splenic lymphoma involvement. Eur J Radiol. 2011;80(2):169–74.
17. Picardi M, Soricelli A, Pane F, Zeppa P, Nicolai E, De Laurentiis M, Grimaldi F, Rotoli B. Contrast-enhanced harmonic compound US of the spleen to increase staging accuracy in patients with Hodgkin lymphoma: a prospective study. Radiology. 2009;251(2):574–82.
18. Valentino M, Serra C, Pavlica P, et al. Blunt abdominal trauma: disgnostic performance of contrast-enhanced ultrasonography in children – initial experience. Radiology. 2008;246:903–9.
19. Oldenburg A, Hohmann J, Skrok J, et al. Imaging of paediatric splenic injury with contrast-enhanced ultrasonography. Pediatr Radiol. 2004;34:351–4.
20. Menichini G, Sessa B, Trinci M, Galluzzo M, Miele V. Accuracy of contrast-enhanced ultrasound (CEUS) in the identification and characterization of traumatic solid organ lesions in children: a retrospective comparison with baseline US and CE-MDCT. Radiol Med. 2015;120(11):989–1001.
21. Poletti PA, Becker CD, Arditi D, Terraz S, Buchs N, Shanmuganathan K, Platon A. Blunt splenic trauma: can contrast enhanced sonography be used for the screening of delayed pseudoaneurysms? Eur J Radiol. 2013;82(11):1846–52.
22. Piccolo CL, Trinci M, Pinto A, Brunese L, Miele V. Role of contrast-enhanced ultrasound (CEUS) in the diagnosis and management of traumatic splenic injuries. J Ultrasound. 2018;21(4):315–27.
23. Rosling M, Trenker C, Neesse A, Görg C. Spontaneous and traumatic splenic rupture: retrospective clinical, B-mode and CEUS analysis in 62 patients. Ultrasound Int Open. 2018;4(1):E30–4.
24. Tagliati C, Argalia G, Polonara G, Giovagnoni A, Giuseppetti GM. Contrast-enhanced ultrasound in delayed splenic vascular injury and active extravasation diagnosis. Radiol Med. 2018;124(3):170–5.
25. Catalano O, Sandomenico F, Vallone P, D'Errico AG, Siani A. Contrast-enhanced sonography of the spleen. Semin Ultrasound CT MR. 2006;27(5):426–33.

14 Contrast-Enhanced Voiding Urosonography (ceVUS): Current Experience and Advanced Techniques

Susan J. Back, Kassa Darge, and Aikaterini Ntoulia

14.1 Background

14.1.1 Vesicoureteral Reflux

Vesicoureteral reflux (VUR) is the retrograde flow of urine from the bladder to the ureter or kidney. VUR occurs due to functional or structural insufficiency of the one-way valve-like mechanism around the ureteric orifice at the vesicoureteral junction [1, 2]. The valve is formed by the oblique insertion of the distal ureter through the bladder wall. This tunnel is compressed as the bladder fills preventing the backflow of urine.

In primary VUR, a congenital defect shortens the length of the ureteric tunnel relative to its diameter, making the valve-like anti-reflux mechanism incompetent [2]. Secondary VUR is an acquired condition that occurs in association with functional abnormalities of the lower urinary tract (e.g., bladder bowel dysfunction or neurogenic bladder) or as a result of anatomic outlet obstruction (e.g., posterior urethral valves).

The estimated prevalence of VUR in the general pediatric population is low ranging from 1% to 2% [3]. However, in children who present with urinary tract infection (UTI), the frequency of VUR can be as high as 25–40% in those under 5 years and up to 50% in those younger than 1 year [3, 4]. A familial prevalence of VUR has been described with a rate of 24–51% in siblings and 66% in children whose parents had VUR [5].

VUR nephropathy may occur due to recurrent UTIs and pyelonephritis and can lead to substantial morbidity including renal scarring, increased risk of hypertension, and end-stage renal disease [6–8].

The management of children with UTI and VUR remains controversial [9]. In most children, even high grades of VUR will spontaneously resolve over time and low grades may not require treatment. Moderate to severe grades of VUR may be treated with antibiotic prophylaxis to prevent recurrent UTIs and correction of bladder and bowel dysfunction if present [10]. Injection of a bulking agent around the vesico-ureteric junction is a minimally invasive approach to treating VUR [11]. Surgical intervention may be needed in children who have recurrent infections along with high-grade VUR [12]. Therefore, VUR imaging

S. J. Back (✉) . K. Darge
Department of Radiology, Children's Hospital of Philadelphia, Perelman School of Medicine, University of Pennsylvania, Philadelphia, PA, USA
e-mail: BackS@email.chop.edu

A. Ntoulia
Department of Radiology, Children's Hospital of Philadelphia, Philadelphia, PA, USA
e-mail: ntouliaa@email.chop.edu

P. S. Sidhu et al. (eds.), *Contrast-Enhanced Ultrasound in Pediatric Imaging*,
https://doi.org/10.1007/978-3-030-49691-3_14

in children is of great importance to determine reflux severity and plan for clinical management.

14.1.2 Imaging of Vesicoureteral Reflux

For many decades, fluoroscopic voiding cystourethrography (VCUG) and radionuclide cystography (RNC) have been the standard modalities for VUR imaging. However, both of these methods expose the ovaries and testes to ionizing radiation.

In the early 1980s, a radiation-free alternative method was developed using ultrasonography and ultrasound contrast agents (UCA), nowadays termed contrast-enhanced voiding urosonography (ceVUS). Initially, first-generation UCA, comprised of air-filled microbubbles stabilized with galactose and palmitic acid, was used for ceVUS [13–15]. Levovist® (Schering AG, Berlin, Germany) was the first of these UCA to obtain approval for intravesical pediatric use in some European countries, but later the pharmaceutical company voluntarily withdrew Levovist® from the market as better UCA emerged.

In the early 2000s second-generation UCA, composed of gas-filled microbubbles, became commercially available. SonoVue® (Bracco Imaging S.p.A., Milan, Italy), or known as Lumason® (Bracco Diagnostics Inc., Monroe Township, NJ, USA) in the United States, is the most commonly used second-generation UCA for ceVUS in children. It consists of sulfur hexafluoride gas microbubbles stabilized within a phospholipid outer shell. The improved physical and chemical characteristics of SonoVue® increased the stability and enhanced echogenic effect of the microbubbles [16, 17]. This combined with the continuous improvement of the ultrasound imaging techniques and contrast-specific software further boosted the diagnostic performance of ceVUS, allowing the detection of extremely small quantities of the UCA.

Since the past 20 years, ceVUS has been performed extensively in Europe and has been shown to be a safe and highly sensitive imaging method for the detection and grading of VUR. More recently ceVUS has been used for urethral pathology. Numerous studies detail the comparative performance of ceVUS with VCUG and RNC with cumulative evidence of the high diagnostic accuracy of ceVUS [18–38]. As a result of this experience, ceVUS is performed as the first and only imaging examination in several radiology departments, completely replacing the two other reflux imaging studies [22, 32, 39].

In 2012, the European Society of Pediatric Radiology (ESPR) endorsed ceVUS examination for the first time in the imaging recommendations and guidelines published in the field of pediatric uroradiology [40]. At the same time, the European Federation of Societies for Ultrasound in Medicine and Biology (EFSUMB) launched an updated set of guidelines on the applications of contrast-enhanced ultrasound including the use of ceVUS in children with an emphasis on the indications, technical performance, safety, and diagnostic efficacy of the examination [41, 42].

In 2014 SonoVue® was introduced for the first time in the United States market under the trade name Lumason®. In 2016 Lumason® received approval by the United States Food and Drug Administration (FDA) for intravesical applications of reflux and urethral imaging studies in children and in 2017 SonoVue® was also approved by the European Medicines Agency (EMA) for the same indication, opening new possibilities for the wider acceptance of this technique. Optison™ (GE Healthcare Inc., Princeton, NJ) is another second-generation UCA commercially available in the United States that has been used off-label for ceVUS in a prospective clinical trial and a couple of case reports [20, 43, 44].

14.1.3 Indications for Reflux Imaging

The National Institute for Health and Clinical Excellence (NICE) in 2007 and the American Academy of Pediatrics (AAP) in 2011 revised their UTI guidelines for febrile infants and young children [45, 46]. The updated guidelines now emphasize on identifying children who are most at risk for UTI and long-term sequelae, tailoring investigations and management to prevent future renal damage.

Imaging investigation for VUR detection is now recommended in children after the first febrile UTI if ultrasonography shows urinary tract dilation,

scarring or other findings that would suggest high-grade VUR or obstructive uropathy, as well as in other atypical or complex clinical circumstances. In view of these updated guidelines, the implementation of ceVUS provides a radiation-free imaging alternative for VUR imaging that can be used for the initial diagnosis, follow up, as well as for screening siblings of children with known reflux.

14.2 How to Perform ceVUS

The ceVUS examination is performed in a similar manner to VCUG [47]. The urinary bladder is catheterized and filled in a retrograde manner with UCA and saline under continuous, real-time ultrasound (US) surveillance using contrast specific, harmonic imaging software with low mechanical index techniques. For newborns and infants, a 2–9 MHz linear or 5–8 MHZ convex transducers are used, whereas for older children a convex multi-frequency (1–5 MHz) transducer is used [22, 47].

Initially, aseptic bladder catheterization is performed using a small catheter without a retention balloon (feeding tube catheter). The size of the catheter varies according to the child's age and usually ranges from 5 to 8 French. Then, the UCA is reconstituted according to the manufacturer's package instructions and it is administered into the bladder. Two techniques have been described in the literature for intravesical UCA administration:

1. Injection technique: UCA is directly injected into the partially filled bladder, which is then filled with normal saline via gravity up to the point of voiding or at least maximum expected bladder capacity in milliliter as calculated by the formula (age + 2) × 30 [48]. In this technique, a bolus dose of 0.5–1 mL of SonoVue® is reported to be sufficient for optimal ceVUS performance [32, 36].
2. Infusion technique: UCA is initially diluted in a normal saline bag and then the solution is infused into the bladder by gravity. Usually, 0.5 or 1 mL of SonoVue® is diluted into a 250 or 500 mL of a normal saline bag, to produce a solution of 0.2% of UCA/normal saline, although a dose up to 1% of the bladder capacity is described [22, 23]. Using Optison™, a 0.2% Optison™/normal saline solution is sufficient [20]. Optimal bladder filling results in a homogenous bladder distribution, which allows for better delineation of the posterior bladder wall and better imaging of a retro-vesical portion of the ureters (Fig. 14.1). The infusion technique is

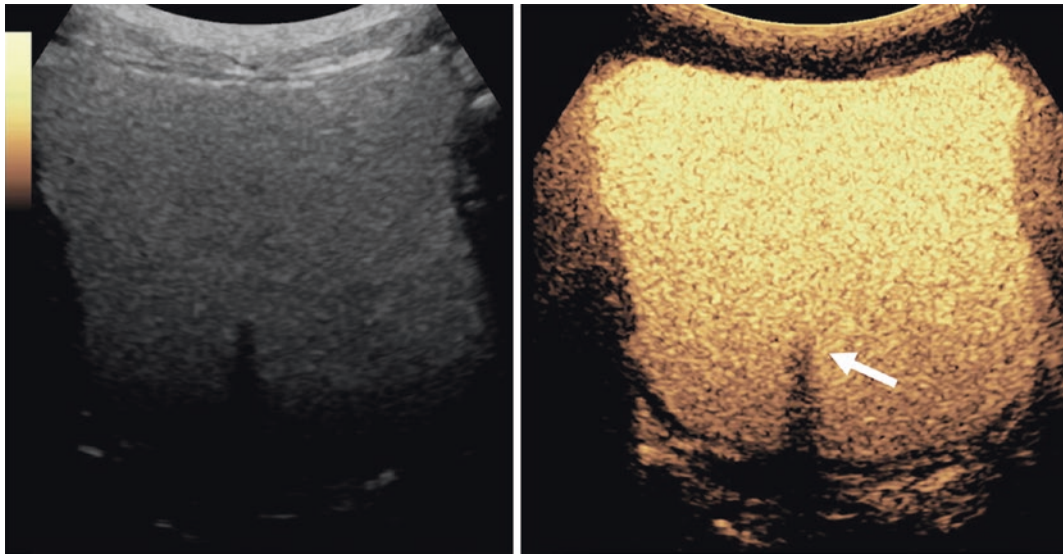

Fig. 14.1 Optimal concentration of the UCA within the urinary bladder. Grayscale (left) and contrast mode (right) with contrast microbubbles homogenously distributed within the bladder. The retro-vesical space is well seen behind the posterior wall of the urinary bladder. A strong acoustic shadow is related to the bladder catheter (arrow)

considered to be advantageous to have a homogenous UCA concentration without causing strong acoustic shadowing [22].

During the filling and voiding phases, real-time scanning of the bladder and right and left kidney is performed alternatively in longitudinal and transverse planes with the child lying in supine, prone, or decubitus positions. A lateral approach in the coronal plane through the flank may enable simultaneous depiction of the entire urinary tract including the bladder, ureters throughout their course and the kidneys in a single image [22] (Fig. 14.2).

When the child voids, the urethra is evaluated, with and without a catheter present, using a suprapubic or trans-perineal/trans-scrotal approach in boys and usually a suprapubic or trans-perineal/trans-labial approach in girls [22, 23, 29, 49] (Figs. 14.3, 14.4, and 14.5). In infants, more than one ceVUS filling/voiding cycle is generally performed with the catheter left in place during voiding [50]. In older children, the catheter can be removed once the expected bladder capacity is reached, and the child voids.

The refluxing UCA is depicted as echogenic microbubbles flowing retrograde within the urinary tract. Depending on the anatomic level of urinary tract involvement and the volume of refluxing UCA, VUR can be graded with ceVUS into a five-grade scale in a similar manner as in VCUG [51].

During continuous US scanning, the region of interest can be depicted in a single image in con-

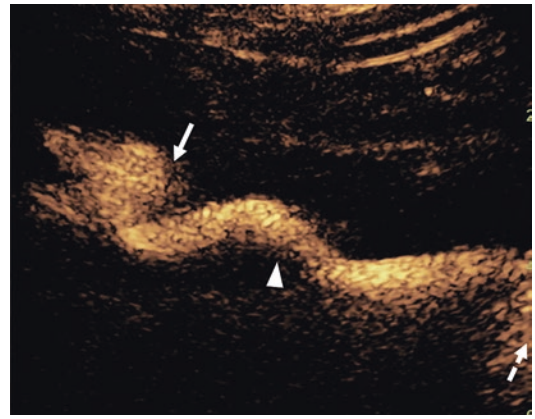

Fig. 14.2 Coronal view from the flank. Contrast mode image. The signal from the background soft tissues has been suppressed and only the bright echoes from the refluxing microbubbles can be identified within the pelvicalyceal system and ureter. The left kidney is scanned in the coronal plane from the flank. From this view, the entire urinary tract from the pelvicalyceal system (arrow) to the bladder dome (dashed arrow) can be visualized in a single image and thus the degree of ureteral tortuosity (arrowhead) is better evaluated

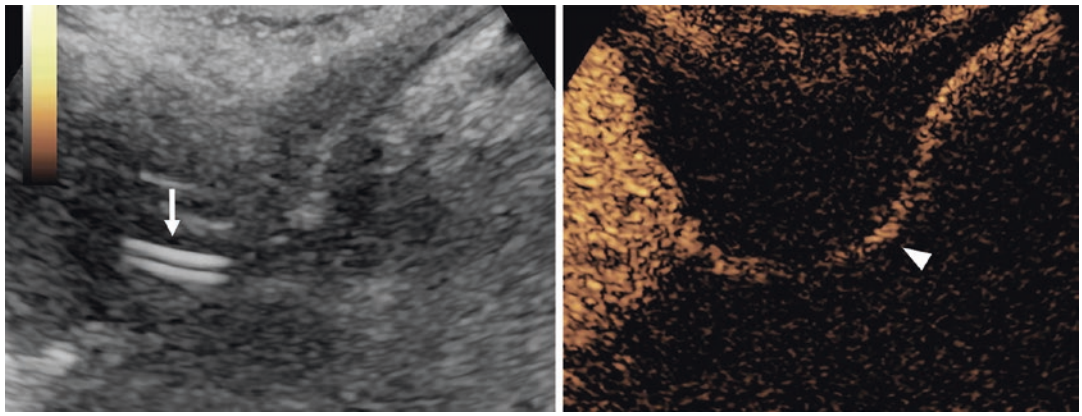

Fig. 14.3 Normal male urethra. Suprapubic approach. Grayscale (left) and contrast mode (right). In this technique, the ultrasound transducer is placed in the low suprapubic region, just above the pubic bone. The structure closer to the ultrasound transducer is the bladder neck. Echogenic microbubbles are seen flowing from the bladder through the urethra lumen (arrow) during micturition. The bladder catheter (arrow) remains in situ during micturition

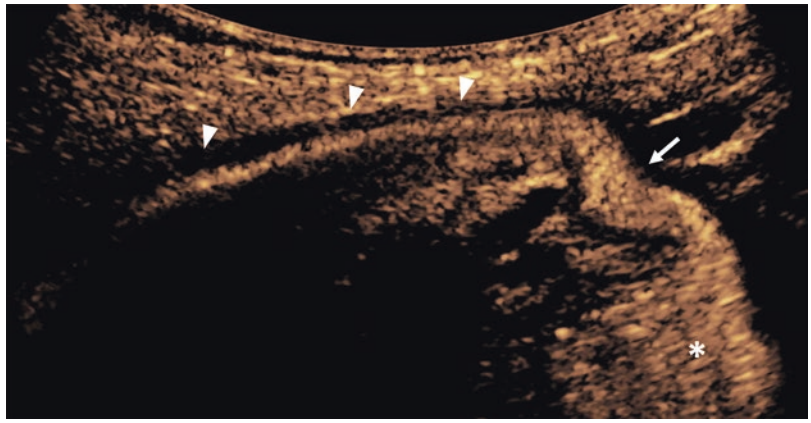

Fig. 14.4 Normal male urethra. Trans-perineal approach. Contrast mode image. In this technique, the ultrasound transducer is placed in the midline of the perineum. The structure closer to the ultrasound transducer is the anterior urethra (arrowheads). The posterior urethra (arrow) is normal. Echogenic microbubbles are seen flowing from the bladder (asterisk) through the urethra lumen during micturition

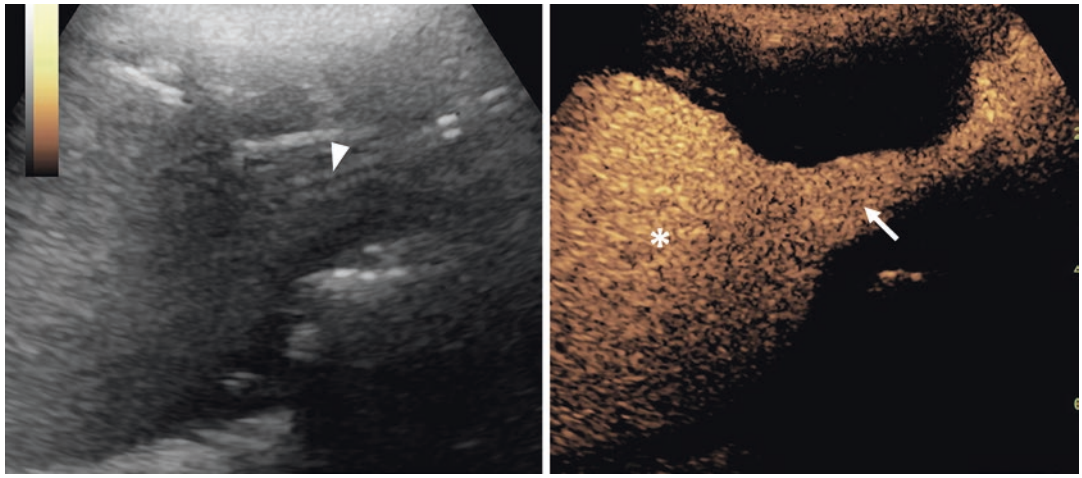

Fig. 14.5 Normal female urethra. Suprapubic approach. Grayscale (left) and contrast mode (right) with echogenic microbubbles are seen flowing from the bladder (asterisk) through the urethral lumen (arrow) during micturition, which appears with normal conical configuration. The bladder catheter remained in situ during micturition (arrowhead)

trast specific mode or as a dual display where the US screen is split into two parts and the region of interest is depicted simultaneously in grayscale and contrast modes. The dual display is helpful to serve as a reference image to maintain transducer positioning over the region of interest. Contrast specific algorithms have been developed to increase the conspicuity of microbubbles. Contrast US technology combines low mechanical index and intermittent pulse US technology that decreases the breakage of the microbubbles under the US acoustic pressure. Subtraction techniques provide effective separation between the background tissues and the contrast agent signals for improved diagnostic information and shortened examination time. Color overlay mode combines the contrast agent and grayscale signal for real-time anatomic and

contrast information display simultaneously in a single image.

14.3 Interpretation of ceVUS Imaging Findings

14.3.1 Reflux Grading

VUR grading for ceVUS was adopted from scoring systems established for other reflux imaging examinations [51]. The most commonly used VUR scoring system was initially proposed for the International Reflux Study in Children (IRSC) to describe findings on VCUG [52]. It uses a 1 (lowest) to 5 (highest) scale based on whether contrast material refluxes only into the ureter or reaches the upper collecting system as well as the degree of ureteral dilation and tortuosity, and upper collecting system dilation. The ceVUS VUR grading proposed by Darge and Troeger is an extrapolated classification derived from the IRSC fluoroscopic scoring and built on earlier authors' experience with voiding sonographic examinations using saline and first-generation UCA [51] (Figs. 14.6, 14.7, 14.8, 14.9, and 14.10). US has the added advantage over VCUG and RNC in that it depicts pre-existing urinary

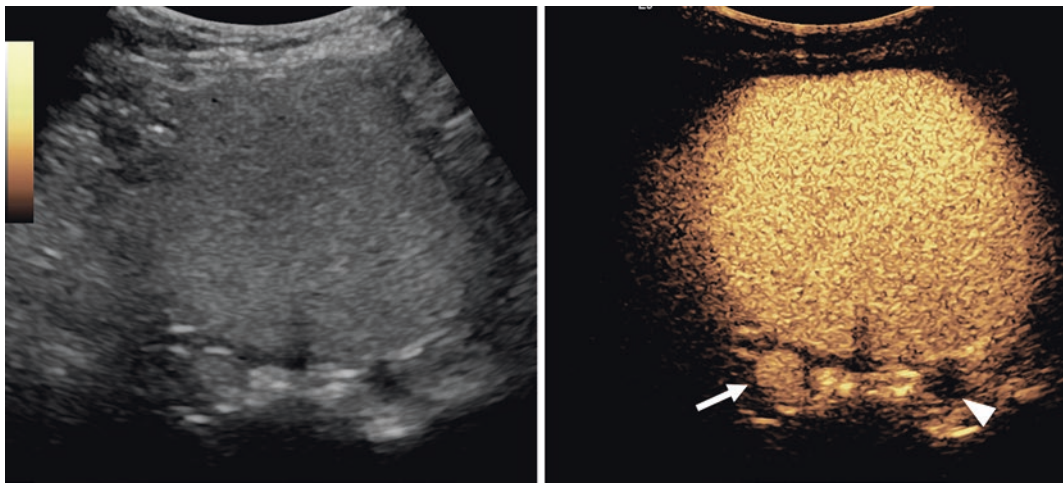

Fig. 14.6 Ureteral reflux. Grayscale (left) and contrast mode (right). Behind the bladder, the retro-vesical part of the right ureter can be visualized moderately distended and filled with echogenic microbubbles (arrow). The dilated left distal ureter is filled with clear anechoic fluid content thus demonstrating the absence of reflux (arrowhead)

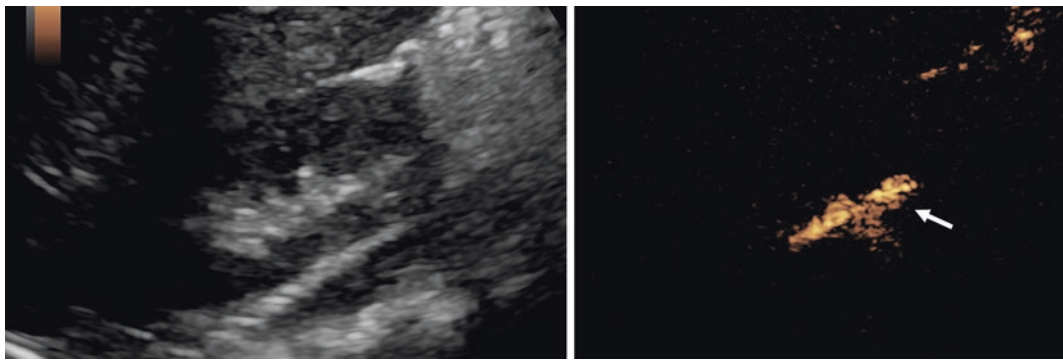

Fig. 14.7 Grade II reflux. Grayscale (left) and contrast mode (right) of the right kidney. Refluxing microbubbles can be identified within the pelvicalyceal system of the right kidney, which is not dilated (arrow)

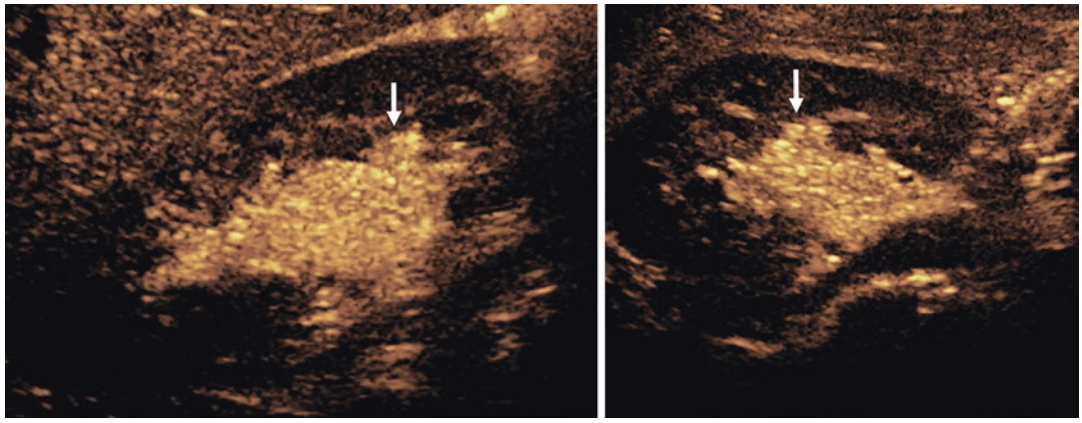

Fig. 14.8 Grade III VUR. Contrast mode images of the right kidney longitudinal (left) and axial (right) planes. There is moderate dilation of the renal pelvis and calyces with minimal blunting of the fornices (arrow)

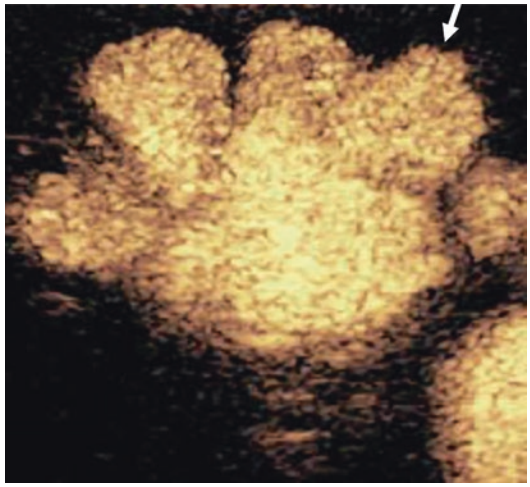

Fig. 14.9 Grade IV VUR. Contrast mode image of the right kidney. Echogenic microbubbles are seen within the dilated pelvis and calyces (arrow) with blunting of fornices. The papillary impressions are preserved

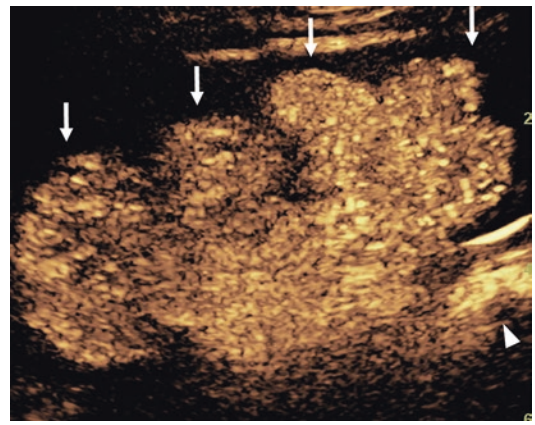

Fig. 14.10 Grade V VUR. Contrast mode image of the right kidney in the longitudinal plane. Echogenic microbubbles are seen within the severely dilated pelvis and calyces (arrows), with loss of the papillary impressions and tortuously dilated proximal ureter (arrowhead)

tract dilation prior to a VUR event. The initial ceVUS scoring system proposed "a" and "b" subcategories for each of the five grades of reflux denoting if the system was primarily nondilated or dilated, however, this notation has not been widely used. The five reflux grades are:

- Grade I: refluxing UCA microbubbles reaches the ureter.
- Grade II: refluxing UCA microbubbles reach up to the pelvicalyceal system, without dilation of the pelvicalyceal system.
- Grade III: refluxing UCA microbubbles reach up to the pelvicalyceal system, which is mildly dilated, but with no significant change of the renal calyceal contour.
- Grade IV: refluxing UCA microbubbles reach up to the pelvicalyceal system, which is moderately dilated with blunting of the renal fornices but papillary impressions still visible.
- Grade V: refluxing UCA microbubbles reach up to the pelvicalyceal system, which is severely dilated with loss of papillary impressions and tortuous course of the ureter.

Less often a three-grade scoring system, such as the one used to grade VUR by RNC, is used for ceVUS [15, 38]. Of note, in an in-vitro experiment, it was shown that UCA microbubbles do not passively ascend into the upper urinary tract, and therefore the demonstration of microbubble in the renal collecting system corresponds to active VUR [53].

The less common phenomenon of intrarenal reflux is detectable by ceVUS and was comparable to detection by VCUG in a small series [43, 54]. With the more advanced contrast specific US modalities, intrarenal reflux appears to be detected more frequently. While not a component of the reflux scoring system, identification of intrarenal reflux may aid in risk stratification for renal scarring [54] (Fig. 14.11). Intrarenal reflux is usually associated with compound papillae, which are more frequently found in the upper pole, and to a lesser extent in the lower pole of the kidney [55].

ceVUS can also provide anatomic details about the morphology of the pelvicalyceal system and detect reflux in cases of complete or partial ureteral duplication (Figs. 14.12 and 14.13).

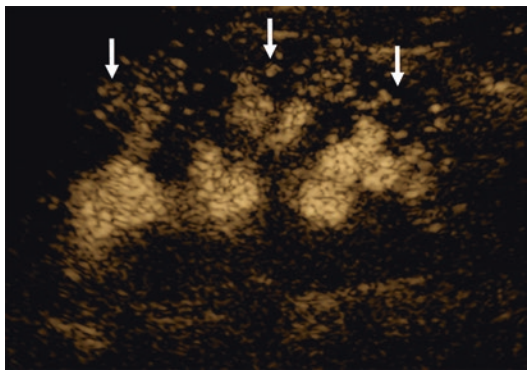

Fig. 14.11 Intrarenal reflux. Contrast mode image. Echogenic microbubbles are extend from the calyces diffusely into the renal parenchyma (arrows)

14.3.2 Urethra

Assessment of the urethra for the presence of posterior urethral valves (PUV) is an important part of the evaluation of the urinary tract in male infants and those with signs and symptoms suggesting lower urinary tract obstruction. Teele and Share [56] and Cohen et al. [57] separately described the utility of trans-perineal US to evaluate the bladder base and urethra in children and showed this approach was complimentary and favorable when compared with trans-pelvic imaging in a non-voiding infant. Using VCUG as a gold standard, Good et al. evaluated the diameter of the obstructed and non-obstructed posterior male urethra at rest and with voiding [58]. They showed significant differences in the diameter of the posterior urethra between non-voiding and voiding in both the non-obstructed and obstructed states. The non-obstructed posterior urethra had a mean diameter of 1 mm pre-void compared with 4 mm while voiding; and obstructed urethras had a mean diameter of 4.5 and 10 mm pre-void and

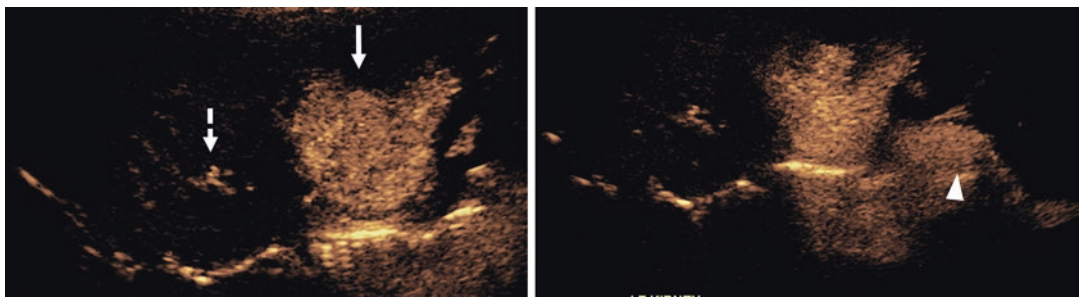

Fig. 14.12 Vesicoureteral reflux into a duplicated collecting system. Contrast mode of a duplex left kidney. There is reflux Grade III to the lower pole of the kidney (arrow) and mild dilation of the proximal ureter (arrowhead). There is no reflux to the upper renal pole (dashed arrow) in keeping with complete duplication of the collecting system

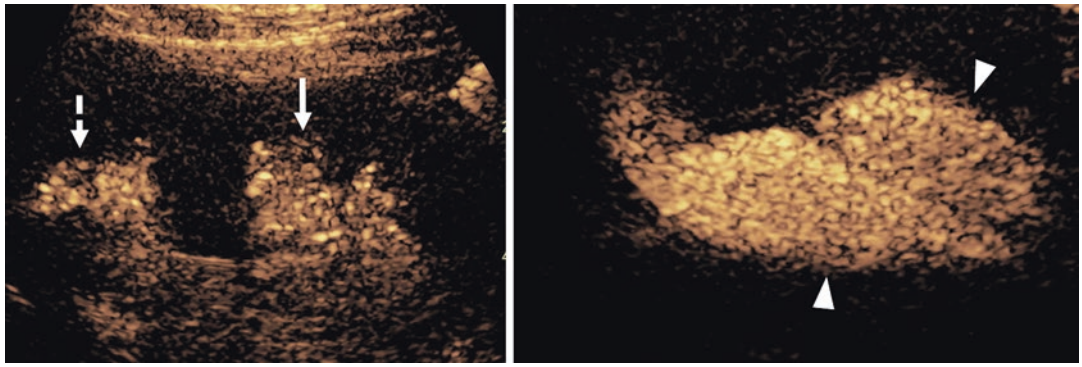

Fig. 14.13 Duplex kidney incomplete duplication. The right kidney has a duplex configuration. Echogenic microbubbles are seen refluxing into the dilated upper (dashed arrow) and lower (arrow) poles. At a lower level, the two separate ureters (arrowheads) are moderately dilated and both filled with echogenic microbubbles. These findings are suggestive of a partially duplicated collecting system with two ureters joined together into one distal ureter inserting into the bladder

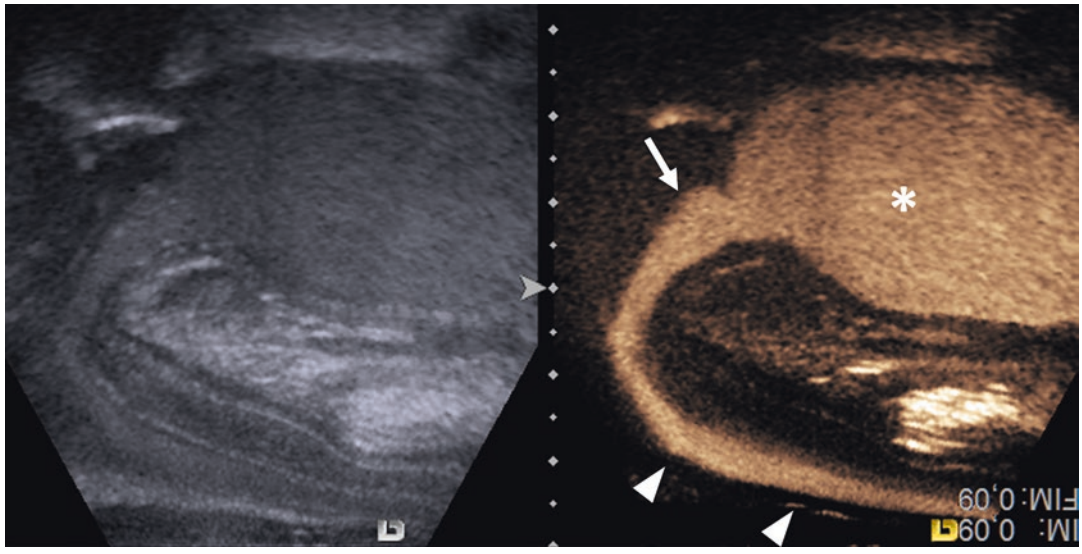

Fig. 14.14 Normal male urethra. Trans-perineal approach. Grayscale (left) and contrast mode (right). The image is rotated 180° to resemble the classic voiding cystourethrography examination. The ultrasound transducer is placed in the midline of the perineum. During micturition, the urethral lumen is filled with echogenic microbubbles which are seen flowing from the bladder (asterisk). The structure closer to the ultrasound transducer is the anterior urethra (arrowheads). The posterior urethra (arrow) is normal in caliber and configuration. The difference in the caliber between the posterior and anterior urethra should not exceed 2 mm. (*Courtesy of Dr. C. Duran. Parc Tauli University Hospital, Sabadell, Barcelona, Spain*)

voiding, respectively [58]. Applying a cut-off of 6 mm for the posterior urethra during voiding yielded a sensitivity of 100% and specificity of 89% for obstruction [58] (Figs. 14.14 and 14.15).

Using Good et al.'s threshold of 6 mm, Mate et al. identified abnormal urethras in 4 of 224 boys, assessing for PUV, examined with the first generation galactose based UCA during ceVUS and confirmed the findings with VCUG [59]. Bosio and Manzoni correctly identified 8 of 100 boys with PUVs using ceVUS by assessing for dilation of the posterior urethra, delayed passage

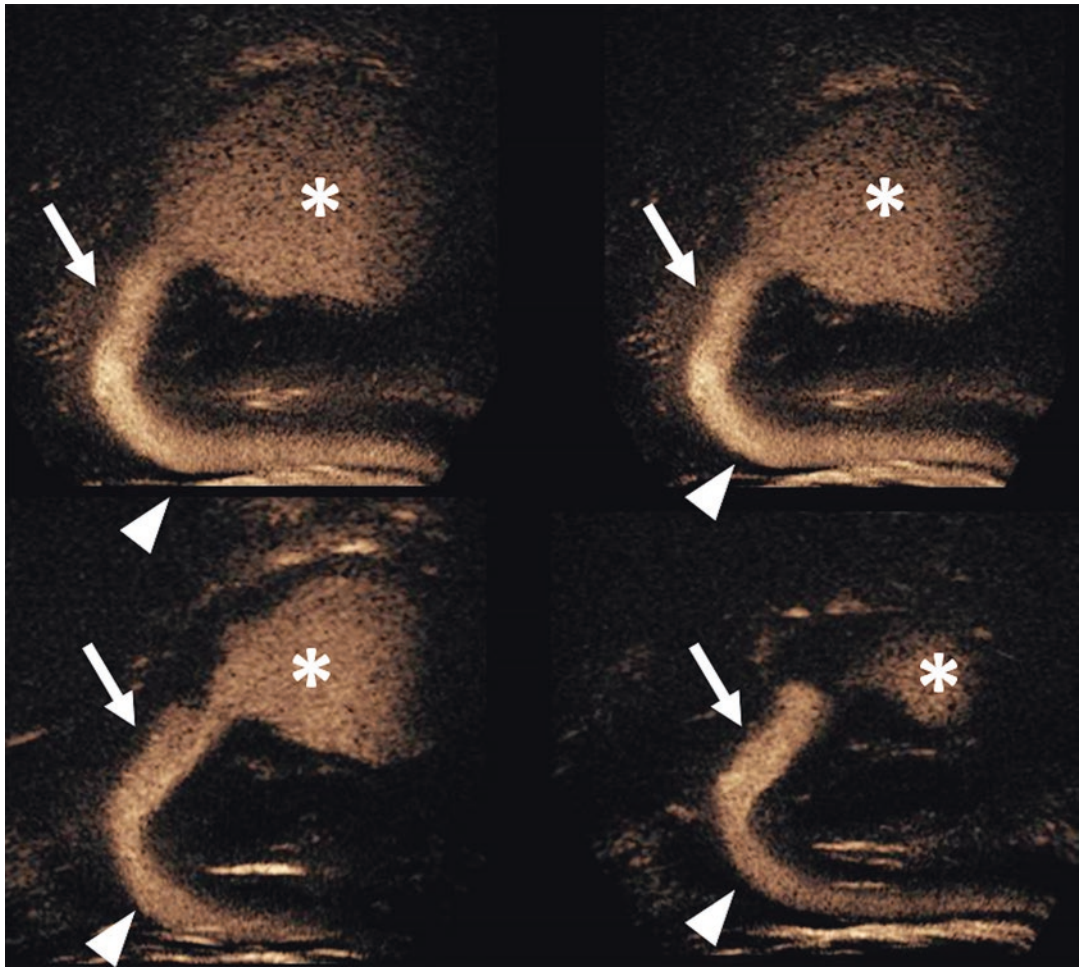

Fig. 14.15 Normal male urethra. Trans-perineal approach. Serial images. Contrast mode serial images. All images are rotated 180° clockwise to resemble the classic voiding cystourethrography examination. The ultrasound transducer is placed in the midline of the perineum. The catheter is withdrawn from the bladder (asterisk) during voiding. The urethra is filled with echogenic microbubbles. The posterior (arrow) and anterior (arrowhead) urethra are normal. The bladder empties completely. (*Courtesy of Dr. C. Duran. Parc Tauli University Hospital, Sabadell, Barcelona, Spain*)

of UCA through a narrowed segment, and less distension of the anterior urethra [60]. Findings were confirmed with VCUG. Following their initial publication, the group added an additional 110 boys in their study and recognized PUV in one child using similar criteria to their initial group. Recently, Duran et al. showed that newer, more stable second-generation UCA could be reliably used to image the urethra [29].

Independently, Berrocal et al. [61] and Duran et al. [29, 49] derived similar normative measurements of the urethra obtained while voiding during ceVUS in boys and girls. They showed that urethral assessment is no longer a limitation to the use of ceVUS as a primary evaluation of the urinary tract in children and particularly in boys. The authors respectively reported normal posterior male urethral measurements during voiding of 6.3 ± 0.66 mm (range: 3.7–7.2 mm) and 6.4 ± 0.78 mm (range: 4–9.2 mm); and anterior male urethral values of 6.1 ± 0.81 mm (range: 2.8–7.1 mm) and 5.8 ± 0.91 mm (range: 3.3–8.9 mm) [29, 61]. For girls, Berrocal et al. reported a mean urethral diameter during voiding of 4.2

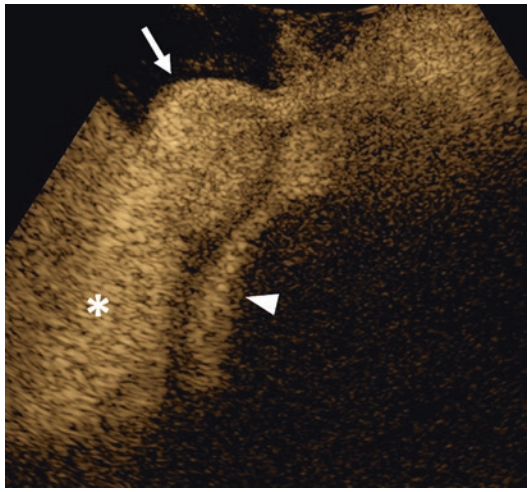

Fig. 14.16 Spinning top urethra and vaginal reflux. Suprapubic approach. Contrast mode image of the urethra during micturition depicting the "spinning top" urethral morphology (arrow) as well as intravaginal reflux (arrowhead). "Spinning top" urethra refers to the non-obstructive widening of the posterior urethra that occurs in girls with a weak bladder neck mechanism and concomitant voluntary contraction of the distal sphincter. It is considered suggestive of functional discoordinate voiding or bladder instability. The bladder (asterisk) is filled with echogenic microbubbles

± 1.01 mm (range: 2.5–7.8 mm) and Duran a mean diameter of 5.9 ± 1.1 mm (range: 4–9 mm) [61].

In addition to posterior urethral valves, ceVUS has depicted urethrovaginal reflux, spinning top urethra, anterior urethral valves, urethral diverticula, prostatic utricles, and bulbar strictures [22, 23, 29, 49, 61] (Fig. 14.16). Patel et al. reported a case of duplicated urethra seen during ceVUS [62].

14.3.3 Diagnostic Comparisons: ceVUS vs VCUG and RNC

Multiple studies have shown that ceVUS has high diagnostic sensitivity and specificity compared to VCUG and RNC for detection and grading or reflux [63]. Up to 2019, 20 original research studies have been published entailing the comparative performance of VCUG and ceVUS with the use of second-generation UCA, most commonly SonoVue® and to a lesser extent Optison™. In these studies, more than 2600 children have been included and more than 5200 pelvi-ureter-units (PUUs) have been analyzed. In most studies, the diagnostic performance of ceVUS was reported to be at least comparable to standard VCUG and RNC and in many studies even higher [18–20, 22–29, 31–34, 36, 39, 43, 44, 64–67]. Overall, it is considered that ceVUS detects approximately 10% more reflux cases compared to VCUG [50, 63]. Most important is to note that 70% of reflux cases detected only on ceVUS were of higher grades (II–V) and thus of higher clinical significance [68]. The high sensitivity of ceVUS might be explained by the fact that even a few refluxing microbubbles can be easily depicted with advanced contrast-specific software, whereas in VCUG, a larger amount of refluxing iodinated contrast is required to be visualized especially in the presence of pre-existing urinary tract dilation. Moreover, the lack of ionizing radiation enables prolonged, real-time examination of each kidney separately and thus higher sensitivity in detecting intermittent or intrarenal reflux [50, 54, 68].

On the other hand, VCUG has a higher sensitivity to detect grade I reflux, because the refluxing retro-vesical ureters may be difficult to delineate from their echogenic surroundings, particularly if these are non-dilated [63]. However, grade I reflux is of uncertain clinical significance and in many cases does not even require treatment.

In a recent meta-analysis including a total of 12 comparative ceVUS studies using VCUG as the reference standard and performed in 953 children, the pooled diagnostic accuracy parameters for ceVUS in detecting VUR in children were as follows: sensitivity 90.43% (95% CI 90.36–90.50), specificity 92.82% (95% CI 92.76–92.87), calculated positive likelihood-ratio 12.59 (95% CI 12.49–12.68), negative likelihood-ratio 0.103 (95% CI 0.102–0.104), and extrapolated pooled diagnostic odds ratio was 122.12 (95% CI 120.75–123.49) [35, 37].

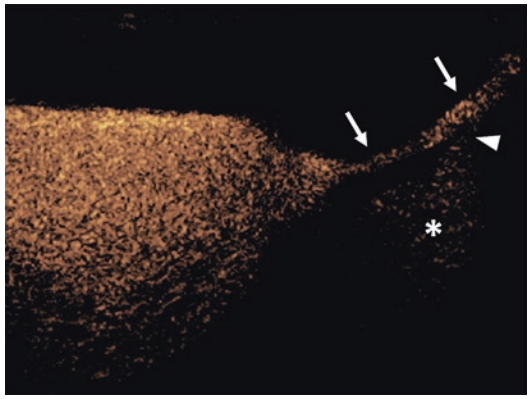

Fig. 14.17 Urogenital sinus. Suprapubic approach. Contrast mode image depicts a long urethra (arrow) in this infant with ambiguous genitalia. A communication (arrowhead) between the posterior urethra and the vagina (asterisk) was seen during the voiding phase of the examination. Contrast material filled the vagina

14.3.4 Retrograde Urethrography

Sonourethrography was first described by McAninch et al. in 1988 [69]. It is performed after catheterization of the urethra and retrograde filling with normal saline. In the literature, its use is primarily described in adults where the detection of strictures is comparable to fluoroscopic retrograde urethrography (RUG) [70]. There is reportedly improved sensitivity for measurement of stricture length and diameter with sonourethrography versus fluoroscopic retrograde urethrography (RUG) when compared with operative findings, especially shorter strictures, which is attributed to differences in positioning and degree of penile stretch during the examination [70, 71]. Some authors found the radiographic technique underestimated stricture length despite concerns about magnification, while others concluded RUG has expected over-measurement of stricture length due to magnification [72]. Because procedures to repair urethral strictures are predicated on their length, accurate measurement is crucial for surgical planning. Sonourethrography can also detect spongiofibrosis, not appreciated by RUG, that can guide surgical management [70, 71]. In a retrospective analysis of 12 adolescent patients, mean age 16.9 years (range 9.5–20.8 years), sonourethrography had similar benefits as shown in adults with improved measurements and detection of fibrosis [73].

The addition of UCA has improved visualization of adult urethras during sonourethrography in the assessment of trauma [74], diverticula and incontinence [75, 76], as well as long, narrow strictures [72].

14.3.5 Complex Genitourinary Anatomy

In a similar manner to RUG and sonourethrography, a persistent genitourinary sinus can be depicted with UCA administration [22]. The UCA instilled in the urinary bladder may reflux into the vagina and show a common channel of the urethra and lower [77, 78] (Fig. 14.17). Rectourethral communication has also been shown after the administration of UCA instilled into the mucous fistula of patients with imperforate anus [79].

14.4 Advanced Techniques

14.4.1 3D/4D ceVUS

Currently, ceVUS procedure is based on the standard two-dimensional (2D) US techniques that provide still images and dynamic cinematic clips of the urinary tract for anatomic imaging and morphological evaluations. However, in recent years, ongoing innovations in sonographic equipment have led to the development of three-dimensional (3D) and four-dimensional (4D) US techniques that are gaining popularity in the field of pediatric uroradiology [33, 80]. 3D/4D US enables static and real-time multiplanar sonographic imaging simultaneously in all orthogonal planes and offline volume rendering reconstructions for selective display of specific tissue components.

These advanced US techniques coupled with contrast imaging options can further expand the diagnostic capability of ceVUS improving volumetric measurements and providing detailed visualization of contrast within the pelvicalyceal

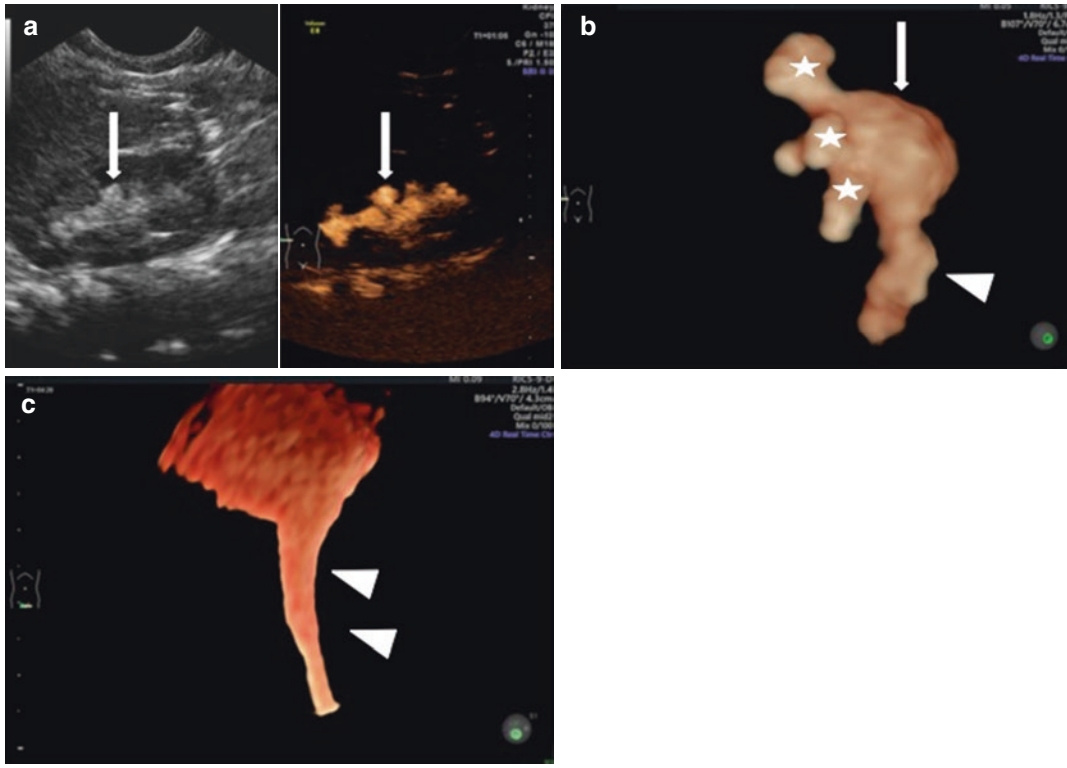

Fig. 14.18 3-D rendering. (**a**) 2D grayscale (left) and contrast-enhanced (right) ultrasound images of the right kidney in the sagittal plane demonstrating contrast material filling the right renal collecting system (arrows) including the renal pelvis and calyces. (**b**) 3D rendered image demonstrating contrast opacification of the right renal collecting system including the pelvis (arrows), calyces (asterisks), and ureter (arrowheads) to better advantage than 2D static images. Improved visualization of the calyceal dilation in multiple angles facilitates grading and gives the ability to upstage the vesicoureteral reflux. (**c**) 3D rendered image demonstrating contrast opacification of the female urethra during voiding (arrowheads). (*Courtesy of Dr. Magdalena Wozniak, Uniwersytet Medyczny w Lublinie, Poland*)

system. A recent study by Wozniak et al. demonstrated that 3D/4D US data acquisition provides increased anatomic information that can potentially improve the diagnosis and predominantly the grading of VUR. In addition, 3D/4D US allows for a more realistic display of reflux thus enhancing comprehensive communication with the clinicians [33, 80] (Fig. 14.18).

14.4.2 Intraoperative ceVUS

ceVUS has been increasingly applied as a useful tool to assess the effectiveness of anti-reflux medical and surgical treatment. Although medical treatment with prophylactic antibiotics remains the mainstay for initial management of VUR, in children with severe reflux and breakthrough pyelonephritis, progressive renal scarring despite antibiotics and associated ureterovesical junction abnormalities surgical management may be required. Laparoscopic or open surgery with reconstruction of the ureterovesical junction is generally considered the gold standard and aims to create a lengthened submucosal tunnel for the ureter. Endoscopic treatment of VUR with an injection of biocompatible bulking agents underneath the intravesical portion of the ureter is an alternative option due to low surgical morbidity and comparable success rates, reserving surgical treatment for persistent or unsuccessful cases. In this technique, the injec-

tion of the bulking agent into the submucosal space under fluoroscopic guidance aims to achieve narrowing of the ureteral lumen to prevent VUR. Subsequent performance of intraoperative ceVUS enables direct monitoring of the effectiveness of the bulking agent within the operation room. This is important in cases of persistent VUR in which repeated injections of the bulking agents can be performed during a single endoscopic treatment session [81]. Finally, ceVUS can be used as a follow-up imaging study in children undergoing medical or anti-reflux surgery to ensure effective management without the risk of further radiation.

14.5 Safety

There is a large volume of published data regarding the safety of intravesical UCA administration. To date, 15 original studies were published on ceVUS with intravesical administration of SonoVue®/Lumason® [18, 23–26, 28, 31–34, 36, 38, 64, 65, 81] and three original studies were published on ceVUS with intravesical administration of Optison™ [20, 43, 44] including in total more than 2300 children. In the majority of these studies, clinical evaluation for possible adverse events was performed, and safety data were collected and reported. There were no serious adverse events reported in any of these studies. In the largest study dedicated to safety, including 1010 children who underwent only ceVUS examination, a few minor adverse events following the procedure occurred in 37 children, accounting for 3.66% of the study population [32]. These symptoms include dysuria, urinary retention, abdominal pain, anxiety and crying during micturition, blood and mucous discharge, increased frequency of micturition, vomiting, perineal irritation, and urinary tract infection. The type and the frequency of these adverse events were similar to those encountered with VCUG or RNC and were most likely related to the inevitable bladder catheterization rather than the contrast agent itself [82].

14.6 Conclusion

ceVUS has come a long way and is now recognized as a modality that can replace VCUG and RNC. It has high diagnostic efficacy coupled with a high safety profile. The added value in terms of patient comfort is an important attribute, too. With the pediatric approval of UCA for reflux diagnosis in children both in the United States and Europe, it is expected that there will be a steady widespread implementation of ceVUS so that it becomes the predominant imaging for VUR in children worldwide.

References

1. Greenbaum LA, Mesrobian HG. Vesicoureteral reflux. Pediatr Clin N Am. 2006;53(3):413–27, vi.
2. Nino F, et al. Genetics of vesicoureteral reflux. Curr Genomics. 2016;17(1):70–9.
3. Cleper R, et al. Prevalence of vesicoureteral reflux in neonatal urinary tract infection. Clin Pediatr (Phila). 2004;43(7):619–25.
4. Carpenter MA, et al. The RIVUR trial: profile and baseline clinical associations of children with vesicoureteral reflux. Pediatrics. 2013;132(1):e34–45.
5. Chertin B, Puri P. Familial vesicoureteral reflux. J Urol. 2003;169(5):1804–8.
6. Shaikh N, et al. Risk of renal scarring in children with a first urinary tract infection: a systematic review. Pediatrics. 2010;126(6):1084–91.
7. Swerkersson S, et al. Urinary tract infection in small children: the evolution of renal damage over time. Pediatr Nephrol. 2017;32(10):1907–13.
8. Wang HH, et al. Why does prevention of recurrent urinary tract infection not result in less renal scarring? A deeper dive into the RIVUR trial. J Urol. 2019;202(2):400–5.
9. Williams G, Hodson EM, Craig JC. Interventions for primary vesicoureteric reflux. Cochrane Database Syst Rev. 2019;2:CD001532.
10. Investigators RT, et al. Antimicrobial prophylaxis for children with vesicoureteral reflux. N Engl J Med. 2014;370(25):2367–76.
11. Diamond DA, Mattoo TK. Endoscopic treatment of primary vesicoureteral reflux. N Engl J Med. 2012;366(13):1218–26.
12. Boysen WR, et al. Multi-institutional review of outcomes and complications of robot-assisted laparoscopic extravesical ureteral reimplantation for treatment of primary vesicoureteral reflux in children. J Urol. 2017;197(6):1555–61.
13. Darge K, et al. Reflux in young patients: comparison of voiding US of the bladder and retrovesical space

with echo enhancement versus voiding cystourethrography for diagnosis. Radiology. 1999;210(1):201–7.
14. Farina R, et al. [Retrograde echocystography: a new ultrasonographic technique for the diagnosis and staging of vesicoureteral reflux]. Radiol Med. 1999;97(5):360–4.
15. Kenda RB, et al. Echo-enhanced ultrasound voiding cystography in children: a new approach. Pediatr Nephrol. 2000;14(4):297–300.
16. Greis C. Technology overview: SonoVue (Bracco, Milan). Eur Radiol. 2004;14(Suppl 8):P11–5.
17. Schneider M. SonoVue, a new ultrasound contrast agent. Eur Radiol. 1999;9(Suppl 3):S347–8.
18. Babu R, Gopinath V, Sai V. Voiding urosonography: contrast-enhanced ultrasound cystography to diagnose vesico-ureteric reflux: a pilot study. J Indian Assoc Pediatr Surg. 2015;20(1):40–1.
19. Battelino N, et al. Vesicoureteral refux detection in children: a comparison of the midline-to-orifice distance measurement by ultrasound and voiding urosonography. Pediatr Nephrol. 2016;31(6):957–64.
20. Ntoulia A, et al. Contrast-enhanced voiding urosonography (ceVUS) with the intravesical administration of the ultrasound contrast agent Optison for vesicoureteral reflux detection in children: a prospective clinical trial. Pediatr Radiol. 2018;48(2):216–26.
21. Darge K, Back SJ. Invited commentary: prime time for contrast-enhanced voiding urosonography after approval of a US contrast agent for children. Radiographics. 2017;37(6):1869–71.
22. Duran C, et al. Contrast-enhanced voiding urosonography for vesicoureteral reflux diagnosis in children. Radiographics. 2017;37(6):1854–69.
23. Duran C, et al. Voiding urosonography including urethrosonography: high-quality examinations with an optimised procedure using a second-generation US contrast agent. Pediatr Radiol. 2012;42(6):660–7.
24. Faizah MZ, et al. Contrast enhanced Voiding Urosonography (ce-VUS) as a radiation-free technique in the diagnosis of vesicoureteric reflux: our early experience. Med J Malaysia. 2015;70(5):269–72.
25. Kis E, et al. Voiding urosonography with second-generation contrast agent versus voiding cystourethrography. Pediatr Nephrol. 2010;25(11):2289–93.
26. Kljucevsek D, et al. A comparison of echo-enhanced voiding urosonography with X-ray voiding cystourethrography in the first year of life. Acta Paediatr. 2012;101(5):e235–9.
27. Kljucevsek D, et al. Potential causes of insufficient bladder contrast opacification and premature microbubble destruction during contrast-enhanced voiding urosonography in children. J Clin Ultrasound. 2019;47(1):36–41.
28. Kuzmanovska D, et al. Voiding urosonography with second-generation ultrasound contrast agent for diagnosis of vesicoureteric reflux: first local pilot study. Open Access Maced J Med Sci. 2017;5(2):215–21.
29. Duran C, et al. Voiding urosonography: the study of the urethra is no longer a limitation of the technique. Pediatr Radiol. 2009;39(2):124–31.
30. Tse KS, et al. Paediatric vesicoureteric reflux imaging: where are we? Novel ultrasound-based voiding urosonography. Hong Kong Med J. 2014;20(5):437–43.
31. Wong LS, et al. Voiding urosonography with second-generation ultrasound contrast versus micturating cystourethrography in the diagnosis of vesicoureteric reflux. Eur J Pediatr. 2014;173(8):1095–101.
32. Papadopoulou F, et al. Contrast-enhanced voiding urosonography with intravesical administration of a second-generation ultrasound contrast agent for diagnosis of vesicoureteral reflux: prospective evaluation of contrast safety in 1,010 children. Pediatr Radiol. 2014;44(6):719–28.
33. Wozniak MM, et al. Two-dimensional (2D), three-dimensional static (3D) and real-time (4D) contrast enhanced voiding urosonography (ceVUS) versus voiding cystourethrography (VCUG) in children with vesicoureteral reflux. Eur J Radiol. 2016;85(6):1238–45.
34. Zhang W, et al. Contrast-enhanced voiding urosonography with intravesical administration of ultrasound contrast agent for the diagnosis of pediatric vesicoureteral reflux. Exp Ther Med. 2018;16(6):4546–52.
35. Chua ME, et al. The evaluation of vesicoureteral reflux among children using contrast-enhanced ultrasound: a literature review. J Pediatr Urol. 2019;15(1):12–7.
36. Papadopoulou F, et al. Harmonic voiding urosonography with a second-generation contrast agent for the diagnosis of vesicoureteral reflux. Pediatr Radiol. 2009;39(3):239–44.
37. Chua ME, et al. Diagnostic accuracy of contrast-enhanced voiding urosonogram using second-generation contrast with harmonic imaging (CEVUS-HI) study for assessment of vesicoureteral reflux in children: a meta-analysis. World J Urol. 2019;37(10):2245–55.
38. Velasquez M, et al. The learning curve of contrast-enhanced 'microbubble' voiding urosonography-validation study. J Pediatr Urol. 2019;15:385.e1–6.
39. Giordano M, et al. Voiding urosonography as first step in the diagnosis of vesicoureteral reflux in children: a clinical experience. Pediatr Radiol. 2007;37(7):674–7.
40. Riccabona M, et al. ESPR Uroradiology Task Force and ESUR Paediatric Working Group—Imaging recommendations in paediatric uroradiology, part V: childhood cystic kidney disease, childhood renal transplantation and contrast-enhanced ultrasonography in children. Pediatr Radiol. 2012;42(10):1275–83.
41. Piscaglia F, et al. The EFSUMB guidelines and recommendations on the clinical practice of contrast enhanced ultrasound (CEUS): update 2011 on non-hepatic applications. Ultraschall Med. 2012;33(1):33–59.
42. Sidhu PS, et al. Role of contrast-enhanced ultrasound (CEUS) in paediatric practice: an EFSUMB position statement. Ultraschall Med. 2017;38(1):33–43.
43. Colleran GC, et al. Intrarenal reflux: diagnosis at contrast-enhanced voiding urosonography. J Ultrasound Med. 2016;35(8):1811–9.

44. Colleran GC, et al. Residual intravesical iodinated contrast: a potential cause of false-negative reflux study at contrast-enhanced voiding urosonography. Pediatr Radiol. 2016;46(11):1614–7.
45. Subcommittee on Urinary Tract Infection, Steering Committee on Quality Improvement and Management, Roberts KB. Urinary tract infection: clinical practice guideline for the diagnosis and management of the initial UTI in febrile infants and children 2 to 24 months. Pediatrics. 2011;128(3):595–610.
46. National Institute for Health and Clinical Excellence. Urinary tract infection in children: diagnosis, treatment, and long-term management: NICE clinical guideline 54. London: National Institute for Health and Clinical Excellence; 2007. Available at: https://www.nice.org.uk/guidance/cg54/evidence/full-guideline-pdf-196566877. Accessed Nov 2019.
47. Darge K. Voiding urosonography with ultrasound contrast agents for the diagnosis of vesicoureteric reflux in children. I. Procedure. Pediatr Radiol. 2008;38(1):40–53.
48. Koff S. Estimating bladder capacity in children. Urology. 1983;21(3):248.
49. Feliubadaló CD, et al. Poster: ECR 2015/C-1387/tips and tricks to evaluate the urethra through serial voiding urosonography (VUS): making it easy. In: ECR 2015; 2015.
50. Papadopoulou F, et al. Cyclic voiding cystourethrography: is vesicoureteral reflux missed with standard voiding cystourethrography? Eur Radiol. 2002;12(3):666–70.
51. Darge K, Troeger J. Vesicoureteral reflux grading in contrast-enhanced voiding urosonography. Eur J Radiol. 2002;43(2):122–8.
52. Lebowitz RL, et al. International system of radiographic grading of vesicoureteric reflux. International Reflux Study in Children. Pediatr Radiol. 1985;15(2):105–9.
53. Darge K, Roessling G, Troeger J. Do microbubbles ascend passively in the ureters? Pediatr Radiol. 2003;33(Suppl 1):S38.
54. Darge K, et al. Intrarenal reflux: diagnosis with contrast-enhanced harmonic US. Pediatr Radiol. 2003;33(10):729–31.
55. Funston MR, Cremin BJ. Intrarenal reflux—papillary morphology and pressure relationships in children's necropsy kidneys. Br J Radiol. 1978;51(609):665–70.
56. Teele RL, Share JC. Transperineal sonography in children. AJR Am J Roentgenol. 1997;168(5):1263–7.
57. Cohen HL, et al. Prenatal sonographic diagnosis of posterior urethral valves: identification of valves and thickening of the posterior urethral wall. J Clin Ultrasound. 1998;26(7):366–70.
58. Good CD, et al. Posterior urethral valves in male infants and newborns: detection with US of the urethra before and during voiding. Radiology. 1996;198(2):387–91.
59. Mate A, et al. Contrast ultrasound of the urethra in children. Eur Radiol. 2003;13(7):1534–7.
60. Bosio M, Manzoni GA. Detection of posterior urethral valves with voiding cystourethrosonography with echo contrast. J Urol. 2002;168(4 Pt 2):1711–5; discussion 1715.
61. Berrocal T, Gaya F, Arjonilla A. Vesicoureteral reflux: can the urethra be adequately assessed by using contrast-enhanced voiding US of the bladder? Radiology. 2005;234(1):235–41.
62. Patel H, Watterson C, Chow JS. Case of urethral duplication seen by voiding urosonography. Clin Imaging. 2018;49:106–10.
63. Darge K. Voiding urosonography with US contrast agents for the diagnosis of vesicoureteric reflux in children. II. Comparison with radiological examinations. Pediatr Radiol. 2008;38(1):54–63; quiz 126–7.
64. Ascenti G, et al. Harmonic US imaging of vesicoureteric reflux in children: usefulness of a second generation US contrast agent. Pediatr Radiol. 2004;34(6):481–7.
65. Darge K, Beer M, Gordjani N. Contrast-enhanced voiding urosonography with the use of a 2nd generation US contrast medium: preliminary results. Pediatr Radiol. 2004;34(S):97.
66. Fernandez-Ibieta M, et al. Voiding urosonography with second-generation contrast as a main tool for examining the upper and lower urinary tract in children. Pilot study. Actas Urol Esp. 2016;40(3):183–9.
67. Piskunowicz M, et al. Premature destruction of microbubbles during voiding urosonography in children and possible underlying mechanisms: post hoc analysis from the prospective study. Biomed Res Int. 2016;2016:1764692.
68. Papadopoulou F, et al. Is reflux missed on fluoroscopic voiding cysteourethrography and demonstrated only by contrast-enhanced voiding urosonography clinically important? Pediatr Radiol. 2007;37(Suppl 2):S105–18.
69. McAninch JW, Laing FC, Jeffrey RB Jr. Sonourethrography in the evaluation of urethral strictures: a preliminary report. J Urol. 1988;139(2):294–7.
70. Choudhary S, et al. A comparison of sonourethrography and retrograde urethrography in evaluation of anterior urethral strictures. Clin Radiol. 2004;59(8):736–42.
71. Gupta N, et al. Urethral stricture assessment: a prospective study evaluating urethral ultrasonography and conventional radiological studies. BJU Int. 2006;98(1):149–53.
72. Babnik Peskar D, Perovic AV. Comparison of radiographic and sonographic urethrography for assessing urethral strictures. Eur Radiol. 2004;14(1):137–44.
73. Gong EM, et al. Sonourethrogram to manage adolescent anterior urethral stricture. J Urol. 2010;184(4 Suppl):1699–702.

74. Czarnecki O, et al. Microbubble-enhanced ultrasound to demonstrate urethral transection in a case of penile fracture. BMJ Case Rep. 2017;2017:220073.
75. Schaer GN, et al. Improvement of perineal sonographic bladder neck imaging with ultrasound contrast medium. Obstet Gynecol. 1995;86(6):950–4.
76. Wang X, et al. Preoperative transurethral contrast-enhanced ultrasonography in the diagnosis of female urethral diverticula. J Ultrasound Med. 2018;37(12):2881–9.
77. Kopac M, Riccabona M, Haim M. Contrast-enhanced voiding urosonography and genitography in a baby with ambiguous genitalia and urogenital sinus. Ultraschall Med. 2009;30(3):299–300.
78. Seranio N, et al. Contrast enhanced genitosonography (CEGS) of urogenital sinus: a case of improved conspicuity with image inversion. Radiol Case Rep. 2018;13(3):652–4.
79. Chow JS, et al. Contrast-enhanced colosonography for the evaluation of children with an imperforate anus. J Ultrasound Med. 2019;38(10):2777–83.
80. Wozniak MM, et al. 3D/4D contrast-enhanced urosonography (ceVUS) in children—is it superior to the 2D technique? J Ultrason. 2018;18(73):120–5.
81. Wozniak MM, et al. Intraoperative contrast-enhanced urosonography during endoscopic treatment of vesicoureteral reflux in children. Pediatr Radiol. 2014;44(9):1093–100.
82. Zerin JM, Shulkin BL. Postprocedural symptoms in children who undergo imaging studies of the urinary tract: is it the contrast material or the catheter? Radiology. 1992;182(3):727–30.

Contrast-Enhanced Ultrasound in the Pediatric Scrotum

15

Vasileios Rafailidis, Dean Y. Huang, Maria E. Sellars, and Paul S. Sidhu

15.1 Introduction

Ultrasound (US) is the first-line imaging modality for assessment of pediatric scrotal disease. Symptoms in both children and adults are often non-specific and associated with abnormalities requiring different therapeutic approaches, either surgical or conservative, with imaging playing a pivotal role in the differential diagnosis. With the multiple US techniques available (grayscale imaging, color and power Doppler techniques), US is capable of readily addressing clinical questions and establishing the diagnosis [1]. The introduction of contrast-enhanced ultrasound (CEUS) has added advantages to conventional US, although conventional US techniques remain the cornerstone of diagnosis [2]. The purpose of this chapter is to discuss the potential benefit of CEUS in the setting of spermatic cord torsion, trauma, complicated inflammation, and other applications. Since the published literature mainly deals with the application of CEUS in adults, we discuss personal experience of the CEUS applications in the pediatric population.

15.2 Technical Aspects of Pediatric Scrotal US and CEUS

Optimal visualization of the pediatric scrotal contents is best achieved with high-frequency linear transducers using a frequency ranging from 9 to 18 MHz. A transducer of lower frequency (9 MHz) might be used to achieve greater depth. Each testis should be assessed in both longitudinal and transverse directions. Of particular importance is the transverse image showing both testes, enabling comparison in terms of echogenicity and vascularity. A small amount of fluid is normally found within the tunica vaginalis. In a painful hemiscrotum, the asymptomatic side should be scanned first, adjusting the imaging settings for comparison with the symptomatic side.

A careful adjustment of the color Doppler settings is crucial since the testes of pre-pubertal boys are small in size and although should normally exhibit vascular flow, this is occasionally poorly visualized; a potential application for CEUS. Adjustments needed for optimal visualization of slow blood flow include:

1. use of a high-frequency transducer
2. reduction of pulse repetition frequency
3. decreasing or disabling the wall filter
4. increasing color gain, avoiding the blooming artifact

V. Rafailidis (✉) · D. Y. Huang · M. E. Sellars
P. S. Sidhu
Department of Radiology, King's College Hospital, London, UK
e-mail: v.rafailidis@nhs.net; dean.huang@nhs.net; maria.sellars@nhs.net; paulsidhu@nhs.net

P. S. Sidhu et al. (eds.), *Contrast-Enhanced Ultrasound in Pediatric Imaging*,
https://doi.org/10.1007/978-3-030-49691-3_15

For the CEUS part of the examination, 4.8 mL of SonoVue™ (Bracco SpA, Milan) should be used as the microbubble physics and size dictates that higher frequency transducers are less sensitive to current ultrasound contrast agents (UCA).

15.3 Clinical Aspects of Pediatric Scrotal Disease

Pain of acute onset and swelling is a common presentation of different types of scrotal disease. Typically, the most common causes of an acute hemiscrotum in a young boy includes:

1. spermatic cord torsion
2. torsion of an appendage
3. inflammatory conditions such as epididymitis and orchitis

Torsion of the testicular appendages is the most frequently encountered cause, estimated at approximately 33% of children with an acute scrotum, with epididymitis being the second most common, accounting for 31% and followed by spermatic cord torsion at 22%. A clinical diagnosis of torsion is paramount, with the loss of the cremasteric reflex on the symptomatic side being suggestive of spermatic cord torsion, but this is insensitive with US far more informative, but should not replace the clinical decision [3]. Different series showed that inflammatory conditions are more common than torsion and confirmed that appendages undergo torsion more frequently than the testis [4].

In *spermatic cord torsion*, the vascular supply of testis is compromised due to rotation of the vascular pedicle. Prompt and accurate diagnosis is crucial; surgery should be rapid to avoid necrosis of the testicular parenchyma. Surgery within the first 6 h after presentation is associated with salvage rates of 100%, while after 12 h surgery rescues <20% of testes [5].

There are two types of testicular torsion: the *extravaginal*, encountered during the first year of life and the *intravaginal* affecting adolescent boys [6]. The *bell clapper anomaly* is a suggested risk factor for intravaginal type of torsion. In the normal scrotum, the epididymis is fully attached to the testis postero-laterally and the parietal layer of the tunica vaginalis is attached to the cranial and caudal end of epididymis. With a bell clapper deformity, the parietal layer of the tunica vaginalis is attached abnormally higher than usual to the spermatic cord, resulting in encirclement of epididymis, testis, and part of the spermatic cord by the tunica vaginalis. On US this may be seen as an absence of posterior attachment of the tunica vaginal parietal layer to the epididymis and disconnection from the lower pole of testis. This allows the scrotal contents to hang freely within the intravaginal space, giving a horizontal position, perpendicular to the contralateral testis, but not if the anomaly is bilateral, occurring in the majority of cases [7]. A recent study reported that in every case of acute spermatic cord torsion, this was intravaginal and caused by bell clapper anomaly [8].

Inflammatory disease of the scrotum includes epididymo-orchitis and is mainly idiopathic when affecting younger children or associated with sexually transmitted disease in adolescents. An underlying anatomic abnormality may be present in children with recurrent episodes of epididymo-orchitis [9].

Scrotal *trauma* is frequent in the pediatric population and usually minor. Common causes include sports activities, motor vehicle or straddle injuries, and falls. Often with only subtle findings of trauma, care is needed to carefully assess for potential coexisting pathology such as spermatic cord torsion or an incidentally found tumor [4, 9].

Intratesticular *masses* affecting children have two peaks in age distribution: one in neonates and children up to 3 years of age and a second at 14 years of age. In children before puberty an important proportion of tumors are benign, with teratoma representing the majority. Adolescents presenting with a painless scrotal mass usually have a malignancy. Scrotal tumors are uncommon in the pediatric age group, occurring in only 2 per 100,000 boys [4]. Both germ cell tumors and non-germ cell tumors are encountered in the pediatric age group [4, 9]. Germ cell tumors include seminoma, embryonal carcinoma, mature

and immature teratoma, choriocarcinoma, yolk sac tumor. Non-germ cell tumors include Leydig cell tumor, Sertoli cell tumor, and gonadoblastoma.

15.4 Conventional US Findings

15.4.1 Torsion of the Spermatic Cord and Appendages

The grayscale US findings of spermatic cord torsion are non-specific, as the testicular parenchyma may appear normal, hypoechoic, or heterogeneous, essentially depending on the duration of onset of symptoms. The presence of a heterogeneous appearance may indicate non-viability of the testis [10]. If segmental infarction is present, then only part of the testicular parenchyma will demonstrate abnormal echogenicity. Other findings that may be present include a twisted spermatic cord (whirlpool sign), hydrocele, and displacement of the epididymis towards the caudal aspect of the testis [3, 6].

The advocated hallmark for the diagnosis of testicular torsion is the absence or reduction in blood flow within the symptomatic testis, in comparison with the unaffected testis essential in the child, where limited Doppler signal is a normal finding (Figs. 15.1 and 15.2). The sensitivity of color Doppler US for the diagnosis of testicular torsion is 95–100%, while specificity is 85–95%. A false-negative diagnosis can be caused by partial torsion, spontaneous detorsion after torsion or erroneous measurement of arterial waveforms from arteries lying at the periphery of the testicle instead of the centripetal intra-parenchymal arteries [5, 11–14]. Color Doppler signals may be visible at the periphery of a torted testis; these originate from capsular vessels and do not exclude the diagnosis of torsion (Fig. 15.2) [9].

The assessment of spermatic cord torsion is problematic in patients with intermittent or partial torsion. Complete torsion refers to the testicular rotation of at least 360°, while in partial torsion the rotation is lower. With spontaneous resolution, symptoms regress and the term "intermittent" is applied. A challenging situation occurs with preserved blood flow, where the affected testis may exhibit symmetric, decreased, or even increased blood flow signals compared with the healthy side (Fig. 15.3) [6].

The "spermatic cord whirlpool sign" is used to describe an abrupt and focal enlargement of the spermatic cord found either within the hemiscrotum or at the level of the external inguinal ring. The spermatic cord appears twisted at the point of enlargement, and there may be a "redundant spermatic cord" or "boggy pseudo-mass" visible (Fig. 15.2a). This is visualized as an elongated spermatic cord appearing bunched up, forming a rounded heterogeneous extra testicular mass with anechoic converging tubes representing blood vessels. Color Doppler US will reveal

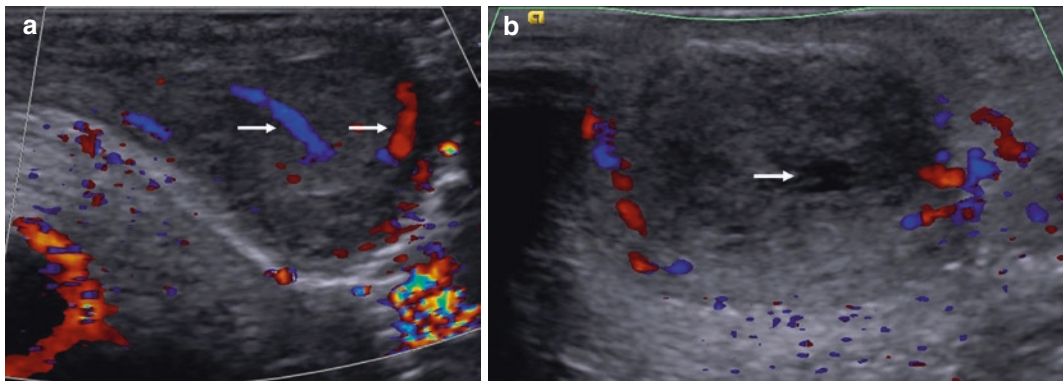

Fig. 15.1 A 4-day-old neonate with extra-vaginal testicular torsion. (**a**) The left testis demonstrates normal good intratesticular color Doppler signal. (**b**) The right testis demonstrates a heterogeneous pattern, with a focal area of possible infarction (arrow), and no color Doppler signal

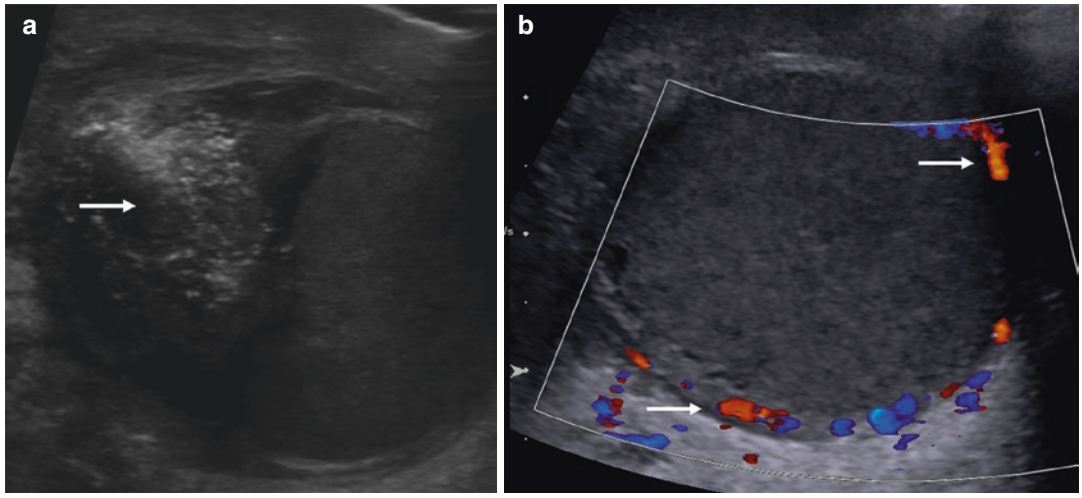

Fig. 15.2 A 17-year-old with a 5-day history of pain and swelling of the left hemi-scrotum, with an infarcted testis following intravaginal spermatic cord torsion. (**a**) There is an echogenic "mass" above the left testis (arrow) likely the twisted spermatic cord, the "whirlpool" sign, with a slightly "mottled" testis noted. (**b**) There is no color Doppler signal demonstrated within the testis, but good signal in the surrounding tissue (arrows)

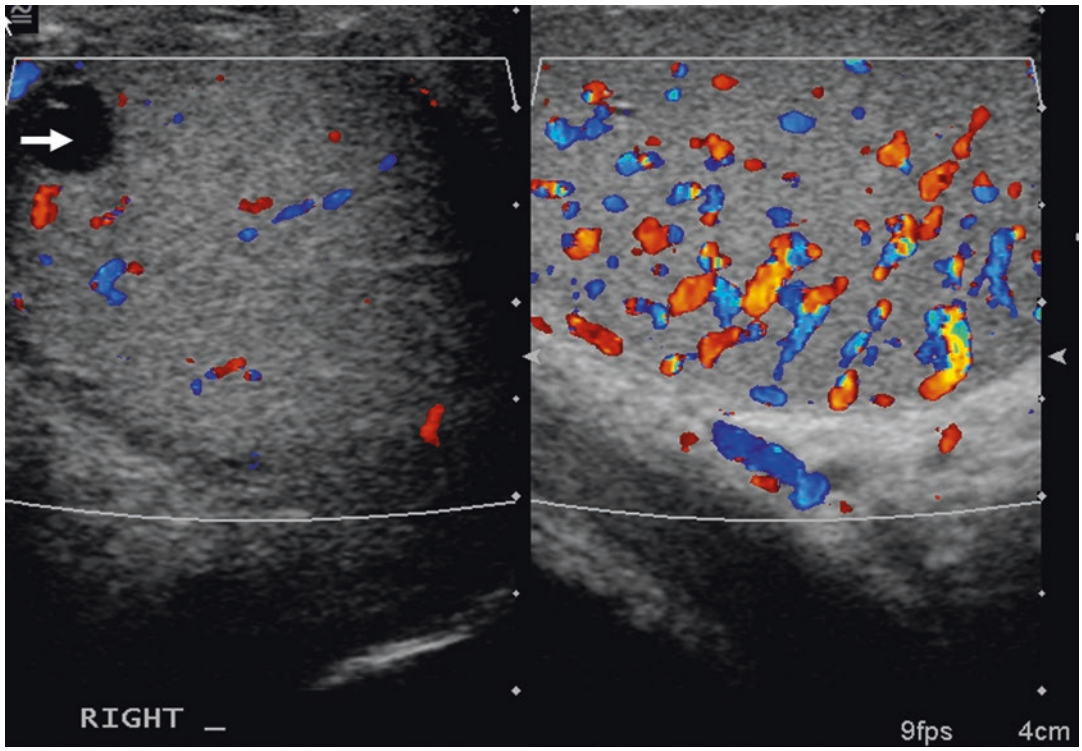

Fig. 15.3 A 17-year-old boy with self-limiting acute left-sided scrotal pain, thought to have spontaneous detorsion. There is increased color Doppler signal in the left testis compared to the right. An incidental intra-testicular cyst is present on the right

blood flow signals in arterial and venous vessels when a partial twist does not completely occlude vascular structures [15]. This "spermatic cord whirlpool sign" is reported to be pathognomonic for the diagnosis of spermatic cord torsion [16].

Spectral Doppler US analysis may be used in the evaluation of suspected spermatic cord torsion. Arteries of the testicular parenchyma normally exhibit a mean resistive index of 0.62, ranging from 0.48 to 0.75 [17]. Asymmetry of waveforms with dampening in the symptomatic side, absence or reversal of blood flow in the diastolic phase are findings suggestive of torsion.

If the torsion affects an appendage, either the appendix testis or appendix epididymis, then hyperemia can be appreciated surrounding the appendage, while normal vascularization is present within the testis. The appendage itself typically appears as an ovoid, avascular, extra-testicular mass of high or mixed echogenicity attached to the testicular parenchyma [18]. Torsion of the appendix testis is usually encountered in pre-pubertal boys presenting with gradual pain and commonly the "blue dot sign," representing a bluish skin discoloration over a palpable nodule in the painful hemi-scrotum. Secondary findings of torsion of an appendage include reactive hydrocele and scrotal skin thickening (Fig. 15.4).

15.4.2 Inflammation and Abscess

Inflammation of the epididymis (epididymitis) appears as epididymal enlargement, a decrease of echogenicity, increase of blood flow signals on color Doppler US and a reduced resistive index of 0.5–0.7 (Fig. 15.5). The head of the epididymis is the most frequently affected part, and may involve the testis, as seen in up to 40% of cases. Reactive hydrocele or scrotal wall thickening can be present. Complications of severe inflammatory disease include abscess and venous testicular infarction, although such entities may be less frequent in the pediatric population [19].

15.4.3 Trauma

There is a wide range of US appearances of scrotal trauma, including testicular rupture and hematoma. A *hematoma* may be located either in the extra-testicular space or within the testicular parenchyma, typically hyperechoic in the acute phase but as the blood products are metabolized and absorbed, gradually becoming hypoechoic, with septations, loculations or fluid–fluid levels. A *testicular fracture* is a linear hypoechoic, avascular line traversing the testicular parenchyma, not reaching the tunica albuginea. Without a

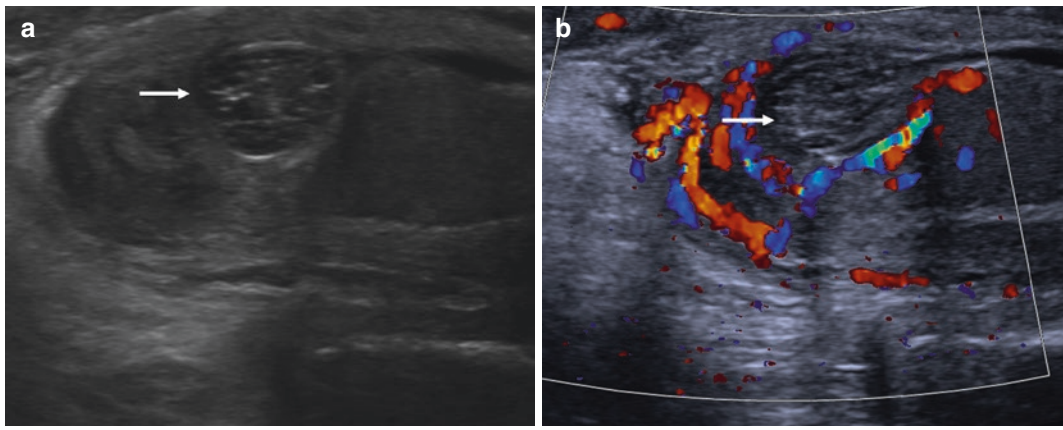

Fig. 15.4 A 9-year-old boy with a 5-day history of left-sided scrotal pain, and a palpated mass, found to have a torted appendix testis. (**a**) At the upper aspect of the left testis is a well-circumscribed area (arrow), with a mixed echogenic pattern, closely related to the epididymis. (**b**) This area demonstrates no color Doppler signal and represents the torted appendix testis

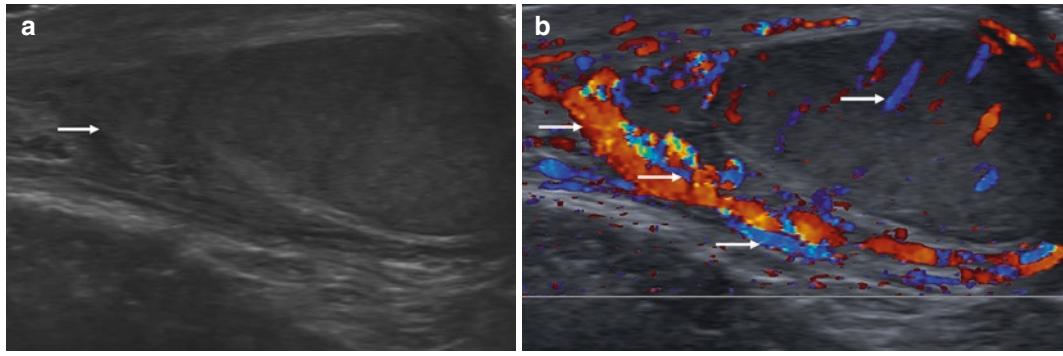

Fig. 15.5 A 13-year-old boy with acute epididymitis. (**a**) A grayscale US image demonstrating the enlargement and heterogeneity of epididymis (arrow). (**b**) The color Doppler US image demonstrating the increased vascularity suggestive of inflammation in the epididymis and the adjacent testis (arrows)

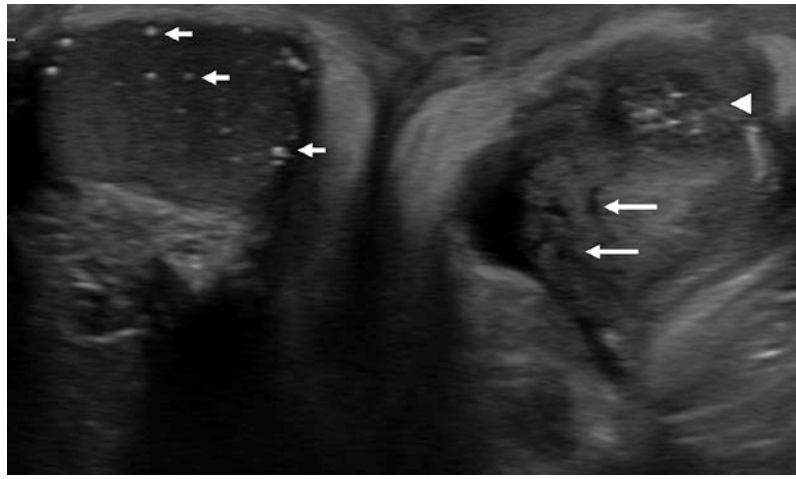

Fig. 15.6 A 11-year-old boy with a direct blunt injury to the left hemi-scrotum, with testicular fractures, and epididymal hematoma. On the right, there is testicular microlithiasis (small arrows) within a normal testis. On the left areas of linear hypo-echogenicity in the testis (arrows) represent fracture lines, and there is disruption to the adjacent tunica albuginea, with a small hematocele. A mixed echogenic epididymal hematoma is also seen (arrowheads)

breech in the tunica albuginea, the testis preserves its normal shape. If the tunica albuginea is disrupted by a fracture line, then an abnormal shape is seen, *testicular rupture* has occurred and is a surgical emergency. Disruption of the tunica albuginea demonstrates on US as poorly defined margins, a focal discontinuity of the echogenic line of the tunica albuginea or the capsular blood vessels and heterogeneity of parenchymal echogenicity [9] (Fig. 15.6).

15.4.4 Tumors and Tumor Mimics

Yolk sac tumors are the most frequent type of germ cell tumor affecting prepubertal children. These tumors appear as heterogeneous, well-defined solid focal masses, although they may occasionally present with diffuse testicular enlargement. Color Doppler US demonstrates increased vascularity with a chaotic internal architecture (Fig. 15.7). Teratomas affecting boys up to 4 years of age are

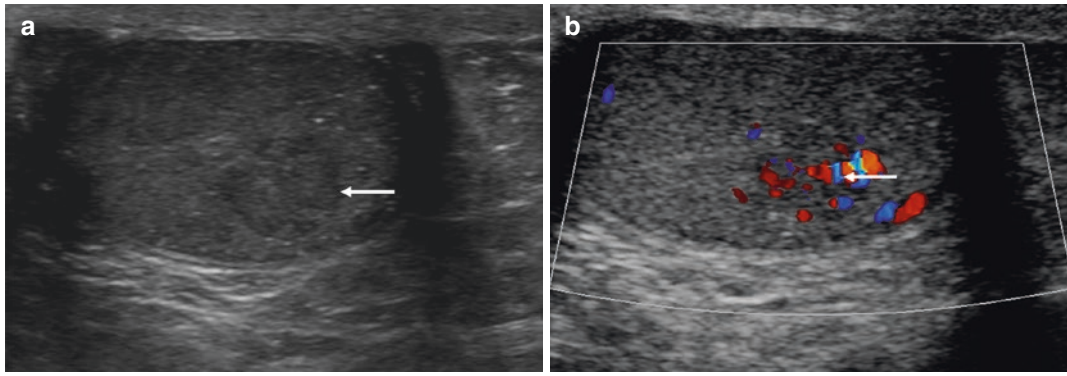

Fig. 15.7 A 11-year-old boy with left groin pain, with an incidental yolk sac tumor of the left testis. (**a**) A mixed reflective circumscribed lesion in the mid aspect of the testis (arrow). (**b**) There is increased color Doppler signal from the lesion indicating a vascularized tumor (arrow)

usually benign, whereas those encountered in post-pubertal boys are malignant. These lesions typically appear solid with heterogeneous echogenicity, cystic components, and calcifications [9].

Gonadal stroma (Leydig cell tumor) and sex cord cells (Sertoli cell tumor) give rise to non-germ cell tumors. Leydig cell tumors usually occur between 3 and 6 years of age and may cause precocious puberty due to androgen secretion. These tumors appear as well-defined and uniformly hypoechoic focal lesions. Any extra-testicular solid lesion is most often a para-testicular rhabdomyosarcoma in a child, usually solid, occasionally cystic with solid nodularity. Other rare but benign entities include lymphangioma, fibrous pseudotumor, lipoma, leiomyoma, and hemangioma [6, 9].

Epidermoid cysts are well-defined, rounded or ovoid lesions typically exhibiting multiple lamellated concentric layers of alternating echogenicity and an outer hyperechoic rim; the "onion ring" sign. If the central part of the lesion is echogenic as well, the so-called target appearance occurs. The number of concentric layers has been associated with the maturity of the epidermoid cyst, with less mature lesions appearing entirely cystic. Calcification of the wall is common finding and can be in the form of scattered foci, dense or complete circumferential. Importantly, no blood flow signals should be documented in color Doppler US as the cyst is devoid of internal vascularity [20, 21].

Simple cysts are rarely found in the pediatric testis and either associated with rete testis or tunica albuginea (Fig. 15.3). Cystic dysplasia of the rete testis is an uncommon congenital malformation commonly coexisting with other anomalies of the genitourinary system such as ipsilateral agenesis of the kidney or multi-cystic kidney. On US, this malformation appears as multiple anechoic areas of cystic dilatation, with irregular shape and measuring up to 5 mm [9].

Primary testicular lymphoma has been reported infrequently, although secondary involvement can be seen in patients with acute lymphoblastic leukemia and non-Hodgkin B-cell lymphoma. On US these may appear either as diffuse involvement of the testis (which will appear enlarged and hypoechoic) or as multiple hypoechoic nodules. Increased vascularity is seen on color Doppler US, mimicking inflammatory conditions [22, 23].

15.5 Potential Roles of CEUS in Pediatric Testis

The published evidence for CEUS in the pediatric population is limited [21, 24–27]. The application of CEUS for the characterization of testicular pathology is off-label both in adults and children, and already established conventional US techniques are well-suited and achieve adequate accuracy. Nonetheless, CEUS could have a

Table 15.1 Summary of potential CEUS applications in pediatric scrotum

Potential CEUS applications in pediatric scrotum
1. Diagnosis of testicular infarction (global or segmental) in children with small testes, where conventional techniques may not be sensitive enough for the normally reduced vascularity in this setting.
2. Detection and differentiation of viable vascularized and non-viable ischemic tissue after trauma, in addition to clearly demonstrating fracture lines.
3. Clear diagnosis and delineation of hematomas following trauma.
4. Confident detection and delineation of abscess borders in the setting of complicated epididymo-orchitis.
5. Definitively demonstrate the absence of internal blood flow in cysts containing echogenic material, confidently excluding the diagnosis of a solid tumor.
6. Qualitative characterization of solid tumors by showing increased enhancement compared to adjacent normal parenchyma and abnormal pattern of vascularization.
7. Quantitative analysis of solid tumors enhancement by use of time-intensity curves analysis.

place in specific fields of pediatric scrotal pathology, as is summarized in Table 15.1. As a general statement, CEUS offers the possibility to accurately assess vascularization, the vascular architecture, and the dynamics of enhancement of any tissue, both normal and abnormal.

The Abdominal Imaging Task Force of the European Society of Pediatric Radiology has suggested that a theoretical risk exists when administering microbubbles and performing CEUS in a poorly perfused organ like the testis, where an increase in cavitation may occur. This risk can be mitigated with scanning at a low MI (<0.4) and balanced with the risk of misdiagnosing an infarcted testis [26].

15.5.1 Spermatic Cord Torsion

Although the US diagnosis of spermatic cord torsion can be readily achieved with conventional US techniques, false-positive results can occur. This may be attributable to the small volume of the testis prior to puberty, and subsequent lower vascularity, limiting color Doppler US to detect blood flow. This may be improved by optimizing the scanning technique (lowering pulse repetition frequency, increasing color gain), comparing findings with the healthy side, using power Doppler US or newer increased color sensitivity techniques.

Contrast-enhanced ultrasound is more sensitive in visualizing vasculature than any other flow visualization technique. In keeping with US Doppler techniques, CEUS should demonstrate absence of intratesticular enhancement in established spermatic cord torsion [7, 28]. In a series evaluating CDUS and CEUS in the assessment of intratesticular flow in various conditions, no clear advantage was found for CEUS, but this was conducted in patients aged 19–61 years of age, where the volume of testicular tissue is greater than in the pre-pubertal boys. However, the study confirmed the lack of perfusion in every case of spermatic torsion using CEUS [29]. It is anticipated that CEUS should improve the ability to detect reduced blood flow in the pediatric testis (Figs. 15.8 and 15.9).

Contrast-enhanced ultrasound is valuable in the characterization and diagnosis of *segmental testicular infarction*, secondary to intermittent spermatic cord torsion or a consequence of severe infection [30–32]. The documentation of lack of enhancement can designate a focal hypoechoic intratesticular region as a segmental infarction, potentially excluding a tumor, where vascularity is expected. In the subacute stage, a rim of peripheral enhancement can be observed, based on appearances in adult patients (Fig. 15.10) [30]. In adult patients with acute scrotal pain and undergoing both color Doppler US and CEUS, the contrast study increased the number of patients with a definitive diagnosis [33]. In a summary of intravenous applications of CEUS in various organs in children, the CEUS examination was used to rule out insufficient testicular perfusion [25].

In an experimental setting, Paltiel et al. have evaluated the use of real-time volumetric CEUS in a rabbit model of testicular torsion, using a two-dimensional matrix phased array US transducer. The changes in CEUS signal intensity had a good correlation with the perfusion values calculated with radiolabelled microspheres [34].

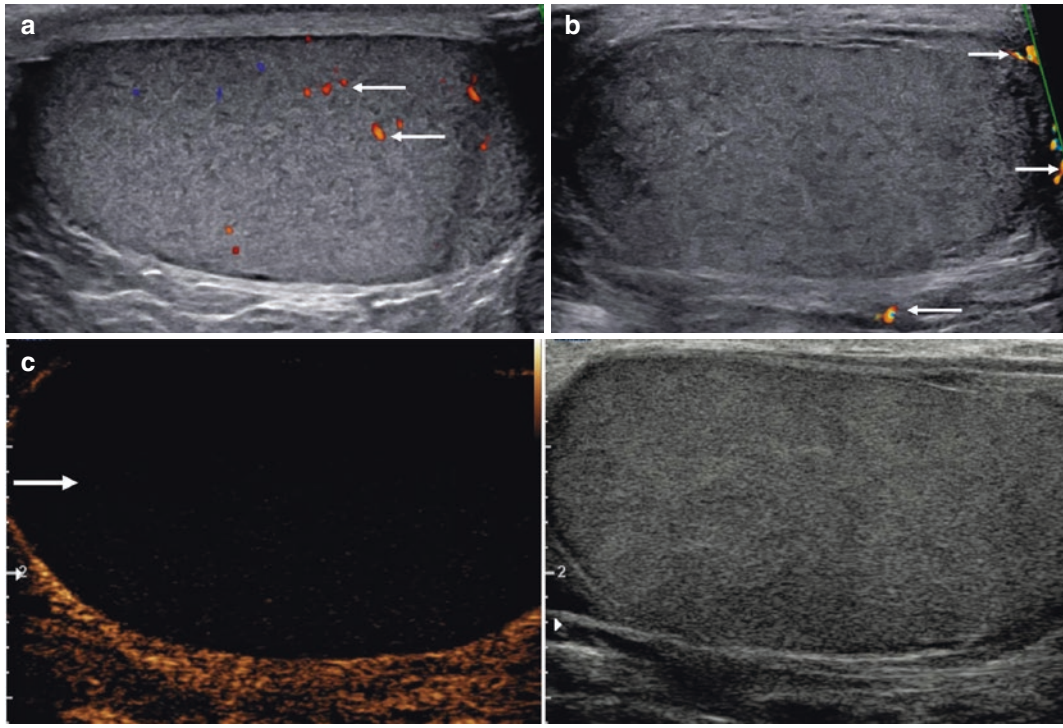

Fig. 15.8 A 17-year old boy with torsion of an undescended inguinal testes. (**a**) Color Doppler US of the normal left testis shows limited blood flow (arrows), a normal appearance. (**b**) A color Doppler US of the right testis (located in the inguinal canal) shows absence of blood flow within the testis, but with flow signal (arrows) in the surrounding tissue. (**c**) On the CEUS examination, there is unequivocally absence of contrast enhancement (arrow) in the testis, establishing the diagnosis of infarction

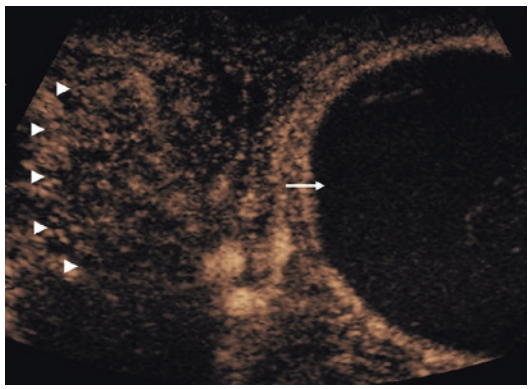

Fig. 15.9 A 17-year-old boy who presented 5 days after the onset of acute testicular pain. The "spectacle" view on the CEUS examination demonstrates no contrast enhancement in the left testis (arrow) and a normal perfusion of the healthy right testis (arrowheads)

This three-dimensional US technique is not widely available and the evaluation of testicular perfusion should be evaluated with a thorough examination of the entire parenchyma, in both the transverse and longitudinal planes with a conventional transducer.

15.5.2 Inflammation

In the setting of *inflammation*, the use of UCA is unnecessary in uncomplicated patients but plays a role in the evaluation of complicated epididymo-orchitis, particularly in the improved delineation and establishment of an abscess, as seen in adult patients [29, 33]. Furthermore, a segmental infarction may also be a complication of severe

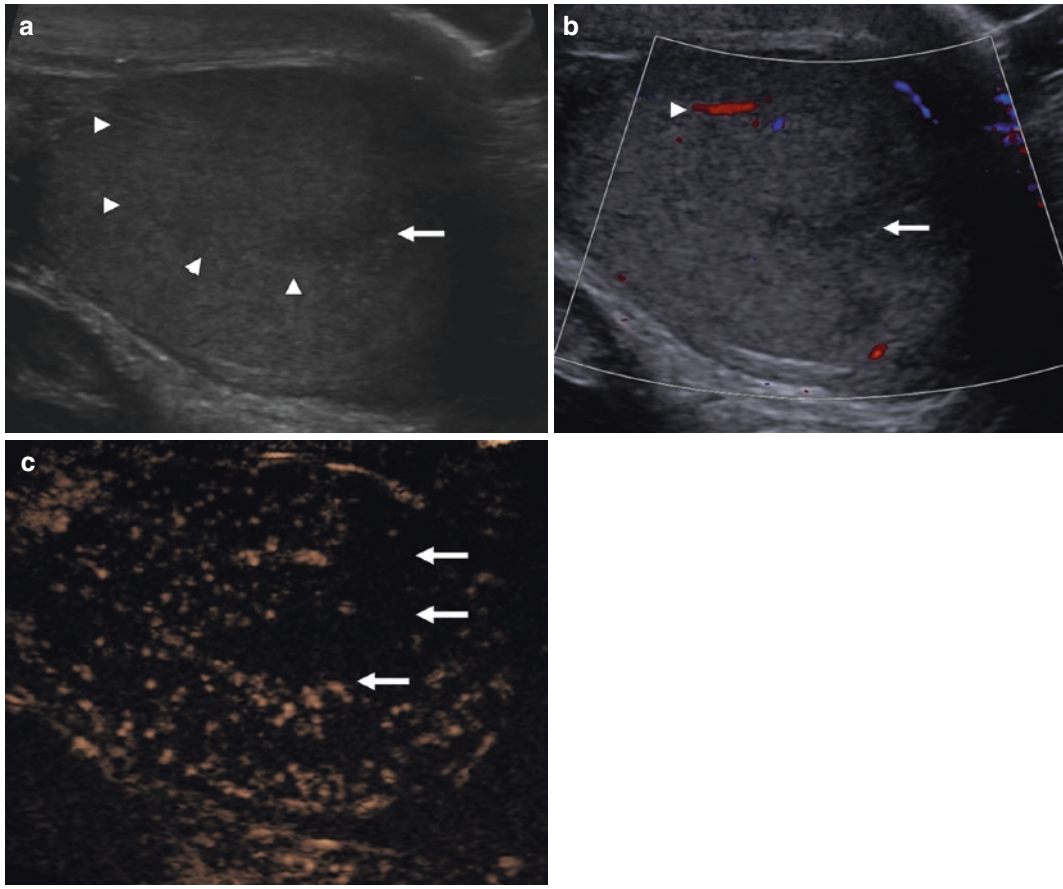

Fig. 15.10 A 15-year-old boy with segmental testicular infarction. (**a**) The B-mode demonstrates a focal area of mixed reflectivity (arrowheads) with a central component of hypo-echogenicity (arrow). (**b**) The color Doppler US demonstrates signal (arrowhead) within the upper aspect of the abnormality but no signal in the hypo-echoic area (arrow). (**c**) On the CEUS examination there is no perfusion within this area (arrows) but normal perfusion of the remaining parenchyma, suggesting this is an area of segmental testicular infarction

inflammation, readily identified with a CEUS examination. An abscess should typically exhibit a rim of increased enhancement but absolute lack of internal enhancement, as is seen with any extra-testicular abscess [16, 35]. A CEUS examination is valuable in improving characterization of non-vascularized tissue and helps to diagnose areas of infarction, abscess, orchitis, and tumor [29].

15.5.3 Trauma

With scrotal *trauma*, UCA can be used to provide clinically useful information, by demonstrating tissue perfusion and establishing the viability of the underlying traumatized testis. This can guide management, with organ-sparing surgery possible with a partially non-perfused testes and orchiectomy performed for a global non-perfused testis (Fig. 15.11). This has been demonstrated in adult patients, where the non-perfused part of an injured testis was identified, allowing for organ-sparing surgery [36]. Beyond examining tissue perfusion after injury, CEUS could be used to confirm the absence of vascularity within hematomas or infarcted testes [14]. The CEUS examination demonstrates absence of internal vascularity in hematomas, with occasional rim and septum enhancement [37].

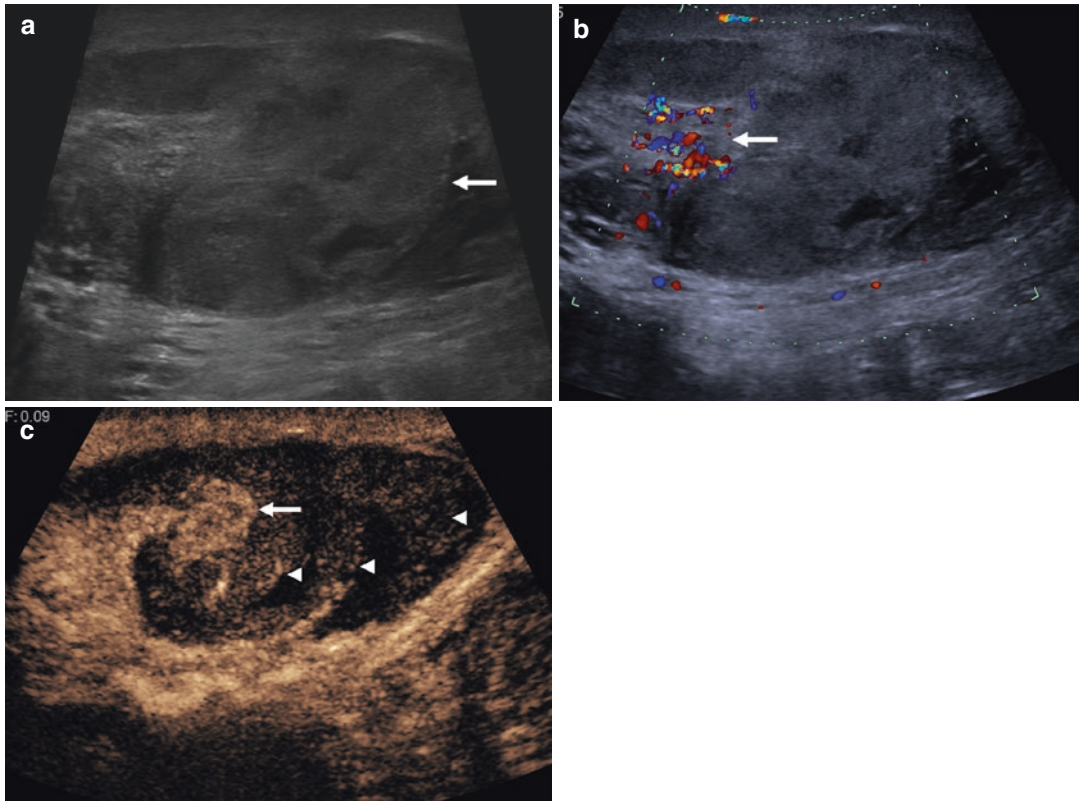

Fig. 15.11 A 24-year-old adult involved in a road traffic accident, with left-sided scrotal trauma. (**a**) The left testis is heterogeneous (arrow), with changes in reflectivity and no well-defined border. (**b**) On the color Doppler image, there is some central color signal (arrow but none elsewhere. (**c**) On the CEUS examination, there is good enhancement (arrow) in the area of increased Doppler signal, and with less well-perfused (arrowheads) patchy areas elsewhere indicating viable testicular parenchyma

15.5.4 Tumors

With *tumor characterization*, US is well-suited with excellent spatial resolution and capability for both anatomical description (grayscale imaging) and physiologic evaluation (assessment of vascularity with Doppler techniques). The key aspects that influence management are:

1. Is the lesion intra-testicular or extra-testicular?
2. Is the lesion solid or cystic?
3. Does the lesion have internal vascularity and if so, what are the vascular characteristics?

Although the findings may be readily interpretable, there are occasions where difficulties arise, e.g., in a complicated cyst-containing proteinaceous content, blood or other forms of echogenic debris. The establishment of the absence of vascularity within the echogenic material, excluding the possibility of solid neoplastic tissue is important. Although Doppler techniques can be useful, CEUS outperforms conventional Doppler US techniques in identifying internal vascularity. The premise of the absence of vascularity as the most sensitive technique is that only a viable tumor will have a blood supply and therefore potentially malignant, requiring surgical management [38, 39]. Contrast-enhanced ultrasound was used to investigate the perfusion pattern of an extra-testicular lesion, which had a similar pattern to the adjacent normal testis, pointing towards the diagno-

sis of a supernumerary testis [27]. A case series of epidermoid cyst, with two cases <18 years of age, demonstrated that CEUS confirmed the complete absence of internal lesion vascularization. A rim of peripheral increased enhancement has been noted due to the aggregation of blood vessels and compression of adjacent testicular parenchyma [21]. Not only with solid tumors, usually germ cell tumors, but also lymphoma deposits or stromal cell tumors (e.g., Leydig cell hyperplasia) are expected to demonstrate higher enhancement than adjacent normal test parenchyma with loss of normal linear pattern of blood vessels. As a result, CEUS using both qualitative and quantitative evaluation of enhancement with time-intensity curve analysis could be useful [40] (Fig. 15.12).

The evaluation of an extra-testicular lesion in the adult is useful for delineation of abscesses and cysts but less useful for the assessment of predominantly benign lesions encountered in the extra-testicular space, i.e., the lipoma or adenomatoid abnormality [35]. In the child, the extra-testicular lesion is often malignant, commonly a rhabdomyosarcoma, and demonstration of vascularity on a CEUS examination may be useful (Fig. 15.13).

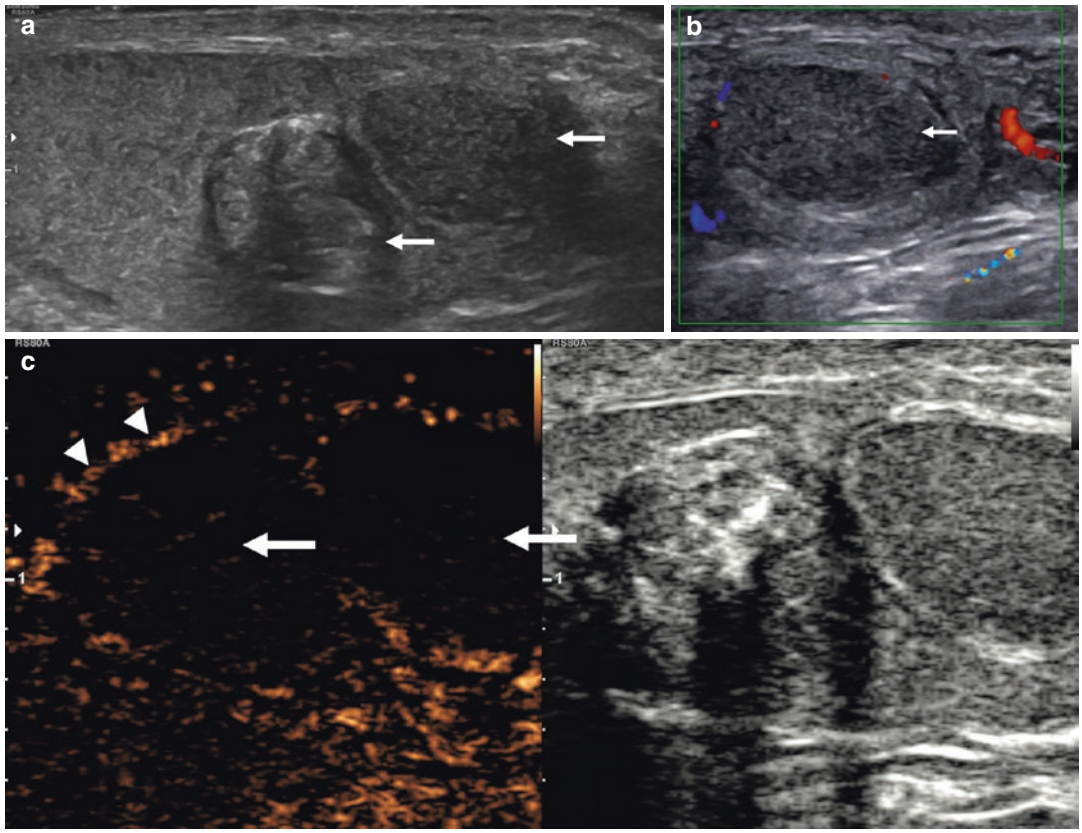

Fig. 15.12 A 11-year-old boy with two testicular epidermoid cysts. (**a**) The B-mode US demonstrates two solid lesions with low and mixed echogenicity (arrows). (**b**) The color Doppler US demonstrates no signal in the uniformly lower reflective lesion (arrow). (**c**) The CEUS examination demonstrates the complete absence of internal vascularity (arrows) with peripheral rim enhancement (arrowheads), suggesting the diagnosis of epidermoid cysts

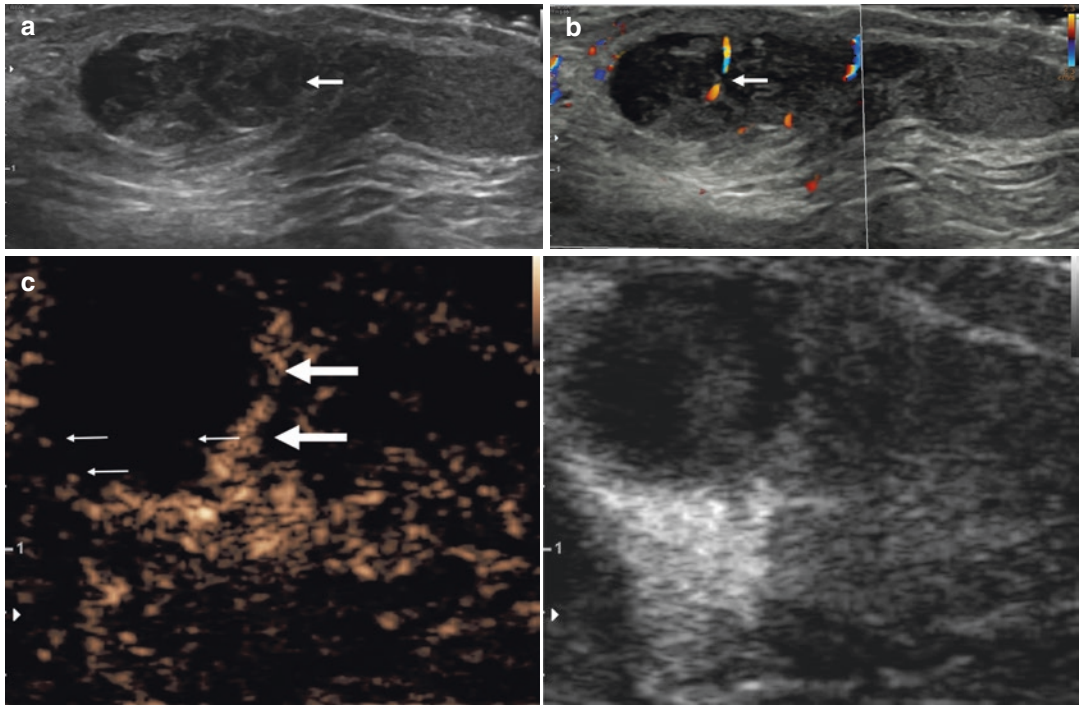

Fig. 15.13 A paratesticular mass in an 8-year-old boy, a rhabdomyosarcoma. (**a**) A mixed reflective predominantly solid lesion at the upper aspect of the left hemi-scrotum (arrow), displacing the left testis inferiorly. (**b**) There is some increase in color Doppler flow to the abnormality (arrow). (**c**) Following the CEUS examination, there is enhancement at the site of increase color Doppler flow (thick arrow) but in addition there are moving microbubbles within the lesion indicating vascularity and likely malignancy

15.6 Conclusion

A conventional US examination with the addition of color Doppler is often very informative when investigating the scrotal contents of a child. The addition of a CEUS examination has the unique ability to assess the detailed vascularity of the testis in spermatic cord torsion, tumor presence, and is invaluable in assessing the post-traumatic testis. Assessment of the dynamic time-intensity curves may be useful in the interpretation of patterns of vascular enhancement in focal testicular tumors.

References

1. Sidhu PS. Multiparametric ultrasound (MPUS) imaging: terminology describing the many aspects of ultrasonography. Ultraschall Med. 2015;36:315–7.
2. Sidhu PS, Cantisani V, Dietrich CF, Gilja OH, Saftoiu A, Bartels E, et al. The EFSUMB guidelines and recommendations for the clinical practice of contrast-enhanced ultrasound (CEUS) in non-hepatic applications: update 2017 (long version). Ultraschall Med. 2018;39:e2–e44.
3. Alkhori NA, Barth RA. Pediatric scrotal ultrasound: review and update. Pediatr Radiol. 2017;47(9):1125–33.
4. Aso C, Enriquez G, Fite M, Toran N, Piro C, Piqueras J, et al. Gray-scale and color Doppler sonography of scrotal disorders in children: an update. Radiographics. 2005;25:1197–214.
5. Sung EK, Setty BN, Castro-Aragon I. Sonography of the pediatric scrotum: emphasis on the Ts—torsion, trauma, and tumors. Am J Roentgenol. 2012;198(5):996–1003.
6. Bandarkar AN, Blask AR. Testicular torsion with preserved flow: key sonographic features and value-added approach to diagnosis. Pediatr Radiol. 2018;48(5):735–44.
7. Sidhu PS. Clinical and imaging features of testicular torsion: role of ultrasound. Clin Radiol. 1999;54:343–52.

8. Martin AD, Rushton HG. The prevalence of bell clapper anomaly in the solitary testis in cases of prior perinatal torsion. J Urol. 2014;191(5S):1573–7.
9. Delaney LR, Karmazyn B. Ultrasound of the pediatric scrotum. Semin Ultrasound CT MRI. 2013;34(3):248–56.
10. Liang T, Metcalfe P, Sevcik W, Noga M. Retrospective review of diagnosis and treatment in children presenting to the pediatric department with acute scrotum. AJR Am J Roentgenol. 2013;200:W444–9.
11. Yang C, Song B, Liu X, Wei G-H, Lin T, He D-W. Acute scrotum in children: an 18-year retrospective study. Pediatr Emerg Care. 2011;27(4):270–4.
12. Altinkilic B, Pilatz A, Weidner W. Detection of Normal intratesticular perfusion using color coded duplex sonography obviates need for scrotal exploration in patients with suspected testicular torsion. J Urol. 2013;189(5):1853–8.
13. Baker LA, Sigman D, Mathews RI, Benson J, Docimo SG. An analysis of clinical outcomes using color Doppler testicular ultrasound for testicular torsion. Pediatrics. 2000;105(3):604.
14. Yusuf GT, Sidhu PS. A review of ultrasound imaging in scrotal emergencies. J Ultrasound. 2013;16:171–8.
15. Hosokawa T, Takahashi H, Tanami Y, Sato Y, Ishimaru T, Tanaka Y, et al. Diagnostic accuracy of ultrasound for the directionality of testicular rotation and the degree of spermatic cord twist in pediatric patients with testicular torsion. J Ultrasound Med. 2020;39(1):119–26.
16. Kitami M. Ultrasonography of pediatric urogenital emergencies: review of classic and new techniques. Ultrasonography. 2017;36(3):222–38.
17. Aziz ZA, Satchithananda K, Khan M, Sidhu PS. High-frequency color Doppler ultrasonography of the spermatic cord arteries: resistive index variation in a cohort of 51 healthy men. J Ultrasound Med. 2005;24:905–9.
18. Sellars MEK, Sidhu PS. Ultrasound appearances of the testicular appendages: pictorial review. Eur Radiol. 2003;13:127–35.
19. Bilagi P, Sriprasad S, Clarke JL, Sellars ME, Muir GH, Sidhu PS. Clinical and ultrasound features of segmental testicular infarction: six-year experience from a single centre. Eur Radiol. 2007;17:2810–8.
20. Atchley JTM, Dewbury KC. Ultrasound appearances of testicular epidermoid cysts. Clin Radiol. 2000;55:493–502.
21. Patel K, Sellars ME, Clarke JL, Sidhu PS. Features of testicular epidermoid cysts on contrast enhanced ultrasound and real time elastography. J Ultrasound Med. 2012;31:1115–22.
22. Bertolotto M, Derchi LE, Secil M, Dogra VS, Sidhu PS, Clements R, et al. Grayscale and color Doppler features of testicular lymphoma. J Ultrasound Med. 2015;34:1139–45.
23. Kachramanoglou C, Rafailidis V, Philippidou M, Bertolotto M, Huang DY, Deganello A, et al. Multiparametric sonography of hematologic malignancies of the testis: grayscale, color Doppler, and contrast-enhanced ultrasound and strain elastographic appearances with histologic correlation. J Ultrasound Med. 2017;36:409–20.
24. AIUM. Practice parameter for the performance of contrast-enhanced ultrasound examinations. J Ultrasound Med. 2020;39(3):421–9.
25. Knieling F, Strobel D, Rompel O, Zapeke M, Menendez-Castro C, Wolfel M, et al. Spectrum, applicability and diagnostic capacity of contrast-enhanced ultrasound in pediatric patients and young adults after intravenous application—a retrospective trial. Ultraschall Med. 2016;37:1–8.
26. Riccabona M, Lobo ML, Augdal TA, Avni F, Blickman J, Bruno C, et al. European Society of Paediatric Radiology Abdominal Imaging Task Force recommendations in paediatric uroradiology, part X: how to perform paediatric gastrointestinal ultrasonography, use gadolinium as a contrast agent in children, follow up paediatric testicular microlithiasis, and an update on paediatric contrast-enhanced ultrasound. Pediatr Radiol. 2018;48(10):1528–36.
27. Rafailidis V, Arvaniti M, Rafailidis D, Sfoungaris D. Multiparametric ultrasound findings in a patient with polyorchidism. Ultrasound. 2017;25(3):177–81.
28. Yusuf T, Sellars ME, Kooiman GG, Diaz-Cano S, Sidhu PS. Global testicular infarction in the presence of epididymitis. Clinical features, appearances on grayscale, color Doppler, and contrast-enhanced sonography, and histologic correlation. J Ultrasound Med. 2013;32:175–80.
29. Moschouris H, Stamatiou K, Lampropoulou E, Kalikis D, Matsaidonis D. Imaging of the acute scrotum; is there a place for contrast-enhanced ultrasonography? Int Braz J Urol. 2009;35:702–5.
30. Bertolotto M, Derchi LE, Sidhu PS, Serafini G, Valentino M, Grenier N, et al. Acute segmental testicular infarction at contrast-enhanced ultrasound: early features and changes during follow-up. AJR Am J Roentgenol. 2011;196:834–41.
31. Lung PF, Jaffer OS, Sellars ME, Sriprasad S, Kooiman GG, Sidhu PS. Contrast enhanced ultrasound (CEUS) in the evaluation of focal testicular complications secondary to epidiymitis. AJR Am J Roentgenol. 2012;199:W345–54.
32. Sriprasad SI, Kooiman GG, Muir GH, Sidhu PS. Acute segmental testicular infarction: differentiation from tumour using high frequency colour Doppler ultrasound. Br J Radiol. 2001;74:965–7.
33. Valentino M, Bertolotto M, Derchi L, Bertaccini A, Pavlica P, Martorana G, et al. Role of contrast enhanced ultrasound in acute scrotal diseases. Eur Radiol. 2011;21:1831–40.
34. Paltiel HJ, Kalish LA, Susaeta RA, Frauscher F, O'Kane PL, Freitas-Filho LG. Pulse-inversion US

imaging of testicular ischemia: quantitative and qualitative analyses in a rabbit model. Radiology. 2006;239:718–29.
35. Rafailidis V, Robbie H, Konstantatou E, Huang DY, Deganello A, Sellars ME, et al. Sonographic imaging of extra-testicular focal lesions: comparison of grey-scale, colour Doppler and contrast-enhanced ultrasound. Ultrasound. 2016;24:23–33.
36. Hedayati V, Sellars ME, Sharma DM, Sidhu PS. Contrast-enhanced ultrasound in testicular trauma: role in directing exploration, debridement and organ salvage. Br J Radiol. 2012;85:e65–8.
37. Yusuf GT, Konstantatou E, Sellars ME, Huang DY, Sidhu PS. Multiparametric sonography of testicular hematomas. Features on grayscale, color Doppler, and contrast-enhanced sonography and strain elastography. J Ultrasound Med. 2015;34:1319–28.
38. Lock G, Schmidt C, Helmich F, Stolle E, Dieckmann K. Early experience with contrast enhanced ultrasound in the diagnosis of testicular masses; a feasibility study. Urology. 2011;77:1049–53.
39. Huang DY, Sidhu PS. Focal testicular lesions: colour Doppler ultrasound, contrast-enhanced ultrasound and tissue elastography as adjuvants to the diagnosis. Br J Radiol. 2012;85:S41–53.
40. Isidori AM, Pozza C, Gianfrilli D, Glannetta E, Lemma A, Pofi R, et al. Differential diagnosis of non-palpable testicular lesions: qualitative and quantitative contrast-enhanced US of benign and malignant testicular tumors. Radiology. 2014;273:606–18.

Contrast-Enhanced Ultrasound in Childhood Pneumonia

16

Vasileios Rafailidis, Annamaria Deganello, Maria E. Sellars, and Paul S. Sidhu

16.1 Introduction

Community-acquired pneumonia (CAP) is a frequent cause of hospitalization, commonly caused by *Staphylococcus aureus*, and normally successfully managed with conservative treatment. In severe cases, CAP may be complicated by necrotizing pneumonia (NP) and abscess formation and parapneumonic effusions can arise, either a simple pleural effusion or an empyema [1]. Imaging plays a central role in the investigation of CAP and is typically based on chest X-rays and ultrasound (US). Both techniques have the potential to assess the lung parenchyma and pleural space, offering information and guiding treatment.

Computed tomography (CT) can also be used to evaluate chest pathology, although ionizing radiation exposure in the pediatric population should be limited. Brenner et al. indicated that CT examinations performed during childhood result in a tenfold increase in the estimated risk for radiation-induced fatal cancer, as compared with adult patients [2]. The life-time increase in cancer mortality risk associated with a CT examination performed in a 1-year old child is 0.18% for abdominal CT and 0.07% for head CT. For the United States, it was calculated that of about 600,000 children younger than 15 years undergoing abdominal and head CT examinations annually, 500 of these could eventually die from cancer attributable to CT radiation [2]. Another recent study has shown increased rates of leukemia and brain cancer following pediatric CT imaging, with the risk of leukemia being three times higher for cumulative absorbed organ doses of approximately 50 mGy as compared to the risk associated with doses below 0.5 mGy [3]. With this risk information, a CT examination should be avoided for the evaluation of pediatric complicated pneumonia, while other modalities should be evaluated and adopted [4].

Contrast-enhanced ultrasound (CEUS) using ultrasound contrast agents (UCA) offers improved sensitivity to vascularity and excellent differentiation between vascularized and non-vascularized tissue. Although widely performed in adults, the intravenous administration of UCA in children remains off-label, with the exception of intravenous administration for pediatric liver applications in the United States, approved by the Food and Drug Administration. The use of UCA in children is equally safe as in adults, with only few adverse reactions being reported either with intravenous or intracavitary administration [5–7]. As a consequence, CEUS could be used as an additional modality in an attempt to reduce the

V. Rafailidis (✉) · A. Deganello · M. E. Sellars
P. S. Sidhu
Department of Radiology, King's College Hospital, London, UK
e-mail: v.rafailidis@nhs.net; adeganello@nhs.net; maria.sellars@nhs.net; paulsidhu@nhs.net

P. S. Sidhu et al. (eds.), *Contrast-Enhanced Ultrasound in Pediatric Imaging*,
https://doi.org/10.1007/978-3-030-49691-3_16

use of CT in children, not only in abdominal applications but in childhood pneumonia as well. The purpose of this chapter is to present the potential applications of CEUS in complicated childhood pneumonia.

16.2 Clinical Aspects and Definitions of Childhood Pneumonia and Complications

Childhood pneumonia may be complicated by NP and abscess formation with a parapneumonic effusion or a pleural effusion developing as a consequence. Pneumonia in children has a reported rate of 30–40 per 100,000 children [8]. Empyema and parapneumonic effusions have an incidence of 3.3 per 100,000 children, affecting more frequently boys, infants, and younger children and occurring usually during winter and spring [9]. An increase in the incidence of empyema has been noted, up to 7 per 100,000 for children younger than 2 years of age and 10.3 per 100,000 in the age group between 2 and 4 years of age [8].

Pleural effusions affecting previously healthy children are usually caused by acute bacterial pneumonia, rather than chronic infections (e.g., pulmonary tuberculosis). The frequency of parapneumonic effusions complicating pneumonia is reported to be 1%, although in adults this may be as high as 40%. This may be an underestimation since small pleural effusions may go undiagnosed [9]. Causative microorganisms of pleural collections include bacteria such as *Streptococcus pneumoniae*, *S. aureus*, *Streptococcus pyogenes*, *Haemophilus influenza*, *Pseudomonas aeruginosa*, and *Klebsiella pneumoniae*. The widespread use of antibiotics has caused the emergence of resistant types like methicillin-resistant *S. aureus*. Other categories of causative organisms include *Mycoplasma pneumonia*, *Legionella pneumophila,* and viruses such as influenza or adenovirus. A virus may not be directly associated with a pleural effusion but rather precede a bacterial infection [8, 9]. In terms of clinical presentations, children suffering from pneumonia present with classic symptoms like cough, fever, dyspnoea, poor appetite, and malaise. If the pneumonia is complicated by a parapneumonic effusion, the symptoms are more pronounced and may be associated with pleuritic chest pain. In the presence of a pleural effusion, clinical examination will reveal reduced or absent breath sounds, dullness on percussion, and scoliosis. In a child already diagnosed with pneumonia, the formation of a parapneumonic effusion may become clinically evident with lack of response to appropriate treatment [8, 9].

A *pleural effusion* refers to the presence of fluid within the pleural cavity while the term *parapneumonic* effusion describes a pleural effusion associated with an underlying lung consolidation. The term *loculation* describes a pleural collection contained by fibrinous pleural adhesions and not freely moving within the pleural space with changes in body posture [10]. A pleural collection containing pus is termed an *empyema.* In essence, infection of the pleural cavity constitutes a continuum of different entities that need to be clearly discriminated [8–10]:

1. An *exudative* collection (or exudate) is a collection of clear fluid containing a limited number of white blood cells, occurring as a reaction to an underlying pneumonia. This type of collection can be referred to also as *simple parapneumonic effusion.*
2. A *fibro-purulent* collection follows the formation of exudate and is characterized by the deposition of fibrin within the pleural cavity, formation of septations with loculations, and an increased number of white blood cells. The term *complicated parapneumonic effusion* can be used as a synonym to fibro-purulent collection while *empyema* describes a collection of overt pus. In some cases, fibrous septations will prevent free movement of fluid within the entire extent of the collection.
3. *Organizational* phase or organized collection is a collection where the previously thin intrapleural membranes become thick and nonelastic. Due to the loss of elasticity, these septations hinder the re-expansion of a compressed lung (the so-called trapped lung). This situation predisposes to the formation of a chronic empyema.

Even more severe infections can be complicated by a broncho-pleural fistula, lung abscess formation or perforation of pus through the thoracic wall, and formation of an empyema, although these conditions are uncommon in the pediatric population [9]. Conservative management including intravenous antibiotics and simple catheter drainage for an effusion, when large enough to compromise respiratory function, will suffice. The subcostal catheter drain should be routinely checked for patency, with removal on resolution of symptoms. The use of intra-pleural fibrinolytics (e.g., urokinase) can shorten the duration of hospital stay and are suggested in complicated parapneumonic effusion (containing loculations) or empyema (collection of pus). If a chest catheter drain, antibiotics, and fibrinolytics fail to resolve the collection, thoracotomy and decortication may be required. A lung abscess coexisting with empyema may not normally be surgically drained [9]. Surgical treatment options should be carefully selected based on clinical and imaging findings as they are associated with increased hospitalization [11]. The characteristics of pleural effusion on US can be used to guide catheter placement with better success in simple anechoic effusions compared to complicated septated effusions [12].

16.3 Imaging of Childhood Pneumonia with US and CT

According to the British Thoracic Society guidelines for management of pediatric pleural infection, a chest X-ray needs to be taken, but no role is recognized for a routine lateral chest X-ray. Classic findings of a pleural effusion include obliteration of the costophrenic angle, a meniscus sign formed by the rim of fluid or diffuse and homogeneous opacification of the hemi-thorax if the X-ray was taken in the supine position. In this latter case of complete opacification of the hemithorax, it is difficult to differentiate pleural collection from underlying consolidation and atelectasis, raising the need for US (Fig. 16.1) [8–10].

An *uncomplicated pneumonia* can be visualized on US as an area of lung parenchyma exhibiting echotexture similar to that of the liver. The bronchial tree can be visualized as linear branching echogenic structures if filled with air (US air bronchogram), or anechoic when filled with fluid or mucus. The use of color Doppler US is crucial for differentiating blood vessels from fluid-filled bronchi and document the vascularization of consolidated parenchyma. The branching pattern of blood vessels visualized within the consolidated lung parenchyma has been referred to as "vascular bronchogram." *Necrotizing pneumonia*, seen as areas of necrosis, can be visualized with conventional US as hypoechoic areas situated within the consolidated parenchyma [13, 14]. According to a meta-analysis, lung US can diagnose childhood pneumonia with a sensitivity of 96% and a specificity of 93% [15]. In a different study assessing the ability of point-of-care US performed by clinicians after 1 h of focused training, it was concluded that US has 86% sensitivity and 89% specificity for diagnosing pneumonia in children and young adults [16]. In a large retrospective analysis of 236 children with CAP examined with US, it was concluded that the degree of impaired perfusion of the lung parenchyma and the occurrence of hypoechoic areas, important features of NP, were similar to CT with high correlation between the two modalities and good diagnostic accuracy for US. Perfusion defects and hypoechoic areas found in US have been associated with a higher risk of pneumatocele formation, longer hospital stay, and higher risk for subsequent need for surgical treatment [1].

It is important to carefully assess the vascularity of the consolidated lung parenchyma, which can be subjectively classified into three categories:

1. Normal perfusion corresponding to homogeneously distributed blood vessels with a branching tree-like pattern.
2. Decreased perfusion with a 50% reduction of the area vascularized with the normal tree-like pattern.
3. Poor perfusion indicating no recognizable color Doppler US blood flow signals within the consolidation [1].

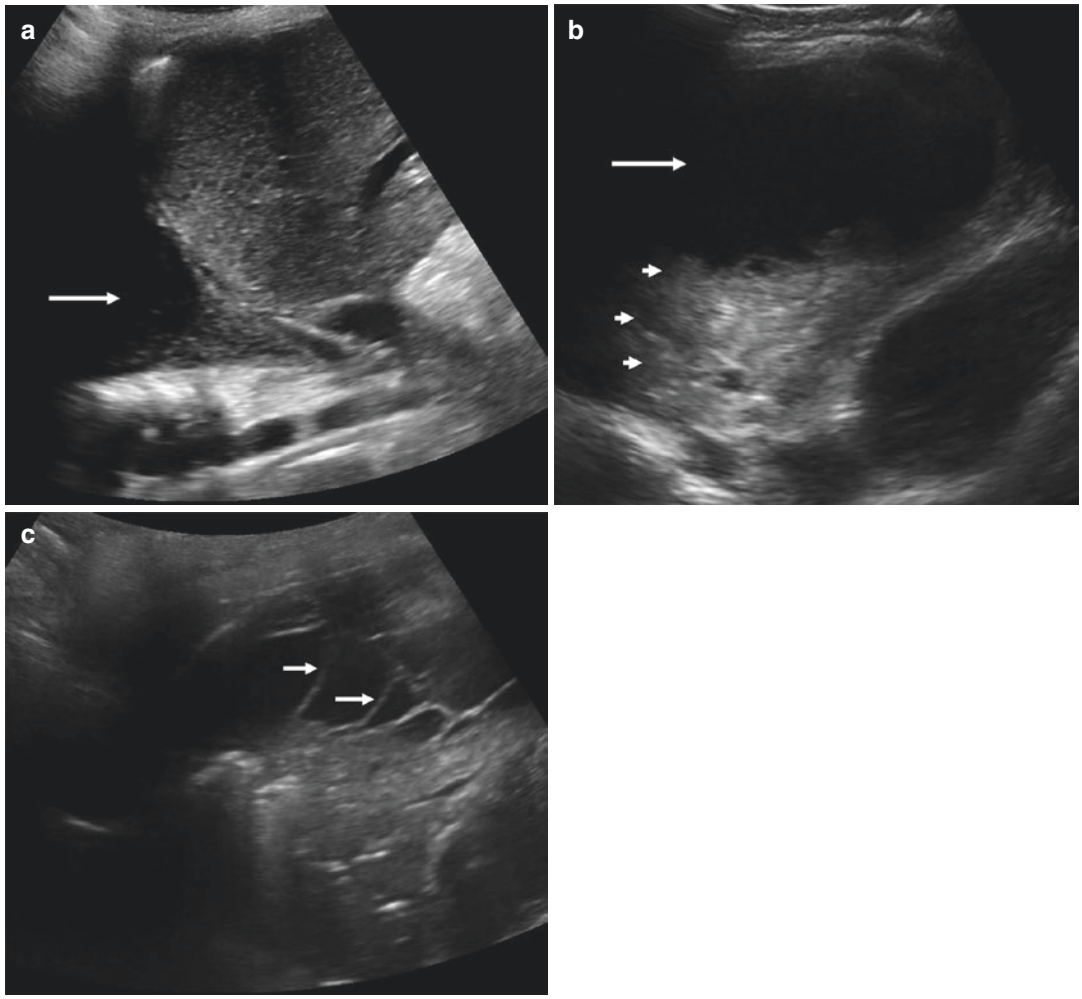

Fig. 16.1 Examples of pleural effusion on conventional B-mode ultrasound. (**a**) A small pleural effusion occupying the costophrenic angle and containing some echogenic debris (arrow). (**b**) A larger anechoic effusion (arrow) extending in the cephalic direction and associated with an area of consolidation (arrowheads). (**c**) A case of parapneumonic effusion containing echogenic septations (arrows)

In a study of 23 children with NP, the finding of peripheral hypoechoic areas within the consolidated lung parenchyma demonstrated a 35% sensitivity, 100% specificity, and 100% positive predictive value, while pneumothorax was more commonly found in these children [17]. Based on these measures of diagnostic accuracy, US with color Doppler US can readily establish the diagnosis of NP if hypoechoic areas are present but cannot exclude this diagnosis if absent.

Ultrasound is indicated for confirmation of a *pleural fluid collection* and guidance of catheter placement, and is able to differentiate parenchymal from pleural abnormalities, outperforming a chest X-ray [8, 9, 18]. Ultrasound evaluation of parapneumonic effusion:

1. determines the size of effusion
2. classifies the collection as free or loculated
3. characterizes the echogenicity of the fluid

Ultrasound is very sensitive in detecting even small pleural fluid collections as little as 3–5 mL. Although US cannot unequivocally determine the stage of pleural effusion, it does provide information about the nature of the fluid [9, 13,

19]. The fluid may be a simple pleural effusion (or transudate) which appears as a homogeneously anechoic or hypoechoic, freely mobile, changing shape with respiration or change in body position. Any type of proteinaceous content within a collection, including blood (hemothorax) or inflammatory debris in exudates, can be visualized as echogenic debris. Complicated fluid collections may appear multi-loculated, containing internal septations, an appearance termed "honeycomb" and are virtually always representing an exudate. However an anechoic pleural effusion could either be a transudate or an exudate, as US cannot always unequivocally determine the nature of a collection [19]. Studies have shown that US is superior to CT imaging for demonstration of internal debris or loculations within parapneumonic effusions [10, 20]. Ultrasound can quantify a pleural effusion by measuring the thickness of fluid content at the costophrenic angle in the posterior sub-axillary area, with the child lying in the supine position. Although subjective, the quantity of a pleural effusion may be characterized as minimal if <1 cm thick, moderate if 1–2 cm thick, and large if >2 cm thick [1]. Depending on the nature of the collection, appropriate treatment including thoracoscopy or drainage placement can be selected for initial treatment. Ultrasound is equally suitable for follow-up of a pleural collection in order to monitor absorption or resolution of septations, confirming the success of management or suggesting the need for further treatment [13].

A chest CT examination should be reserved only for problematic cases or pre-operative planning [8, 21], despite CT imaging offering more diagnostic information than a chest X-ray, including detection of abscess and NP. However, CT imaging does not alter management or predict length of hospital stay [21]. Contrast-enhanced CT is thought to be essential for differentiation of parenchymal and pleural disease, potentially identifying effusion loculation and thickening of the pleura [20]. On a CT examination, NP presents as an area of consolidated lung parenchyma with no volume loss (excluding atelectasis) in combination with a centrally located non-enhancing hypodense area. A subjective estimation of NP severity can be calculated from the relative area of necrotic consolidation. Mild necrosis affects <30% of the consolidated lung, moderate between 30% and 80% and massive if >80% being necrotic [1]. The CT findings of empyema include pleural enhancement and thickening, chest wall edema, and increased density of adjacent extra-thoracic fat [10, 22]. A study assessing the value of CT for diagnosing empyema in children has indicated that none of these findings can accurately differentiate transudates from an empyema, stressing the superiority of US for this purpose [22].

Pneumatoceles can be detected on CT as air-containing cysts with sharply demarcated thin walls, occurring during pneumonia resolution, while bronchopleural fistula can be suspected based on the occurrence of pneumothorax or persistent air leakage from chest tubes [1]. A CT examination may be used to differentiate an intrapulmonary abscess from an empyema: clinically significant as an abscess should be treated medically (catheter drainage would entail the risk of forming a bronchopleural fistula). On CT, an abscess will appear thick-walled and forming acute angle with the chest wall, whereas an empyema may demonstrate the split pleura sign (with pleural enhancement) and compression of the adjacent lung parenchyma [10].

16.4 Contrast-Enhanced Ultrasound in Childhood Pneumonia

There is limited evidence for the use of thoracic CEUS [23–33], particularly in the pediatric age group [27, 32, 33]. The CEUS examination for thoracic pathology, both in adults and children remains off-label. Nonetheless, there are potential applications in the field of childhood pneumonia. As with conventional US techniques, sound absorption from air in lung parenchyma and sound reflection by the ribs may prevent adequate imaging.

A lung US examination for a pleural-based lesion can be performed using a linear high-frequency (9–17 MHz) transducer with a supra-

clavicular, suprasternal, intercostal, or transdiaphragmatic–transabdominal approach, depending on the position of the lesion under examination. A CEUS examination using a high-frequency transducer would be limited for technical reasons, surrounding the physics of the microbubble interaction with high-frequency US waves. When an effusion is present in the costophrenic angle, then a lower frequency curvilinear transducer can be used and will readily image the underlying consolidated lung [13].

The UCA dose suggested for intravenous administration is similar to any other pediatric intravenous application (e.g., liver) and varies according to age, but would apply only when using a lower frequency transducer; higher doses are required with the linear higher frequency transducers. The UCA can be administered via a 20-gauge cannula inserted into an antecubital fossa vein and then flushed with 10 mL of 0.9% normal saline. For the intracavitary application of CEUS, where the UCA is administered via the catheter into the pleural space, a single drop of SonoVue™ (Bracco SpA, Italy) can be diluted into 20–50 mL of 0.9% normal saline solution depending on the patient's body size and then administered via the catheter.

Lung lesions that have a vascular supply from the pulmonary arteries will enhance prior to the liver and spleen which are supplied by the systemic circulation, while lesions supplied by the bronchial or intercostal arteries will show enhancement simultaneously with the liver and spleen. The timing of enhancement is an important parameter for the CEUS examination of the lung, as well as the level and homogeneity of enhancement as compared to liver or spleen. More importantly, CEUS can readily and accurately differentiate vascularized from non-vascularized tissue. Consequently, pleural effusions exhibit no enhancement, regardless of any echogenic content. An area of uncomplicated compression atelectasis and pneumonia demonstrates homogeneous enhancement, predominantly from pulmonary arterial supply. A lung abscess should show hyper-enhancing walls but no internal contrast enhancement [23, 28, 30]. These lung abscess characteristics were confirmed in an experimental study in small animals, where CEUS was able to differentiate benign from malignant lesions based on the arrival time of the UCA [34].

16.4.1 Intravenous CEUS

The UCA can be administered intravenously for investigation of lung tissue perfusion, or via a chest catheter to evaluate the pleural space. Intravenous CEUS can readily and accurately differentiate vascularized from ischemic tissue and delineate pleural effusions, while the intracavitary CEUS examination can detect loculations or free diffusion of a pleural collection. A decision to perform CEUS in a child with pneumonia should be made along with the pediatric physician, with clinical deterioration and suspicion of NP suggesting the need for intravenous CEUS, while malfunction of chest catheter indicating the need for intracavitary CEUS. This experience with both intravenous and intracavitary CEUS in children with complicated pneumonia has been summarized in a study of ten patients with age range from 1 to 12 years [33]. No adverse reactions were observed, with no sedation required, and the CEUS procedure was well-tolerated.

The US examination with color Doppler is detailed for the diagnosis of NP but lacks sensitivity, potentially missing this clinically important diagnosis [17]. Using CEUS increases the ability to depict tissue perfusion with confidence. Intravenous CEUS identifies NP based on the presence of non-enhancing areas within the consolidated lung parenchyma, where conventional US techniques are inconclusive (Figs. 16.2, 16.3, 16.4, and 16.5). Moreover, intravenously administered UCA helps to exclude any residual empyema. Intracavitary CEUS was performed where the tip of the chest drainage could not be detected with conventional US, detecting loculation of the fluid around the drain tip, with clinical deterioration and complete lung opacification on chest radiography. Urokinase administration via the

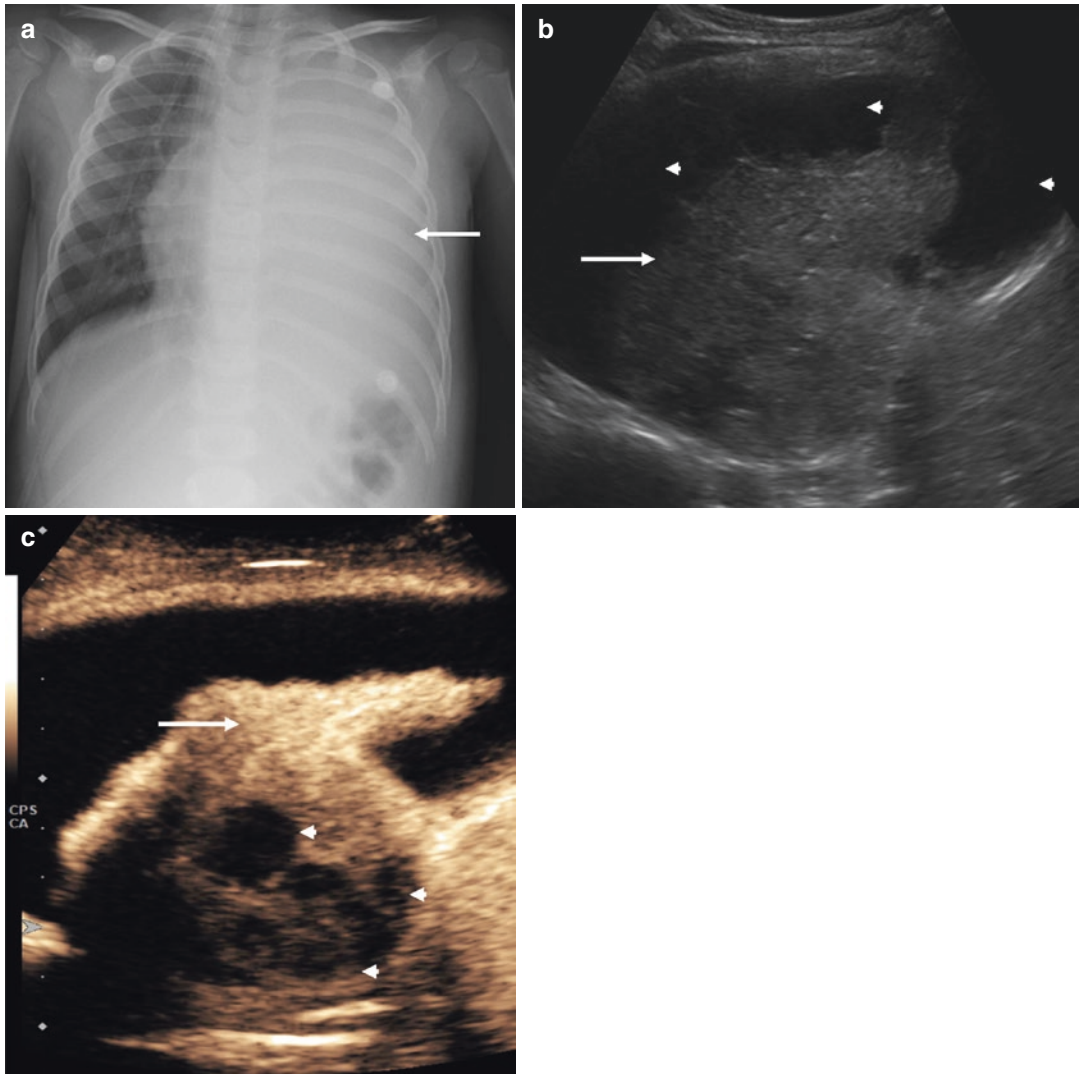

Fig. 16.2 A 4-year-old girl with complicated pneumonia. (**a**) Chest X-ray shows the classic "complete white out" (arrow) appearance of the left hemithorax, where consolidation and pleural effusion cannot be readily differentiated. (**b**) B-mode ultrasound shows the consolidated lung parenchyma (arrow) and the anechoic parapneumonic effusion (arrowheads). (**c**) The CEUS examination shows the enhancement of consolidated lung (arrow), delineated the effusion as anechoic but importantly an area of internal absence of enhancement within the consolidation is present, suggesting there is necrotizing pneumonia or abscess formation (arrowheads)

catheter and follow-up intracavitary CEUS, the UCA demonstrated disappearance of loculation, with free flow of the UCA within the cavity.

A CEUS examination outperformed conventional US for the clear demarcation of the lung border and diagnosis of NP, while CEUS offered improved diagnostic confidence for this diagnosis [33]. CEUS can also differentiate NP from a pleural effusion with better delineation of collection borders and lung parenchyma blood vessels, helping avoid catheter placement within a necrotic part of the lung parenchyma, avoiding a complicating bronchopleural fistula (Figs. 16.6 and 16.7). The potential applications of CEUS in childhood pneumonia are summarized in Table 16.1.

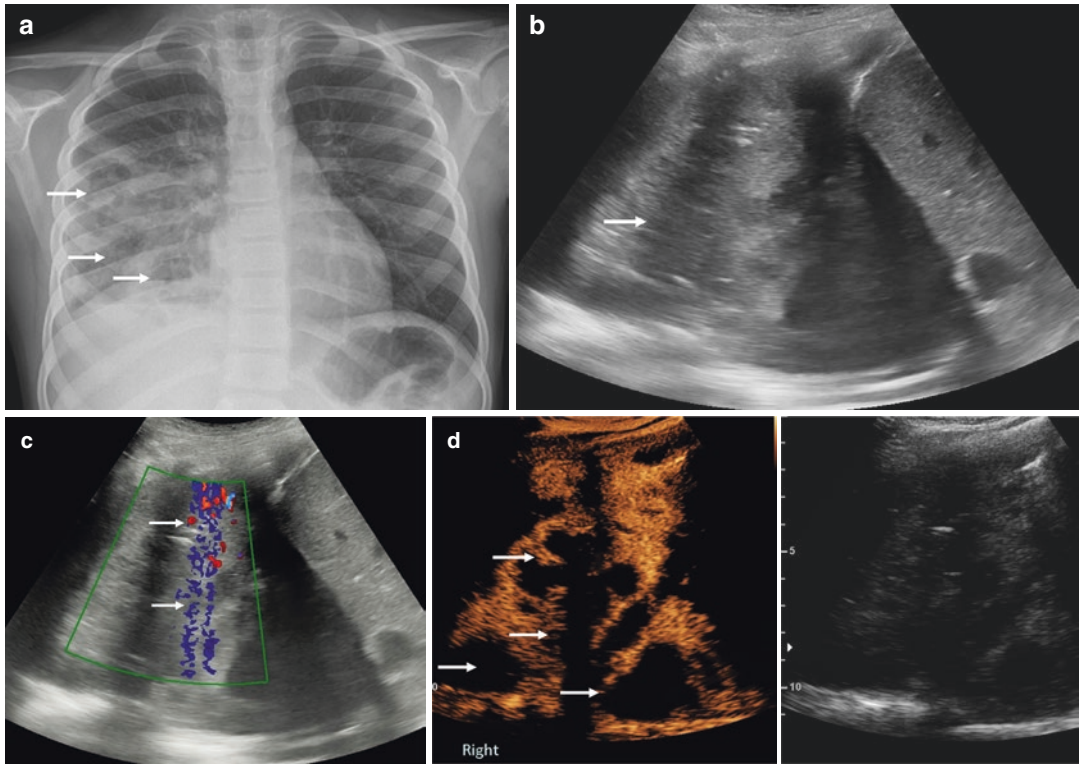

Fig. 16.3 A 8-year-old boy with necrotizing pneumonia. (**a**) The chest X-ray shows effusion with underlying airspace disease containing some gas locules, suggesting necrosis (arrows). (**b**) A B-mode ultrasound shows the echogenic consolidation of the lung parenchyma (arrow). (**c**) The color Doppler ultrasound fails to assess vascularity as image quality was degraded by movement artifact (arrows). (**d**) The CEUS examination (dual screen) shows enhancement of the consolidated parenchyma but an internal area of lack of enhancement, in keeping with necrotizing pneumonia (arrows)

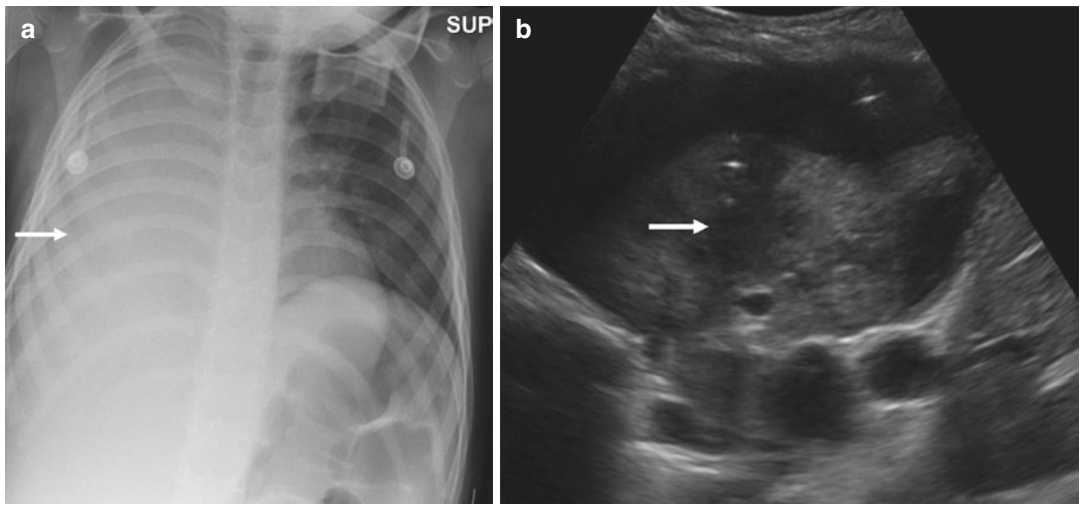

Fig. 16.4 A 3-year-old girl with necrotizing pneumonia and parapneumonic effusion. (**a**) A chest X-ray shows again the "complete white-out" appearance of the right hemi-thorax (arrow). (**b**) A B-mode ultrasound shows the anechoic effusion and the consolidated lung parenchyma with some heterogeneity including hypoechoic areas (arrow), raising suspicion of necrosis. (**c**) The CEUS examination confidently shows the lack of enhancement in areas of necrosis, diagnosing necrotizing pneumonia, extending close to the lung surface. Note that the effusion appears completely anechoic

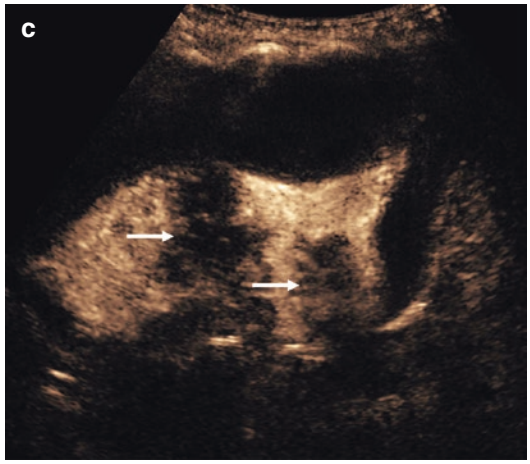

Fig. 16.4 (continued)

Further applications of lung CEUS, based on adult studies, have potential use in differentiating neoplastic from non-neoplastic pleuro-pulmonary lesions, with a delayed lesion enhancement or a high imaging-based score suggesting a neoplastic abnormality [23]. In the investigation of atelectasis, CEUS has shown the different perfusion characteristics demonstrated by obstructive atelectasis and compression atelectasis, with the former exhibiting a delayed time to enhancement [25]. In the investigation of alveolar pneumonia, using CEUS, the majority exhibited pulmonary arterial enhancement and a homogeneously isoechoic level of enhancement, as compared

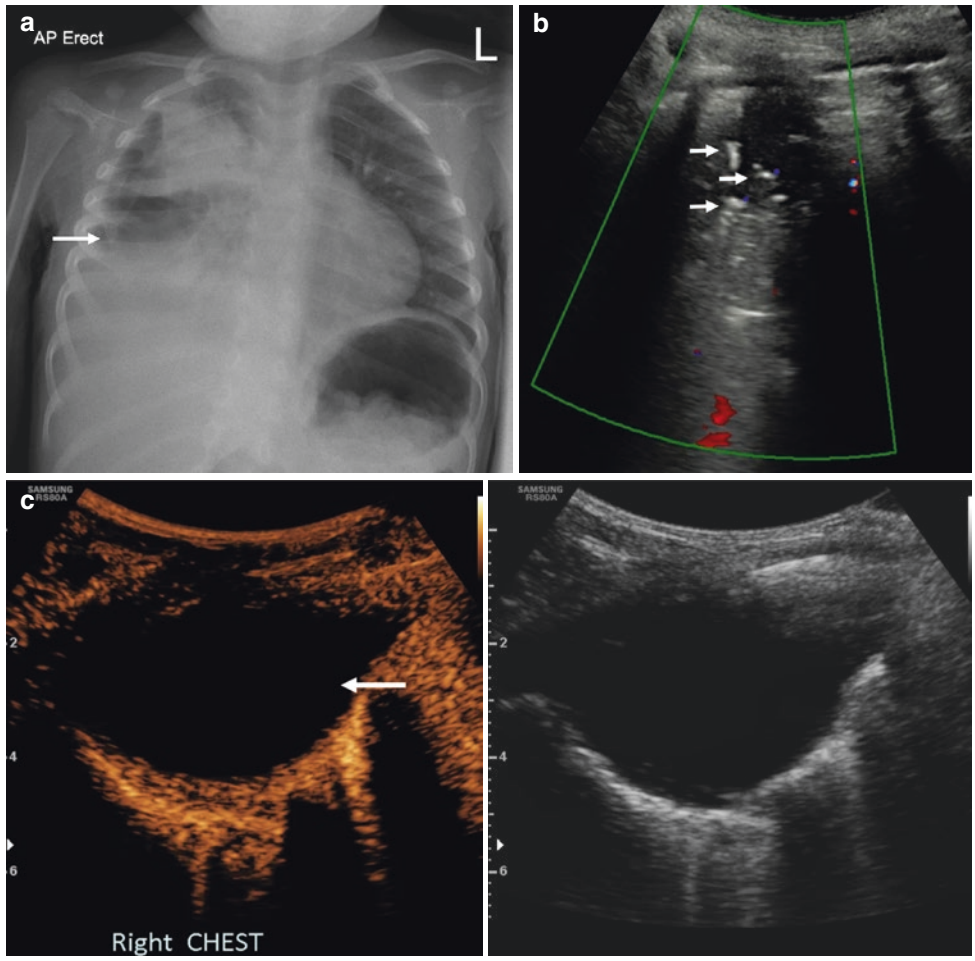

Fig. 16.5 A 3-year-old boy with a lung abscess. (**a**) The chest X-ray shows the extensive consolidation of the right lung with an air–fluid level of a lung abscess (arrow). (**b**) The color Doppler ultrasound shows no vascularity within the consolidated lung, while bright echogenic reflections with reverberation artifact likely represent gas bubbles (arrows). (**c**) The CEUS examination shows peripheral lung enhancement surrounding an anechoic abscess (arrow)

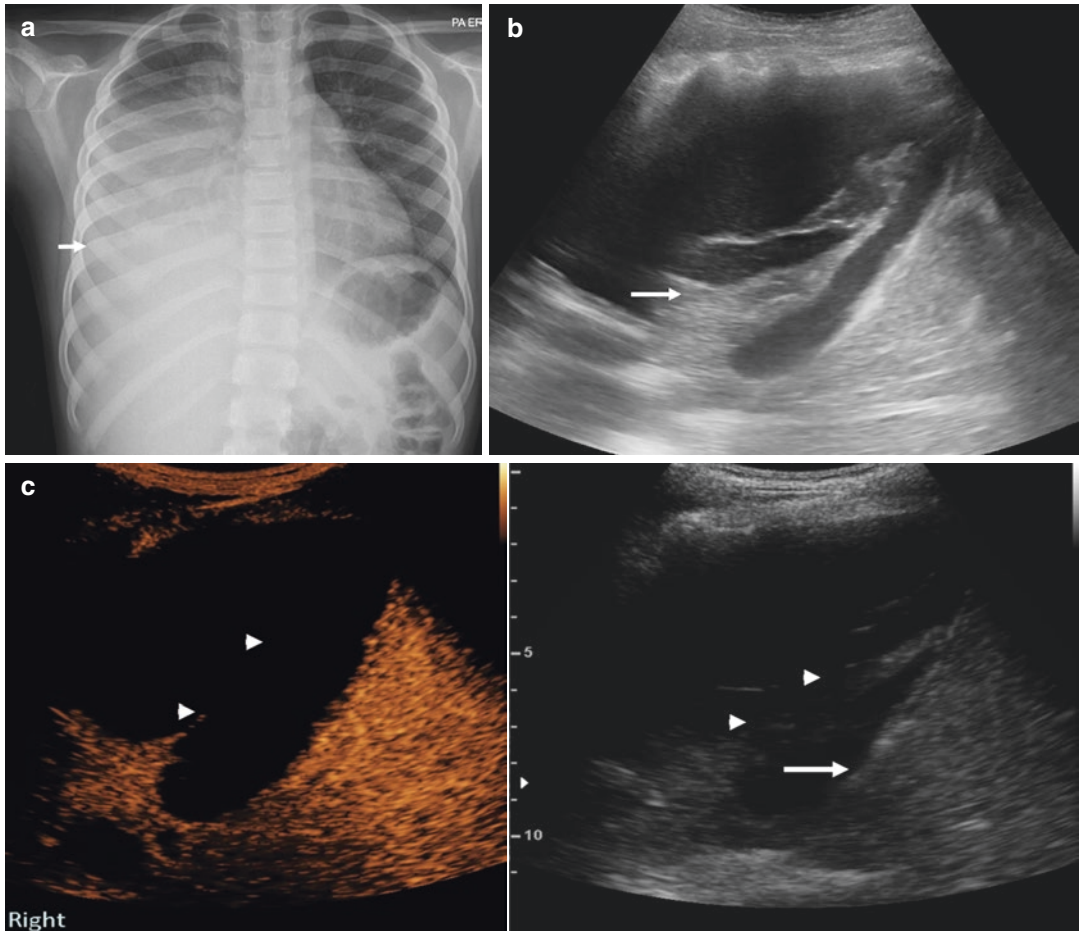

Fig. 16.6 An 8-year-old girl with complicated community-acquired pneumonia. (**a**) Chest X-ray shows opacification of the right middle and lower lung field suggesting there is a pleural effusion (arrow). (**b**) The B-mode ultrasound of the costophrenic angle shows anechoic fluid with some echogenic septations (arrow) and atelectasis of the lung parenchyma. (**c**) The CEUS examination is better at delineating the collection which appears anechoic, with no septal enhancement (arrowheads), as opposed to the collapsed parenchyma, showing homogeneous enhancement (arrow)

with the spleen as an "in vivo" reference. Findings such as bronchial artery supply, enhancement heterogeneity, or decreased level of enhancement did not show any prognostic value regarding length of hospitalization, comorbidity, complications, and the presence of pleural effusion [31].

Furthermore, CEUS has been used to investigate a wide variety of pleural-based lesions, including malignancy, pneumonia, pulmonary atelectasis, and compression atelectasis, using time to enhancement, extent and homogeneity of enhancement as indicators. Although some characteristic patterns were identified, CEUS was not able to accurately discriminate malignant from benign lesions. Compression atelectasis tended to show a short time to marked enhancement, while pulmonary embolism was characterized by delayed and reduced enhancement; no specific enhancement patterns were distinguished for malignant or benign lesions [26]. In a study of adult patients with pleural-based lesions, CAP and lung cancer did not differ in terms of time, duration, or washout of enhancement [29].

Despite the limited value in establishing a precise diagnosis, CEUS can still distinguish pulmonary arterial from bronchial arterial supply in a pleural-based lesion providing additional information [28]. For example, a case report describes

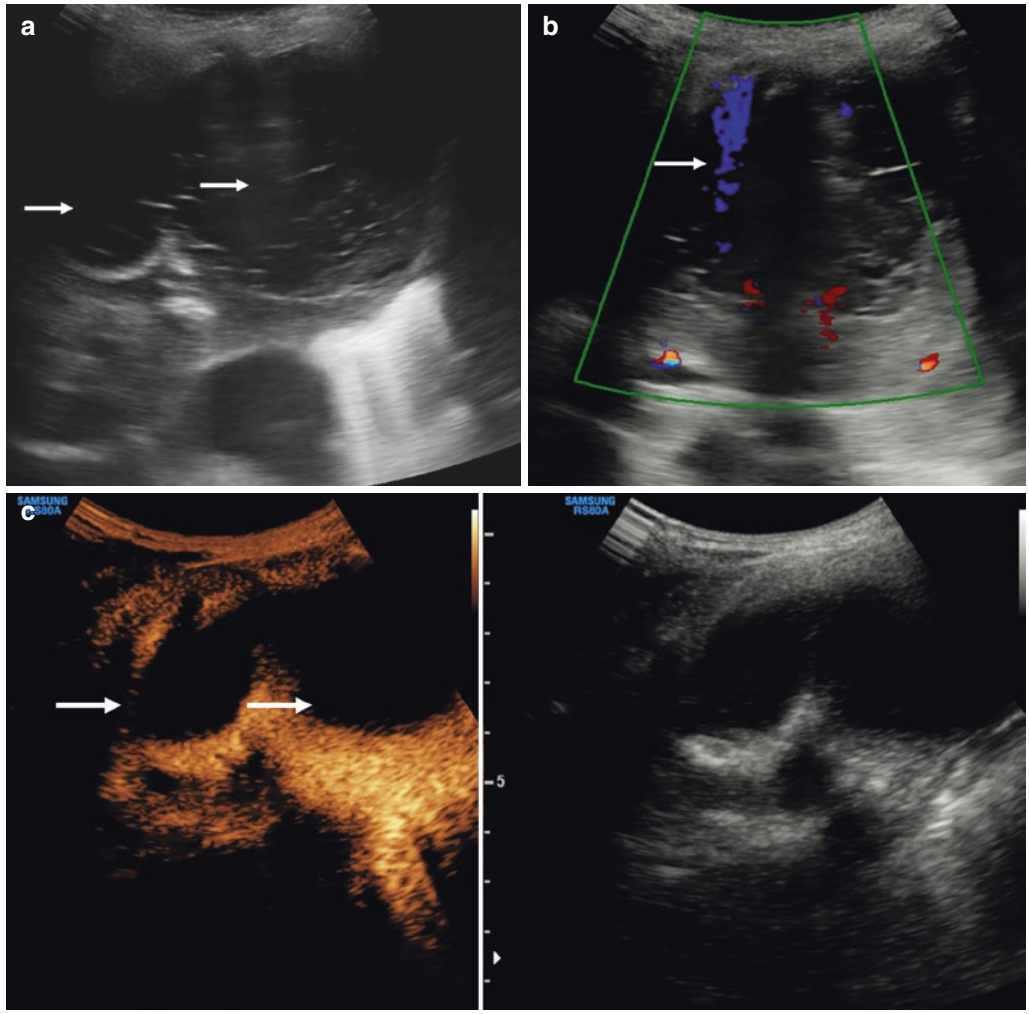

Fig. 16.7 A 3-year-old girl with pneumonia complicated with empyema. (**a**) The B-mode ultrasound shows a parapneumonic collection with two convexities (arrows) and internal echo reflections. (**b**) The color Doppler ultrasound shows no internal vascular flow signals, only artifact (arrow). (**c**) On the CEUS examination, a note is made of increased enhancement of the adjacent lung parenchyma but no enhancement within the parapneumonic collection, suggesting this was an empyema

Table 16.1 Potential contrast-enhanced ultrasound (CEUS) applications in childhood pneumonia

Intravenous	Intracavitary
• *Pneumonia vs. empyema*: Better delineation of pleural effusion borders and demonstration of necrotic lung and pleural effusion (either empyema or clear collection). • Identification of areas of *necrotizing pneumonia* as lack of enhancement within consolidation. • *Residual empyema vs. simple consolidated lung (post drainage)*: The enhancement pattern with blood vessels extending up to the periphery of the lung indicates absence of residual collection and thus safe drainage removal.	• Detection of *catheter position.* • Confirmation of *catheter patency.* • Quantitative information of *volume* of fluid effectively drained, possible *communication* of the collection with the surrounding structures (e.g., a fistula). • Demonstration of *loculations* formed by fibrous septa within a pleural effusion and hindering complete drainage of effusion. Instillation of fibrinolytics could be recommended. • *Post fibrinolytics*, the filling of a larger cavity with microbubbles can be demonstrated, thanks to the resolution of septations.

the use of CEUS in distinguishing active bleeding into the pleural cavity in a sub phrenic located hepatocellular carcinoma, undergoing radiofrequency ablation [24]. A further application is reported with a lung abscess, where CEUS a biopsy towards the necrotic interior part of the abscess and the hyper-vascularized rim [30].

16.4.2 Intracavitary CEUS

The intracavitary use of CEUS, as previously described for lung applications in children, is well described in a number of applications. This technique has the potential to evaluate the internal architecture of any physiological or non-physiological cavity, in a real-time manner, similar to the conventional fluoroscopy examination. Moreover, it also provides valuable information about the patency and location of any catheter into which the UCA is injected (Figs. 16.8 and 16.9). Potential fields of application in pediatrics include intra-abdominal fluid collections, the biliary tract, urinary tract, gastrointestinal applications, and vascular lines [35].

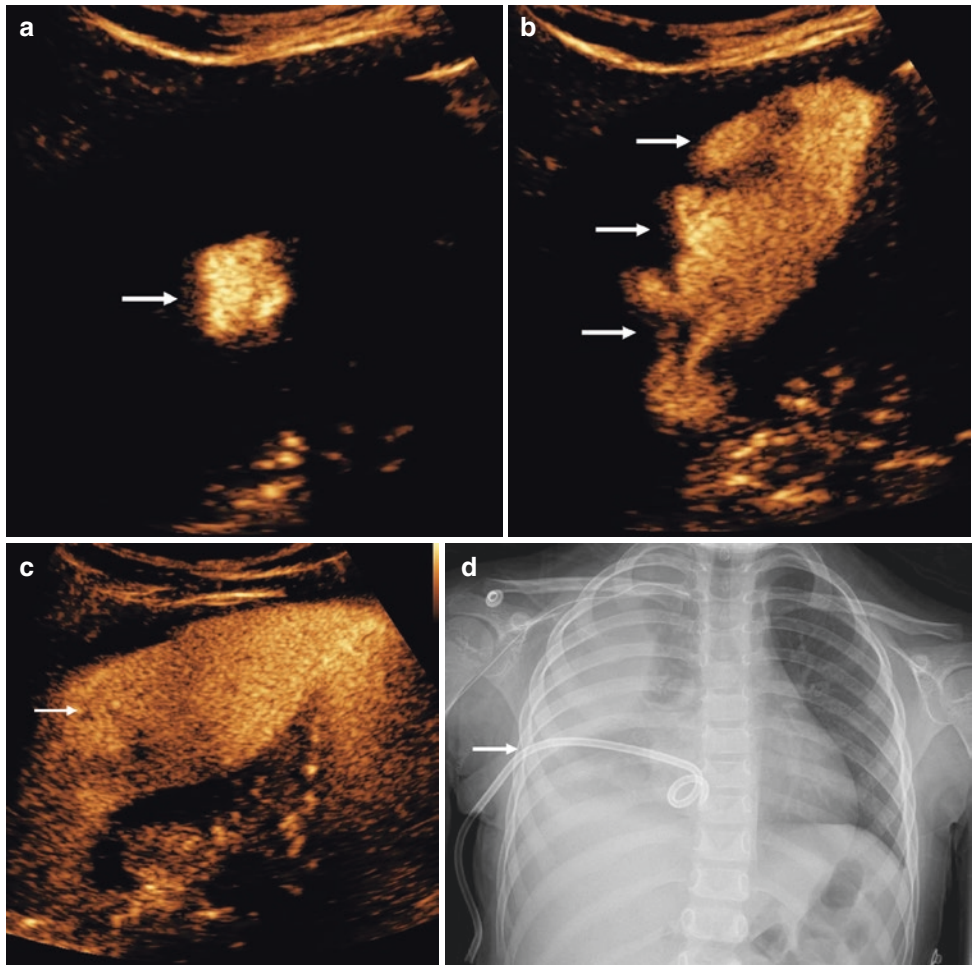

Fig. 16.8 A 4-year-old girl with parapneumonic effusion. (**a**) An intracavitary CEUS was performed for evaluation of catheter patency, location, and effusion internal architecture. Note the initial appearance of microbubbles, documenting the location of catheter tip inside the effusion (arrow). (**b**) A few seconds later, the microbubbles delineate the pleural space, showing there are no septations (arrows). (**c**) A further image shows the exact extent of effusion and the collapsed parenchyma (arrow). (**d**) A chest X-ray confirms the location of the catheter (arrow)

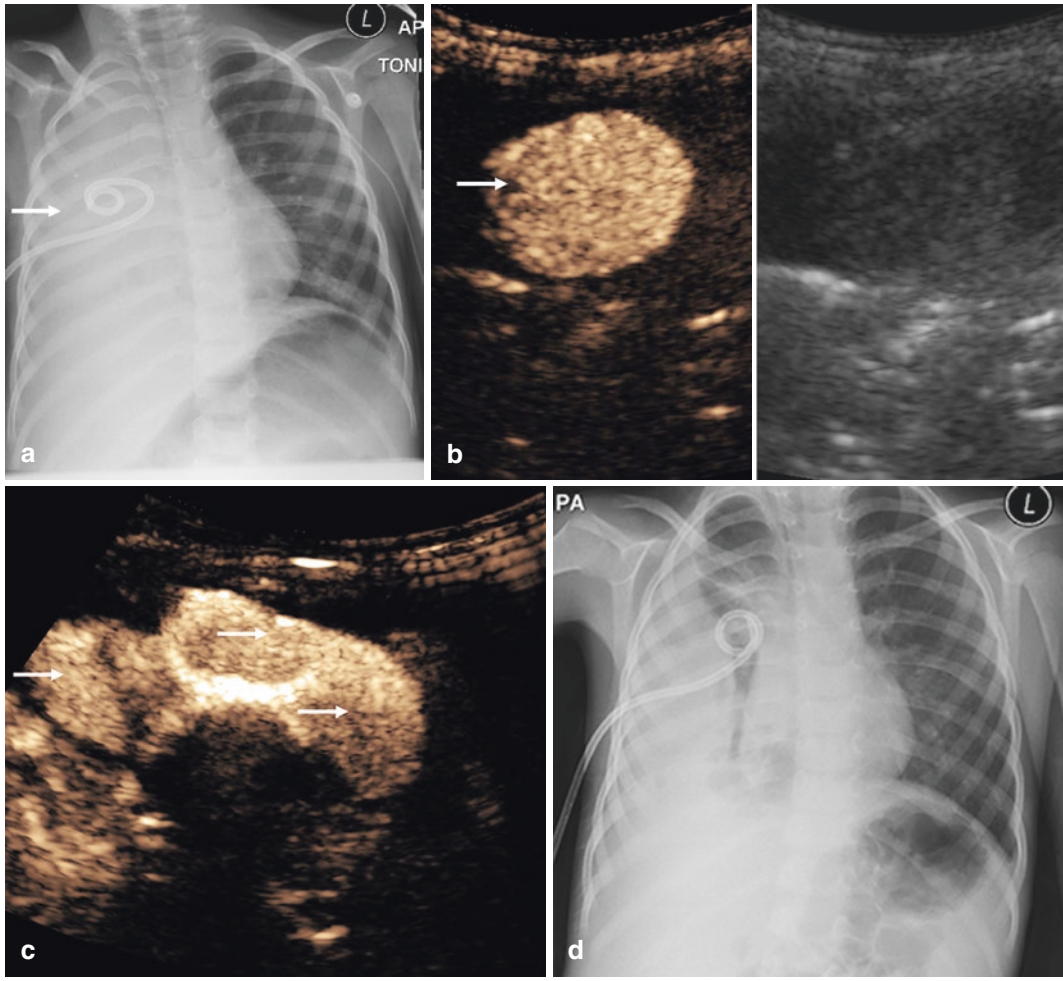

Fig. 16.9 A 3-year-old boy with parapneumonic empyema not resolving after chest drainage insertion. (**a**) A chest X-ray shows an adequately positioned catheter (arrow), which did not effectively drain the pleural effusion. (**b**) The intracavitary CEUS examination detected the tip of a catheter inside a loculation, delineated by a rounded collection of microbubbles (arrow). (**c**) Post fibrinolytics intracavitary insertion, an intracavitary CEUS was repeated, showing free movement of the microbubbles within the pleural cavity (arrows). (**d**) A chest X-ray acquired the following day shows the reduction of the pleural effusion which eventually completely resolved

16.5 Conclusion

The ability to add a CEUS examination to the imaging of a complicated pneumonia is useful for a number of reasons. The clear identification of the limits of underlying consolidated lung from an echogenic pleural effusion aids the confident placement of a drainage catheter, the delineation of necrotic lung aids management, the position of the catheter can be identified with an intracavitary injection. Most importantly, the ability to use a safe imaging technique that is child friendly and portable is an attractive option.

References

1. Lai SH, Wong KS, Liao SL. Value of lung ultrasonography in the diagnosis and outcome prediction of pediatric community-acquired pneumonia with necrotizing change. PLoS One. 2015;10(6):e0130082. https://doi.org/10.1371/journal.pone.0130082.
2. Brenner D, Elliston C, Hall E, Berdon W. Estimated risks of radiation-induced fatal cancer from pediatric CT. AJR Am J Roentgenol. 2001;176(2):289–96. https://doi.org/10.2214/ajr.176.2.1760289.
3. Pearce MS, Salotti JA, Little MP, McHugh K, Lee C, Kim KP, Howe NL, Ronckers CM, Rajaraman P, Sir Craft AW, Parker L, Berrington de González A. Radiation exposure from CT scans in childhood and subsequent risk of leukaemia and brain tumours: a retrospective cohort study. Lancet (London, England). 2012;380(9840):499–505. https://doi.org/10.1016/S0140-6736(12)60815-0.
4. Kutanzi KR, Lumen A, Koturbash I, Miousse IR. Pediatric exposures to ionizing radiation: carcinogenic considerations. Int J Environ Res Public Health. 2016;13(11):1057. https://doi.org/10.3390/ijerph13111057.
5. Rosado E, Riccabona M. Off-label use of ultrasound contrast agents for intravenous applications in children: analysis of the existing literature. J Ultrasound Med. 2016;35(3):487–96. https://doi.org/10.7863/ultra.15.02030.
6. Darge K, Papadopoulou F, Ntoulia A, Bulas DI, Coley BD, Fordham LA, Paltiel HJ, McCarville B, Volberg FM, Cosgrove DO, Goldberg BB, Wilson SR, Feinstein SB. Safety of contrast-enhanced ultrasound in children for non-cardiac applications: a review by the Society for Pediatric Radiology (SPR) and the International Contrast Ultrasound Society (ICUS). Pediatr Radiol. 2013;43(9):1063–73. https://doi.org/10.1007/s00247-013-2746-6.
7. Piskunowicz M, Kosiak W, Batko T, Piankowski A, Polczynska K, Adamkiewicz-Drozynska E. Safety of intravenous application of second-generation ultrasound contrast agent in children: prospective analysis. Ultrasound Med Biol. 2015;41(4):1095–9. https://doi.org/10.1016/j.ultrasmedbio.2014.11.003.
8. Islam S, Calkins CM, Goldin AB, Chen C, Downard CD, Huang EY, Cassidy L, Saito J, Blakely ML, Rangel SJ, Arca MJ, Abdullah F, St Peter SD. The diagnosis and management of empyema in children: a comprehensive review from the APSA Outcomes and Clinical Trials Committee. J Pediatr Surg. 2012;47(11):2101–10. https://doi.org/10.1016/j.jpedsurg.2012.07.047.
9. Balfour-Lynn IM, Abrahamson E, Cohen G, Hartley J, King S, Parikh D, Spencer D, Thomson AH, Urquhart D, Paediatric Pleural Diseases Subcommittee of the BTSSoCC. BTS guidelines for the management of pleural infection in children. Thorax. 2005;60(Suppl 1):i1–i21. https://doi.org/10.1136/thx.2004.030676.
10. Calder A, Owens CM. Imaging of parapneumonic pleural effusions and empyema in children. Pediatr Radiol. 2009;39(6):527–37. https://doi.org/10.1007/s00247-008-1133-1.
11. Gates RL, Hogan M, Weinstein S, Arca MJ. Drainage, fibrinolytics, or surgery: a comparison of treatment options in pediatric empyema. J Pediatr Surg. 2004;39(11):1638–42.
12. Chiu CY, Wong KS, Huang YC, Lai SH, Lin TY. Echo-guided management of complicated parapneumonic effusion in children. Pediatr Pulmonol. 2006;41(12):1226–32. https://doi.org/10.1002/ppul.20528.
13. Goh Y, Kapur J. Sonography of the pediatric chest. J Ultrasound Med. 2016;35(5):1067–80. https://doi.org/10.7863/ultra.15.06006.
14. Stadler JAM, Andronikou S, Zar HJ. Lung ultrasound for the diagnosis of community-acquired pneumonia in children. Pediatr Radiol. 2017;47(11):1412–9. https://doi.org/10.1007/s00247-017-3910-1.
15. Pereda MA, Chavez MA, Hooper-Miele CC, Gilman RH, Steinhoff MC, Ellington LE, Gross M, Price C, Tielsch JM, Checkley W. Lung ultrasound for the diagnosis of pneumonia in children: a meta-analysis. Pediatrics. 2015;135(4):714–22. https://doi.org/10.1542/peds.2014-2833.
16. Shah VP, Tunik MG, Tsung JW. Prospective evaluation of point-of-care ultrasonography for the diagnosis of pneumonia in children and young adults. JAMA Pediatr. 2013;167(2):119–25. https://doi.org/10.1001/2013.jamapediatrics.107.
17. Chiu CY, Wong KS, Lai SH, Huang YH, Tsai MH, Lin YC. Peripheral hypoechoic spaces in consolidated lung: a specific diagnostic sonographic finding for necrotizing pneumonia in children. Turk J Pediatr. 2008;50(1):58–62.
18. Luri D, De Candia A, Bazzocchi M. Evaluation of the lung in children with suspected pneumonia: usefulness of ultrasonography. Radiol Med. 2009;114(2):321–30. https://doi.org/10.1007/s11547-008-0336-8.
19. Yang PC, Luh KT, Chang DB, Wu HD, Yu CJ, Kuo SH. Value of sonography in determining the nature of pleural effusion: analysis of 320 cases. AJR Am J Roentgenol. 1992;159(1):29–33. https://doi.org/10.2214/ajr.159.1.1609716.
20. Kurian J, Levin TL, Han BK, Taragin BH, Weinstein S. Comparison of ultrasound and CT in the evaluation of pneumonia complicated by parapneumonic effusion in children. AJR Am J Roentgenol. 2009;193(6):1648–54. https://doi.org/10.2214/ajr.09.2791.
21. Jaffe A, Calder AD, Owens CM, Stanojevic S, Sonnappa S. Role of routine computed tomography in paediatric pleural empyema. Thorax. 2008;63(10):897–902. https://doi.org/10.1136/thx.2007.094250.
22. Donnelly LF, Klosterman LA. CT appearance of parapneumonic effusions in children: findings are not specific for empyema. AJR Am J Roentgenol. 1997;169(1):179–82. https://doi.org/10.2214/ajr.169.1.9207521.

23. Sartori S, Postorivo S, Vece FD, Ermili F, Tassinari D, Tombesi P. Contrast-enhanced ultrasonography in peripheral lung consolidations: What's its actual role? World J Radiol. 2013;5(10):372–80. https://doi.org/10.4329/wjr.v5.i10.372.
24. Sugihara T, Koda M, Tokunaga S, Matono T, Nagahara T, Ueki M, Murawaki Y, Kaminou T. Contrast-enhanced ultrasonography revealed active thoracic bleeding. J Med Ultrason. 2010;37(3):143–5. https://doi.org/10.1007/s10396-010-0257-8.
25. Gorg C, Bert T, Kring R. Contrast-enhanced sonography of the lung for differential diagnosis of atelectasis. J Ultrasound Med. 2006;25(1):35–9.
26. Gorg C, Bert T, Kring R, Dempfle A. Transcutaneous contrast enhanced sonography of the chest for evaluation of pleural based pulmonary lesions: experience in 137 patients. Ultraschall Med. 2006;27(5):437–44. https://doi.org/10.1055/s-2006-927021.
27. Rafailidis V, Deganello A, Watson T, Sidhu PS, Sellars ME. Enhancing the role of paediatric ultrasound with microbubbles: a review of intravenous applications. Br J Radiol. 2017;90(1069):20160556. https://doi.org/10.1259/bjr.20160556.
28. Görg C. Transcutaneous contrast-enhanced sonography of pleural-based pulmonary lesions. Eur J Radiol. 2007;64(2):213–21. https://doi.org/10.1016/j.ejrad.2007.06.037.
29. Sperandeo M, Rea G, Grimaldi MA, Trovato F, Dimitri LM, Carnevale V. Contrast-enhanced ultrasound does not discriminate between community acquired pneumonia and lung cancer. Thorax. 2017;72(2):178–80. https://doi.org/10.1136/thoraxjnl-2016-208913.
30. Di Vece F, Tombesi P, Ermili F, Sartori S. Contrast-enhanced ultrasound (CEUS) and CEUS-guided biopsy in the diagnosis of lung abscess in a patient with achalasia: case report. Interv Med Appl Sci. 2013;5(1):31–3. https://doi.org/10.1556/imas.5.2013.1.6.
31. Linde HN, Holland A, Greene BH, Gorg C. [Contrast-enhanced sonography (CEUS) in pneumonia: typical patterns and clinical value—a retrospective study on n = 50 patients]. Ultraschall Med. 2012;33(2):146–51. https://doi.org/10.1055/s-0031-1273280.
32. McCarville MB, Coleman JL, Guo J, Li Y, Li X, Honnoll PJ, Davidoff AM, Navid F. Use of quantitative dynamic contrast-enhanced ultrasound to assess response to antiangiogenic therapy in children and adolescents with solid malignancies: a pilot study. AJR Am J Roentgenol. 2016;206(5):933–9. https://doi.org/10.2214/AJR.15.15789.
33. Deganello A, Rafailidis V, Sellars ME, Ntoulia A, Kalogerakou K, Ruiz G, Cosgrove DO, Sidhu PS. Intravenous and intracavitary use of contrast-enhanced ultrasound in the evaluation and management of complicated pediatric pneumonia. J Ultrasound Med. 2017;36(9):1943–54. https://doi.org/10.1002/jum.14269.
34. Linta N, Baron Toaldo M, Bettini G, Cordella A, Quinci M, Pey P, Galli V, Cipone M, Diana A. The feasibility of contrast enhanced ultrasonography (CEUS) in the diagnosis of non-cardiac thoracic disorders of dogs and cats. BMC Vet Res. 2017;13(1):141. https://doi.org/10.1186/s12917-017-1061-0.
35. Yusuf GT, Fang C, Huang DY, Sellars ME, Deganello A, Sidhu PS. Endocavitary contrast enhanced ultrasound (CEUS): a novel problem solving technique. Insights Imaging. 2018;9(3):303–11. https://doi.org/10.1007/s13244-018-0601-x.

Contrast-Enhanced Ultrasound in Inflammatory Bowel Disease

17

Damjana Ključevšek

17.1 Introduction and Background

Inflammatory bowel disease (IBD) is a lifelong chronic inflammatory disease of the gastrointestinal tract. Due to the natural fluctuating course, periods of inflammation alternate with periods of remission, frequent re-evaluation and monitoring of inflammatory activity are required in order to plan appropriate therapy and to evaluate the response to treatment. Imaging surveillance must be safe, readily available, child-friendly, effective, and inexpensive. Incidence of pediatric-onset IBD is increasing; the peak age of onset is in adolescence, but 18% of IBD patients are younger than 10 years and 4% younger than 5 years [1].

The gold standard in the assessment of the degree of Crohn's disease is upper and lower gastrointestinal (GI) endoscopy (endoscopic severity score) with biopsy, but considered an invasive method, which also requires anesthesia or deep sedation in pediatric patients. There are several surrogate markers for the disease activity that clinicians have traditionally used, including the clinical pediatric Crohn's disease activity index (PCDAI), laboratory markers of inflammation C-reactive protein (CRP), and fecal markers such as fecal calprotectin. Various imaging methods including ultrasound (US), with color and pulsed Doppler, and magnetic resonance (MR) enterography, rarely computed tomography (CT) enterography, play a significant role in the evaluation of the disease activity [2–4]. Wireless capsule endoscopy (WCE) is a useful alternative to identify small bowel lesions in children with suspected Crohn's disease, in whom conventional endoscopy and imaging tools have been nondiagnostic [5]. Each of these modalities for disease assessment has its own numerous limitations [6].

IBD phenotype in children differs from adults. The Paris classification recognizes a different expression of pediatric IBD between patients <10 years and those 10–17 years of age [7]. In addition, the monogenic disorders in very young children (<2 years) with severe IBD-like disease have been recognized. Assa et al. showed that the Paris classification for pediatric IBD has clear predictive properties [8].

The European Society for Pediatric Gastroenterology, Hepatology and Nutrition (ESPGHAN) revisited the Porto criteria for the diagnosis of IBD in children and adolescents and developed the criteria to meet present challenges and developments in pediatric-onset IBD [9]. US was found to be a valuable screening tool in the preliminary diagnostic workup of pediatric patients with suspected IBD, but US should be complemented by a more sensitive imaging of the small bowel, in most cases MR enterography.

D. Ključevšek (✉)
University Medical Center Ljubljana,
Ljubljana, Slovenia

P. S. Sidhu et al. (eds.), *Contrast-Enhanced Ultrasound in Pediatric Imaging*,
https://doi.org/10.1007/978-3-030-49691-3_17

The use of oral anechoic contrast solution (isoosmolar polyethylene glycol) to perform small intestine contrast-enhanced US (SICUS) is mentioned as an option, but there is currently no data on bowel contrast-enhanced ultrasonography (CEUS). In every day clinical practice, the determination of the disease activity depends on the results specified by the various complementary markers and imaging methods depending on local capabilities.

Guidelines on IBD management and follow-up suggest a more regular disease assessment and surveillance in order to guide treatment adjustments and provide more personalized care. In general, the main goal for imaging in pediatric patients with IBD is to find an accurate and objective non-invasive method for the assessment of the disease activity, which is simple, quick, widely available, well tolerated by patients, and safe (avoiding harmful radiation or risks of endoscopy). US imaging techniques are the closest to these requirements, and thus US plays an important role in evaluating the bowel wall in children with IBD [2, 10–15]. High-resolution B-mode US can evaluate the localization and the length of the affected intestinal segments and can identify intra-abdominal complications. Doppler US techniques can visualize and semi-quantify the bowel wall vascularization. However, color Doppler ultrasound (CDUS) reflects large blood vessels with fast flow (macro-vascularization), but is not sensitive enough to show the blood flow at the capillary level (micro-vascularization), which is important for the determination of the disease activity. Sometimes CDUS does not show Doppler signals due to technical reasons. The use of UCA upgrades the evaluation of the bowel wall micro-vascularization due to the microbubble properties (smaller than erythrocytes, true blood pool agent). It is well-known that early pathological change in patients with active Crohn's disease is intense neovascularization and angiogenesis of the bowel wall, characterized by the development of new capillary vessels in the lamina propria and submucosa, which results in increased regional perfusion [16]. Also, the autoregulation of the blood supply in the bowel wall is dysfunctional in these patients [17]. US is frequently criticized for operator dependency, therefore, the use of more objective parameters for the assessment of IBD activity is important in order to overcome the subjective nature of the sonographic determination of the disease activity. Another promising complementary US method in the evaluation of the intestinal fibrosis is sonoelastography [18]. However, the new sonographic methods, bowel CEUS and bowel sonoelastography, have not been systematically investigated in children with IBD.

The initial studies for the evaluation of the bowel wall perfusion with CEUS were done in the early 2000s using first-generation UCA [19], followed by studies using second-generation UCA; SonoVue® (Bracco, Milan, Italy), Definity® (Lantheus Medical Imaging, Bellerica MA), and Optison® (GE Healthcare, St. Louis, MO). The goal was to determine inflammatory activity as manifest by different enhancement patterns of the bowel wall and quantification of the degree of bowel wall enhancement. Serra et al. described four different enhancement patterns in the arterial phase of bowel CEUS and correlated them to clinical disease activity [20]. Patients with complete transmural enhancement of the bowel wall or enhancement of the inner layers were more likely to have the active disease. The quantification of the disease activity by the quantitative assessment of the bowel wall enhancement was found to be an inaccurate CEUS technique, because the degree of the contrast-enhancement depends on several confounding factors, such as type of contrast agent and equipment used, anatomical position of the bowel segment (depth of the segment, location of the bowel—upper or lower abdominal quadrant), body composition (particularly the fat content) and shadowing from bowel air, or arteries filled with the UCA. Absolute numbers of degree of enhancement, "cut-off points," could not be determined.

Dynamic CEUS is a step forward in the quantification of the bowel wall enhancement and perfusion. It allows real-time examination of the bowel wall perfusion on capillary level (microvascularization) and enables an objective quantitative measurement of the enhancement by analyzing the parameters of the time–intensity

curve (TIC) [21]. Medellin et al. integrated CEUS within the global assessment as an additional objective parameter of the disease activity for adults [22]. Quantification analyses diminish the operator dependency and allow for more reliable intra- and inter-patient correlation.

17.2 Dynamic Contrast-Enhanced Ultrasound of Bowel Wall Protocol and Time Intensity Curve Analysis

The dynamic CEUS technique should be standardized; the UCA dose, the equipment, and the transducers are selected for use. Many different systems for TIC analysis are available and comparison is difficult. In general, a multiple-step protocol for bowel CEUS in children is practically the same as in adults [23, 24].

17.2.1 Patient Preparation

The purpose of the examination and the basic information regarding the examination performance should be explained to parents and child. Dynamic CEUS has to be performed on a fasting patient. The main purpose of fasting is to reduce bowel blood flow and lumen content. Intravenous access should be obtained, using a left-arm vein as the most suitable access. A child should be trained to shallow breathe, not to move or speak during the recording period. For a non-cooperating child, light sedation is an option.

17.2.2 Pre-Acquisition US Examination, US Machine, and UCA Preparation

Baseline US and CDUS of the bowel are performed using a high-frequency linear transducer to detect the location and extension of the IBD. The most abnormal segment is selected on the basis of bowel wall thickening, hyperemia detected with CDUS, the presence and amount of inflammatory fat, and mesenteric lymphadenopathy. In <10% of adults, the use of an anti-peristaltic drug is needed to reduce the peristalsis [22]. Anti-peristaltic drugs can be used in children at the same dose as for MR enterography [25].

Once the bowel segment is selected, the contrast-specific US program is switched on. A dual-screen image, contrast and B-mode US image, is necessary for viewing the abnormal area of bowel. Both images should be optimized: mechanical index (0.04–0.08, varies based on the machine), frame rate (should be kept low at about 10 fps), focal zone depth (beneath the desirable segment of the bowel), and dynamic range/compression (around 55–65, any reduction in dynamic range will produce the higher signal intensity, increase the risk of oversaturation) [24].

Transducer orientation is also important. A long orientation of the transducer face to the bowel wall is preferred as this allows for more placement opportunities for the region of interest (ROI) placement. To minimize the effects of respiration, which causes excessive movement of the bowel segment, the transducer should be aligned with the plane of movement (sagittal orientation of the transducer).

UCA should be prepared according to manufacturer's instructions. The dose depends on the child's weight, the transducer frequency, the quality of US contrast-specific software, and the type of second-generation UCA. High-frequency linear transducers provide a better image resolution, but on the contrast image there is less backscatter signal intensity, more microbubble destruction, and more signal attenuation. At our institution, we use SonoVue® in dose 0.04–0.05 mL/kg for a high-frequency linear transducer. Application of UCA is followed by 10 mL of saline solution flush. A convex transducer is rarely used (half a dose of UCA compared to linear transducer up to 1.2 mL). In addition, we need to be aware that the way UCA is administered affects the UCA enhancement; the cannula should be at least 22G, the UCA should be injected perpendicular to the cannula, and neutral displacement connectors should be avoided [26].

17.2.3 Acquisition

The child lies comfortably in a supine position with his/her parents sitting at the bedside, breathing under instruction in a quiet, shallow manner without physical movement. The transducer is held in a fixed position during the continuous acquisition of data. Recording starts at the time of UCA administration and lasts at least 90 s. The examination is stored on digital video clip. A subjective evaluation of the enhancement (the pattern of transmural enhancement, vascularization of the mesentery—enhancement and comb sign) may be performed during and immediately after acquisition. An initial quantitative analysis of data can be performed directly on many US machines.

17.2.4 Post-Processing with Time–Intensity Curve Analysis

The examination data are transferred to a workstation, where an analysis of the TIC is undertaken. At our institution, we use CHI-Q™ software by Canon (previously Toshiba) (Fig. 17.1). The system is vendor-specific and limited. Another vendor-specific system is Q-laboratory™ (Philips Healthcare Ultrasound). A more general and neutral platform for data analysis is VueBox® (Bracco, Software, Genova, CH), using DICOM header information.

An ROI is drawn manually at the most visually enhanced part of the thickened bowel wall. The lumen and perivisceral tissues should not be included. It is better to use a large ROI size as a larger ROI size shows better approximation of the overall disease activity. Conversely, a large ROI size may cover less affected layers or segments of the bowel, which could result in a lower peak enhancement (Fig. 17.2) [24]. The ROI is drawn using free hand and a size of approximately 1.5 cm^2 is recommended. We suggest controlling the position and movement of ROI by watching a video clip to estimate the position of ROI and possible moving artifacts.

A TIC is drawn by calculating the change in mean ROI intensity over time. The time is displayed in seconds on the *X* axis, and contrast

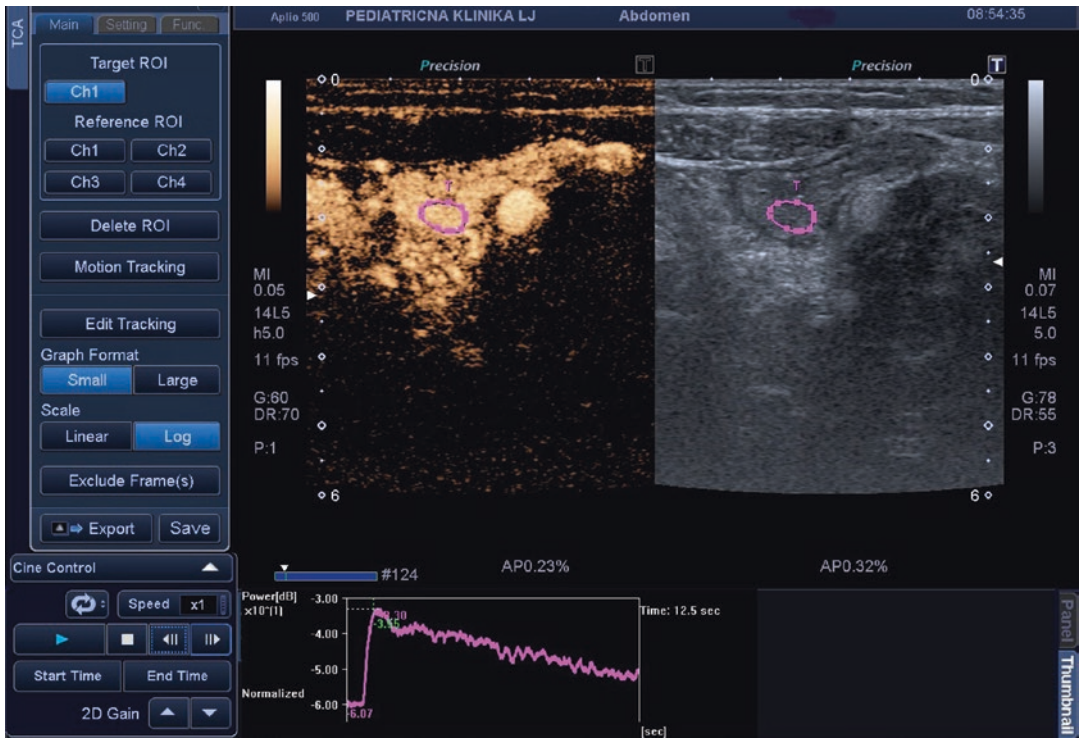

Fig. 17.1 CHI Q®, Canon (Toshiba) software program for time–intensity curve analysis. A region of interest (ROI) is placed over the enhancing bowel segment and a time–intensity curve generated automatically

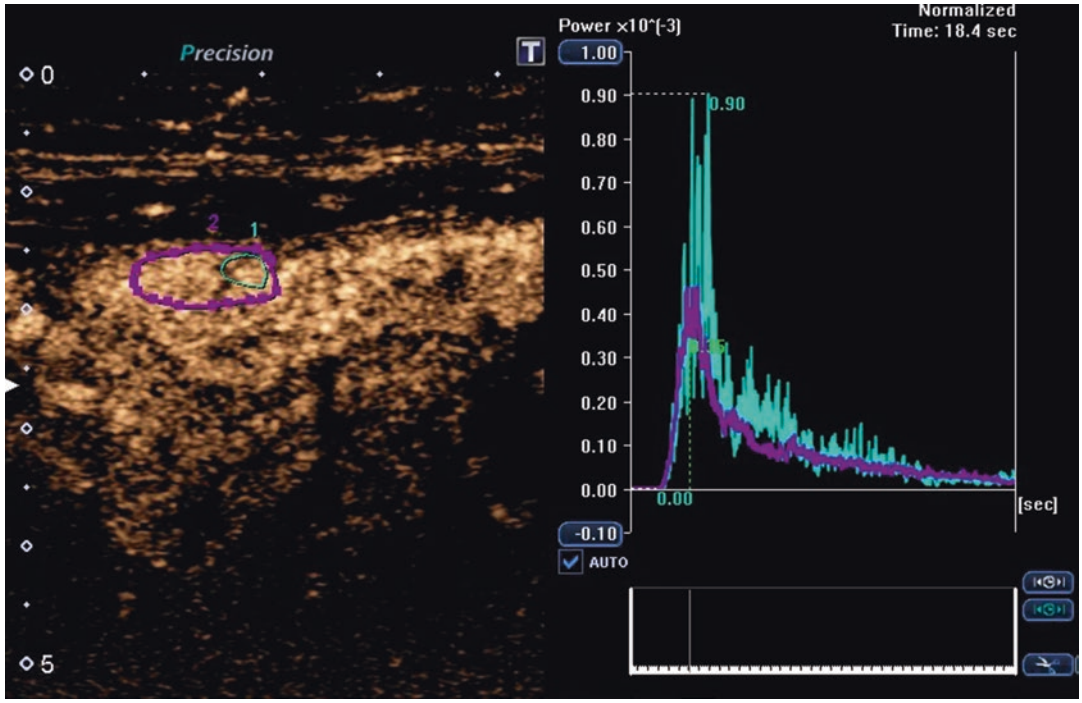

Fig. 17.2 The effect of the size of the region of interest (ROI) on time–intensity curve (linear data) after tracking motion corrections: the larger ROI (purple) shows a lower peak enhancement and less signal fluctuations compared to the smaller ROI (blue)

intensity (arbitrary units) on the *Y* axis. CHI-Q™ software uses raw linearized data to generate a TIC. The interval of observation within an ROI is generated from the raw linearized or DICOM data depending on the type of software used for analysis [24]. An automatic calculation of TIC parameters is completed from the fitted curve on linear data [21]. The peak intensity/enhancement (PE) can be log-converted by most software programs.

17.2.5 Interpretation

The interpretation may be semi-quantitative (subjective), or quantitative (objective). The subjective evaluation includes the pattern of the enhanced bowel wall and perivisceral tissue (degree of enhancement, enhanced part of the bowel wall, homogeneity of the enhancement). There are many difficulties with the objective interpretation of the TIC. Our experience, and the experience of other centers dealing with bowel CEUS, is that the shape and the height of the TIC give the most important information regarding disease activity. However, currently the shape of the TIC cannot be objectively evaluated by any given parameters.

Objective assessment of dynamic CEUS of the bowel wall deals with many potential issues; the first is standardization of the procedure. Many internal (body composition, position of bowel loop, active peristalsis, etc.) and external factors (dose, intravenous administration equipment set-ups, respiratory and patient movement of the abdominal wall) influence the quality of the examination. The second issue is that different software programs used for TIC analysis are not completely comparable. In addition, the definition of parameters varies based on the software program and the fitted curve model. For example, the time to peak (TTP) on one software analysis is commenced from the first microbubble appearance in the bowel wall to its maximum intensity.

Others define TTP as the time from the injection to the peak enhancement (PE). In addition, there are different definitions of the mean transit time (mTT). The third issue arises as there is no single parameter which can describe the perfusion pattern and thus be represented by different curve types. There are no widely accepted cut-off values for quantification, each center is accustomed to the reliability of their own measurement system which diminishes the objectivity of the perfusion quantification. Therefore, more studies or a wide multicentric study are needed, with the optimal standardization of all steps of the examination, including uniform or more comparable post-processing software. In the future, the validation should include a combination of two or more parameters and a subjective enhancement pattern represented by the height and shape of TIC.

17.3 Position Statements for Bowel Dynamic CEUS

Dynamic CEUS is proven in adults to be a valuable addition to the performance of bowel US allowing a more objective evaluation of bowel perfusion and is a potential biomarker for disease activity. In the current European Federation of Societies for Ultrasound in Medicine and Biology (EFSUMB) guidelines on CEUS for non-liver studies, recommendations clarify the current position accepted by EFSUMB for adult studies [27]. The EFSUMB position statement for the use of bowel CEUS in children is practically identical [28], although the level of evidence is based on adult studies and there are no dedicated CEUS studies for the evaluation of IBD in children, stating that CEUS can be used as an alternative imaging modality for the follow-up of the children with known IBD to differentiate between active and quiescent disease and to evaluate the outcome of therapeutic strategies.

The first joint European Society of Gastrointestinal and Abdominal Radiology (ESGAR) and European Society of Pediatric Radiology (ESPR) consensus statement reached an agreement statement on the technical performance of the cross-sectional small bowel and colonic imaging [25]. The routine use of bowel CEUS in children by these organizations is currently not recommended, but they open to include CEUS examination when the evidence base grows.

17.4 Indications, Advantages, and Limitations of Bowel CEUS

The current status (indications), advantages, and limitations of bowel CEUS regarding the recommendations are presented [6, 27, 28].

17.4.1 Evaluation of the Disease Activity

EFSUMB Recommendation 35 states that CEUS can be used to estimate disease activity in IBD in adults [27]. The use of UCA helps to assess the degree, direction, and behavior of the enhancement (Figs. 17.3, 17.4, and 17.5).

Serafin et al. have recently published the biggest systematic review and meta-analysis focused specifically on the role of bowel CEUS in the detection of the acute phase of Crohn's disease in adults [29]. A pooled sensitivity and specificity of CEUS in this regard were 0.94 (95% CI 0.87–0.97) and 0.79 (96% CI 0.67–0.88), respectively. Despite the difference in methods used by multiple researchers, CEUS consistently shows a good correlation with disease activity. The biggest problem with the current evidence regarding the imaging of the active Crohn's disease with CEUS is the technical and methodological quality of the studies. In addition, current evidence indicates that parameters obtained from TIC analysis have limited accuracy.

Most common TIC evaluating parameters which are related to the bowel wall perfusion are the total area under curve (AUC), the mean intensity of AUC (IMA), maximum peak inten-

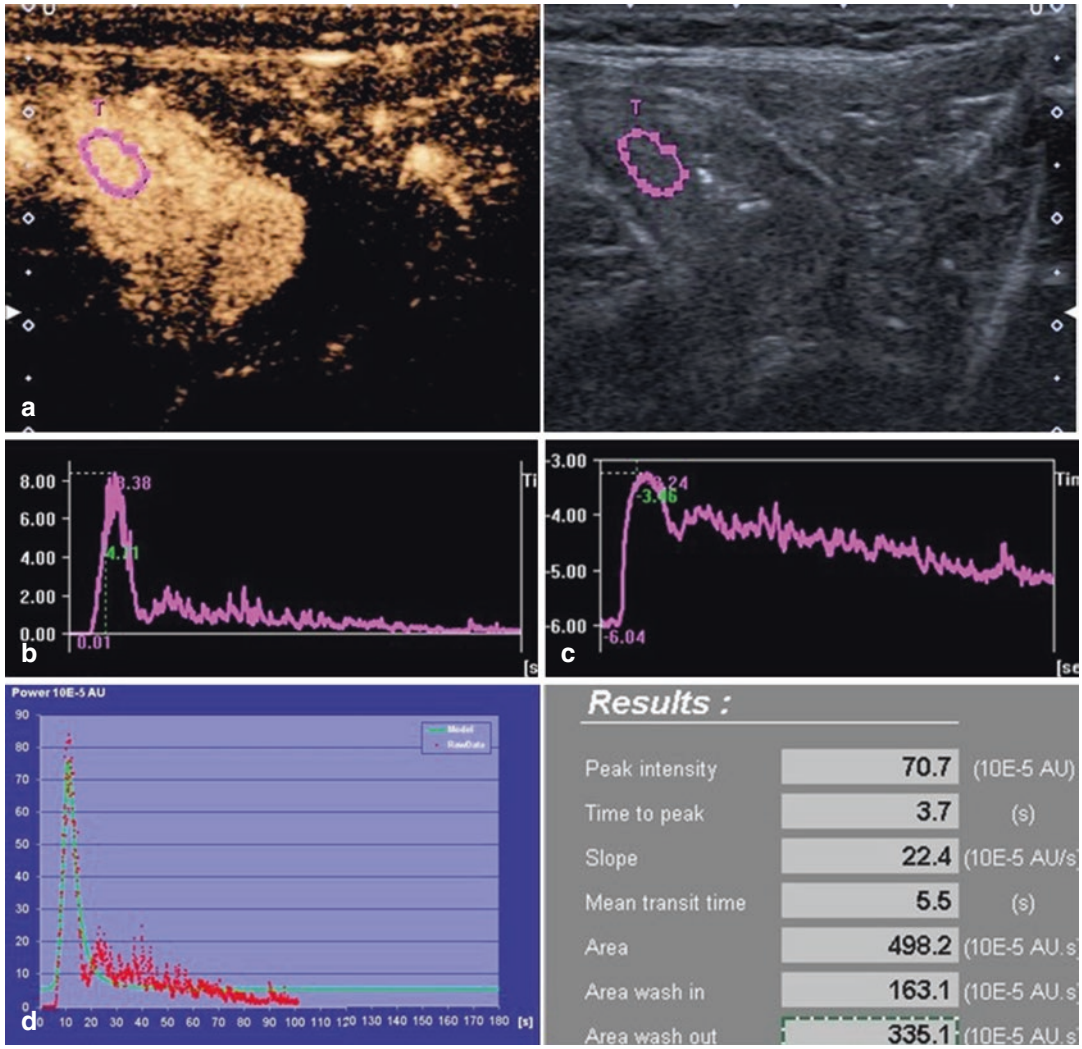

Fig. 17.3 Dynamic CEUS of the bowel wall in a 10-year-old girl with Crohn's disease and severe inflammation of the bowel wall (histologically proved): (**a**) strong enhancement of the bowel wall with a region of interest placed appropriately, (**b**) linear time-intensity curve (TIC), (**c**) logarithmic TIC, and (**d**) adjusted TIC, and the parameters calculated

sity (MPI—reflected the strength of intestine perfusion), and β coefficient of the slope (correlated with TTP enhancement). No single parameter can describe the perfusion pattern and be represented by different curve types. High activity is consistent with a high PE, a short and step wash-in and a slow wash out and an increase in AUC [24]. Relative intestine wall enhancement had the highest diagnostic value. The diagnostic threshold for the diagnosis of active Crohn's disease that could endorse CEUS as an objective modality is not determined from the study.

Medellin-Kowalewski et al. proposed that quantitative CEUS parameters could be integrated into inflammatory assessments with US to improve disease activity level determination and to reduce indeterminate results [30]. Prospective

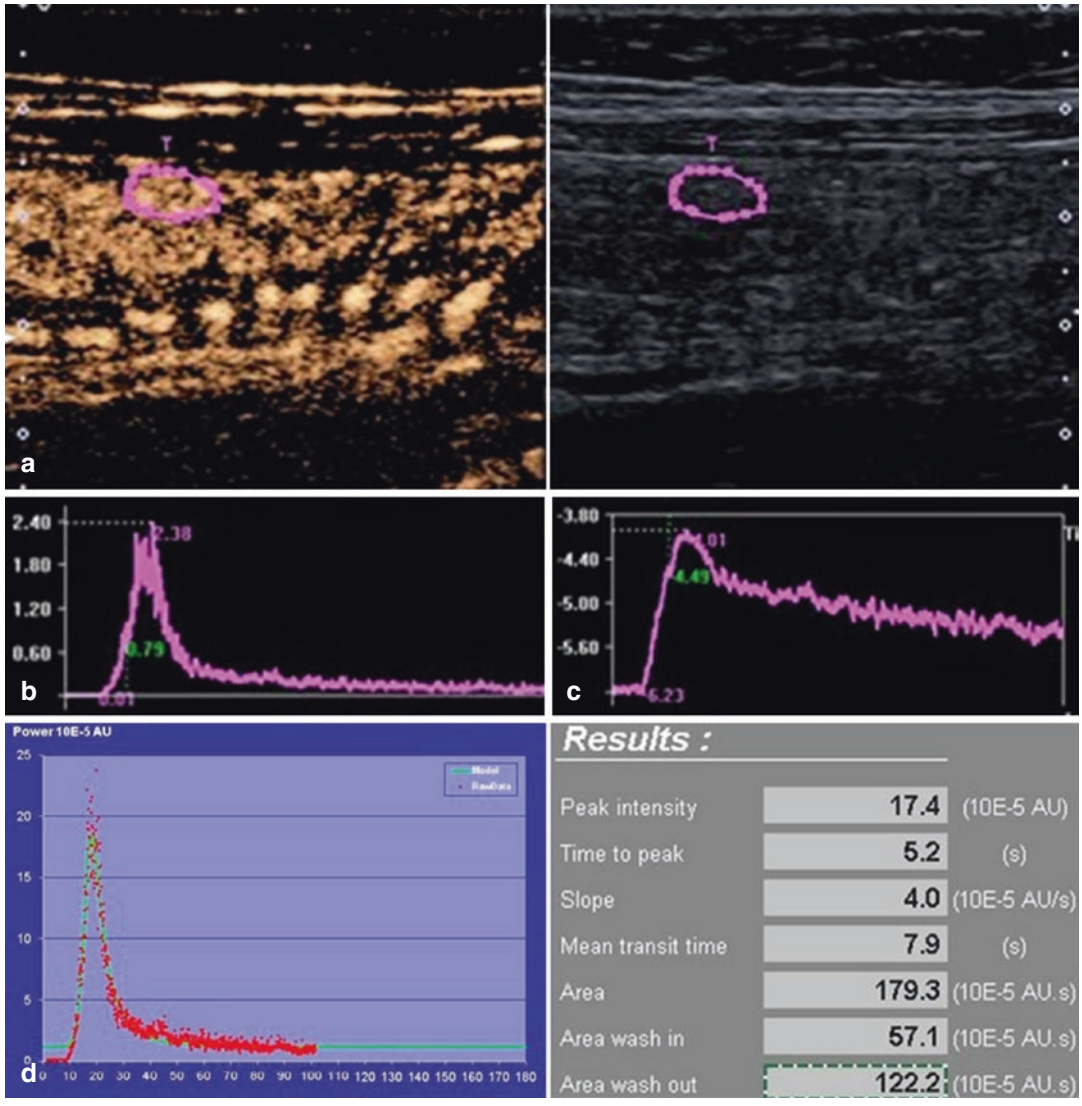

Fig. 17.4 Dynamic CEUS of the bowel wall in a 14-year-old girl with Crohn's disease and moderate inflammation of the bowel wall (histologically proved): (**a**) moderate enhancement of the bowel wall with region of interest placed, (**b**) linear time–intensity curve (TIC), (**c**) logarithmic TIC, and (**d**) adjusted TIC and the parameters calculated

studies have to be performed to develop an US index for Crohn's disease activity that combines the US global assessment and CEUS parameters. Ripollés et al. published a study dealing with when CEUS would be justified on the basis of US and CDUS findings in patients with IBD for detecting disease activity [31]. They concluded that the use of UCA is probably not justified to assess disease activity for patients with CDUS grade 2/3.

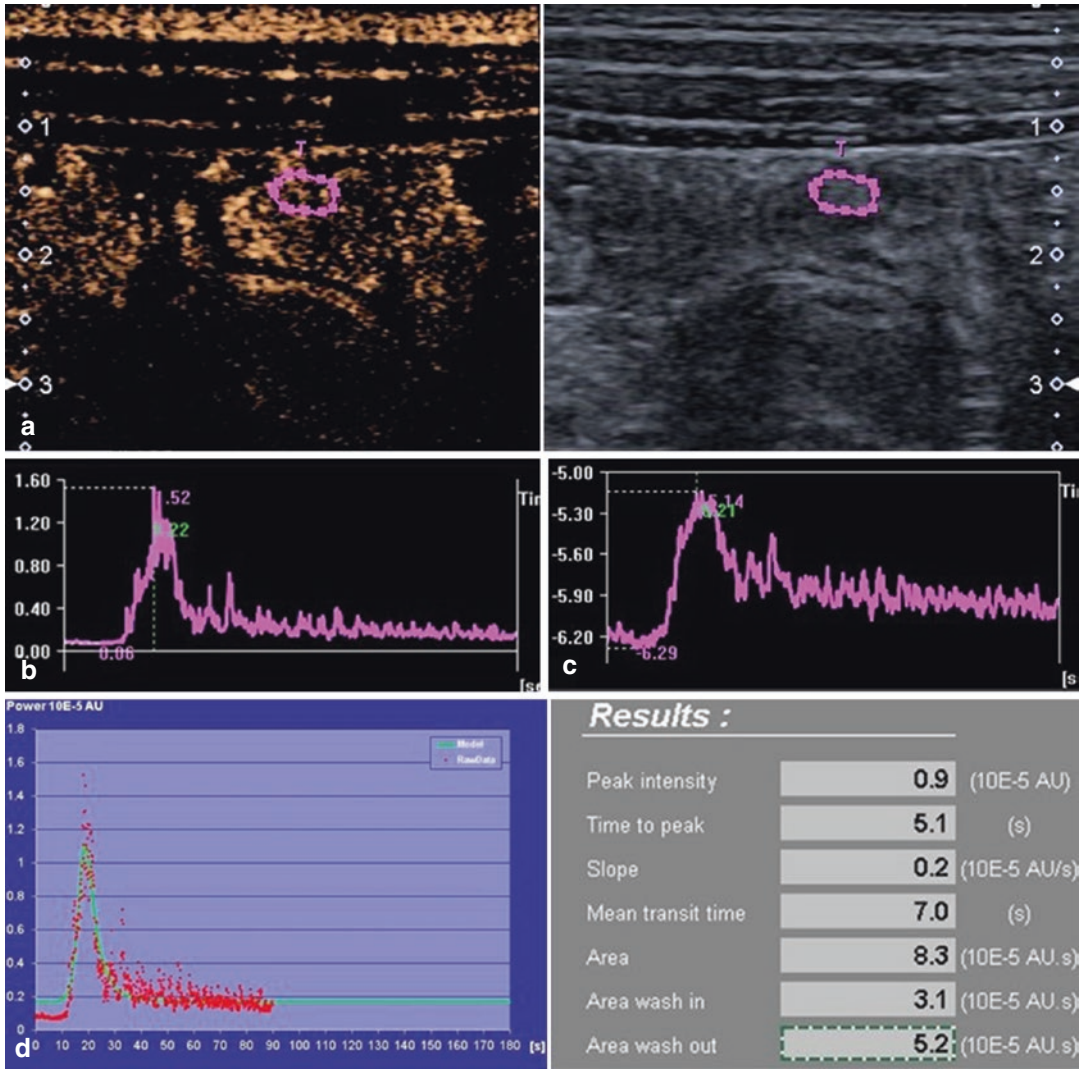

Fig. 17.5 Dynamic CEUS of the bowel wall in a 13-year-old boy with Crohn's disease and a mild inflammation of the bowel wall (histologically proved): (**a**) mild enhancement of the bowel wall with a region of interest placed, (**b**) linear time–intensity curve (TIC), (**c**) logarithmic TIC, and (**d**) adjusted TIC and the parameters calculated

17.4.2 Differential Diagnosis Between Fibrotic and Inflammatory Stenosis in Order to Select Patients for Medical Therapy or Surgery

CEUS can be used to discern between fibrous and inflammatory strictures in Crohn's disease, Recommendation 35 [30]. In theory and according to some studies, the active inflammatory components of the bowel wall will enhance using UCA, whereas the fibrotic stricture will not [32, 33]. On the other hand, CEUS quantitative perfusion parameters failed to reliably detect bowel wall fibrosis in the setting of superimposed inflammation in a Crohn's disease animal model [34]. These findings question the ability of CEUS to detect and quantify bowel wall fibrosis of human Crohn's strictures, which commonly contain both substantial inflammation and fibrosis. Further prospective studies are needed.

17.4.3 Extraintestinal Complications of Crohn's Disease

Extraintestinal complications of Crohn's disease include the development of a fistula, the formation of an inflammatory mass or phlegmon or the presence of an abscess. CEUS can be used to detect abscesses and to confirm and track the route of fistulae according to EFSUMB Recommendation 37 [27]. It is often difficult to differentiate between phlegmon mass and abscess on B-mode US. However, the distinction is very important as management, prognosis, and therapy differ. CEUS is of benefit in this situation; a phlegmon mass shows diffused hyperenhancement during CEUS examination, while abscess shows regions of avascularity (pockets of necrosis and pus) surrounded by peripheral areas of enhancement.

17.4.4 Follow-Up of IBD Patients

CEUS can be used to monitor the effect of a treatment in Crohn's disease, EFSUMB Recommendation 36 [27]. An evaluation of the treatment response is very important regardless of the type of treatment and extent of IBD [35–39]. The most valuable quantitative parameters are PE and AUC. The pre-treatment values and percentage changes of the PE, AUC, AUC during wash-in, and AUC during wash-out were found to be predictors ($P < 0.05$) of the long-term therapeutic outcome [38]. Changes of the enhancement parameters will occur prior to changes in the gross morphology of the bowel noted on baseline and changes in other US activity parameters (density of vascular signals and changes in flow in larger blood vessels on color Doppler imaging) [39]. The follow-up results of CEUS are important, particularly when expensive biological drugs are used, because about 30% of patients have an incomplete response or even no response to biological therapy. Therefore, CEUS has the ability to provide a quick answer regarding treatment response in case the dose should be increased, or biological drug should be changed, or other treatment is necessary (Fig. 17.6).

CEUS is also very useful in children with clinically suspected relapse of the disease and mild (borderline) thickness of the bowel wall (Fig. 17.7). In the case of an active inflammation the bowel wall enhances.

17.4.5 Advantages and Limitations

There are numerous advantages of bowel CEUS. The method has a high safety profile. It is non-invasive, non-nephrotoxic, radiation-free, well-tolerated by patients and accessible (wide availability and portability of US machines) [40]. The whole examination takes 10–15 min, which is significantly less compared to the time-consuming MR enterography. There is no need for sedation. The size and body composition in children are more favorable for a CEUS examination than in adults [40]. It is easily repeatable, and there are no limits to perform frequent serial examinations at short intervals (important in follow-up patients with insufficient response to treatment). In addition, it is cost-effective examination.

The main limitations are inadequate technical performance of dynamic CEUS and differences in the post-processing evaluation of the examination as discussed above (Sect. 2.5). The whole bowel cannot be evaluated at once and each intestinal segment evaluation needs an injection of UCA.

17.4.6 When Is a Bowel CEUS Justified in Pediatrics?

According to our experience, bowel CEUS in children should be done when the diagnosis of Crohn's disease is first established. The disease activity in the most affected bowel segments and baseline TIC curve (height and shape) with calculated parameters are obtained. This baseline information is important for disease activity follow-up. Follow-up CEUS is not required with a good response to treatment (clinical, laboratory, and US improvement). CEUS can give valuable and objective data around the dynamics of

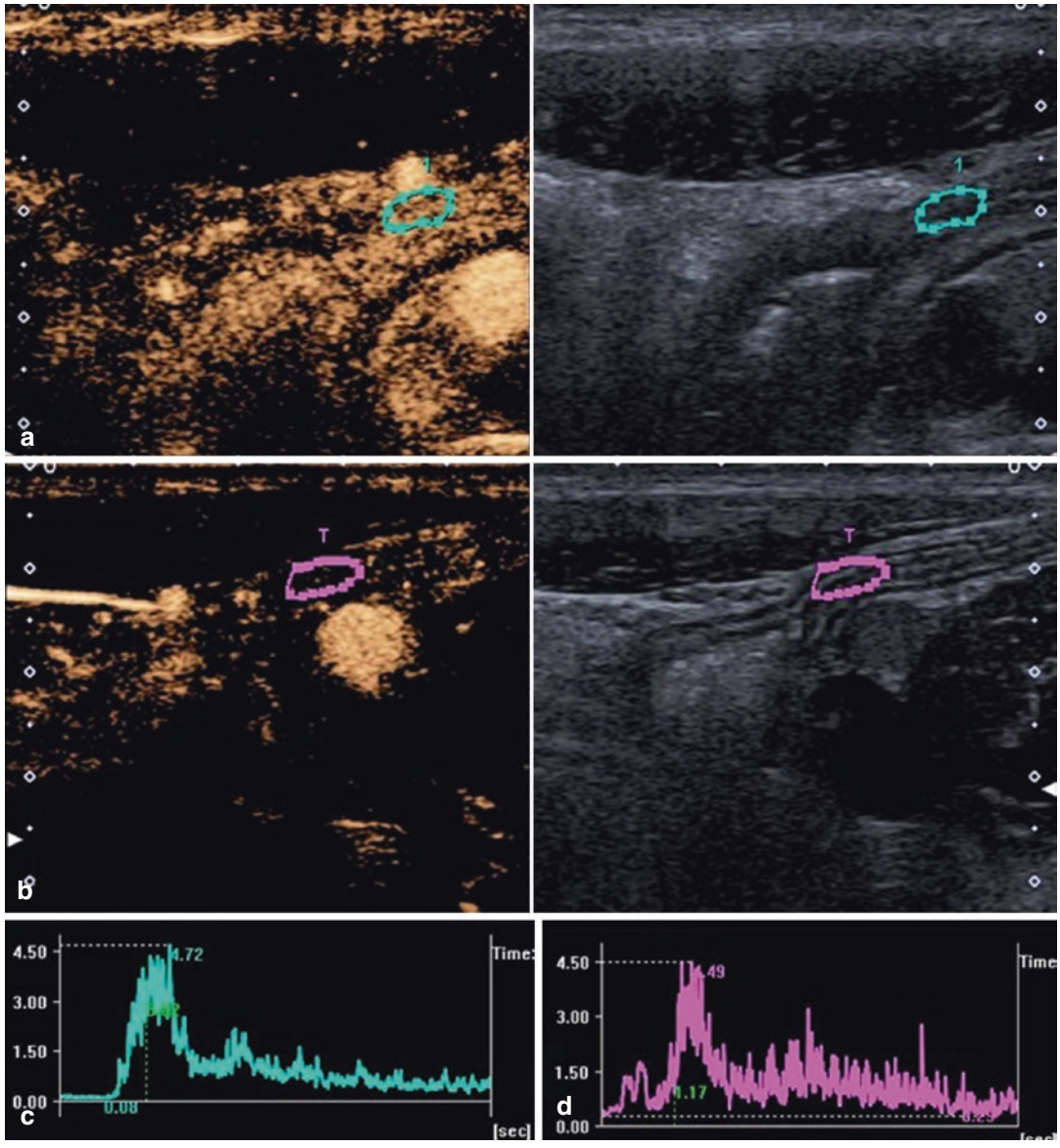

Fig. 17.6 A 14-year-old boy with an early onset of Crohn's disease and sigmoid stenosis found on ultrasound and confirmed on colonoscopy. Bowel CEUS of this segment was performed to evaluate the activity of the inflammation to optimize the treatment with infliximab; (**a**) CEUS showed a moderate enhancement of the stenotic segment. The dose of infliximab (anti-TNFα) was increased, (**b**) a follow-up CEUS 3 weeks later with a diminished enhancement of the stenotic segment showed a good response to the treatment and diminished activity of the disease. Colonoscopy balloon dilation of the stenotic part was done. The peak enhancement (PE) obtained from the logarithmic time–intensity curve from (**c**) the first and (**d**) a follow-up bowel CEUS showed diminished values of PE

inflammation, compared with the baseline examination in cases with insufficient response and help when making a decision about further treatment. We should consider CEUS of the bowel wall as a complementary method in evaluating Crohn's disease activity and treatment response.

We are aware that there is no ideal imaging method for children and any additional imaging

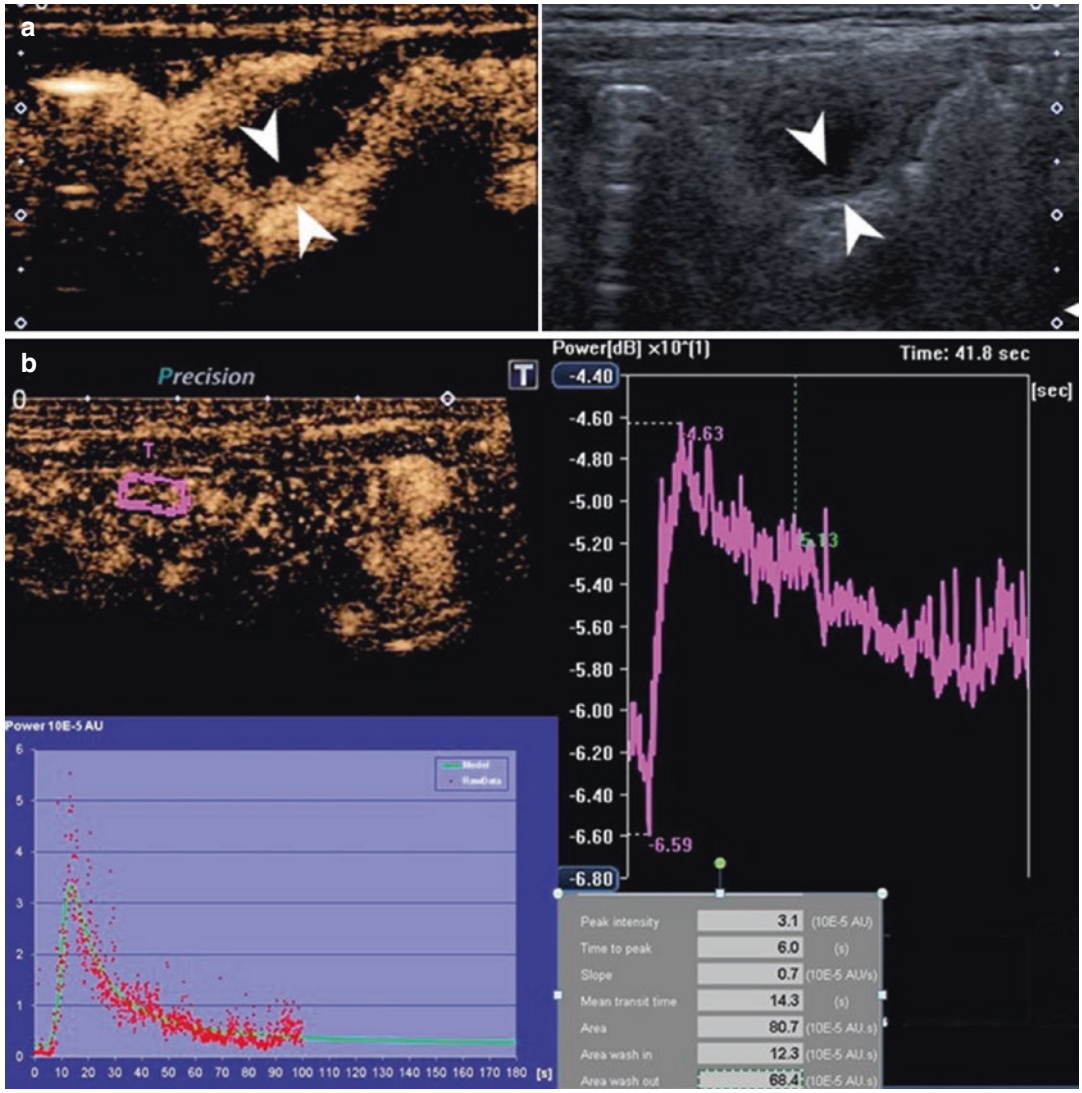

Fig. 17.7 (**a**) Bowel CEUS in a 3.8-year-old boy with suspected Crohn's disease. Enhancement of the ascending colon bowel wall is seen. The time–intensity curve (TIC) analysis could not be performed due to extensive respiratory movement. On the bases of CEUS enhancement pattern and elevated fecal calprotectin (179.8 mg/kg) colonoscopy was performed, which showed no abnormalities of the colon mucosa. However, the histological analysis of the ascending colon bowel wall reported a mild inflammation concordant with an indeterminate inflammatory bowel disease. He was treated by diet modification. (**b**) Follow-up bowel CEUS after 5 months in the same boy; fecal calprotectin is even higher (451.8 mg/kg); moderate transmural bowel wall enhancement of the ascending colon with TIC analysis suggested a mild inflammation, which was confirmed by a histology analysis (mild to moderate inflammation). Complete enteral nutrition was introduced

technique that resolves the problem is welcome. There are many studies of bowel CEUS in adults, and they should be extended to children. In addition, we are aware of advantages and limitations of the examination and have a good, solid base for more standardized and thus comparable studies. Child-friendly, safe, and available examination surely is mandatory in this young population with a potential lifelong disease [41].

In conclusion bowel CEUS has great potential to become a complementary method in more

objective disease activity assessment in children with IBD that might have positive implications for patient management and monitoring of disease activity after a precise standardization of the examination and after solving some technical and interpretation issues.

References

1. Rosen MJ, Dhawan A, Saeed SA. Inflammatory bowel disease in children and adolescents. JAMA Pediatr. 2015;169(11):1053–60.
2. Duigenan S, Gee MS. Imaging of pediatric patients with inflammatory bowel disease. AJR Am J Roentgenol. 2012;199:907–15.
3. Anupindi SA, Podberesky DJ, Towbin AJ, et al. Pediatric inflammatory bowel disease: imaging issues with targeted solutions. Abdom Imaging. 2015;40(5):975–92.
4. Maltz R, Podberesky DJ, Saeed SA. Imaging modalities in pediatric inflammatory bowel disease. Curr Opin Pediatr. 2014;26(5):590–6.
5. Kopylova U, Yungb DE, Engela T, et al. Diagnostic yield of capsule endoscopy versus magnetic resonance enterography and small bowel contrast ultrasound in the evaluation of small bowel Crohn's disease: systematic review and meta-analysis. Dig Liver Dis. 2017;49:854–63.
6. Pecere S, Holleran G, Ainora ME, et al. Usefulness of contrast-enhanced ultrasound (CEUS) in inflammatory bowel disease (IBD). Dig Liver Dis. 2018;50(8):761–7.
7. Levine A, Griffiths A, Markowitz J, et al. Pediatric modification of the Montreal classification for inflammatory bowel disease: the Paris classification. Inflamm Bowel Dis. 2011;17(6):1314–21.
8. Assa A, Rinawi F, Shamir R. The long-term predictive properties of the Paris classification in pediatric inflammatory bowel disease patients. J Crohns Colitis. 2018;12(1):39–47.
9. Levine A, Koletzko S, Turner D, et al. ESPGHAN revised Porto criteria for the diagnosis of inflammatory bowel disease in children and adolescents. J Pediatr Gastroenterol Nutr. 2014;58:795–806.
10. Francavilla ML, Anupindi SA, Kaplan SL, et al. Ultrasound assessment of the bowel: inflammatory bowel disease and conditions beyond. Pediatr Radiol. 2017;47(9):1082–90.
11. Chiorean L, Schreiber-Dietrich D, Braden B, et al. Ultrasonographic imaging of inflammatory bowel disease in pediatric patients. World J Gastroenterol. 2015;21(17):5231–41.
12. Chiorean L, Schreiber-Dietrich D, Braden B, et al. Transabdominal ultrasound for standardized measurement of bowel wall thickness in normal children and those with Crohn's disease. Med Ultrason. 2014;16(4):319–24.
13. Maffè GC, Brunetti PE, Corazza GR. Ultrasonographic findings in Crohn's disease. J Ultrasound. 2015;18:37–49.
14. Biko DM, Rosenbaum DG, Anupindi SA. Ultrasound features of pediatric Crohn disease: a guide for case interpretation. Pediatr Radiol. 2015;45(10):1557–66.
15. Maconi G, Nylund K, Ripolles T, et al. EFSUMB recommendations and clinical guidelines for intestinal ultrasound (GIUS) in inflammatory bowel disease. Ultraschall Med. 2018;39:304–17.
16. Danese S, Sans M, de la Motte C, et al. Angiogenesis as a novel component of inflammatory bowel disease pathogenesis. Gastroenterology. 2006;130:2060–73.
17. Hatoum OA, Binion DG, Otterson MF, et al. Acquired microvascular dysfunction in inflammatory bowel disease: loss of nitric oxidemediated vasodilation. Gastroenterology. 2003;125:58–69.
18. Coelho R, Ribeiro H, Maconi G. Bowel thickening in Crohn's disease: fibrosis or inflammation? Diagnostic ultrasound imaging tools. Inflamm Bowel Dis. 2017;23(1):23–34.
19. Di Sabation A, Fulle I, Ciccocioppo R, et al. Doppler enhancement after intravenous Levovist injection in Crohn's disease. Inflamm Bowel Dis. 2002;8:251–7.
20. Serra C, Menzzi G, Labate AM, et al. Ultrasound assessment of vascularization of the thickened terminal ileum wall in Crohn's disease patients using a low-mechanical index real-time scanning technique with a second-generation ultrasound contrast agent. Eur J Radiol. 2007;62:114–21.
21. Dietrich CF, Averkiou MA, Correas JM, et al. An EFSUMB introduction into dynamic contrast-enhanced ultrasound (DCE-US) for quantification of tumour perfusion. Ultraschall Med. 2012;33:344–51.
22. Medellin A, Merrill C, Wilson SR. Role of contrast-enhanced ultrasound in evaluation of the bowel. Abdom Radiol. 2018;43:918–33.
23. Ključevšek D, Vidmar D, Urlep D, et al. Dynamic contrast-enhanced ultrasound of the bowel wall with quantitative assessment of Crohn's disease activity in childhood. Radiol Oncol. 2016;50(4):347–54.
24. Wilkens R, Pournazari P, Wilson RS. CEUS of the bowel in inflammatory bowel disease. In: Weskott HP, editor. Contrast-enhanced ultrasound. 2nd ed. Bremen: UNI-MED Verlag AG; 2013. p. 222–36.
25. Taylor SA, Avni F, Cronin CG, et al. The first joint ESGAR/ESPR consensus statement on the technical performance of cross-sectional small bowel and colonic imaging. Eur Radiol. 2017;27:2570–82.
26. Kramer MR, Bhagat N, Back SJ, et al. Influence of contrast-enhanced ultrasound administration setups on microbubble enhancement: a focus on pediatric applications. Pediatr Radiol. 2018;48(1):101–8.
27. Sidhu PS, Cantisani V, Dietrich CF, et al. The EFSUMB guidelines and recommendations for the clinical practice of contrast-enhanced ultrasound (CEUS) in non-hepatic applications: update 2017 (short version). Ultraschall Med. 2018;39(2):154–80.
28. Sidhu PS, Cantisani V, Deganello A, et al. Role of contrast-enhanced ultrasound (CEUS) in pediatric

practice: an EFSUMB position statement. Ultraschall Med. 2017;38:33–43.
29. Serafin Z, Białecki M, Białecka A, et al. Contrast-enhanced ultrasound for detection of Crohn's disease activity: systematic review and meta-analysis. J Crohns Colitis. 2016;10(3):354–62.
30. Medellin-Kowalewski A, Wilkens R, Wilson A, et al. Quantitative contrast-enhanced ultrasound parameters in Crohn disease: their roe in disease activity determination with ultrasound. AJR. 2016;206:64–73.
31. Ripollés T, Martínez-Pérez MJ, Paredes JM, et al. The role of intravenous contrast agent in the sonographic assessment of Crohn's disease activity: is contrast agent injection necessary? J Crohns Colitis. 2018;13:585. https://doi.org/10.1093/ecco-jcc/jjy204. [Epub ahead of print].
32. Nylund K, Sævik F, Leh S, et al. Interobserver analysis of CEUS-derived perfusion in fibrotic and inflammatory Crohn's disease. Ultraschall Med. 2018;40:76. https://doi.org/10.1055/s-0044-100492. [Epub ahead of print].
33. Quaia E, Gennari AG, van Beek EJR. Differentiation of inflammatory from fibrotic ileal strictures among patients with Crohn's disease through analysis of time-intensity curves obtained after microbubble contrast agent injection. Ultrasound Med Biol. 2017;43(6):1171–8.
34. Dillman JR, Rubin JM, Johanson LA, et al. Can contrast-enhanced sonography detect bowel wall fibrosis in mixed inflammatory and fibrotic Crohn disease lesions in an animal model? J Ultrasound Med. 2017;36:523–30.
35. Socaciu M, Ciobanu L, Diaconu B, et al. Non-invasive assessment of inflammation and treatment response in patients with Crohn's disease and ulcerative colitis using contrast-enhanced ultrasonography quantification. J Gastrointestin Liver Dis. 2015;24(4):457–65.
36. Saevik F, Nylund K, Hausken T, et al. Bowel perfusion measured with dynamic contrast-enhanced ultrasound predicts treatment outcome in patients with Crohn's disease. Inflamm Bowel Dis. 2014;20(11):2029–37.
37. Romanini L, Passamonti M, Navarria M, et al. Quantitative analysis of contrast-enhanced ultrasonography of the bowel wall can predict disease activity in inflammatory bowel disease. Eur J Radiol. 2014;83(8):1317–23.
38. Quaia E, Gennari AG, Cova MA. Early predictors of the long-term response to therapy in patients with Crohn disease derived from a time-intensity curve analysis after microbubble contrast agent injection. J Ultrasound Med. 2018;38:947. https://doi.org/10.1002/jum.14778. [Epub ahead of print].
39. Quaia E, Cabibbo B, De Paoli L, et al. The value of time-intensity curves obtained after microbubble contrast agent injection to discriminate responders from non-responders to anti-inflammatory medication among patients with Crohn's disease. Eur Radiol. 2013;23(6):1650–9.
40. Darge K, Papadopoulou F, Ntoulia A, et al. Safety of contrast enhanced ultrasound in children for non-cardiac applications. Pediatr Radiol. 2013;43:1063–73.
41. Sidhu PS, Cantisani V, Deganello A, et al. Authors' reply to letter: role of contrast-enhanced ultrasound (CEUS) in pediatric practice: an EFSUMB position statement. Ultraschall Med. 2017;38(4):447.

Contrast-Enhanced Ultrasound in Childhood Oncology

18

Judy Squires, Abhay Srinivasan, and M. Beth McCarville

18.1 Introduction

Ultrasound (US) has many positive attributes in pediatric imaging; it is non-invasive, portable, provides Doppler capabilities for vascular assessment, does not require sedation, and, most importantly, does not expose the child to the potentially harmful effects of ionizing radiation. The avoidance of radiation and sedation is of heightened concern in pediatric oncology because these children undergo innumerable imaging examinations at diagnosis, for staging, to monitor treatment response, to assess acute and chronic treatment-related complications, and to assess for tumor recurrence after completion of therapy. A recent study showed an association between radiation exposure from computed tomography (CT) imaging and an increased risk of developing brain tumors and leukemia in children [1]. Those investigators reported that brain tumor risk was comparable to observed risk estimates for brain tumors following childhood radiation exposure in Japanese nuclear blast survivors. These findings underscore the importance of minimizing radiation exposure in children whenever possible.

In children with cancer, US is often the first-line imaging modality to identify and localize pathology in the abdomen, pelvis, and extremities. However, B-mode US has recognized limitations and further imaging with CT, magnetic resonance (MR), and nuclear medicine imaging is required for diagnosis and staging. The addition of a contrast agent to US imaging offers the opportunity to improve lesion conspicuity, better characterize lesions, distinguish benign from malignant features, and improve diagnostic confidence. The current role of contrast-enhanced ultrasound (CEUS) in pediatric oncology is to guide interventional procedures and for use as a problem-solving tool at the time of diagnosis or when complications arise during and after therapy. In some circumstances, CEUS could replace CT or MR imaging, which exposes the patient to radiation and sedation, adds cost, can create anxiety, and usually necessitates the administration of an intravenous contrast agent. An added benefit of CEUS is that ultrasound contrast agents (UCA) are not metabolized by the kidneys and can be safely administered to patients with renal insufficiency. Additionally, rates of adverse reactions

J. Squires
Department of Radiology,
Children's Hospital of Pittsburg, Pittsburg, PA, USA
e-mail: judy.squires@chp.edu

A. Srinivasan
Department of Radiology, Children's Hospital of Philadelphia, Perelman School of Medicine, University of Pennsylvania, Philadelphia, PA, USA
e-mail: srinivasaa@email.chop.edu

M. B. McCarville (✉)
Department of Diagnostic Imaging, St. Jude Children's Research Hospital, Memphis, TN, USA
e-mail: Beth.McCarville@STJUDE.ORG

P. S. Sidhu et al. (eds.), *Contrast-Enhanced Ultrasound in Pediatric Imaging*,
https://doi.org/10.1007/978-3-030-49691-3_18

to UCA are low, similar to that of gadolinium agents for MR imaging. With the recent US FDA approval of a UCA for children, coupled with an increasing emphasis on medical cost containment and radiation and anesthesia reduction, the role of this important alternative imaging modality is expanding in pediatric clinical practice. In this chapter, we illustrate the value of CEUS in pediatric oncology, specifically in the diagnosis and management of pediatric malignancies, in assessing complications of therapy and in guiding interventional procedures. The potential role of CEUS in assessing tumor response to therapy and as a treatment modality is also presented.

18.2 CEUS of Pediatric Solid Tumors

In the pediatric oncology patient setting, CEUS has tremendous potential for diagnostic problem-solving, given its excellent safety and cost profile compared to CT and MR imaging, both of which utilize contrast agents that may be contraindicated in patients with renal insufficiency. Compared to CT, major advantages of CEUS are its lack of ionizing radiation, excellent temporal resolution and the ability to easily image during all phases of contrast enhancement. Compared to MR imaging, the major advantages of CEUS are increased accessibility, faster examination, lower cost, and the ability to perform the examination without sedation. In young patients (usually between 6 months and 7 years), sedation is almost always necessary to provide MR images that are of diagnostic quality, and general anesthesia would be required to obtain sequences that require breath holds. Anesthesia or sedation medications carry a risk of adverse events in this patient population, and this may be avoided with CEUS.

The use of CT or MR imaging contrast agents also poses potential risks for pediatric oncology patients, as renal excretion of contrast agents may be impaired due to concomitant use of chemotherapeutic agents, and this may increase the risk of further injury or nephrogenic systemic fibrosis. The deposition of gadolinium in the body has also been described, although there is currently no known clinical significance. Finally, these patients usually undergo multiple imaging evaluations during the course of diagnosis, treatment, and disease surveillance, and repeat imaging may compound the aforementioned risks [2, 3].

There are limitations to CEUS imaging in the pediatric oncology setting. Most importantly, tumor staging is not possible with CEUS. Although CEUS can confidently diagnose malignancy, once a diagnosis of malignancy has been made, further evaluation with CT and/or MR imaging for tumor staging is mandatory. In patients who have multiple, non-adjacent lesions with different appearances (and therefore potentially several different coexistent types of lesions), multi-phase CT and/or MR imaging should be considered to allow easier characterization of each lesion. It should be noted that although evaluation of only up to two lesions is possible in the arterial phase at CEUS, scanning through the entire organ is possible in the delayed phase of contrast enhancement, which enables limited evaluation of additional lesions.

In the pediatric oncology setting, CEUS may be most helpful to determine if a newly detected liver lesion is benign or malignant [4]. Specifically, although there are various appearances of different malignancies in the arterial phase, liver lesions that do not retain contrast compared to the background liver parenchyma in the delayed phase may be confidently diagnosed as malignant with high specificity [5, 6]. Conversely, liver lesions that retain contrast on the delayed phase of CEUS may confidently be diagnosed as benign, with sensitivity of up to 98% and negative predictive value of 100% in pediatric patients [4]. Specific examples of the use of CEUS to characterize different types of pediatric liver tumors are detailed below, as is the use of CEUS to characterize lesions in other organs.

18.3 Malignant Liver Lesions

18.3.1 Hepatoblastoma

Hepatoblastoma is the most common primary pediatric liver tumor and is usually diagnosed within the first 3 years of life [7]. Although many associated conditions have been described, including Beckwith–Wiedemann syndrome, very low birth weight and premature infants, most cases of hepatoblastoma are sporadic [8–10]. Histologically, hepatoblastoma is composed either entirely of epithelial cells or a mixture of epithelial and mesenchymal cells. There are several subtypes of hepatoblastoma, including fetal, embryonal, pleomorphic epithelial, small cell undifferentiated, and cholangioblastic. Tumors with more histologically mature cell lines usually have a better prognosis than tumors with undifferentiated or immature cell lines [11]. Hepatoblastoma staging relies on the PRE-Treatment EXTent of Tumor (PRETEXT) staging system to standardize the imaging evaluation and to stratify tumors that may be surgically resectable and those which are unresectable. The PRETEXT group (I, II, III, or IV) is based on the number of contiguous tumor-free liver sections. Several annotation factors were recently updated, which define areas of extrahepatic involvement including tumor involvement of the inferior vena cava, hepatic veins, and portal veins [12, 13].

Contrast-enhanced ultrasound can be used to risk stratify patients who have a liver lesion into malignant or non-malignant categories. Although the appearance of hepatoblastoma at CEUS is not well described [14], like other non-hepatocellular primary liver tumors, the washout phase of contrast enhancement is likely most helpful to confirm a diagnosis of malignancy (Fig. 18.1). No characteristic arterial phase or portal venous

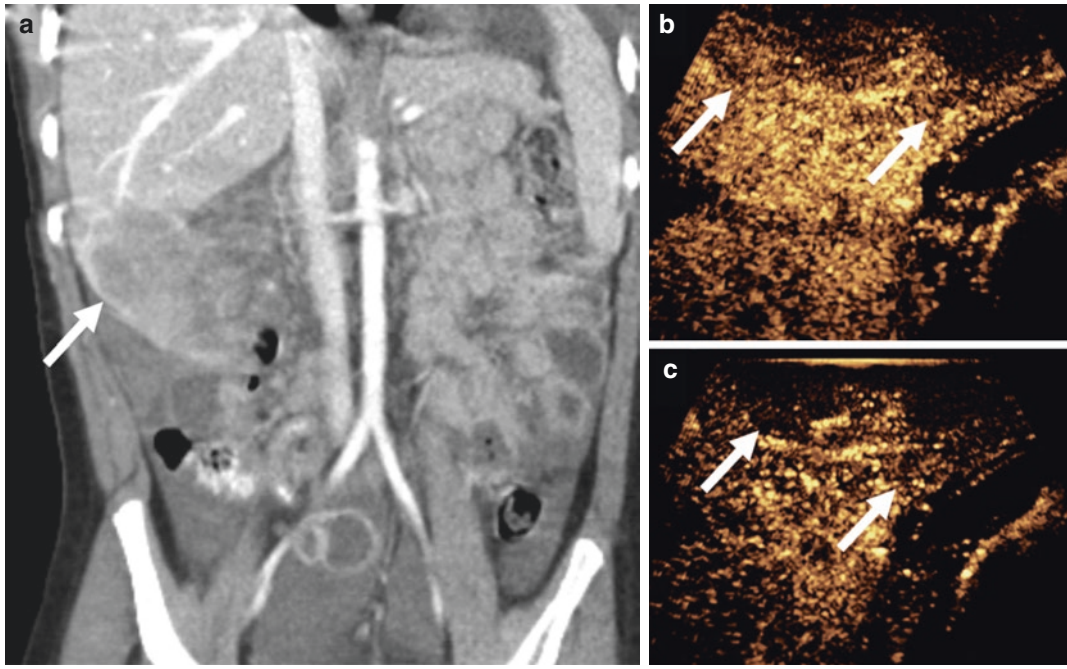

Fig. 18.1 A 2-year-old male with a hepatoblastoma. (**a**) Coronal contrast-enhanced CT demonstrates the pedunculated primary tumor arising from the inferior right hepatic lobe (arrow). (**b**) Contrast-enhanced ultrasound obtained at 11 s demonstrates hypo-enhancement of the mass in the arterial phase. (**c**) The lesion demonstrates early portal venous peripheral washout at 28 s

appearance has yet been described for hepatoblastoma. Once a diagnosis of hepatoblastoma is suspected or confirmed, further evaluation with CT or MR imaging is required for appropriate PRETEXT staging of the tumor beyond the liver. Chest CT is required to evaluate the lungs, which is the most common site of hepatoblastoma metastasis [13]. CEUS may be beneficial for evaluating vascular involvement of the tumor, if questions remain after either CT or MR imaging, as it may demonstrate enhancement of tumor thrombus with good temporal and spatial resolution.

18.3.2 Hepatocellular Carcinoma

Hepatocellular carcinoma (HCC) is the second most common primary pediatric liver tumor after hepatoblastoma, and usually affects children 10–14 years of age. In distinction to hepatoblastoma, HCC is rarely encountered in children less than 5 years of age [15]. Unlike in adults, the majority (almost 70%) of cases of HCC in pediatric patients occur in patients with no underlying liver disease [16]. However, cirrhosis increases the risk of developing HCC. Causes of cirrhosis in children include Alagille syndrome, glycogen storage diseases, Hepatitis B and C, progressive familial intrahepatic cholestasis (PFIC) types 2 and 3, Wilson disease, biliary atresia, Fanconi syndrome, and tyrosinemia [17]. Also in distinction to HCC in adults, pediatric HCC usually presents with larger tumor size, more advanced disease, and higher rates of both locoregional and distant metastatic disease at presentation [18]. However, pediatric HCC usually has a better response to chemotherapy compared to adults. Additionally, whereas adults must often meet specific criteria for liver transplantation, children with unresectable HCC may be treated by liver transplantation regardless the size of the tumor or number of tumor lesions in the liver, as long as there is no vascular invasion or extrahepatic disease [17, 19].

Fibrolamellar HCC is considered a distinct entity from HCC. Of all types of HCC encountered under the age of 20 years, fibrolamellar accounts for almost 30% [20, 21]. Serum alpha fetoprotein level is almost always normal, and there is typically no underlying hepatocellular disease in these patients. Unless resectable, fibrolamellar HCC has a poor prognosis. Another variant tumor of HCC is the recently described hepatocellular malignant neoplasm not otherwise specified (NOS), formerly referred to as transitional liver cell tumor because of the admixture of both hepatocellular and hepatoblastoma histopathologic components [22]. These tumors have been described to have highly elevated serum alpha fetoprotein levels and worse outcomes than traditional hepatoblastoma [22, 23].

The CEUS appearance of HCC in children has not yet been well described. However, the appearance is likely to be similar to that described in adults. In adults, HCC classically demonstrates early arterial enhancement, with late-phase subtle washout [24]. In contradistinction, metastatic liver tumors and non-HCC primary liver tumors have much more prominent and earlier washout than HCC.

18.3.3 Liver Metastases

Metastasis is the most frequently encountered pediatric liver neoplasm and the most common pediatric tumors to metastasize to the liver include neuroblastoma, Wilms tumor, and lymphoma [15]. Identification of a primary malignancy aids in diagnosing a focal liver lesion as a metastasis, particularly at initial diagnosis. However, it should be noted that almost 20% of children treated for a solid malignancy develop focal liver lesions after therapy [25] and they are often discovered on routine surveillance imaging raising concern for tumor recurrence. In such cases, CEUS provides a rapid, low-risk, low cost, and highly accurate method of distinguishing benign from malignant etiologies. This approach allows almost immediate feedback to the physician and parent/care giver, thus alleviating anxiety and avoiding the need for additional imaging and delays in treatment. Liver metastases are characterized by early, marked washout of the UCA, normally by 1 min after injection (Fig. 18.2) [24].

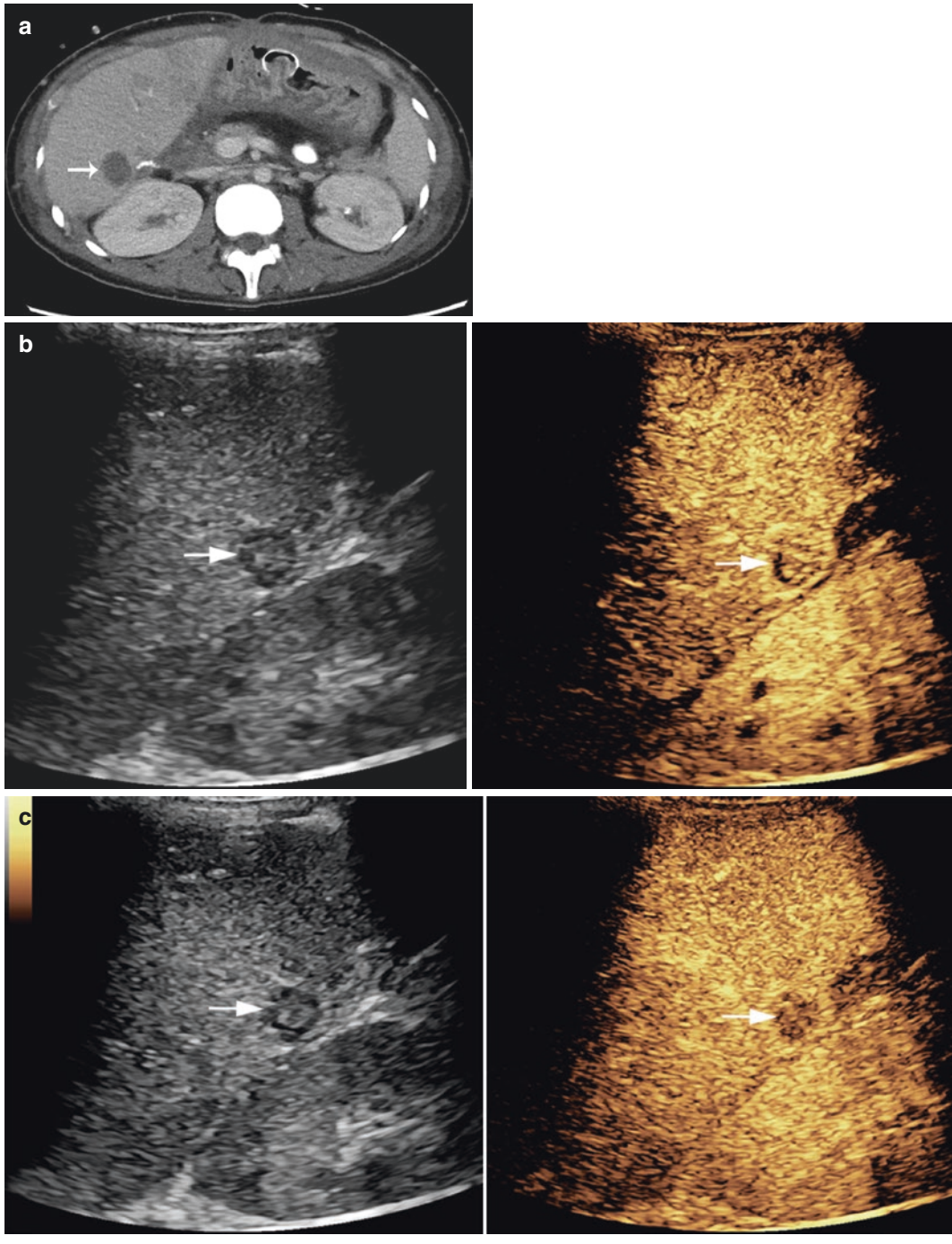

Fig. 18.2 A 20-year-old male with desmoplastic small round cell tumor. (**a**) Axial contrast-enhanced CT shows a liver lesion (arrow) that was suspicious for metastatic disease. (**b**) Contrast-enhanced ultrasound split screen image of the liver lesion (arrows) in the early arterial phase demonstrates patchy iso-enhancement compared to surrounding normal liver. (**c**) In the early portal venous phase, the lesion (arrow) demonstrates early washout. (**d**) In the late portal venous phase the lesion (arrow) shows clear washout compared to surrounding normal liver. Early washout, such as seen here, is typical of metastatic disease in the liver

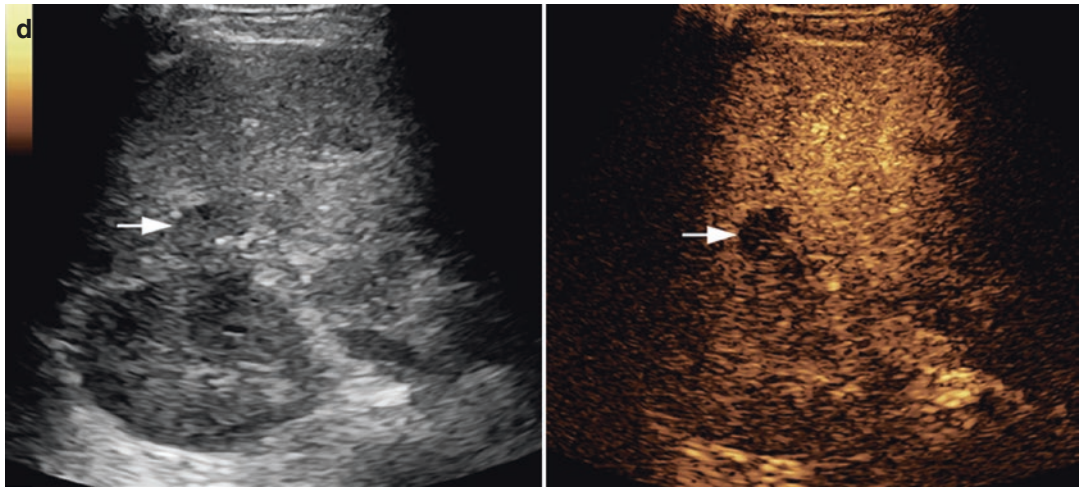

Fig. 18.2 (continued)

18.4 Benign Liver Lesions

18.4.1 Hemangioma

Infantile hepatic hemangioma is the most common benign liver mass in children [26–28]. Infantile hemangiomas are true vascular neoplasms that develop within a few weeks to months of life and are not present at birth. These lesions demonstrate GLUT1 staining on pathology. The CEUS appearance of infantile hemangioma is not well reported, however, the CEUS enhancement pattern is expected to follow that seen on other modalities, including early peripheral arterial enhancement, enhancement through the portal venous phase, and complete isoenhancement in the delayed phase, with minimal subtle washout possible (Fig. 18.3) [5, 29]. The primary differential considerations for infantile hemangiomas are metastases and multifocal hepatoblastoma, which will demonstrate early (<1 min) and pronounced washout. Marked washout has not been described with infantile hepatic hemangioma at CEUS.

Congenital hepatic hemangiomas are usually solitary lesions. Unlike infantile hepatic hemangioma, congenital hepatic hemangiomas are present, and fully proliferated, at birth. These lesions are GLUT1 negative and most commonly spontaneously involute by 1 year of life [30]. Like infantile hemangioma, the CEUS appearance of congenital hemangioma is not well described. Limited reports describe these lesions as heterogeneously enhancing in the arterial phase with either complete or incomplete fill-in on delayed phases. Areas of contrast fill-in will have sustained enhancement in delayed phases [5]. The primary differential consideration for congenital hemangioma is hepatoblastoma, which is expected to have early contrast washout, an appearance not described with congenital hemangioma.

18.4.2 Focal Nodular Hyperplasia

Focal nodular hyperplasia (FNH) is a regenerative mass and is typically asymptomatic. Focal nodular hyperplasia is the second most common benign liver lesion in older children and young adults, but is very uncommon in young children. The exception is that FNH is frequently encountered in childhood cancer survivors [25]. Ultrasound is often used for screening and follow-up of patients with a known primary malignancy, but because FNH has a non-specific conventional grayscale US appearance, additional imaging is necessary for characterization. The major advantage of CEUS over CT and MR imaging is that FNH can be confidently diag-

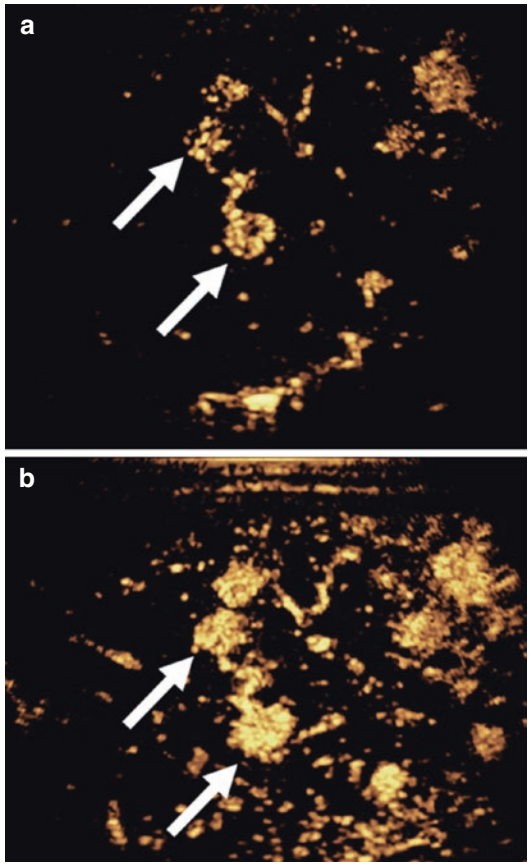

Fig. 18.3 A 4-month-old female with multiple cutaneous infantile hemangiomas. (**a**) Contrast-enhanced ultrasound images obtained in the early arterial phase at 10 s, showing two (arrows) rapidly enhancing lesions (arrows), with centripetal flow. (**b**) Contrast-enhanced ultrasound images in the later arterial phase demonstrates the complete centripetal fill-in (arrows), compatible with infantile hepatic hemangiomas

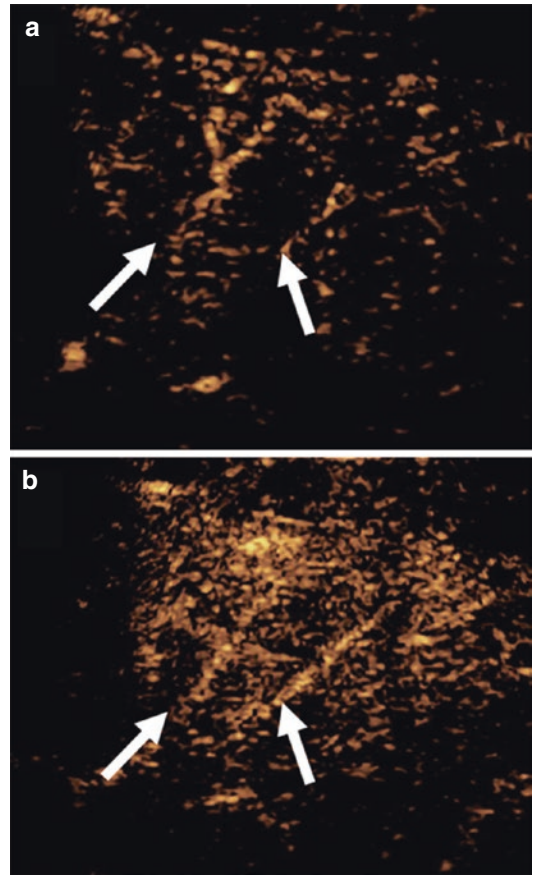

Fig. 18.4 A 10-year-old female with non-alcoholic fatty liver disease. (**a**) Contrast-enhanced ultrasound early arterial phase images obtained at 12 s, showing initial spoke wheel pattern of arterial enhancement to the central aspect of the lesion (arrows). (**b**) In the later arterial phase, at 15 s, the spoke-wheel pattern is more established with the beginnings of diffuse lesion enhancement (arrows), diagnostic of focal nodular hyperplasia. The lesion will remain hyperenhancing to background liver in all vascular phases

nosed with CEUS the same day a new liver lesion is discovered, which is not always possible with CT and/or MR imaging [31]. This rapid and definitive diagnosis of FNH with CEUS offers the additional benefit of decreasing patient and parental anxiety about the unknown etiology of a new liver lesion in a patient who is at risk for metastatic disease [25, 32].

At CEUS, FNH are hypervascular lesions that have a stellate appearance of early arterial enhancement (Fig. 18.4). A tortuous feeding artery may additionally be seen. An FNH typically has complete or incomplete centrifugal pattern contrast fill-in during the portal venous phase, with a central scar possible, as seen with other modalities. An FNH has sustained enhancement about 90% of the time, again unlike metastases which will have early and noticeable washout [33–36].

18.5 Benign and Malignant Renal Lesions

Intravenous CEUS for characterization of renal lesions is much less well described than hepatic lesions. However, CEUS may aid in the diagnosis of certain renal lesions.

18.5.1 Complex Renal Cysts

Simple renal cysts, including those with an imperceptible wall, posterior acoustic enhancement, and no internal septations, can usually be easily diagnosed with grayscale ultrasound. This is particularly true in pediatric patients, in whom a smaller body habitus allows visualization of the kidneys with higher resolution than in adults. However, when adequate visualization of simple and complex renal cysts is not possible, CEUS may be helpful for additional evaluation. Specifically, CEUS can demonstrate the presence of internal septations with greater sensitivity than CT and can more easily demonstrate the thin or nodular character of septations (Fig. 18.5) [37]. When present, thick nodular septations raise concern for possible malignancy and additional imaging may be necessary.

18.5.2 Renal Tumors

Primary renal tumors encountered in childhood, including Wilms tumor, rhabdoid tumor, and clear cell sarcoma, have not yet been described to have a characteristic appearance on CEUS. Currently, CEUS for renal tumors is often reserved for problem-solving and surgical planning, including better delineation of vascular involvement.

18.5.3 Renal Pseudotumor

Pseudotumor, including a hypertrophied column of Bertin or dromedary hump, is often easily diagnosed with grayscale and color Doppler US. However, CEUS may increase diagnostic confidence and provide better reassurance that a contour abnormality is not neoplastic. On CEUS, these lesions follow the enhancement appearance of the background renal parenchyma throughout all contrast phases, unlike a true renal tumor [38].

18.6 CEUS in Pediatric Oncologic Interventions

Interventional oncology involves application of interventional radiology techniques to the diagnosis and treatment of cancer and relies on image guidance to increase the efficacy and precision of targeted minimally invasive therapy. Broadly, the role of interventional radiology in the care of cancer can be subdivided into three categories:

(a) Interventions for diagnosis: biopsy (tumors of soft tissue and bone, and marrow), lumbar puncture.
(b) Interventions for supportive care: venous access (temporary and long term), drainage procedures (pleural and peritoneal fluid, abscesses), additional interventions for less common complications such as venous thrombosis.
(c) Interventions to treat the primary tumor or palliate metastasis: tumor ablation, tumor embolization.

Interventions in the first two categories are commonly applied in pediatrics. However, the third category, while an established pillar of cancer therapy in adults, is only recently gaining recognition in pediatric oncology.

Ultrasound has been established as a core modality in pediatric image guidance because of the advantages it offers over other modalities (multiplanar imaging, excellent temporal and good spatial resolution, portability, lack of ionizing radiation) previously described in this chapter. Contrast-enhanced ultrasound adds to these advantages, by improving contrast resolution for procedure guidance, given the lower contrast resolution of grayscale US relative to CT or MR imaging. Contrast-enhanced ultrasound can play in guiding procedures in pedi-

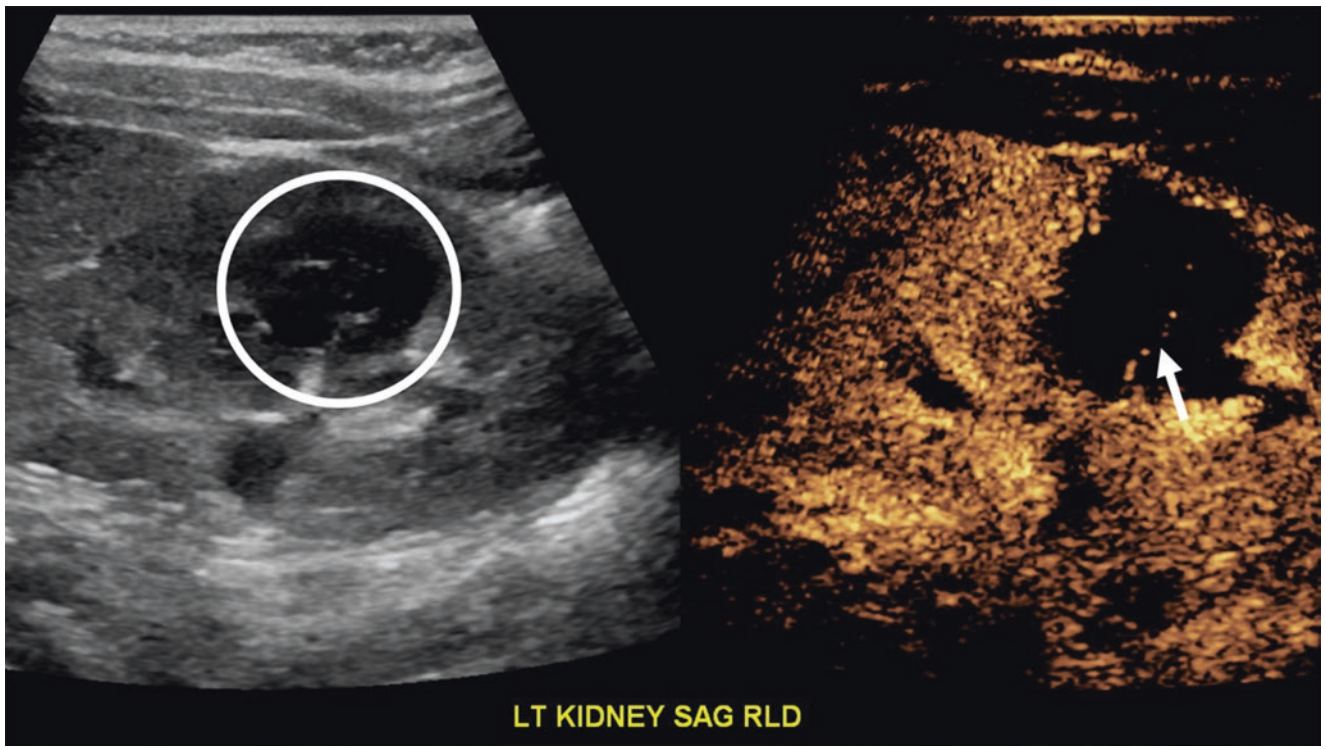

Fig. 18.5 A 5-year-old male with autosomal dominant polycystic kidney disease. A split screen image during contrast-enhanced ultrasound demonstrates a complex-appearing cyst (circle), with internal echoes, and a thin linear enhancing septation (arrow), compatible with a benign cyst, Bosniak Type 2

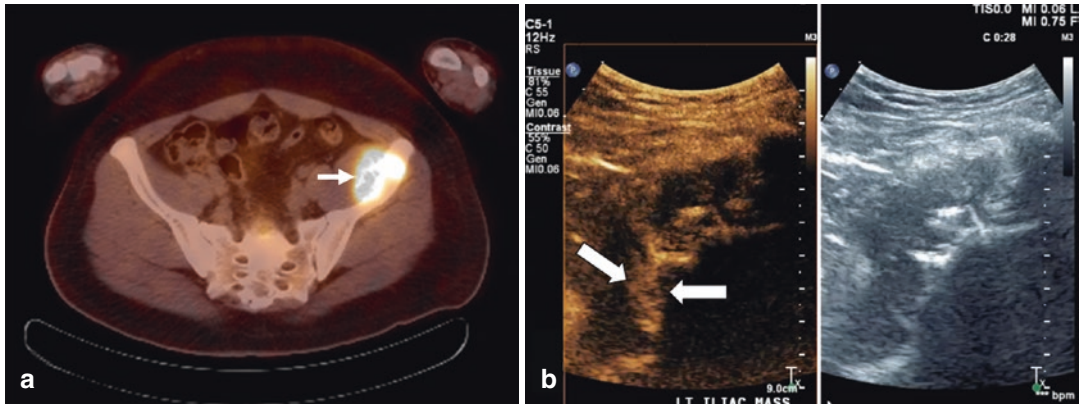

Fig. 18.6 A 19-year-old male with a mass in the left iliac fossa. (**a**) A left-sided mass is demonstrated on an ^{18}F-fluorodeoxyglucose positron emission tomography (FDG-PET)-CT scan, as avid uptake (arrow). A biopsy of the superficial component yielded only necrotic tissue. (**b**) On the CEUS examination, the lesion shows enhancement of only the deep component alongside the bone (arrows). This was targeted for biopsy, and on histology was a deposit of Hodgkin lymphoma

atric oncology, with a focus on biopsy and tumor ablation, which are among the best-supported indications for the use of CEUS in interventional radiology [39]. These procedures involve intravascular administration of the UCA, which enables the visualization of perfusion at the microvascular level, and thus provides a reliable assessment of tumor vascularity and viability. Technical aspects of CEUS in interventional radiology, as well as applications of CEUS in the above-noted procedures for supportive care, are discussed in Chap. 20.

18.6.1 Biopsy

Ultrasound contrast agents are sometimes useful to increase the conspicuity of small lesions in the liver. In children, this is often in the setting of a concern for metastasis, as primary liver neoplasms, while less common in children, are frequently large and readily visible on sonography at presentation. More frequently, CEUS is used to determine the optimum site of biopsy within the tumor, as enhancement indicates regions of intact microvasculature, suggestive of areas of most tumor viability and least necrosis (Fig. 18.6). Biopsy of non-necrotic regions should increase diagnostic yield, and the need for high-viability may be particularly salient if next-generation sequencing for characterization of signal transduction defects is desired. In this regard, CEUS can shorten the procedure, as it can increase the confidence of adequate sampling, thereby decreasing the number of passes the interventionist would make, and also decrease the need for frozen section analysis during the procedure. If there is concern for significant post-procedure hemorrhage, this can be assessed by CEUS of the region of biopsy, often faster and with less logistical complexity than CT [39]. The excellent depiction of vasculature allows the easy detection of pseudoaneurysms and active extravasation [40].

Contrast-enhanced ultrasound may also be used to guide decisions during the procedure, and this entails applying diagnostic principles of CEUS, particularly of liver lesions, described in Chap. 8 and in the prior section of this chapter. It is, therefore, important that the CEUS technique applied in interventional radiology be consistent with that used for diagnostic applications. As children who undergo interventional procedures have venous access established and are under sedation or anesthesia, diagnostic characterization of a lesion can be performed in a manner that is more con-

trolled and convenient for the radiologist. One illustrative scenario is that a lesion may be demonstrated to be benign in the interventional suite, therefore obviating the need for biopsy and sedation (Fig. 18.7).

18.6.2 Tumor Ablation

Tumor ablation involves the application of probes that induce thermal injury (radiofrequency ablation, microwave ablation, cryoablation, high-intensity focused ultrasound) or the injection of chemicals (ethanol ablation) in the

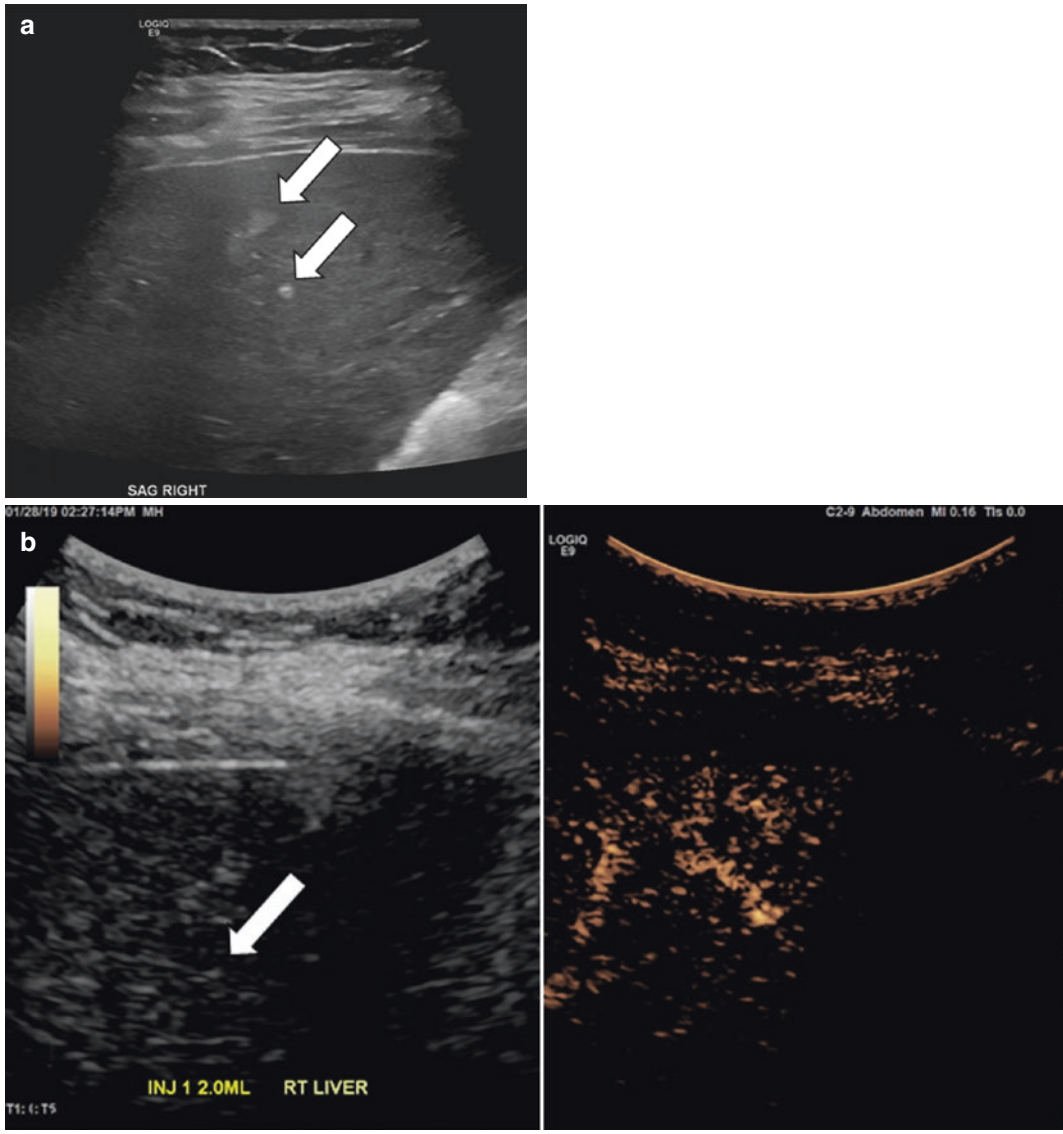

Fig. 18.7 A 6-year-old male with history of neuroblastoma. (**a**) Grayscale US demonstrating multiple echogenic lesions (arrows), and the patient was referred for a biopsy. (**b**) The CEUS of the liver performed by the interventionist just prior to biopsy, which showed no enhancement of the lesion (arrows) in the arterial phase. (**c**) In the portal venous phase, the lesions (arrows) are isoenhancing with the remainder of the liver, consistent with focal fat infiltration and no biopsy was performed

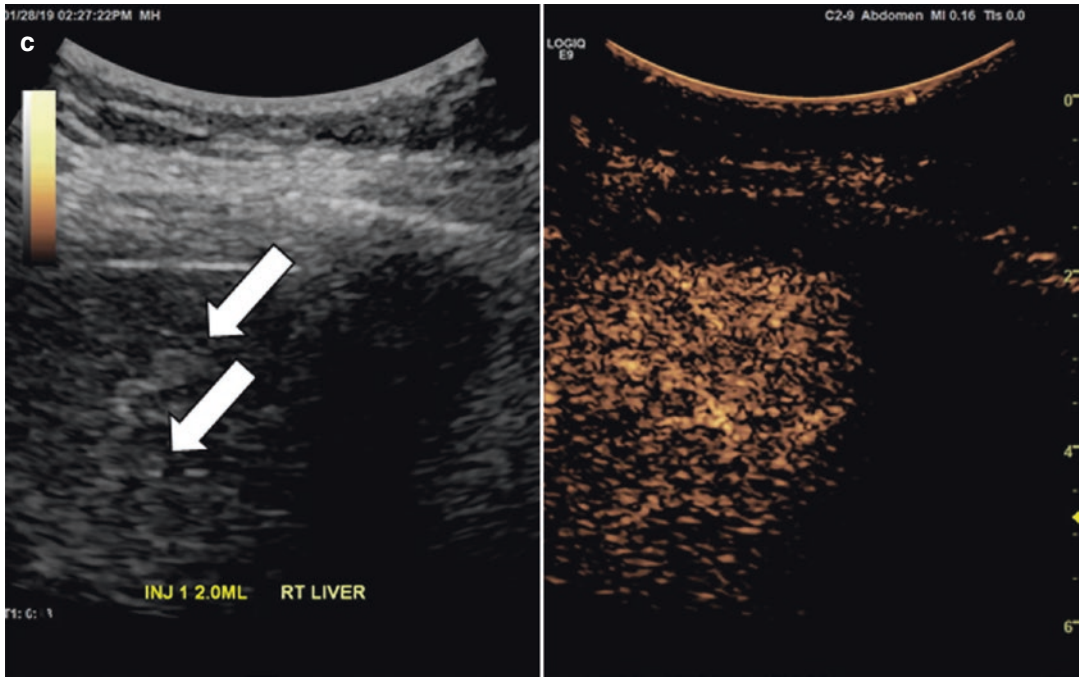

Fig. 18.7 (continued)

tumor. For technical success, the ablation procedure must precisely treat the tumor and a surrounding margin of normal tissue; it is also important to avoid injury to surrounding organs. The most common application of CEUS in this realm is intra-procedural feedback: tumor vascularity is assessed before and after ablation. A lack of contrast enhancement provides strong confirmation of adequacy of treatment (Figs. 18.8 and 18.9), and residual perfusion of the tumor would indicate that further ablation is necessary. For this purpose, CEUS provides superior spatial and temporal resolution of tissue perfusion than CT or MR imaging, as perfusion can be visualized in real-time and with a small field-of-view. In adults undergoing ablation of hepatocellular carcinoma, the absence of perfusion after ablation has shown to be highly predictive of therapeutic success, and residual tumor detection has been shown to be at least commensurate with other imaging modalities [39]. It should be noted that the immediate post-ablation assessment of tissue perfusion is best suited for cryoablation, as collection of gas in the treatment area from tissue vaporization will hinder US assessment immediately after radiofrequency or microwave ablation [39]. In the latter settings, CEUS assessment may have to be performed shortly after the procedure. Selective trans-arterial embolization of tumors, most frequently in the liver, is an established procedure in interventional oncology, and specific subsets include "bland" particle embolization, chemoembolization, embolization with drug-eluting beads, and radioembolization with beta-emitting particles. Tumor embolization is much less frequently performed in children, largely due to the different spectrum of pediatric cancers and efficacy of conventional treatment, but is occasionally indicated. During trans-arterial embolization of liver tumors, intra-procedural CEUS with arte-

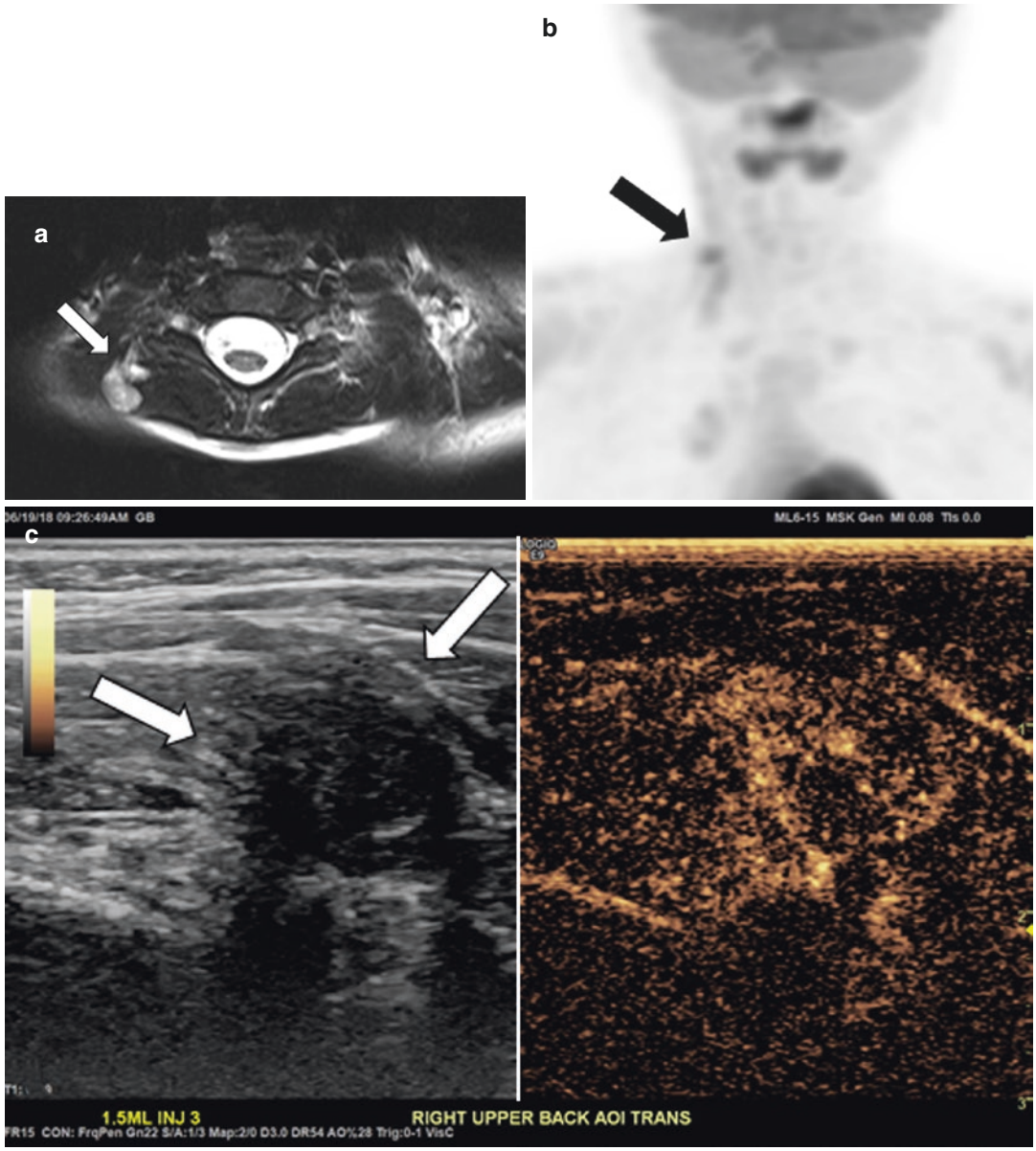

Fig. 18.8 An 8-year-old male with history of a right paraspinal rhabdomyosarcoma. (**a**) A lobulated metastatic recurrence (arrow) in the right posterior supraclavicular soft tissues on axial single T2-weighted MR image. (**b**) On the ^{18}FDG PET, there is uptake in the mass (arrow). (**c**) On the corresponding transverse, arterial phase CEUS shows enhancement of the lesion (arrows). (**d**) The corresponding sagittal CEUS 3 months after percutaneous cryoablation of the metastatic lesion (arrows) show no residual uptake or contrast enhancement

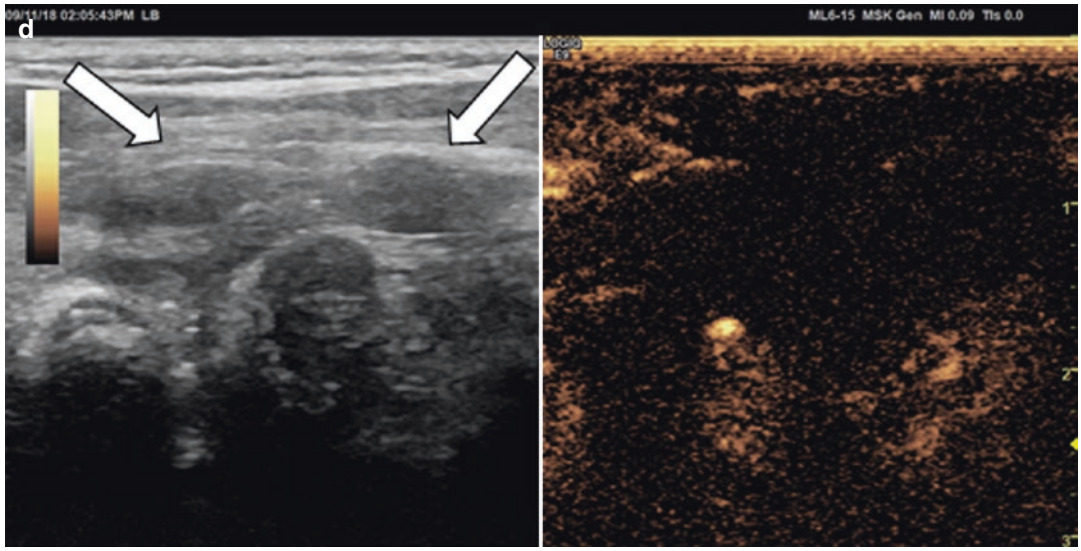

Fig. 18.8 (continued)

rial administration of a UCA has been used to guide embolization (confirm appropriate subselectivity prior to embolization) and to determine adequacy of treatment, similar to tumor ablation [41].

18.7 Future Directions of CEUS in Oncology

The role of CEUS in oncology is rapidly evolving and there are a wide variety of potential applications in the management of adult and pediatric oncology patients. Because pediatric malignancies are relatively rare, much of the clinical research in this area is occurring in the adult population. However, the principles can be easily applied to the pediatric population which is the ideal population for the use of ultrasound in general. Adult clinical investigators have reported the value of CEUS in distinguishing benign from malignant thyroid nodules, endometrial hyperplasia from neoplasms, benign from malignant soft tissue masses, low from high-grade bladder carcinoma, benign from malignant lymph nodes, benign prostatic hypertrophy from prostate carcinoma and to monitor response to therapy in breast cancer, liver metastases, and liver tumors treated with trans-arterial chemoembolization and radiofrequency ablation [42–64]. Clearly, there is considerable interest in the development of CEUS to diagnose malignancies and assess treatment response in the oncology population.

Angiogenesis (the development of new blood vessels) is essential for tumor development, growth, and metastasis and accurate imaging and quantitation of tumor vascularity is an important area of investigation [65, 66]. Contrast-enhanced ultrasound has unique attributes that make it more appealing for measuring tumor blood flow than other imaging modalities and it is emerging as a reliable method of quantitating tumor vascularity and assessing response of a variety of adult malignancies [67–76]. Because UCAs remain in the vascular space, the pharmacodynamics is less complex than those for CT and MR contrast agents that freely diffuse across the vascular membrane. Additionally, CEUS is less expensive than contrast-enhanced CT and MR imaging, can be performed at the bedside, does not require sedation, and, most importantly in the pediatric population, does not expose the patient to the harmful effects of ionizing radiation. With the use of contrast-specific software, several perfu-

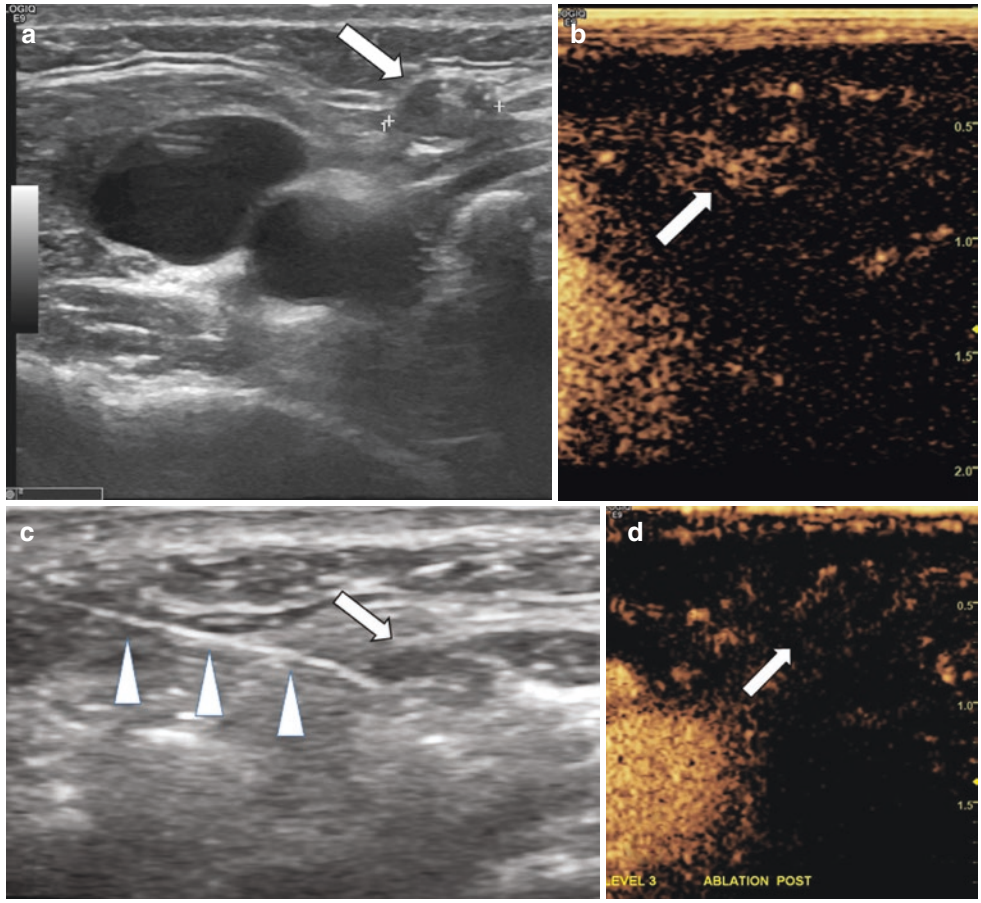

Fig. 18.9 A 16-year-old female with relapsed papillary cell thyroid cancer. (**a**) A lymph node with a metastatic deposit shown on the grayscale US (arrow). (**b**) The corresponding CEUS in arterial phase (arrow) showing arterial enhancement, with patchy areas of non-enhancement, early washout occurred later in the study. (**c**) Grayscale image during the US-guided ethanol ablation of the metastasis (arrow); needle shown with arrowheads. (**d**) The CEUS of the lesion (arrow) immediately after the procedure showing no residual enhancement, consistent with complete ablation. (Case courtesy of Dr. Fernando Escobar)

sion parameters can be quantitated. These include peak enhancement intensity, rise time, mean transit time, and area under the curve. These parameters can be quantitated at baseline (before initiation of therapy) and then remeasured at specific time points during therapy to assess change. The baseline values or the change between baseline and follow-up time points, may provide unique insight into the biological behavior of tumors that could ultimately be predictive of patient outcome.

The role of CEUS in oncology is also expanding beyond diagnosis and treatment response into molecular imaging and targeted therapy. Several methods of UCA-mediated drug delivery are under investigation in preclinical and clinical trials, including for direct and indirect drug delivery and development of nano-scaled UCAs. By applying an ultrasound pulse, a UCA can be destroyed to create microjets or be excited to physically interact with the vascular wall and create pores in the vascular membrane. This approach results in enhanced vessel permeability allowing co-administered drugs to extravasate into the tumor interstitial space (indirect drug delivery). Alternatively,

the UCA shell itself can be loaded with a drug that is released during microbubble destruction and then extravasates, through US-mediated, permeabilization of the vascular membrane (direct drug delivery). However, with these techniques, it is difficult to achieve high enough doses of the therapeutic agent. Nanobubble, nanoparticle, and nanodroplet UCA are capable of passing through the damaged endothelium of tumor vessels and accumulate in the extracellular space without the need to enhance vessel permeability. Once in the extracellular space they can be manipulated to cause tissue cavitation and release drugs directly into the tumor. This approach could be especially advantageous in treating brain tumors because the nanoparticles could pass through the blood–brain barrier. Although some of these agents have a short shelf life and handling difficulties, they provide promising future clinical directions and exciting research opportunities [77].

18.8 Conclusions

Contrast-enhanced ultrasound is especially well suited for pediatric use because the contrast agents are safe in children, do not require prior laboratory testing or sedation, the equipment is accessible, and, importantly, does not expose the patient to the harmful effects of ionizing radiation. The latter benefit is particularly relevant to the pediatric cancer population because these children undergo innumerable imaging examinations during diagnosis and staging, throughout treatment, and during surveillance after the completion of therapy. We have presented information to promote the use of CEUS in pediatric oncology patients and have described current clinical applications including distinguishing benign from malignant liver and renal masses, guidance of interventional procedures, and the assessment of tumor ablation. There is ongoing research investigating the value of CEUS to quantitatively assess the effect of cancer therapy and as a therapeutic tool in oncology. These developments will likely significantly expand the role and increase the impact of CEUS in the management of pediatric oncology patients in the near future.

References

1. Berrington de Gonzalez A, Salotti JA, McHugh K, Little MP, Harbron RW, Lee C, et al. Relationship between pediatric CT scans and subsequent risk of leukemia and brain tumors: assessment of the impact of underlying conditions. Br J Cancer. 2016;114(4):388–94.
2. Ruggiero A, Ferrara P, Attina G, Rizzo D, Riccardi R. Renal toxicity and chemotherapy in children with cancer. Br J Clin Pharmacol. 2017;83(12):2605–14.
3. Latham GJ, Greenberg RS. Anesthetic considerations for the pediatric oncology patient—part 2: systems-based approach to anesthesia. Paediatr Anaesth. 2010;20(5):396–420.
4. Jacob J, Deganello A, Sellars ME, Hadzic N, Sidhu PS. Contrast enhanced ultrasound (CEUS) characterization of grey-scale sonographic indeterminate focal liver lesions in pediatric practice. Ultraschall Med (Stuttgart, Germany: 1980). 2013;34(6):529–40.
5. Anupindi SA, Biko DM, Ntoulia A, Poznick L, Morgan TA, Darge K, et al. Contrast-enhanced US assessment of focal liver lesions in children. Radiographics. 2017;37(6):1632–47.
6. Sidhu PS, Cantisani V, Deganello A, Dietrich CF, Duran C, Franke D, et al. Role of contrast-enhanced ultrasound (CEUS) in pediatric practice: an EFSUMB position statement. Ultraschall Med (Stuttgart, Germany: 1980). 2017;38(1):33–43.
7. Czauderna P, Lopez-Terrada D, Hiyama E, Haberle B, Malogolowkin MH, Meyers RL. Hepatoblastoma state of the art: pathology, genetics, risk stratification, and chemotherapy. Curr Opin Paediatr. 2014;26(1):19–28.
8. Shuman C, Beckwith JB, Weksberg R. Beckwith-Wiedemann syndrome. In: Adam MP, Ardinger HH, Pagon RA, Wallace SE, Bean LJH, Stephens K, et al., editors. GeneReviews®. Seattle, WA: University of Washington; 1993.
9. Spector LG, Birch J. The epidemiology of hepatoblastoma. Paediatr Blood Cancer. 2012;59(5):776–9.
10. Trobaugh-Lotrario AD, Lopez-Terrada D, Li P, Feusner JH. Hepatoblastoma in patients with molecularly proven familial adenomatous polyposis: clinical characteristics and rationale for surveillance screening. Paediatr Blood Cancer. 2018;65(8):e27103.
11. Sharma D, Subbarao G, Saxena R. Hepatoblastoma. Semin Diagn Pathol. 2017;34(2):192–200.

12. Roebuck DJ, Aronson D, Clapuyt P, Czauderna P, de Ville de Goyet J, Gauthier F, et al. 2005 PRETEXT: a revised staging system for primary malignant liver tumors of childhood developed by the SIOPEL group. Paediatr Radiol. 2007;37(2):123–32; quiz 249–50.
13. Towbin AJ, Meyers RL, Woodley H, Miyazaki O, Weldon CB, Morland B, et al. 2017 PRETEXT: radiologic staging system for primary hepatic malignancies of childhood revised for the pediatric hepatic international tumor trial (PHITT). Paediatr Radiol. 2018;48(4):536–54.
14. McCarville MB. Contrast-enhanced sonography in pediatrics. Paediatr Radiol. 2011;41(Suppl 1):S238–42.
15. Chung EM, Lattin GE Jr, Cube R, Lewis RB, Marichal-Hernandez C, Shawhan R, et al. From the archives of the AFIP: Pediatric liver masses: radiologic-pathologic correlation. Part 2. Malignant tumors. Radiographics. 2011;31(2):483–507.
16. Czauderna P, Mackinlay G, Perilongo G, Brown J, Shafford E, Aronson D, et al. Hepatocellular carcinoma in children: results of the first prospective study of the International Society of Pediatric Oncology group. J Clin Oncol. 2002;20(12):2798–804.
17. Walther A, Tiao G. Approach to pediatric hepatocellular carcinoma. Clin Liver Dis. 2013;2(5):219–22.
18. Lau CS, Mahendraraj K, Chamberlain RS. Hepatocellular carcinoma in the pediatric population: a population based clinical outcomes study involving 257 patients from the surveillance, epidemiology, and end result (SEER) database (1973–2011). HPB Surg. 2015;2015:670728.
19. Elshamy M, Aucejo F, Menon KV, Eghtesad B. Hepatocellular carcinoma beyond Milan criteria: management and transplant selection criteria. World J Hepatol. 2016;8(21):874–80.
20. Lopez-Terrada D, Alaggio R, de Davila MT, Czauderna P, Hiyama E, Katzenstein H, et al. Towards an international pediatric liver tumor consensus classification: proceedings of the Los Angeles COG liver tumors symposium. Mod Pathol. 2014;27(3):472–91.
21. Weeda VB, Murawski M, McCabe AJ, Maibach R, Brugieres L, Roebuck D, et al. Fibrolamellar variant of hepatocellular carcinoma does not have a better survival than conventional hepatocellular carcinoma—results and treatment recommendations from the Childhood Liver Tumor Strategy Group (SIOPEL) experience. Eur J Cancer (Oxford, England: 1990). 2013;49(12):2698–704.
22. Prokurat A, Kluge P, Kosciesza A, Perek D, Kappeler A, Zimmermann A. Transitional liver cell tumors (TLCT) in older children and adolescents: a novel group of aggressive hepatic tumors expressing beta-catenin. Med Paediatr Oncol. 2002;39(5):510–8.
23. Zhou S, Venkatramani R, Gupta S, Wang K, Stein JE, Wang L, et al. Hepatocellular malignant neoplasm, NOS: a clinicopathological study of 11 cases from a single institution. Histopathology. 2017;71(5):813–22.
24. Burrowes DP, Medellin A, Harris AC, Milot L, Wilson SR. Contrast-enhanced US approach to the diagnosis of focal liver masses. Radiographics. 2017;37(5):1388–400.
25. Smith EA, Salisbury S, Martin R, Towbin AJ. Incidence and etiology of new liver lesions in pediatric patients previously treated for malignancy. AJR Am J Roentgenol. 2012;199(1):186–91.
26. Chung EM, Cube R, Lewis RB, Conran RM. From the archives of the AFIP: Pediatric liver masses: radiologic-pathologic correlation part 1. Benign tumors. Radiographics. 2010;30(3):801–26.
27. Merrow AC, Gupta A, Patel MN, Adams DM. 2014 Revised classification of vascular lesions from the International Society for the study of vascular anomalies: radiologic-pathologic update. Radiographics. 2016;36(5):1494–516.
28. McLean CK, Squires JH, Reyes-Mugica M, McCormick A, Mahmood B. Hepatic vascular tumors in the neonate: angiosarcoma. J Paediatr. 2018;193:245–248.e1.
29. Stenzel M. Intravenous contrast-enhanced sonography in children and adolescents—a single center experience. J Ultrasonogr. 2013;13(53):133–44.
30. Christison-Lagay ER, Burrows PE, Alomari A, Dubois J, Kozakewich HP, Lane TS, et al. Hepatic hemangiomas: subtype classification and development of a clinical practice algorithm and registry. J Paediatr Surg. 2007;42(1):62–7; discussion 7–8.
31. Rumack CLD. Diagnostic ultrasound. Philadelphia, PA: Elsevier Health Sciences; 2017.
32. Masetti R, Colecchia A, Rondelli R, Martoni A, Vendemini F, Biagi C, et al. Benign hepatic nodular lesions after treatment for childhood cancer. J Paediatr Gastroenterol Nutr. 2013;56(2):151–5.
33. Dietrich CF, Schuessler G, Trojan J, Fellbaum C, Ignee A. Differentiation of focal nodular hyperplasia and hepatocellular adenoma by contrast-enhanced ultrasound. Br J Radiol. 2005;78(932):704–7.
34. Strobel D, Seitz K, Blank W, Schuler A, Dietrich CF, von Herbay A, et al. Tumor-specific vascularization pattern of liver metastasis, hepatocellular carcinoma, hemangioma and focal nodular hyperplasia in the differential diagnosis of 1,349 liver lesions in contrast-enhanced ultrasound (CEUS). Ultraschall Med (Stuttgart, Germany: 1980). 2009;30(4):376–82.
35. Ungermann L, Elias P, Zizka J, Ryska P, Klzo L. Focal nodular hyperplasia: spoke-wheel arterial pattern and other signs on dynamic contrast-enhanced ultrasonography. Eur J Radiol. 2007;63(2):290–4.
36. Kim TK, Jang HJ, Burns PN, Murphy-Lavallee J, Wilson SR. Focal nodular hyperplasia and hepatic adenoma: differentiation with low-mechanical-index contrast-enhanced sonography. AJR Am J Roentgenol. 2008;190(1):58–66.
37. Kapur JOH. Contrast-enhanced ultrasound of kidneys in children with renal failure. J Med Ultrasound. 2015;23(2):86–97.
38. Sparchez Z, Radu P, Sparchez M, Crisan N, Kacso G, Petrut B. Contrast enhanced ultrasound of renal

masses. A reappraisal of EFSUMB recommendations and possible emerging applications. Med Ultrason. 2015;17(2):219–26.
39. Nolsoe CP, Nolsoe AB, Klubien J, Pommergaard HC, Rosenberg J, Meloni MF, et al. Use of ultrasound contrast agents in relation to percutaneous interventional procedures: a systematic review and pictorial essay. J Ultrasound Med. 2018;37(6):1305–24.
40. Huang DY, Yusuf GT, Daneshi M, Ramnarine R, Deganello A, Sellars ME, et al. Contrast-enhanced ultrasound (CEUS) in abdominal intervention. Abdom Radiol (New York). 2018;43(4):960–76.
41. Lekht I, Nayyar M, Luu B, Guichet PL, Ho J, Ter-Oganesyan R, et al. Intra-arterial contrast-enhanced ultrasound (IA CEUS) for localization of hepatocellular carcinoma (HCC) supply during transarterial chemoembolization (TACE): a case series. Abdom Radiol (New York). 2017;42(5):1400–7.
42. D'Onofrio M, Crosara S, De Robertis R, Canestrini S, Cantisani V, Morana G, et al. Malignant focal liver lesions at contrast-enhanced ultrasonography and magnetic resonance with hepatospecific contrast agent. Ultrasound (Leeds, England). 2014;22(2):91–8.
43. Quaia E, De Paoli L, Angileri R, Cabibbo B, Cova MA. Indeterminate solid hepatic lesions identified on non-diagnostic contrast-enhanced computed tomography: assessment of the additional diagnostic value of contrast-enhanced ultrasound in the non-cirrhotic liver. Eur J Radiol. 2014;83(3):456–62.
44. Trillaud H, Bruel JM, Valette PJ, Vilgrain V, Schmutz G, Oyen R, et al. Characterization of focal liver lesions with SonoVue-enhanced sonography: international multicenter-study in comparison to CT and MRI. World J Gastroenterol. 2009;15(30):3748–56.
45. Zhang Y, Luo YK, Zhang MB, Li J, Li J, Tang J. Diagnostic accuracy of contrast-enhanced ultrasound enhancement patterns for thyroid nodules. Med Sci Monit. 2016;22:4755–64.
46. Defortescu G, Cornu JN, Bejar S, Giwerc A, Gobet F, Werquin C, et al. Diagnostic performance of contrast-enhanced ultrasonography and magnetic resonance imaging for the assessment of complex renal cysts: a prospective study. Int J Urol. 2017;24(3):184–9.
47. Wei SP, Xu CL, Zhang Q, Zhang QR, Zhao YE, Huang PF, et al. Contrast-enhanced ultrasound for differentiating benign from malignant solid small renal masses: comparison with contrast-enhanced CT. Abdom Radiol (New York). 2017;42(8):2135–45.
48. Sanz E, Hevia V, Gomez V, Alvarez S, Fabuel JJ, Martinez L, et al. Renal complex cystic masses: usefulness of contrast-enhanced ultrasound (CEUS) in their assessment and its agreement with computed tomography. Curr Urol Rep. 2016;17(12):89.
49. Barr RG, Peterson C, Hindi A. Evaluation of indeterminate renal masses with contrast-enhanced US: a diagnostic performance study. Radiology. 2014;271(1):133–42.
50. Edenberg J, Gloersen K, Osman HA, Dimmen M, Berg GV. The role of contrast-enhanced ultrasound in the classification of CT-indeterminate renal lesions. Scand J Urol. 2016;50(6):445–51.
51. Putz FJ, Erlmeier A, Wiesinger I, Verloh N, Stroszczynski C, Banas B, et al. Contrast-enhanced ultrasound (CEUS) in renal imaging at an interdisciplinary ultrasound Centre: possibilities of dynamic microvascularisation and perfusion. Clin Hemorheol Microcirc. 2017;66(4):293–302.
52. Liu Y, Xu Y, Cheng W, Liu X. Quantitative contrast-enhanced ultrasonography for the differential diagnosis of endometrial hyperplasia and endometrial neoplasms. Oncol Lett. 2016;12(5):3763–70.
53. Gruber L, Loizides A, Luger AK, Glodny B, Moser P, Henninger B, et al. Soft-tissue tumor contrast enhancement patterns: diagnostic value and comparison between ultrasound and MRI. AJR Am J Roentgenol. 2017;208(2):393–401.
54. Guo S, Xu P, Zhou A, Wang G, Chen W, Mei J, et al. Contrast-enhanced ultrasound differentiation between low- and high-grade bladder urothelial carcinoma and correlation with tumor microvessel density. J Ultrasound Med. 2017;36(11):2287–97.
55. Cantisani V, Bertolotto M, Weskott HP, Romanini L, Grazhdani H, Passamonti M, et al. Growing indications for CEUS: the kidney, testis, lymph nodes, thyroid, prostate, and small bowel. Eur J Radiol. 2015;84(9):1675–84.
56. Knieling F, Strobel D, Rompel O, Zapke M, Menendez-Castro C, Wolfel M, et al. Spectrum, applicability and diagnostic capacity of contrast-enhanced ultrasound in pediatric patients and young adults after intravenous application—a retrospective trial. Ultraschall Med (Stuttgart, Germany: 1980). 2016;37(6):619–26.
57. Seitz K, Strobel D. A milestone: approval of CEUS for diagnostic liver imaging in adults and children in the USA. Ultraschall Med (Stuttgart, Germany: 1980). 2016;37(3):229–32.
58. Seitz K, Strobel D, Bernatik T, Blank W, Friedrich-Rust M, Herbay A, et al. Contrast-enhanced ultrasound (CEUS) for the characterization of focal liver lesions—prospective comparison in clinical practice: CEUS vs. CT (DEGUM multicenter trial). Parts of this manuscript were presented at the Ultrasound Dreilandertreffen 2008, Davos. Ultraschall Med (Stuttgart, Germany: 1980). 2009;30(4):383–9.
59. Mori N, Mugikura S, Takahashi S, Ito K, Takasawa C, Li L, et al. Quantitative analysis of contrast-enhanced ultrasound imaging in invasive breast Cancer: a novel technique to obtain histopathologic information of microvessel density. Ultrasound Med Biol. 2017;43(3):607–14.
60. Tai CJ, Huang MT, Wu CH, Tai CJ, Shi YC, Chang CC, et al. Contrast-enhanced ultrasound and computed tomography assessment of hepatocellular carcinoma after transcatheter arterial chemoembolization: a systematic review. J Gastroint Liver Dis. 2016;25(4):499–507.
61. Ishii T, Numata K, Hao Y, Doba N, Hara K, Kondo M, et al. Evaluation of hepatocellular carcinoma tumor

vascularity using contrast-enhanced ultrasonography as a predictor for local recurrence following radiofrequency ablation. Eur J Radiol. 2017;89:234–41.
62. Bartolotta TV, Taibbi A, Picone D, Anastasi A, Midiri M, Lagalla R. Detection of liver metastases in cancer patients with geographic fatty infiltration of the liver: the added value of contrast-enhanced sonography. Ultrasonography (Seoul, Korea). 2017;36(2):160–9.
63. Pandey P, Lewis H, Pandey A, Schmidt C, Dillhoff M, Kamel IR, et al. Updates in hepatic oncology imaging. Surg Oncol. 2017;26(2):195–206.
64. Granata V, Fusco R, Catalano O, Avallone A, Palaia R, Botti G, et al. Diagnostic accuracy of magnetic resonance, computed tomography and contrast enhanced ultrasound in radiological multimodality assessment of peribiliary liver metastases. PLoS One. 2017;12(6):e0179951.
65. Maj E, Papiernik D, Wietrzyk J. Antiangiogenic cancer treatment: the great discovery and greater complexity (review). Int J Oncol. 2016;49(5):1773–84.
66. Hendry SA, Farnsworth RH, Solomon B, Achen MG, Stacker SA, Fox SB. The role of the tumor vasculature in the host immune response: implications for therapeutic strategies targeting the tumor microenvironment. Front Immunol. 2016;7:621.
67. Lassau N, Bonastre J, Kind M, Vilgrain V, Lacroix J, Cuinet M, et al. Validation of dynamic contrast-enhanced ultrasound in predicting outcomes of antiangiogenic therapy for solid tumors: the French multicenter support for innovative and expensive techniques study. Investig Radiol. 2014;49(12):794–800.
68. Atri M, Hudson JM, Sinaei M, Williams R, Milot L, Moshonov H, et al. Impact of acquisition method and region of interest placement on inter-observer agreement and measurement of tumor response to targeted therapy using dynamic contrast-enhanced ultrasound. Ultrasound Med Biol. 2016;42(3):763–8.
69. Amioka A, Masumoto N, Gouda N, Kajitani K, Shigematsu H, Emi A, et al. Ability of contrast-enhanced ultrasonography to determine clinical responses of breast cancer to neoadjuvant chemotherapy. Jpn J Clin Oncol. 2016;46(4):303–9.
70. Saracco A, Szabo BK, Tanczos E, Bergh J, Hatschek T. Contrast-enhanced ultrasound (CEUS) in assessing early response among patients with invasive breast cancer undergoing neoadjuvant chemotherapy. Acta Radiol (Stockholm, Sweden: 1987). 2017;58(4):394–402.
71. Matsui S, Kudo M, Kitano M, Asakuma Y. Evaluation of the response to chemotherapy in advanced gastric cancer by contrast-enhanced harmonic EUS. Hepato-Gastroenterology. 2015;62(139):595–8.
72. Peng C, Liu LZ, Zheng W, Xie YJ, Xiong YH, Li AH, et al. Can quantitative contrast-enhanced ultrasonography predict cervical tumor response to neoadjuvant chemotherapy? Eur J Radiol. 2016;85(11):2111–8.
73. Jia WR, Tang L, Wang DB, Chai WM, Fei XC, He JR, et al. Three-dimensional contrast-enhanced ultrasound in response assessment for breast Cancer: a comparison with dynamic contrast-enhanced magnetic resonance imaging and pathology. Sci Rep. 2016;6:33832.
74. Ohno N, Miyati T, Yamashita M, Narikawa M. Quantitative assessment of tissue perfusion in hepatocellular carcinoma using perflubutane dynamic contrast-enhanced ultrasonography: a preliminary study. Diagnostics (Basel, Switzerland). 2015;5(2):210–8.
75. Mogensen MB, Hansen ML, Henriksen BM, Axelsen T, Vainer B, Osterlind K, et al. Dynamic contrast-enhanced ultrasound of colorectal liver metastases as an imaging modality for early response prediction to chemotherapy. Diagnostics (Basel, Switzerland). 2017;7(2):35.
76. Wu Z, Yang X, Chen L, Wang Z, Shi Y, Mao H, et al. Anti-angiogenic therapy with contrast-enhanced ultrasound in colorectal cancer patients with liver metastasis. Medicine. 2017;96(20):e6731.
77. Guvener N, Appold L, de Lorenzi F, Golombek SK, Rizzo LY, Lammers T, et al. Recent advances in ultrasound-based diagnosis and therapy with micro- and nanometer-sized formulations. Methods (San Diego, CA). 2017;130:4–13.

19 Intraoperative Contrast-Enhanced Ultrasound in the Pediatric Neurosurgical Patient

Ignazio G. Vetrano, Laura Grazia Valentini, Francesco DiMeco, and Francesco Prada

19.1 Introduction

19.1.1 Contrast-Enhanced Ultrasound in Neurosurgery

The routine application of contrast-enhanced ultrasound (CEUS) during adult neurosurgical procedures is a relatively recent introduction and is not yet widely practiced [1–4]. In 2005, Kanno et al. first described the application of a contrast agent during intra-operative power Doppler ultrasound, aiding the surgical resection of 40 brain tumors [1]. Even if this experience was based on a first-generation ultrasound contrast agent (UCA) it demonstrated that intraoperative CEUS (iCEUS) could facilitate intraoperative orientation and the assessment of intra-tumoral and peritumoral vessels. Since that preliminary experience, several groups have explored different applications of iCEUS in neurosurgery. Engelhardt et al. demonstrated the opportunity to attain time–intensity curves with continuous imaging using newer techniques [2]. Hölscher et al. focused studies on vascular neurosurgery (e.g., aneurysms, arteriovenous malformation) demonstrating with "angiosonography" the real-time flow dynamics [4]. With this technique, the ability of iCEUS to highlight tumor and tumor margins, aiding in differentiating between tumor and surrounding brain parenchyma, was established [3].

Several other studies demonstrated the usefulness of iCEUS [5–7], leading to the introduction and application of iCEUS in neurosurgery, with incorporation in the European Federation of Societies for Ultrasound in Medicine and Biology (EFSUMB) guidelines [8]. Intraoperative CEUS is particularly suited for neurosurgery application for a number of reasons: during surgery, there are no obstacles (skin, subcutaneous tissues, muscles) between the transducer and the brain, of which the tissue composition allows optimal

I. G. Vetrano · L. G. Valentini
Department of Neurosurgery, Fondazione IRCCS Istituto Neurologico Carlo Besta, Milan, Italy
e-mail: ignazio.vetrano@istituto-besta.it; laura.valentini@istituto-besta.it

F. DiMeco
Department of Neurosurgery, Fondazione IRCCS Istituto Neurologico Carlo Besta, Milan, Italy

Department of Pathophysiology and Transplantation, University of Milan, Milan, Italy

Department of Neurological Surgery, Johns Hopkins Medical School, Baltimore, MD, USA
e-mail: fdimeco@istituto-besta.it

F. Prada (✉)
Department of Neurosurgery, Fondazione IRCCS Istituto Neurologico Carlo Besta, Milan, Italy

Department of Neurological Surgery, University of Virginia Health Science Center, Charlottesville, VA, USA
e-mail: FUP5A@hscmail.mcc.virginia.edu; francesco.prada@istituto-besta.it

P. S. Sidhu et al. (eds.), *Contrast-Enhanced Ultrasound in Pediatric Imaging*,
https://doi.org/10.1007/978-3-030-49691-3_19

mechanical properties for ultrasound (US) propagation. Furthermore, cerebral blood flow is sustained by a terminal circulation with multiple arteries and different anastomosis, with a complex venous draining system, where the UCA behave as purely intravascular contrast media not spreading into the interstitial space, taking advantage of the terminal circulation of the brain. This allows the UCA to demonstrate and characterize all phases of tumor/brain perfusion: arterial, parenchymal, and venous. Usually, normal brain parenchyma does not enhance strongly, except for the basal ganglia, but with alteration of enhancement findings seen with different pathological conditions.

We have described applications of CEUS in neurosurgery: intraoperative neoplastic evaluation and characterization and the so-called *angiosonography* for vessel visualization [5, 9]. Intraoperative CEUS is able to highlight tumor parenchyma and tumor–brain interface with great accuracy in nearly all tumors, but particularly with poorly defined tumor borders, or when the surrounding parenchyma is the edematous brain. Ultimately, this allows for assessment of lesion distribution and to visualize potential residual tumor during each phase of the surgical resection. The degree and pattern of contrast enhancement depend on the density and distribution of capillaries in the region of interest and on the neoplastic vascular supply. Consequently, each pathological entity demonstrates a specific enhancement pattern, according to the specific vascular organization of afferent and efferent vessels, allowing characterization of tumor behavior [10].

19.1.2 Contrast-Enhanced Ultrasound: Pediatric Applications in Neurosurgery

The first application of iCEUS in the pediatric neurosurgical field was a 14–year-old child with an intramedullary cervical spine tumor [6]. Following that other clinical cases have been reported, without any prospective case series published. Kastler, in 2014, presented a small cohort of neonates and infants with hemorrhage, hydrocephalus, and hypoxic-ischemic injuries, evaluated in an emergency setting with trans-fontanellar CEUS (TCEUS) [11]. They compared TCEUS with a B-mode trans-fontanellar US and with magnetic resonance (MR) imaging. TCEUS showed abnormalities not depicted on B-mode US and were concordant with the MR imaging findings. In particular, TCEUS allowed for the assessment of brain perfusion, without adverse events of the contrast agent administration of other imaging modalities. Hwang et al. presented feasibility of brain CEUS studies in neonates and infants [12, 13], describing the enhancement intensity in the region of interest changing during the wash-in and wash-out phases of the UCA, from which brain perfusion could be quantified [13]. Evaluating the evolution of cerebral perfusion in this manner is useful, particularly in brain injury, where it is valuable for prognosis and guidance of therapeutic intervention. The neurosurgical application of iCEUS can also be modified in real time according to the surgical strategy, i.e., in order to increase the extent of resection for tumors, or to avoid normal surrounding structures or to verify the blood flow and tissue perfusion in vascular malformation applications [12, 14].

Ultrasound applications have not been fully exploited by the neurosurgical community to date, with the main pre- or intraoperative imaging tools used being computed tomography (CT) and magnetic resonance (MR) imaging, performed in three panoramic orthogonal planes: axial, sagittal, and coronal. Intra-operative US (ioUS) generates a unique tomographic representation in a precise moment during insonation a consequence of the transducer positioning, coupled with the surgical approach. The transducer is usually rotated, changing the orientation with multiplanar and sectorial imaging, all unique in the information provided. B-mode US examination shows inherent limitations in distinguishing between tumor and surrounding edematous parenchyma, improved with CEUS, but is deployed in pediatric neurosurgery relying on experience in adults [9, 15, 16]. The EFSUMB statement [17] considers the uncertainty surrounding the long-term

effects of gadolinium brain deposition in adult and children [18, 19], the need to reduce radiation exposure, and use of iodinated contrast medium.

There are potential issues using iCEUS in pediatric neurosurgery. Occasionally it is necessary to enlarge the bone access to adapt to the transducer size, more evident in infants. The craniotomy or laminotomy/laminoplasty must be large enough to guarantee trans-dural examination and to allow transducer free tilting and change of orientation of the transducer. Moreover, in craniovertebral junction or spinal surgery, examination can only be possible in the axial and sagittal planes. This will also affect Doppler US imaging, reducing the possibility to identify vessels that run perpendicular to the insonation angle. With posterior fossa access, the sitting position is adopted, making the use of ioUS and iCEUS difficult. This is due to the inherent difficulty in obtaining an acoustic coupling with irrigation, with fluid quickly draining away. In addition, hemostatic agents or the presence of diffuse bleeding, both hyper-echoic, can prejudice the US examination [20]. Previous surgery may present artifacts on the CEUS examination.

We describe and illustrate the deployment of iCEUS in different intra-operative settings in pediatric neurosurgical patients and define various conditions in which iCEUS is feasible and useful for, particularly in cerebral and spinal cord malformation, neoplastic and vascular diseases.

19.2 Instruments and Technique

An ultrasound machine equipped with various transducers, able to perform CEUS, with elastography and fusion imaging (for virtual navigation), enables the peri-operative exploration of almost all neurosurgical conditions [7, 21–23]. Normally a linear array multifrequency (3–11 MHz) transducer with linear or trapezoidal views for both superficial and deep-seated lesions, and for very superficial lesions, a linear high-frequency transducer (10–22 MHz) should be available. Spinal lesions may be examined with a high-frequency linear transducer. A small micro-convex multi-frequency transducer can be used for small craniotomies or to explore surgical cavities while undertaking tumor resection. Once the craniotomy or the laminoplasty/laminotomy has been secured, and the operculum or the spinal flap has been removed, an initial B-mode US examination is performed through the intact dura mater, with the transducer placed on the meningeal surface that is continuously irrigated with saline solution. Prior to an iCEUS study, a detailed baseline examination is performed with standard B-mode and Doppler US imaging, adding elastography as required [23]. The baseline examination allows for the identification of the principal anatomical landmarks and the vascularity, in order to adequately understand the plane of insonation and structure orientation. Variation of the transducer position is performed with slow movements in a standardized manner; from left to right for the sagittal plan, or from anterior to posterior for the coronal plan or from top to bottom for the axial plan, according to the region being explored. With spinal surgery, only axial and sagittal planes are required.

19.2.1 Ultrasound Contrast Agent

SonoVue™ (Bracco SpA, Milan, Italy) is normally used and adult doses are established. In the pediatric population, there is a lack of pediatric studies to establish dosage. Based on the kinetics and distribution of the UCA in the brain and spinal cord, with dose adjustment based on the adult dose of 2.4 mL (SonoVue™), Hwang et al. [12, 13] have used the FDA-recommended Lumason™ (Bracco Diagnostics Inc., Monroe Township, NJ) dosage of 0.03 mL/kg for the pediatric population, with optimal image quality. We have adapted the dose calculating 0.5 mL/10 kg bodyweight. However there are many dose schedules used by other practitioners; e.g., 0.1 mL SonoVue™ for each year of age [11, 13, 24]. The UCA is normally injected by the anesthesiologist, via a peripheral or central vein, followed by a flush of normal saline. Following intravenous injection, the contrast agent lasts for up to 5 min, a second injection may be administered. US imaging

parameters including mechanical Index (MI), gain, frequency, and depth will need to be adapted for each case.

19.3 Practical CEUS Applications in Pediatric Neurosurgery

19.3.1 Brain Tumors

Central nervous system (CNS) solid malignant and non-malignant tumors are common in children and are the leading cause of cancer death from the ages 0 through 14 years in the United States, with a tumor incidence of 5.54 per 100,000 [25]. According to the records of the Central Brain Tumor Registry of the United States (CBTRUS), gliomas are the most common histologic group in all ages (52.9%), of which the majority are pilocytic astrocytoma (33.2%) and other low-grade gliomas (27.1%), but glioblastomas also occur [26]. In infants <1 year of age, gliomas, and embryonal tumors are the most common tumor type, while in children 5–9 years of age, medulloblastoma represents almost all embryonal tumors, of which there are three embryonal tumor types; (1) primitive neuroectodermal tumor, (2) medulloblastoma, and (3) atypical teratoid/rhabdoid tumor. Pilocytic astrocytoma, deriving from glial cells, represents 17% of all CNS tumors in 0- to 14-year-old age group.

The histopathological origin affects the US visualization; sometimes it is difficult to distinguish between the glioma and surrounding normal parenchyma, in particular, if edematous. Intraoperative CEUS is beneficial, in this instance, highlighting tumor parenchyma and tumor–brain interface with great precision in most situations, and can identify the active/viable and the necrotic/cystic areas within the tumor. For example, during glioma surgery, iCEUS is capable of differentiating low- and high-grade gliomas and can show anaplastic areas in low-grade tumors (Fig. 19.1). In tumors with ill-defined borders, e.g., glioblastomas, iCEUS can show tumor extension clearly against healthy edematous brain (Fig. 19.2). In highly vascularized tumors, it is possible to identify deep feeder vessels, allowing rapid devascularization of the tumor, reducing bleeding. Avoiding excessive blood loss is more important in children because rapid blood loss can cause severe hemodynamic dysfunction (Fig. 19.3). Furthermore, a brain abscess (Fig. 19.4), possibly in the differential diagnosis with intracranial tumors, may also be depicted with the use of iCEUS.

In our experience, CEUS can help to visualize tumor remnants after resection, providing valuable biological information about tumor perfusion and vascularization, possibly changing the surgical strategy for tumor removal. Increasing the extent of resection, moreover, has an impact on efficacy of adjuvant therapies and progression-free survival or overall survival.

19.3.2 Epilepsy Surgery

With medical refractory epilepsy, or if seizures are secondary to a cortical malformation, surgery for disconnection or resection can be performed. Focal cortical dysplasia, an alteration of cortical development, is the most common cause of symptomatic drug-resistant epilepsy, and surgery can achieve seizure control. Even if, pre-operative imaging modalities are able to detect cortical disorders, the intra-operative identification and visualization remain a challenge [27]. For these patients, the most important factor in terms of seizure freedom is the complete removal of the dysplastic tissue, and a poor outcome may be explained by the lack of direct identification of boundaries between dysplastic and normal parenchyma. The use of iCEUS used at our institution enables better visualization of the dysplastic area, in order to achieve a total resection. Some drug-resistant seizures are due to the presence of other lesion types, such dysembryoplastic neuroepithelial tumor (DNET). A DNET is a Grade I WHO tumors described as a neuronal and mixed neuronal–glial tumor [28]. A simple "lesionectomy" is often sufficient for seizure control, and the use of iCEUS to delineate and identify a DNET (Fig. 19.5) is essential, even when surgery is a simple disconnective procedure, where the resection of parenchyma should include the lesion (Fig. 19.6).

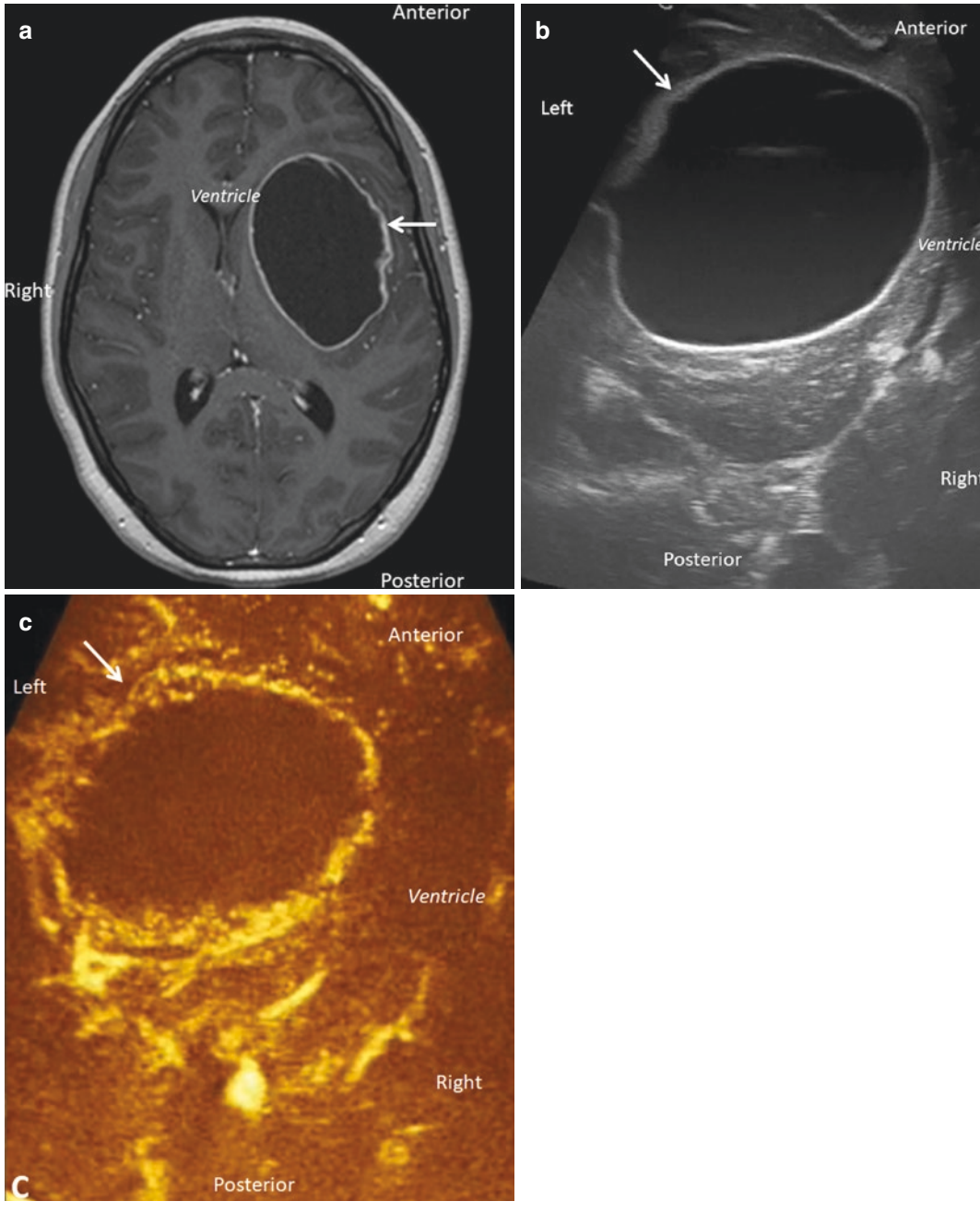

Fig. 19.1 High-grade glioma in a 13-year-old female. (**a**) Axial T1 MR image with contrast, showing a left fronto-temporo-insular intra-parenchymal tumor, with annular enhanced ring (arrow) and large cystic component. (**b**) Intraoperative visualization on B-mode US (arrow) of the cystic tumor. (**c**) The corresponding iCEUS imaging showing the cystic tumor and enhancing rim (arrow). The iCEUS images show the rich peri-tumor vascularization, confirming the lack of intra-tumor vessels, with a fluid fulfilled cystic component. Histology confirmed the suspected intraoperative diagnosis of glioblastoma multiforme

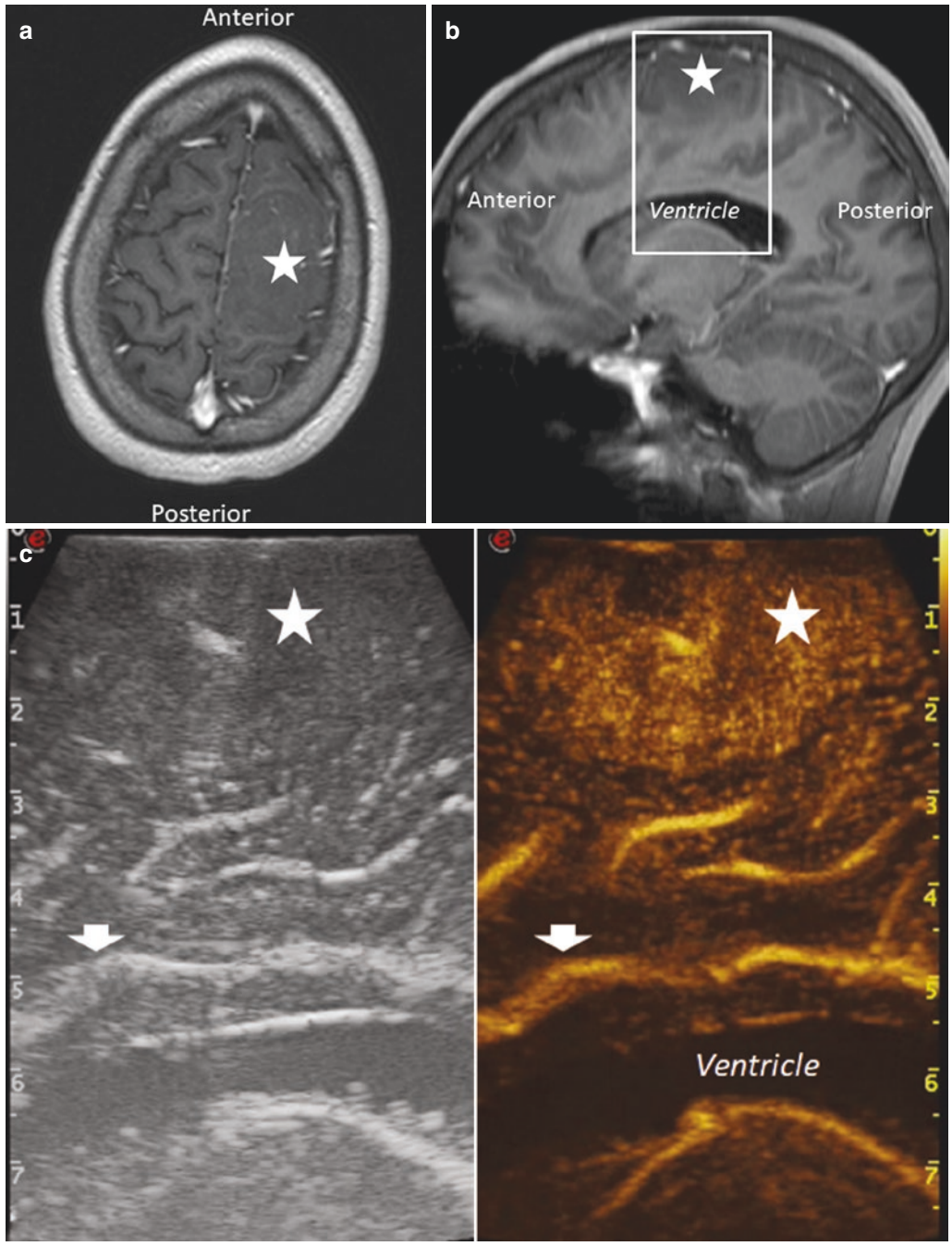

Fig. 19.2 Frontal glioblastoma in a 16-year-old male. (**a**) Axial T1-weighted contrast MR image shows a left frontal para-sagittal intra-parenchymal tumor no enhancement with contrast (star). (**b**) Sagittal T1-weighted contrast MR image shows a left frontal para-sagittal intra-parenchymal tumor no enhancement with contrast (star). (**c**) Dual screen mode. On the B-mode US examination, the tumor was slight hypoechoic (star). Following CEUS, arterial feeders and macro-vessels related to tumor neo-angiogenesis within the lesion are clearly visible (star), along with the typical peripheral centripetal enhancement recognizable. The distal branches of anterior cerebral artery were identifiable around corpus callosum (arrow-head). Histology confirmed a glioblastoma multiforme. Glioblastoma multiforme and high-grade glioma usually demonstrate brief contrast enhancement (20–30 s after UCA injection) with a rapid arterial phase (2–3 s), rapid time to peak, and a disordered intra-lesion flow pattern

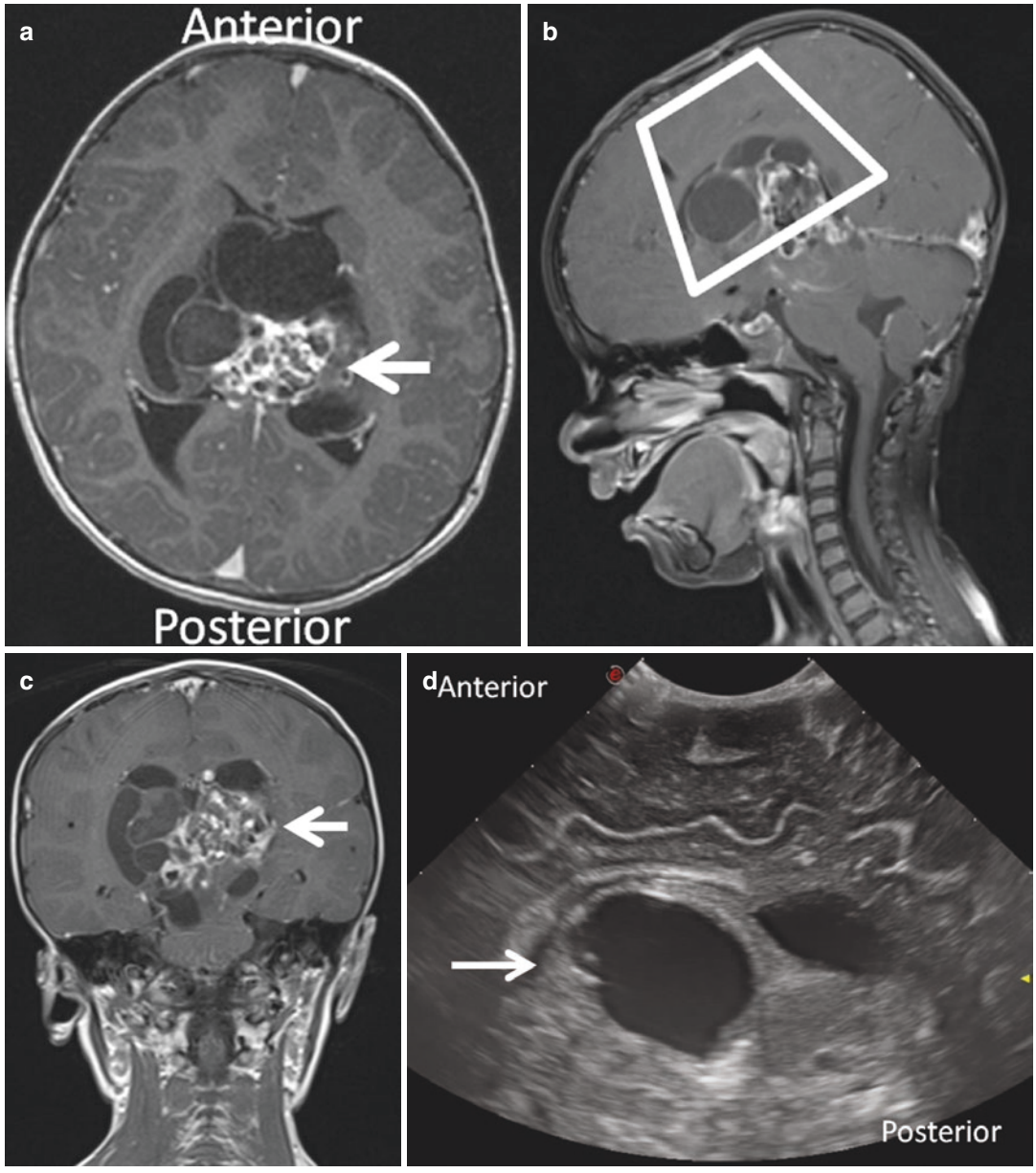

Fig. 19.3 Teratoma in a 3-year-old boy with previous multiple subtotal tumor resections. (**a**–**c**) Multiplanar (**a**; axial, **b**; Sagittal, and **c**; Coronal) MR T1-weighted images following contrast administration demonstrate a large multi-cystic, inhomogeneous tumor (arrow) arising from mesencephalic region with endo-ventricular extension. (**d**) On the B-mode US in a sagittal plane, the variegate tumor composition (arrow) is demonstrated, with anechoic and hyperechoic structures. (**e**) Intraoperative CEUS confirms the heterogeneous appearances, with multiple cystic and solid areas, with a slow–moderate arterial phase, the degree of enhancement reflecting the heterogeneous composition (likely due to the coexistence of cystic, fatty, and calcified elements). Patient in the sitting position adversely affects the quality of the iCEUS examination (see text)

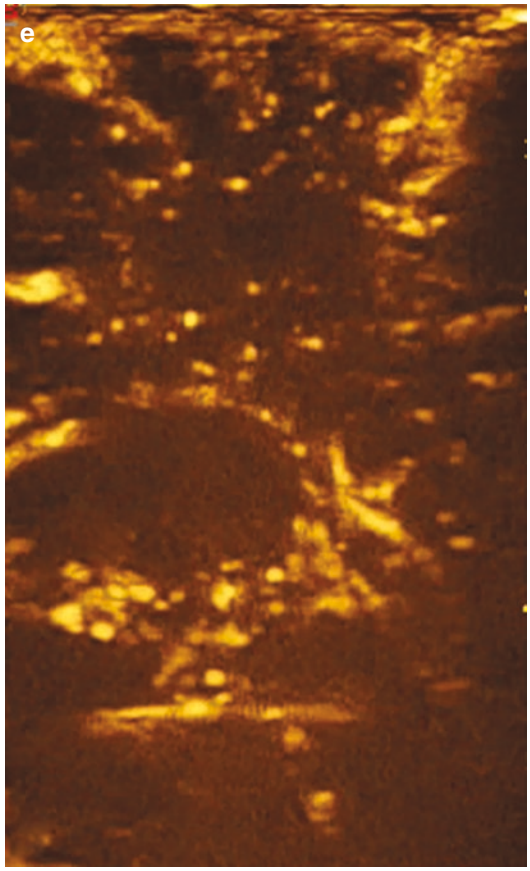

Fig. 19.3 (continued)

With drug-resistant seizures not secondary to cortical malformation or other lesions, disconnection or resection procedures can be performed. The most common procedure is the anteromesial temporal lobectomy; the resection includes anterior temporal lobe, along with resection of mesial structures: the uncus, a large part of the amygdala, and approximately a 3 cm length of the hippocampus/para-hippocampus. Intraoperative CEUS can be helpful to identify the middle cerebral artery branches and other anatomical landmarks that represent the margin of resection, as well as the choroid plexus or anterior choroidal artery.

19.3.3 Chiari Malformation

Chiari malformation Type I (CM-I) is a congenital disease in which the cerebellar tonsils herniate below the foramen magnum, causing an obstruction to normal cerebro-spinal fluid (CSF) circulation between brain and spinal compartment; a strain headache is the most common symptom [29, 30]. The incidence and prevalence are variable, estimated at 8 per 1000 live births. The incidence of symptomatic cases of a CM is low compared with a variant low tonsillar position. The cases of CM found incidentally on imaging are asymptomatic; the prevalence of low tonsillar position is higher in children compared with older adults and can disappear with growth [31]. A Chiari malformation can be associated with spinal cord syrinx, a dilatation of central ependymal canal; a further sign of CSF flow alteration [29]. The presence of syringomyelia is considered an indication for treatment usually by an osteo-dural decompression of the posterior fossa, with the aim to establish and restore adequate CSF flow. There is no consensus on the optimal technique: the extension of bone decompression, dural opening with duraplasty, arachnoid debridement, coagulation, and sometimes also resection of the cerebellar tonsils should be adapted specifically to each single patient.

Intraoperative US has been used to better define the cranio-vertebral junction and the surrounding structures, as well as retro-cerebellar space and cisterna magna, and particularly to identify CSF dynamic and real-time flow through the foramen magnum, prior to opening the dura and subsequent dural closure or duraplasty [32, 33]. Intraoperative CEUS is superior to B-mode US in the evaluation of the dynamic pathophysiology and venous engorgement, which can contribute to the intramedullary alteration. Intraoperative CEUS can also identify and delineate arterial structures, such as the vertebral artery, in association with Doppler examination (Fig. 19.7).

19.3.4 Moyamoya, Arteriovenous Malformation, and Other Neurovascular Diseases

Vascular neurosurgery using iCEUS may be applied in patients with aneurysms, arteriovenous malformations (AVM), and whenever a vessel undergoes prolonged surgical manipulation.

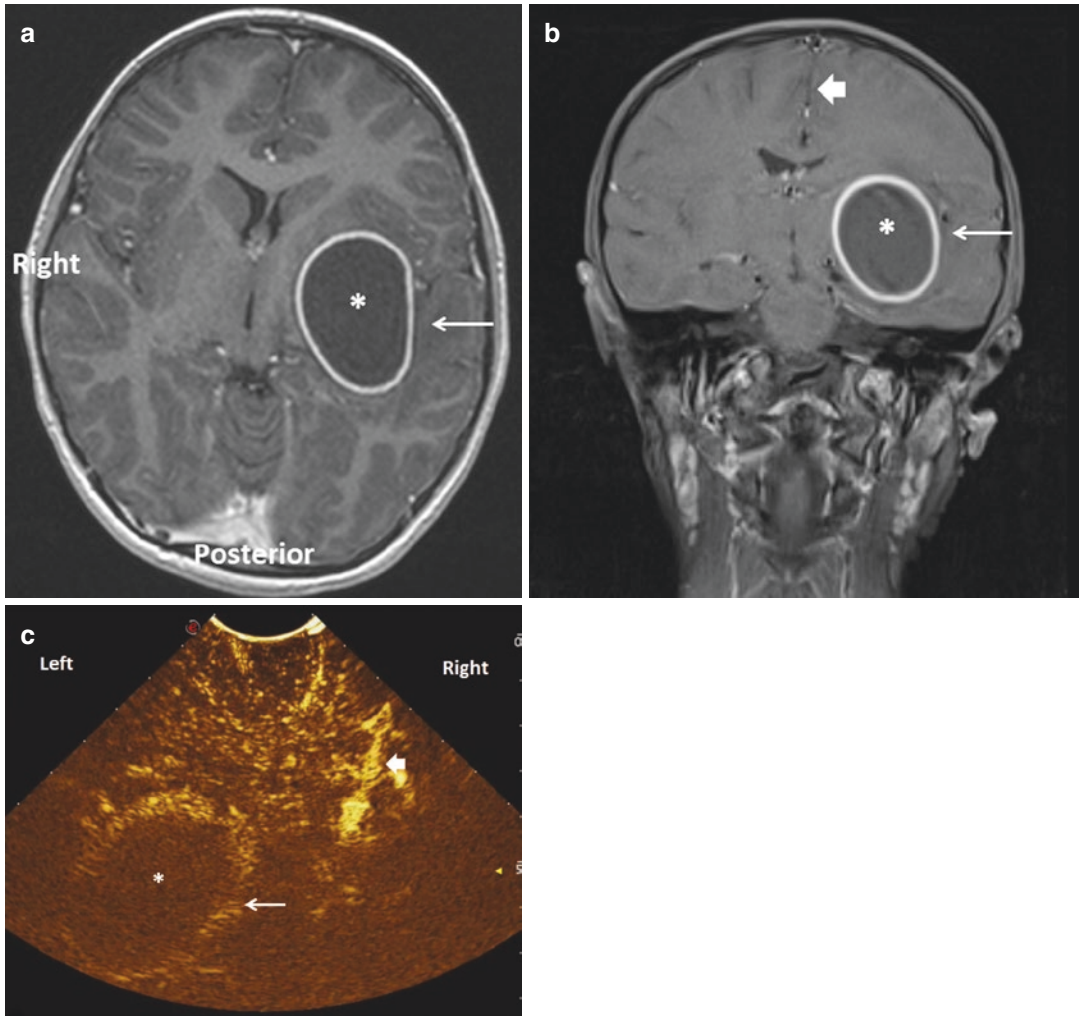

Fig. 19.4 Fronto-temporal abscess in a 9-year-old boy. (**a**) An abscess is seen as a peripheral enhancing rim (arrow) with a large, homogeneous anechoic center (asterisk) corresponding to the fluid component, on the axial contrast T1-weighted MR image. (**b**) The abscess (asterisk) is also demonstrated in the coronal contrast T1-weighted MR image. (**c**) Intraoperative CEUS was performed after an unsuccessful stereotactic evacuation (due to the thickness of the capsule, abscess; asterisk, small arrow enhancing abscess wall). A small craniotomy was fashioned during the procedure and, without CT evaluation, there was an appreciation that no dissemination of the abscess material had occurred. A small convex transducer was used to accommodate the limited dimensions of the bone flap. Cerebral falx (large arrow) is seen as intense CEUS enhancement

Intraoperative CEUS can help to estimate cerebral perfusion based on the UCA flow dynamics, in aneurysm surgery iCEUS can evaluate morphology and spatial orientation of the sac, assessing proximal and distal vessels, even prior to direct surgical exposure. After aneurysm clipping, iCEUS can assess distal flow and vessel patency. In AVM surgery, iCEUS identifies the nidus, feeding and draining vessels, and finally permits assessment of any residual cavity.

Another application of iCEUS is in the evaluation of any revascularization surgery. Moyamoya disease is a cerebrovascular syndrome characterized by progressive stenosis of the intracranial internal carotid arteries and their proximal branches, predisposing to ischemic and hemorrhagic events [34, 35]. Moyamoya is the most common pediatric cerebrovascular disease in Japan, with a prevalence of 3 per 100,000 children, while the incidence in Europe appears to be about

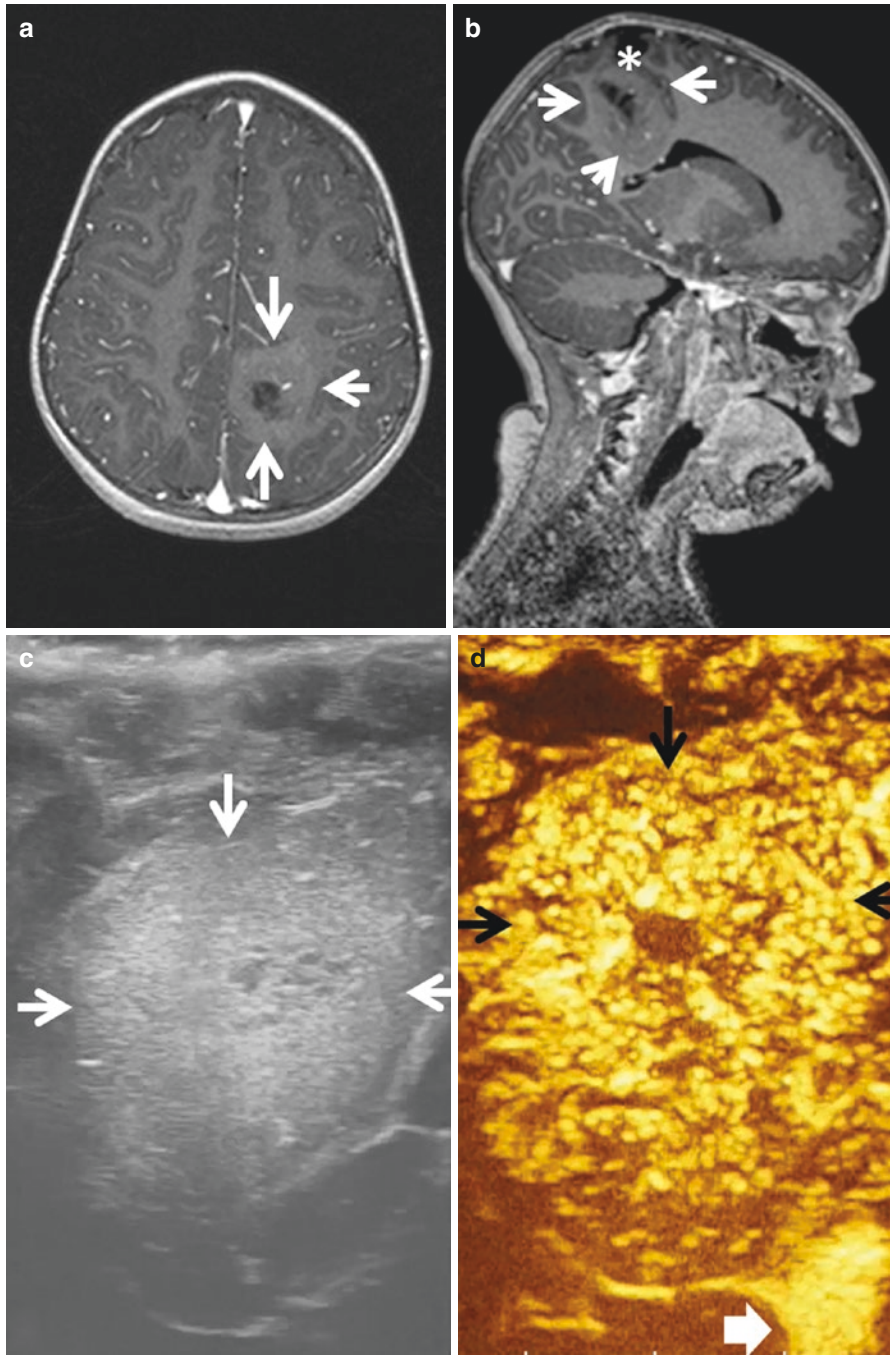

Fig. 19.5 A 4-year-old female affected by seizures previously underwent a biopsy without a diagnosis established. (**a**) An axial contrast MR image depicts a solid left parietal tumor (arrows) with cystic intra-tumor component and only partial, moderate contrast enhancement. The previous biopsy site (asterisk) is noted. (**b**) A sagittal contrast MR image depicts a solid left parietal tumor (arrows) with cystic intra-tumor component and only partial, moderate contrast enhancement. The previous biopsy site (asterisk) is noted. (**c**) The B-mode US illustrates a hyperechoic, slight homogeneous tumor (arrows). (**d**) The iCEUS confirms findings of slow enhancement diffusing to the entire tumor (black arrows). The large arrow demonstrates venous vascular enhancement. Histology following total resection was of dysembryoplastic neuroepithelial tumor

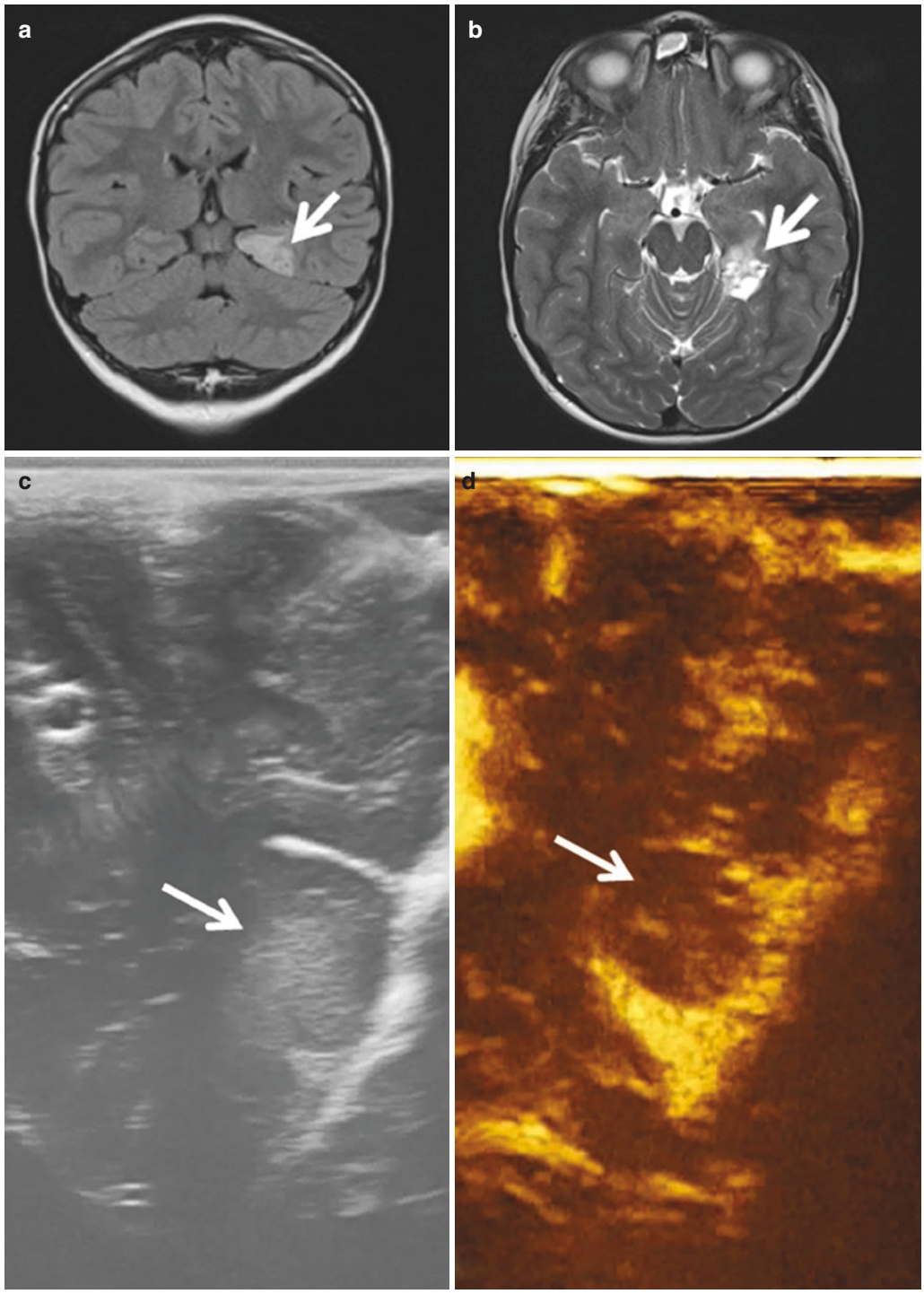

Fig. 19.6 A 9-year old boy with a mesial temporal ganglioglioma. (**a**) A coronal fluid-attenuated inversion recovery MR image of a left mesial temporal ganglioglioma (arrow). (**b**) An axial T2-weighted MR image of a left mesial temporal ganglioglioma (arrow). (**c**) The tumor appears hyper-echoic on the B-mode US (arrow). (**d**) On the iCEUS absence of contrast enhancement is noted in the lesion (arrow). Absence of contrast enhancement is also absent on traditional neuroradiological examinations

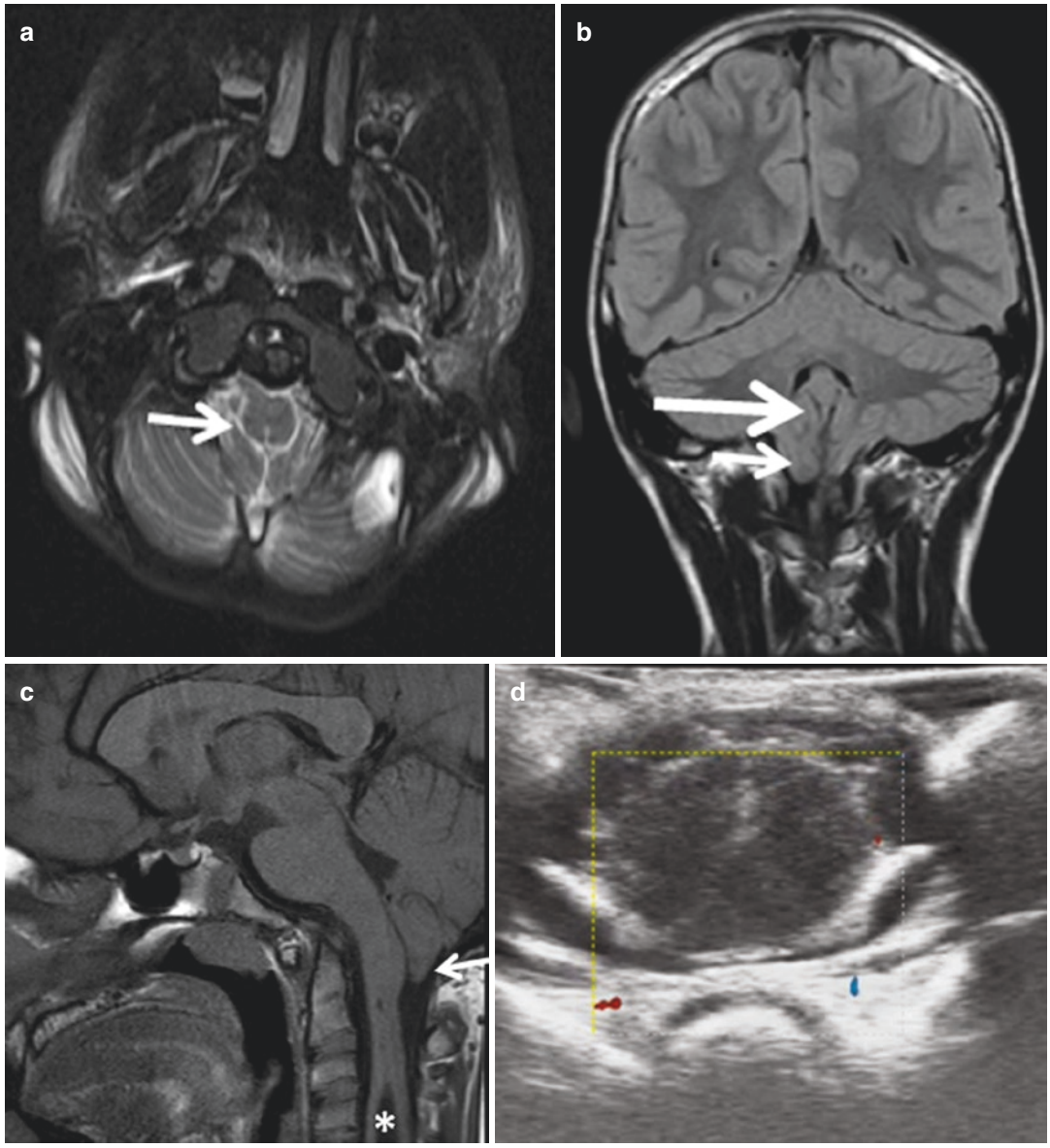

Fig. 19.7 An 8-year-old girl with the Chiari syndrome; cervical syringomyelia, cerebellar tonsillar ectopia through the foramen magnum. (**a**) Axial T2-weighted image of a Chiari syndrome and cerebellar tonsillar ectopia through the foramen magnum and a syrinx is seen (arrow). (**b**) Coronal T2-weighted image of a Chiari syndrome and cerebellar tonsillar ectopia through the foramen magnum (arrow). (**c**) A syrinx (asterisk) is visible on the pre-operative sagittal T1-weighted sequence. Tonsillar herniation is evident (arrow). (**d**) A color Doppler US demonstrating some CSF flow (box). (**e**) Intraoperative CEUS in an axial plane is useful during surgery to confirm partial subarachnoid space occlusion and abnormal cerebellar tonsils motion. (**f**) Intraoperative CEUS identifies vascular structures (arrows) and allows demonstration of the variation of CSF dynamics following dura-plasty. Less visible color Doppler US

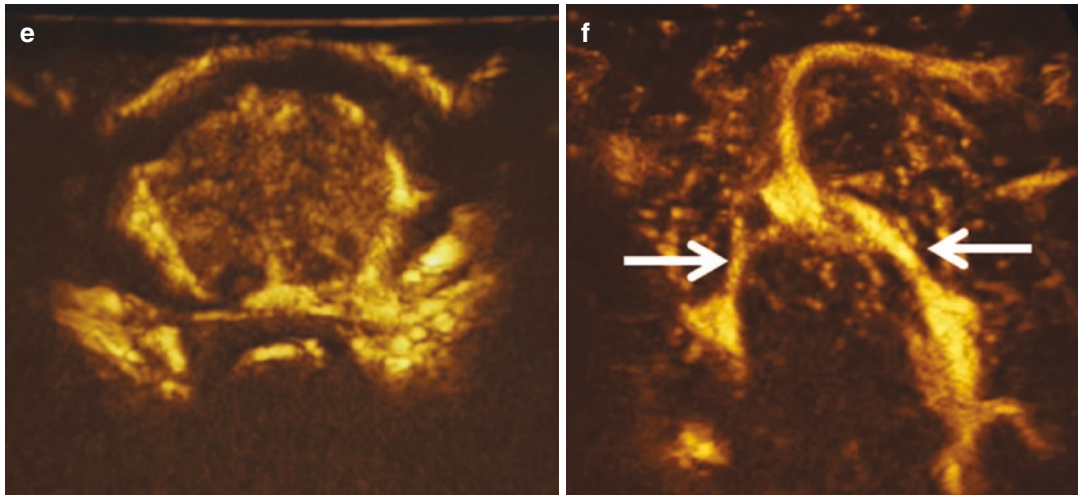

Fig. 19.7 (continued)

1/10th of the Japanese population. Symptoms are related to ischemic events, while in children the rate of hemorrhage is less than in adults [35, 36]. The diagnosis is based on imaging with arteriography definitive. Surgical treatment is revascularization of the cortical surface, based on direct and indirect pathways to restore valid circulation from the external carotid artery. Direct revascularization is with an extra-intracranial bypass, with the superficial temporal artery directly anastomosed to a cortical artery arising from the middle cerebral artery; the indirect revascularization is based on encephalo-duro-arterio-synangiosis or encephalo-myo-arterio-synangiosis, which requires some time to establish blood flow. This is a consequence of the revascularized tissue (dura and temporalis muscle) being directly placed on cortical surface. Traditionally, the two techniques are performed together during the same surgical procedure.

Intra-operative CEUS may be used to confirm pre-operative findings, demonstrating stenosis or occlusion of an internal carotid artery and the distal branches, and may also identify the most appropriate cortical arteries to accept the external carotid artery following extra-intracranial bypass (Fig. 19.8). Intra-operative CEUS may also confirm the patency of a temporal artery-middle cerebral artery bypass. Post-operative CEUS can be considered for non-invasive follow-up, to avoid other more invasive or time-consuming examinations while assessing the patency of bypass or the neo-cortical flow, with the added advantage of reducing radiation exposure and iodinated contrast agents in children [17].

19.3.5 Intramedullary Tumors

Primary pediatric spinal cord tumors are rare neoplasms in childhood, with a frequency of 0.19 per 100,000 person-years. The incidence varies by age, and increases between the 0–4 years (0.17 per 100,000 person-years) and to the ages of 15–19 years (0.28 per 100,000 person-years). Pediatric intramedullary spinal cord lesions also differ from adult tumors in a number of aspects [37–39]. Astrocytomas and ependymomas constitute the most common intramedullary spinal lesions in children, with developmental tumors predominating in the first decade [37, 39, 40]. Children usually present with good functional grades pre-operatively and maintain this following surgery. Long-term functional outcome depends on the pre-operative neurological status and histopathology of the lesion. Surgical excision is the standard treatment option, although with a considerable risk of neurological deficits, in particular when myelotomy is performed. Intra-operative US improves outcome, allowing a reduction of neural structure manipulation, which may lead to worsening of neurological symptoms. Intramedullary pediatric tumors appear

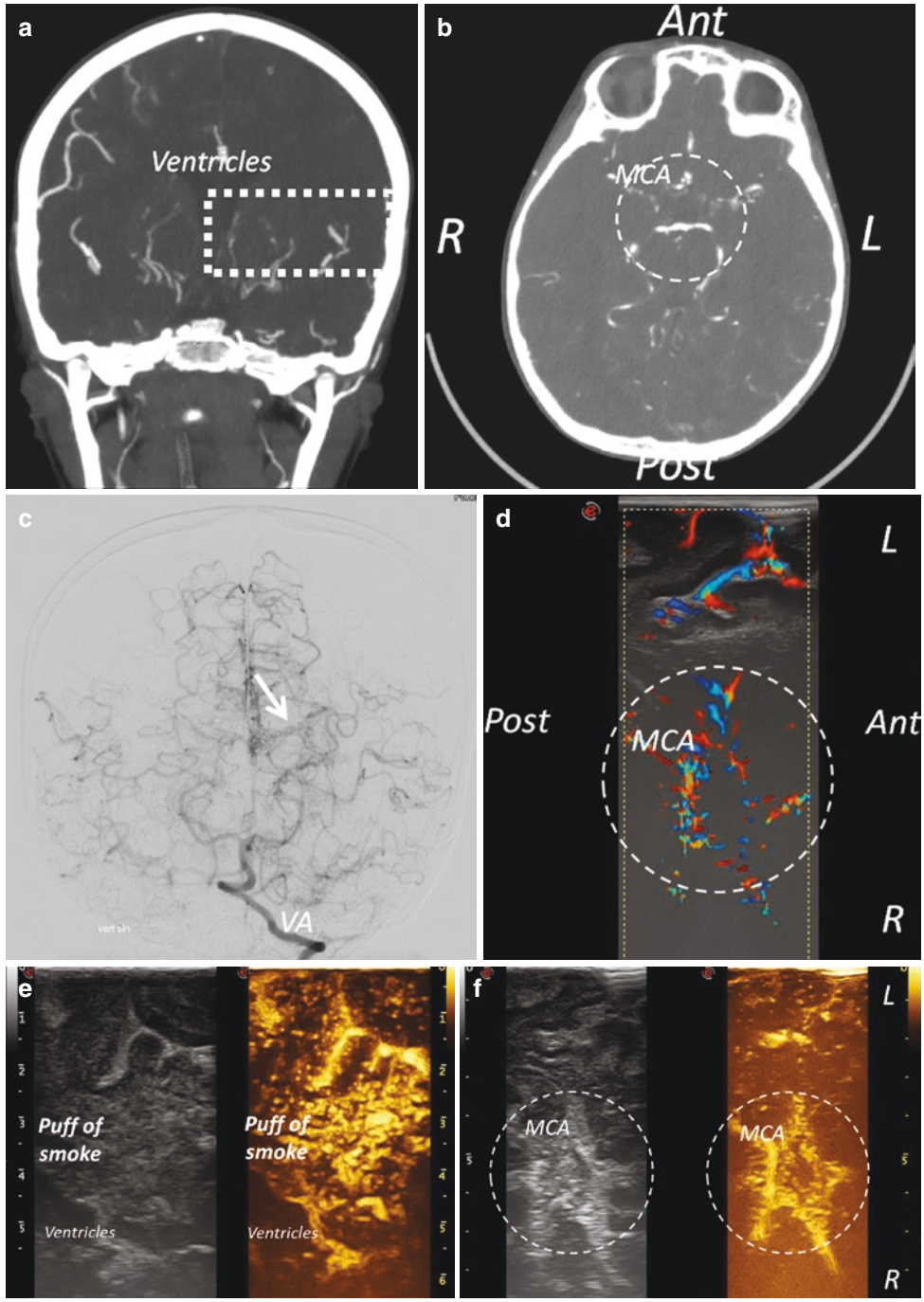

Fig. 19.8 A 6-year-old girl affected by bilateral Moyamoya disease and suffering from multiple ischemic attacks. (**a**) The coronal CT angiogram images show rarefaction of fronto-temporal vascularization (square box). (**b**) The axial CT angiogram images show rarefaction of fronto-temporal vascularization (circle, MCA: middle cerebral artery). (**c**) Vertebral artery angiography confirms partial revascularization by the posterior circle of Willis (VA: vertebral artery), with the typical "puff of smoke" appearance of lenticulostriate arteries (arrow). (**d**) Intraoperative color Doppler US demonstrates an incompletely visualized circle of Willis (circle). (**e**) A B-mode US and iCEUS (dual image) confirm the "puff of smoke" appearance. (**f**) Intraoperative CEUS is able to depict flow reduction of the anterior circulation (MCA). The circle of Willis polygon is clearly identifiable (circle)

variably hyper-echoic compared to the spinal cord, with a circumscribed and homogeneous aspect, sometimes with intra-lesion or peri-lesion cysts or dilation of the central ependymal canal. The spinal cord, if normal, usually appears hypo-echoic and homogeneous. The presence of edema obscures the delineation of the hyper-echoic aspect of the tumor, making it difficult to distinguish between the lesion and the surrounding compressed and/or infiltrated spinal cord. Some intramedullary tumors such as hemangioblastoma or ependymomas present cystic intra-tumor or peri-tumor structures (Fig. 19.9). Tumor-related syrinx may also be present and be

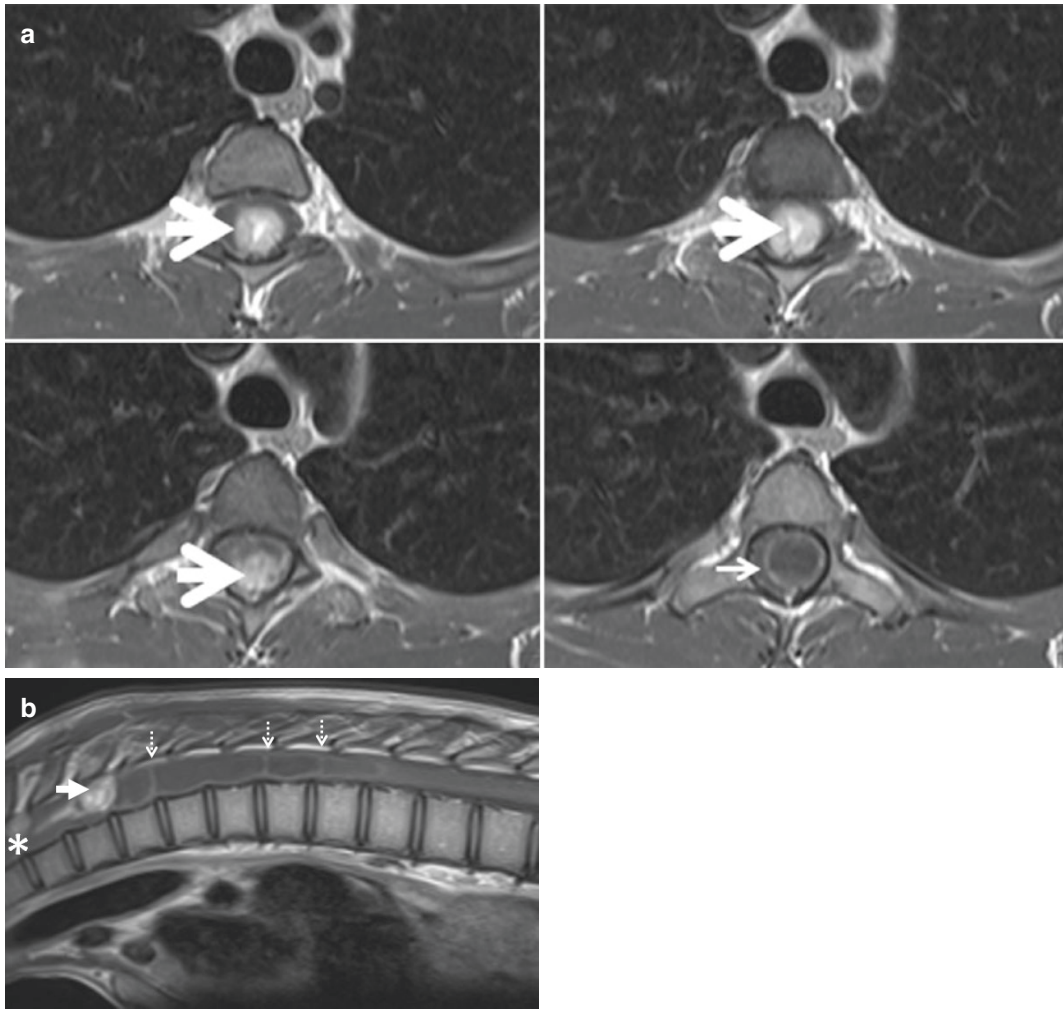

Fig. 19.9 Intramedullary cervico-thoracic hemangioblastomas in a 14-year-old boy. (**a**) Axial multi-slice T1-weighted post-contrast MR images show a D3 nodular tumor (thick arrow) with homogenous contrast enhancement, surrounded by a cystic cavity with septations (thin arrow). Cyst capsules and the altered spinal cord in between the nodules show enhancement after contrast. (**b**) Sagittal (rotated image of 90° to the left of (**a**)) T1-weighted post-contrast MR images show a D3 nodular tumor (thick arrow) with homogenous contrast enhancement, surrounded by a cystic cavity with septations (thin arrow). A further smaller and upper oval lesion is visible (asterisk). The pre-operative imaging was unclear if this was a syrinx or a peri-tumor cyst. (**c**) Axial trans-dural IOUS confirms the presence of hyperechoic tumor (large arrow), but it was not possible to clearly differentiate edematous spinal cord (triple arrows) from the tumor, particularly as the spinal cord appeared hyperechoic, due to edema. Intra-operative CEUS clearly identified tumor–myelon interface (triple arrows). (**d**) Sagittal trans-dural IOUS confirms the presence of hyperechogenic tumor, but it was not possible to clearly differentiate edematous spinal cord (triple arrows) from the tumor, particularly as the spinal cord appeared hyperechoic, due to edema. CEUS clearly identified tumor–myelon interface (triple arrows)

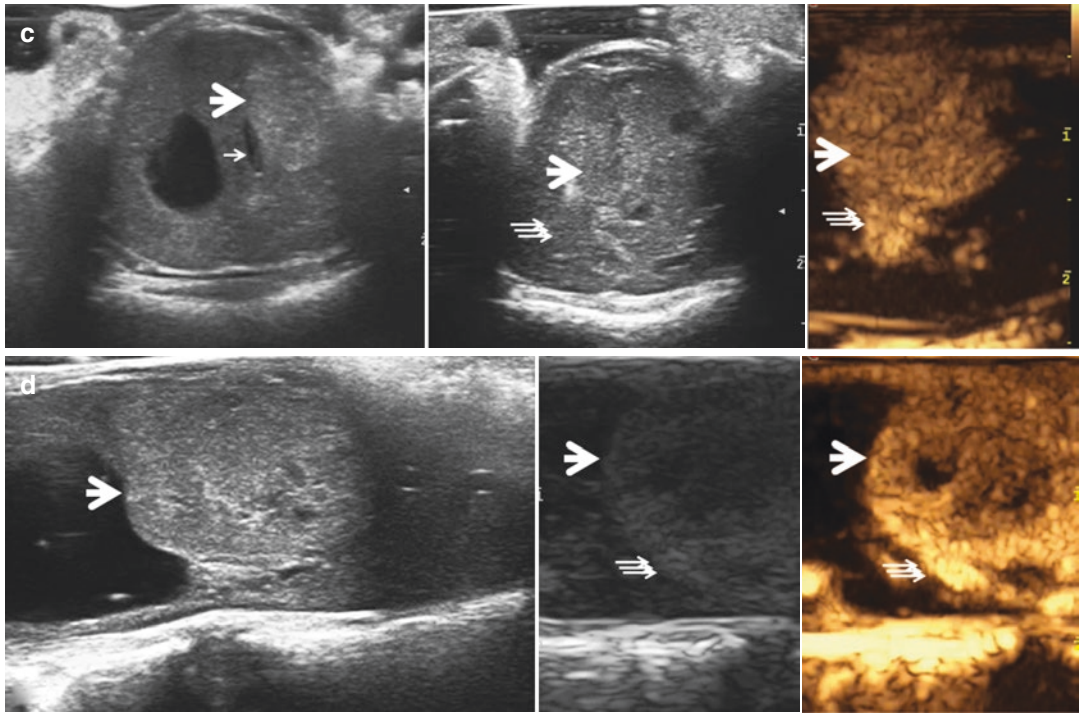

Fig. 19.9 (continued)

difficult to distinguish from tumor cysts, even when septations within tumor-derived cysts are thicker and more nodular than the thin partitions that are common with a syrinx. Astrocytomas can appear isoechoic to the spinal cord, and the surface between tumor and myelin is not clearly delineated. Intraoperative CEUS can be helpful to better delineate the nodular aspect of the tumor or distinguish an intramedullary glioma with respect to the spinal cord.

19.3.6 Spinal Dysraphism and Other Spinal Alterations

Spinal dysraphism is a group of developmental anomalies characterized by malformations in the embryonal dorsum, comprising also neural tube defects. Dysraphism comprises a subset of different malformations, characterized by caudal lesions affecting the spinal cord, vertebrae, and skin in different grades, all of them consequences of failure of fusion of the caudal neural tube [41, 42]. The prevalence of spinal dysraphism varies across time, by region, and by ethnicity. These conditions can carry severe neurological morbidity, with arm and leg weakness and paralysis, sensory loss, bowel and bladder dysfunction, and orthopedic abnormalities. Filum lipoma results from a developmental error in mesodermal cell migration, arising from the filum terminale. A fatty filum can become symptomatic if resulting in a tethered cord syndrome, with a low-lying conus (tip of the conus at or below the midpoint of L2). Intraoperative CEUS can aid to better identify the lipoma of the filum and to delineate the lipoma with respect to surrounding nerves. A spinal arachnoid cyst may cause spinal cord compression [43] with trans-dural CEUS showing the boundaries between the spinal cord surface, and vascularization, to better delineate the cyst boundaries and evaluating intra-cystic septations; these septations need to be fragmented to establish CSF circulation (Fig. 19.10).

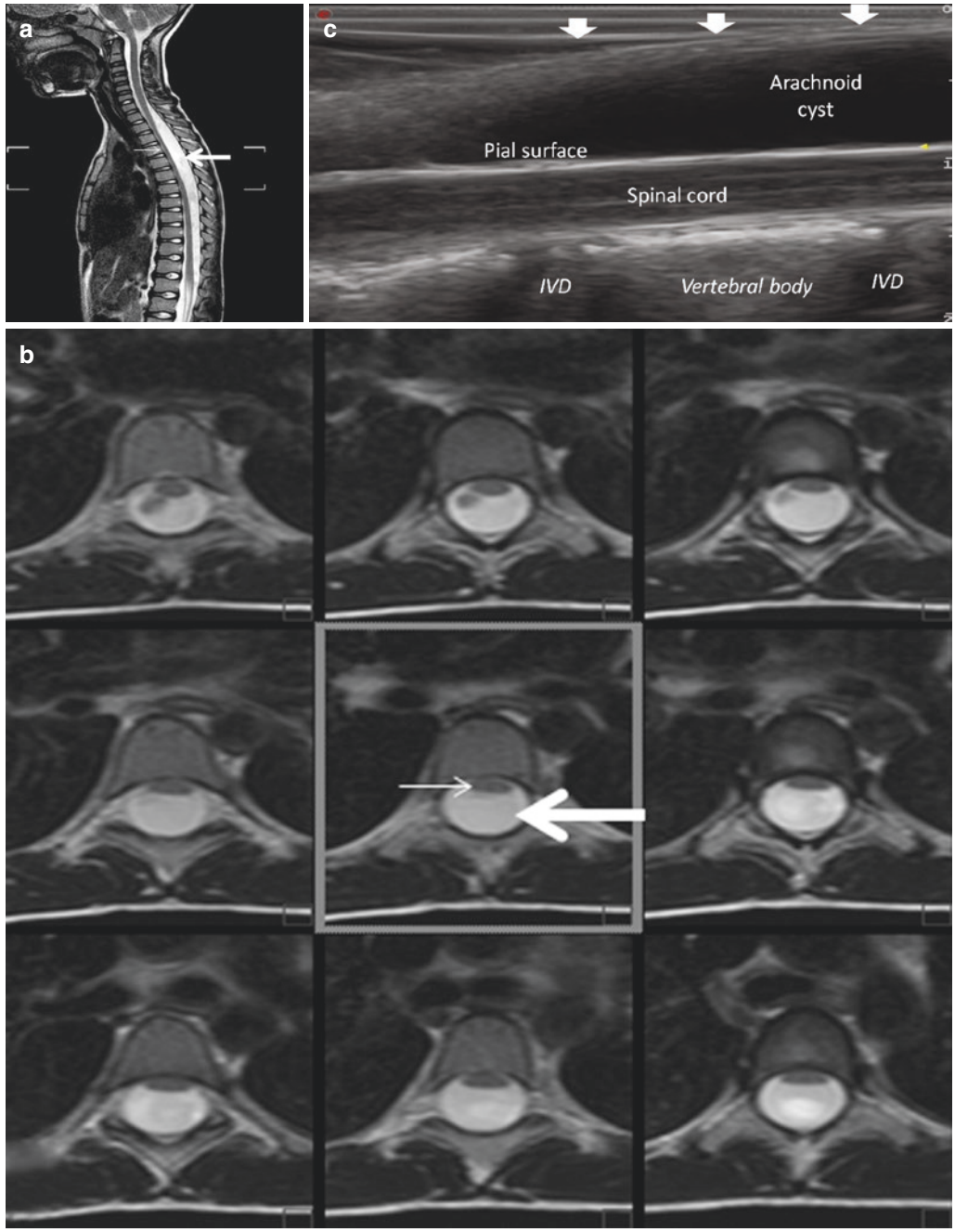

Fig. 19.10 A 10-year-old girl harboring a dorsal arachnoid cyst. (**a**) Sagittal T2-weighted MR images demonstrate an extensive hyperintense olodorsal arachnoid cyst (large arrow), causing an anterior dislocation of the spinal cord (hypointense, thin arrow). (**b**) Multi-slice axial T2-weighted MR images demonstrate an extensive hyperintense olodorsal arachnoid cyst (large arrow), causing an anterior dislocation of the spinal cord (hypointense, thin arrow). Due to the severe compression and subsequent neurological symptoms, the patient underwent surgery for cyst fenestration. (**c**) On the B-mode US the cyst appears hypoechoic, compressing the iso-echoic spinal cord. The vertebral bodies and intervertebral discs (IVD) are clearly recognizable. (**d**) Intraoperative CEUS further delineated the interface between cyst and dorsal spinal cord surface, without intra-cystic vessels or solid structures. The dura mater presented an intense and homogeneous enhancement (arrows)

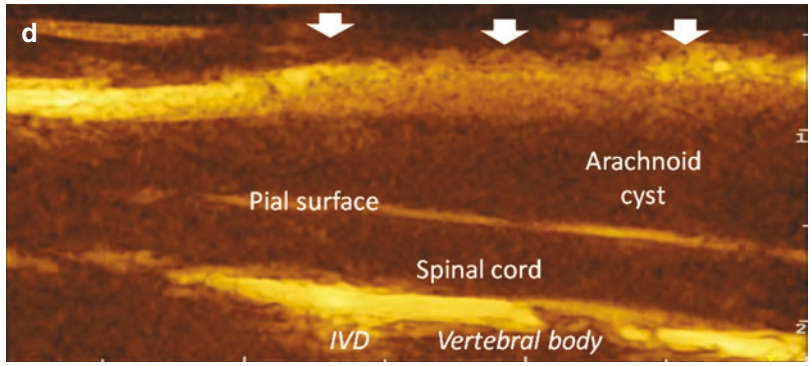

Fig. 19.10 (continued)

19.4 Conclusions

Intra-operative CEUS represents a promising technique to assess and guide neurosurgical procedures in the pediatric population. This technique can help intraoperative definition and relationship between tumor and surrounding structures, and visualize brain and spinal tumor remnants after resection. Intra-operative CEUS provides valuable biological information about tumor perfusion and vascularization, possibly changing the surgical strategy for tumor removal. Intra-operative CEUS can be useful also for non-invasive follow-up in neurovascular disease. Despite the anecdotal application of iCEUS in pediatric neurosurgery, further studies can confirm the usefulness, with the aim to better understand the pathophysiological substrate of different CNS afflictions.

References

1. Kanno H, Ozawa Y, Sakata K, Sato H, Tanabe Y, Shimizu N, Yamamoto I. Intraoperative power Doppler ultrasonography with a contrast-enhancing agent for intracranial tumours. J Neurosurg. 2005;102:295–301.
2. Engelhardt M, Hansen C, Eyding J, Wilkening W, Brenke C, Krogias C, Scholz M, Harders A, Ermert H, Schmieder K. Feasibility of contrast-enhanced sonography during resection of cerebral tumours: initial results of a prospective study. Ultrasound Med Biol. 2007;33:571–5.
3. He W, Jiang X, Wang S, Zhang M, Zhao J, Liu H, Ma J, Xiang D, Wang L. Intraoperative contrast-enhanced ultrasound for brain tumors. Clin Imaging. 2008;32:419–24.
4. Hölscher T, Ozgur B, Singel S, Wilkening WG, Mattrey RF, Sang H. Intraoperative ultrasound using phase inversion harmonic imaging. Oper Neurosurg. 2007;60:382–7.
5. Prada F, Bene MD, Casali C, et al. Intraoperative navigated angiosonography for skull base tumor surgery. World Neurosurg. 2015;84:1699. https://doi.org/10.1016/j.wneu.2015.07.025.
6. Vetrano IG, Prada F, Nataloni IF, Del Bene M, DiMeco F, Valentini LG. Discrete or diffuse intramedullary tumor? Contrast-enhanced intraoperative ultrasound in a case of intramedullary cervicothoracic hemangioblastomas mimicking a diffuse infiltrative glioma: technical note and case report. Neurosurg Focus. 2015;39:E17. https://doi.org/10.3171/2015.5.FOCUS15162.
7. Prada F, Mattei L, Del Bene M, et al. Intraoperative cerebral glioma characterization with contrast enhanced ultrasound. Biomed Res Int. 2014;2014:1. https://doi.org/10.1155/2014/484261.
8. Sidhu P, Cantisani V, Dietrich C, et al. The EFSUMB guidelines and recommendations for the clinical practice of contrast-enhanced ultrasound (CEUS) in non-hepatic applications: update 2017 (long version). Ultraschall Med—Eur J Ultrasound. 2018;39:e2–e44.
9. Prada F, Del Bene M, Saini M, Ferroli P, DiMeco F. Intraoperative cerebral angiosonography with ultrasound contrast agents: how I do it. Acta Neurochir. 2015;157:1025–9.
10. Prada F, Perin A, Martegani A, et al. Intraoperative contrast-enhanced ultrasound for brain tumor surgery. Neurosurgery. 2014;74:542–52.
11. Kastler A, Manzoni P, Chapuy S, Cattin F, Billon-Grand C, Aubry S, Biondi A, Thiriez G, Kastler B. Transfontanellar contrast enhanced ultrasound in infants: initial experience. J Neuroradiol. 2014;41:251–8.
12. Hwang M, De Jong RM, Herman S, et al. Novel contrast-enhanced ultrasound evaluation in neo-

natal hypoxic ischemic injury: clinical application and future directions. J Ultrasound Med. 2017;36:2379–86.
13. Hwang M. Introduction to contrast-enhanced ultrasound of the brain in neonates and infants: current understanding and future potential. Pediatr Radiol. 2018;49:254. https://doi.org/10.1007/s00247-018-4270-1.
14. Bailey C, Huisman TAGM, de Jong RM, Hwang M. Contrast-enhanced ultrasound and elastography imaging of the neonatal brain: a review. J Neuroimaging. 2017;27:437–41.
15. Prada F, Del Bene M, Mattei L, Lodigiani L, DeBeni S, Kolev V, Vetrano I, Solbiati L, Sakas G, DiMeco F. Preoperative magnetic resonance and intraoperative ultrasound fusion imaging for real-time neuronavigation in brain tumor surgery. Ultraschall Med—Eur J Ultrasound. 2014;36:174–86.
16. Vetrano IG, Prada F, Erbetta A, DiMeco F. Intraoperative ultrasound and contrast-enhanced ultrasound (CEUS) features in a case of intradural extramedullary dorsal schwannoma mimicking an intramedullary lesion. Ultraschall Med. 2015;36:307–10.
17. Sidhu P, Cantisani V, Deganello A, et al. Role of contrast-enhanced ultrasound (CEUS) in Pediatric practice: an EFSUMB position statement. Ultraschall Med—Eur J Ultrasound. 2016;38:33–43.
18. Rossi Espagnet MC, Bernardi B, Pasquini L, Figà-Talamanca L, Tomà P, Napolitano A. Signal intensity at unenhanced T1-weighted magnetic resonance in the globus pallidus and dentate nucleus after serial administrations of a macrocyclic gadolinium-based contrast agent in children. Pediatr Radiol. 2017;47:1345–52.
19. Costa AF, van der Pol CB, Maralani PJ, McInnes MDF, Shewchuk JR, Verma R, Hurrell C, Schieda N. Gadolinium deposition in the brain: a systematic review of existing guidelines and policy statement issued by the Canadian Association of Radiologists. Can Assoc Radiol J. 2018;69:373–82.
20. Selbekk T, Jakola AS, Solheim O, Johansen TF, Lindseth F, Reinertsen I, Unsgård G. Ultrasound imaging in neurosurgery: approaches to minimize surgically induced image artifacts for improved resection control. Acta Neurochir. 2013;155:973–80.
21. Prada F, Del Bene M, Moiraghi A, et al. From grey scale B-mode to elastosonography: multimodal ultrasound imaging in meningioma surgery-pictorial essay and literature review. Biomed Res Int. 2015;2015:925729.
22. Prada F, Del Bene M, Mattei L, et al. Fusion imaging for intra-operative ultrasound-based navigation in neurosurgery. J Ultrasound. 2014;17:243. https://doi.org/10.1007/s40477-014-0111-8.
23. Prada F, Del Bene M, Rampini A, et al. Intraoperative strain elastosonography in brain tumor surgery. Oper Neurosurg. 2018;17:227. https://doi.org/10.1093/ons/opy323.
24. Ntoulia A, Anupindi SA, Darge K, Back SJ. Applications of contrast-enhanced ultrasound in the Pediatric abdomen. Abdom Radiol. 2018;43:948–59.
25. Ostrom QT, de Blank PM, Kruchko C, et al. Alex's Lemonade stand foundation infant and childhood primary brain and central nervous system tumors diagnosed in the United States in 2007-2011. Neuro-Oncology. 2015;16(Suppl 10):x1–x36.
26. Ostrom QT, Gittleman H, Liao P, Vecchione-Koval T, Wolinsky Y, Kruchko C, Barnholtz-Sloan JS. CBTRUS statistical report: primary brain and other central nervous system tumors diagnosed in the United States in 2010-2014. Neuro-Oncology. 2017;19:v1–v88.
27. Tringali G, Bono B, Dones I, Cordella R, Didato G, Villani F, Prada F. Multimodal approach for radical excision of focal cortical dysplasia by combining advanced magnetic resonance imaging data to intraoperative ultrasound, electrocorticography, and cortical stimulation: a preliminary experience. World Neurosurg. 2018;113:e738–46.
28. Louis DN, Perry A, Reifenberger G, von Deimling A, Figarella-Branger D, Cavenee WK, Ohgaki H, Wiestler OD, Kleihues P, Ellison DW. The 2016 World Health Organization classification of tumors of the central nervous system: a summary. Acta Neuropathol. 2016;131:803–20.
29. Strahle J, Muraszko KM, Kapurch J, Bapuraj JR, Garton HJL, Maher CO. Chiari malformation type I and syrinx in children undergoing magnetic resonance imaging. J Neurosurg Pediatr. 2011;8:205–13.
30. Curone M, Valentini LG, Vetrano I, Beretta E, Furlanetto M, Chiapparini L, Erbetta A, Bussone G. Chiari malformation type 1-related headache: the importance of a multidisciplinary study. Neurol Sci. 2017;38:91. https://doi.org/10.1007/s10072-017-2915-8.
31. Smith BW, Strahle J, Bapuraj JR, Muraszko KM, Garton HJL, Maher CO. Distribution of cerebellar tonsil position: implications for understanding Chiari malformation. J Neurosurg. 2013;119:812–9.
32. Brock RS, Taricco MA, de Oliveira MF, de Lima OM, Teixeira MJ, Bor-Seng-Shu E. Intraoperative ultrasonography for definition of less invasive surgical technique in patients with Chiari type I malformation. World Neurosurg. 2017;101:466–75.
33. McGirt MJ, Attenello FJ, Datoo G, Gathinji M, Atiba A, Weingart JD, Carson B, Jallo GI. Intraoperative ultrasonography as a guide to patient selection for duraplasty after suboccipital decompression in children with Chiari malformation type I. J Neurosurg Pediatr. 2008;2:52–7.
34. Scott RM, Smith ER. Moyamoya disease and moyamoya syndrome. N Engl J Med. 2009;360:1226–37.
35. Ibrahimi DM, Tamargo RJ, Ahn ES. Moyamoya disease in children. Childs Nerv Syst. 2010;26:1297–308.
36. Smith ER, Scott RM. Spontaneous occlusion of the circle of Willis in children: Pediatric moyamoya summary with proposed evidence-based practice guidelines. A review. J Neurosurg Pediatr. 2012;9:353–60.

37. Sahu RK, Das KK, Bhaisora KS, Singh AK, Mehrotra A, Srivastava AK, Sahu RN, Jaiswal AK, Behari S. Pediatric intramedullary spinal cord lesions: pathological spectrum and outcome of surgery. J Pediatr Neurosci. 2015;10:214–21.
38. Steinbok P, Cochrane DD, Poskitt K. Intramedullary spinal cord tumors in children. Neurosurg Clin N Am. 1992;3:931–45.
39. Crawford JR, Zaninovic A, Santi M, Rushing EJ, Olsen CH, Keating RF, Vezina G, Kadom N, Packer RJ. Primary spinal cord tumors of childhood: effects of clinical presentation, radiographic features, and pathology on survival. J Neuro-Oncol. 2009;95:259–69.
40. Guss ZD, Moningi S, Jallo GI, Cohen KJ, Wharam MD, Terezakis SA. Management of Pediatric spinal cord astrocytomas: outcomes with adjuvant radiation. Int J Radiat Oncol Biol Phys. 2013;85:1307–11.
41. Mitchell LE, Adzick NS, Melchionne J, Pasquariello PS, Sutton LN, Whitehead AS. Spina bifida. Lancet. 2004;364:1885–95.
42. Northrup H, Volcik KA. Spina bifida and other neural tube defects. Curr Probl Pediatr. 2000;30:313–32.
43. Bond AE, Zada G, Bowen I, McComb JG, Krieger MD. Spinal arachnoid cysts in the Pediatric population: report of 31 cases and a review of the literature. J Neurosurg Pediatr. 2012;9:432–41.

Contrast-Enhanced Ultrasound in Pediatric Intervention

20

Abhay Srinivasan and Dean Y. Huang

20.1 Principles of Contrast-Enhanced Ultrasound in Pediatric Interventional Radiology

Image guidance when performing any intervention greatly increases the efficacy and precision of targeted therapy, and it allows minimally invasive procedures that limit post-procedure morbidity. Current modalities used for procedure guidance are fluoroscopy, ultrasonography (US), computed tomography, and magnetic resonance imaging. The choice of modality is often based on criteria which include ease of use, availability, spatial resolution, contrast resolution, and temporal resolution.

Significant benefits of US are the ability to perform imaging in any plane, excellent temporal resolution—one can visualize the intervention in "real-time" and easy availability, with the ability to perform procedures away from the interventional suite. For pediatric interventions, US has the added benefit of superior spatial resolution, as smaller patients allow the visualization of deep tissues with high-frequency transducers, a luxury often not afforded with adult interventions. Also, particularly important for children is that the US does not produce any ionizing radiation, and therefore carries no carcinogenic risk. Limitations of US in comparison to other modalities include operator-dependent performance, limited visualization in patients with large habitus, inability to see through the bone cortex and bowel gas, a decreased field-of-view, and less contrast resolution than computed tomography (CT) and magnetic resonance (MR) imaging. While these first two limitations are constitutional to the US, the final limitation has greatly been ameliorated by the advent contrast-enhanced US (CEUS) [1].

20.2 Technique

There are a variety of ultrasound contrast agents (UCA) on the market. With regard to pediatric applications, sulfur hexafluoride lipid-type A microspheres (SonoVue™/Lumason™, Bracco, Milan/Monroe Township NJ) is the most widely used UCA in Europe and Asia and has been approved by the US Food and Drug Administration for the characterization of pediatric liver lesions and for intracavitary use in voiding sonourography. Imaging is begun immediately after administration of the UCA and often viewed in a split-screen display, or alternatively in overlay

A. Srinivasan
Department of Radiology, Children's Hospital of Philadelphia, Perelman School of Medicine, University of Pennsylvania, Philadelphia, PA, USA
e-mail: srinivasaa@email.chop.edu

D. Y. Huang (✉)
Department of Radiology, King's College Hospital, London, UK
e-mail: Dean.huang@nhs.net

P. S. Sidhu et al. (eds.), *Contrast-Enhanced Ultrasound in Pediatric Imaging*,
https://doi.org/10.1007/978-3-030-49691-3_20

mode wherein the contrast image is overlaid on the B-mode (grayscale) image, with activation of the contrast timer.

Contrast-enhanced ultrasound is performed with low MI (<0.2), and this allows imaging down to a depth of 12 cm, which is generally adequate for most pediatric interventions. Default settings of the contrast software are often adequate for imaging during the intervention, but additional setting packages such as "resolution" or "penetration" (which adjust transmit frequency) are available on most machines for simple optimization. The focal zone should be positioned just deep to the target tissue, and the gain should be set so that, before contrast infusion, the image is dark, but with only a slight amount of noise. The dynamic range may be tailored for the procedure; a small range will accentuate vessels, but a wider range will allow different degrees of tissue enhancement [2].

20.2.1 Intravascular Administration

In contrast to diagnostic applications, establishing venous access is rarely a logistical hurdle for interventional CEUS. Children often present for an interventional radiology procedure with venous access already established, as procedures are often done with moderate sedation or general anesthesia. In patients with no venous access, venous access can be obtained in the interventional suite. To aid patient comfort, this can be done after the induction of anesthesia or with US guidance.

Ultrasound contrast agents may be administered through a central venous catheter or peripheral venous cannula. For the latter, it is advised that the cannula be at least 22 gauge in size and preferably 20 gauge. Using standard sterile technique, the UCA is injected gently via a three-way connector through the in-line port, with the orthogonal port connected to normal saline to allow the saline flush. It is preferred that the UCA is not injected through a hemostatic "clave" connector, as this may prematurely burst the microbubbles. In addition, connectors and valves in central venous catheters may burst the UCA, necessitating a higher dose.

Intravascular UCA dose is dependent on the specific agent and may have to be further adjusted depending on the US transducer used, contrast software, and size of the patient [2]. Linear transducers may require higher UCA doses, as scattering from microbubbles is less efficient at high frequencies. The standard intravenous dose is 0.03 mL/kg of sulfur hexafluoride reconstituted in 5 mL of sterile normal saline. To allow more prolonged UCA enhancement, additional boluses of UCA may be given, and if necessary, a continuous slow infusion may be performed. For sulfur hexafluoride lipid, the reconstituted UCA is infused by the pump at 1 mL/min.

The major absolute contraindication to UCA use is a history of hypersensitivity to the agent. Anaphylaxis is rare (about 1 in 7000), but an increased incidence of a serious allergic reaction to sulfur hexafluoride has been reported [3, 4]. Resuscitation medications and equipment must be readily available.

20.2.2 Intracavitary Administration

Intracavitary administration of UCA requires a prior needle or catheter access. For access, UCA may be useful to increase visualization of the needle, which is achieved by flushing a few drops of dilute UCA through the hub and shaft. Access is performed in dual-screen or overlay mode, and successful cannulation is confirmed when UCA diffuses into the target or is pushed out of the needle by fluid egress from the target.

UCA may be infused into either physiologic or pathologic cavities. As the enclosed space is much smaller than the blood pool, the UCA must be significantly diluted. A dilution of 1:100 (i.e., 1 mL of reconstituted microspheres in 100 mL normal saline) is reasonable. For enteric administration, the UCA is diluted in water at room temperature. The injection is performed with a sterile technique, and post-contrast administration imaging is performed as described in the prior section. Microbubbles remain stable in the cavity longer than in the blood pool, 20–30 min for

sulfur hexafluoride lipid. If an immediate repeat examination is necessary, the UCA may either be aspirated out of the cavity or the microbubbles burst by repeated high mechanical index (MI) pulses, before a fresh injection.

20.3 Applications

With either the intravascular and intracavitary applications, the distribution of UCA within the target improves visualization of the region of interest and provides valuable guidance during the procedure. Besides, CEUS is often used as a problem-solving tool to guide decisions in patent management after completion of the procedure.

20.3.1 Intravascular Applications

Microbubbles within the UCA measure 2–6 μm in diameter, and when administered in the blood pool, UCA remains in the blood pool without entering the interstitial space, and therefore offers an excellent characterization of the "target" vascularity.

20.3.1.1 Biopsy

A primary application of CEUS in interventional radiology is biopsy guidance. A UCA is sometimes useful to increase the conspicuity of the lesion, given the lower contrast resolution of grayscale US relative to computed tomography (CT) or magnetic resonance (MR) imaging. This may be particularly useful for small lesions in homogeneous solid viscera such as the liver. In children, this is frequently in the setting of concern for metastasis, as primary liver neoplasms, while uncommon, are frequently large at presentation and readily visible on conventional sonography. More frequently, CEUS is used in biopsy guidance to determine the optimum site of biopsy within the tumor, as enhancement indicates most viable regions of the tumor. Biopsy of nonnecrotic regions would increase diagnostic yield (Fig. 20.1). Acquisition of viable tissue may be of

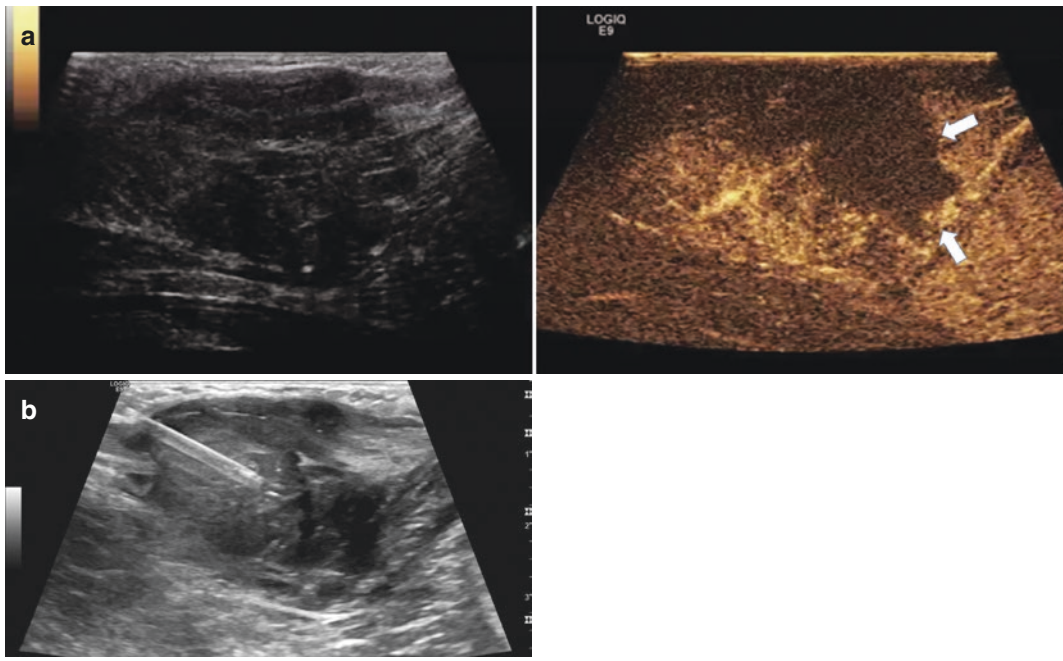

Fig. 20.1 (**a**) A split-screen display of a CEUS examination (left: grayscale. Right: CEUS) demonstrates a mass in the right lower quadrant of the abdomen. An area of necrosis, demonstrated as a non-enhancing area within the mass, is demonstrated on CEUS (arrows). (**b**) On US-guided biopsy, the necrotic area within the lesion was avoided, guided by the CEUS findings

particular concern if genetic analysis of tissue for next-generation sequencing is desired. The use of CEUS can shorten the procedure, as it can increase the confidence of adequate sampling, thereby decreasing the number of passes the interventionist would make, and also decrease the need for frozen section analysis during the procedure. Similarly, the assessment of perfusion during a biopsy can help avoid large vessels coursing through or around the tumor, therefore decreasing the risk of hemorrhage after a biopsy. If there is a concern for significant post-procedure hemorrhage, this can be assessed by CEUS of the region of intervention, often faster and with less logistical complexity than CT [5]. The excellent depiction of vasculature allows for the easy detection of pseudoaneurysms [6].

CEUS may also be used to guide decisions during the procedure, and this aspect would apply diagnostic principles of CEUS. Illustrative scenarios include use of CEUS to distinguish complex fluid collections (which may have a questionable solid appearance on the grayscale US) from solid tumors, and this would determine whether the procedure is a drainage or a biopsy, without having to perform a CT or MR examination (Fig. 20.2). Furthermore, based on the enhancement pattern, a lesion may be demonstrated to be benign in the interventional suite, therefore obviating the need for biopsy [1].

20.3.1.2 Interventional Oncology

Interventional oncology, the application of interventional radiology towards targeted destruction of tumors, is an established pillar of cancer therapy in adults, and these techniques, while less frequently indicated in children, are gaining recognition in pediatric oncology. A practical application of CEUS would be for intra-procedural and post-procedural feedback: tumor vascularity is assessed before and after ablation (radiofrequency ablation, cryoablation, microwave ablation, ethanol ablation, high-frequency focused ultrasound, and irreversible electroporation). The demonstration of cessation of contrast enhancement provides strong confirmation of the adequacy of treatment (Fig. 20.3), and the lack thereof would indicate further ablation is necessary. Contrast-enhanced ultrasound provides superior spatial and temporal resolution of tissue perfusion than other modes of cross-sectional imaging. In adults undergoing ablation of hepatoma, the absence of perfusion after ablation has shown to be highly predictive of therapeutic success, and residual tumor detection is at least commensurate with other imaging modalities [5]. Immediate post-ablation assessment of tissue perfusion is best suited for cryoablation, as a collection of gas in the treatment area from tissue vaporization will

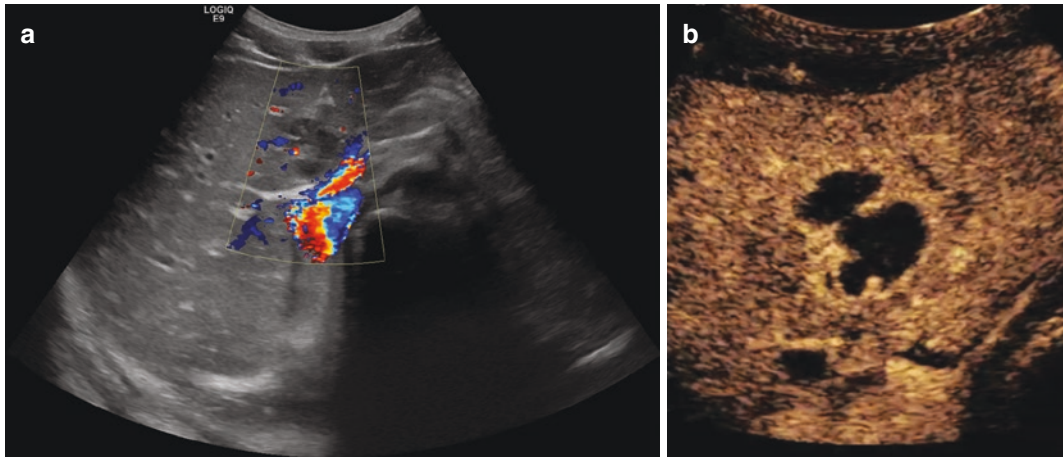

Fig. 20.2 (**a**) Color Doppler US examination in a boy with a history of neuroblastoma revealed an indeterminate hypoechoic focal abnormality. (**b**) CEUS performed in the interventional suite showed the rim-enhancement of the lesion, consistent with abscess, and a drainage, instead of a biopsy, was performed

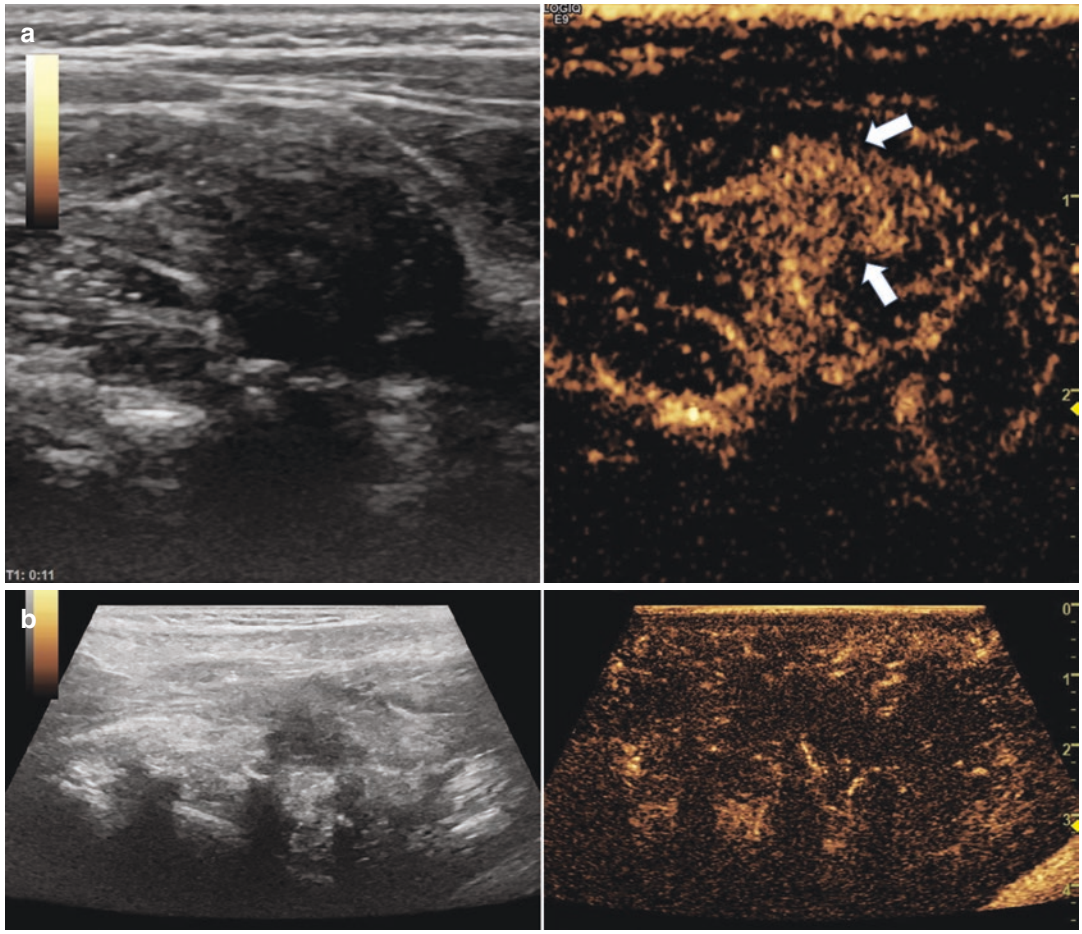

Fig. 20.3 (**a**) A split-screen display of a CEUS examination (left: grayscale. Right: CEUS) in a 3-year-old male demonstrates a metastatic rhabdomyosarcoma at the right shoulder. The lesion demonstrates enhancement (arrows) relative to the surrounding structures on CEUS, and there was early washout. (**b**) A split-screen display of a CEUS examination (left: grayscale. Right: CEUS) was performed immediately following cryoablation, showing absence of enhancement of the ablated lesion and indicating a successful ablation

hinder US assessment immediately after radiofrequency or microwave ablation [5]. Similarly, intra-arterial administration of UCA has been used to guide embolization (confirm appropriate sub-selectivity) and to determine adequacy treatment during trans-arterial embolization of liver tumors [7].

20.3.1.3 Vascular Access

CEUS may be used for planning in cases of challenging venous access. Patients with a history of multiple or long-term central venous access often develop central venous stenosis or occlusion. Smaller children are particularly susceptible to these complications, as the catheter occupies a larger cross section of the venous lumen, reducing flow and predisposing to thrombosis and intimal hyperplasia, which then evolves to stenosis or occlusion. This can significantly complicate venous access [8]. To date, at-risk patients are commonly assessed by CT or MR venography, interventional venography, or Doppler sonography. CEUS venography may demonstrate central venous stenosis to good advantage (Fig. 20.4) and has the added benefit of ease-of-use and the lack of ionizing radiation.

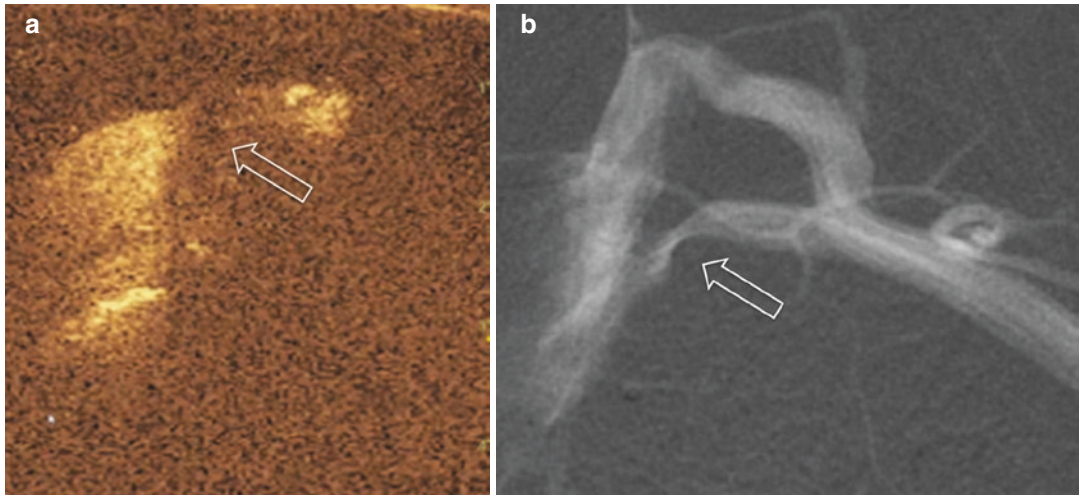

Fig. 20.4 (**a**) CEUS and the corresponding (**b**) venography of the left subclavian vein. Both examinations demonstrate a focal stenosis (block arrow) at the distal left subclavian vein

20.3.2 Intracavitary Applications

The distribution of the contrast agent within a cavity can provide valuable information to determine the adequacy of intervention and post-procedure management. Endocavitary CEUS can also be used as a problem-solving tool to assess complications related to interventions (e.g., catheter dislodgement) or the underlying disease process (e.g., fistula formation). These applications often enhance or supplant conventional fluoroscopic or CT techniques, and can facilitate the care of critically ill children, as they can be performed at the bedside and also without ionizing radiation. While some of these applications may be performed with agitated saline infusion and the grayscale US, CEUS offers improved visualization and the ability to see delayed filling of communications and compartments, as the microbubbles in the UCA are more stable than those of agitated saline [3].

20.3.2.1 Drainage

CEUS gives an excellent definition of the cavity size and shape. Large abscesses are often multiloculated and may require multiple drains. After the initial catheter placement, demonstrated filling of the entire volume of a multiloculated collection may confirm procedure endpoint without fluoroscopy, and obviate the need for additional catheter placement.

Concerning management post-procedure, CEUS of the drained cavity can be used to verify the position of the drain, demonstrate fistulous communication, and characterize the state of the cavity before drain removal (Fig. 20.5). For example, inflammatory collections such as empyema contain complex proteinaceous material that forms membranes/loculations and greatly increase fluid viscosity, limiting the efficacy of drainage. The fluid can be mobilized by intracavitary infusion of a fibrinolytic agent (e.g., urokinase or tissue plasminogen activator), but the response to fibrinolysis must be monitored to ensure adequate management. The progress of adequate fibrinolysis can be assessed with good confidence by infusion of UCA into the cavity (Fig. 20.6). In cases of high or abnormal output after drainage, CEUS provides an excellent depiction of fistulae and can be used to track resolution. CEUS can be easily performed at the bedside and allows imaging in multiple planes with greater spatial and contrast resolution than fluoroscopy.

20.3.2.2 Sclerotherapy

Endocavitary CEUS can minimize or obviate the use of fluoroscopy for certain slow-flow vascular

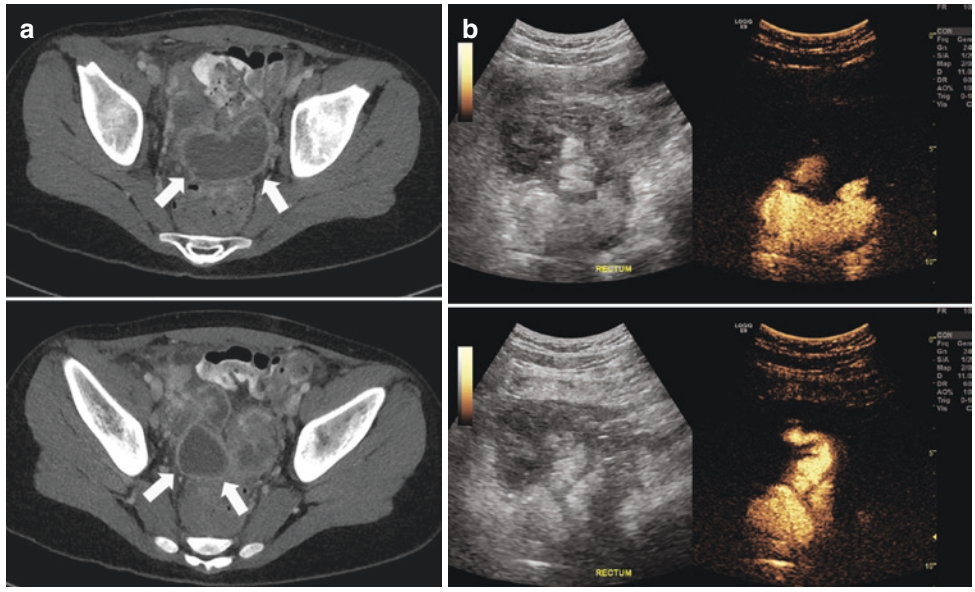

Fig. 20.5 (**a**) CT images of a multi-loculated pelvic abscess (arrows). (**b**) A split-screen display of an intracavitary CEUS examination (left: grayscale. Right: CEUS) confirms adequacy of treatment from a single trans-rectal drain, with all loculations within the collection filled with microbubbles after instilling the contrast

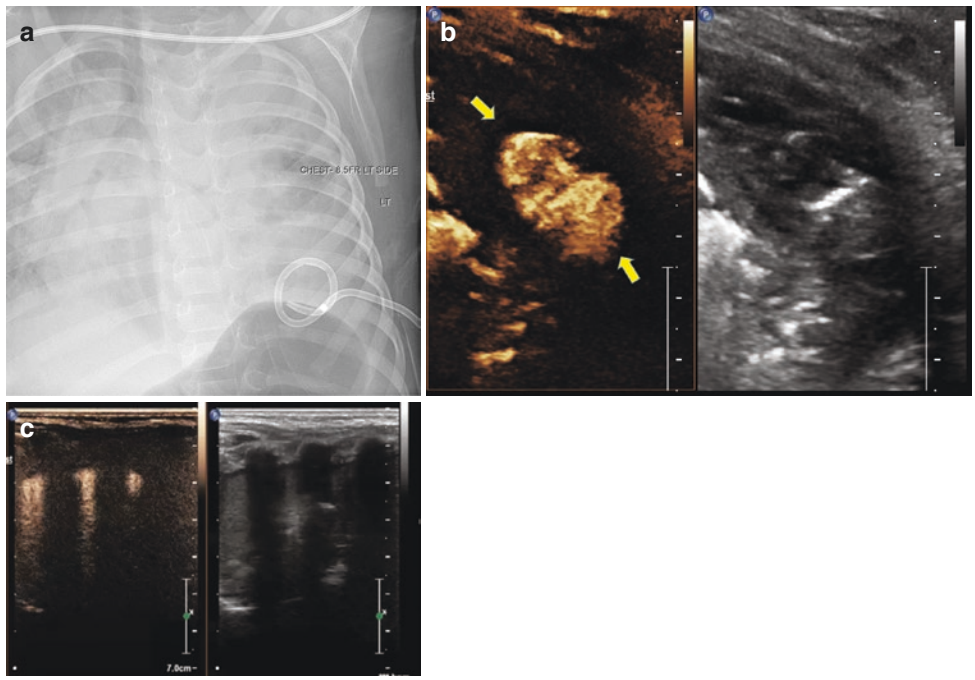

Fig. 20.6 (**a**) A chest radiograph demonstrates a left empyema with a pleural drain in situ. (**b**) A split-screen display of an intracavitary CEUS examination (left: CEUS. Right: grayscale), with contrast instilled through the pleural drain, demonstrates a loculated empyema, with microbubbles confined within a loculated collection around the pleural drain (arrows). (**c**) Following fibrinolytic infusion through the pleural drain, a repeat intracavitary CEUS (left: CEUS grayscale. Right: grayscale; coronal image) demonstrates microbubbles diffusing through the pleural space

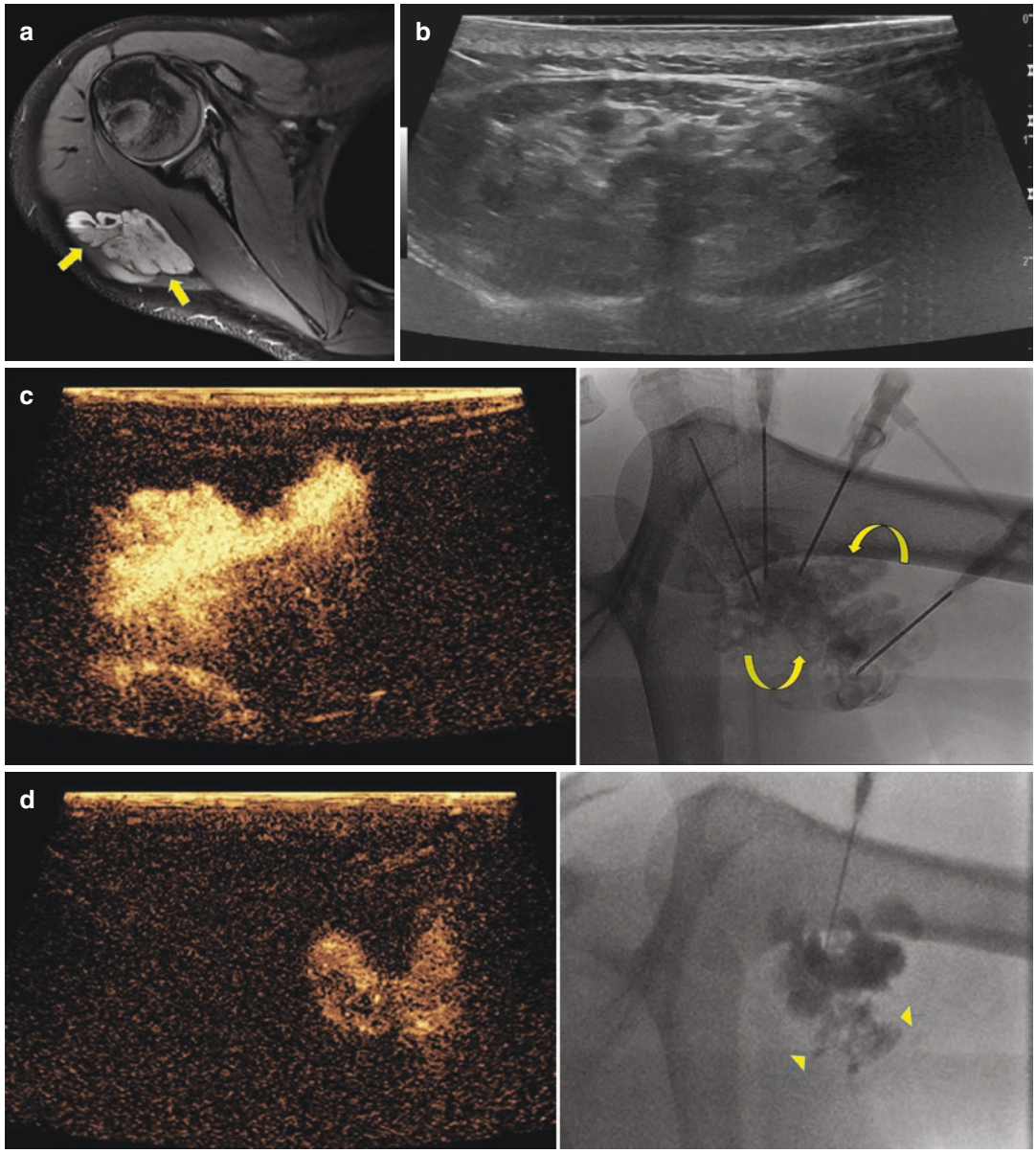

Fig. 20.7 (**a**) A T2-weighted MRI image showing the high signal intramuscular vascular malformation (arrows). (**b**) The grayscale US image demonstrates an intramuscular vascular malformation at the right shoulder as mixed echogenicity areas in the subcutaneous tissue. (**c**, **d**) CEUS (left) and corresponding fluoroscopic (right) images during CEUS-guided sclerotherapy. CEUS can be used to assess for complete treatment, as injection into separate sites shows microbubble filling of the different compartments of the larger lesion, as depicted on the fluoroscopic images (curved arrows and arrowheads)

malformations (specifically, lymphatic and non-diffuse venous malformations which lack robust outflow into deep veins). Using principles similar to those highlighted with drainage, the distribution of UCA in the malformation can be used to determine whether all components of the malformation have been filled. If areas of the malformation do not fill with UCA, this would mandate separate access to these areas (Fig. 20.7). CEUS allows excellent characterization of the lesion before installation of the sclerosant; the sclerosant is often constituted as a foam, and once it

is injected, the lesion may no longer be adequately seen on the US.

In instances of sclerotherapy of cysts that are not strictly vascular malformations, CEUS may be useful in documenting the lack of communication with normal parenchyma. For example, this utility may be beneficial in sclerotherapy of a symptomatic renal cyst if there is a question of communication with the collecting system, before instilling an offending sclerosant (Fig. 20.8).

20.3.2.3 Urinary and Biliary Tracts

Access to non-dilated collecting systems can be greatly aided by CEUS [9]. As described above, instilling UCA into the needle before access improves needle visualization. With successful access to the renal collecting system, the UCA will flow away from the needle and fill the calyx, allowing access with the US instead of fluoroscopy. However, if UCA is injected without adequate access to the calyx or a bile duct, the UCA will remain in the parenchyma, but stagnant microbubbles can be destroyed with high MI scanning. Therefore, a failed access attempt will not result in a "blob" that impedes visualization in subsequent attempts, as can be encountered with fluoroscopy [6].

Once access is obtained, CEUS cholangiography or antegrade nephrostogram (Fig. 20.9) can

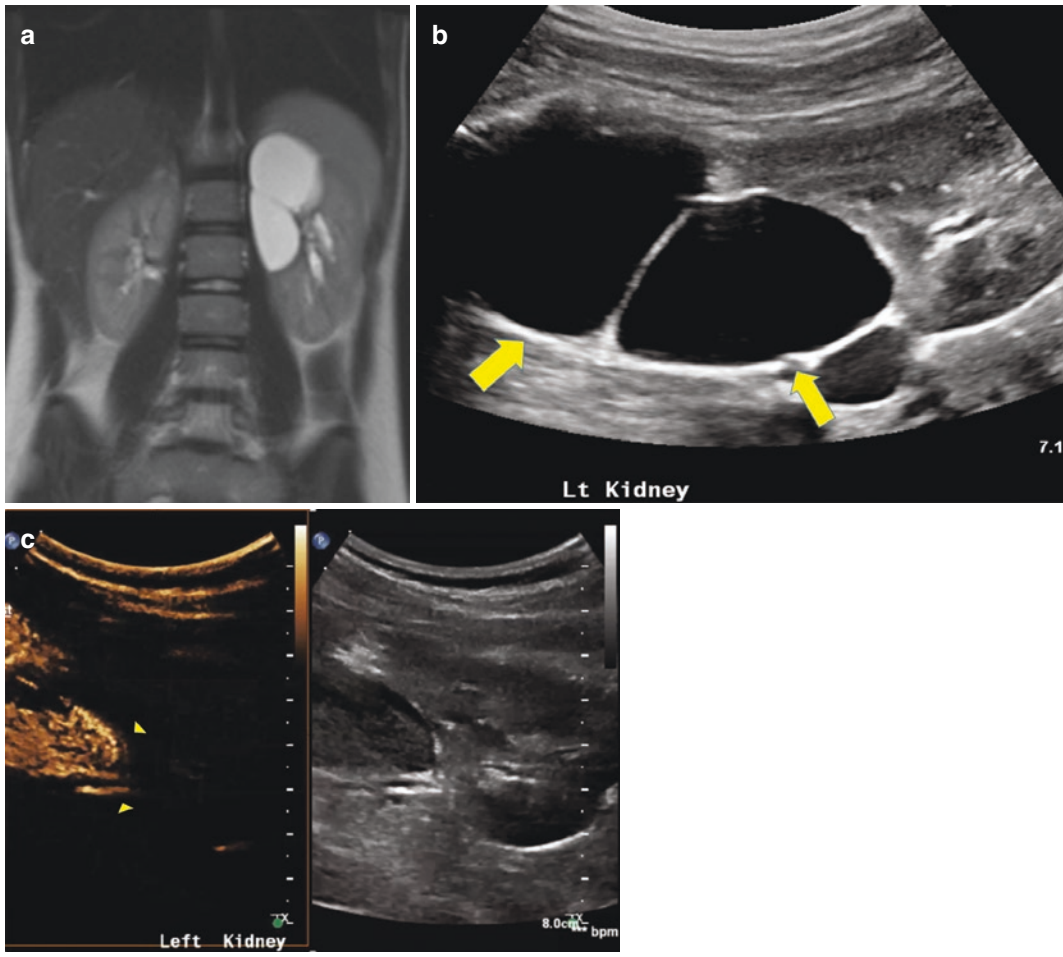

Fig. 20.8 (**a**) A coronal T2-weighted image of the abdomen and (**b**) a grayscale US image of the left kidney demonstrate a large cystic structure within the left kidney (arrows). (**c**) A split-screen display of an intracavitary CEUS examination (left: CEUS. Right: grayscale) confirms no communication (arrowheads) between this cyst with the renal collecting system. The CEUS finding permits sclerotherapy to be safely performed

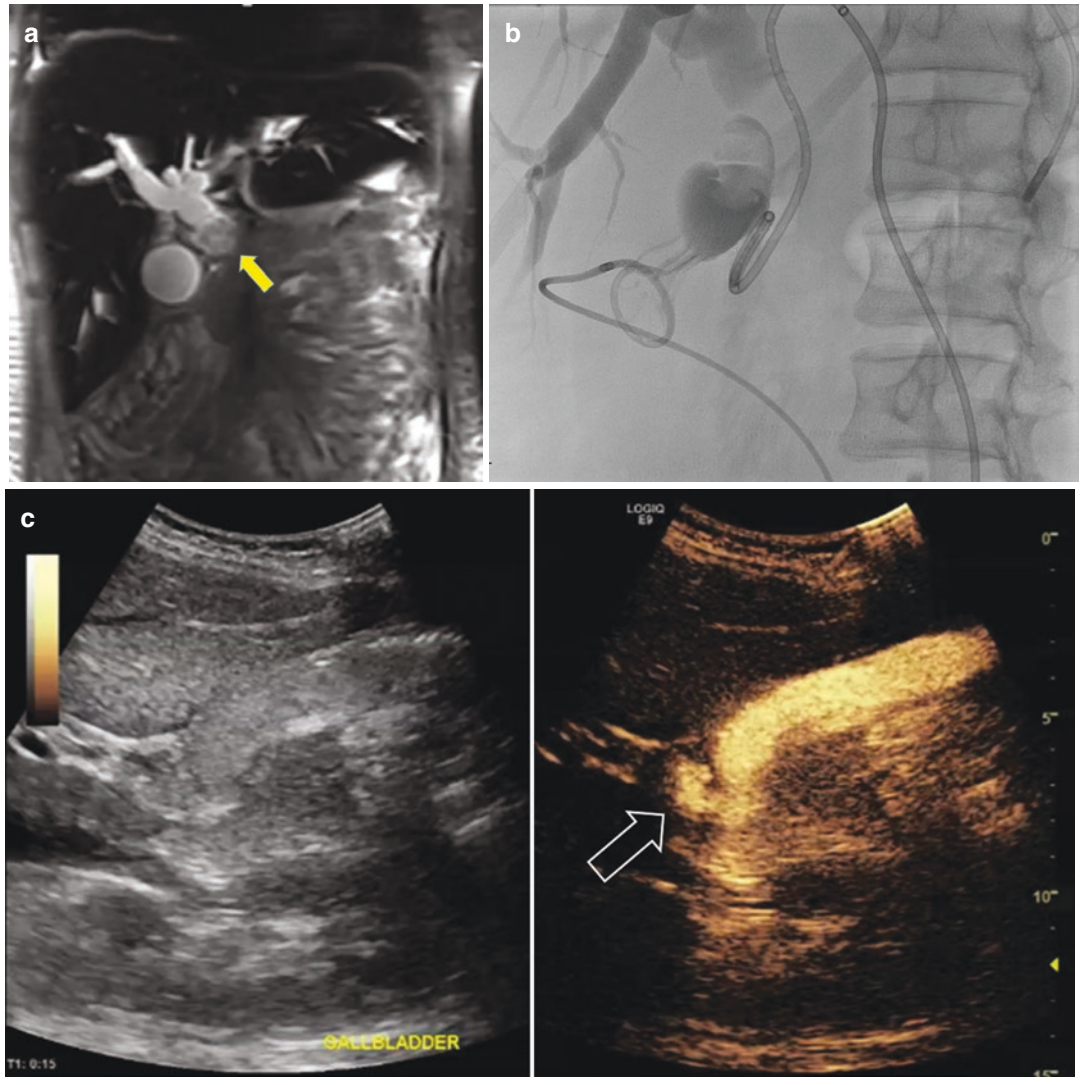

Fig. 20.9 (**a**) A coronal MR cholangiogram image demonstrates biliary dilation and cystic duct debris (arrow) of Mirrizi syndrome. (**b**) A biliary drain and percutaneous cholecystostomy were placed. (**c**, **d**) Resolution of the obstructing debris was followed with bedside CEUS (split-screen display, left: CEUS. Right: grayscale) with contrast flowing into the cystic duct and duodenum (open arrows)

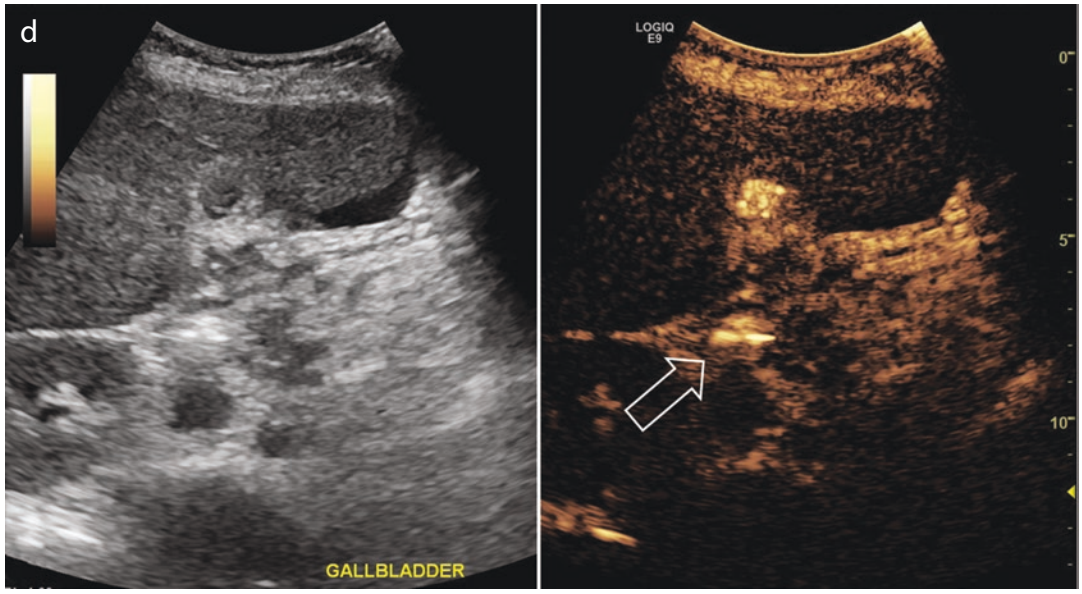

Fig. 20.9 (continued)

be performed, with all the previously described advantages over fluoroscopy. The ureter and the site of any obstruction can be well visualized, as can the central biliary ductal system—UCA can also be followed into the small bowel (Fig. 20.10) [5]. As with drainage of other collections, CEUS can be used to assess post-procedure complications such as catheter dislodgement, leakage, fistula, and hemorrhage.

20.3.2.4 Other Intracavitary Applications

Myriad other endocavitary applications have been described. In the enteric system, a UCA enema may be performed with primary gastrostomy placement to delineate the large bowel in relation to the stomach. The advantage over fluoroscopy is that one can easily determine whether the colon is superficial or deep to the stomach. Injection of UCA into the stoma can confirm appropriate tube placement and assess complications [10].

Additional applications of "endocavitary" CEUS include assessment of ducts of the parotid glands (CEUS sialography). Contrast-enhanced ultrasound access techniques can also be employed to access joints for steroid injections in children with juvenile idiopathic arthritis.

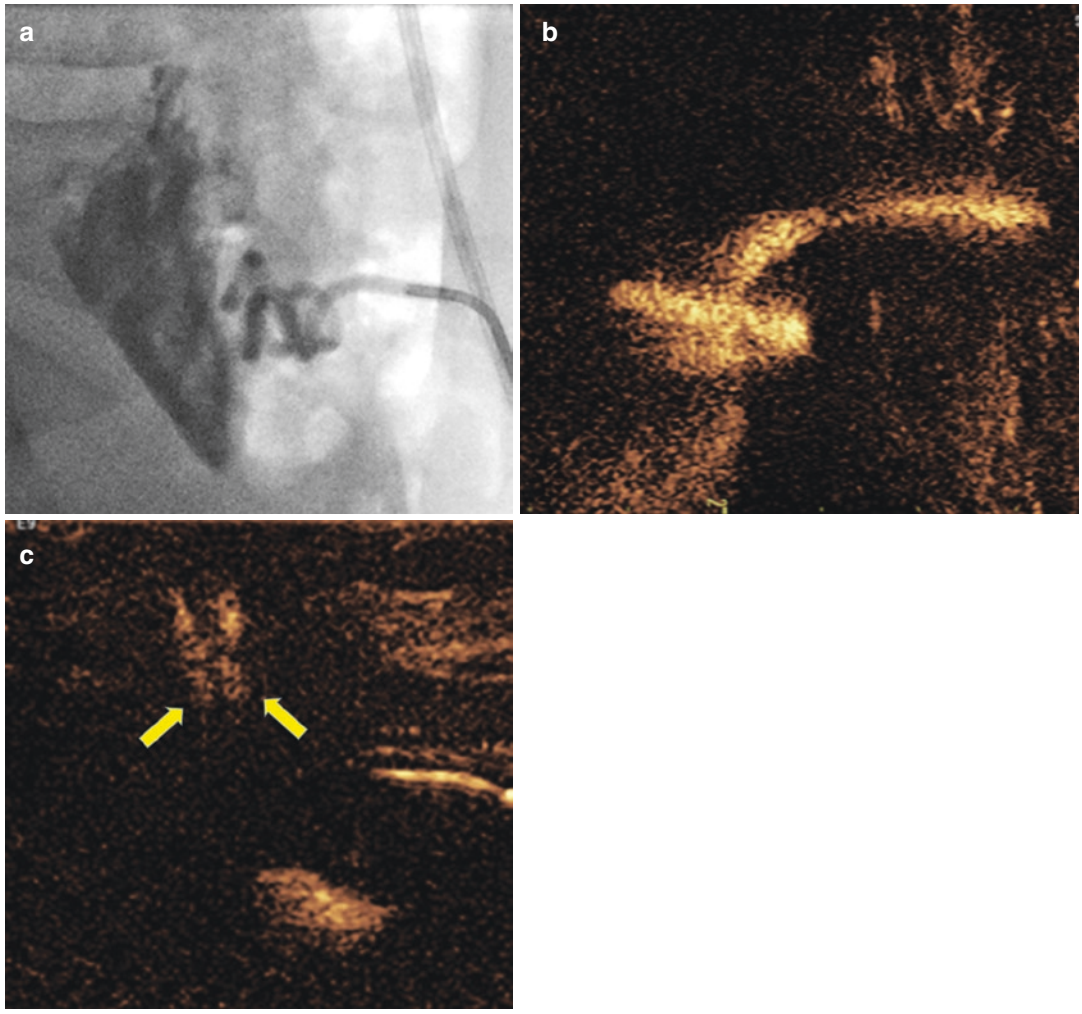

Fig. 20.10 Images from (**a**) fluoroscopic and (**b**) US contrast injection of a cecostomy tube in a teenager with constant fecal leakage from the site. (**c**) CEUS of tract injection after tube removal shows two parallel tracks (arrows). One of the tracks is the stoma and the other an enterocutaneous fistula

20.4 Conclusion

Contrast-enhanced ultrasound is an asset to interventional radiology and offers manifold advantages that can facilitate the procedure and enhance patient care. While currently US contrast is best indicated for biopsy guidance, ablation control, and follow-up and drainage procedures, these are by no means limitations to the impactful use of CEUS in pediatric interventions. With added experience, new applications will undoubtedly be found, and these would only be bounded by the inventiveness of the enterprising interventional radiologist.

References

1. Huang DY, Yusuf GT, Daneshi M, Husainy MA, Ramnarine R, Sellars MEK, Sidhu PS. Contrast-enhanced US-guided interventions: improving success rate and avoiding complications using US contrast agents. Radiographics. 2017;37:652–64.
2. Dietrich CF, Averkiou M, Nielsen MB, Barr RG. How to perform contrast-enhanced ultrasound (CEUS). Ultrasound Int Open. 2018;4:E2–E15.
3. Muller T, Blank W, Leitlein J, Kubicka S, Heinzmann A. Endocavitary contrast-enhanced ultrasound: a technique whose time has come? J Clin Ultrasound. 2015;43:71–80.

4. Kessner R, Nakamoto DA, Kondray V, Partovi S, Ahmed Y, Azar N. Contrast-enhanced ultrasound guidance for interventional procedures. J Ultrasound Med. 2019;38:2541. https://doi.org/10.1002/jum.14955.
5. Nolsøe CP, Nolsøe AB, Klubien J, Pommergaard HC, Rosenberg J, Meloni MF, Lorentzen T. Use of ultrasound contrast agents in relation to percutaneous interventional procedures: a systematic review and pictorial essay. J Ultrasound Med. 2018;37:1305–24.
6. Huang DY, Yusuf GT, Daneshi M, Ramnarine R, Deganello A, Sellars ME, Sidhu PS. Contrast-enhanced ultrasound (CEUS) in abdominal intervention. Abdom Radiol. 2018;43:960–76.
7. Lekht I, Nayyar M, Luu B, Guichet PL, Ho J, Ter-Oganesyan R, Katz M, Gulati M. Intra-arterial contrast-enhanced ultrasound (IA CEUS) for localization of hepatocellular carcinoma (HCC) supply during transarterial chemoembolization (TACE): a case series. Abdom Radiol. 2017;42:1400–7.
8. Forauer AR, Theoharis C. Histologic changes in the human vein wall adjacent to indwelling central venous catheters. J Vasc Interv Radiol. 2003;14:1163–8.
9. Liu BX, Huang GL, Xie XH, Zhuang BW, Xie XY, Lu MD. Contrast-enhanced US-assisted percutaneous nephrostomy: a technique to increase success rate for patients with nondilated renal collecting system. Radiology. 2017;285:293–301.
10. Yusuf GT, Fang C, Huang DY, Sellars ME, Deganello A, Sidhu PS. Endocavitary contrast enhanced ultrasound (CEUS): a novel problem-solving technique. Insights Imaging. 2018;9:303–11.

Cost-Effectiveness of CEUS in Pediatric Practice

21

Gibran T. Yusuf, Annamaria Deganello, Maria E. Sellars, and Paul S. Sidhu

21.1 Introduction

Imaging has become an essential part of modern medical practice, both in adult and pediatric practice. Increasingly sophisticated methods have been developed for both detection and characterization of pathology through invasive and non-invasive means. Cross-sectional imaging with magnetic resonance (MR) or computed tomography (CT) imaging has come to the forefront, with the latter being of dominant use. Both modalities are useful in providing tissue characteristic detail and dynamic vascular imaging. However, disadvantages exist, CT while providing rapid panoramic assessment, utilizes ionizing radiation and nephrotoxic iodinated contrast. MR imaging provides superb tissue characteristic detail, with new techniques, including elastography, spectroscopy, or functional imaging further improving imaging. Unfortunately, MR imaging is often a prolonged procedure, suffering severely with movement artifact and frequently requiring sedation or general anesthesia in the pediatric population. Furthermore, the potential long-term effects of the contrast agent used in MR imaging, gadolinium, are still questionable, with deposition proven within the bone and brain without an understanding of the possible long-term consequences [1–3].

Conventional ultrasound (US) offers a radiation-free technique of examining a patient without the need to provide sedation/general anesthetic and can be performed at the bedside. While color and spectral Doppler US imaging allow for detailed assessment of hemodynamics, there is a lack of temporal vascular assessment. Contrast-enhanced ultrasound (CEUS) provides an adjunct to traditional US assessment with real-time vascular imaging to a microvascular level. Contrast-enhanced ultrasound lends itself well to pediatric practice, given an established safety record [4–6]. The critical aspect to CEUS coming into widespread utility is that it is considered equivalent in diagnostic imaging with CT or MR imaging, which has been demonstrated in many areas [7–10].

The majority of healthcare services worldwide face escalating expenses, with an increasing population and longer survival with multiple comorbidities. Healthcare systems, therefore, are finding novel ways of reducing cost without compromising patient care. Diagnostic imaging is a prime target for improving expenditure levels, primarily due to the marked increase in patient numbers, requirement for detailed imaging, and the need for highly skilled staff to operate the imaging modalities. It is generally accepted that CT and MR are the mainstays of imaging in adults. In the pediatric population, the desire to

G. T. Yusuf (✉) · A. Deganello · M. E. Sellars
P. S. Sidhu
Department of Radiology, King's College Hospital, London, UK
e-mail: Gibran.yusuf@nhs.net

P. S. Sidhu et al. (eds.), *Contrast-Enhanced Ultrasound in Pediatric Imaging*,
https://doi.org/10.1007/978-3-030-49691-3_21

reduce radiation exposure has meant that US is of dominant use, with the added benefit of being an economical modality [11].

21.2 Cost Implications

Few studies have examined the cost-effectiveness of CEUS often due to the difficulty in comparison directly between modalities, and only a solitary study to date has evaluated the cost-effectiveness of CEUS in pediatric use [6]. The majority of the literature evaluating the cost of CEUS is based on adult hepatic studies [12, 13].

The earliest study evaluating the economic impact of CEUS was performed in 2007 as part of a multicenter study in Italy [14]. Indeterminate liver lesions on US were examined at three Italian centers with the aim of evaluating both the ability to characterize a focal liver lesion and assess the economic impact. Within the Italian National Health Service, the authors describe a minimal capped payment for outpatient care with all care beyond this delivered free. Hospital reimbursement is based on regional tariffs and in this study was compared with the true cost to each hospital. Conventional diagnostic imaging pathways resulted in a reduction in the need for CT by 89% and MR in 77% and indeed preventing the need for any further imaging in 89%. The resulting cost saving equated to €162 per patient, in total a sum of €78,902. While the authors describe inadequate reimbursement from the National Health System, the deficit was less for CEUS than for conventional diagnostic pathways. The authors also clearly allude to the principle of CEUS being as effective diagnostically as the usual imaging pathways.

A similar study was conducted in the Czech Republic (a primarily insurance-based healthcare system) and identified a similar pattern of cost saving with CEUS [15]. However, there was a discrepancy between CT and MR imaging. Contrast-enhanced ultrasound showed only a modest reduction in cost for incidentally discovered focal liver lesions of 4% while a cost reduction of 406% was present for CEUS compared to MR imaging. Similar outcomes in two studies, despite differences in healthcare provision lead to the impression of CEUS as a cost-effective modality.

A further group evaluated the cost of CEUS in respect to incidental focal liver lesions, but interestingly broke down the cost of the pathway using CEUS by lesion type [16]. Factors contributing to cost were also considered including equipment costs and depreciation, consumables costs, and staff costs. Contrast-enhanced ultrasound was found to be more expensive than conventional US (€46.36 vs €101.51) but was less than half as expensive as CT imaging (€211.48). The primary difference in cost between US and CEUS was associated with the contrast media charge as well as radiologist and nursing staff cost. Comparatively, CT contrast media was similar in cost, but the cost of CT staff was considerably increased. Overall, the utility of CEUS to characterize a focal liver lesion resulted in €47,055.33 saved over a 2-year period, with CT costing 208% that of CEUS [16].

Within this evaluation is an important abnormality, the pseudo-lesion. The pseudo-lesion is described as either focal fatty infiltration or sparing, importantly these are benign but often indistinguishable from a malignant lesion on conventional US. By performing CEUS examination, resultant cost savings alone of €17,352 over 4 years were established [16, 17]. Zaim et al. [18] analyzed the wider picture of a patient pathway and included CEUS as a second-line technique in addition to baseline US and conventional CT and/or MR imaging. The cost analysis was inclusive of all diagnostic tests as well as hospital stay and treatments (including ablation, chemo-embolization, transplantation, and resection). Over the period of follow-up (2 years), a €452 saving was found in using the CEUS pathway which was broken down to include €160 saving on the diagnostic pathway. With a cost-effectiveness threshold set at €20,000, the CEUS pathway was effective in 90% compared to only 10% in the MR/CT imaging pathway [18].

21.3 NICE Guidelines

The rapid growth of CEUS in Europe encouraged the National Institute of Clinical Excellence in the United Kingdom (NICE UK) to undertake a health technology assessment of the dominant ultrasound contrast agent, SonoVue™ (Bracco, Milan) [19]. The assessment identified three areas: characterization of focal liver lesions found in surveillance of cirrhotic patients, detection of colorectal metastases, and characterization of incidental liver lesions. Three individual models were used with separate assumptions made for the analysis. Cost was based upon physician opinion combined with the additional time and disposable costs of CEUS compared to conventional US yielding a figure of £65. For surveillance in cirrhosis, CEUS was found to be inferior in sensitivity to MR imaging but when factored in the cost increase per MR of £1063 more per scan, this resulted in an incremental cost-effectiveness ratio (ICER) per quality-adjusted life year (QALY) of £48,454 (above the typical acceptable threshold of £30,000). CEUS was found equivalent to CT but marginally cheaper in the assessment by NICE [19].

In the model for colorectal liver metastases, detection with CEUS was equivalent in diagnostic capability to CT and was calculated to be £1 more expensive, while MR was significantly more costly. The authors point out that although technically CT is cheaper the difference is small without differing clinical adequacy. When incidental liver lesions were examined, there was a reduction in cost of £52 versus CT and £131 for MR, with further improvement noted if the consequences of an incorrect etiology were found (benign or malignant). Importantly the analysis also considered that immediate CEUS was highly accessible, given the directly prior performed conventional US, contributing to reducing the anxiety associated with the unknown diagnosis from a patient perspective, with a wait for further investigations and consultations. It was acknowledged that there remains some uncertainty over patients who are given an incorrect diagnosis following CEUS. It is considered that patients with a false-negative result are likely to become symptomatic within a year and so little cost effect would be encountered. The situation becomes more complex and with it more costly, particularly in the case of colorectal metastases where treatment in all cases was assumed. Overall, it was considered that the major use of CEUS was in the rapid exclusion of malignancy, and it is expected that CEUS can reduce costs without reducing quality of life or survival.

While the data for adults and in particular hepatic use appear convincing for a cost-effective modality, CEUS efficiency has comparatively little evidence in the pediatric population. A solitary study of cost-effectiveness has been performed in pediatrics [6]. A single center, experienced in Pediatric CEUS, analyzed 8 years' worth of studies in children under the age of 18 years for a range of indications including hepatic, renal, trauma, vascular, testicular, and endocavitary use in 305 patients. Utilizing figures quoted within the NICE assessment, the traditional pathways for the specified indications were assessed in each case with utility of CT or MR imaging assessed. Overall, a $16,000 saving was achieved over the study period; however, this figure was likely an under-estimate as the figures used were based on adults in the NICE assessment [19]. The authors redefine doses in pediatric practice, based on age and utility, allowing a single vial of UCA to be not solely for a single use, decreasing the cost per examination.

Furthermore, the expense of MR imaging in pediatrics can be variable depending on the degree of sedation/anesthesia required. In addition to drug costs and supportive care staff, costs associated with trained anesthetic personnel will escalate the cost of MR imaging in many cases beyond the quoted ($180). Costs associated with CT ($94) are less than that of MR imaging but still represent an increased cost compared to CEUS, and sedation/anesthesia may still be required particularly for younger children [6]. In cases of trauma, serial CT imaging would be needed for a variable length of time. In a number of cases, such as testicular CEUS, there will simply be no other means of effective imaging.

21.4 Conclusion

There is no doubt in the utility of CEUS, and deep seated within any consideration of cost-effectiveness, is the principle that CEUS is equivalent to CT or MR imaging for diagnostic purposes. This has been generally accepted for pediatric focal liver lesion characterization. Further uses are less well studied, but the dynamic nature of CEUS and the degree of spatial resolution have led to increasing enthusiasm for its use as a "problem-solving" tool [7, 9, 10, 20]. The benefits CEUS confers; absence of radiation, a safe contrast agent and bedside imaging, make it ideal for use in pediatrics. The advent of such an imaging modality may lead to more widespread uptake in cases where imaging would not be normally performed, e.g., low-velocity trauma. In addition, the changing attributes of the pediatric population lead to changing disease prevalence, particularly fatty liver disease which in turn leading to increased recognition of pseudo-lesions and hepatocellular lesions. In combination, CEUS in pediatric use is likely to become a part of routine imaging pathways and must represent a cost-effective modality for successful integration. Consensus from studies seems to suggest CEUS offers an overall reduction in the cost for traditional imaging pathways in both the adult and pediatric population, particularly for hepatic use.

References

1. Khawaja AZ, Cassidy DB, Al Shakarchi J, McGrogan DG, Inston NG, Jones RG. Revisiting the risks of MRI with gadolinium based contrast agents—review of literature and guidelines. Insights Imaging. 2015;6:553–8.
2. Ramalho J, Semelka RC, Ramalho M, Nunes RH, AlObaidy M, Castillo M. Gadolinium-based contrast agent accumulation and toxicity: an update. AJNR Am J Neuroradiol. 2016;37:1192.
3. Elbeshlawi I, AbdelBaki MS. Safety of gadolinium administration in children. Pediatr Neurol. 2018;86:27–32.
4. Piskunowicz M, Kosiak W, Batko T, Piankowski A, Polczynska K, Adamkiewicz-Drozynska E. Safety of intravenous application of second generation ultrasound contrast agent in children: prospective analysis. Ultrasound Med Biol. 2015;41:1095–9.
5. Piscaglia F, Bolondi L. The safety of SonoVue in abdominal applications: retrospective analysis of 23188 investigations. Ultrasound Med Biol. 2006;32:1369–75.
6. Yusuf GT, Sellars ME, Deganello A, Cosgrove DO, Sidhu PS. Retrospective analysis of the safety and cost implications of pediatric contrast-enhanced ultrasound at a single center. AJR Am J Roentgenol. 2016;208:446–52.
7. Sidhu PS, Cantisani V, Deganello A, Dietrich CF, Duran C, Franke D, et al. Role of contrast-enhanced ultrasound (CEUS) in Pediatric practice: an EFSUMB position statement. Ultraschall Med. 2017;38:33–43.
8. Sidhu PS, Cantisani V, Deganello A, Dietrich CF, Duran C, Franke D, et al. Authors reply to letter: role of contrast-enhanced ultrasound (CEUS) in Pediatric practice: an EFSUMB position statement. Ultraschall Med. 2017;38:447–8.
9. Sidhu PS, Cantisani V, Dietrich CF, Gilja OH, Saftoiu A, Bartels E, et al. The EFSUMB guidelines and recommendations for the clinical practice of contrast-enhanced ultrasound (CEUS) in non-hepatic applications: update 2017 (long version). Ultraschall Med. 2018;39:e2–e44.
10. Rafailidis V, Deganello A, Watson T, Sidhu PS, Sellars ME. Enhancing the role of Pediatric ultrasound with microbubbles: a review of intravenous applications. Br J Radiol. 2016;90(1069):20160556.
11. Pearce MS, Salotti JA, Little MP, McHugh K, Lee C, Kim KP, et al. Radiation exposure from CT scans in childhood and subsequent risk of leukaemia and brain tumours: a retrospective cohort study. Lancet. 2012;380:499–505.
12. Leen E, Moug S, Horgan P. Potential impact and utilization of ultrasound contrast media. Euro Radiol Suppl. 2004;14:P16–24.
13. Strobel D, Seitz K, Blank A, Schuler A, Dietrich C, von Herbay A, et al. Contrast-enhanced ultrasound for the characterization of focal liver lesions—diagnostic accuracy in clinical practice (DEGUM multicenter trial). Ultraschall Med. 2008;225:499–505.
14. Romanini L, Passamonti M, Aiani L, Cabassa P, Raieli G, Montermini I, et al. Economic assessment of contrast-enhanced ultrasonography for evaluation of focal lesions: a multicenter Italian experience. Eur Radiol Suppl. 2007;17:F99–F106.
15. Smajerova M, Petrasova H, Little J, Ovesna P, Andrasina T, Valek V, et al. Contrast-enhanced ultrasonography in the evaluation of incidental focal liver lesions: a cost-effectiveness analysis. World J Gastroenterol. 2016;22:8605–14.
16. Faccioli N, D'Onofrio M, Comai A, Cugini C. Contrast-enhanced ultrasonography in the characterization of benign focal liver lesions: activity-based cost analysis. Radiol Med. 2007;112:810–20.
17. Jacob J, Deganello A, Sellars ME, Hadzic N, Sidhu PS. Contrast enhanced ultrasound (CEUS) characterization of grey-scale sonographic indeterminate focal liver lesions in Pediatric practice. Ultraschall Med. 2013;34:529–40.

18. Zaim R, Taimr P, Redekop W, Uyl-de Groot C. Economic evaluation of contrast-enhanced ultrasound (CEUS) in the characterization of focal liver lesions (FLL) in the Netherlands. Rotterdam: Institute for Medical Technology Assessment, Department of Health Policy and Management, Erasmus University; Department of Gastroenterology and Hepatology, Erasmus MC University Hospital; 2011.
19. Westwood M, Joore M, Grutters J, Redekop K, Armstrong N, Lee K, et al. Contrast-enhanced ultrasound using SonoVue® (sulphur hexafluoride microbubbles) compared with contrast-enhanced computed tomography and contrast-enhanced magnetic resonance imaging for the characterization of focal liver lesions and detection of liver metastases: a systematic review and cost-effectiveness analysis. Health Technol Assess (Winchester, England). 2013;17(16):1.
20. Claudon M, Dietrich CF, Choi BI, Kudo M, Nolsoe C, Piscaglia F, et al. Guidelines and good clinical practice recommendations for contrast enhanced ultrasound (CEUS) in the liver—update 2012. Ultraschall Med. 2013;34:11–29.

Recent Advances in Neonatal CEUS

22

Misun Hwang

22.1 Introduction

Due to the enhanced diagnostic sensitivity, portability, and safety, contrast-enhanced ultrasound (CEUS) has emerged as a promising modality for pediatric patients. Increasing numbers of CEUS examinations are being performed for emerging indications, previously unexplored, and are benefiting clinical care. This chapter reviews recent advances in neonatal CEUS applications beyond the commonly used indications and present new clinical directions.

22.2 Neonatal Imaging

Neonates represent a specific group in the pediatric population with disease processes that are distinct and unique. Their vulnerability to prenatal and perinatal insults in the background of immature physiology produces a constellation of neonatal diseases including hypoxic ischemic injury, necrotizing enterocolitis, and hip dysplasia. For this population, moreover, the optimal imaging choice is not always magnetic resonance (MR) imaging for several reasons. Firstly, patient transport and sedation pose a higher risk to neonates than in older children. Secondly, the resolution of MR imaging is suboptimal for the evaluation of any small abnormality. Thirdly, gadolinium contrast as an addition to conventional MR imaging for functional characterization of tissues has an additional risk. In this regard, CEUS has emerged as a valuable alternative to MR imaging examination; a CEUS examination is portable, obviating the need for patient transport. The CEUS examination is independent of patient movement with a contrast agent that allows for repeated examinations without compromise to safety, using a modality, ultrasound (US), which has high resolution. The need for any patient sedation or general anesthetic is obviated, with time and cost implications.

22.3 Clinical Applications

22.3.1 Hypoxic Ischemic Injury

More recently, CEUS has been used to diagnose and characterize neonatal hypoxic ischemic injury [1–3] (Fig. 22.1). There are three major patterns of hypoxic ischemic injury: watershed (or cortical), central, and mixed. The watershed hypoxic ischemic injury is the most common pattern of injury and can be subtle on grayscale US. The central pattern hypoxic ischemic injury, which involves the central gray nuclei, is less common but signifies poor prognosis, and can be

M. Hwang (✉)
Department of Radiology, Children's Hospital of Philadelphia, University of Pennsylvania, Philadelphia, PA, USA
e-mail: HWANGM@email.chop.edu

P. S. Sidhu et al. (eds.), *Contrast-Enhanced Ultrasound in Pediatric Imaging*,
https://doi.org/10.1007/978-3-030-49691-3_22

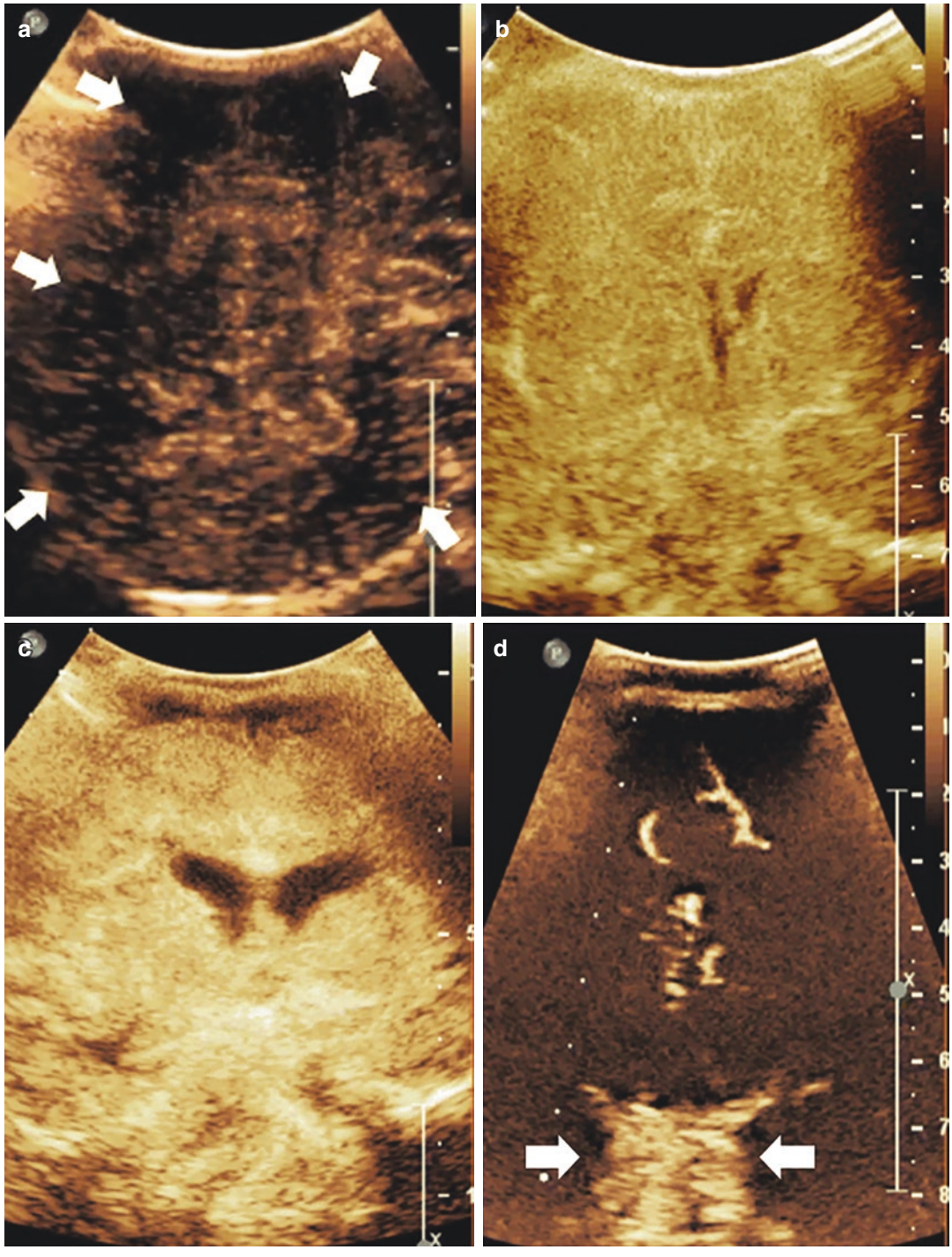
a
b
c
d

Fig. 22.1 Brain CEUS: hypoxic ischemic injury. Multifocal and symmetrical diffuse perfusion abnormalities are shown on contrast-enhanced ultrasound (CEUS). A coronal scan through the posterior parieto-occipital lobes (**a**) in a 4-day-old boy with hypoxic ischemic injury was obtained at 27 s after ultrasound contrast agent (UCA) injection at peak intensity. Generalized hypoperfusion with multifocal perfusion abnormalities is noted as evidenced by the paucity of UCA in scattered areas (*arrows*). In a 14-day-old boy and a 5-month-old boy with symmetrical diffuse hypoxic ischemic injury (**b, c**), both obtained at 18 s after UCA injection, resulting generalized hyperperfusion to the brain, as seen in the immediate post-injury period. An image (**d**) in a 6-month-old boy post prolonged cardiac arrest demonstrates diffuse hypoperfusion to the brain. Images obtained with an EPIQ scanner, Philips Healthcare, Bothell, WA: (**a**) was obtained with C5-1 transducer and settings of 12 MHz, mechanical index (MI) 0.06; (**b**) with C9-2 transducer and settings of 13 MHz, MI 0.06; (**c**) with C9-2 transducer and settings of 7 MHz, MI 0.06, and (**d**) with C9-2 transducer and settings of 12 MHz, MI 0.06 (Reproduced with permission from Pediatric Radiology 2019 Feb;49(2):254–262)

manifested as altered echogenicity of the thalamus and/or basal ganglia, which can be diagnostically challenging depending on the severity and extent of injury. Similar to the watershed type injury, mixed pattern injury which involves both the cortex and central gray nuclei can be difficult to subjectively discern on grayscale US. In such settings, perfusion abnormalities highlighted by CEUS can be helpful to improve the diagnostic sensitivity for hypoxic ischemic injury. In the hyperacute phase of hypoxic ischemic injury, a perfusion defect is expected in the affected brain regions. In the acute to subacute phases of hypoxic ischemic injury, hyperperfusion is typically seen in the affected brain regions due to the reperfusion response. In the chronic phase, perfusion can be decreased, normalized, or increased depending on the presence or absence of permanent brain damage. Future research will reveal additional insights into the extent to which CEUS can enhance the diagnostic sensitivity and prognostic value of US.

With the scanning protocol for brain CEUS specifically to screen for hypoxic ischemic injury [2], open fontanelles, as present in neonates, serve as acoustic windows. The anterior fontanelle is initially used to acquire a cine clip of washin and early washout of the ultrasound contrast agent (UCA) in the coronal plane of the basal ganglia (Fig. 22.2). The acquisition of the initial cine clip in the plane of the basal ganglia ensures that the central pattern hypoxic ischemic injury can be detected. After the initial cine clip, coronal and optimal sagittal sweeps through the brain are performed to screen for perfusion abnormalities. Note that these sweeps are done immediately after the confirmation of early washout such that sufficient contrast signal is seen in the remainder of the brain. In some cases, dedicated posterior fontanelle or transmastoid views may be used to delineate germinal matrix/periventricular white matter or cerebellar abnormalities, respectively. In the setting of acute to subacute hypoxic ischemic injury, both the cortex and central gray nuclei demonstrate delayed washout of contrast, and this can be either qualitatively or quantitatively evaluated. The delayed washout parameter is similar to delayed mean transit time in perfusion MR imaging.

Similar to other CEUS examinations, the imaging parameters should be optimized for harmonic imaging of the UCA. The mechanical index (MI) is set low at <0.2 in order to enhance the contrast signal while minimizing microbubble destruction. The focal zone is placed low in the field of view so that microbubble destruction is minimized in the brain. Either the dual display (CEUS image adjacent to Grayscale US image), single display (CEUS image only), or CEUS overlay onto Grayscale US image may be adopted for scanning approach. The dual display or CEUS overlay ensures real-time localization between perfusion and anatomic region, whereas single display slightly increases the frame rate and highlights the microbubble signal in the absence of background grayscale US image. The injection method is similar to other CEUS examinations, and the injection dose may be as per standard dosing for liver evaluation. It should be noted however that scanners with higher sensitivity to

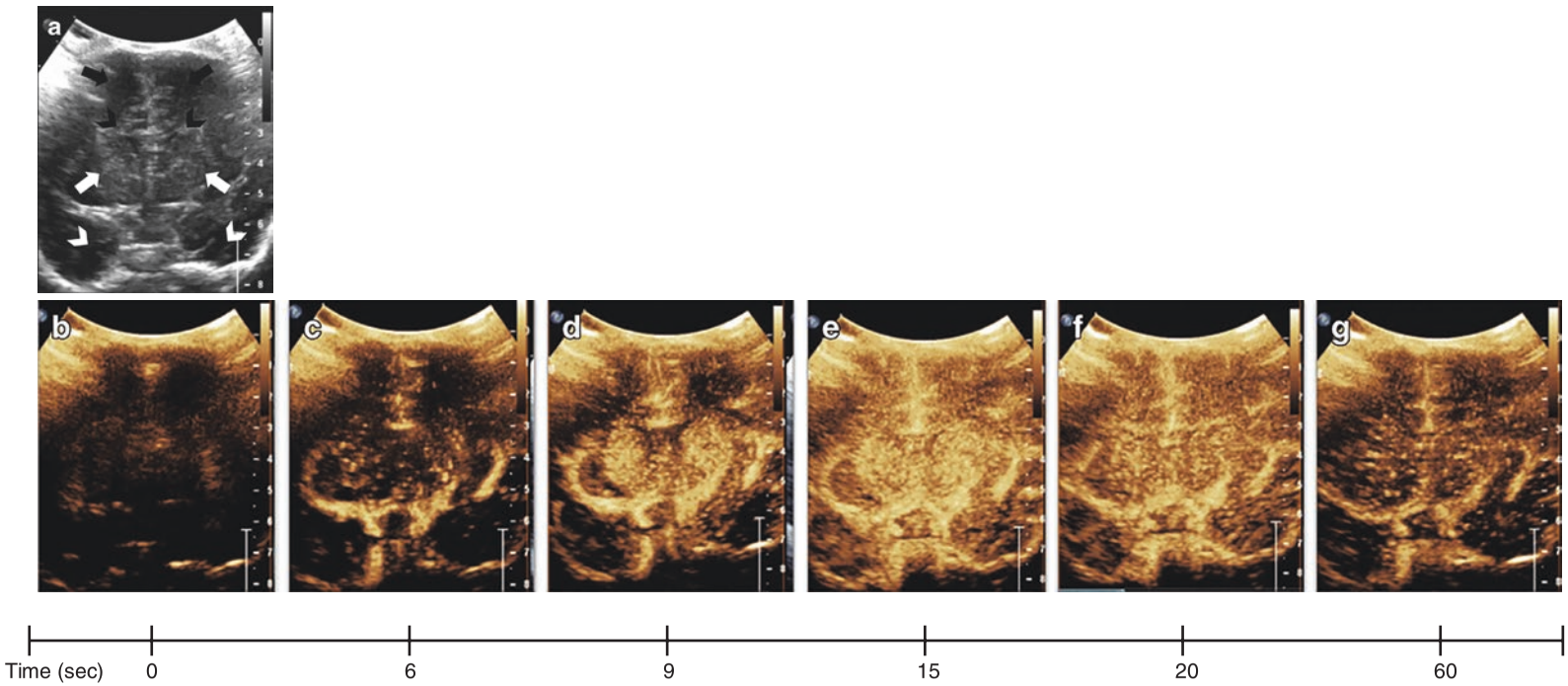

Fig. 22.2 Brain CEUS: Protocol. Dynamic UCA washin on mid-coronal brain scan in a normal 1-month-old boy. A mid-coronal Grayscale US image (**a**) through the brain of a normal subject shows bilateral frontal lobes (black arrows), frontal horns (black arrowheads), basal ganglia (white arrows), and temporal lobes (white arrowheads). (**b**–**g**) Dynamic UCA washin through the mid-coronal slice through the brain on a contrast specific mode from the time of injection (time 0) to 1 min is illustrated. Note that the UCA flow into the partially visualized Circle of Willis by 6 s. By 9 s, relatively more avid enhancement to the basal ganglia with respect to the remainder of the brain. Further enhancement of the cortex but with relative hyperenhancement of the basal ganglia is noted at 15 s. Washout of contrast from both the basal ganglia and cortex begins at 20 s and further washout is noted at 60 s. Images obtained with an EPIQ scanner, Philips Healthcare, Bothell, WA, with C5-1 transducer and settings of 12 MHz, mechanical index (MI) 0.06. (Reproduced with permission from Pediatric Radiology 2019 Feb;49(2):254–262)

UCA signal may enable decreased contrast dose especially in small neonates. As the dose is often ≤0.1–2 mL in neonates, it is useful to prepare a smaller caliber syringe in order to avoid under- or over-injection of the UCA. Care should be taken in the neonatal brain when performing a CEUS examination; avoid switching from CEUS setting (MI of <0.2) to grayscale setting (MI approximately 1.0) prior to complete contrast washout. This is due to the possibility of causing unwanted microbubble destruction in the presence of immature vasculature in select brain regions such as the germinal matrix. Hence, complete washout of the UCA prior to resuming grayscale or color Doppler US evaluation is recommended.

22.3.2 Brain Death

The extreme case of hypoxic ischemic injury is brain death. While brain death is a clinical diagnosis based on the apnea test, an infant's inability to tolerate test necessitates clinicians to rely on ancillary imaging tests. In the 2011 revised pediatric brain death guidelines, the two most commonly used ancillary studies for validation of circulatory arrest (CCA) were a radionuclide examination and four-vessel cerebral angiography [4]. Note that both studies require transportation out of the intensive care unit, which can be challenging during the critical period. Not all hospitals are equipped with to perform such studies outside the working day. Compared to these studies, brain CEUS can be performed at the bedside and promptly at the time of suspicion of CCA. Furthermore, the examination is cost-effective and can readily be adopted into existing clinical practice.

While further work is needed to introduce CEUS as an alternative tool to a radionuclide examination or cerebral angiography in validating brain death, there is evidence that it may help confirm the absence of brain perfusion and therefore the diagnosis of brain death. In a case report of an infant with cardiac arrest, brain CEUS was performed to assess for brain perfusion [5]. In this infant, perfusion was nearly absent in the whole brain except for few parasagittal vessels, and the typical prompt washin and washout of the UCA (lasting less than 10 min total) were not observed (Fig. 22.3). Instead, UCA washin was significantly delayed and washout did not occur up to 30 min at which point the examination was terminated. Likely, the near absent brain perfusion state was accompanied by increased intracranial pressure due to the severe hypoxic ischemic injury, which altered both the washin and washout perfusion kinetics parameters. Future studies comparing brain CEUS with the reference standard nuclear examination for the diagnosis of brain death will be necessary to advance this novel application.

22.3.3 Intracranial Lesions

In the presence of an acoustic window, such as the fontanelle or open cranial window during surgery or craniotomy, CEUS can be valuable for detailed evaluation of benign and malignant intracranial lesions. Contrast-enhanced ultrasound offers dynamic perfusion kinetics of intracranial lesions with excellent spatial and temporal resolution and enhances the conspicuity of lesional borders [6]. In the case of a tumor, CEUS can be valuable for distinguishing benign from malignant tumors, discerning the tumor–parenchymal border, differentiating edema from tumor, grading tumor, guiding biopsy, and following treatment response [7–18] (Fig. 22.4). There is preliminary evidence that CEUS may aid with tumor grading although its accuracy needs to be further validated. In the case of vascular malformation, the extent of shunting and blood volume within the lesion can be qualitatively and quantitatively evaluated with CEUS. In infants or in the case of cranial window, CEUS permits quantitative assessment of residual flow post endovascular intervention of vascular malformation without the need for contrast-enhanced computed tomography (CT), MR imaging, or angiography. In the case of multiple lesions such as with abscesses or vascular malformations not readily apparent with conventional grayscale US, CEUS can enhance the conspicuity of these lesions.

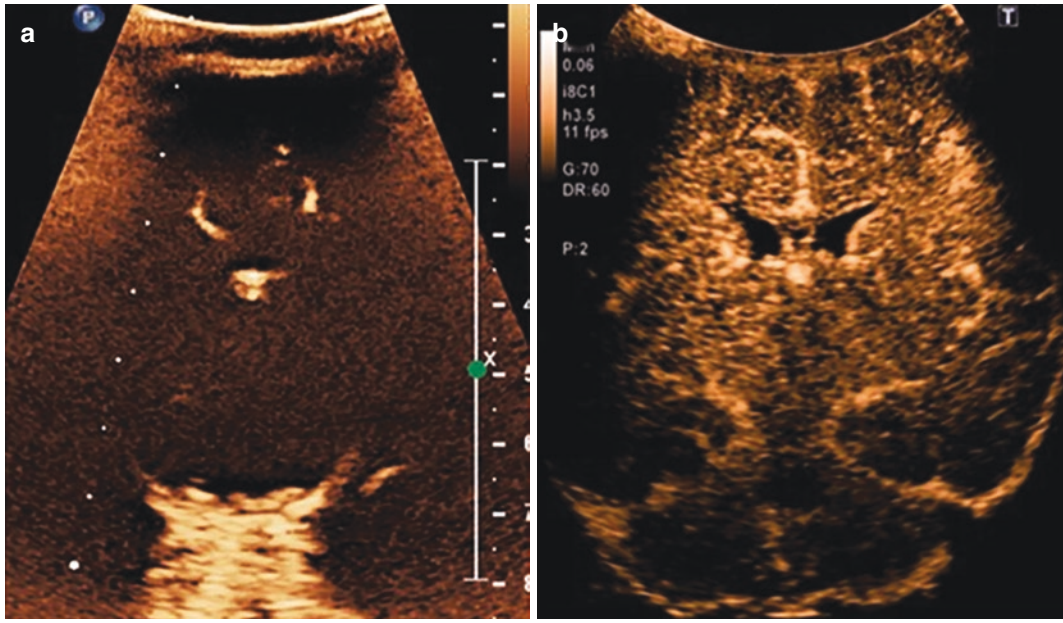

Fig. 22.3 Brain CEUS: near brain death. A midcoronal CEUS image (**a**) shows avid enhancement of the cervical extracranial vessels (arrows). For comparison, (**b**) is a coronal slice from a 2-month-old male admitted for respiratory distress but without intracranial injury showing normal enhancement of brain. Within 7 min of administration, the UCA had a near-complete washout in the comparison case; however, washout from few intracranial vessels had not occurred 30 min after administration in the post-cardiac arrest patient, signifying extremely poor cerebral circulation. There was no further imaging possible following the death (declared dead as per clinical assessment for brain death) of the child. (Reproduced with permission from Neuroradiology Journal 2018 Dec;31(6):578–580)

22.3.4 Bowel Disease of Prematurity

Bowel disease of prematurity encompasses a wide variety of bowel pathology affecting preterm infants, including necrotizing enterocolitis, prenatal volvulus, or atresia. Etiologies could be due to prenatal or perinatal insult leading to compromise of the blood supply to the bowel. While conventional grayscale and color Doppler US have enhanced the diagnostic sensitivity of bowel disease of prematurity as compared to a radiograph alone, there are limitations. There is an inability to quantitate bowel perfusion with color Doppler US in the presence of an oscillator or other external vibrator, which is common in the intensive care unit setting, due to motion degradation. In such case, CEUS which is relatively motion insensitive can be performed to better characterize bowel perfusion.

Necrotizing enterocolitis affects up to one in 2000 births and occurs in approximately 10% of preterm infants, although rare in term infants. Etiology is thought to be due to intestinal invasion of bacteria followed by local infection and inflammation leading to bowel wall destruction, perforation, overwhelming sepsis, and death. Diagnosis is made using the Bell's staging criteria aided by radiographic findings, which can vary in manifestation to fixed and/or dilated bowel loops, pneumatosis, portal venous air, and/or pneumoperitoneum. The diagnostic sensitivity of the clinical and radiographic criteria combined is low, and many cases of even advanced necrotizing enterocolitis can be missed. In this regard, color Doppler US has been used to characterize the evolution of necrotizing enterocolitis to potentially augment the diagnostic sensitivity. Prior studies have shown that in the evolution of necrotizing enterocolitis, avid perfusion to the bowel wall has been observed. The hyperperfusion seen during the evolution of necrotizing enterocolitis could be attributable to local inflam-

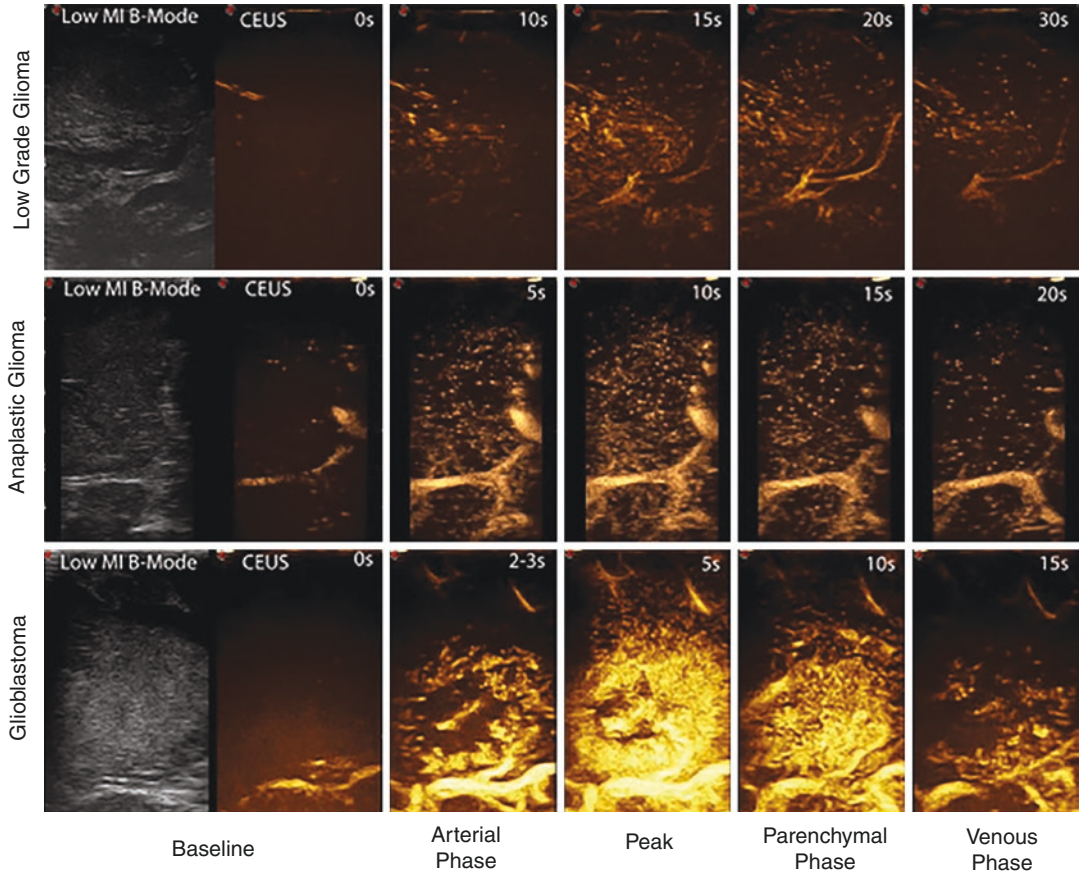

Fig. 22.4 CEUS for tumor characterization. Time frame of how different grades of glioma are visualized with CEUS. In the first column of each row, low mechanical index US and baseline CEUS (CA arrival − *t*0) are displayed; then different CEUS phases (time is shown in the top right corner of each image) are displayed only. The image clearly shows the differences in terms of timing, degree of enhancement, and CEUS patterns for different types of glioma, with a continuous and dynamic modality. (Reproduced with permission from Biomedical Research International 2014;2014:484261)

mation leading to vasodilatation, reperfusion response to ischemic insult, and/or alterations in vaso-regulatory mechanisms.

With CEUS a case series has demonstrated that in necrotizing enterocolitis bowel hyperperfusion, as previously demonstrated with color Doppler US, follows a similar pattern [19]. The hyperperfused bowel segment demonstrated hypoperistalsis and dilatation, as compared to other bowel loops in the abdomen. On surgical pathology, both viable and ischemic bowel were observed. The exact timing and extent of perfusion changes in the affected bowel segment are not known, but further studies to gather information regarding CEUS behavior would greatly augment the diagnostic sensitivity of CEUS in necrotizing enterocolitis (Fig. 22.5). A diagnosis of early disease can help institute therapies preventing further cascade of infection/inflammation.

In the same CEUS case series, a preterm infant with total bowel ischemia due to prenatal volvulus was illustrated (Fig. 22.6). Color Doppler US evaluation in this case was equivocal due to the presence of an oscillator. Grayscale US of the bowel loops demonstrated decreased peristalsis but without evidence of pneumatosis or significant thickening. With a UCA injection, complete lack of enhancement of the bowel walls throughout the abdomen was demonstrated, confirming

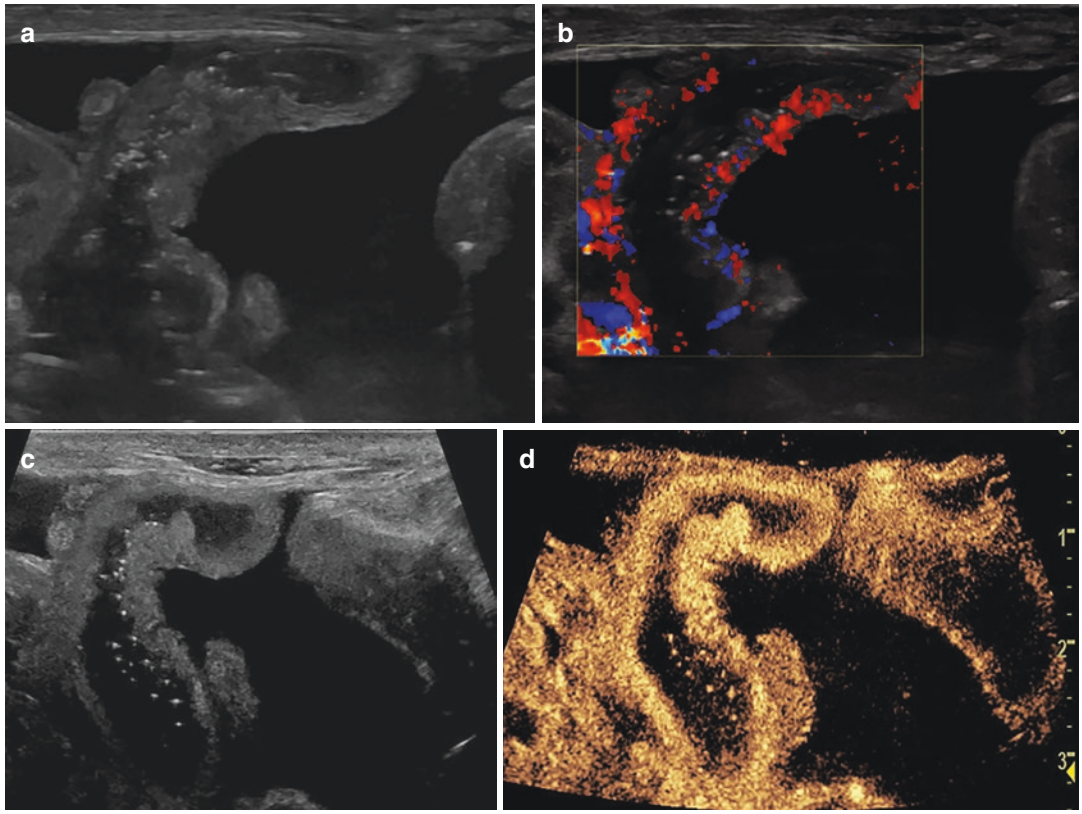

Fig. 22.5 CEUS for necrotizing enterocolitis. A 39-day-old formerly premature girl was born at 26 weeks with abdominal distention and bloody stool. (**a**) Grayscale US of the right lower quadrant shows a distended loop of bowel with wall thickening that was hypoperistaltic in real time. (**b**) Corresponding color Doppler US image shows hyperemia within the thickened bowel wall. (**c**, **d**), Dual-screen display with grayscale US (**c**) and corresponding CEUS (**d**) reveals hyperemia of the bowel wall. On all images, large volume ascites is present. (Permission to reproduce from Journal of Ultrasound in Medicine 2019 Nov 9. https://doi.org/10.1002/jum.15168)

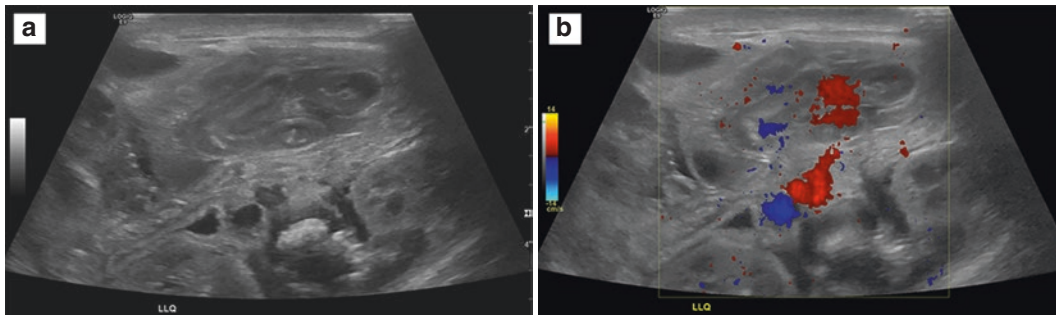

Fig. 22.6 CEUS for bowel ischemia of prematurity. A 1-day-old formerly premature girl was born at 29 weeks with gaseous distention on abdominal radiography. (**a**) Grayscale US in the left upper quadrant shows multiple dilated loops of bowel with wall thickening and hypoperistalsis to aperistalsis in real time. (**b**) Corresponding color Doppler US image shows apparent flow in the mesentery but no appreciable flow in the bowel. However, the interpretation was limited by pulsatile motion from the patient's high-frequency oscillator. (**c**, **d**) Dual-screen CEUS display shows loops of bowel (**c**, arrowheads) in the right upper quadrant that do not enhance (**d**, arrowheads) regardless of the high-frequency oscillator. (Permission to reproduce from Journal of Ultrasound in Medicine 2019 Nov 9. https://doi.org/10.1002/jum.15168)

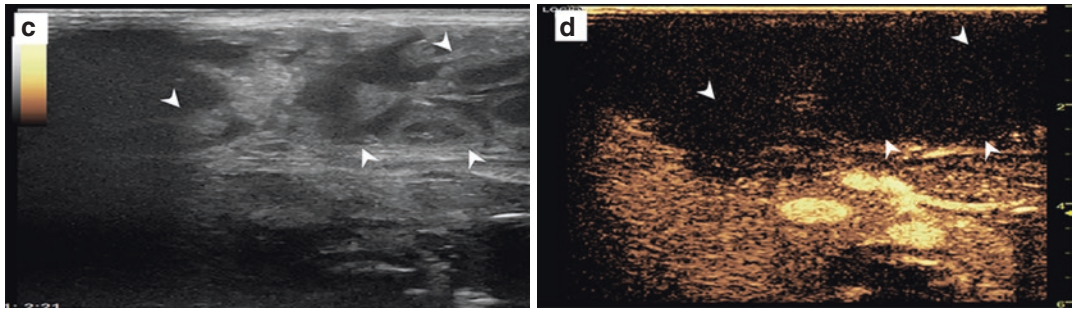

Fig. 22.6 (continued)

global bowel ischemia, confirmed at subsequent surgery. Likewise, CEUS can be a useful troubleshooting tool for confirmation of bowel perfusion in cases where prenatal ischemic insult is suspected and color Doppler US is suboptimal.

22.3.5 Developmental Dysplasia of the Hip

Development dysplasia of the hip (DDH) is the most common developmental deformity of the lower extremity in children. It affects 28.5 per 1000 infants [20, 21] and timely diagnosis and correction are critical to preventing worsening dysplasia and associated morbidity. While approximately 80% of infants with frankly dislocated hips can be successfully reduced with a Pavlik harness or other bracing treatment, some do not respond to nonsurgical treatment and need to undergo closed or open reduction followed by Spica cast immobilization in the operating room. A major source of morbidity in patients requiring surgical intervention is iatrogenic avascular necrosis (AVN), which could result from excessive hip abduction within the cast [22]. AVN can disrupt normal epiphyseal growth and lead to premature osteoarthritis, ultimately requiring total hip arthroplasty [23, 24].

In order to confirm the preservation of femoral head perfusion post reduction, postoperative gadolinium-enhanced MR imaging can be performed. It has been shown that decreased enhancement of the femoral head on postoperative MR imaging is strongly correlated with the future development of AVN [25]. However, there are challenges with relying on postoperative MR imaging including the need to leave the operating room and decreased sensitivity to microcirculatory flow, which is below the resolution of MR imaging. The potential discovery of compromised femoral head perfusion immediately post reduction could lead to prompt surgical intervention prior to departure from the operating room. In this regard, CEUS may serve as an effective alternative to contrast-enhanced MR imaging that can be used in the operating room pre and post hip reduction.

A prior article described preliminary experience with intraoperative hip CEUS in 17 children with DDH [26]. A scoring system used to quantify the number of vessels visualized in the femoral head revealed a decrease in vessel number post reduction as qualitatively evaluated using CEUS, while all CEUS showed preserved blood flow in the femoral epiphysis before and after reduction. All MR imaging studies were similar to the CEUS examination and showed femoral head enhancement post reduction. The article not only demonstrates the feasibility of safely performing intraoperative hip CEUS in infants but also suggests the need for a larger prospective study exploring the long-term implications of the femoral head perfusion patterns observed on intraoperative CEUS (Fig. 22.7).

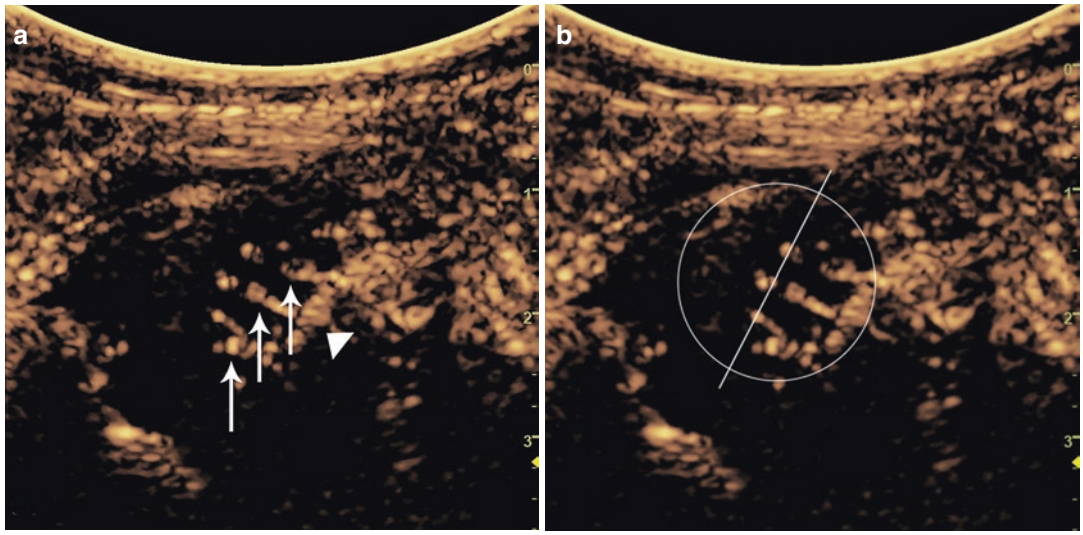

Fig. 22.7 CEUS for hip dysplasia. Imaging landmarks for epiphyseal blood flow assessment with CEUS in a 20-month-old boy before reduction: CEUS images of the left hip in a coronal plane. (**a**) Landmarks used to assess the vascular flow in the femoral epiphysis. (**b**) Circle drawn over the epiphysis, bisected by a line parallel to the epiphysis, traversing the ossific nucleus when visible. Arrowhead indicates epiphysis; and arrows, epiphyseal vessels. (Reproduced with permission Journal of Ultrasound in Medicine 2019 Jul 23. https://doi.org/10.1002/jum.15097)

22.4 Conclusion and Future Directions

Due to the convenience of CEUS combined with the improved diagnostic sensitivity it provides over the conventional grayscale and color Doppler US, the advantages of CEUS for the neonatal population are clear. In the future, the neonatal applications of CEUS will continue to increase and improve the clinical care by obviating the need for transport, sedation, and costly examinations. The ability of CEUS to discern microvascular flow at much higher spatial resolution than advanced imaging modalities such as CT or MR imaging can also help characterize the unique pathophysiology in neonates. Likewise, the future applications of CEUS in neonates seem promising.

References

1. Hwang M. Novel contrast ultrasound evaluation in neonatal hypoxic ischemic injury: case series and future directions. J Ultrasound Med. 2017;36:2379–86.
2. Hwang M. Introduction to contrast-enhanced ultrasound of the brain in neonates and infants: current understanding and future potential. Pediatr Radiol. 2019;49:254–62.
3. Hwang M, et al. Novel quantitative contrast-enhanced ultrasound detection of hypoxic ischemic injury in neonates and infants: pilot study 1. J Ultrasound Med. 2019;38:2025–38.
4. Nakagawa TA, et al. Guidelines for the determination of brain death in infants and children: an update of the 1987 Task Force recommendations. Crit Care Med. 2011;39:2139–55.
5. Hwang M, Riggs BJ, Saade-Lemus S, Huisman TA. Bedside contrast-enhanced ultrasound diagnosing cessation of cerebral circulation in a neonate: a novel bedside diagnostic tool. Neuroradiol J. 2018;31:578–80.

6. Cheng LG, et al. Intraoperative contrast enhanced ultrasound evaluates the grade of glioma. Biomed Res Int. 2016;2016:2643862.
7. Kanno H, et al. Intraoperative power Doppler ultrasonography with a contrast-enhancing agent for intracranial tumors. J Neurosurg. 2005;102:295–301.
8. Holscher T, et al. Intraoperative ultrasound using phase inversion harmonic imaging: first experiences. Neurosurgery. 2007;60:382–6; discussion 386–7.
9. Engelhardt M, et al. Feasibility of contrast-enhanced sonography during resection of cerebral tumours: initial results of a prospective study. Ultrasound Med Biol. 2007;33:571–5.
10. He W, et al. Intraoperative contrast-enhanced ultrasound for brain tumors. Clin Imaging. 2008;32:419–24.
11. Prada F, et al. Intraoperative contrast-enhanced ultrasound for brain tumor surgery. Neurosurgery. 2014;74:542–52; discussion 552.
12. Mattei L, et al. Neurosurgical tools to extend tumor resection in hemispheric low-grade gliomas: conventional and contrast enhanced ultrasonography. Childs Nerv Syst. 2016;32:1907–14.
13. Vetrano IG, et al. Discrete or diffuse intramedullary tumor? Contrast-enhanced intraoperative ultrasound in a case of intramedullary cervicothoracic hemangioblastomas mimicking a diffuse infiltrative glioma: technical note and case report. Neurosurg Focus. 2015;39:E17.
14. Prada F, et al. Intraoperative cerebral glioma characterization with contrast enhanced ultrasound. Biomed Res Int. 2014;2014:484261.
15. Prada F, et al. Intraoperative navigated angiosonography for skull base tumor surgery. World Neurosurg. 2015;84:1699–707.
16. Vetrano IG, Prada F, Erbetta A, DiMeco F. Intraoperative ultrasound and contrast-enhanced ultrasound (CEUS) features in a case of intradural extramedullary dorsal schwannoma mimicking an intramedullary lesion. Ultraschall Med. 2015;36:307–10.
17. Prada F, Del Bene M, Saini M, Ferroli P, DiMeco F. Intraoperative cerebral angiosonography with ultrasound contrast agents: how I do it. Acta Neurochir. 2015;157:1025–9.
18. Prada F, et al. Contrast-enhanced MR imaging versus contrast-enhanced US: a comparison in glioblastoma surgery by using intraoperative fusion imaging. Radiology. 2017;285:242–9.
19. Benjamin JL, et al. Improved diagnostic sensitivity of bowel disease of prematurity on contrast-enhanced ultrasound. J Ultrasound Med. 2020;39:1031–6.
20. Dezateux C, Rosendahl K. Developmental dysplasia of the hip. Lancet. 2007;369:1541–52.
21. Duppe H, Danielsson LG. Screening of neonatal instability and of developmental dislocation of the hip. A survey of 132,601 living newborn infants between 1956 and 1999. J Bone Joint Surg Br. 2002;84:878–85.
22. Rosenbaum DG, Servaes S, Bogner EA, Jaramillo D, Mintz DN. MR imaging in postreduction assessment of developmental dysplasia of the hip: goals and obstacles. Radiographics. 2016;36:840–54.
23. Holman J, Carroll KL, Murray KA, Macleod LM, Roach JW. Long-term follow-up of open reduction surgery for developmental dislocation of the hip. J Pediatr Orthop. 2012;32:121–4.
24. Gornitzky AL, Georgiadis AG, Seeley MA, Horn BD, Sankar WN. Does perfusion MRI after closed reduction of developmental dysplasia of the hip reduce the incidence of avascular necrosis? Clin Orthop Relat Res. 2016;32:121–4.
25. Tiderius C, et al. Post-closed reduction perfusion magnetic resonance imaging as a predictor of avascular necrosis in developmental hip dysplasia: a preliminary report. J Pediatr Orthop. 2009;29:14–20.
26. Back SJ, et al. Intraoperative contrast-enhanced ultrasound imaging of femoral head perfusion in developmental dysplasia of the hip: a feasibility study. J Ultrasound Med. 2020;39:247–57.